The role of HLA-C-specific alloantibodies in enhancing NK cell-mediated responses against tumour cells

Amandeep Johal Kaur

A thesis submitted to the University of Birmingham for the degree of DOCTOR OF PHILOSOPHY

Institute of Immunology & Immunotherapy
College of Medical & Dental Sciences
University of Birmingham
2020

UNIVERSITY OF
BIRMINGHAM

University of Birmingham Research Archive

e-theses repository

This unpublished thesis/dissertation is copyright of the author and/or third parties. The intellectual property rights of the author or third parties in respect of this work are as defined by The Copyright Designs and Patents Act 1988 or as modified by any successor legislation.

Any use made of information contained in this thesis/dissertation must be in accordance with that legislation and must be properly acknowledged. Further distribution or reproduction in any format is prohibited without the permission of the copyright holder.

ABSTRACT

Engagement between the highly polymorphic human leukocyte antigen-C (HLA-C) and the inhibitory killer immunoglobulin-like receptors (KIRs) proteins acts to supress Natural killer (NK) cell function, which may facilitate tumour cell evasion and promote disease progression. It was hypothesised that overexpression of HLA-C in cancer, and its interaction with KIRs might be disrupted by human HLA-C-specific alloantibodies to enhance NK cell function against tumour cells. Firstly, alloantibodies against HLA-C alleles from the sera of allo-sensitised individuals were confirmed by luminex microbead assay and flow cytometry staining of single HLA-C allele transfected cell lines. Secondly, affinity-purified alloantibodies from sera were applied in an *in vitro* cell model and NK cell cytotoxicity against HLA-C-specific antibody-coated transfected cells, solid tumour cell lines and primary B-CLL cells was significantly improved. Antibody-dependent cellular cytotoxicity (ADCC) mechanism played a role in enhancing target cell lysis in the presence of purified HLA-C-specific antibodies, which was inhibited by anti-CD16 treatment of NK cells. An ADCC-independent NK cell activation mechanism was also involved as the cytotoxic effect was retained after anti-CD16 treatment of NK cells and in the absence of Fc fragment. Such observations indicate that HLA-C:KIR blockade with HLA-C-specific antibodies can promote NK cell activation. Lastly, attempts to generate recombinant antibodies were hampered by low frequencies of memory B cells within allo-sensitised patients. Immortalisation of B cells by EBV, however, led to the detection of HLA Class I-specific antibodies, confirming the presence of circulating HLA-specific memory B cells. Monoclonal antibodies were generated from $CD27^{+}CD38^{+}$ plasmablasts from transplant patients with active graft rejection to investigate the alloreactive antibody repertoire during an active immune response, but their specificity was not determined. This study implicates the role of HLA-C in tumour immune resistance and for the first time, demonstrates the potential of HLA-C:KIR blockade with HLA-C-specific alloantibodies to enhance NK cell function.

ACKNOWLEDGEMENTS

First and foremost, I would like to sincerely thank my primary supervisor, Professor Paul Moss for his continuous support and encouragement during my PhD and allowing me the freedom to make this project my own. I am also grateful for his efforts in setting up collaborations with Professor Antonio Lanzavecchia and Professor Gavin Screaton to support my project and encourage my growth as a scientist. Thank you for being an inspiration and always full of enthusiasm and excitement about my project, Paul.

I would also like to express my gratitude to my second supervisor Dr Jianmin Zuo, who has been there since the beginning of this project, guiding me and always keeping me on my toes. His advice, scientific knowledge and expertise has been invaluable during this journey. Thank you for always helping me Jianmin, even at a moment's notice, especially with all the proofreading during the write-up process.

I am also extremely grateful to my third supervisor Professor David Briggs, for his constant support, his patience and his enthusiasm for all-things HLA. I always learned a lot during our meetings and your wealth of transplant and HLA knowledge is unmatched. Thank you for allowing me to use the H&I laboratory, answering all my questions and guiding me through the HLA-related side of the project.

Great appreciation is due to College of Medical and Dental Sciences, University of Birmingham for funding this PhD. I would like to acknowledge Mrs Surinder Jandu for her hard work in collecting samples from various dialysis centres around Birmingham for my study and the serology lab staff at the H&I laboratory for their willingness to include my samples for testing during their daily operations. More specifically, I want to thank Miss Emily Halford for helping me navigate through the world of H&I laboratory techniques with patience and good humour. I would also like to express my gratitude to Mr Michael Kramer, Dr Luca Piccoli, Professor Antonio Lanzavecchia at the IRB, Bellinzona and Dr Hua Wongwiwat at Oxford University for providing me with an incredible opportunity to collaborate with them and learn from experts in the field.

I am greatly indebted to the members of the Moss research group. Thank you so much for being the most wonderful, fun and supportive colleagues during this long journey. I would like to sincerely thank Mrs Sam Nicol for her molecular biology expertise and for really helping me during the antibody cloning process. Your patience, humour and willingness to help will never be forgotten. I want to acknowledge Dr Rachel Bruton for her guidance in all things research ethics (oh, the fun times!) and answering any administrative, organisational question known to man. The Moss group is very lucky to have you. I want to say thank you to Dr Hayden Pearce, for letting me borrow 'his technician' every now then, and to Dr Kriti Verma for her invaluable help with presentations and career advice.

And to all the former members of the Moss group – Dr Louise Hosie, Dr Suzy Eldershaw, Dr Fara Hassan, Mr Jimmy van Hear and Mrs Tanuja Rai, I am very grateful to have met you during this journey. The fun, the laughs and the tears will stay with me forever. Thank you for being great colleagues and more importantly, friends over the last couple of years.

My greatest gratitude goes to my friends and family. Miss Sonam Rhaud, thank you for your incredible support over the years, for our long and serious conversations about anything and everything, never changing, and for always checking in with me when I needed it the most. Miss Lily Cao, thank you for being an amazing friend and soul sister. May our love for science, skincare and boba never die. I'm so grateful to have you both in my corner!

And lastly, I want to sincerely thank my family for being my personal champions during this long journey. Thank you, Sheldon, for being the best furry friend and study companion anyone could have ever asked for and my sister for her continuous pep talks, never failing to make me laugh and for feeding me boba for the rest of my life. I want to thank my dad for always encouraging me and my sister to pursue our goals, and for asking on a weekly basis whether I was nearly done with my PhD. After nearly 4 years, I can say that yes, I'm almost there. And last but not least, I want to thank my mum, who has been my personal rock throughout this journey. Your unwavering support and faith in me are beyond words. Thank you.

TABLE OF CONTENTS

CHAPTER IV | ANTIBODIES AGAINST HLA-C ENHANCE NK CELL FUNCTION

CHAPTER V | THERAPEUTIC POTENTIAL OF HLA-C-SPECIFIC ANTIBODIES IN CANCER

LIST OF FIGURES

LIST OF TABLES

CHAPTER I

GENERAL

INTRODUCTION

1.1. The human immune response

The immune system has primarily evolved to defend the host from invading pathogens and abnormal cells. Defence mechanisms such as the ability to distinguish between self and non-self is critical in ensuring that the immune system functions to offer continuous surveillance as well as maintains tolerance to the host's own cells (Actor, 2014). The immune response to pathogen-infected or transformed cells is divided into innate and adaptive immunity (Figure 1.1).

1.1.1. The innate immune response

The innate immune response is rapid and more primitive than the adaptive immune response by providing the first line of defence within minutes to hours from infection. Innate immunity comprises physical (skin) and microbiological barriers (mucosal surfaces); cellular elements including phagocytic cells, basophils, mast cells and eosinophils which release inflammatory mediators and natural killer (NK) cells; molecular elements including complement, cytokines and acute phase proteins (Delves and Roitt, 2000). Discrimination between self and non-self by innate immunity is regulated by three mechanisms of recognition – (i) microbial non-self, (ii) missing self and (iii) induced or aberrant self (Janeway and Medzhitov, 2002).

1.1.1.1. Recognition of microbial non-self

Conserved microbial signatures which are absent in the host are recognised by a range of germline-encoded pattern recognition receptors (PRRs) (Janeway, 1989). PRRs are defined by the ability to recognise specific microbial components which are key to survival of the microorganisms and therefore, cannot be altered by the microorganisms (Akira et al., 2006). The best-known examples of microbial components defined as pathogen-associated molecular patterns (PAMPs) include the gram-negative bacteria-specific lipopolysaccharide (LPS) and proteins such as bacterial flagellin.

Recognition of PAMPs by PRRs facilitates discrimination between self and microbial non-self, which leads to the activation of the innate immune response mediated by Toll-like receptors (TLRs). TLRs are expressed on the cell surface of antigen presenting cells (APCs), macrophages, fibroblast and epithelial cells, and localise to intracellular components including endosomes, endoplasmic reticulum, lysosome or endolysosome (Kawasaki and Kawai, 2014).

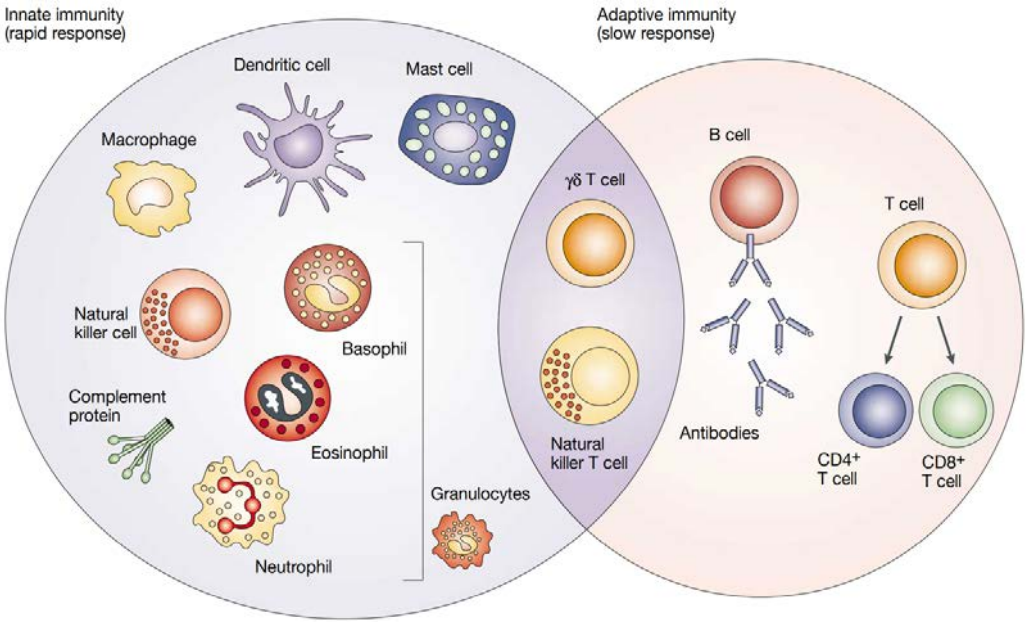

Figure 1.1. | Innate and adaptive immunity.

The rapid innate immune response is composed of soluble factors e.g. complement proteins and a range of granulocytes i.e. basophils, eosinophils and neutrophils, natural killer cells, macrophages, dendritic cells and mast cells. The slower adaptive immune response develops over time but demonstrates increased antigenic specificity and memory. Adaptive immunity consists of B cells and T cells ($CD4^+$ and $CD8^+$). The overlap between innate and adaptive immunity involves the function of γδ T cells and natural killer T cells (Dranoff, 2004). Permission to reuse content in this thesis obtained from Nature Reviews Cancer via RightsLink. Licence number 4861970885666.

1.1.1.2. Recognition of missing self

The absence of self-proteins or the 'missing self' hypothesis was first proposed to describe the regulation of NK cell function as a key player of innate immunity (Kärre et al., 1986a). It was hypothesised that in comparison to healthy cells with normal levels of self-proteins (i.e. major histocompatibility complex or MHC) virally infected and transformed cells downregulate their self-protein expression level to escape the adaptive immune response. Consequently, the missing self-scenario facilitates selective elimination of abnormal cells by NK cells (Janeway and Medzhitov, 2002). Recognition of missing self by NK cells is described in detail in section 1.5.1.

Other immune receptors involved in missing self-recognition include the sialic acid binding immunoglobulin lectins (siglecs), which recognise sialoside glycans as self-ligands. Like the inhibitory receptors on NK cells, siglecs negatively regulate the immune response by recognising sialic acids on normal, self-cells and thus, maintaining immune homeostasis (Lanoue et al., 2002; Paulson et al., 2012).

In addition to NK cell-based activation of the innate immune response, the alternative pathway (AP) of the complement system is also a major mechanism recognising and elimination missing self-cells. C3 is a serum protein that plays a central role in AP activation as it indiscriminately binds to self and non-self-cells due to the spontaneous and slow hydrolysis of thioester bond in C3 (Janeway and Medzhitov, 2002). An active protease complex called C3 convertase is formed on the surface of non-self-cells only, activating the complement cascade to eliminate non-self-cells by lysis of phagocytosis. Self-cells ubiquitously express membrane-bound complement regulatory proteins (mCRPs) such as CD46, CD55 and CD59. mCRP expression tightly regulates the complement cascade by inhibiting the formation of the C3 convertase complex and thus

prevents over-activation of AP. In diseases such as cancer, however, mCRP expression on tumour cells renders the extensively regulated complement cascade ineffective at eliminating tumours (Geller and Yan, 2019).

1.1.1.3. Recognition of altered self

The induction of altered or stressed self molecules as markers of an infection or cellular transformation is recognised by the innate immune system. Natural killer group 2 member D (NKG2D) is a transmembrane activating receptor on NK cells which recognises ligands such as major histocompatibility complex class I-related chain (MIC) A or B that are commonly upregulated on the surface of bacterial or virally infected cells, tumour cells and 'stressed' cells compared to normal healthy cells (Diefenbach and Raulet, 1999). Instead of the immune system discriminating between self and non-self-cells, upregulation of NKG2D ligands is a recognition strategy dependent on abnormal cells to reveal themselves as potential targets for an immune response (Diefenbach and Raulet, 2003).

1.1.2. The adaptive immune response

Due to rapidly evolving pathogens, the innate mechanisms of defence cannot recognise and mount an efficient and robust response. Instead the adaptive or 'acquired' immune response is generated over days and weeks following functional recognition of pathogens which escape the innate defence system (Cohn, 2004). The initial encounter with a pathogenic antigen leads to a highly specific adaptive immune response mediated by the antigen-specific receptors on T and B lymphocytes. In contrast to innate immunity and the germline-encoded receptors that have evolved over time, immunological specificity is a key component of adaptive immunity as the antigen-specific receptors are specifically tailored and selected through the process of somatic recombination. Moreover, these

antigen-specific receptors persist during the lifetime of the host, generating immunological memory. Consequently, repeated antigen exposure leads to a stronger and more rapid adaptive immune response (Bonilla and Oettgen, 2010).

T and B lymphocytes of adaptive immunity develop in the primary lymphoid organs. Whilst B cell precursors continue to mature in the bone marrow, T cell precursors migrate out of the bone marrow and mature in the thymus. Both T and B lymphocytes undergo variable (V), diversity (D) and joining (J) gene rearrangements to generate a broad range of T cell receptors (TCRs) and B cell receptors (BCRs) (McBlane et al., 1995). As many as 10^{11} clones of T and B lymphocytes are thought to arise from this process of somatic recombination expressing distinct antigen receptors (Fearon and Locksley, 1996).

Antigen-naïve T and B lymphocytes traffic to secondary lymphoid organs i.e. lymph nodes and the spleen to encounter specific antigens from the lymph and blood, respectively (Bonilla and Oettgen, 2010). Antigen-experienced T and B lymphocytes differentiate and initiate immune responses by different non-self-antigen recognition mechanisms. The innate immune system orchestrates the adaptive immune response by providing signals to generate a tailored response to a pathogen (reviewed by Jain and Pasare, 2017). The responses mediated by T and B lymphocytes are fundamentally different.

1.1.2.1. The cellular response to non-self

The cellular or T cell mediated response to non-self-antigens is predominantly initiated by cytotoxic T cells ($CD8^+$) and T helper cells ($CD4^+$). Under the influence of the innate immune response, APCs i.e. dendritic cells (DCs) and macrophages engulf pathogens by phagocytosis and migrate to the closest draining lymph nodes to stimulate T cell mediated-adaptive immune response. DCs are critical in linking innate and adaptive

immunity in their role as APCs, whilst also maintaining peripheral tolerance to self-cells (Steinman et al., 2005). Engulfed pathogens undergo degradation into short, continuous 8-10 amino acid sequences, also known as peptide fragments, which are subsequently presented by an MHC molecule to TCR, initiating an effector T cell response.

1.1.2.2. The humoral response to non-self

The humoral or B cell mediated response to non-self-antigens is, however, regulated by antibodies secreted by plasma cells. B cells matured in the fetal liver or bone marrow encounter antigens in the spleen, lymph nodes and mucosal lymphoid tissues. B cells recognise whole proteins, cell surface and soluble forms of antigen, unlike T cells which recognise and bind to peptides to trigger an immune response (Otagiri and Giam Chuang, 2016).

The activation of mature naïve B cells is characterised by two signals to allow differentiation into antibody-secreting plasma cells and memory B cells. Signal 1 is delivered as the antigen (whole proteins, polysaccharides, lipids and nucleic acids) binds to the BCR. In the absence of T cell help, a T independent B cell activation response involves the antigen-bound BCR engaging with TLRs and initiating a rapid IgM antibody response within 1-3 days of antigen exposure (Hoffman et al., 2016). Therefore, antibodies generated in the absence of T cell help tend to be less functionally versatile and of low affinity compared to those generated under the influence of T cell signalling i.e. signal 2 (Liu et al., 1988; Shih et al., 2002). Signal 2 is delivered when T cells recognise antigen-bound BCR, stimulating B cell survival and proliferation to induce and antibody response to an antigen (Goodnow et al., 2010; Dorak, 2002).

The generation of memory B cells and plasma cells which persist during the lifetime of the host and produce high affinity, isotype switched antibodies upon stimulation are a hallmark of humoral immunity and a vital defence mechanism against non-self or altered-self molecules (Hoffman et al., 2016). In addition, humoral immune responses are perpetuated and sustained by B cells serving as APCs; by forming tertiary lymphoid organs and by secreting pro- and anti-inflammatory cytokines to modulate T cell responses (Karahan et al., 2017a).

1.1.2.3. T cell-dependent activation of B cells

The multi-step process involving the B cell response to non-self or altered-self antigens is initiated at the SLOs (Figure 1.2A). SLOs provide a suitable platform for B cells to encounter both T cell help and antigen and large immune complexes presented by follicular DCs and macrophages (Cyster et al., 2000). Cellular interaction between T cells and B cells is crucial to stimulate an antibody response which occurs when activated B cells migrate to the margin between primary follicles and T cell zone in SLOs (Bonilla and Oettgen, 2010). The migration of B cells is facilitated by the upregulation of chemokine receptors expression including CXCR5 (Förster et al., 1996), whilst CCR7 expression promotes homing and migration of T cells (Sharma et al., 2015). B cells are also efficient APCs that internalise and present processed antigens in HLA Class II restricted manner to stimulate $CD4^+$ T helper cells.

Antigenic peptide-HLA Class II-complexes on B cells are recognised by $CD4^+$ T helper cells that respond to the same antigen by the process of linked recognition (Rock et al., 1984; Lanzavecchia, 1985). To stimulate B cells into generating an antibody response, firstly, pathogen peptide-specific T cells are primed following antigen presentation by DCs to produce a pool of appropriately armed T helper cells. T cells must recognise a peptide that is a physical part of the antigen recognised by the B cell. It is, however, not necessary for the linked armed T helper cell and the B cell to recognise identical epitopes (Ploegh, 2007; Murphy and Weaver, 2017).

T helper cell interaction with B cells is analogous to T cell interaction with DCs. Therefore, subsequent co-stimulatory signalling is required for B cell activation and differentiation. Of note, activation of CD40 on B cells and APCs by TCR-induced CD40 ligand (CD40L) (Elgueta et al., 2009) and production of cytokines including IL-21, IL-6, TGF-β, IFN-γ and IL-4 promote B cell survival and proliferation. IL-21 stimulates B cell differentiation into plasma cells and memory B cells (Kuchen et al., 2007). Once T cell help is received, B cells either migrate from the T/B zone to the extrafollicular areas and differentiate into transient low affinity IgM antibody-producing plasmablasts or proceed to establish a germinal center (GC) (Figure 1.2B).

1.1.2.4. Germinal center reactions

GC reactions take place in the primary follicles of SLOs which can be divided into light and dark zones defined by B cells at different stages of cell division (Karahan et al., 2017a). GC B cells that transiently interact with follicular T helper cells are further selected based on the high affinity BCRs (affinity maturation) and subsequently differentiated into long-lived plasma cells and memory B cells. The antibody encoding genes of the activated GC B cells undergo class switch recombination (light zone) from IgM to IgG, IgA and IgE as well as acquire somatic hypermutations (dark zone) to diversify the BCR repertoire (McHeyzer-Williams and McHeyzer-Williams, 2005; Karahan et al., 2017a). Affinity-matured plasma cells migrate to the bone marrow (Phan et al., 2006) and secrete antigen-specific antibodies for three days, whilst memory B cells enter circulation and remain quiescent independent of continuous antigen stimulation (Maruyama et al., 2000). Repeat exposure to specific antigens, however, results in the rapid recall of memory B cells that also proliferate and differentiate into plasma cells (Figure 1.2C) and therefore maintain serological memory (Bernasconi et al., 2002).

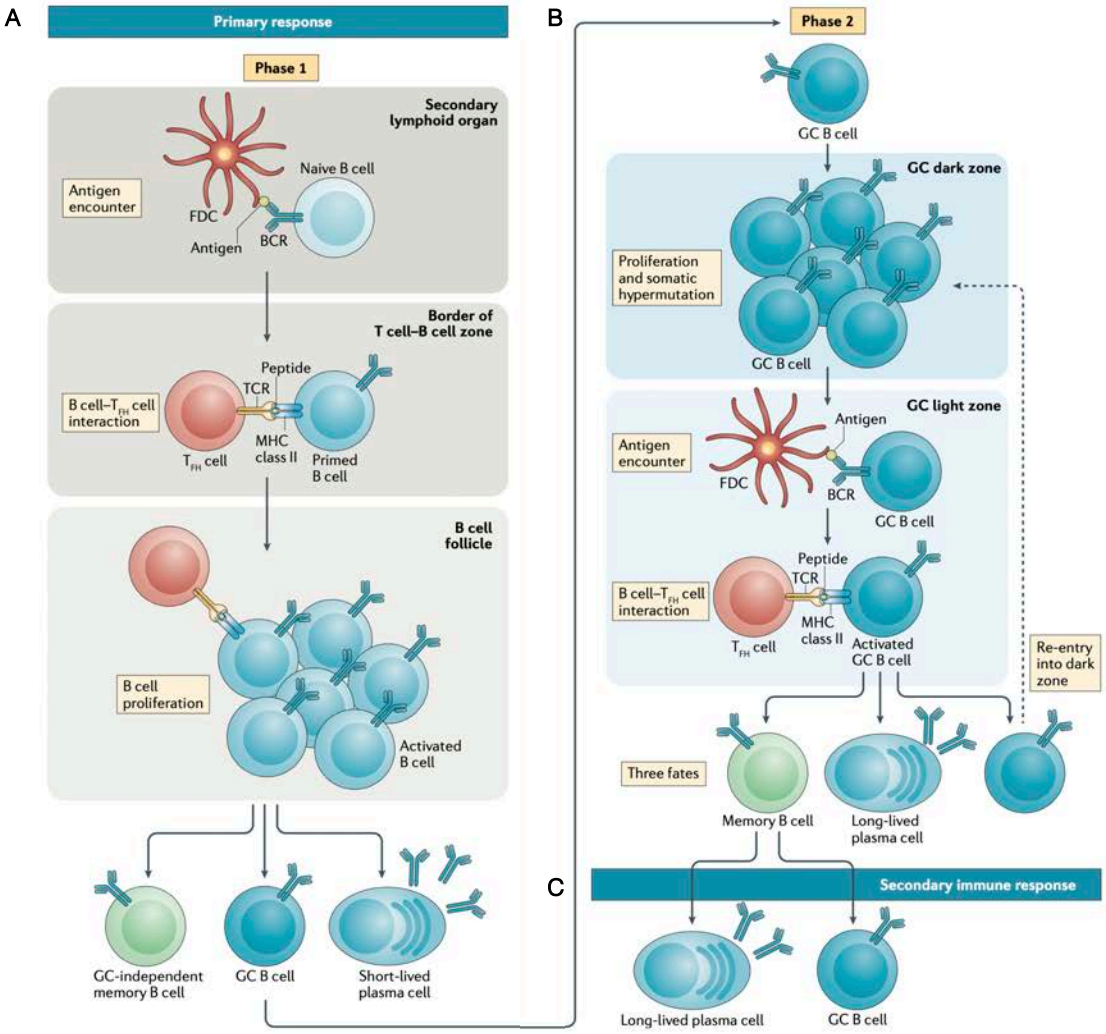

Figure 1.2. | Generation of memory B cells during a response to an antigen.

A | In phase 1 of the primary response to an antigen, naïve B cells enter the secondary lymphoid organs (SLOs), where they encounter antigen on follicular dendritic cells (FDC). B cells are activated via B cell receptor (BCR) and T follicular helper cell (T_{FH}) interaction at the T cell-B cell border. Naïve B cells proliferate and differentiate into germinal center (GC)-independent memory B cells, GC B cells or short-lived plasma cells.

B | In phase 2 of the primary response to an antigen, GC B cells form GCs. In the dark zone, GC B cells proliferate and undergo somatic hypermutation, whilst in the light zone, GC B cells encounter antigen on FDCs and interact with T_{FH} cells to differentiate into memory B cells or long-lived plasma cells or re-enter the GC dark zone.

C | In a secondary recall response to antigens, memory B cells differentiate into long-lived plasma cells or re-enter the GC reaction.

Adapted from Akkaya et al., (2020). Permission to reuse content in this thesis obtained from Nature Reviews Immunology via RightsLink. Licence number 4861980968452.

1.2. Antibodies

Antibodies, also known as immunoglobulins (Ig), are the soluble and secreted form of the BCR (Murphy and Weaver, 2017). In a membrane-bound form, the BCR permits cell signalling and activation whilst in a soluble form, immunoglobulins behave as effector molecules that bind and neutralise or lyse a target cell. There are five main isotypes or classes of Ig heavy chains – IgA, IgD, IgE, IgG and IgM, and each Ig isotype confers different effector function.

1.2.1. IgG antibody structure

Structurally, an IgG antibody molecule is a Y-shaped heterodimeric protein composed of four polypeptide chains (Figure 1.3) – two heavy (H) and two light (L) chains (Edelman and Gally, 1962). As large glycoproteins, the molecular weight of an IgG antibody molecule is approximately 150kDa – 50kDa for each heavy chain and 25kDa for each light chain. A disulphide bond connects the heavy chains, and each heavy chain is also connected to a light chain with a disulphide bond (Murphy and Weaver, 2017).

IgG antibody molecule can be cleaved enzymatically to produce two functionally distinct fragments – fragment antigen binding (Fab) and fragment crystallisable (Fc). The Fab fragment is composed of two heavy (V_H) and two light (V_L) chain variable regions which determine antigen binding specificity and a heavy (C_H1) and a light (C_L) constant domains that confer biological activity of the IgG antibody molecule (Putnam et al., 1979). Digestion at the disulphide bond results in the $F(ab')_2$ fragment whereby the antibody binding parts of the antibody molecule remained linked (Murphy and Weaver, 2017). The Fc fragment, however, comprises paired C_H2 and C_H3 domains, which are not involved in interactions

with antigens but effector molecules and cells to stimulate an immune response (Poljak et al., 1973).

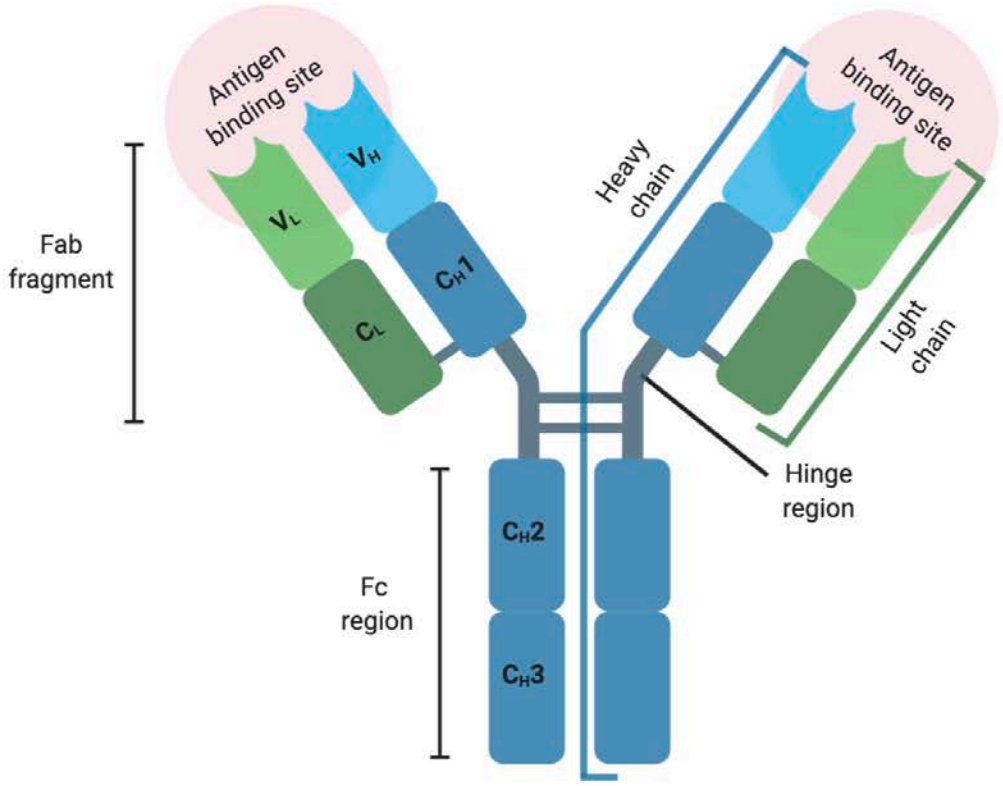

Figure 1.3. | Structure of an IgG antibody molecule.

An IgG molecule is composed of four polypeptide chains – two heavy (blue) and two light (green) which are joined by disulphide bonds at the hinge region. The heavy and light chains comprise constant (C_L, C_H1, C_H2 and C_H3) and variable (V_H and V_L) regions. The tips of the Fab fragment constitute the variable region which binds to antigens. The Fc fragment containing the C_H2 and C_H3 domains interact with effector molecules and cells to induce an immune response. Adapted from Murphy and Weaver (2017).

1.2.2. Antibody domains

The Ig heavy chain locus is located on chromosome 14 (Croce et al., 1979) and comprises 75 variable (V), 30 diversity (D) and 6 joining (J) gene segments (Pascual and Capra, 1991). There are two types of light chains – kappa (κ) and lambda (λ). An antibody molecule comprises a heavy chain and either kappa or lambda light chain as the genes encoding the κ and λ isotypes are located on different chromosomes. Transient B cells undergoing light chain isotype switching, however, have shown κ and λ simultaneous surface expression (Pauza et al., 1993).

The genes for the Igκ locus are encoded on the short arm of chromosome 2 (Malcolm et al., 1982), whilst the Igλ locus is encoded on chromosome 22 (Erikson et al., 1981). In the case of the kappa chain, there are 52 V and 5 J gene segments (Barbié and Lefranc, 1998) whereas the lambda chain comprises 30 V and 7 J gene segments (Pallares et al., 1998). Due to the chromosomal location and greater number of variable genes, the kappa locus rearrangement precedes the lambda locus rearrangement. As a result, more kappa antibodies are detected in the peripheral blood compared to lambda antibodies at 2:1 ratio (Bräuninger et al., 2001).

1.2.3. Antibody diversity

The V domain of the heavy and light chains is functionally divided into three hypervariable regions, also known as complementarity-determining regions (CDR1, CDR2 and CDR3). CDR3 is a highly diverse CDR which plays an important role in determining antigen specificity (Xu and Davis, 2000). The four regions between the CDRs are less variable and are known as the framework regions (FR) that provide structural support for the CDRs as well as antigen binding (Murphy and Weaver, 2017).

Antibody diversity is produced by a complex process known as V(D)J recombination (also somatic recombination) involving rearrangements of the heavy and light chain V, D and J genes during B cell development (Tonegawa, 1983). Progenitor (pro) B cells in the bone marrow undergo somatic recombination of the Ig heavy chain genes first, followed by the Ig light chain genes. This process is initiated by two key enzymes – recombination activation genes 1 and 2 (RAG-1 and RAG-2) (Oettinger et al., 1990). In the variable region of the heavy chain, one D and one J segment join, bringing the constant region in close proximity to the V gene segment. Next, the fused D and J segment binds to one V segment to form a recombined VDJ domain. The resulting primary transcript consists of the rearranged VDJ domain of the heavy chain and the constant *mu* (C_{μ}) and *delta* (C_{δ}) domains. As the most 5' C region includes the exons of the μ chain, the mRNA complete with C_{μ} gene segment is translated to produce the IgM (Igμ) heavy chain which is expressed on the surface of the pro-B cells during maturation (Schroeder and Cavacini, 2010).

The same process is repeated to rearrange the light chain genes, with the exception of V segment recombining with J segment as the light chain loci lack D gene segments (Abbas et al., 2015; Murphy and Weaver, 2017). Somatic recombination of the light chain genes results in Igκ and Igλ light chain proteins to stabilise the expression of BCR on the surface of pre-B cells. In addition to V(D)J gene rearrangement, nucleotide deletion and insertions (Nadel and Feeney, 1997), exclusion of allelic forms of Ig to confer monospecificity (Chess, 1998) and receptor editing to prevent immature B cells from expressing autoreactive receptors (Nemazee, 2006) are other mechanisms that contribute to the diversity of the light chain repertoire (reviewed by Collins and Watson, 2018).

1.2.4. Antibody effector functions

Antibody function is determined by the biological effect of an antibody molecule against a pathogen or infected cells. Examples of antibody functions include neutralisation of infectious agents such as viruses and toxins; opsonisation of non-self antigens or pathogens; activation of the complement cascade and Fcγ receptor-dependent effector mechanisms (Murphy and Weaver, 2017).

Neutralising antibodies bind to a pathogenic antigen and prevent pathogen entry into the host cells. For example, during an antibody response to virus infections, envelope spikes on the virion are coated with antibody molecules. This process of coating inhibits attachment to the target cell or blocks virion fusing with the target cell membrane (Burton et al., 2000). Antibody opsonisation involves opsonins i.e. antibody molecules bind to an epitope on a pathogen and coat the surface to promote their ingestion by phagocytes. The Fc fragments of antibody isotypes such as IgG_1 and IgG_3 can bind to high affinity receptor FcγRI (CD64) expressed on the surface of macrophages and neutrophils to further facilitate phagocytosis (Abbas et al., 2015). Fcγ receptors link effector cells of innate immunity to antibodies of adaptive immunity to initiate target cell lysis by a number of mechanisms including antibody-dependent cell-mediated phagocytosis (ADCP), antibody-dependent cell-mediated cytotoxicity (ADCC), cell-cell tethering and degranulation (Hickey et al., 2016).

Alternatively, antibody-antigen complexes are recognised by complement components C1, C2 and C4. The sequential cleavage of complement proteins amplifies the cascade of signals, which lead to the generation of activated effector proteins that trigger pathogen elimination by opsonisation, cell lysis or by promoting inflammation. There are three

pathways by which complement activation mediates effector function – classical, alternative and lectin pathways.

The classical pathway is triggered when the complement component C1 actively recognises pathogenic antigen or an antibody-coated pathogen. The alternative pathway is initiated by the spontaneous hydrolysis of complement protein C3, which binds directly to the surface of the pathogen. Finally, the lectin pathway is not triggered by antibodies but by engagement of soluble carbohydrate-binding proteins, mannose-binding lectin (MBL) to pathogens. This, in turn, activates the cleavage of the complement proteins and stimulates the effector function (Murphy and Weaver, 2017). It is vital to note that the antibody-independent alternative and lectin pathways of the complement cascade are mechanisms of innate immunity against non-self antigens, whereas the antibody-dependent classical pathway presents as a mechanism of adaptive humoral immunity (Abbas et al., 2015).

1.2.5. Antibodies as therapeutics

Monoclonal antibodies as therapeutic agents are predominantly used in oncology as a targeted therapy. Compared to small molecule drugs, therapeutic antibodies are expensive, complex to design and manufacture, but the advantages of antibody therapy are demonstrated by the high selectivity, stability and favourable pharmacokinetic properties. For example, the half-life of a therapeutic antibody is 3.1-7.8 days, while small molecule drugs retain a half-life of 36-48 hours (Imai and Takaoka, 2006). Moreover, therapeutic antibodies require weekly dosing compared to once-daily dosing of small molecules drugs, demonstrating their potential to offer a biologically longer, more specific and effective form of treatment than small molecule drugs (Huang et al., 2004). Therefore, the development of antibodies is more favourable and lucrative for pharmaceutical

companies, particularly with rapid advancements in technologies that facilitate humanisation of antibodies for therapy (Baker, 2005).

1.2.5.1. Humanisation of antibodies

Since the discovery of hybridoma technology (Köhler and Milstein, 1975), murine monoclonal antibodies have demonstrated limited therapeutic benefits with short half-lives, inefficient effector function and their rapid clearance from the body by human anti-mouse antibodies (HAMAs) (Klee, 2000). Thus, humanisation of murine antibodies and/or alterations to the antibody structure to improve their functional characteristics are popular and credible alternatives to antibodies produced in other species.

The immunogenicity of murine antibodies is significantly reduced and the availability of antibodies as therapeutics is increased following humanisation. Early attempts of genetically engineering to humanise murine antibodies led to the generation of 'chimeric' monoclonal antibodies. Chimeric antibodies were produced by fusing murine variable V(D)J gene segments to human constant domains (Morrison et al., 1984). Subsequent antibody humanisation work involved replacing CDR regions on a human variable region framework with those from a mouse antibody (Jones et al., 1986). More recently, pembrolizumab (Keytruda®), a humanised antibody that prevents the ligation of immune checkpoint receptor PD-1 to its ligands PD-L1 and PD-L2 has been approved for therapy in many cancers (Lee et al., 2019). This therapeutic antibody was generated by grafting the variable gene segments of a mouse anti-human PD-1 antibody onto a human IgG_4 isotype framework, which was further stabilised by introducing amino acid mutations in the Fc region (Patnaik et al., 2015). Moreover, substituting mouse constant domains with those of human may not completely resolve the issue of immunogenicity also arising from humanised antibodies (Harding et al., 2010), but there is evidence to suggest that the

severity of human anti-antibody response is significantly reduced (Hwang and Foote, 2005).

1.2.5.2. Antibody-drug conjugates

The development of antibody-drug conjugate (ADC) biobetters incorporate cytotoxic molecules that aim to combine the therapeutic potency of small molecule drugs with the highly selective and favourable pharmacokinetic characteristics of humanised therapeutic antibodies (Beck et al., 2017). Key properties of ADCs include the availability of target antigen for antibody binding; the ability to internalise the ADC complex into the target cells to release the drug and the use of stable linkers to minimise off-target effects and maximise the exposure of drugs in target cells (Thomas et al., 2016). ADCs are becoming increasingly popular forms of anti-cancer drugs with many ADCs undergoing clinical trials for solid and haematological malignancies (reviewed by Birrer et al., (2019).

1.2.5.3. Modifications to antibody structure

As monoclonal antibodies predominantly induce cytotoxicity by CDC and ADCC, antibody engineering to improve functional characteristics of therapeutics antibodies are referred to as 'biobetters' or next-generation antibodies (Elgundi et al., 2017). A biobetter is characterised by modifications to the antibody structure including humanisation, glycoengineering and drug conjugation to enhance effector function of antibodies. For instance, glycosylation modifications and mixed human antibody chimeric isotypes demonstrated a significantly improved complement-dependent cytotoxic function against target cells (Natsume et al., 2008, 2009).

Modifications to the Fc region of antibodies to increase affinity for the low affinity FcγRIIIa also impact the binding and biological activity of therapeutic antibodies. Introduction of amino acid mutations in the human IgG_1 constant domain significantly improved binding and cellular cytotoxicity of IgG_1 variants (Shields et al., 2001). More specifically, generation of trastuzumab antibody variants, an anti-HER2 antibody for breast cancer treatment, with triple mutations (Ser293Asp/Ile332Glu/Ala330Leu) within the Fc region presented a considerably enhanced ADCC response against target cells (Lazar et al., 2006).

In contrast, engineering Fc regions to decrease or eliminate undesirable host effector functions is often a preferential form of antibody mode of action for therapy. IgG_4 antibodies present a poor ability to induce cytotoxicity via complement fixation and Fc receptor-mediated ADCC (van der Zee et al., 1986), and thus offer a favourable solution for minimising antibody-mediated cytotoxicity involving delivery of antibody-drug conjugates or inhibition of receptors without depleting target cells (Labrijn et al., 2008). The ability of IgG_4 antibodies to undergo Fab-arm exchange *in vivo* has limited their use as therapeutics (Kolfschoten et al., 2007; Labrijn et al., 2009). Nonetheless nivolumab, a humanised IgG_4 PD-1 immune checkpoint blocking antibody has demonstrated promising therapeutic activity as a single agent and in combination with other checkpoint blockade antibodies in advanced melanoma patients (Johnson et al., 2015). It is important to note that a fine balance between optimal effector function with absent or reduced off-target response and therapeutic efficacy is imperative when generating monoclonal antibodies that target key molecules of an immune signalling pathway. Other mechanisms by which the desired antibody cytotoxic function can be achieved has been extensively reviewed by Weiner (2015) and Beers et al. (2016).

1.2.6. Generation of monoclonal antibodies

There are several methods available by which human monoclonal antibodies can be produced *in vitro* following isolation of memory or antigen-specific B cells, including the immortalization of B cells with Epstein-Barr virus (EBV) and toll-like receptor (TLR) agonist; mouse hybridoma technology using myeloma cells; phage display libraries or by amplifying immunoglobulin genes from antigen-specific B cells and expression vector cloning.

1.2.6.1. Immortalisation of B cells by EBV

Human monoclonal antibodies can be produced efficiently by EBV which immortalizes B cells to generate a lymphoblastoid cell line (LCL) that maintains the characteristics of the primary B cells, including the ability to secrete antibodies and expression of surface immunoglobulins at variable levels (Traggiai et al., 2004). The limitation to this approach requires continuous growth of specific clones in culture over time. Risk of infection, contamination or cell death caused by cellular exhaustion and passages may affect LCL viability in cell culture. Optimal use of this method has been reported to generate high levels of IgG, reaching up to 30% in cell culture medium (Corti and Lanzavecchia, 2014).

1.2.6.2. Mouse hybridoma technology

As an effective method to expand B cells *in vitro*, EBV transformation is also often used prior to the generation of human hybridoma. Originally used to immortalize mouse B cells, transformed B cell cultures secreting antibody of interest are fused with a myeloma cell line. Despite the lack of suitable fusion counterparts available for human B cells (Kwakkenbos et al., 2016), recent technological advances such as electrofusion

maximises the production of B cell-myeloma cell fusions by eliminating unfused B cells and myeloma cells. The generation of heterohybridomas (murine myeloma cell lines fused with human cells) have been successful in producing fully human monoclonal antibodies against viruses, including influenza (Yu et al., 2008) and dengue (Smith et al., 2012).

1.2.6.3. Phage display

Antibody phage display (APD) technology is based on the physical link formed between bacteriophage phenotype and genotype via genetic engineering. Therefore, fragment of interest expressed on phage surface and the corresponding genetic information is presented within the bacteriophage (Smith, 1985). This allows the generation of monoclonal antibodies *in vitro* defined by any specificity and affinity, particularly against rare antigens (Hammers and Stanley, 2014). Phage display is a useful technique to generate antibodies, but efficiency can be limited by many factors including access to suitable phage display libraries and maintaining their stability and quality (Wu et al., 2016).

1.2.6.4. Isolation of human antibody-secreting B cells

To overcome the limitations of obtaining specific human monoclonal antibodies from hybridoma technology and EBV transformed B cells, a strategy involving cloning and expression of antibodies from single human antigen-specific B cells has emerged (Wardemann et al., 2003; Tiller et al., 2008). This technology allows for the rapid generation of fully humanised monoclonal antibodies specific to an immunogen by isolating B cells from immunised and/or recovered donors (Wrammert et al., 2008). A large library of antibodies with a broad range of specificities against an immunogen can be interrogated using this technique by isolating antibody-secreting cells (ASCs) and cloning the immunoglobulin genes in a mammalian expression system. This technology also leads

to the production of large amounts of human monoclonal antibodies in a short amount of time (Smith et al., 2009).

Other approaches negate the need for fresh whole blood samples for generation of antibodies as the history of previous antigen exposure can be retrospectively interrogated from frozen peripheral blood mononuclear cells (PBMCs), this rapid ASC-based antibody development technique is mostly suited for efficient detection and isolation of short-lived activated plasmablasts at the height of an ongoing immune response to an antigen e.g. exposure to allogeneic tissue or vaccination event (Xu et al., 2012).

Therefore, this technology provides an opportunity for a thorough and more robust analysis of an antibody repertoire to an immunogen during an active immune response. Moreover, in the context of therapy and diagnostic research, rare broadly neutralising antibodies against viruses such as HIV-1 and influenza (Karlsson Hedestam et al., 2008) can be isolated, whilst using antibodies to eliminate antibiotic-resistant bacteria (Motley and Fries, 2017) presents as a favourable alternative form of treatment.

1.2.6.5. Next-generation Sequencing (NGS)

Over the last decade, the analysis of Ig repertoire using next-generation sequencing (NGS) has rapidly gain popularity. NGS, also known as high throughput or deep sequencing was first used in 2009 to bulk sequence B-cell populations (Weinstein et al., 2009). Compared with Sanger sequencing, NGS analysis of Ig genes (Ig-Seq) for antibody profiling produces a much broader and comprehensive account of the antibody repertoire (Georgiou et al., 2014). As a result, NGS technology has been applied to study paired Ig heavy and light chain repertoires (Dekosky et al., 2013) in antigen-specific B cells (Goldstein et al., 2019; Waltari et al., 2019); to discover more diverse antibody clones from

a phage library (Yang et al., 2017) and to perform an in-depth analysis of T- and B-cell receptor repertoires in response to an infection (Schultheiß et al., 2020).

Ig-Seq is now a well-established method that offers high throughput characterisation of Ig gene sequences from bulk B cell populations, but fails to provide information on cognate heavy and light chain pairing (Georgiou et al., 2014). To achieve optimal antibody stability, expression and antigen binding properties, it is imperative to obtain VH and VL pairing (Kovaltsuk et al., 2017). Although difficult to achieve initially, several studies have showed paired VH:VL sequencing is feasible in combination with high resolution protein mass spectrometry approaches from serum (Cheung et al., 2012; Lavinder et al., 2014) and single B cells (Dekosky et al., 2013; DeKosky et al., 2015; Tan et al., 2014; Lu et al., 2014). Compared with unpaired VH:VL sequences from bulk B cells, paired Ig-Seq yield smaller data sets, but offer >97% pairing precision from a finite pool of short-lived antibody secreting cells (DeKosky et al., 2015).

The four most commonly used NGS platforms for Ig-Seq are Illumina, PacBio, IonTorrent and Roche454 (Kovaltsuk et al., 2017). Given the complexity of NGS, errors involving library preparation material and quantification biases introduced by PCR into the high-throughput Ig-Seq process leads to inaccurate estimation of the number of unique clones in a data set (Georgiou et al., 2014; Khan et al., 2016). Nonetheless, the recent development of paired VH:VL analysis by NGS that links to antibody functionality is a favourable approach for antibody discovery and deep analysis of antibody diversity and repertoire in health and disease.

1.3. The Human Leukocyte Antigen (HLA) family

The Human Leukocyte Antigen (HLA) is a superfamily of membrane-bound glycoproteins that regulate the binding and presentation of antigens to the adaptive immune system. Also known as the major histocompatibility complex (MHC) in other species, the highly polymorphic collection of genes in this family likely represent many variants of primordia genes that have duplicated and evolved to overcome pathogen escape mechanisms and maintain a fully functioning immune system. Located in the short arm of chromosome 6 at position 21, the HLA locus spans approximately 3.6Mbp of DNA (Beck and Trowsdale, 2000) and encodes three subclasses of genes which regulate immune function and thus, play an important role in health and disease.

The HLA Class I region includes the classical (Ia) and highly polymorphic *HLA-A, HLA-B* and *HLA-C* genes as well as the non-classical (Ib) and less polymorphic *HLA-E, HLA-F* and *HLA-G* genes. The HLA Class II region comprises *HLA-DP, HLA-DQ* and *HLA-DR* genes. Compared to HLA Class I and II regions, the HLA Class III region is poorly defined, and is thought to be predominantly involved in inflammatory responses, maturation of leucocytes and the complement cascade (Dendrou et al., 2018).

The HLA Class I molecules are ubiquitously expressed on the surface of nucleated cells and also found in plasma and urine in soluble form (Puppo et al., 1995). HLA Class II molecules, however, are only found on activated T cells and APCs, including B cells, DCs, monocytes and macrophages (Choo, 2007). Both subclasses of the HLA family are also heavily involved in adaptive immunity by presenting self and non-self-antigens as peptides to TCRs in an HLA-restricted manner (Zinkernagel and Doherty, 1974). Although the Class I and Class II molecules are functionally closely related, they differ in structure and tissue expression levels and distribution.

1.3.1. Structure and Function: HLA Class I

The HLA Class I molecule is a heterodimer composed of glycosylated heavy (α) chains which are non-covalently associated with the extracellular β_2-microglobulin (β_2m) (Figure 1.4). The peptide binding groove of the Class I molecule, which determines the antigen specificity of the molecule, is formed by two helical structures – α1 and α2 domains. The immunoglobulin-like α3 domain connected to the cytoplasmic tail of the molecule dimerises with the invariant β_2m to interact with the CD8 co-receptor of T lymphocytes during antigen presentation. HLA-A2 was the first HLA molecule whose structure was revealed in detail using X-ray crystallography (Bjorkman et al., 1987a, 1987b).

Early studies investigating responses to HLA-matched bone marrow transplantation (Goulmy et al., 1977) and influenza epitopes (Townsend et al., 1986) demonstrated that cytotoxic T cells were HLA Class I restricted. As markers of self, HLA Class I molecules function to act as ligands to inhibit NK cell activation towards normal cells (innate immunity) as well as present 8-10 amino acids long peptides deriving from endogenous proteins to the cytotoxic $CD8^+$ T cells (adaptive immunity). Endogenous proteins include intracellular self-proteins, proteins entering the cytosol by phagosomes and viral proteins (Wyatt et al., 2019). Due to the mechanisms of self-tolerance, most peptides presented by Class I molecules are self-peptides which do not induce T cell responses.

The less polymorphic non-classical HLA Class Ib molecules differ in tissue distribution and function. Like the classical HLA Class Ia molecules, HLA-E is expressed on nucleated cells. HLA-G expression, however, is limited to the trophoblast, thymus, cornea and endothelial precursor cells. The less widely known HLA-F exists as an intracellular protein in the spleen, tonsils, thymus and villous trophoblast (Petersdorf, 2011).

Structurally, HLA-E and HLA-G molecules are similar to the classical Ia molecules which are loaded with a short peptide. The HLA-E peptide complex is recognised by the heterodimeric-lectin CD94/NKG2C (activating) and CD94/NKG2A (inhibitory) receptors found on NK cells and $CD8^+$ T cells (Braud et al., 1998a; Lee et al., 1998). HLA-G peptide complexes exert immunomodulatory functions by binding to multiple receptors including leucocyte immunoglobulin-like receptors (LILR), LILRB1 (ILT2) and LILRB2 (ILT4) and KIR2DL4 to modulate the activity of $CD8^+$ T cells, NK cells and DCs (Alegre et al., 2014).

Due to its differential expression in pregnancy sites, HLA-G protects the foetus from an immune attack by inhibitory defence mechanisms. Some tumours, however, take advantage of the inhibitory nature of HLA-G expression to escape immune surveillance (reviewed by Morandi et al., 2016). Like HLA-G, HLA-F is thought to be involved in maintaining tolerance at the fetal-maternal interface and responsible in infection and autoimmunity. Structurally, however, HLA-F molecule can exist in two forms – with β_2m and without β_2m (open conformer free of peptide) (Goodridge et al., 2010). HLA-F regulates immunity by interacting with activating and inhibitory KIRs on NK cells (Dulberger et al., 2017).

1.3.2. Structure and Function: HLA Class II

The HLA Class II molecule is also a heterodimer composed of a non-covalent complex of two polypeptide chains - heavy (α) and β_2m chains, spanning the membrane (Figure 1.4). Unlike the HLA Class I molecule, the peptide binding groove is more open and formed by α1 and β1 domains. Due to the open-ended peptide binding groove, the ends of the peptides are less likely to be buried within the molecule and thus the Class II molecule binds longer peptides (15-24 amino acid residues) than HLA Class I binding nonameric peptides (Brown et al., 1993). Early studies investigating macrophage-dependent T cell

responses demonstrated that T helper cells (CD4) were restricted by HLA Class II (Bergholtz and Thorsby, 1977; Ziegler and Unanue, 1981). HLA Class II molecules present exogenous proteins e.g. non-self or altered-self proteins as digested peptide fragments on the surface of APCs to form peptide:HLA II complexes and initiate T cell and B cell-dependent adaptive immune responses.

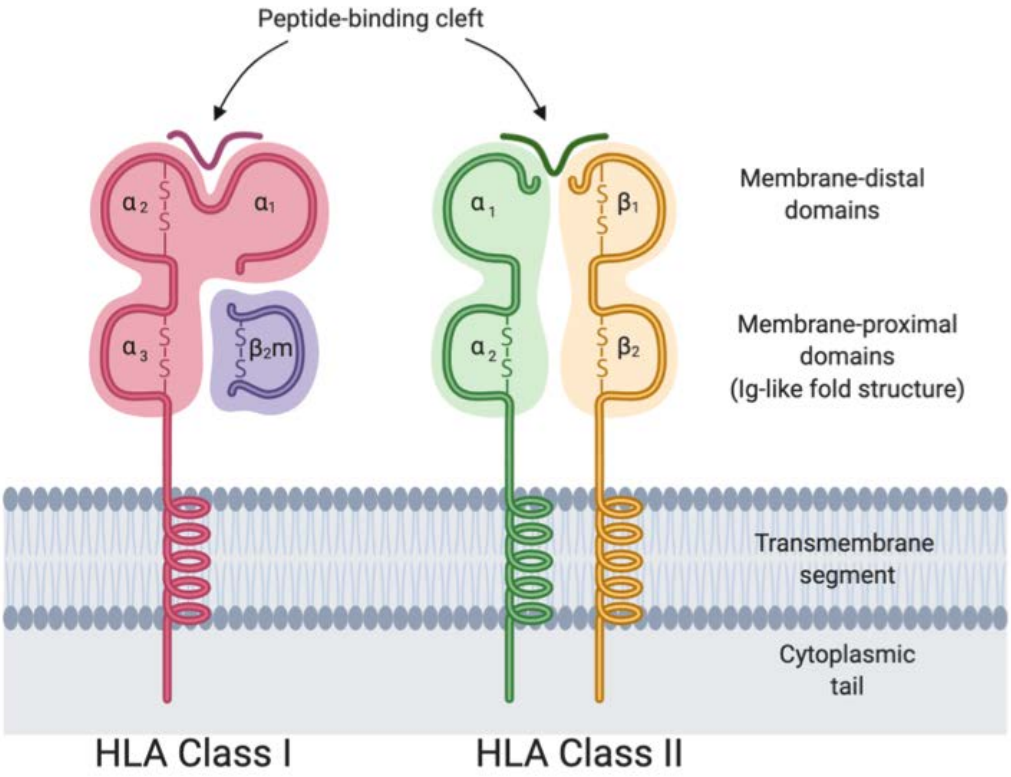

Figure 1.4. | Structure of HLA molecules.

HLA Class I (left) and HLA Class II (right) are heterodimeric transmembrane proteins. HLA Class I comprises a heavy chain and three globular domains (α_1, α_2 and α_3) that are non-covalently linked to β_2m. HLA Class II contains two heavy (α and β), each comprising two globular domains (α_1 and α_2; β_1 and β_2). The processed antigen is presented as a peptide which sits in the peptide binding cleft of the HLA Class I (α_1 and α_2 domains) and HLA Class II (α_1 and β_1 domains) molecules. Adapted from Hickey et al., (2016) and Murphy and Weaver (2017).

1.3.3. HLA polymorphisms

The HLA system has evolved rapidly during evolution and is highly polymorphic. HLA polymorphisms are primarily driven by pathogens which enforces selection of HLA alleles that offer protection and thus, ensures survival. This pathogen-driven diversity, therefore generates HLA diversity in the population (Prugnolle et al., 2005). During antigen presentation, the domains responsible for interacting with the components of the TCR and co-receptor are generally conserved. Extensive polymorphisms occur within the peptide-binding groove and the domains interacting with the variable regions of the TCR. This demonstrates that the functional domains of the HLA molecules have evolved under the effect of selective epitopes and presentation of an enormously diverse range of degraded pathogenic peptides (Jin and Wang, 2003).

To date (June 2020), *HLA-B* genes are the most polymorphic genes (7,255 alleles) in the classical *HLA* family, followed by *HLA-A* (6,082 alleles) and *HLA-C* (5,842 alleles) (Figure 1.5A). In evolutionary terms, the origin of the HLA-C locus is the most recent and consequently less polymorphic compared to HLA-A and –B loci (Zemmour and Parham, 1992). Of the *HLA Class II* genes, *HLA-DRB1* is the most polymorphic locus with 3,357 alleles (European Bioinformatics Institute, 2020) (Figure 1.5B). Approximately 20 HLA-A, 50 HLA-B, 10 HLA-Cw, 18 HLA-DR and 7 HLA-DQ antigens have been identified at the serologic level (Hickey et al., 2016). HLA polymorphisms are implicated in a range of infectious diseases (reviewed by Blackwell et al., 2009); autoimmune conditions (reviewed by Simmonds and Gough, 2009) and cancer. More importantly, HLA molecules also play a central role in transplantation as histocompatibility antigens that have the capacity to induce an immune response in genetically dissimilar environment, and this can ultimately lead to rejection of allograft by the recipient.

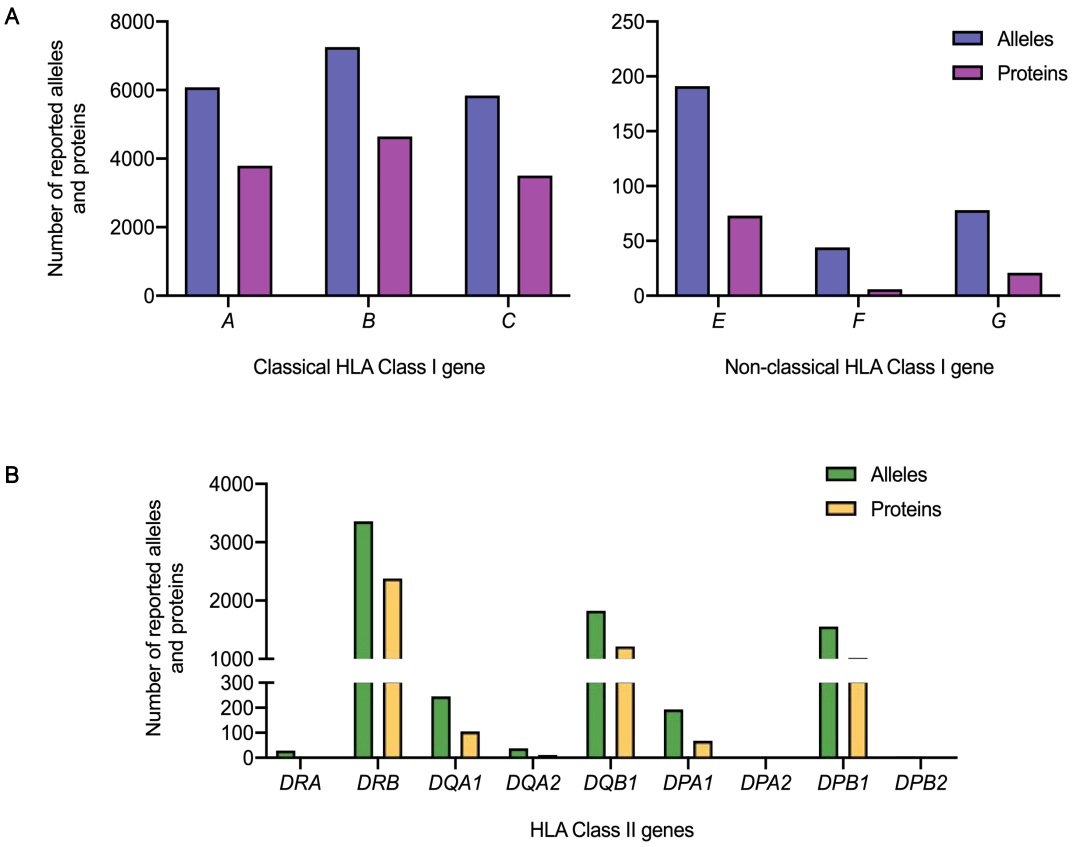

Figure 1.5. | Allelic polymorphism of the *HLA* genes.

The number of sequences identified that encode distinct **A |** alleles (purple) and proteins (pink) of *HLA Class I* classical and non-classical genes, and **B |** alleles (green) and proteins (yellow) that encode *HLA Class II* genes are shown. The statistics were obtained from the IPD-IMGT/HLA database (http://www.ebi.ac.uk/ipd/imgt/hla/stats.html).

1.3.4. HLA nomenclature

HLA nomenclature, albeit complicated and confusing at times, is critical in understanding the HLA system in terms of DNA sequences, serologic specificities and cellular responses (Hurley, 2020). Since 1968, World Health Organisation (WHO) sponsored Nomenclature Committee for factors of the HLA system meet regularly to discuss and document HLA genes and alleles. The first report from the committee agreed to use the term 'HL-A', which was a contraction of 'Hu-1' and 'LA' systems proposed by pioneers of the HLA field, Dausset and Payne and Bodmer (Bernard Amos, 1991). The first HLA antigens were identified serologically by using sera from multiparous women against a panel of leucocytes in agglutination assays - 4a (HLA-Bw4) and 4B (HLA-Bw6) (Van Roodj and Van Leeuwen, 1963) and LA1 (HLA-A1) and LA2 (HLA-A2) (Payne et al., 1964) were detected.

During the 1970s, the presence of a lower case 'w' between the gene and antigen number e.g. HLA-Aw23 indicated provisional specificity until the antigen was confirmed by the Nomenclature Committee (Torres and Moraes, 2011). The asterisk (*) was introduced to separate the gene name (HLA-**A***02) and the serologically determined allele group (HLA-A***02**), whilst the colon is used as a field separator (Figure 1.6). For example, the first field indicates the allele family (HLA-A***02**); the second field describes the protein encoded by the allele (HLA-A*02:**101**); the third field distinguishes between alleles based on silent (non-coding) nucleic substitutions (HLA-A*02:101:**01**) which differ in DNA sequences but the resulting protein is identical to the normal gene and the fourth field indicates nucleotide polymorphisms in the introns or 5' and 3' untranslated regions (HLA-A*02:101:01:**02**) (Mehra et al., 2010; Antony Nolan Research Institute, 2020). Optional suffixes are also included to describe the expression status of the allele (Table 1.1).

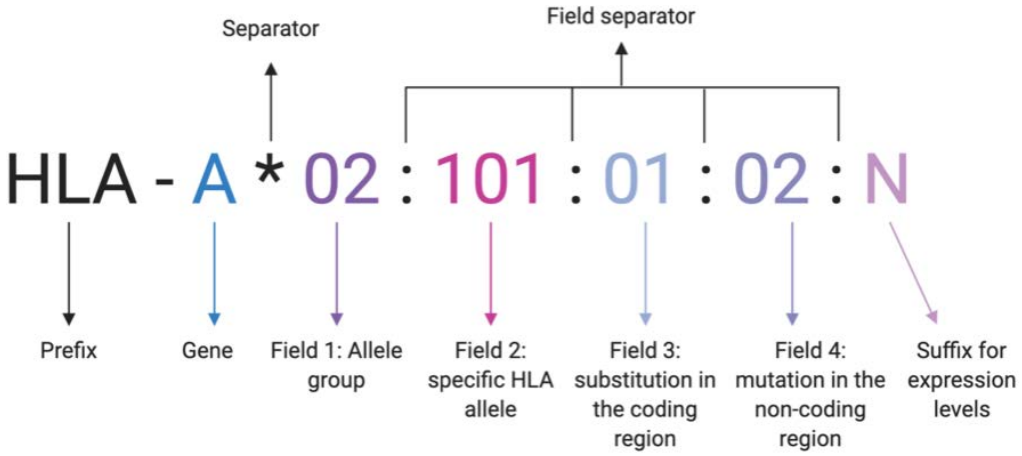

Figure 1.6. | Annotated HLA nomenclature. Adapted from Marsh, 2010, Antony Nolan Research Institute (http://hla.alleles.org/nomenclature/naming.html)

Table 1.1. | Summary of HLA allele nomenclature with examples[1]

Nomenclature	Explanation
HLA	prefix for the HLA gene
HLA-C	HLA locus i.e. C
*HLA-C*08*	an allele group that encodes the C antigen
*HLA-C*08:01*	a specific HLA allele or protein
*HLA-C*08:01:02*	an allele that differs by a synonymous mutation from *C*08:01:01*
*HLA-C*08:01:01:02*	an allele containing a mutation in the non-coding region from *C*08:01:01:01*
*HLA-A*24:09N*	'N' suffix indicates null alleles that are not expressed
*HLA-A*30:14L*	'L' suffix indicates low or significantly reduced expression of the allele
*HLA-A*24:02:01:02L*	an allele with low or significantly reduced expression with a mutation in the non-coding region
*HLA-B*44:02:01:02S*	'S' suffix indicates the allele encoding a protein is expressed as secreted molecule only
*HLA-A*32:11Q*	'Q' suffix indicates questionable where an allele with a mutation has previously shown to significantly affect normal expression levels but this has not been confirmed

[1] Adapted from Antony Nolan Research Institute (2019)

1.4. Immune response to solid organ transplantation

HLA molecules play a dominant role in the clinical outcome of transplantation. Due to the highly diverse genetic nature of the HLA system, these polymorphisms can stimulate immune responses in genetically non-identical individuals and ultimately affect transplant outcome. Therefore, in order to minimise these responses, it is important that the donor and recipient are matched at the MHC loci, in addition to the selection of other favourable donor-recipient matching characteristics such as sex, donor biological sibling and age (Sasazuki et al., 1998; Milner et al., 2016). However, the degree to which HLA loci need to be matched between the donor and recipient varies according to the nature of the transplant procedure. Liver allografts, for instance, tolerate very broad HLA mismatches (Jucaud et al., 2018). In most cases, the immune response defined as rejection is largely mediated by adaptive immunity (Murphy and Weaver, 2017). HLA mismatches in solid organ transplantation (SOT) present with a higher incidence of graft rejection and thus, graft loss (Tinckam et al., 2016; Williams et al., 2016). Non-HLA antigens such as ABO blood group antigens and minor histocompatibility antigens (MiHA) that are endogenous peptides occupying the antigen binding site of donor HLA molecules are also involved in generating an alloimmune response against the graft (Mehra et al., 2010).

In SOT, a non-specific inflammatory response is activated by the physiological stress experienced during the process of organ harvesting, storage, implantation and ischaemia-reperfusion injury (Ball and Dallman, 2014). This inflammatory environment provides the context for the innate immune system to initiate a response involving activation of the complement cascade, leucocyte migration to the site of inflammation and secretion of chemokines and cytokines, which recruit other key players of innate immunity (Kumbala and Zhang, 2013).

HLA antigenic differences between the donor and recipient triggers non-self recognition strategies of innate immunity (section 1.1.1), and also leads to increased HLA antigen presentation to T cells by mechanisms of allorecognition, stimulating a strong adaptive alloimmune response.

1.4.1. Allorecognition in transplantation

The phenomenon known as allorecognition requires the activation of recipient $CD4^+$ T helper cells. This, in turn, activates the cytotoxic $CD8^+$ T cells and stimulates the generation of HLA-specific alloantibodies following transplantation, resulting in the formation of the germinal center and alloantibody-producing memory B cells (Hickey et al., 2016).

1.4.1.1. Direct allorecognition by T cells

The direct allorecognition pathway mediated by T cells is the most dominant and direct pathway of alloantigen recognition, which takes place early on post-transplant, potentially leading to acute allograft rejection (Pietra et al., 2000). This pathway involves donor APCs to present intact donor-derived HLA molecules directly to recipient (alloreactive) T cells. Studies have shown that APCs residing in the graft, also known as passenger leucocytes, migrate through the lymphatics to nearby lymph nodes, following graft reperfusion (Steinmuller, 1980; Okuda et al., 2002). Consequently, recipient $CD4^+$ T helper cells in the lymph nodes become activated by recognising non-self HLA molecules presented by the donor APCs. This interaction initiates an inflammatory immune response against the allograft.

The direct polyclonal T cell-mediated alloresponse is vigorous as up to 10% of the allospecific T cells can engage with intact allogeneic HLA-peptide complexes (Sherman and Chattopadhyay, 1993). The frequency of precursor T cells within the T cell pool with the capacity for direct alloreactivity is likely to result in TCRs specific for self-HLA cross-reacting with allogeneic HLA-peptide complexes by changing the peptide recognition requirements (Daniel et al., 1998). It has also been demonstrated that T cells involved in direct alloresponses display a predominant memory phenotype due to previous priming by non-self antigen presented by self-HLA molecules (Lombardi et al., 1991). The role of B cells in direct allorecognition is generally absent due to the lack of cognate interaction between allospecific $CD4^+$ T helper cells and B cells (Taylor et al., 2007).

1.4.1.2. Indirect allorecognition by T cells

Indirect pathway of allorecognition occurs during the lifetime of a graft. Donor antigens that are shed by the graft are processed as peptides and presented by recipient APCs to alloreactive $CD4^+$ T helper cells in a HLA Class II restricted manner by B cells (Lechler and Batchelor, 1982). This pathway is more akin to the classical mechanism of non-self antigen uptake and presentation by HLA Class II molecules to T cells as donor peptides derive from exogenous proteins. The immune response generated by this pathway involves $CD4^+$ T cells providing help to cytotoxic $CD8^+$ T cells and activating B cells to produce alloantibodies, which mediate chronic rejection of the allograft (Ball and Dallman, 2014).

1.4.1.3. Semi-direct allorecognition by T cells

The semi-direct pathway proposes an alternative role for donor passenger leucocytes whereby intact allogeneic HLA-peptide complexes are transferred between recipient and donor APCs (Markey et al., 2014). There is further evidence that in addition to providing the intact version of the HLA molecule to $CD8^+$ T cells, HLA Class II molecules on recipient APCs present the same antigen as processed allopeptides to $CD4^+$ T helper cells by the indirect pathway (Sivaganesh et al., 2013). An overview of the B cell response to non-self antigens is described in section 1.1.2.3. Like the direct pathway, the semi-direct pathway of allorecognition is thought to dominate during the early immune responses to the graft as it is directed primarily against donor HLA antigens (Afzali et al., 2008).

1.4.1.4. Allorecognition by B cells

As described in the previous section, the role of B cells in initiating an alloresponse is not essential. Instead, B cells play a secondary role to T cells during allorecognition. Nevertheless, B cells are thought to be heavily involved in chronic rejection of the allograft by facilitating long term presentation of alloantigen to $CD4^+$ T helper cells via the indirect pathway (Lakkis and Lechler, 2013). In addition, B cells contribute to the immunological response and rejection of the graft by producing donor-specific HLA alloantibodies by the processes (Figure 1.7). Moreover, the release of soluble HLA Class I alloantigens by the graft can be taken up by DCs and subsequently presented in intact, unprocessed form to B cells to stimulate an alloantibody response against the graft (Curry et al., 2007).

The generation of HLA-specific alloantibody occurs following exposure to non-self or allogeneic tissue by three main sensitising events – exposure of non-self paternal antigens in the foetus during pregnancy, blood transfusions and previous transplants. Healthy, non-sensitised individuals can also develop HLA-specific antibodies, which is likely in response to cross-reactive epitopes on allergens, ingested proteins, infections and vaccines (Morales-Buenrostro et al., 2008; D'Orsogna et al., 2011). For the purpose of this thesis, HLA-specific antibodies generated in the context of renal transplants will be discussed.

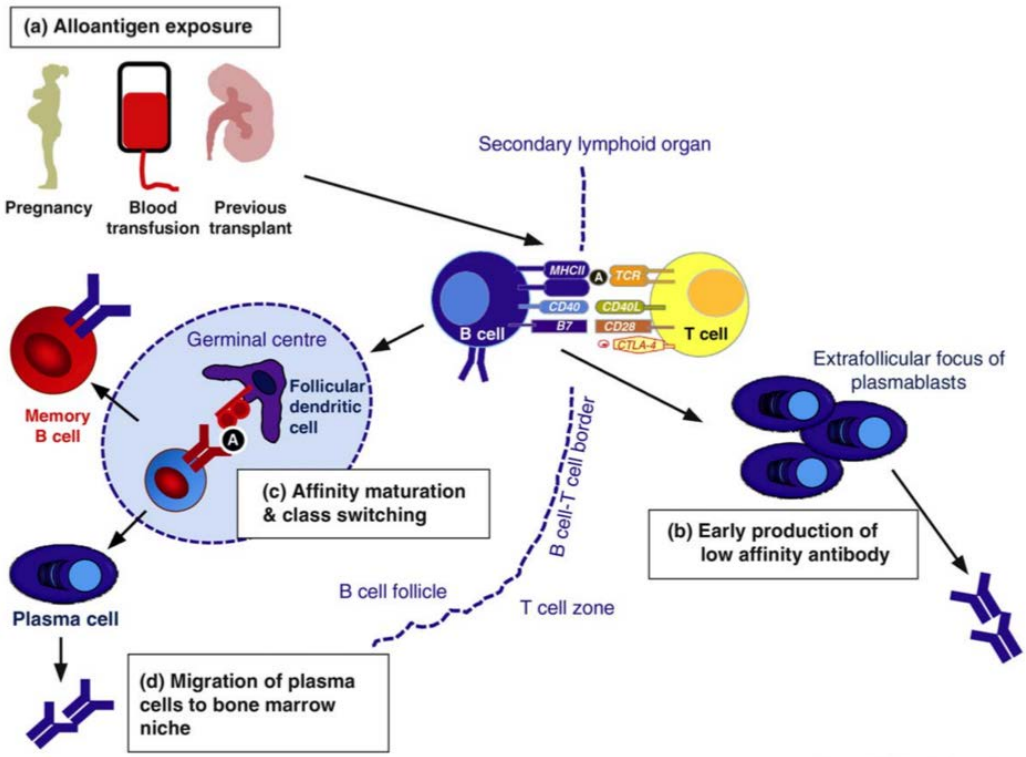

Figure 1.7. | The generation of an alloantibody response.

a | Exposure to alloantigen occurs via pregnancy, blood transfusion and previous transplants. B cells are activated in SLOs by BCR interacting with cognate antigen A, and migrate to the T/B cell border to present antigen A in the context of HLA Class II molecules to $CD4^+$ T helper cells. Activated $CD4^+$ T cells provide costimulatory signals (CD40-CD40L and CD28-B7) to B cells and mediate cytokine secretion. Following T-dependent activation, B cells either **b |** migrate out of the B cell follicle of SLO and differentiate into low affinity antibody producing plasmablasts, or **c |** undergo somatic hypermutation in the germinal center and class-switch recombination. B cell clones positively selected with high affinity for antigen A differentiate into memory B cells or plasma cells. **d |** A proportion of plasma cells from the germinal center migrate to the bone marrow to become long-lived plasma cells that maintain antibody titres (Clatworthy et al., 2010). Permission to reuse content in this thesis obtained from Current Opinion in Immunology via RightsLink. Licence number 4844220359875.

1.4.2. Immunogenicity of HLA

HLA-specific alloantibodies are commonly raised in SOT due to the minor differences in HLA types of the recipient and donor. Large retrospective studies provide evidence to support the importance of matching or compatible HLA alleles between donor and recipient to prolong graft survival, particularly in SOT (Held et al., 1994; Opelz and Wujciak, 1994; Takemoto et al., 2000).

The immunogenicity of HLA varies between molecules. The antibody response to mismatched HLA antigens can result in sensitisation (Claas et al., 2006; Lucas et al., 2015). As the first HLA antigens were characterised as broad antigens using serologic techniques, these molecules were later discovered to be shared epitopes between multiple HLA molecules rather than individual HLA molecules. These shared epitopes or cross-reactive epitope groups (CREGs) give rise to antibodies that react broadly to multiple epitopes on any relevant HLA molecule. Therefore, the immunogenicity of HLA molecules that initiate alloantibody production is likely to be controlled by the immunogenicity of CREGs (McKenna and Takemoto, 2000; Lucas et al., 2015).

Exposure to CREGs that may differ from self by one amino acid can result in intra-locus and inter-locus HLA-specific antibodies, which are found in the sera as well as in the graft (Milongo et al., 2017). For example, HLA-A11 molecule shares a specific epitope with HLA-A1, A3, A9 (23 and 24), A36 and A80 antigens. Therefore, an antibody arising following exposure to HLA-A11 would demonstrate a broad intra-locus specificity to the HLA-A antigens mentioned (Marrari and Duquesnoy, 2010).

Inter-locus cross-reactivity is best demonstrated by the closely related HLA-B and HLA-C loci as the HLA-C locus is shown to have evolved as a duplication of HLA-B locus (Yeager and Hughes, 1996; McKenzie et al., 1999). In addition to producing alloantibodies specific to non-self HLA molecules at the serological level, alloantibodies may also rise against other alleles of the self HLA antigen. The generation of HLA-allele specific alloantibodies is dependent on the differences between the amino acid residues at key positions of the HLA antigen (Hickey et al., 2016). This issue can be circumvented by performing higher resolution HLA typing at the allelic level. For example, a patient serologically typed as HLA-DQ6 is further defined as HLA-DQB1*06:01 with high resolution typing. Exposure to other HLA alleles e.g. HLA-DQB1*06:04 would result in allele-specific alloantibody production (Muro et al., 2010).

1.4.3. HLA-specific alloantibodies and mechanisms of graft damage

HLA-specific alloantibodies impact the graft by numerous mechanisms (reviewed by Thomas et al., 2015), which includes cross-linking of antibody molecules upon binding to HLA target proteins on vascular cells and inducing a cascade of intracellular signalling. This, in turn, leads to functional changes in the graft vascular cells such as increased cell migration, rearrangement of cell cytoskeleton and increased recruitment of immune cells into the graft (Valenzuela and Reed, 2015). The initiation of the classical pathway of the complement cascade triggers damage to the graft which can lead to acute rejection. The pro-inflammatory effects of complement activation include stimulation of neutrophils and macrophages. Complement activation and subsequent graft damage is further potentiated by the Fc fragments of the donor HLA-specific alloantibodies bound to the graft (reviewed by Wasowska et al., 2007; Murata and Baldwin, 2009). FcγR-related graft injury is mediated by FcγRs on monocytes, macrophages and NK cells by ADCC.

HLA-specific alloantibodies initiate ADCP by macrophages and neutrophils, which leads to enhanced T cell responses mediated by presentation of non-self HLA allopeptides (Thomas et al., 2015). Alloantibodies bound to the graft trigger NK cell degranulation and target cell cytotoxicity by ADCC to mediate antibody-mediated rejection (AMR) (Toyoda et al., 2012).

1.4.4. HLA-specific alloantibodies and graft rejection

AMR is the most common cause of kidney allograft loss following transplantation. It is now well known that antibodies to donor HLA antigens, or donor-specific HLA antibodies (DSAs) are clinically implicated in graft survival outcome. The frequency of HLA-specific DSAs have been reported as low as 4.4% to up to 68% (Pelletier et al., 2002; Cardarelli et al., 2005). The incidence of HLA-specific antibodies includes HLA Class I and II-specific antibodies. Therefore, the role of HLA-specific DSAs in causing allograft loss is universally accepted in all types of rejection, including hyperacute rejection which primarily results from the presence of HLA-specific antibodies pre-transplantation (Patel and Terasaki, 1969; Kannabhiran et al., 2015), and chronic failure with DSAs arising five to ten years post-transplantation (Lee et al., 2002; Hourmant et al., 2005).

Previous studies have highlighted the importance of HLA matching specific to the HLA-DR locus, followed by HLA-A and -B loci (Moen et al., 1980; Opelz et al., 2017; Leeaphorn et al., 2018). Due to the extensive polymorphisms of the HLA family and shared epitopes (CREGs) of HLA-A and -B antigens, there is evidence that matching at these dominant loci is the most beneficial to heart, renal and liver transplant recipients with increased graft survival (Opelz and Wujciak, 1994; Laux and Opelz, 2004; Balan et al., 2008).

The role of HLA-C mismatches on allograft survival, however, remains unclear. Due to low cell surface expression, the HLA-C locus is defined as 'weakly immunogenic' in comparison to HLA-A and -B loci (McCutcheon et al., 1995). In the context of solid organ transplantation, an early study by Solheim et al. (1977) reported that matching at the HLA-C locus did not improve graft survival. Similarly, a prospective study by Albrechtsen et al. (1978) found that matching for HLA-C antigens did not give a predictive value for allograft survival. However, there is evidence that in addition to HLA-A, -B and -DR alloreactive T cells, cytotoxic clones specific to HLA-C locus mismatches were detected in kidney transplantation (Bonneville et al., 1988) and bone marrow transplantation (Pei et al., 2001). Frohn et al. (2001) reported that HLA-C mismatches in renal transplants are significantly correlated with acute AMR, particularly in the presence of an HLA-B antigen mismatch. Moreover, individual case reports demonstrate a causative link between HLA-C-specific antibodies and hyperacute rejection (Chapman et al., 1986; Bachelet et al., 2011; Bosch et al., 2014).

1.4.5. HLA-specific memory B cells

An immune response against donor HLA antigens on the allograft leads to the generation of plasma cells, which produce high affinity circulating alloantibodies that can persist for decades in the form of serological memory (Elgueta et al., 2010), while memory B cells can also contribute to HLA-specific alloantibody production by rapidly differentiating into antibody secreting cells i.e. plasmablasts and plasma cells upon re-exposure to antigen (Bernasconi et al., 2002; Crotty and Ahmed, 2004). In HLA-sensitised transplant patients, circulating alloreactive memory B cells and plasma cells derived from the bone marrow have been detected (Zachary et al., 2007; Han et al., 2009; Heidt et al., 2012; Snanoudj et al., 2015; Karahan et al., 2019).

Several methods have been used to detect peripheral HLA-specific memory B cells in individuals immunised by pregnancy and/or transplantation. The identification of HLA-specific alloreactive B cells have been reported by using HLA-specific tetramers (Mulder et al., 2003; Zachary et al., 2007). The caveat to this method is often demonstrated by B cells reacting non-specifically to the non-HLA components of the tetramer (Pape et al., 2011; Taylor et al., 2012), and thus, frequencies up to 10^5 HLA tetramer$^+$ B cells have been detected in females immunised by pregnancy (Mulder et al., 2001, 2003).

HLA-specific antibody-secreting B cells have also been identified and quantified by enzyme linked immunospot (ELISpot) assays (Heidt et al., 2012; Lúcia et al., 2015; Karahan et al., 2017b). *In vitro* polyclonal activation of B cells leads to differentiation into antibody-secreting cells (Bernasconi et al., 2002; Crotty et al., 2004; Cao et al., 2010), which allows subsequent detection of memory B cells using the ELISpot technology. This method reportedly detected very low frequencies of HLA Class I-specific alloantibody (less than 150 B cells) and HLA Class II-specific alloantibody (less than 100 B cells) per 10^6 B lymphocytes (Heidt et al., 2012; Karahan et al., 2017b).

Degauque and colleagues (2013) analysed the frequency of alloreactive B cells in renal transplant patients by using single HLA antigen-coated polystyrene luminex beads. As expected, an increased frequency of B cells (less than 2% of total B cells) binding to beads coated with single HLA antigen were detected in immunised recipients compared to non-immunised healthy controls. Single HLA antigen-coated polystyrene luminex beads can also be used to screen for HLA-specific alloantibody specificity in the serum. This method has been used to screen the culture supernatants of *in vitro* activated B cells for HLA-specific antibodies to determine the presence of circulating HLA-specific memory B cells (Han et al., 2009; Snanoudj et al., 2015; Karahan et al., 2019).

Studies have shown that whilst donor-specific HLA antibodies were detectable in B cell culture supernatants deriving from immunised individuals, specificities of HLA alloantibodies from cultured B cells were not identical to the serum HLA antibody profiles (Han et al., 2009; Karahan et al., 2019). Snanoudj and colleagues (2015) reported that HLA-specific alloantibodies secreted by memory B cells show a restricted HLA specificity pattern compared to serum antibodies that present broad specificities. This further suggested that the strength of HLA alloantigen exposure plays a critical role in the *in vitro* proliferation and survival of alloreactive memory B cells.

Together, these data demonstrate that memory B cells secreting alloantibodies following HLA immunisation can be identified and quantified, although the frequencies of alloreactive memory B cells are reportedly very low in the peripheral blood compartment, which is likely related to the number, the dose and/or duration of alloantigen exposure.

1.5. Natural Killer cells

Natural Killer (NK) cells are key players of the immune system which, unlike T and B lymphocytes, do not require antigenic priming to eliminate infected and cancerous cells. Following the discovery of murine lymphocytes with 'natural' cytotoxicity in the 1970s (Kiessling et al., 1975), subsequent studies demonstrated the cytotoxic potential of human NK cells from healthy donors *in vitro* at efficiently lysing tumour cells (Peter et al., 1975; Becker et al., 1978; Trinchieri et al., 1978; Main et al., 1985).

NK cells comprise up to 15% of all circulating lymphocytes and are phenotypically defined as CD3-negative and CD56 and Fcγ receptor III (CD16) expressing lymphocytes. CD56 is an isoform of neural cell adhesion molecule (NCAM) or Leu-19 that is stringently associated with NK cells, but is also observed on DCs, activated $CD8^+$ and gamma delta (γδ) T cells (Cooper et al., 2001a; Van Acker et al., 2017). On the basis of CD56 and CD16 expression, NK cells can be further divided into two subsets. $CD56^{dim}$ mature NK cells with high levels of CD16 constitute up to 90% of peripheral blood NK cells that display a potent cytotoxic effector function upon stimulation (Lanier et al., 1986, 1988). The immature and poorly cytolytic $CD56^{bright}$ $CD16^{+/-}$ NK cells, however, predominantly reside in tissues and SLOs, that secrete immunoregulatory cytokines including interferon (IFN)-γ, tumour necrosis factor (TNF)-β, interleukin (IL)-10 and IL-13 and granulocyte-macrophage colony-stimulating factor (GMCSF) in response to stimulation (Cooper et al., 2001b).

1.5.1. The 'missing-self' hypothesis

Early studies demonstrated that the effector function of NK cells was mediated against target cells with reduced or deleted expression of self-MHC (Kärre et al., 1986) Downregulation of MHC expression is a hallmark of infection or cellular transformation. Therefore the 'missing-self' hypothesis postulated that host MHC Class I molecules engaging with inhibitory receptors were vital in dampening NK cell activation (Ljunggren and Kärre, 1990). Thus, the lack of self MHC Class I molecules renders target cells more susceptible to NK cell mediated lysis (Figure 1.8). This hypothesis was directly validated when MHC Class I-deficient target cells that were initially NK cell sensitive demonstrated resistance to NK cell cytolytic activity following the transfection of MHC Class I genes (Storkus et al., 1989a). Subsequent studies revealed that the α_1 and α_2 domains of the MHC Class I molecule conferred resistance to NK cell mediated lysis (Storkus et al., 1989b, 1991).

To explain the role of MHC Class I molecules in conferring resistance or susceptibility to NK cells, two models were proposed. The effector inhibition model suggested that MHC Class I molecules mediated inhibitory signals that prevented NK cell activation. The target interference model suggested that upregulation of MHC Class I molecules would mask NK cell activating ligands on target cells, limiting NK cell effector function (Ljunggren and Kärre, 1990; Borrego, 2006). However, a simplistic view of the missing-self hypothesis would suggest that the absence or mutated forms of self MHC Class I proteins is enough to trigger NK cell activation. By extension, this effect would lead to autoimmune disorders in Class I-deficient individuals, but this is not the case (Furukawa et al., 1999; Vitale et al., 2002). Instead, the lack of engagement of cognate self MHC Class I and inhibitory receptor interaction results in uneducated NK cells, which are ineffective against Class I-deficient target cells.

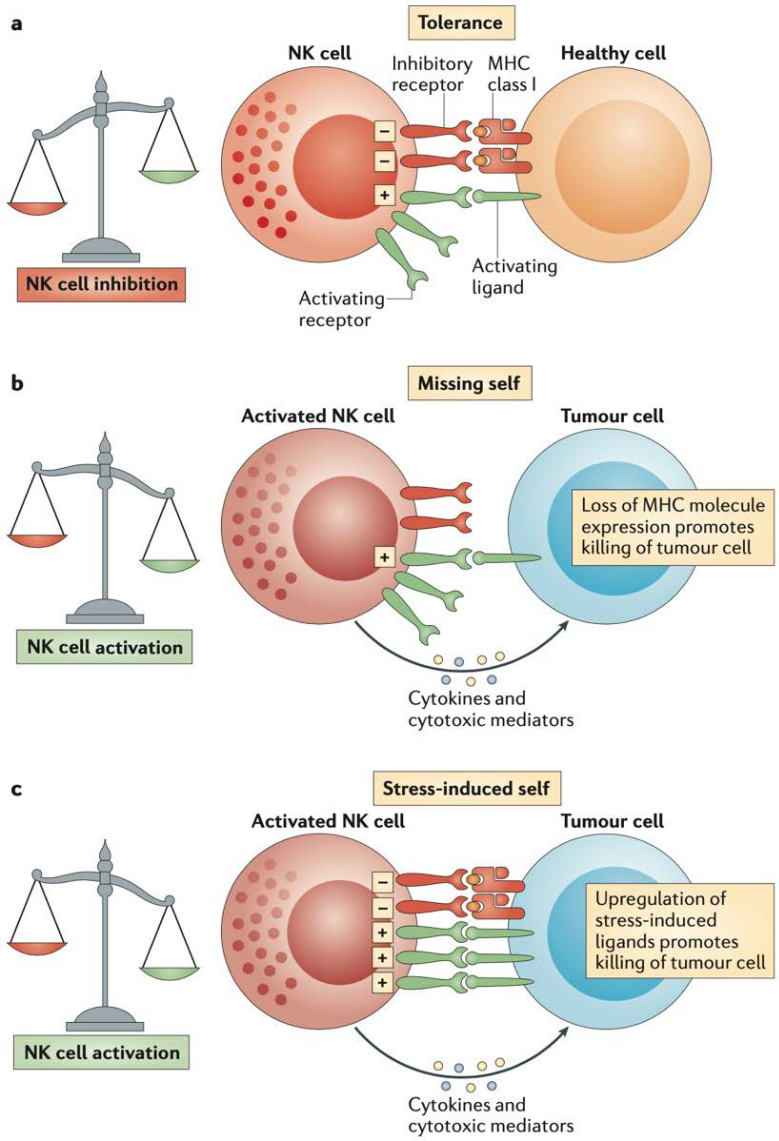

Figure 1.8. | NK cell recognition of abnormal cells.

a | NK cells are tolerant to healthy cells as the engagement of inhibitory receptors dampen the activating signals received by NK cell and healthy cell interaction.

b | In the context of tumour cells, loss of MHC Class I molecules leads to NK cell activation as the inhibitory signals delivered by the MHC Class I molecules ligating with inhibitory NK cell receptors are absent. This is known as 'missing-self'-induced NK cell activation.

c | Selective activation of NK cells by 'stressed' cells e.g. tumour cells is mediated by the upregulation of activating NK cell ligands which overcome the inhibitory signals delivered by the MHC Class I molecules.

NK cell activation by these mechanisms leads to tumour cell elimination directly via NK cell mediated cytotoxicity, or indirectly by producing pro-inflammatory cytokines. Adapted from Vivier et al., (2012). Permission to reuse content in this thesis obtained from Nature Reviews Immunology via RightsLink. Licence number 4862011157156.

1.5.2. NK cell integration of signals

NK cells express a range of inhibitory and activating receptors that tightly regulate NK cell activity by binding to cognate ligands on target cells. NK cell activation is also controlled by the dynamic equilibrium of signals that exists between these negative and positive mechanisms (Vivier et al., 2004).

To date, several germline-encoded activating NK cell receptors have been characterised such as NKG2D, natural cytotoxicity receptors (NCRs) including NKp30, NKp44 and NKp46, which receive signals and induce diverse signalling cascades to lyse abnormal and non-self target cells (Vivier et al., 2004; Bryceson et al., 2006). Experimental studies have shown that despite MHC Class I expression, this inhibitory signalling can be overridden when potent activating NK cell receptors are stimulated involving the recruitment of activating signalling molecules such as Vav1 and PLC-γ2 (Cerwenka et al., 2001). Nonetheless, when encountering 'self' cells, inhibitory signals are dominant over activation signals when inhibitory receptors are co-ligated with an inhibitory signalling motif (Bléry et al., 1997). But NK cell response outcomes are not completely dependent on the simple balance of signals. Inhibitory signalling blocks inside-out and outside-in signals mediated by co-activating receptors such as DNAM-1, 2B4 and CD2, possibly explaining the domination of inhibition over activating signals (Long et al., 2013).

1.5.3. NK cell-mediated effector function

1.5.3.1. Natural killer cytotoxicity

The primary mechanism of natural killer cytotoxicity involves the exocytosis of preformed lytic granules (or secretory lysosomes), perforin and granzymes. Perforin is a multi-domain pore-forming protein that targets the cell membrane (Young et al., 1986). Granzymes are a family of serine proteases that work synergistically with perforin to induce programmed cell death (Trapani, 1995).

The exocytosis of perforin and granzymes is a tightly regulated process which can be divided into four stages. Firstly, the formation of an immunological synapse (IS) between the target cell and NK cell triggers the reorganisation of the actin cytoskeleton. Secondly, the microtubule organising center (MTOC) and associated cytotoxic granules are translocated (or polarised) towards the IS. Thirdly, the secretory lysosomes dock with the plasma membrane of NK cells at the IS and subsequently fuse with the target cell membrane to release the cytotoxic granules in the final stage (reviewed in detail by Topham and Hewitt, 2009). This process of degranulation induces the transient expression of lysosomal-associated membrane protein-1 (LAMP-1 or CD107a) and LAMP-2 (or CD107b), which can be used to indirectly measure the cytolytic function of NK cells (Alter et al., 2004).

NK cells can also induce cell death by TNF-related apoptosis inducing ligand (TRAIL) by binding to TRAIL-R1 (DR4) and TRAIL-R2 (DR5). In addition, the ligation of Fas ligand (CD178) on target cells to Fas receptor (CD95) is another mechanism by which NK cells induce apoptosis (Chan et al., 2014).

1.5.3.2. Regulation of pro-inflammatory cytokines

The effector function of NK cells is also regulated by pro-inflammatory cytokines such as IL-2, IL-15, IL-18, IL-21 and IFN-α (Lanier, 2005). Perforin expression is upregulated by IFN-α and IL-2, which leads to enhanced NK cell cytotoxicity (Jewett and Bonavida, 1995; Zhang et al., 1999; Kwaa et al., 2018). Both IL-2 and IL-15 stimulate NK cell proliferation and effector function by inducing the expression of activating c-lectin receptor NKG2D and NKp44 (de Rham et al., 2007). In contrast, IL-18 is not involved in NK cell proliferation, cytotoxicity or cytokine secretion, but facilitates the migration of NK cells to DCs and serve as a bridge between innate and adaptive immune systems (Mailliard et al., 2005; Senju et al., 2018).

1.5.3.3. ADCC

ADCC is another mechanism by which NK cells mediate a cytolytic response against IgG-coated target cells. The process involves the ligation of the Fc fragment of an antibody molecule to the low affinity FcγRIIIa (CD16a). This leads to the phosphorylation of the CD3-ζ transmembrane-anchored protein containing immunoreceptor tyrosine-based activating motifs (ITAMs) (O'Shea et al., 1991). The subsequent signal transduction mechanisms leads to NK cell degranulation and secretion of pro-inflammatory cytokines that mediate target cell lysis (Anegón et al., 1988; Morrison et al., 2017). Cross-linking of FcγRIIIa by IgG also induces a rapid increase in Ca^{2+} mobilisation, followed by the increased expression of *IFN-γ* and *TNF-α* genes (Cassatella et al., 1989).

1.5.4. NK cell self-tolerance and licensing

To ensure that the NK cell receptor repertoire is functional yet tolerant to self, NK cells undergo an educational process also termed as licensing. It is generally accepted that in humans, NK cell tolerance is acquired in the host, rather than germline encoded, which is achieved when each NK cell expresses at least one or more self-HLA-specific inhibitory receptor (Valiante et al., 1997). The 'at least one' receptor hypothesis implies that NK cells undergo education during development to ensure the survival of this self-HLA-specific inhibitory receptor-expressing subset (Raulet et al., 2001).

The functional importance of self-MHC in NK cell education and tolerance is further highlighted by murine studies. Fernandez and colleagues (2005) demonstrated that NK cells lacking inhibitory receptors specific for host-MHC achieved self-tolerance but responded poorly to Class I-deficient target cells. Similarly, NK cells from humans with TAP-deficiency were inefficient at lysing Class I-deficient target cells (Furukawa et al., 1999; Vitale et al., 2002), most likely a result of uneducated NK cells. This hyporesponsive NK cell activity is reversed when NK cell inhibitory murine Ly49 receptors (Kim et al., 2005) and KIRs in humans have undergone licensing with self-MHC molecules become functionally competent (Anfossi et al., 2006). These findings suggest that there are two forms of self-tolerant NK cells. Self-HLA educated NK cells acquire functional competence during the licensing process, whereas in the absence of cognate HLA Class I ligand and inhibitory receptor interaction, the unlicensed or uneducated NK cells are hyporesponsive against stimuli. However, the unlicensed phenotype is not necessarily fixed as transferring hyporesponsive unlicensed murine NK cells from MHC Class I-deficient donors to MHC Class I-sufficient hosts results in a gain of functional donor NK cells, indicating the process of licensing occurring beyond the NK cell developmental stage (Elliott et al., 2010).

The mechanisms underlying NK cell education are not well established but several models have been proposed (reviewed by Yokoyama and Kim, 2006; Raulet and Vance, 2006). The arming model postulates that the engagement of inhibitory receptors and HLA Class I molecules stimulates a coordinated signalling event whereby molecular mechanisms and activating receptors raise the NK cell state of responsiveness to stimuli (Kim et al., 2005; Orr et al., 2010). This licensing event is a hallmark of a mature and educated NK cells (Boudreau and Hsu, 2018a).

The disarming model, however, offers an alternative view to the arming model that argues inhibitory receptors are not necessary for NK cell education. It was hypothesised that all NK cells initially exist in a state of hyperresponsiveness but become disarmed following chronic stimulation by self-HLA-expressing cells. This loss of responsiveness in NK cells is similar to inducing anergy in T and B lymphocytes (Raulet and Vance, 2006).

The rheostat model offers a quantitative view on NK cell education. It postulates that the responsiveness of an NK cell is tuned by the number of interactions between self-HLA and specific inhibitory receptors (Raulet and Vance, 2006; Brodin et al., 2009b). Additional studies have shown that the density of inhibitory receptors, co-expression of multiple self-HLA- specific inhibitory receptors and the presence of self-HLA ligands influence NK cell education and thus, NK cell responsiveness to stimuli (Yu et al., 2007; Brodin et al., 2009b, 2009a; Jonsson et al., 2010).

The differences in the activity of licensed NK cells are attributed to differences in signalling rather than changes in gene expression. Forslund and colleagues (2015) reported that educated NK cells possessing a single inhibitory receptor demonstrated increased migration and contact with target cells and thus, increased target cell lysis compared to inhibitory receptor-deficient NK cells. Transferring mature NK cells expressing self-HLA-

specific inhibitory receptors from one HLA environment to another replete of cognate HLA ligands led to increased NK cell reactivity to stimuli (Boudreau et al., 2016). The higher responsiveness would be expected following the removal of inhibitory signals from licensed NK cells as this lowers the threshold of activation leading to the subsequent depletion of accumulated cytolytic granules (Goodridge et al., 2019).

The rheostat model is applicable to both arming and disarming models as it suggests NK cell education and activation can be increased in proportion to the inhibitory signals received by the cell (Boudreau and Hsu, 2018a). Collectively, licensed (or educated) and unlicensed (or uneducated) NK cells present a well-coordinated system of responsiveness that confers tolerance to self-HLA-expressing cells and reactivity against non-self or downregulated self-HLA plays an important role in health and disease (Boudreau and Hsu, 2018b).

1.5.5. NK cell inhibitory receptors

NK cells express a range of inhibitory receptors that negatively regulate their activation. Some inhibitory receptors recognise classical HLA Class I molecules as ligands, while other receptors bind non-classical HLA Class I molecules. Nonetheless, these receptors are vital in distinguishing between autologous, normal cells and non-self or transformed cells. The killer immunoglobulin-like receptors (KIRs) are the most well-known example of NK cell inhibitory receptors, which recognise allelic groups, particularly HLA-C of the HLA Class I family (Bottino et al., 1995). The c-type lectin inhibitory receptor complex CD94/NKG2A binds to the non-classical HLA-E proteins (reviewed by Borrego et al., 2005). Human inhibitory receptors Ig-like transcript 2 (ILT2) and ILT4 are considered more promiscuous as they recognise a range of classical and non-classical HLA Class I

molecules, but preferentially bind to HLA-G (Shiroishi et al., 2003). Given that this thesis focusses on alloantibodies against HLA-C, KIRs will be described in further detail.

1.5.6. KIRs

KIRs are a family of highly homologous transmembrane glycoproteins that are mainly expressed on the surface of NK cells, γδ T cells and $CD8^+$ T cells transitioning from naïve to effector phenotype (Anfossi et al., 2004). As a set of highly diverse and rapidly evolving NK cell receptors, KIRs bind determinants of the polymorphic HLA Class I ligands through direct recognition (Vilches and Parham, 2002). The interaction between specific self HLA Class I molecules and KIR isotypes inhibit NK cell effector activity against normal, healthy cells. Therefore, NK cell recognition and the ability to distinguish between self and non-self is partially dependent on KIR and HLA Class I complexes.

Structurally, the extracellular region of the KIR proteins comprise either two (KIR2D) or three (KIR3D) Ig-like domains which function to recognise and bind their cognate HLA Class I ligand (D'Andrea et al., 1995; Wagtmann et al., 1995) (Figure 1.9). Determined by the length of the cytoplasmic tail, KIRs exist in two functional forms. Long-tailed KIRs (KIR2DL or KIR3DL) confer an inhibitory effect via two immunoreceptor tyrosine-based inhibitory motifs (ITIM), with the exception of KIR2DL4 and KIR3DL3 which possess one ITIM. HLA ligand binding to inhibitory KIRs lead to the phosphorylation of the dual ITIMs by the Src family kinases. The subsequent recruitment of Src homology region 2 (SH2)-containing protein tyrosine phosphatase (SHP-1) and SHP-2 prevents NK cell activation (Burshtyn et al., 1996; Yusa and Campbell, 2003).

The short-tailed KIRs (KIR2DS or KIR3DS) lack ITIMs and instead possess two immunoreceptor tyrosine-based activating motifs (ITAM) associated with adaptor proteins such as DAP12 that mediate activating signalling. Activating KIR ITAMs are phosphorylated following binding with cognate ligand, leading to the recruitment of tyrosine kinases, Syk and ZAP70 that propagate NK cell activation (McVicar et al., 1998).

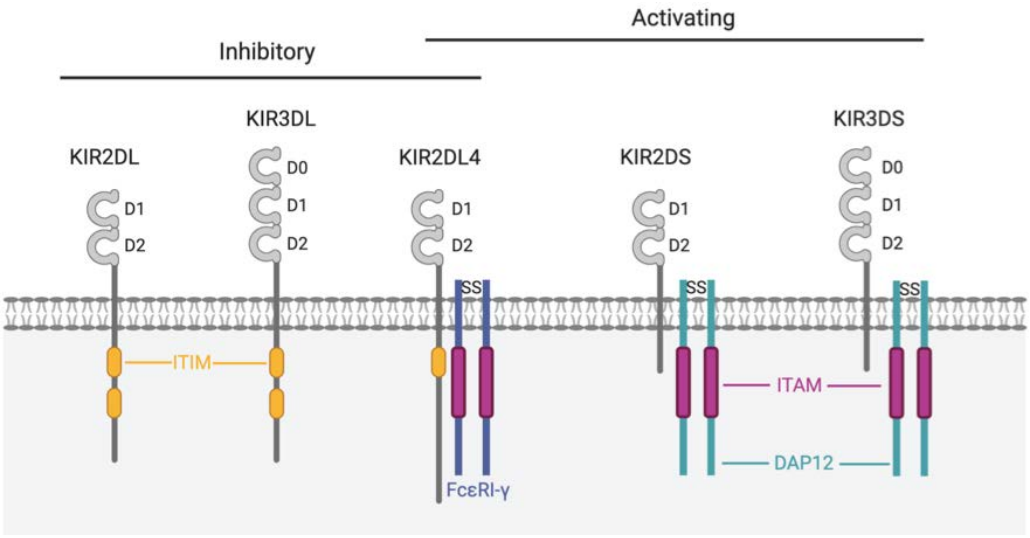

Figure 1.9. | Structural differences between KIRs.

KIR nomenclature is based on the number of extracellular Ig-like domains (2D or 3D) and the length of the cytoplasmic tail (L – long; S – short). Inhibitory KIRs (KIR2DL and KIR3DL) are characterised by long cytoplasmic tails with two ITIMs (yellow) that mediate inhibitory signals. Activating receptors, KIR2DS and KIR3DS contain short cytoplasmic tails while activating KIR2DL4 is long-tailed to confer weak inhibitory function. Specific amino acid residues in the transmembrane domains of signalling adaptor proteins FcεRI-γ (purple) and DAP12 (blue), respectively, provide ITAMs (pink) signals to induce NK cell activation. Adapted from Campbell and Purdy (2011).

1.5.7. KIR diversity

In humans, the *KIR* gene locus is located within the leucocyte receptor complex (LRC) encoded on chromosome 19 (Trowsdale, 2001). The *KIR* gene group can be divided into two haplotypes – A and B (Parham, 2005). Haplotype A mainly encodes inhibitory KIRs – *KIR2DL1, KIR2DL3, KIR2DL4, KIR3DL1, KIR3DL3* and *KIR3DL3* and one activating KIR – *KIR2DS4*. In contrast, haplotype B is characterised by various combinations of activating and inhibitory KIRs including *KIR2DL2, KIR2DL5, KIR3DS1, KIR2DS1, KIR2DS2, KIR2DS5* and *KIR2DS5* (Uhrberg et al., 1997). Variation in KIRs is a result of a highly polymorphic gene and allele content which leads to haplotypic and allelic diversity, that also affects KIR interaction with HLA Class I ligands (Fan et al., 2001; Boyington and Sun, 2002). The *KIR* genotype of an individual can comprise six or more different *KIR* genes and the KIR phenotype can be different by combinations of two to nine receptors determined during NK cell maturation (Uhrberg et al., 1997; Valiante et al., 1997).

1.5.8. KIR ligands

KIRs are able to distinguish between HLA Class I molecules by recognising specific polymorphic determinants (Table 1.2). Inhibitory KIRs bind to HLA-C alleles which can be further divided into two groups of KIR ligands – HLA-C1 and HLA-C2, based on the amino acid present at key positions of the α_1 helix. HLA-C1 alleles bind to KIR2DL2/3 and are defined by serine (Ser) at position 77 and asparagine (Asn) at position 80, while HLA-C2 possess Asn and lysine (Lys) at positions 77 and 80, respectively (Colonna et al., 1993a; Mandelboim et al., 1996) and bind to KIR2DL1.

KIR3DL1 binds to approximately 40% of HLA-B allotypes with the Bw4 serological motif (Cella et al., 1994; Gumperz et al., 1995). However, KIRs recognising the Bw6 serological motif, which differs from Bw4 at residues 77-83, are yet to be identified. KIR3DL2 specifically recognises HLA-A*03 and HLA-A*11 alleles (Pende et al., 1996; Hansasuta et al., 2004), and HLA-F (Goodridge et al., 2013). Unlike the other inhibitory KIRs, KIR2DL4 which resides in endosomes, displays weak inhibitory function when engaged with soluble HLA-G (Faure and Long, 2002; Rajagopalan and Long, 2012).

In contrast to inhibitory KIRs, the activating KIRs present a weaker affinity to the putative HLA Class I ligands. For example, due to similarities in the sequences, the activating KIR2DS1 and KIR2DS2 are expected to recognise the same HLA-C allotypes as KIR2DL1 and KIR2DL2/3, respectively. KIR2DS1, however, weakly recognises HLA-C2 allotypes (Stewart et al., 2005; Foley et al., 2008), whereas the presence of specific amino acid residues at key positions prevent KIR2DS2 recognition of the HLA-C1 epitope at Asn^{80} (Saulquin et al., 2003). KIR2DS2 binding to HLA-A*11 has been reported (Liu et al., 2014). KIR2DS3 and KIR2DS5 have no known ligands, although KIR2DS5*006 in the African population has shown reactivity to HLA-C2 allotypes (Blokhuis et al., 2017). KIR2DS4 also binds HLA-C2 alleles - HLA-C*04 (Katz et al., 2001) and HLA-C*05:01 (Sim et al., 2019) and HLA-F (Goodridge et al., 2013) as well as non-HLA Class I molecules (Katz et al., 2004). As KIR3DL1 and KIR3DS1 share 97% amino acid sequence homology, KIR3DS1 recognises HLA-Bw4-associated specificity HLA-B*57 (O'Connor et al., 2015) and open conformers of HLA-F (Garcia-Beltran et al., 2016).

Table 1.2. | KIRs, their function, known ligands, allelic and protein forms

KIR	Function	Ligand	Number of alleles[1]	Number of proteins[1]
2DL1	Inhibitory	HLA-C group 2	111	36
2DL2	Inhibitory	HLA-C groups 1, 2[2]	34	15
2DL3	Inhibitory	HLA-C groups 1, 2[2, 3]	64	35
2DL4	Inhibitory and Activating	HLA-G	107	54
2DL5	Inhibitory	Unknown	57	24
2DS1	Activating	HLA-C group 2[4]	16	8
2DS2	Activating	HLA-A*11	24	9
2DS3	Activating	Unknown	16	7
2DS4	Activating	HLA-A*11, HLA-C, HLA-F, non-HLA	37	18
2DS5	Activating	Unknown	24	17
3DL1	Inhibitory	HLA-Bw4 specificity	183	92
3DS1	Activating	HLA-B*57, HLA-F	39	22
3DL2	Inhibitory	HLA-A*03, A*11, HLA-F	164	114
3DL3	Inhibitory	Unknown	165	92

[1]Statistics collected from Immuno Polymorphism Database (IPD) for KIRs (2019) (https://www.ebi.ac.uk/ipd/kir/stats.html)

[2]KIR2DL2 and KIR2DL3 display weak binding affinity for HLA-C group 2 allotypes than group 1 allotypes

[3]KIR2DL2 binds HLA-C ligands with greater affinity than KIR2DL3

[4]KIR2DS1 binds HLA-C2 allotypes with very low affinity

1.5.9. HLA-C allotype recognition by KIR2DL

The inhibitory KIR2DL1, KIR2DL2 and KIR2DL3 proteins bind HLA-C alleles based on the dimorphism at position 80. HLA-C1 allotypes are recognised by KIR2DL2 and KIR2DL3, whereas HLA-C2 allotypes bind to KIR2DL1. The direct engagement between an HLA-C allele and inhibitory KIR offer target cells selective protection from NK cell mediated lysis (Ciccone et al., 1992; Colonna et al., 1993a). Vitale and colleagues (1995) reported that KIR2DL1 and KIR2DL2/3 recognised by EB6 and GL183 antibody clones respectively, were two independent receptors for two groups of HLA-C alleles. NK cell clones expressing KIR2DL1 were unable to lyse HLA-C2^{+} allotype target cells (Asn^{77} Lys^{80}). Similarly, KIR2DL2^{+} and KIR2DL3^{+} NK cell clones were not reactive against HLA-C1 allotype-expressing target cells (Ser^{77} Asn^{80}), demonstrating the HLA-C ligand specificity for the inhibitory KIRs, which upon ligation regulate NK cell function.

Amino acid residues at positions 44-46 of the KIR molecule determine the ability to distinguish between the two HLA-C allotype groups (Winter and Long, 1997). Single amino acid substitutions at positions 77 and 80 of the HLA-Cw3 allele (HLA-C1 allotype) with those defining HLA-Cw4 (HLA-C2 allotype) resulted in a mutated HLA-Cw3 allele, which was not recognised by KIR2DL2/3^{+} NK cells but recognised by KIR2DL1^{+} NK cells (Biassoni et al., 1995). Similarly, amino acid substitutions at position 70, a critical site for KIR and HLA-C interaction, have shown changes in the ligand binding affinities (Biassoni et al., 1997).

HLA-C1 and HLA-C2 allotype recognition by certain KIR2DL receptors is more permissive than originally reported as KIR2DL2, and to a weaker extent KIR2DL3, also display affinity for the HLA-C2 epitope at Lys^{80}. These observations suggested that compared to KIR2DL2, KIR2DL3 is a weaker but more specific HLA-C1 receptor (Winter et al., 1998;

Moesta et al., 2008). Additional mutagenesis analyses by Hilton and colleagues (2012) showed that KIR2DL3 has broader HLA-C ligand specificity and lower avidity than KIR2DL1. The authors postulated that the HLA-C1 allotype interactions with KIR2DL2/3 evolved first, followed by HLA-C2 allotypes that were selected by novel KIR variants that interacted with the HLA-C2 epitope. The ligand binding specificities of the KIRs suggest that HLA-C and KIR systems are continually evolving as the older KIR2DL2/3 receptors demonstrate a weak functional ability to interact with HLA-C2 epitope, whereas the more recently evolved KIR2DL1 bind exclusively to HLA-C2 allotypes (Kulkarni et al., 2008; Moesta et al., 2008; Hilton et al., 2012).

1.5.10. Peptide selectivity of KIRs

To date, studies have shown all HLA-C binding KIRs demonstrate a degree of peptide selectivity based on the residues at positions 7 and 8 of the peptide. For example, HLA-Cw4 ligand recognition by KIRs was peptide-dependent as selectivity of the peptide bound to the HLA molecule was conferred by positions 7 and 8. Amino acid substitutions at these positions abolished KIR recognition of HLA-Cw4 with mutant peptides (Rajagopalan and Long, 1997). The importance of peptides as a component of the HLA-C-KIR complex was demonstrated by NK cell clones that did not recognise HLA-Cw03*04-expression alone. Further functional analyses revealed that not all forms of isolated peptides deriving from HLA-Cw03*04 conferred the same degree of protection, but in fact provided a variable response in protecting target cells from NK cell lysis (Zappacosta et al., 1997). These data show that functionally, NK cells expressing HLA-C-specific KIRs are sensitive to changes in the amino acid residues of the peptide, further suggesting that the inhibitory signalling mediated by the KIRs is possibly dependent on the peptide content of the HLA-C molecule.

The crystal structure of HLA-Cw3 and KIR2DL2 complex revealed that the KIR-HLA-C binding interface involved direct contact with peptide positions 7 and 8 at the C-terminal (Boyington et al., 2000). The HLA-Cw4-KIR2DL1 crystal structure further revealed that the KIR-HLA-C binding was dependent on the interactions between the complementary charged residues. Methionine at position 44 of KIR2DL1 is situated in an electronegatively charged pocket that interacts with lysine at residue 80 of the HLA-Cw4 molecule to confer HLA-C2 specificity (Fan et al., 2001). In contrast, the HLA-C1 specificity of KIR2DL2 is mediated by a hydrogen bond between Lys^{44} of the KIR molecule and Asn^{80} of the HLA-Cw3 ligand (Boyington et al., 2000). These crystal structure studies also report that KIR-HLA-C recognition interface differs in only 4 out of 17 residues. Additionally, minimal contact was observed between HLA-Cw3 peptide and KIR2DL2 and HLA-Cw4 peptide and KIR2DL1, questioning the role of peptides in the specific recognition of HLA-C alleles by KIR2D molecules (Boyington et al., 2000; Fan et al., 2001; Boyington and Sun, 2002).

It is thought that peptide-specific recognition by KIRs to achieve discrimination between self and non-self is unlikely because the peptide binding rules differ for each KIR and HLA ligand pairs (Malnati et al., 1995; Peruzzi et al., 1996; Rajagopalan and Long, 1997). HLA Class I is extensively polymorphic whereas the KIR repertoire is limited. Therefore, KIR recognition to specific HLA ligands is unlikely to be restricted by peptides (Rajagopalan and Long, 2005). Nevertheless, several functional studies have shown NK cell activation is regulated by the peptide presented in activating and inhibitory KIR-HLA ligand interactions (Stewart et al., 2005; Fadda et al., 2010; Sim et al., 2017, 2019).

1.5.11. KIR blockade enhances NK cell function

In cancer, tumour cells exhibit variable levels of HLA Class I antigens predominantly to avoid T cell mediated lysis (Demanet et al., 2004). This, in turn, makes them prime targets for NK cell mediated cytolysis, but by upregulating cognate HLA ligands for NK inhibitory KIRs, despite the expression of NK cell activating ligands, facilitates tumour cell escape from NK cell immunosurveillance and ensures survival (Benson and Caligiuri, 2014; Freund-Brown et al., 2018). Therefore, NK cell immune checkpoint blockade has emerged as a treatment whereby blocking the interaction between the inhibitory KIR and HLA-C ligands would induce 'missing-self' to improve NK cell function against tumour cells.

Pre-clinical characterization of the first anti-KIR2D antibody, IPH2101 (1-7F9) that functions to antagonize inhibitory KIR signalling (Romagné et al., 2009) found that resting NK cells in PBMCs did not break tolerance to normal self-tissue in acute myeloid leukaemia (AML) patients. IPH2101 lowered NK cell activation threshold *in vitro* by blocking inhibitory KIR2DL signalling, which led to NK cells to being more easily activated but not in the presence of healthy tissue. Therefore, potential NK cell-mediated autoimmunity with IPH2101 was not observed. Moreover, it is highly possible that normal healthy cells may express low levels of NK activating ligands as their upregulation is usually a result of stress or DNA damage. It is important to note that Romagné and colleagues (2009) characterised these effects in KIR-HLA Class I mismatched AML patients. The clinical relevance of this treatment may be optimally effective in specifically engineered KIR-HLA mismatches, particularly in the context of HSCT. Therefore, it is vital to investigate favourable patient and donor KIR/HLA genotype combinations aiming to promote NK cell mediated responses in solid and haematological malignancies.

IPH2101 treatment also yielded similar results in multiple myeloma (MM) patients without significant toxicity or autoimmune events (Benson et al., 2011). Inhibitory KIR blockade with IPH2101 also induced ADCC *in vitro* and improved patient-derived NK cell cytotoxicity against autologous tumour cells, whilst sparing normal cells (Romagné et al., 2009; Benson et al., 2011). *In vivo*, however, as a monotherapeutic agent IPH2101 lacked clinical efficacy due to the loss of surface KIR2D molecules by trogocytosis following antibody binding, leading to NK cell hyporesponsiveness (Carlsten et al., 2016). A recombinant version of IPH2101, IPH2102 (lirilumab) was produced by introducing point mutations in the IgG_4 heavy chain constant region. The preserved epitope reactivity of lirilumab demonstrated no trogocytosis, a satisfactory safety profile with sustained KIR blockade in patients with various types of cancers (Vey et al., 2012).

Subsequent pre-clinical studies of lirilumab in combination with anti-CD20 antibodies enhanced NK cell mediated and rituximab-mediated ADCC against murine lymphoma cells in *in vitro* and *in vivo* models (Kohrt et al., 2014). A phase I trial of lirilumab and lenalidomide in MM patients has shown acceptable safety and tolerability of the dual treatment as no adverse autoimmune events were observed (Benson et al., 2015). However, a phase II trial (EFFIKIR) with lirilumab as a monotherapeutic agent in the maintenance therapy of elderly patients with acute myeloid leukaemia (AML) failed to meet its primary efficacy endpoint and did not demonstrate a difference in response compared to the placebo arm (Vey et al., 2017).

1.6. Thesis rationale

NK cells play an important role in controlling tumour development and have also shown their versatility in cancer immunotherapy (reviewed by Hu et al. (2019)). Several studies implicate KIRs and their ligand expression levels and genotypes in cancer disease progression and prognosis (Jobim et al., 2013; Kim et al., 2014; Zhao et al., 2014; Morales-Estevez et al., 2016). For instance, in patients with metastatic melanoma, inhibitory KIR2DL2/3 and HLA-C1 ligand interaction is increased, thus facilitating tumour evasion and disease progression (Naumova et al., 2005). Whilst the frequency of activating and inhibitory *KIR* genes was comparable between healthy donors and melanoma patients, distinct HLA/KIR combinations may be relevant as prevalence of inhibitory signals over activating signals in melanoma was observed.

Similarly, increased frequency of inhibitory KIR2DL2 in leukaemic patients compared to healthy individuals further implicate the role of inhibitory KIRs and their ligands in tumour escape and NK cell immunity (Verheyden et al., 2004). This study further suggests that susceptibility of leukaemia was partially influenced by the inhibitory NK cell receptor phenotype, indicating the major inhibitory capacity of haematological malignancies to escape NK cell control. By extension, the presence of cognate HLA-C ligands may also be critical in this immune escape response. In the context of haematopoietic stem cell transplant (HSCT), however, overall survival of recipients lacking HLA-C1 molecules specific for inhibitory KIR2DL2/3 is significantly impaired, particularly in donors carrying the activating *KIR2DS2* gene (Cook et al., 2004). This demonstrated the importance of specific *HLA-C/KIR* genotype to achieve a positive clinical transplant outcome. Detailed analyses of different HLA and KIR combinations in cancer and other diseases have been reviewed (Rajagopalan and Long, 2005; Velardi, 2008; Kulkarni et al., 2008; Khakoo and Jamil, 2011; Augusto, 2016).

Collectively, these reports demonstrate the importance of KIRs and their association with cognate HLA-C ligands potentially facilitate tumour escape from the immune system. Therefore, in light of the recent developments in anti-KIR treatment and the role HLA-C and inhibitory KIR proteins in cancer, this thesis aimed to investigate the potential of HLA-C-specific alloantibodies *ex vivo* to exploit and enhance NK cell effector function against tumour cells (Figure 1.10).

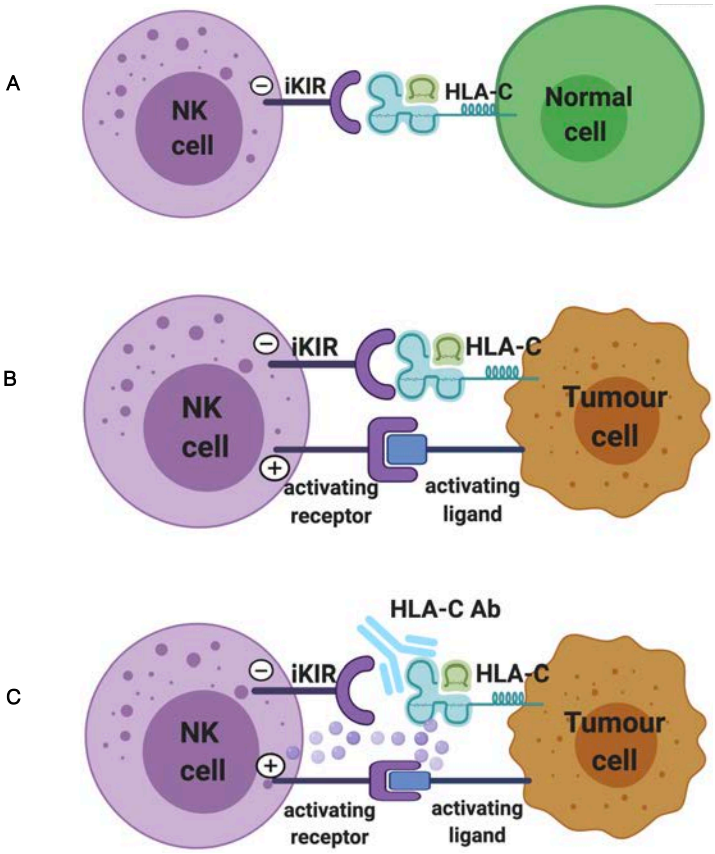

Figure 1.10. | NK cell tolerance mediated by HLA-C ligand and inhibitory KIR interactions.

A | On autologous normal cell, cognate HLA-C ligand binds to inhibitory KIR on NK cells. A balance of signals favour inhibition over NK cell activation to prevent target cell lysis.

B | Tumour cells that retain or upregulate their HLA-C expression also interact with inhibitory KIRs, while NK cell activating ligand on tumour cells bind with NK cell activating receptor. Due to inhibitory HLA-C and KIR interactions, NK cells do not elicit a cytotoxic response against the tumour cell.

C | The inhibitory KIR and HLA-C interactions between NK cells and tumour cells can be disrupted using human HLA-C-specific antibodies to skew the balance of signals within NK cells in favour of activation. The interaction between NK cell activating receptor and ligand facilitate a cytotoxic response against the tumour cell.

1.7. Objectives and aims

The primary objective of this study was to investigate the functional potential of enriched human alloreactive antibodies in enhancing NK cell cytotoxicity against tumour cells. More specifically, HLA-C-specific alloantibodies from renal transplant patient sera were enriched and tested against HLA-C-specific allele transfected cell lines and primary tumour cells in NK cell cytotoxicity assays. The secondary objective was to isolate HLA Class I antibody-producing B cell subsets at the single cell level and clone the immunoglobulin genes to subsequently generate recombinant HLA Class I-specific monoclonal antibodies. To address these objectives, the specific aims of this thesis were as follows:

I | To enrich and prepare KIR ligand groups (HLA-C1 and HLA-C2)-specific alloantibodies from sera deriving from allo-sensitised renal transplant patients

II | To investigate whether enriched alloantibodies against HLA-C can enhance NK cell effector function by performing HLA-C:KIR blockade on single HLA-C allele transfected cell lines and NK cells

III | To analyse the surface HLA-Class I expression levels, including HLA-C and HLA-E on primary tumour cells from Chronic Lymphocytic Leukaemia patients

IV | To determine the functional potential of HLA-C:KIR blockade in increasing primary CLL tumour cell lysis by the enhanced function of NK cells

V | To generate HLA-Class I-specific monoclonal antibodies from two B cell subsets – plasmablasts and memory B cells using PBMCs from renal transplant recipients

CHAPTER II

METHODS

AND MATERIALS

This project used a range of cell culture, molecular biology and protein purification techniques. The following sections in this chapter describe all relevant materials, methods and techniques in detail. Assays performed using commercially available kits were followed according to the manufacturers' protocols and recommendations. Any modifications are described accordingly. Routine clinical assays employed by the Birmingham Histocompatibility and Immunogenetics (H&I) laboratory are also described in this chapter.

2.1. Materials and reagents

2.1.1. Materials

The materials and kits used throughout this study are outlined in Table 2.1.

2.1.2. Buffers and reagents

Individual reagents used throughout this study are outlined in Table 2.2.

Culture media used throughout this study are outlined in Table 2.3.

Buffers used throughout this study are outlined in Table 2.4.

Table 2.1. | A list of materials and kits used in this study

Materials	Manufacturer
Multiwell plates (6, 12, 24 and 48 wells)	Corning, Sigma-Aldrich, U.K.
96 well flat bottom microtitre plates	Corning, Sigma-Aldrich, U.K.
96 well round bottom microtitre plates	Corning, Sigma-Aldrich, U.K.
Tissue culture flasks (25, 75 and 150 cm)	Corning, Sigma-Aldrich, U.K.
96 well filter microplates	Nunc, Thermo Fisher Scientific, U.K.
1ml Cryovials	Alpha Laboratories, U.K.
Mr. Frosty™ Freezing Container	Thermo Fisher Scientific, U.K.
2ml Cryovials	Nunc, Thermo Fisher Scientific, U.K.
Amicon® Ultra-15 centrifugal filter unit	Millipore, U.K.
CELLSTAR™ 15cm vented cell culture dish	Greiner Bio-One, Austria
0.4mm gap electroporation cuvette	Geneflow, U.K.
15ml falcon tubes	Sarstedt, Inc. Fisher Scientific, U.S.A.
50ml conical tubes	Corning, Sigma-Aldrich, U.K.
0.2ml microcentrifuge tubes	Sarstedt, Inc. Fisher Scientific, U.S.A.
0.5ml microcentrifuge tubes	Sarstedt, Inc. Fisher Scientific, U.S.A.
5mL polypropylene FACS tubes	BD Biosciences, U.S.A.
5mL polystyrene FACS tubes	BD Biosciences, U.S.A.
0.2mL domed PCR tubes	Star Labs, U.K.
0.45µM syringe filter	Corning, Sigma-Aldrich, U.K.
72 well Terasaki typing trays	VH Bio Ltd, U.K.
96 well PCR plates	Bio-Rad Laboratories, U.S.A.
Domed 12-cap strips	Bio-Rad Laboratories, U.S.A.
Microseal foil	Bio-Rad Laboratories, U.S.A.
384-well plates	Corning, Sigma-Aldrich, U.K.
Costar® Spin-X® centrifuge tube filters	Corning, Sigma-Aldrich, U.K.

Kits	Manufacturer
Cytotoxicity Detection Kit (LDH)	Roche, Sigma-Aldrich
EasySep™ Human NK cell Enrichment Kit	Stemcell Technologies
EasySep™ Human B cell Enrichment Kit	Stemcell Technologies
VersaComp Antibody Capture Bead Kit	Beckman Coulter, Inc.
LABScreen Single HLA Class I	One Lambda
LABScreen Single HLA Class II	One Lambda
QIAquick Gel Extraction Kit	Qiagen
QIAquick PCR Purification Kit	Qiagen
QIAprep Spin Miniprep Kit	Qiagen
EndoFree Plasmid Maxi Kit	Qiagen
Alkaline phosphatase substrate kit	Bio-Rad Laboratories
Pierce™ BCA Protein Assay Kit	Thermo Fisher Scientific
OneStep RT-PCR Kit	Qiagen
T4 DNA Ligase	New England BioLabs (NEB) Inc.
Gibson Assembly® Cloning Kit	New England BioLabs (NEB) Inc.
Quick Ligation™ Kit	New England BioLabs (NEB) Inc.

Table 2.2. | A list of reagents used in this study

Reagent	Manufacturer
Lympholyte®	Cedarlane, Canada
FastRead Counting Slides	Immune Systems, U.K.
Countbright™ Absolute Counting Beads	Life Technologies, Thermo Fisher Scientific, U.K.
Alexa Fluor™ 647 NHS Ester (Succinimidyl Ester)	Invitrogen, Thermo Fisher Scientific, U.K.
MabThera® Rituximab	Roche, Switzerland
CFSE	eBioscience, Thermo Fisher Scientific, U.K.
Recombinant Human IFN-α	PeproTech, U.S.A.
Recombinant Human IL-2	PeproTech, U.S.A.
Recombinant Human IL-21	PeproTech, U.S.A.
IgG Elution Buffer	Pierce™, Thermo Fisher Scientific, U.K.
10x Ultrapure™ TBE buffer	Invitrogen, Thermo Fisher Scientific, U.K.
Ethidium Bromide solution	Sigma-Aldrich, U.K.
Terrific Broth, modified powder	Sigma-Aldrich, U.K.
Polyethylenimine, Linear, MW 25000,	Polysciences Inc, U.S.A.
Protein A Agarose Beads	Thermo Fisher Scientific, U.K.
Opti-MEM Medium	Gibco, Thermo Fisher Scientific, U.K.
Lipofectamine 2000, transfection agent	Invitrogen, Thermo Fisher Scientific, U.K.
Human serum	Invitrogen, Thermo Fisher Scientific, U.K.
Polybrene	Sigma-Aldrich, U.K.
Luria Bertani (LB) Broth, tablet	Sigma-Aldrich, U.K.
LB with Agar, tablet	Sigma-Aldrich, U.K.
100bp DNA Ladder	New England BioLabs (NEB) Inc.
1kb DNA Ladder	New England BioLabs (NEB) Inc.
AgeI-HF	New England BioLabs (NEB) Inc.
SalI-HF	New England BioLabs (NEB) Inc.
BsiWI-HF	New England BioLabs (NEB) Inc.
XhoI	New England BioLabs (NEB) Inc.
BamHI	New England BioLabs (NEB) Inc.
EcoRI	New England BioLabs (NEB) Inc.
HindIII	New England BioLabs (NEB) Inc.
DH5α competent *E. coli* cells	New England BioLabs (NEB) Inc.
TrypLE™ Express Enzyme (1x), phenol red	Gibco, Thermo Fisher Scientific, U.K.
Geneticin™ Selective Antibiotic (G418 Sulfate)	Gibco, Thermo Fisher Scientific, U.K.
IdeS protease	Promega, U.S.A.
Fluoroquench	One Lambda, U.S.A.
Phytohaemagglutinin (PHA)	Invitrogen, Thermo Fisher Scientific, U.K.
CpG ODN 2006	InvivoGen, U.S.A.
6x gel loading dye	New England BioLabs (NEB) Inc.
Propidium Iodide (PI)	Miltenyi Biotec, Germany

Table 2.3. | A list of culture media, individual components and sources used in this study

Culture media	Components	Source
General medium (GM)	Roswell Park Memorial Institute (RPMI)-1640 10% Fetal Calf Serum (FCS) 1% Penicillin/streptomycin 1% L-glutamine	Merck, Sigma-Aldrich, Germany Invitrogen, Thermo Fisher, U.S.A. Invitrogen, Thermo Fisher, U.S.A. Invitrogen, Thermo Fisher, U.S.A.
DMEM-GM	Dulbecco's Modified Eagle Medium (DMEM) 10% Fetal Calf Serum (FCS) 1% Penicillin/streptomycin 1% L-glutamine	Merck, Sigma-Aldrich, Germany Invitrogen, Thermo Fisher, U.S.A. Invitrogen, Thermo Fisher, U.S.A. Invitrogen, Thermo Fisher, U.S.A.
NK92-GM	GM 10% Horse serum 5% Human serum 400 IU/ml Interleukin-2 (IL-2)	In house Invitrogen, Thermo Fisher, U.S.A. Invitrogen, Thermo Fisher, U.S.A. Peprotech, U.S.A
DMEM-Wash	DMEM	Merck, Sigma-Aldrich, Germany
Transfection medium	DMEM 10% FCS	Merck, Sigma-Aldrich, Germany Invitrogen, Thermo Fisher, U.S.A.
Protein-free medium	BioWhittaker™ UltraDOMA Protein-free medium 1% Penicillin/streptomycin 1% L-glutamine	Lonza, Switzerland Invitrogen, Thermo Fisher, U.S.A. Invitrogen, Thermo Fisher, U.S.A.
Freezing medium	90% FCS 10% Dimethyl sulfoxide (DMSO)	Invitrogen, Thermo Fisher, U.S.A. Merck, Sigma-Aldrich, Germany
B cell culture medium	IMDM with GlutaMAX 10% FCS 0.2% Mycozap-PR 10,000 IU/ml IL-2 100µg/ml IL-21	Invitrogen, Thermo Fisher, U.S.A. Invitrogen, Thermo Fisher, U.S.A. Lonza, Switzerland Peprotech, U.S.A Peprotech, U.S.A

Table 2.4. | A list of buffers, individual components and sources used in this study

Buffer	Components	Source
Phosphate Buffered Saline (PBS)	1 PBS tablet 100ml dH_2O	Sigma-Aldrich, U.K. In house
MACS Buffer	1x PBS 0.5% BSA 2mM EDTA	In house Sigma-Aldrich, U.K. In house
Catch Buffer	5ml RNAse-free H_2O 50µl 1M Tris pH 8.0 125µl Rnasin	Ambion™, Thermo Fisher, U.S.A. Invitrogen, Thermo Fisher, U.S.A. Promega, U.S.A.
Carbonate Buffer	1 Carbonate-Bicarbonate Buffer capsule 25ml dH_2O	Sigma-Aldrich, U.K. In house
PBS-T	PBS 0.1% Tween® 20	In house Sigma-Aldrich, U.K.
Blocking Buffer	PBS 3% BSA	In house Sigma-Aldrich, U.K.

2.2. Tissue Culture

2.2.1. Suspension cell lines

Suspension cell lines were routinely cultured in 25cm^2 tissue culture flasks in a total of 10mL of GM/NK-92 culture media. Cell lines were passaged at 1:5 dilution, every two to three days by discarding 8mL of cells and replacing with fresh medium. The final volume was maintained at 10mL. The various suspension cell lines used throughout this study have been listed in detail in Table 2.5.

2.2.2. Adherent cell lines

Adherent cell lines were routinely cultured in 25cm^2 tissue culture flasks in 5mL of GM or DMEM-GM. Cell lines were passaged every two to three days by removing the culture medium in the flask and rinsing the cell layer with 1mL of sterile PBS. Following the removal of PBS, 1mL of Trypsin was added to the flask and incubated at 37°C. To deactivate the trypsin once the cells had detached, fresh GM or DMEM-GM was added to disaggregate the cells and achieve a single cell suspension. According to the passage dilution, an appropriate amount of medium was removed and replaced with 5mL of fresh medium. The various adherent cell lines used throughout this study have been listed in detail in Table 2.5.

Table 2.5. | A list of suspension and adherent cells used in this study and their sources

Suspension cell lines	
Name	**Source**
721.221	Professor John Trowsdale, University of Cambridge, U.K.
721.221-Cw1	
721.221-Cw6	
K562	Professor E.J.H.J. (Emmanuel) Wiertz, Utrecht University, Netherlands
K562-A2	
K562-Cw01*02	
K562-Cw08*01	
NK-92	Dr Jianmin Zuo, University of Birmingham, U.K.
Lymphoblastoid cell line (LCL)	Dr Heather Long, University of Birmingham, U.K.
B95-8	

Adherent cell lines	
Name	**Source**
HEK293T	Dr Steve Lee, University of Birmingham, U.K.
GP2-293	Dr Jianmin Zuo, University of Birmingham, U.K.
CFPAC-1	Dr Francesca Marcon, University Hospitals Birmingham, U.K.
SUIT-2	
PANC-1	
A431	Dr Jason Yap, University of Birmingham, U.K.
OVCAR-3	
A2780	
SKOV-3	
A375	Dr Guido Frumento, University of Birmingham, U.K.

2.3. Generation of cell lines

2.3.1. Transfection by electroporation

High voltage electric shocks were used to introduce single HLA-Cw06*02 allele plasmid DNA into K562 cells. The plasmid DNA was generated in-house using the methods described by Forrest et al., (2018). Approximately $2.0x10^7$ K562 cells were suspended in 1mL Opti-MEM medium, of which 0.5mL (~$1.0x10^7$ cells) was transferred to a 0.4mm gap electroporation cuvette. 10µg of HLA-Cw06*02 plasmid DNA was added to the cells in the cuvette and mixed by gentle pipetting. The cells were subjected to voltage at 270V and 950µF capacitance settings. The cuvette was left to stand at room temperature for 10 minutes before gently transferring the cells to 9.5mL fresh GM in a 6-well plate. The plate was incubated at 37°C in 5% CO_2 overnight.

The next day, HLA-Cw06*02 surface expression was checked using flow cytometry. 1mL of the transfected cell suspension was transferred to a 5mL FACS tube containing 1mL of PBS. The tube was centrifuged at 1,500rpm for 5 minutes and the supernatant was discarded. Cells were suspended in 100µL of PBS and 3µL of W6/32 antibody conjugated to APC was added, followed by an incubation at 4°C for 30 minutes. The cells were washed in 2mL PBS and the supernatant was removed. For flow cytometry analysis, the cells were suspended in 200µL of PBS and 2µL of PI was added prior to sample acquisition. Following confirmation of cell surface expression, HLA-Cw06*02 transfected K562 cells were purified using BD FACS Canto (BD Biosciences, U.S.A.) and transferred to GM containing Geneticin (G418) (125mg/mL) for propagation into a cell line.

2.3.2. Viral transduction: Lentivirus system

2.3.2.1. Generation of KIR constructs

Nucleotide sequences for KIR2DL2 (accession number: NM_014219.2) and KIR2DL3 (NM_015868.2) were obtained from the NCBI reference sequence directory. *KIR2DL2* and *KIR2DL3* gene fragments (Integrated DNA Technologies, U.S.A.) were purchased and resuspended at a concentration of 25ng/μL, followed by an incubation at 50°C for 20 minutes. To ligate *KIR2DL2* and *KIR2DL3* gene fragments with digested pLV-MCS-IRES-Puromycin vector (a kind gift from Dr Hayden Pearce, University of Birmingham, U.K.), a 2:1 insert-to-vector molar ratio was used. 10μL of Gibson assembly master mix was added and the reaction mix volume was adjusted to 20μL with nuclease-free water, followed by an incubation at 50°C for 30 minutes.

The ligation reaction (2μL) was transformed into 50μL of DH5α competent *E. coli* cells using the method outlined in section 2.10.3.4. Following an overnight incubation, bacteria growth medium was inoculated with a bacterial colony and grown overnight in an orbital shaker at 37°C, 160rpm. Plasmid DNA from overnight cultures was extracted using the QIAprep spin mini-prep kit by following the manufacturer's protocol. DNA was eluted in 30μL volume and subsequently tested for the presence of *KIR2DL2* and *KIR2DL3* insert by restriction digestion analysis.

2.3.2.2. Restriction digestion analysis

To 4µL of KIR2DL2 and KIR2DL3 plasmid DNA, 0.2µL of EcoRI-HF and 0.2µL of BamHI, 1µL of Cutsmart buffer and 4.6µL of nuclease-free water (NEB) was added. The reaction mixes were incubated at 37°C for 60 minutes and later loaded onto 1% w/v Ethidium Bromide (EtBr) agarose gel to separate the digested plasmid DNA fragments based on size by electrophoresis (section 2.10.2.3) at 120V voltage for 50 minutes. 1kb DNA ladder was also loaded onto the gel. The DNA fragments were visualised under UV light.

High concentrations of plasmid DNA containing KIR2DL2 and KIR2DL3 gene fragments were prepared by inoculating 100mL of Terrific Broth (TB) and purifying DNA using the Endofree plasmid maxi kit and following the manufacturer's protocol. The final concentration of dissolved plasmid DNA was adjusted to 1µg/µL with nuclease-free water.

2.3.2.3. Generating KIR2DL2 and KIR2DL3 lentiviruses

To generate KIR2DL2 and KIR2DL3 lentiviruses, HEK293T cells were seeded at $2.0x10^6$ cells in 5mL of DMEM-GM in two $25cm^2$ flasks to achieve approximately 80-90% confluency. The following day, transfection mixes were prepared for KIR2DL2 and KIR2DL3. Firstly, 20µL of lipofectamine 2000 was added to 600µL of Opti-MEM medium and incubated at room temperature for 5 minutes. Secondly, 4µg of either KIR2DL2 or KIR2DL3 plasmid DNA, 2µg of envelope VSV-G plasmid and 6µg of packaging plasmid psPAX2 (gag-pol) were mixed in 600µL of Opti-MEM medium. The lipofectamine 2000 and plasmid DNA reaction mixes were combined and incubated at room temperature for 20 minutes. DMEM-GM from HEK293T flasks was removed, transfection complexes were added and incubated 5-6 hours at 37°C in 5% CO_2. Following incubation, 5mL of DMEM-GM was added to each flask and incubated at 37°C in 5% CO_2 for a further 48-72 hours.

2.3.2.4. Transduction of NK92 cells

Following the generation of lentiviruses using HEK293T cells, the supernatant containing the virus was collected and centrifuged at 2,000rpm for 10 minutes to remove the cell debris. The virus supernatant was filtered using a 0.45μM syringe filter into a new 15mL falcon tube. To transduce NK92 cells, approximately $5.0x10^5$ cells were removed from culture, centrifuged at 1,500rpm for 5 minutes and the cell pellet was resuspended in 2mL of the filtered lentivirus, supplemented with 8μg/mL polybrene. The cells were transferred to one well of a 24 well plate and centrifuged at 2,250 rpm for 2 hours at 33°C. Following centrifugation, the plate was incubated overnight at 37°C in 5% CO_2. The next day, the supernatant was removed and replaced with 1mL of fresh NK92 medium.

2.3.2.5. Confirmation of KIR expression

To determine the transduction of KIR2DL2 and KIR2LD3 into NK92 cells, the surface expression levels were assessed using flow cytometry. Approximately 100μL of transduced cell culture was removed, washed in 2mL of PBS at 1,500rpm for 5 minutes and the supernatant was discarded. 5μL of KIR2DL2/KIR2DL3-PE/Cy7 antibody (Beckman Coulter) was added to 100μL of cell pellet and incubated at 4°C for 30 minutes. The cells were washed, suspended in 200μL of PBS and surface expression was analysed on the Gallios™ flow cytometer. The KIR transduced NK92 population was isolated using BD FACSMelody™ (BD Biosciences, U.S.A) and maintained in NK92-medium for propagation into cell lines.

2.3.3. Viral transduction: Retrovirus system

2.3.3.1. Generation of KIR2DL1 construct

Nucleotide sequence for KIR2DL1 (accession no NM_014218.2) was obtained from the NCBI reference sequence directory. KIR2DL1 nucleotide sequence was synthesised into using pMX vector (GeneArt Gene Synthesis, Invitrogen). 5µg of KIR2DL1 vector DNA was reconstituted in 50µL of nuclease-free water. 2µg (10µL) of DNA was digested using 1µL of EcoRI-HF, 1µL of XhoI, 5µL of cutsmart buffer (NEB) and nuclease-free water in a 50µL final volume, followed by an incubation at 37°C for 60 minutes. The digested product was separated into DNA fragments based on size by gel electrophoresis and subsequently purified using the QIAprep gel extraction kit. The concentration of the purified KIR2DL1 gene fragment was measured with the Nanodrop™ spectrophotometer.

Using 2:1 vector-to-insert molar ratio, appropriate volumes of GFP-PLZRS vector and KIR2DL1 purified gene fragment were mixed with 10µL of quick ligase buffer and 1µL of ligase in a 20µL ligation reaction, followed by incubation at 25°C for 6 minutes. 5µL of ligation reaction was transformed into 50µL of DH5α competent *E. coli* cells (section 2.10.3.4). Bacterial colonies were selected and grown overnight in TB. Positive clone plasmid DNA determined by restriction digestion analysis (section 2.10.3.6) was produced and purified from large volumes of bacterial cultures. The final concentration of the KIR2DL1 plasmid DNA was adjusted to 1µg/µL with nuclease-fee water.

2.3.3.2. Generation of KIR2DL1 retrovirus

To generate KIR2DL1 retrovirus, $6.0x10^6$ GP2-293 cells were seeded in 30mL of DMEM-GM in 75cm^2 flask to achieve 80-90% confluency for transfection. The next day, KIR2DL1 transfection mix was prepared. 60µL of lipofectamine 2000 was added to 1.5mL of Opti-MEM medium and incubated at room temperature for 5 minutes. 6µg of KIR2DL1 plasmid DNA and 6µg of envelope VSV-G plasmid was mixed in 1.5mL Opti-MEM medium. The lipofectamine 2000 and KIR2DL1 plasmid DNA transfection mixes were combined and incubated at room temperature for 20 minutes. DMEM-GM from the flask was removed, transfection complex was added and incubated 5-6 hours at 37°C in 5% CO_2. Following incubation, 15mL of DMEM-GM was added to the flask and incubated at 37°C in 5% CO_2 for a further 48-72 hours.

2.3.3.3. Concentration of virus and NK92 transduction

The supernatant containing KIR2DL1 retrovirus was collected, centrifuged and filtered as described in section 2.3.2.3. The virus was concentrated using ultracentrifugation in a SW40-rotor at 19,500rpm for 2 hours at 16°C. 0.5mL of the concentrated virus, supplemented with 8µg/mL polybrene, was used to transduce $5.0x10^5$ NK92 cells following the method described in section 2.3.2.4. KIR2DL1 transduction into NK92 cells was determined by staining NK92 cells with KIR2DL1/2DS1-PC5.5 antibody (Beckman Coulter). Dual GFP-KIR2DL1$^+$ NK92 cells were isolated using BD FACSMelody™ and maintained in NK92-medium for propagation into a cell line.

2.4. Research study and recruitment of donors

2.4.1. Ethics approval

Ethics approval for this study was obtained from the West Midlands-Edgbaston Research Ethics Committee (ref 15/WM/0440). Blood samples were obtained from fully informed and consented healthy volunteers and HLA antibody-incompatible renal transplant recipients from University Hospitals Birmingham. This study was sponsored by the University of Birmingham.

2.4.2. Healthy volunteer cohort

Healthy volunteers used as controls for flow cytometry staining or as sources of NK cells were recruited for the study among the staff and students at the Institute of Immunology and Immunotherapy, University of Birmingham. Up to 50mL of blood was collected from volunteers by a trained phlebotomist.

2.4.3. Leucocyte (apheresis) cones

Leucocyte (apheresis) cones containing a plentiful supply of white blood cells were obtained from platelet donors attending NHS Blood and Transplant Services Birmingham Donor Centre.

2.4.4. Renal transplant recipient cohort

Samples from a total of 13 allo-sensitised renal transplant recipients were used in this study. Patients were selected based on their HLA-specific antibody profiles generated from routine serum antibody testing at the Birmingham H&I laboratory. Informed consent was obtained under study guidelines and 40mL of blood anti-coagulated in heparin and 10mL of clotted blood was collected. Patients were recruited from the Queen Elizabeth Hospital, Birmingham and several NHS dialysis centres across the Birmingham area. All patient sensitive information was anonymised and uniquely coded according to the study guidelines by NHS staff before releasing the samples for research.

Ten renal transplant recipients receiving dialysis treatment and awaiting re-transplantation were recruited. One patient initially gave consent but refused at the time of donation and later withdrew from the study. Two patients undergone transplant nephrectomy were recruited before the procedure and samples were obtained seven days later. Two patients were asked to donate one follow up sample, volume not exceeding 50mL. Serum from a deceased patient was obtained from a set of historical samples previously collected from patients in a University Hospitals Coventry and Warwickshire (UHCW) study to investigate HLA-specific antibodies (REC 13/WM/090).

2.4.5. B-CLL patient cohort

Patients with Chronic lymphocytic leukaemia (CLL) were recruited from the outpatient haematology clinics at QEHB and Birmingham Heartlands Hospital (BHH) (REC 10/H1206/58). All patients were medically untreated. Approximately 10mL of blood anti-coagulated in heparin was received for processing.

2.5. Processing of samples

2.5.1. Isolation of PBMCs

Within 24 hours of sample collection, peripheral blood mononuclear cells (PBMCs) were isolated, under sterile conditions, from whole blood by density gradient centrifugation. Up to 15mL of whole blood in heparinised vacutainers were diluted with 15mL of RPMI-wash medium at a 1:1 ratio. The diluted whole blood was layered over 15mL of Lympholyte® at 2:1 ratio and centrifuged at 2,000 x g for 25 minutes with the brake off. The PBMC layer in the separated cellular fractions of whole blood was aspirated and transferred to a new 50mL conical tube. Up to 50mL of RPMI-wash medium was added and centrifuged at 1,500rpm for 10 minutes. The supernatant was discarded and the PBMC pellet was suspended in RPMI-wash medium to determine the total number of cells using FastRead disposable counting slides (Immune Systems, U.K.) and a microscope. The PBMCs were either prepared for cryopreservation or used fresh for experiments.

2.5.2. Cryopreservation, storage and thawing of PBMCs

PBMCs suspended in RPMI-wash medium were centrifuged at 1,500rpm for 5 minutes. The cell pellet was resuspended in freezing medium at a maximum of $5.0x10^7$ cells per mL (healthy donor PBMCs) or $2.0x10^7$ cells per mL (patient PBMCs) and subsequently transferred to cryovials. The cryovials were stored overnight in a Mr. Frosty™ freezing container with isopropanol at -80°C. Storage in Mr. Frosty allows optimal rate of cooling of cells at -1°C per minute for cell preservation. For short-term storage, cryovials containing frozen PBMCs were transferred to -80°C freezer. For long-term storage, cryovials were transferred to liquid nitrogen tanks with -140°C to -180°C temperatures. Frozen cells were

recovered by thawing cryovials at room temperature. Thawed PBMCs (1mL) were added to 9mL of appropriate pre-warmed medium or buffer and centrifuged at 1,500rpm for 5 minutes. Supernatant was discarded, the cell pellet was suspended in an appropriate volume of medium/buffer and cells were counted.

2.5.3. Serum collection and storage

To collect serum, vacutainers with clotting factor containing whole blood were processed within 1-2 hours of receiving the samples. Vacutainers were centrifuged at 2,000 x g for 10 minutes. The serum was aspirated and transferred to 2mL cryovials which were directly stored at -80°C.

2.6. HLA-specific antibody screening and adsorption

2.6.1. Single HLA antigen luminex® microbead assay

To determine recipient and donor suitability for transplantation, HLA-specific antibodies from the sera of sensitised individuals are routinely detected using solid phase assays e.g. microbead analysis by Luminex®. The polystyrene microbeads are coupled with purified single HLA antigens and are internally labelled with varying ratios of two fluorophores. Following incubation with serum, any HLA-specific antibodies react and bind to the beads and a fluorochrome-conjugated anti-human IgG secondary antibody is added to detect the antibody-bound microbeads using the Luminex® platform. For this project, these microbeads assays were carried out using the LABScreen Single Antigen kits (One Lambda, U.S.A.) by the serology laboratory staff at NHS Blood and Transplant, Birmingham.

Prior to testing, the wash buffer (supplied with the LABScreen kit) and serum test samples were brought to room temperature. The wells required for testing in a 96 well filter microplate were prepared by adding 200µL of wash buffer. The plate was then shaken on a plate agitator for 5 minutes at room temperature and later placed on a vacuum manifold to aspirate the wash buffer. Luminex beads were vortexed for 10 seconds. To the test wells, 20µL of wash buffer, 2µL of beads and 8µL of patient or control (positive and negative) sera were added. Control sera included positive control serum which comprised sera from multiple sensitised individuals with HLA-specific antibodies, and negative control serum which consisted of a pool of A/B male blood donors' sera that previously showed no anti-HLA reactivity during Luminex® analysis. The plate was covered and incubated on a plate agitator in the dark for 30 minutes at room temperature.

Following incubation, 200µL of wash buffer was added to the test wells and the plate was placed on a vacuum manifold to aspirate the wash buffer. This wash step was repeated an additional three times to achieve a total of 4 washes. To identify the antibody-bound beads, PE conjugated goat anti-human IgG secondary antibody (supplied with the LABScreen kit) was used. The stock concentration 1mg/mL of the secondary antibody was diluted 1:100 to achieve a working concentration of 10µg/mL and 40µL of the diluted antibody was added to each well. The plate was covered and incubated on a plate agitator in the dark for 30 minutes at room temperature.

After incubation, the plate was washed four times with 200µL of wash buffer. Prior to analysis, 80µL of wash buffer was added to each well to resuspend the reaction mix. The plate was placed on a plate agitator for 2-3 minutes. Samples were acquired using the Luminex® two colour laser xMap 100 platform (Luminex Corp, U.S.A). The data were analysed using the HLA Fusion software (One Lambda Inc, U.S.A) to determine serum antibody reactivity to the beads at the HLA allelic level.

2.6.2. Adsorption of HLA-C-specific antibodies from serum

2.6.2.1. Immobilised chromatography column

2mg of soluble HLA-Cw08 protein was coupled to 1mL of sepharose and packed into 2mL chromatography column (Figure 2.1) to selectively deplete or isolate HLA-Cw08-specific antibodies from patient sera or plasma samples. This immobilised chromatography column was a kind gift from Dr Rico Buchli, Pure Protein, L.L.C (U.S.A.) (McMurtrey et al., 2014).

To prepare the column for antibody selection, the flow tap was opened and PBS (containing 0.01% NaN_3, pH 7.4) in the column was released. The flow tap was closed before the PBS level reached the level of sepharose and 1mL of PBS was added. To wash the column, the PBS and sepharose were resuspended with a transfer pipette. The flow tap was opened to release the PBS and the wash step was repeated an additional four times for a total of five washes.

2mL of patient serum containing HLA-Cw08 (HLA-C1)-reactive antibodies were thawed and diluted in 4mL of PBS. Following the final wash step, the flow tap was closed and 1mL of diluted serum was loaded into the column reservoir. The serum was allowed to flow through by gravity. Before the diluted serum level dropped below the level of sepharose, another 1mL of the sample was loaded. This step was repeated until 6mL of the diluted sample was applied to the column. The flow through was collected in a universal tube and discarded. The column was washed with 7mL of PBS to remove residual serum and non-specific antibody binding to the sepharose.

To recover the HLA-Cw08-specific antibodies bound to the sepharose, 5mL of an alkaline elution buffer of glycine (0.1M, pH 11.0) was loaded in the column reservoir in 1mL fractions. The eluate (flow through) was collected in a universal tube containing 1mL of neutralisation buffer (1M Tris-HCl, pH 7.0). HLA-Cw08 protein-bound sepharose was washed and re-equilibrated by adding and releasing 10mL of PBS to the column. For long term storage, 2mL of PBS (containing 0.01% NaN_3, pH 7.4) was added to the column and stored at 4°C.

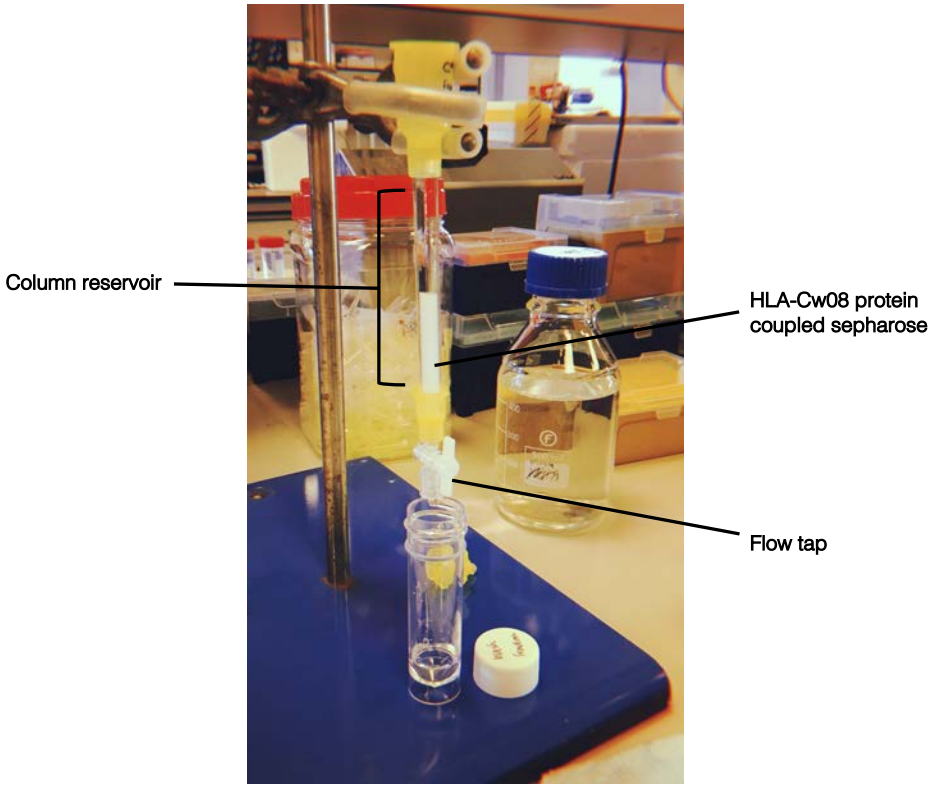

Figure 2.1. | Immobilised HLA-Cw08 protein coupled chromatography column.

The antibody removal/adsorption column uses sepharose as a carrier matrix and soluble HLA-Cw08 protein as the immobilised target antigen to which patient serum or plasma is applied. 1ml of patient serum diluted in PBS is loaded into the column reservoir. The diluted serum travels through the column by gravity as the flow tap is released and the flow through is collected for analysis.

2.6.2.2. Concentration of antibody eluate

The Amicon® Ultra-15 centrifugal filter unit was prepared by adding 15mL of PBS and centrifugation at 4,300rpm for 20 minutes. The flow through was discarded and the antibody eluate fraction was made up to 15mL with PBS and loaded into the unit reservoir. The filter unit was centrifuged at 4,300rpm for 20-30 minutes or until a volume between 0.5-0.7mL was reached. Under sterile conditions, the concentrated antibody eluate fraction was transferred to a Spin-X® centrifuge tube filter to remove bacteria and other particles. Using a table-top microcentrifuge, the Spin-X® filters were centrifuged at 13,000rpm for 1 minute. The antibody eluate flow through was recovered and transferred to a 1.2mL microcentrifuge tube and stored at 4°C. The Amicon® filter unit was washed two times with 15mL of PBS. The flow through was discarded and PBS containing 0.01% NaN_3 was added to preserve the filter unit for repeated use up to two additional times.

2.6.2.3. Antibody adsorption using HLA-C2 allele-transfected cell line

To adsorb HLA-C2 specific antibodies from patient serum, parental and HLA-Cw6 transfected 721.221 cell lines were used. Parental 721.221 cells express high levels of HLA Class II (Drukker et al., 2002). Therefore, a pre-adsorption step was performed with 721.221 cells to deplete HLA Class II-specific antibodies from serum and allow a more efficient HLA-C2-specific antibody adsorption process. Frozen patient serum containing HLA-C2-specific antibodies, determined by Luminex®, was thawed at room temperature. 721.221 and 721.221-Cw6 cells were removed from culture and a cell count was performed.

Approximately $1x10^7$ cells were suspended in PBS and centrifuged at 1,500rpm for 5 minutes. Under sterile conditions, the supernatant was discarded, the cell pellet was resuspended in 1mL of PBS and transferred to a 1.5mL microcentrifuge tube, which were centrifuged at 13,000rpm for 2 minutes. The supernatant was discarded and the 100µL of serum was added to the 721.221 cells only. The serum and cell reaction was mixed and incubated at room temperature for 30 minutes. Following incubation, the 721.221 cell and patient serum mix was centrifuged at 13,000rpm for 2 minutes. The serum supernatant was collected and applied to 721.221-Cw6 cell pellet in another microcentrifuge tube. After a 30 minutes incubation at room temperature, 1.5mL of PBS was added to wash the cells and the microcentrifuge tube was centrifuged at 13,000rpm for 2 minutes. The supernatant was removed, and the wash step was repeated for an additional two times.

To elute the HLA-C2-specific antibodies bound to the 721.221-Cw6, 100µL of IgG Elution Buffer was added. The buffer and cell reaction mixture was resuspended and the microcentrifuge tube was placed in a table top agitator for 30 minutes at room temperature. Following incubation, the tube was centrifuged at 13,000rpm for 2 minutes. The antibody eluate supernatant was carefully collected and transferred to a new 1.5mL microcentrifuge tube, which was also centrifuged at 13,000rpm for 2 minutes to remove any residual 721.221-Cw6 cells. The antibody eluate was transferred to another 1.5mL microcentrifuge tube and neutralised with 42µL of neutralisation buffer (1M Tris, pH 9.5). The enriched HLA-C2-specific antibody eluate was stored at 4°C.

2.6.3. Digestion of Fc fragment using IdeS protease

To cleave IgG molecule below the hinge region to obtain $F(ab')_2$ and Fc fragments, enriched HLA-C-specific antibody eluates were incubated with 1 unit of IdeS (Immunoglobulin-degrading enzyme from *S. pyogenes*) protease at 37°C for 1 hour. Following incubation, IdeS-digested antibody eluates were stored at 4°C.

2.7. Flow cytometry

Flow cytometry was used throughout this study as a means of analysing antigenic expression levels on PBMCs and cell lines; to measure target cell cytotoxicity in functional experiments and to identify and isolate populations of interest. This section describes setting up flow cytometry analysis, the antibody panels used in this study and the methods for cell surface staining.

2.7.1. Flow cytometer and compensation

In this study, flow cytometry analyses were carried out using the Gallios™ flow cytometer (Beckman Coulter, Inc.) unless stated otherwise. Fluorescence-activated cell sort (FACS) was performed for different experiments using either BD FACSAria™ Fusion or BD FACSMelody™ (BD Biosciences). The Gallios™ flow cytometer is a 10-colour system with four lasers (red, blue, violet and green). All flow cytometry analyses were performed using Kaluza software (version 2.1; Beckman Coulter, Inc.) unless stated otherwise.

Prior to carrying out compensation, optimal voltages for each fluorescence channel were set up using unstained target cells for each antibody panel. To correct the fluorescence compensation and minimise the spectral overlap of fluorochromes, a compensation protocol involving the use of VersaComp Antibody Capture Kit. 100µL of PBS was added to 5mL polypropylene tubes and one drop of positive and negative beads. The number of tubes used for compensation were equivalent to the number of fluorochromes used in an antibody panel.

Next, 5µL of a single fluorochrome-antibody conjugates were added to individual tubes containing antibody capture beads and mixed well. The tubes were incubated for 30 minutes at room temperature and in the dark. 2mL of PBS was added to each tube and centrifuged at 2,000 x g for 10 minutes. The supernatant was aspirated using transfer pipettes and approximately 200µL of supernatant was left behind to avoid disturbing the bead pellet. An additional 300µL of PBS was added to each tube and vortexed. Compensation tubes were freshly made prior to acquisition on the Gallios™ and/or stored at 4°C up to two weeks for re-use. Compensation was performed following the manufacturer's protocols and the resulting compensation matrix was analysed using the Kaluza software, which was subsequently applied to all the samples acquired on the Gallios™ using the same antibody panel.

2.7.2. Immunophenotyping - PBMCs

Frozen or freshly isolated PBMCs (~ $1x10^6$) were analysed for cell surface expression by co-incubating with the relevant antibody panel. The samples were incubated at 4°C for 30 minutes. 2mL of PBS was added to each tube and the cells were washed by centrifugation at 1,500rpm for 5 minutes. The supernatant was discarded, and the cells were suspended in 200µL of PBS prior to sample acquisition on the Gallios™.

Antibody panels analysing the KIR2D and KIR3D expression on NK cells from healthy donors are described in Tables 2.6 and 2.7, respectively.

Antibody panels analysing the HLA surface expression on $CD5^+$ $CD19^+$ tumour cells from B-CLL patients are described for HLA-C (Table 2.8), HLA Class I (Table 2.9) and HLA-E (Table 2.10).

Table 2.6. | Antibody panel for cell surface staining to analyse NK cell KIR2D expression

Channel	Antibody	Clone	Fluorophore	Manufacturer	Catalogue No.
FL1	KIR2DL1/2DS1	EB6	FITC	Miltenyi Biotec	130-118-973
FL2	KIR2DL1	REA284	PE	Miltenyi Biotec	130-120-446
FL3	KIR2DS4	REA860	PE-Vio615	Miltenyi Biotec	130-114-780
FL5	KIR2DL2/3	REA1006	PE-Vio770	Miltenyi Biotec	130-116-835
FL6	KIR2DL1/2DS5	143211	APC	R&D Systems	FAB1844A-100
FL7	KIR2DL3	180701	AF700	R&D Systems	FAB2014N-100ug
FL8	CD56	REA196	APC-Cy7	Miltenyi Biotec	130-114-739
FL9	CD3	REA613	Pacific Blue	Miltenyi Biotec	130-114-710
FL10	CD14	REA599	VioGreen	Miltenyi Biotec	130-110-583
FL10	CD19	REA675	VioGreen	Miltenyi Biotec	130-114-175

Table 2.7. | Antibody panel for cell surface staining to analyse NK cell KIR3D expressi

Channel	Antibody	Clone	Fluorophore	Manufacturer	Catalogue No.
FL1	CD3	REA613	FITC	Miltenyi Biotec	130-113-700
FL2	KIR3DL2	539304	PE	R&D Systems	FAB2878P-100
FL3	KIR2DS4	REA860	PE-Vio615	Miltenyi Biotec	130-114-780
FL5	KIR2DL2/3	REA1006	PE-Vio770	Miltenyi Biotec	130-116-835
FL6	KIR3DL1/3DS1	REA168	APC	Miltenyi Biotec	130-104-534
FL7	KIR3DL3-1136B	1136B	AF700	Novus Biologicals	FAB8919N-100UG
FL8	CD56	REA196	APC-Cy7	Miltenyi Biotec	130-114-739
FL9	KIR3DL1	REA1005	Pacific Blue	Miltenyi Biotec	130-116-943
FL10	CD14	REA599	VioGreen	Miltenyi Biotec	130-110-583
FL10	CD19	REA675	VioGreen	Miltenyi Biotec	130-114-175

Table 2.8. | Antibody panel for cell surface staining to analyse HLA-C expression

Channel	Antibody	Clone	Fluorophore	Manufacturer	Catalogue No.
FL1	CD5	UCHT2	FITC	Biolegend	300606
FL2	HLA-C	DT-9	PE	BD Pharmingen	566372
FL3	CD14	RM052	ECD	Beckman Coulter	IM2707U
FL6	CD19	HIB19	APC	Biolegend	302212
FL9	CD3	HIT3a	PB	Biolegend	300330

Table 2.9. | Antibody panel for cell surface staining to analyse totsl HLA Class I expression

Channel	Antibody	Clone	Fluorophore	Manufacturer	Catalogue No.
FL1	CD5	UCHT2	FITC	Biolegend	300606
FL2	CD19	HIB19	PE	Biolegend	302208
FL3	CD14	RM052	ECD	Beckman Coulter	IM2707U
FL6	HLA Class I	W6/32	APC	Biolegend	311410
FL9	CD3	HIT3a	PB	Biolegend	300330

Table 2.10. | Antibody panel for cell surface staining to analyse HLA-E expression

Channel	Antibody	Clone	Fluorophore	Manufacturer	Catalogue No.
FL1	CD5	UCHT2	FITC	Biolegend	300606
FL2	CD19	HIB19	PE	Biolegend	302208
FL3	CD14	RM052	ECD	Beckman Coulter	IM2707U
FL6	HLA-E	3D12	APC	Miltenyi Biotec	130-096-846
FL9	CD3	HIT3a	PB	Biolegend	300330

2.7.3. Immunophenotyping - cell lines

To identify the expression levels of specific proteins on the surface of cell lines, approximately $2.0x10^5$ cells were incubated with 5µL of single fluorochrome-conjugated antibody or isotype control at 4°C for 30 minutes. 2mL of PBS was added to each tube and the cells were washed by centrifugation at 1,500rpm for 5 minutes. The supernatant was discarded, and the cells were suspended in 200µL of PBS prior to sample acquisition on the Gallios™.

2.7.4. Immunophenotyping with serum and enriched antibodies

2.7.4.1. Flow cytometry cross match

Isolated lymphocytes from donors with HLA genotype corresponding to the patient serum HLA-specific antibody profiles were suspended in PBS at $12.0x10^6$ cells per mL. To 5mL polystyrene tubes, 25µL of patient or control sera (section 2.6.1) and 25µL of lymphocytes (~ $3.0x10^5$ cells) were mixed and incubated for 30 minutes at room temperature.

Following incubation, a cell washing centrifuge (Diacent-CW, Diamed, U.S.A.) was used to wash the sample tubes three times with PBS. The supernatant was discarded and to each tube, 100µL of diluted FITC-conjugated goat anti-human IgG (1:220), 5µL of CD14-ECD and 5µL of CD3-PE were added. The tubes were vortexed and incubated at 4°C for 15 minutes. Following incubation, the tubes were washed in PBS using the cell washing centrifuge. The supernatant was removed, and the samples were suspended in 200µL of PBS. Prior to sample acquisition on the Gallios™ flow cytometer, 2µL of PI (viability dye) was added. Approximately 50,000 cell events were acquired per sample.

2.7.4.2. Cell lines

Parental and single HLA-C allele transfected cell lines were removed from culture and a cell count was performed. Depending on the number of tests, cells were suspended in PBS at $1.0x10^7$ cells per mL and 20µL of cell suspension (~$2.0x10^5$ cells) was transferred to a 5mL polystyrene FACS tube. To 20µL of cells, 20µL of serum or enriched antibody eluate was added (1:2 final dilution) and incubated at room temperature for 30 minutes. Following incubation, cell washing centrifuge (Diacent-CW, Diamed, U.S.A.) was used to wash the sample tubes three times with PBS.

The supernatant was discarded and to each tube, 100µL of diluted FITC-conjugated goat anti-human IgG (1:200) was added. The tubes were vortexed and incubated at 4°C for 15 minutes. Following incubation, the tubes were washed in PBS using the cell washing centrifuge. The supernatant was removed, and the samples were suspended in 200µL of PBS. Approximately 30,000 cell events were acquired per sample on the Gallios™ flow cytometer.

2.8. Cytotoxicity assays

2.8.1. Lactate Dehydrogenase (LDH) assay

NK cells from healthy donors and NK92-KIR2DL1 cytotoxic activity against solid tumour cell lines, A431 and A375, was detected by the release of LDH in cell culture supernatants following an overnight assay. LDH cytotoxicity detection kit was used as a non-radioactive colorimetric assay to quantify target cell lysis based on the measurement of LDH activity released by damaged cells into the culture supernatant. Data were analysed in Microsoft Excel and statistical analyses were performed using the Graphpad Prism 8 software.

2.8.1.1. Optimisation

Optimal cell concentration of A431 and A375 target cell lines and primary NK cells and NK92-KIR2DL1 as effector cells was determined by titrating cell number for this assay. Firstly, the optimal target cell number was determined by seeding 100µL of target cells in 96 well flat-bottom microtiter plates at various concentrations, reaching up to $1.0x10^5$ cell per well. 100µL of GM was added and after an overnight incubation at 37°C in 5% CO_2., optimal cell concentration was determined with a monolayer of cells by microscopic evaluation. Each assay condition was performed in triplicate wells. The optimal target cell concentration for both A431 and A375 cell lines was $1.0x10^4$ cells per well which doubled overnight, ready for use in the assay.

Secondly, enriched NK cells from healthy donors pre-activated with IFN-α and NK92-KIR2DL1 cells cultured in medium conditioned with IL-2 were used to optimise effector cell concentration. GM (200µL) were removed from the wells and replaced with fresh medium (100µL), following overnight incubation to achieve a monolayer of target cells

(approximately 2.0x10^4 cells) for experiment. Different effector cell concentrations (100µL) were suspended in GM and added to target cells at E:T ratios varying from 1:1-10:1 and incubated overnight at 37°C in 5% CO_2. Of note, primary NK cells and NK92-KIR2DL1 cells were tested against A431 and A375 cell lines, respectively. The optimal effector cell concentration was 1.0x10^5 cells per well (5:1 E:T ratio).

In addition, each experimental setup included controls. Background control (BGC) provided measurement of LDH activity of the assay culture medium (GM). The absorbance value from this control was subtracted from all other values in the experiment. The low control (LC) involved measuring spontaneous LDH activity from wells containing 100µL of target cells and 100µL of GM. The high control (HC) provided maximum LDH activity from wells containing 100µL of target cells and 100µL of GM supplemented with 1% Triton-X-100 solution.

2.8.1.2. Experimental set up

Following an overnight incubation of target cells to achieve optimal cell density, 200µL of culture supernatant in each well was removed and cells were washed with 100µL of GM. For each experimental well, 10µL of enriched HLA-C1 or HLA-C2-specific antibody eluate was diluted in 90µL of GM. Wash medium were aspirated from the wells, 100µL of diluted antibody eluate was added to relevant wells and incubated at 37°C in 5% CO_2 for 3-4 hours. Effector cells i.e. primary NK cells for A431 target cells and NK92-KIR2DL1 cells for A375 target cells were added at 1.0x10^5 cells per well. The experiment was incubated overnight at 37°C in 5% CO_2.

2.8.1.3. Determining LDH activity

To determine LDH activity, 10µL of cell free supernatant was collected and transferred to a new 96 well flat-bottom microtiter plate containing 90µL of culture media per well. 100µL of LDH reaction mix was added to each well containing the diluted supernatant (1:10) and kept at room temperature and in the dark for 15 minutes. The absorbance of samples was measured at 490nm using an ELISA plate reader (Bio-Rad, U.K.). Absorbance values were corrected for 1:10 dilution and an average value of the triplicate wells per condition (Table 2.11). was used to determine target cell cytotoxicity by the following calculation:

$$\left(\frac{experimental\ LDH - low\ control\ LDH}{high\ control\ LDH - low\ control\ LDH}\right)\ x\ 100 = \%\ target\ cell\ cytotoxicity$$

Table 2.11. | Representative example of LDH assay percentage cytotoxicity

		Well replicate					
		1	2	3	Average	Exp value	Cyto (%)
	BGC	3.26	3.21	3.24	3.24		
	HC	5.69	5.81	5.7	5.73	2.50	
	LC	3.34	3.36	3.41	3.37	0.13	
E:T Ratio	1:1	3.82	3.69	3.72	3.74	0.51	15.80
	2:1	4.08	3.84	3.95	3.96	0.72	24.82
	5:1	4.49	4.45	4.3	4.41	1.18	44.15
	10:1	5.61	5.73	5.58	5.64	2.40	96.05

2.8.2. K562 and NK cell cytotoxicity assay

This flow cytometry-based assay measures NK cell cytotoxicity activity by quantifying the number of viable CFSE-labelled target cells i.e. K562 cells following an overnight co-incubation with primary NK cells from healthy individuals with specific KIR repertoires. The *in vitro* model was further modified to assess the effect of HLA-C-specific alloantibodies on NK cell cytotoxicity activity. Data were analysed in Microsoft Excel and statistical analyses were performed using the Graphpad Prism 8 software.

2.8.2.1. NK cell enrichment and activation

Using the EasySep™ human NK cell enrichment kit, NK cells were negatively enriched from previously frozen or freshly isolated PBMCs from healthy donors. A maximum of $25.0x10^6$ PBMCs were used in a 15mL falcon tube for each round of enrichment. Approximately $5x10^4$ PBMCs were set aside to determine purity of NK cells at the end of the process using flow cytometry. The remaining PBMCs were centrifuged at 1,500rpm for 5 minutes and the supernatant was discarded.

Following the manufacturer's instructions, PBMCs were suspended in sterile PBS at a concentration of $5.0x10^7$ PBMCs per mL. The suspension volume was calculated based on the number of PBMCs available for enrichment. For example, $25.0x10^6$ PBMCs were suspended at a concentration of $5.0x10^7$ cells/mL in 0.5mL of sterile PBS ($25.0x10^6$ / $5.0x10^7$ = 0.5). Unwanted non-NK cells were targeted for removal by adding 25µL of EasySep™ human NK cell enrichment cocktail (50µL/mL of sample), containing antibodies that recognised specific cell surface markers. The reaction mix was incubated at room temperature for 10 minutes. Vortexed 50µL of EasySep™ D magnetic particles were added to the sample (100µL/mL). The sample was mixed and incubated at room

temperature for 5 minutes. The final volume of the sample was made up to 2.5mL, which was transferred to a 5mL polystyrene falcon tube. The sample tube was placed in an EasySep™ magnet for 2-3 minutes and unwanted non-NK cells labelled with antibodies and magnetic particles were separated to the sides of the 5mL falcon tube touching the magnet. The NK cells retained in the clear sample were transferred to a new 15mL falcon tube using a pipette and a cell count was performed. Approximately $5.0x10^4$ NK cells were set aside to determine purity of the enriched NK cells using flow cytometry. The enriched NK cell suspension was centrifuged at 1,500rpm for 5 minutes and the supernatant was discarded. In a 24 well plate, NK cells were resuspended at $2.0x10^6$ cells/mL in GM and IFN-α was added (2µg/mL) for overnight activation at 37°C in 5% CO_2. Non-IFN-α activated NK cells in GM were included as control condition for the optimisation experiments.

2.8.2.2. NK cell enrichment purity analysis

To determine the purity of the NK cell enrichment process, PBMCs and NK cells were incubated with CD3-AF700 and CD56-PE/Cy7 antibodies at 4°C for 30 minutes. Each test tube was washed using 2mL of PBS followed by centrifugation at 1,500rpm for 5 minutes and the supernatant was discarded. The cell pellets were suspended in 0.2mL PBS and 2µL of PI was added before acquiring samples on the flow cytometer.

2.8.2.3. CFSE-labelling of K562 target cells

Target cells i.e. parental K562 and single HLA-C allele transfected K562 cell lines were labelled with Carboxyfluorescein succinimdyl ester (CFSE) to discriminate between target cells and effector cells during flow cytometry analysis of the cytotoxicity assay. Up to $2.0x10^6$ target cells were removed from culture and centrifuged an appropriate volume of

PBS at 1,500rpm for 5 minutes. From a 5mM stock solution, CFSE dye was diluted (1:50) in PBS. Following target cell centrifugation, the supernatant was discarded and 10µL of the diluted CFSE dye (0.1mM) was added to the suspended cell pellet (final concentration 0.5µM) and incubated at 37°C in 5% CO_2 for 10 minutes. The cells were mixed after 5 minutes of incubation to allow even labelling of cells. 10mL of GM was added to the CFSE and cell sample mixture and washed by centrifuging at 1,500rpm for 5 minutes. The supernatant was removed. 5mL of GM was added to the labelled target cells and incubated at 37°C in 5% CO_2 for 30-45 minutes.

2.8.2.4. Optimisation of E:T ratios

The effector-to-target (E:T) ratios were optimised in this assay by using non-IFN-α and IFN-α activated NK cells as effector cells and CFSE-labelled parental K562 cell line as target cells in a U-bottom 96 well microtiter plate. A fixed number of CFSE-labelled K562 cells were used during the NK cell cytotoxicity assay, while the number of effector cells varied depending on the E:T ratio being tested (0.1:1, 0.2:1, 0.5:1 and 1:1) (Figure 2.2).

Following incubation, a count of CFSE-labelled K562 cells in GM was performed and cells were centrifuged at 1,500rpm for 5 minutes. Likewise, NK cells from overnight IFN-α activation and control NK cells were counted and centrifuged at 1,500rpm for 5 minutes. The target cells and effector cells were suspended at a final concentration of $5.0x10^5$ cells/mL in GM. 100µL of target cell suspension containing approximately $5.0x10^4$ cells were added to each well of a U-bottom 96 well microtiter plate and co-cultured with varying numbers of effector cells corresponding to E:T ratio. For example, for 0.1:1 E:T ratio, 10µL of effector cell suspension containing approximately $5x10^3$ cells were added to 100µL of $5.0x10^4$ target cells in a well.

A control condition was also included whereby the wells did not contain any effect cells but only 100µL of $5.0x10^4$ target cells and 100µL of GM. All assay optimisation conditions contained a final volume of 200µL comprising GM, CFSE-labelled target cells and either non-IFN-α (control) or IFN-α activated effector cells per well. Each assay condition was performed in triplicate wells and the experiment was incubated at 37°C in 5% CO_2 overnight (16-18 hours).

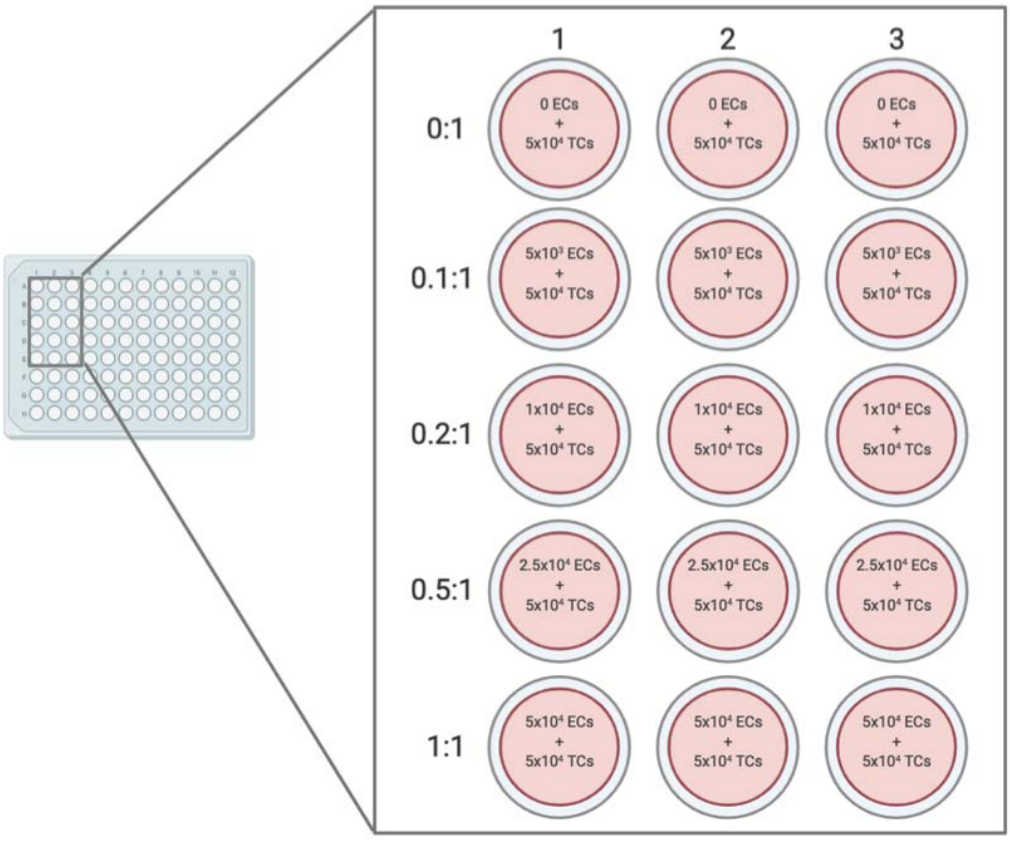

Figure 2.2. | Schematic of E:T ratio optimisation for K562-NK cell cytotoxicity assay.

Varying numbers of effector (NK) cells were added to a fixed number ($5.0x10^4$) of target (K562) cells in a U-bottom 96 well microtiter plate. The final volume in each well was standardised to 200µL with GM.

2.8.2.5. Measuring NK cell cytotoxicity by flow cytometry

Following overnight incubation, 200µL of target and effector cell co-cultures were harvested. The contents of each well were transferred to an individual 5mL polypropylene FACS tube. 200µL of non-sterile PBS was also added to each well to aspirate and collect any residual cell contents before adding to the corresponding tube. Each tube containing 400µL of harvested co-cultures was further prepared by adding 5µL of Countbright™ absolute counting beads and 2µL of PI for acquisition on the Gallios™ flow cytometer. An automated set up of protocol facilitated sample acquisition of approximately 200µL for 2 minutes.

A specific volume of Countbright™ counting beads (Figure 2.3A) containing a known concentration of beads was added to each sample tube so that the ratio of sample volume to bead volume was known. For example, 50µL of the bead suspension contained 49,500 beads as per manufacturer's instructions. In this study, however, 5µL of beads were used which contained 4,950 beads (assigned bead count). At least 1,000 bead events were acquired per test (Figure 2.3B). Variation in bead counts between experiments was very low (Figure 2.3C) and the number of beads quantified from one experiment (Figure 2.3D) show that these calibration beads validate this analysis method whereby flow cytometry is used to quantify target cell population.

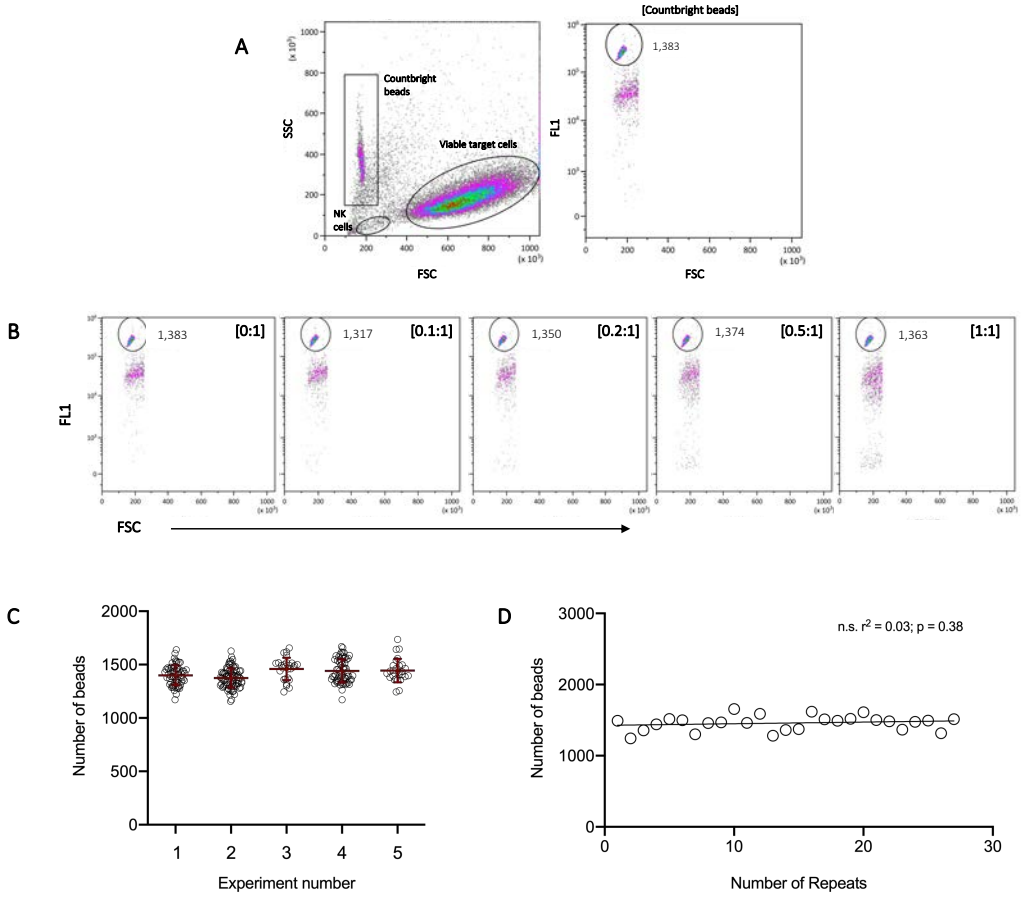

Figure 2.3. | Validation of flow cytometry-based analysis of NK cell cytotoxicity assay.

A | Countbright™ counting beads and viable target cells were detected based on their forward and side scatter parameters. Counting beads were further analysed and quantified by forward scatter profile and fluorescence channel 1 (FL1).

B | Representative examples of individual scatter plots demonstrating the consistent quantification of counting beads under different E:T ratio test conditions from one experiment.

C | The number of beads quantified by flow cytometry across five independent experiments. Red line indicates mean±SD.

D | A series of repeated bead counts (n=27) from one experiment. Simple linear regression analysis; r^2=0.03; p=0.38; not significant

Therefore, to calculate the percentage of target cell cytotoxicity, the absolute number of live K562 cells (A) were quantified from flow cytometry analyses and standardised using the bead count (B) from the same sample. The concentration of the assigned bead count (4,950) (C) was also determined in the total sample volume (D). The calculation used to determine the absolute number of viable K562 cells is as follows:

$$\left(\frac{No.\,of\ live\ K562\ events}{No.\,of\ bead\ events}\right) x \left(\frac{Assigned\ bead\ count}{Volume\ of\ sample}\right)$$

$$= concentration\ of\ sample\ as\ cells/\mu l$$

An example, using the above equation is outlined in Table 2.12. To determine percentage of target cell cytotoxicity (Table 2.13), the absolute counts of live K562 cells were used in the following calculation:

$$100\ x \left(\frac{No.\,of\ live\ cells\ from\ E{:}T\ ratio\ (D)}{Mean\ of\ live\ cells\ from\ control\ (0{:}1)\ (E)}\right) = \%\ live\ cells\ (F)$$

$$100 - \%\ of\ live\ cells = \%\ target\ cell\ cytotoxicity$$

Table 2.12. | Representative example of standardising live target cell count using Countbright™ counting beads

E:T Ratio	Replicate	No. of cells (A)	No. of bead count (B)	(A/B) = X	(C/D) = Y	cells/µl (X*Y = Z)	Total Z*200µl	Mean
0:1 (Control)	1	11026.00	1490.00	7.40	12.38	91.58	18315.00	19351.75
	2	10550.00	1244.00	8.48	12.38	104.95	20989.75	
	3	10273.00	1356.00	7.58	12.38	93.75	18750.50	
0.1:1	1	9149.00	1396.00	6.55	12.38	81.10	16220.47	15756.32
	2	8658.00	1396.00	6.20	12.38	76.75	15349.96	
	3	8899.00	1403.00	6.34	12.38	78.49	15698.52	
0.2:1	1	7780.00	1356.00	5.74	12.38	71.00	14200.22	13865.14
	2	7566.00	1380.00	5.48	12.38	67.85	13569.46	
	3	7748.00	1387.00	5.59	12.38	69.13	13825.74	
0.5:1	1	5195.00	1406.00	3.69	12.38	45.72	9144.83	8736.89
	2	4942.00	1445.00	3.42	12.38	42.32	8464.67	
	3	4980.00	1433.00	3.48	12.38	43.01	8601.19	
1:1	1	2251.00	1355.00	1.66	12.38	20.56	4111.61	3399.28
	2	1573.00	1255.00	1.25	12.38	15.51	3102.13	
	3	1735.00	1439.00	1.21	12.38	14.92	2984.10	

Table 2.13. | Representative example of calculating percentage target cell cytotoxicity

E:T Ratio	Replicate	No. of live cells (D)	Mean Control no. of cells (E)	% live cells 100*(D/E) = F	% cyto (100-F)	Mean % cyto
0.1:1	1	16220.47	19351.75	83.82	16.18	18.58
	2	15349.96		79.32	20.68	
	3	15698.52		81.12	18.88	
0.2:1	1	14200.22	19351.75	73.38	26.62	28.35
	2	13569.46		70.12	29.88	
	3	13825.74		71.44	28.56	
0.5:1	1	9144.83	19351.75	47.26	52.74	54.85
	2	8464.67		43.74	56.26	
	3	8601.19		44.45	55.55	
1:1	1	4111.61	19351.75	21.25	78.75	82.43
	2	3102.13		16.03	83.97	
	3	2984.10		15.42	84.58	

2.8.2.6. Set-up of experimental conditions

Once the optimal 0.5:1 E:T ratio was determined, the assay setup was modified to test the effect of HLA-C-specific antibodies and CD16 blockade on NK cell function. Following overnight activation with IFN-α, NK cells were counted and divided into two fractions – CD16-specific antibody-treated and control NK cells. To inhibit FcγRIIIα on NK cells, 5μL of purified CD16 antibody (Biolegend, U.K.) was added to a maximum of $1.0x10^6$ NK cells and incubated at room temperature for 30 minutes. No wash step by centrifugation was performed to remove CD16-specific antibody.

In parallel, approximately $2.0x10^5$ CFSE-labelled target cells were incubated with 20μL of either intact HLA-C1-specific (K562 and K562-Cw08*01 cells) or HLA-C2-specific (K562 and K562-Cw06*02 cells) enriched antibodies for 30 minutes at room temperature. The same procedure was followed when incubating IdeS-digested HLA-C-specific antibodies with target cell lines. After incubation, 1mL of GM was added to each tube and centrifuged at 1,500rpm for 5 minutes. The supernatant was aspirated using a pipette tip to minimise disturbance to the target cell pellet. GM was added to both HLA-C-specific antibody-treated CFSE-labelled target cells and control and CD16-specific antibody-treated NK cells to reach a concentration of $5.0x10^5$ cells/mL and $2.5x10^4$ cells/mL, respectively. 100μL of target cells and effector cells were mixed according to experimental condition and co-cultured overnight (16-18 hours) at 37°C in 5% CO_2. The assay was analysed using flow cytometry and the method is described in section 2.8.2.5.

2.8.3. K562 and NK92-KIR2DL1 cell cytotoxicity assay

Data were analysed in Microsoft Excel and statistical analyses were performed using the Graphpad Prism 8 software.

2.8.3.1. Preparing NK92 and NK92-KIR2DL1 cells

To prepare NK92 and NK92-KIR2DL1 cells for an experiment, the day before assay set up, 10mL of NK92 and NK92-KIR2DL1 were removed from culture and centrifuged at 1,500rpm for 5 minutes. The supernatant was discarded and replaced with fresh 10mL of NK92 culture medium to both effector cell lines. The medium was supplemented with an additional 400IU/mL of IL-2.

2.8.3.2. Optimisation of E:T ratios and assay conditions

Following the method outlined in section 2.8.2.4, E:T ratios (1:1, 2:1, 5:1, 10:1 and 20:1) were optimised using $5.0x10^4$ Alexa Fluor 647 dye-labelled K562 cells and varying concentrations of NK92-KIR2DL1 cells. To determine the importance of IL-2 to activate the effector function, NK92 cells were grown in either culture medium conditioned with IL-2 or GM (contained no IL-2) for 7 days, prior to co-culture with labelled K562 cells for 16-18 hours at 37°C in 5% CO_2.

E:T ratios (2:1, 5:1 and 10:1) were also optimised using IL-2 pre-conditioned NK92-KIR2DL1 as effector cells and K562-Cw06*02 cell line as target cells, followed by a 16-18 hours incubation at 37°C in 5% CO_2. Flow cytometry analysis described in sections 2.8.2.5 was used to determine target cell cytotoxicity.

2.8.3.3. Alexa Fluor 647-labelling of K562 target cells

Target cells i.e. parental K562 and K562-Cw06*02 cell lines were labelled with Alexa Fluor 647 dye to discriminate between target cells and GFP-transduced NK92-KIR2DL1 effector cells during flow cytometry analysis. Up to $2.0x10^6$ target cells were removed from culture and centrifuged with an appropriate volume of PBS at 1,500rpm for 5 minutes. The Alexa Fluor 647 dye was diluted (1:50) in PBS. Following target cell centrifugation, the supernatant was discarded and 10µL of the diluted Alexa Fluor 647 dye was added to the suspended cell pellet and incubated at 37°C in 5% CO_2 for 10 minutes. The cells were mixed after 5 minutes of incubation to allow even labelling of cells. 10mL of GM was added to the cells and washed by centrifuging at 1,500rpm for 5 minutes. The supernatant was removed, and the wash step was repeated twice. 5mL of GM was added to the labelled target cells and incubated at 37°C in 5% CO_2 for 30-45 minutes.

2.8.3.4. Set-up of experimental conditions

Once the optimal 5:1 E:T ratio was determined, the assay setup was modified to test the effect of HLA-C-specific antibodies on NK92-KIR2DL1 effector cell function. A cell count was performed of Alexa Fluor 647 dye-labelled target cells and NK92-KIR2DL1 cells. Firstly, following the method outlined in section 2.8.2.6, HLA-C1 and HLA-C2-specific enriched antibodies were incubated with parental K562 and K562-Cw06*02 cells and subsequent co-culture with NK92-KIR2DL1 cells for 16-18 hours at 37°C in 5% CO_2.

A second experiment was performed whereby K562-C2 target cells were co-incubated with either intact or IdeS-digested HLA-C2-specific antibody eluate. Antibody-bound K562-C2 cells were co-cultured with NK92-KIR2DL1 cells at 5:1 E:T ratio for 16-18 hours

at 37°C in 5% CO_2. All experimental conditions were set up in triplicate wells. Flow cytometry analysis described in sections 2.8.2.5 was used to determine target cell cytotoxicity.

2.8.4. B-CLL and NK cell cytotoxicity assay

This flow cytometry-based assay aimed to measure primary B-CLL tumour cell lysis by using allogeneic and autologous NK cells from healthy donors and B-CLL patients, respectively. The *in vitro* model involved enriching B cells from B-CLL patient PBMCs, treating isolated B cells with HLA-C-specific antibodies and subsequently co-incubating target cells with primary NK cells. NK cell cytotoxicity was measured using flow cytometry analyses. Data were analysed in Microsoft Excel and statistical analyses were performed using the Graphpad Prism 8 software.

2.8.4.1. Serological HLA typing of B-CLL PBMCs

A complement-dependent cytotoxicity (CDC) or microlymphocytotoxicity assay was performed to assign HLA-C group 1 and/or group 2 expression on B cells from ten B-CLL patients. This serological typing method provided low resolution typing for HLA-C by using the Terasaki HLA-C tissue typing trays. The principle involved testing lymphocytes with a panel of sera containing characterised HLA-C-specific alloantibodies. The addition of rabbit serum as a source of complement led to the lysis of B cells bound to the antibodies in the wells by complement activation.

Negatively enriched B cells from previously frozen B-CLL PBMCs were standardised to a concentration of $2.0x10^6$ cells/mL in PBS. The 72 well Terasaki typing trays were thawed at room temperature and used within 30 minutes. Each well contained 1µL of HLA-C-

specific anti-serum and 5μL of heavy mineral oil. Positive and negative control sera wells were also included in each tray. Approximately 2,000 B cells from 1μL of the B cell suspension were added to each well using a Hamilton syringe (Hamilton Company, U.S.A.). One typing tray was assigned to one B-CLL patient. The anti-serum and cell droplets were mixed and incubated at room temperature for 30 minutes.

Following incubation, 5μL of rabbit anti-serum was added to each well and the plates were incubated at room temperature for 60 minutes. After incubation with rabbit serum, 5μL of Fluoroquench, a mixture of fluorescent dyes that stain lymphocytes, quench background fluorescence and stop the reaction was added to each well. The trays were left to stand for 15 minutes at room temperature to prepare for ultra-violet (UV) microscopic evaluation. Live (negative) B cells lacking the HLA-C antigen stained green, whilst dead (positive) B cells possessing particular HLA-C antigen in a well stained red. The negative and positive controls in each tray were used to standardise percentage cell death in the test wells to obtain consistent and accurate grading.

2.8.4.2. Staining B-CLLs with enriched antibodies

Freshly isolated PBMCs from B-CLL patients were tested for HLA-C allelic expression with enriched HLA-C-specific antibody eluates. To approximately $5.0x10^5$ lymphocytes, 20μL of either HLA-C1 or HLA-C2-specific antibody eluate was added, and the samples were incubated for 30 minutes at room temperature. 2mL of PBS was added to each tube and centrifuged at 1,500rpm for 5 minutes. The supernatant was discarded and 100μL of diluted FITC-conjugated goat anti-human IgG (1:200) and 5μL of CD19-APC and CD5-BV510 (Biolegend, U.K.). Following a 30 minutes incubation at 4°C, cells were washed with PBS at 1,500rpm for 5 minutes. The supernatant was discarded, and cells were

suspended in 200µL of PBS. 2µL of PI was added to each tube prior to sample acquisition on the Gallios™.

2.8.4.3. Enrichment of target and effector cells

NK cells were negatively enriched from healthy donor PBMCs with specific KIR repertoires and B-CLL patient autologous PBMCs using the method described in section 2.8.2.1. In a 24 well plate, the isolated NK cells were resuspended at $2.0x10^6$ cells/mL in GM and IFN-α was added (2µg/mL) for overnight activation at 37°C in 5% CO_2.

B cells were negatively enriched, from previously frozen or freshly isolated PBMCs from B-CLL patients by using the EasySep™ human B cell enrichment kit. A maximum of $2.0x10^7$ PBMCs were used in a 15mL falcon tube for each round of enrichment, which were suspended in sterile PBS and centrifuged at 1,500rpm for 5 minutes. The supernatant was discarded and following the manufacturer's instructions, PBMCs were suspended in sterile PBS at a concentration of $5.0x10^7$ PBMCs per mL. The suspension volume was calculated based on the number of PBMCs available for enrichment. For example, $2.0x10^7$ PBMCs were suspended at a concentration of $5.0x10^7$ cells/mL in 0.4mL of sterile PBS ($2.0x10^7$ / $5.0x10^7$ = 0.4). Unwanted non-B cells were targeted for removal by adding 20µL of EasySep™ human B cell enrichment cocktail (50µL/mL of sample), containing antibodies that recognised specific cell surface markers. The reaction mix was incubated at room temperature for 10 minutes. Vortexed 30µL of EasySep™ D magnetic particles were added to the sample (75µL/mL). The sample was mixed and incubated at room temperature for 5 minutes. The final volume of the sample was made up to 2.5mL, which was transferred to a 5mL polystyrene falcon tube. The sample tube was placed in an EasySep™ magnet for 2-3 minutes and unwanted non-B cells labelled with antibodies and magnetic particles were separated to the sides of the 5mL falcon tube touching the

magnet. B cells retained in the clear sample were transferred to a new 15mL falcon tube using a pipette and a cell count was performed. The enriched B cell suspension was centrifuged at 1,500rpm for 5 minutes, the supernatant was discarded, and B cells were suspended in GM at an appropriate concentration.

2.8.4.4. Optimisation of cytotoxicity assay

To measure NK cell cytotoxicity against CLL tumour cells, a flow cytometry-based cytotoxicity assay was optimised using lymphoblastoid cells (LCLs) as target cells. Using the method described in section 2.8.2.4, 0.5:1, 1:1, 2:1, 5:1 and 10:1 E:T ratios were tested. IFN-α activated NK cells from healthy donors were co-cultured with CFSE-labelled LCLs ($5.0x10^4$ cells) at varying concentrations for 16-18 hours incubation at 37°C in 5% CO_2. Flow cytometry analysis described in section 2.8.2.5 was used to determine target cell cytotoxicity (Figure 2.4).

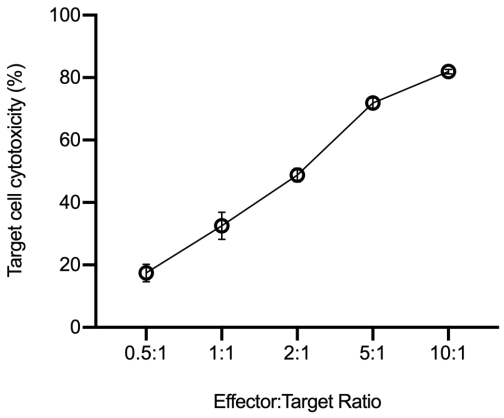

Figure 2.4. | Optimisation of E:T ratio for B-CLL and NK cell cytotoxicity assay.

The optimal E:T ratio was determined by co-incubating varying number of NK cells from healthy donor with enriched B cells from CLL patient PBMCs. NK cells were pre-activated with IFN-α overnight. Each circle represents the average percentage cytotoxicity calculated from triplicate wells for each assay condition. Data from one independent experiment.

Using 5:1 E:T ratio, enriched B cells from CLL patient PBMCs were exposed to varying concentrations of an anti-CD20 antibody, MabThera® rituximab (Roche, Switzerland) which was included as a positive control in each assay. Rituximab concentration was diluted from a working stock of 10mg/mL in GM to achieve final test concentrations of 1µg/mL, 0.1µg/mL and 0.01µg/mL. Enriched B cells and IFN-α activated NK cells were counted and centrifuged at 1,500rpm for 5 minutes. The supernatant was discarded and the target and effector cells were suspended in GM to reach a concentration of $5.0x10^5$ cells/mL and $2.5x10^6$ cells/mL, respectively. 100µL of target cells ($5.0x10^4$ cells) and effector cells ($2.5x10^5$ cells) were mixed according to experimental condition in U-bottom 96 well microtiter plates at 5:1 E:T ratio and a final volume of 200µL in GM. 20µL of diluted rituximab antibody was added to the wells to reach a final concentration of 1µg/mL, 0.1µg/mL and 0.01µg/mL. The different rituximab concentrations were set up in triplicate wells. The assay was incubated for 16-18 hours at 37°C in 5% CO_2.

2.8.4.5. Measuring B-CLL target cell cytotoxicity

Following an overnight incubation, 200µL of target and effector cell co-cultures were harvested. The contents of each well were transferred to an individual 5mL polypropylene falcon tube. 200µL of non-sterile PBS was also added to each well to aspirate and collect any residual cell contents before adding to the corresponding tube. Antibodies against CD5-BV510 and CD19-APC were added to each tube to identify the B-CLL or $CD5^+$ $CD19^+$ tumour cell subset during flow cytometry analysis of the experiment. After the addition of the antibodies, tubes were incubated at 4°C for 30 minutes. 2mL of non-sterile PBS was added to each tube and cells were washed by centrifugation at 1,500rpm for 5 minutes. The supernatant was discarded, and the cells were suspended in a final volume of 200µL of non-sterile PBS. 2µL of PI was added to each tube prior to sample acquisition on the Gallios™ flow cytometer. Countbright™ counting beads were not added since the method

of quantifying live target cells by flow cytometry was previously validated in section 2.8.2.5. An automated set up of protocol facilitated sample acquisition of approximately 200µL for 2 minutes.

2.8.4.6. Experimental set up using HLA-C-specific antibodies

The experimental setup was modified to test the effect of B-CLL coated with HLA-C-specific antibodies and CD16 blockade on NK cell function. Following overnight activation with IFN-α, NK cells were counted and divided into two fractions – CD16-specific antibody-treated and control NK cells. CD16 blockade was performed using the method described in section 2.8.2.6.

In parallel, enriched B cells were also counted and divided into two fractions – control and HLA-C-specific antibody-treated B cells. An appropriate number of B cells were incubated with 20µL of either intact HLA-C1-specific or HLA-C2-specific enriched antibodies for 30 minutes at room temperature. The same procedure was followed when incubating IdeS-digested HLA-C-specific antibodies with target B cells. Control B cells were set aside to for 5:1 E:T control ratio and to test the rituximab-treatment of B cells in the presence of NK cells. After incubation, 1mL of GM was added to each tube and centrifuged at 1,500rpm for 5 minutes. The supernatant was aspirated using a pipette tip to minimise disturbance to the target cell pellet. GM was added to both control and HLA-C-specific antibody-treated target B cells and control and CD16-specific antibody-treated NK cells to reach a concentration of $5.0x10^5$ cells/mL and $2.5x10^6$ cells/mL, respectively. 100µL of target cells ($5.0x10^4$ cells) and effector cells ($2.5x10^5$ cells) were mixed according to experimental condition. 0.1µg/mL of diluted rituximab was also added to each well. The assay was incubated overnight (16-18 hours) at 37°C in 5% CO_2 and analysed by flow cytometry the following day using the method is described in section 2.8.4.5.

2.9. Detection of HLA-specific memory B cells

2.9.1. Single HLA antigen luminex beads

Approximately $4.0x10^6$ freshly isolated PBMCs from healthy donors were divided into two tubes. One tube containing $2.0x10^6$ PBMCs were treated with 20µL of autologous serum for 15 minutes at room temperature. 2mL of PBS was added and the tubes were centrifuged at 1,500rpm for 5 minutes. The supernatant was discarded and the PBMCs were stained with 5µL of CD19-PE antibody at 4°C for 30 minutes.

2mL of PBS was added and the tubes were centrifuged at 1,500rpm for 5 minutes. The supernatant was discarded and the CD19-labelled PBMCs were further divided into eight tubes - 0µL (control), 1µL, 2µL and 3µL, with and without autologous serum treatment, to test the optimal luminex microbead volume to use in this immunoassay. The single HLA Class I antigen coated microbeads (LIFECODES, Immucor, U.S.A.) were briefly vortexed and co-incubated with CD19-labelled PBMCs in the dark at room temperature for 30 minutes. The tubes were gently mixed at regular intervals and later washed with PBS by centrifugation at 1,500rpm for 5 minutes. The supernatant was discarded, and the cell-bead pellet was suspended in 200µL of PBS. 2µL of PI was added to each tube prior to sample acquisition on the Gallios™ flow cytometer.

Following optimisation, HLA-specific B cells reacting to luminex microbeads were identified in patient PBMCs in the absence of autologous serum treatment and by using 1µL of microbeads for analysis. Cell surface staining was performed with 5µL of IgM-FITC, IgD-FITC, CD19-PE, CD14-ECD, CD27-APC/Cy7 and IgA-VioBlue antibodies according to the method described in section 2.7.2.

Samples were suspended in 0.5mL of PBS and 2µL of PI was added prior to sample acquisition on the BD FACSAria™ Fusion. SAB-bound $CD19^+$ $CD27^+$ memory B cells were identified and sorted at the single cell level in a flat bottom 96 well microtiter plate containing a layer of CD40-L expressing feeder cell line and medium conditioned with IL-2 and IL-21.

2.9.2. HLA Class I tetramers

HLA Class I-specific tetramers (Moss research group, University of Birmingham, U.K.) used in this study were obtained from the National Institutes of Health (NIH) Tetramer Core Facility, Emory University, U.S.A. The CMV peptides were purchased from Alta Bioscience, U.K. The tetramers were conjugated to APC and are listed in Table 2.14.

Previously frozen patient PBMCs were thawed at room temperature. Approximately $1x10^6$ PBMCs were suspended in PBS and 1µL of APC-conjugated tetramer was added. The tubes were incubated at 37°C for 30 minutes, followed by a wash step by adding 2mL of PBS and centrifuging at 1,500rpm for 5 minutes. This wash step was repeated. The PBMCs were incubated with 5µL of the antibody panel described in Table 2.15 and incubated at 4°C for 30 minutes. The method for cell surface staining of PBMCs were followed as described in section 2.7.2. Samples were suspended in 0.5mL of PBS and 2µL of PI was added prior to sample acquisition on the BD FACSAria™ Fusion. $Tetramer^+$ $CD19^+$ $CD27^+$ memory B cells were identified and sorted at the single cell level in a 96 well plate containing a layer of CD40-L expressing feeder cell line and medium conditioned with IL-2 and IL-21.

Table 2.14. | HLA Class I-specific tetramers used for cell surface staining

HLA Class I Restriction	Epitope Sequence	Abbreviation	Fluorophore	CMV protein (gene)	Amino acid location	Concentration (mg/ml)
A*01:01	VTEHDTLLY	VTE	APC	pp50 (UL44)	245-253	1.5
A*03:01	IMREFNSYK	IMR	APC	gB (UL55)	683-691	1.5
B*07:02	TPRVTGGGAM	TPR	APC	pp65 (UL183)	417-426	1.5
B*08:01	ELRRKMMYM	ELR	APC	IE-1 (UL123)	199-207	1.5
B*35:01	FPTKDVAL	FPT	APC	pp65 (UL183)	188-195	1.5

Table 2.15. | Antibody panel for cell surface staining to identify IgG+ memory B cells

Channel	Antibody	Clone	Fluorophore	Manufacturer	Catalogue No.
FL1	IgD	IA6-2	FITC	Biolegend	348206
FL1	IgM	MHM-88	FITC	Biolegend	314506
FL2	CD19	HIB19	PE	Biolegend	302208
FL3	CD14	RM052	ECD	Beckman Coulter	IM2707U
FL5	CD38	HB-7	APC	Biolegend	356608
FL8	CD27	O323	APC/Cy7	Biolegend	302816
FL9	IgA	IS11-8E10	VioBlue	Miltenyi Biotec	130-113-479

2.9.3. Culture of single memory B cells

To culture memory B cells, the method described by Huang and colleagues (2013) was used in this study. The day before FACS of antigen-specific B cells, L cells were removed from culture and suspended in DMEM-GM for irradiation with a dose of 10kGγ. Following irradiation, a cell count was performed, and L cells were suspended at $2.0x10^5$ cells/mL in DMEM-GM. Approximately, $2.0x10^4$ cells (100µL) were added to each well of a flat bottom 96 well microtiter plate and incubated for 18-20 hours at 37°C in 5% CO_2. Sterile dH_2O was added to the outer wells of the plate to prevent evaporation of medium from the inner wells.

The next day, prior to FACS, the media from the wells were removed and 50µL of PBS was added to gently wash the wells. The PBS and remaining media were aspirated and 200µL of B cell culture medium was added. HLA-specific B cells using either SABs (sec 2.9.1) or HLA-specific tetramers (section 2.9.2), were selected and single antigen-specific B cells were directly sorted into individual wells using FACS. The plates were incubated at 37°C in 5% CO_2 up to 12 days.

2.9.4. EBV transformation of B cells

The method to immortalise B cells using Epstein-Barr virus (EBV) described in this section has been reported by Traggiai and colleagues (2004). A modified version of this method optimised for 384 well plates and performed at the Institute of Research in Biomedicine (IRB), Bellinzona, Switzerland during a collaboration. This experiment was also later repeated at the University of Birmingham, U.K.

2.9.4.1. Generation of PHA blasts

Previously frozen PBMCs from healthy donors were thawed at room temperature. PBMCs were washed in GM by centrifugation at 1,500rpm for 5 minutes and the supernatant was discarded. PBMCs were suspended in 2mL of GM and transferred to a 24 well plate for overnight incubation at 37°C in 5% CO_2.

The rested PBMCs were suspended at a concentration of $2.5x10^6$ cells per mL in GM and approximately $5.0x10^5$ PBMCs were seeded in a final volume of 200µL per well in flat bottom 96 well microtiter plates. The PBMCs were stimulated with 2% Phytohaemagglutinin (PHA) (1µg/mL) and 500 IU IL-2, followed by incubation at 37°C in

5% CO_2. IL-2 was supplemented every 2-3 days for two weeks of culture. PHA blast cultures were expanded and passaged as necessary.

2.9.4.2. Patient serum staining of PHA blasts

At IRB, PHA blasts from healthy donors and Expi293 (Thermo Fisher Scientific, U.S.A.) cells were incubated with either patient or control (positive and negative) sera to determine HLA-specific antibody reactivity to the alloreactive T cell blasts. Control sera used in this assay are described in section 2.6.1.

PHA blasts and Expi293 cells were counted and mixed at a ratio of 4:1. For example, $16.0x10^4$ cells were used per test sample, which comprised $128.0x10^3$ PHA blasts and $32.0x10^3$ Expi293 cells. Patient and control sera were tested at varying three-fold dilutions (1:2, 1:6, 1:18, 1:54, 1:162, 1:486, 1:1,458 and 0).

To 40µL of mixed PHA blasts and Expi293 cells in in U-bottom 96 well microtiter plates, 40µL of serum was added and incubated at 4°C for 30 minutes. 200µL of MACS was added to each well and the plate was centrifuged at 1,000rpm x g for 4 minutes. The supernatant was discarded, and the wash step was repeated two more times. 50µL of diluted (1:400) Alexa-Fluor647 goat anti-human IgG secondary antibody (Jackson ImmunoResearch Laboratories, Inc, U.S.A.) was added to all test wells and incubated at 4°C for 15 minutes. The wells were washed two times and the cells were suspended in 65µL of MACS for sample acquisition on the BD FACS Canto flow cytometer.

2.9.4.3. B cell immortalisation by EBV

Isolated PBMCs from renal transplant patients were stained with CD19-PE/Cy7 (BD Biosciences, U.S.A.) and anti-human IgG-Alexa-Fluor647 at 1:20 and 1:400 final dilutions, respectively, using the method described in section 2.7.2. Feeder cells i.e. allogeneic PBMCs from a healthy donor were irradiated with a dose of 45Gγ. IgG^+ $CD19^+$ lymphocytes were identified and isolated using FACS into a 5mL falcon tube containing 1mL of GM. Depending on the number of sorted cells, IgG^+ $CD19^+$ B cells were manually seeded at a density of 1.5 or 3 cells per well in 384 well plates, containing 50µL GM supplemented with 2.5µg/mL CpG 2006 in the presence of 30% EBV (supernatant of B95-8 cell line) and 15,000 irradiated feeder cells. The 384 well plates were incubated at 37°C in 5% CO_2 for two weeks.

At UoB, this experiment was set up using the IRB method described above, with a few exceptions - negatively isolated (IgM^- IgD^- IgA^-) IgG^+ $CD19^+$ $CD27^+$ memory B cells were sorted using FACS from freshly isolated PBMCs. Memory B cells were manually seeded at a density of 4 cells per well.

2.9.4.4. Screening pooled supernatants

To screen for HLA-specific antibodies against PHA blasts, culture supernatants were pooled from multiple 384 well plates. At IRB, using the JANUS® liquid handling automated workstation (Perkin Elmer, U.S.A.), 5µL of supernatant from a set number of individual wells were combined. For example, 5µL of supernatant from well A1 in plates 1-7 were pooled in a 384 well plate to provide 35µL of supernatant cocktail for screening.

PHA blasts from multiple healthy donors and parental K562 cells were mixed at an equal ratio. A total of $8.0x10^4$ cells (15µL) were added to each well containing pooled supernatant in a 384 well plate. The addition of cell suspension to 35µL of supernatant resulted in a 1:10 dilution for each supernatant comprising the pool. The plate was incubated at 4°C for 30 minutes. No cell wash was performed and 15µL of anti-human IgG-Alexa-Fluor647 secondary antibody was added to each well using MicroFlo Select automated dispenser (Bio Tek, U.S.A.) to achieve the recommended 1:2,000 dilution. The plate was incubated at 4°C for 15 minutes. Following incubation with the secondary antibody, approximately 6µL of samples were acquired directly from the 384 well plate using BD FACS Canto flow cytometer. The data was analysed using FlowJo™ (Tree Star, Inc., U.S.A.) analysis software.

During the repeat experiment at UoB, however, 50µL of manually pooled supernatant was screened against pooled PHA blasts and CFSE-labelled K562 cells. The staining process and sample acquisition were carried out in U-bottom 96 well microtiter plates. Flow cytometry analyses were performed on the CytoFLEX (Beckman Coulter, U.S.A.) and data were analysed using FlowJo™ v10.6.2.

2.9.4.5. Screening unpooled supernatants

After identifying prime pooled supernatant candidates that react to PHA blasts, individual supernatants from wells comprising the pool were tested. K562 cells were CFSE-labelled (section 2.8.2.3) and mixed with one donor PHA blasts at an equal ratio. 20µL of PHA blasts from one healthy donor and CFSE-labelled K562 cells (total number $16.0x10^4$) were added to U-bottom 96 well microtiter plates containing 10µL of supernatant from individual culture wells. This results in a 1:3 final dilution, which provides a more concentrated testing condition for HLA-specific antibodies compared to pooled supernatants. The plate was

incubated at 4°C for 30 minutes and washed three times (section 2.9.4.2). To the cell pellet, 50µL of 1:400 diluted anti-human IgG-Alexa-Fluor647 secondary antibody was added. The plate was incubated at 4°C for 15 minutes and washed two times. The cells were suspended in 120µL of MACS and analysed using BD FACS Canto flow cytometer.

The same procedure was followed during the UoB repeat experiment with the exception of using mixed donor PHA blasts instead of individual donor PHA blasts for screening due to low cell number available for the assay.

2.10. Generation of monoclonal antibodies from single B cells

To generate monoclonal antibodies from single B cells, the protocols and primer sequences used in this study were adapted from methods outlined by Tiller et al., (2008) and Smith et al., (2009).

2.10.1. Isolation of plasmablasts

Freshly isolated PBMCs from whole blood collected 7 days after transplant nephrectomy were stained with the antibody panel described in Table 2.16. Using the method outlined in section 2.7.2, the antibody-secreting cells (ASCs) were selected on the basis of high $CD19^+$ $CD27^+$ $CD38^+$ expression and were directly single cell sorted into PCR plates loaded with RNAse-inhibiting catch buffer. One row per plate did not contain any sorted cells and was used as a negative control. The plates were immediately covered in microseal foil centrifuged at 2,000rpm for 2 minutes and stored at -80°C.

Table 2.16. | Antibody panel for cell surface staining to identify ASCs

Channel	Antibody	Clone	Fluorophore	Manufacturer	Catalogue No.
FL2	CD19	HIB19	PE	Biolegend	302208
FL3	CD14	RM052	ECD	Beckman Coulter	IM2707U
FL3	CD56	HCD56	PE-Dazzle 594	Biolegend	318348
FL5	CD38	HB-7	APC	Biolegend	356608
FL8	CD27	O323	APC/Cy7	Biolegend	302816

2.10.2. Amplification of immunoglobulin genes

2.10.2.1. One step RT-PCR

To amplify the immunoglobulin (Ig) genes from a single cell, one step reverse-transcriptase polymerase chain reaction (RT-PCR) was performed to allow both reverse transcription and PCR amplification of Ig genes to take place in one step. Single ASC containing PCR plates were thawed at room temperature and centrifuged briefly at 400 x g for 1 minute. The microseal was removed carefully and 15µL of one step master mix (Table 2.17) was added to each well. 1µL of cDNA generated from healthy donor B cells was added to 15µL of master mix and used a positive control. The wells were sealed with 12-strip dome caps (Bio-Rad). The plate was loaded into the Labnet MultiGene™ Optimax thermal cycler and RT-PCR was performed using the program described in Table 2.18. Primer sequences (Alta Bioscience, U.K.) used in this initial RT-PCR step that cover as many heavy and light chain variable regions as possible are listed in Table 2.19.

Table 2.17. | Preparation of master mix for OneStep RT-PCR

Master mix component	Volume/reaction (µl)
Forward primer mix (10µM)	1
Reverse primer mix (10µM)	1
dNTP mix (10mM)	1
OneStep RT-PCR Buffer (5x)	5
RNase-free water	6.5
OneStep RT-PCR Enzyme Mix	0.5

Table 2.18. | OneStep RT-PCR conditions

Stage	Time	Temperature (°C)	Number of cycles
Reverse Transcription	30 mins	50	1
Initial PCR activation step	15 mins	95	1
Denaturation	30 secs	94	50
Annealing	30 secs	58	
Extension	1 min	72	
Final extension	10 mins	72	1
	∞	4	

Table 2.19. | Ig genes variable region-specific primer sequences for RT-PCR

		Primer Name	Sequence 5' - 3'
HEAVY CHAIN (IgH)	Forward primers	5' L VH1	ACAGGTGCCCACTCCCAGGTGCAG
		5' L VH2	GACCATCCCTTCATCAGATCACC
		5' L VH3	AAGGTGTCCAGTGTGARGTGCAG
		5' L VH4/6	CCCAGATGGGTCCTGTCCCAGGTGCAG
		5' L VH5	CAAGGAGTCTGTTCCGAGGTGCAG
		5' L VH7	GGCAGCAGCAACAGCAGGTGCAGC
	Reverse primer	3' Cγ CH1	GGAAGGTGTGCACGCCGCTGGTC
KAPPA CHAIN (IgK)	Forward primers	5' L VK1/2	ATGAGGSTCCCYGCTCAGCTGCTGG
		5' L VK3	CTCTTCCTCCTGCTACTCTGGCTCCCAG
		5' L VK4	ATTTCTCTGTTGCTCTGGATCTCTG
	Reverse primer	3' CK 543	GTTTCTCGTAGTCTGCTTTGCTCA
LAMBDA CHAIN (Igλ)	Forward primers	5' L Vλ1	GGTCCTGGGCCCAGTCTGTGCTG
		5' L Vλ2	GGTCCTGGGCCCAGTCTGCCCTG
		5' L Vλ3	GCTCTGTGACCTCCTATGAGCTG
		5' L Vλ4/5	GGTCTCTCTCSCAGCYTGTGCTG
		5' L Vλ6	GTTCTTGGGCCAATTTTATGCTG
		5' L Vλ7	GGTCCAATTCYCAGGCTGTGGTG
		5' L Vλ8	GAGTGGATTCTCAGACTGTGGTG
	Reverse primer	3' Cλ	CACCAGTGTGGCCTTGTTGGCTTG

2.10.2.2. Nested PCR

Using the primers listed in Table 2.20, semi-nested PCR (IgK) and nested PCR for cloning (IgH and Igλ) master mixes were prepared Table 2.21. The RT-PCR product was diluted 1:50 using RNase-free water in a 96 well PCR plate (Star Labs). 3µL of the diluted PCR product was used as template and added to each well containing 37µL of semi-nested or nested PCR master mix. Nested PCR for each antibody gene was performed separately i.e. three PCR reactions per well. The plates were loaded into the thermal cycler and run according to the program described in Table 2.22.

Table 2.20. | Primer sequences for semi-nested and nested PCRs

		Primer Name	Sequence 5' - 3'
IgH (Nested PCR)	Forward primers	5' AgeI VH1/5	CTGCAACCGGTGTACATTCCGAGGTGCAGCTGGTGCAG
		5' AgeI VH3	CTGCAACCGGTGTACATTCTGAGGTGCAGCTGGTGGAG
		5' AgeI VH4	CTGCAACCGGTGTACATTCCCAGGTGCAGCTGCAGGAG
		5' AgeI VH3-23	CTGCAACCGGTGTACATTCTGAGGTGCAGCTGTTGGAG
		5' AgeI VH4-34	CTGCAACCGGTGTACATTCCCAGGTGCAGCTACAGCAGTG
		5' AgeI VH 1–18	CTGCAACCGGTGTACATTCCCAGGTTCAGCTGGTGCAG
		5' AgeI VH 1–24	CTGCAACCGGTGTACATTCCCAGGTCCAGCTGGTACAG
		5' AgeI VH 3–9/30/33	CTGCAACCGGTGTACATTCTGAAGTGCAGCTGGTGGAG
		5' AgeI VH 6–1	CTGCAACCGGTGTACATTCCCAGGTACAGCTGCAGCAG
		5′ AgeI VH4–39	CTGCAACCGGTGTACATTCCCAGCTGCAGCTGCAGGAG
		5′ AgeI VH1	CTGCAACCGGTGTACATTCCCAGGTGCAGCTGGTGCAG
		5′ AgeI VH3–33	CTGCAACCGGTGTACATTCTCAGGTGCAGCTGGTGGAG
	Reverse primers	3' SalI JH1/2/4/5	TGCGAAGTCGACGCTGAGGAGACGGTGACCAG
		3' SalI JH3	TGCGAAGTCGACGCTGAAGAGACGGTGACCATTG
		3' SalI JH6	TGCGAAGTCGACGCTGAGGAGACGGTGACCGTG
IgK (Semi-nested PCR)	Forward primers	5' Pan VK	ATGACCCAGWCTCCABYCWCCCTG
	Reverse primer	3' CK 494	GTGCTGTCCTTGCTGTCCTGCTC
Igλ (Nested PCR)	Forward primers	5' AgeI Vλ1	CTGCTACCGGTTCCTGGGCCCAGTCTGTGCTGACKCAG
		5' AgeI Vλ2	CTGCTACCGGTTCCTGGGCCCAGTCTGCCCTGACTCAG
		5' AgeI Vλ3	CTGCTACCGGTTCTGTGACCTCCTATGAGCTGACWCAG
		5' AgeI Vλ4/5	CTGCTACCGGTTCTCTCTCSCAGCYTGTGCTGACTCA
		5' AgeI Vλ6	CTGCTACCGGTTCTTGGGCCAATTTTATGCTGACTCAG
		5' AgeI Vλ7/8	CTGCTACCGGTTCCAATTCYCAGRCTGTGGTGACYCAG
	Reverse primer	3' XhoI Cλ	CTCCTCACTCGAGGGYGGGAACAGAGTG

Table 2.21. | Preparation of master mix for semi-nested and nested PCR

Master mix component	Volume/reaction (µl)
Forward primer mix (10µM)	1
Reverse primer mix (10µM)	1
dNTP mix (25µM)	0.5
HotStarTaq Buffer (10x)	4
RNase-free water	30.25
HotStarTaq DNA Polymerase (1.25U)	0.25
DNA template (RT-PCR product)	3

Table 2.22. | Program conditions for semi-nested and nested PCR

Stage	Time	Temperature (°C)	Number of cycles
Initial PCR activation step	15 mins	95	1
Denaturation	30 secs	94	50
Annealing	30 secs	58	
Extension	55 secs	72	
Final extension	10 mins	72	1
	∞	4	

2.10.2.3. Separation of Ig DNA fragments

To visualise IgH, IgK and Igλ DNA fragments, 10µL of semi-nested (IgK) and nested (IgH and Igλ) PCR products were analysed by gel electrophoresis, which separates DNA by size using an electrical field.

1% w/v agarose gel was prepared by weighing out 1g of agarose (Bioline, U.K.) and mixing with 100mL of 1x Ultrapure™ TBE buffer in an Erlenmeyer flask. The agarose and buffer mix was melted by placing the flask in a microwave until the agarose was

completely dissolved. The agarose was cooled and ethidium bromide (EtBr) was added at a final concentration of 0.5µg/mL, before pouring the molten agarose into the gel tray mould holding an appropriate size comb for sample loading. The agarose was left to set at room temperature, followed by the removal of the gel comb and moulds. The agarose gel was subsequently submerged in 1x TBE buffer in the gel box.

2µL of gel loading dye was mixed with 10µL of PCR product and then pipetted into individual wells in the agarose gel. 5µL of 100bp DNA ladder was also loaded into a well alongside the test samples. The gel was subjected to an electrical voltage at 120V for 45 minutes. Following electrophoresis, the gel was viewed and analysed by exposing to UV light in GeneFlash UV gel documentation system (Syngene, U.K.).

2.10.2.4. Purifying Ig PCR products

To purify the amplified antibody genes, DNA fragments ranging between 380-450bp (IgH), 510-540bp (IgK) and 405-450bp (Igλ) in length were excised from the agarose gel and placed in a labelled 1.5mL microcentrifuge tube. Using the QIAquick gel extraction kit, the Ig PCR products were purified by following the manufacturer's instructions. IgH and Igλ DNA was eluted in a final volume of 45µL buffer EB, while IgK DNA was eluted in 20µL volume in new 1.5mL microcentrifuge tubes. The DNA was collected and later quantified by placing 1.2µL of DNA on the Nanodrop™ UV spectrophotometer (Thermo Fisher Scientific). The samples were stored at -20°C.

2.10.2.5. IgK PCR product sequencing

Following purification of IgK DNA fragments from the agarose gel, the sample concentrations were adjusted to 10ng/µL in RNase-free water. The primer 3' Ck494

concentration was standardised to 3.2pmol/µL. IgK PCR products were sequenced using Source Genomics Sanger Sequencing service (Source BioScience, U.K.). Sequencing results were analysed using the Chromas software (Technelysium, Australia) and IgK sequences were determined using the IMGT/V-QUEST online tool.

2.10.2.6. IgK nested PCR for cloning

IgK forward and reverse primers required for nested PCR were determined from the sequence analyses. Using the nested PCR master mix (Table 2.23), including individual or a mix of forward and reverse primers, 3µL of diluted RT-PCR product was added as DNA template to amplify IgK gene and incorporate restriction sites for cloning. Following gel electrophoresis, the PCR products were visualised using UV light and fragments 510-540bp in length were excised for purification. The DNA was eluted in a final volume of 45µL.

Table 2.23. | Primer sequences for IgK nested PCR for cloning

	Primer Name	Sequence 5' - 3'
Forward primers	5'AgeIVk1	CTGCAACCGGTGTACATTCTGACATCCAGATGACCCAGTC
	5'AgeIVk1_9_1–13	TTGTGCTGCAACCGGTGTACATTCAGACATCCAGTTGACCCAGTCT
	5'AgeIVk1D_43_1_8	CTGCAACCGGTGTACATTGTGCCATCCGGATGACCCAGTC
	5'AgeIVk2	CTGCAACCGGTGTACATGGGGATATTGTGATGACCCAGAC
	5'AgeIVk2_28_2_30	CTGCAACCGGTGTACATGGGGATATTGTGATGACTCAGTC
	5'AgeVk3_11_3D_11	TTGTGCTGCAACCGGTGTACATTCAGAAATTGTGTTGACACAGTC
	5'AgeVk3_15_3D_15	CTGCAACCGGTGTACATTCAGAAATAGTGATGACGCAGTC
	5'AgeVk3_20_3D_20	TTGTGCTGCAACCGGTGTACATTCAGAAATTGTGTTGACGCAGTCT
	5'AgeVk4_1	CTGCAACCGGTGTACATTCGGACATCGTGATGACCCAGTC
Reverse primers	3'BsiWIJk1_2_4	GCCACCGTACGTTTGATYTCCACCTTGGTC
	3'BsiWIJk3	GCCACCGTACGTTTGATATCCACTTTGGTC
	3'BsiWIJk5	GCCACCGTACGTTTAATCTCCAGTCGTGTC

2.10.3. Expression vector cloning

2.10.3.1. Ig PCR product digestion

Purified IgH, IgK and Igλ PCR products were digested for expression vector cloning using relevant restriction enzymes (Table 2.24). 5µL of master mix prepared to each heavy and light chain product digestion was added to 45µL of purified PCR product in 0.2mL domed PCR tubes. The tubes were placed in a thermal cycler at 37°C for 60 minutes, followed by heat inactivation at 65°C for 20 minutes, and then replaced on ice for 5 minutes.

Following restriction enzyme digestion, the PCR products were purified using the QIAquick PCR purification kit (Qiagen, Germany) and by following the manufacturer's protocol. The resulting purified PCR products were eluted in a final volume of 25µL and the concentration was quantified using the Nanodrop™. The concentration of digested heavy and light chain inserts was adjusted to 27ng/µL with RNase-free water.

2.10.3.2. Vector digestion

Human $Igγ_1$ (heavy chain), IgK (kappa chain) and Igλ (lambda chain) expression vectors used in this study were a kind gift from Professor H. Wardemann at the Max Planck Institute for Infection Biology, Berlin, Germany. To prepare the vectors for cloning, restriction digestions were set up (Table 2.25). Approximately 1µg of vector DNA was added to master mix containing 5' enzyme 1 AgeI-HF in 0.2mL domed PCR tubes and incubated overnight at 37°C. Vector linearisation was checked the following day by loading 1µL of the digested sample onto 1% w/v EtBr agarose gel and performing gel electrophoresis. The DNA fragments were visualised using UV light.

The linearised vectors were digested with relevant 3' enzyme 2 (NEB) overnight at 37°C, followed by heat inactivation at 65°C for 20 minutes. 2µL of alkaline phosphatase, calf intestinal (CIP) was added to each digested vector and the tubes were incubated at 37°C for 60 minutes. Vector DNA was isolated by loading the digestion reaction mixes onto 1.5% w/v EtBr agarose gel and performing electrophoresis at 100V for 60 minutes. The digested DNA fragments were purified using the QIAquick gel extraction kit and following manufacturer's instructions. The concentration of the purified vector DNA was quantified using the Nanodrop and standardised to 100ng/µL with RNase-free water.

Table 2.24. | Preparation of reaction mixes for Ig PCR product restriction digestion

	IgH	IgK	Igλ
PCR product	45µl	45µl	45µl
5' enzyme 1 AgeI-HF	0.125µl	0.125µl	0.125µl
3' enzyme 2 SalI-HF	0.125µl		
3' enzyme 2 BsiWI-HF		0.5µl	
3' enzyme 2 XhoI			0.5µl
Cutsmart buffer (10x)	5µl	5µl	5µl
BSA			0.5µl
Final volume	~50µl	~50µl	~50µl

Table 2.25. | Preparation of reaction mixes for Ig expression vector restriction digestion

	IgH	IgK	Igλ
Vector DNA	1µg	1µg	1µg
Cutsmart buffer (10x)	10µl	10µl	10µl
5' enzyme 1 AgeI-HF	1µl	1µl	1µl
Rnase-free water	up to 100µl	up to 100µl	up to 100µl
Incubate at 37°C overnight			
3' enzyme 2 SalI-HF	1µl		
3' enzyme 2 BsiWI-HF		1µl	
3' enzyme 2 XhoI			1µl
Incubate at 37°C overnight			
CIP	2µl	2µl	2µl
Incubate at 37°C for 60 mins; heat inactivation at 65°C for 20 mins			

2.10.3.3. Vector and insert ligation

The length of expression vectors was approximately 5,500bps and the insert was typically between 350-510bp due to the differences in the CDR3 region. Therefore, a 3:1 vector-to-insert molar ratio was used for ligation. In 0.2mL domed PCR tubes, 100ng of heavy and light chain vector and 27ng of corresponding Ig insert were mixed with 2µL of T4 DNA ligase buffer, 1µL of T4 DNA ligase and nuclease-free water in a final volume of 20µL. The ligation reactions were incubated at 16°C in a thermal cycler overnight.

2.10.3.4. Transformation of DH5α cells

A vial of DH5α competent *E. coli* cells were thawed on ice. 10µL of ligation reaction was added to 100µL of competent cells in a fresh 1.5mL microcentrifuge tube. The tubes were placed on ice for 30 minutes, followed by heat shock in a 42°C water bath for 45 seconds, and again placed on ice for 5 minutes. 900µL of SOC medium (NEB, U.S.A.) was added to each tube and incubated at 37°C in an orbital shaker for 45 minutes at 160rpm. The tubes were centrifuged at 13,000rpm for 1 minutes and the supernatant was discarded. The cell pellet was suspended in 100µL of SOC medium and plated onto 10cm^2 LB agar plate containing 100µg/mL ampicillin. The plates were incubated overnight at 37°C. The following day, universal tubes containing 5mL of TB, supplemented with100µg/mL ampicillin were inoculated with one bacterial colony and incubated at 37°C in an orbital shaker overnight at 160rpm. A total of three colonies per plate were selected to prepare overnight cultures.

2.10.3.5. Plasmid DNA purification

Using the QIAprep Spin miniprep kit, plasmid DNA from overnight bacterial cultures were isolated. Approximately 4mL of the overnight cultures were centrifuged at 3,000rpm for 5 minutes. Glycerol stock of each culture were prepared by mixing 700µL of the confluent culture and 300µL of glycerol and freezing at -80°C for further work. The supernatant of the centrifuged bacterial cultures was discarded and following the manufacturer's protocol, plasmid DNA was purified from the cell pellets. DNA was eluted in a final volume of 25µL. The concentration was quantified using the Nanodrop™ and adjusted to 300ng/µL with nuclease-free water.

2.10.3.6. Testing for insert-positive bacterial clones

Approximately 300ng of purified plasmid DNA was digested with restriction enzymes to confirm the presence of heavy and light chain insert. 1µL of plasmid DNA was added to the master mix (Table 2.26) in 0.2mL domed PCR tubes and incubated at 37°C for 60 minutes. The reaction mixes containing gel loading dye were transferred to 1% w/v EtBr agarose gel for electrophoresis at 120V for 45 minutes. The DNA fragments were visualised under UV light.

2.10.3.7. Plasmid DNA sequencing

Purified plasmid DNA concentration was adjusted to 100ng/µL in RNase-free water. Using Source Genomics Sanger Sequencing service (Source BioScience, U.K.), plasmid DNA was sequenced with 5' Absense forward primer and 3' IgG internal (IgH), 3' Ck494 (IgK) and 3' Cλ (Igλ) (Table 2.27). The primer concentrations were standardised to 3.2pmol/µL. Sequencing results were analysed using the IMGT/V-QUEST online tool.

Table 2.26. | Preparation of reaction mixes for plasmid DNA restriction digestion

	IgH	IgK	Igλ
Plasmid DNA	4µl	4µl	4µl
5' enzyme 1 EcoRI-HF	0.1µl		
3' enzyme 2 SalI-HF	0.1µl		
5' enzyme 1 EcoRI-HF		0.1µl	
3' enzyme 2 HindIII-HF		0.1µl	
5' enzyme 1 AgeI-HF			0.1µl
3' enzyme 2 XhoI			0.1µl
Cutsmart buffer (10x)	2µl	2µl	2µl
Nuclease-free water	13.8µl	13.8µl	13.8µl
Final volume	20µl	20µl	20µl

Table 2.27. | Primer sequences for plasmid DNA sequencing

	Primer Name	Sequence 5' - 3'
Forward	5'Ab sense	GCTTCGTTAGAACGCGGCTAC
Reverse	3' IgG (internal)	GTTCGGGGAAGTAGTCCTTGAC
	3' CK 494	GTGCTGTCCTTGCTGTCCTGCTC
	3' Cλ	CACCAGTGTGGCCTTGTTGGCTTG

2.10.4. Transient mammalian cell line expression

2.10.4.1. Transfection of HEK293T cells: small-scale

In 24 well plates, $2.0x10^5$ HEK293T cells were seeded per well in 0.5mL of transfection medium and incubated overnight at 37°C in 5% CO_2, until the cells were 70-90% confluent. The next day, the transfection medium was decanted from the wells carefully and 0.1mL of DMEM was added to wash the cells. The plate was replaced at 37°C in 5% CO_2, whilst the transfection mixes were prepared.

In a U-bottom 96 well microtiter plate, 100µL of DMEM and an appropriate volume of paired heavy and light chain plasmid DNA (~300ng each) and 3µL of polyethylenimine (PEI) was mixed. The plate was placed on a shaker for 5 minutes and incubated at room temperature for 20 minutes. DMEM medium in the 24 well plate containing HEK293T cells were carefully removed. The heavy and light chain transfection mix were added to each well in a dropwise manner to cover the well surface area and the plate was incubated at 37°C in 5% CO_2 overnight.

The following day, transfection mixes were removed and 0.5mL of protein-free medium was added to each well. The plate was incubated at 37°C in 5% CO_2 and after 5 days, the supernatant was harvested for downstream assays, including IgG quantification (section 2.10.6) and cell line staining (section 2.7.4.2).

2.10.4.2. Transfection of HEK293T cells: large-scale

High concentrations of plasmid DNA were purified from large volume bacterial cultures. An Erlenmeyer flask containing approximately 100mL of TB supplemented with 100µg/mL ampicillin was inoculated with heavy or light chain colony of choice from the frozen glycerol stock and incubated in an orbital shaker overnight at 37°C and 160rpm. Using the EndoFree Plasmid Maxi Kit, plasmid DNA was purified by following the manufacturer's protocol and dissolved in a final volume of 0.5mL of nuclease-free water. The concentration was adjusted to 1µg/µL.

In a 15cm vented cell culture dish, approximately $8.0x10^6$ HEK293T cells were seeded in a volume of 20mL of transfection medium. The culture plates were incubated at 37°C in 5% CO_2. The next day, the medium was carefully removed, and the cells were washed with 5mL DMEM and the plates were replaced at 37°C (5% CO_2). Transfection mixes were prepared in 2mL DMEM containing 15µg heavy chain plasmid DNA, 15µg light chain plasmid DNA and 100µL PEI. The reaction mixes were vortexed and incubated at room temperature for 15 minutes. The DMEM wash medium was removed from the plates and replaced with 20mL of fresh medium. The transfection mixes were added to the plates in a dropwise manner to cover the plate area and incubated overnight at 37°C in 5% CO_2. The following day, the transfection mix medium was removed and replaced with 25mL of protein free-medium. The plates were incubated at 37°C in 5% CO_2 and the supernatant was harvested after five days.

2.10.5. Antibody purification

To purify antibodies from large-scale transfection culture supernatants, protein A agarose beads were firstly prepared. 1.5mL of beads were added to 50mL of PBS in conical tubes and centrifuged for 10 minutes at 4,300rpm at room temperature with no brake. The PBS supernatant was removed with a pipette controller and the beads were washed again. Secondly, the culture supernatants were collected and prepared for antibody purification by removing cell debris via centrifugation at 2,000rpm for 10 minutes. Approximately 50mL of culture supernatant (from two plates) was incubated with 1.5mL of prepared agarose beads overnight at 4°C with slow agitation using a speed angle rocker.

The next day, the tubes were centrifuged, and the media was removed using a pipette controller. 35mL of 1M NaCl was added to each tube and centrifuged. The 1M NaCl was removed and the beads were washed with 35mL of PBS twice. 5mL of IgG elution buffer was added to each tube and incubated on a table-top shaker for 30 minutes. The tubes were centrifuged, and the IgG eluate supernatant was transferred to a new conical tube. The pH of the IgG eluate was adjusted to 7-7.4 with 1M Tris-HCl and the neutralised sample was applied to a prepared Amicon protein concentrator (section 2.6.2.2). the antibody eluate was buffer exchanged with PBS twice and concentrated to a volume between 0.5-1.0mL. The purified antibody eluates were stored at 4°C.

2.10.6. Total IgG quantification

2.10.6.1. IgG ELISA

To quantify the total IgG concentration from small-scale HEK293T transfections, an enzyme-linked immunosorbent assay (ELISA) was performed. This protocol was obtained from Dr W Dejnirattisai and Professor Gavin Screaton at Imperial College London, U.K. Therefore, all reagents and test conditions were previously optimised.

Monoclonal anti-human IgG (γ-chain specific) antibody produced in mouse (Sigma, U.K.) was diluted 1:10,000 in dissolved carbonate buffer solution. 50µL of the diluted coating antibody was added to each well of a Nunc Maxisorp ELISA plate and incubated at 4°C overnight. The following day, the plate was washed twice by adding 200µL of PBS-T to each well. 200µL of blocking buffer was added and the plate was incubated on a plate shaker at room temperature for 60 minutes.

Test and standard curve samples were prepared in PBS. Supernatant test samples were diluted 1:100, while standard curve samples were prepared from 1000ng/mL stock concentration of IgG from human serum (Sigma, U.K.) and performing two-fold dilutions – 125ng/mL, 62.5ng/mL, 31.25ng/mL, 15.6ng/mL, 7.8ng/mL, 3.9ng/mL, 0.98ng/mL and 0ng/mL. Following incubation with blocking buffer, the plate was washed three times with PBS-T and 50µL of the diluted test and standard curve samples were added in duplicate wells, followed by an incubation at 37°C for 60 minutes. The plate was washed three times with PBS-T and 50µL of goat anti-human IgG (Fc) alkaline phosphatase (ALP) conjugate (Sigma, U.K.) prepared at 1:10,000 dilution in blocking buffer was added to each well. To test for light chain specificity, 50µL of goat anti-human IgK chain or Igλ chain antibody

conjugated to ALP (Sigma, U.K.) was added instead. The plate was incubated at 37°C for 60 minutes, followed by four washed with PBS-T.

Using the ALP substrate kit, 100µL of the prepared p-Nitrophenylphosphate (PNPP) solution was added to each well and the plate was incubated at room temperature in the dark until a bright yellow colour of reaction product developed. 100µL of 0.4M NaOH solution was added to stop the reaction and the plate was read at 415nm using the ELISA plate reader.

2.10.6.2. IgG ELISA: data analysis

The average of absorbance values for duplicate wells were calculated (Table 2.28). The average of 0ng/mL (blank) absorbance values was subtracted from the average of standard curve values. Whereas the average of negative control (NC) (culture or protein-free medium) was subtracted from the average of test sample absorbance values (Table 2.28; B). The standard curve values were analysed by performing Log_{10} function and plotting the transformed values against log_{10} IgG standard concentration values (Figure 2.5).

A polynomial trendline with an order of 2 was used to account for any fluctuations in the data and the r^2 value closest to 1 was observed. Using the trendline equation, the log_{10} IgG concentration (ng/mL) for test samples were calculated (Table 2.28; C), which were later converted with antilog function (Table 2.28; D). The values were multiplied by 100 to achieve total IgG concentration (ng/mL). All data were analysed in Microsoft Excel.

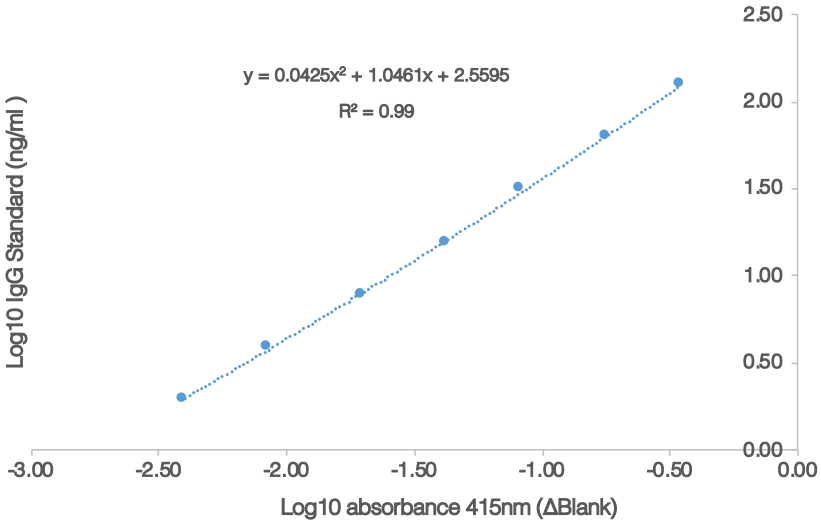

Figure 2.5. | Representative example of a standard curve generated from IgG ELISA.

Log_{10} absorbance values measured at 415nm were plotted for varying concentrations of log_{10} IgG standard (µg/ml). A polynomial trendline with r^2 value of 0.99 was observed. The trendline equation was used to quantify total IgG protein concentration.

Table 2.28. | Representative example of calculating total IgG concentration from ELISA analysis

Test sample	Absorbance at 415nm			Average (ΔNC) = B	Log10 (B) = C	Log10 IgG C (ng/ml) = D	Antilog D (ng/ml) = E	Corrected IgG Conc (µg/ml)
	1	2	Average					
1	0.70	0.72	0.71	0.63	-0.20	2.35	223.08	22.31
2	0.79	0.78	0.79	0.70	-0.15	2.40	250.31	25.03
3	0.09	0.10	0.09	0.01	-2.22	0.45	2.79	0.28
4	0.09	0.09	0.09	0.00	-2.40	0.30	1.97	0.20
NC	0.09	0.09	0.09	0.00	0.00	0.00	0.00	0.00

2.10.6.3. BCA protein assay

Concentrations of IgG produced by large-scale preparations were quantified using the Bicinchoninic acid (BCA) assay. Following the manufacturer's protocol, the bovine serum albumin (BSA) standard curve samples were prepared by two-fold dilutions in a working concentration range of 2,000µg/mL to 25µg/mL. Concentration IgG test samples were diluted in ten-fold dilutions – 1:10, 1:100 and 1:1000. Absorbance values of the duplicate wells were measured at 550nm.

2.10.6.4. BCA protein assay: data analysis

The average of absorbance values was calculated for this assay and the average value of 0µg/mL (blank) was subtracted from the average values of standard and IgG test samples (Table 2.29). The standard curve was generated by plotting the corrected absorbance values (y axis) against the concentrations of the BSA standard (µg/mL) (x axis) (Figure 2.6). A linear trendline was added and an r^2 value of 0.99 was obtained. Using the trendline equation, the corrected protein concentration of the IgG test samples was determined (Table 2.30). The data were analysed in Microsoft Excel.

Table 2.29. | Representative example of calculating BCA assay standard curve values

BSA standard (ng/ml)	Absorbance at 550nm			Average (Δblank) = A
	1	2	Average	
125	0.45	0.43	0.44	0.35
62.5	0.27	0.26	0.26	0.18
31.25	0.17	0.16	0.17	0.08
15.6	0.13	0.12	0.13	0.04
7.8	0.10	0.10	0.10	0.02
3.9	0.09	0.09	0.09	0.01
1.95	0.09	0.09	0.09	0.00
0.98	0.09	0.09	0.09	0.00
0 (blank)	0.08	0.08	0.08	0.00

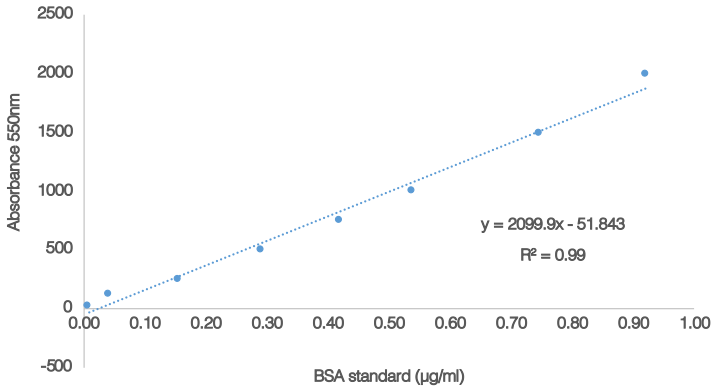

Figure 2.6. | Representative example of a standard curve generated from BCA assay.

Absorbance values measured at 550nm were plotted for varying concentrations of BSA standard (µg/ml). A linear trendline with r^2 value of 0.99 was observed. The trendline equation was used to quantify total IgG protein concentration.

Table 2.30. | Representative example of calculating total IgG concentration from BCA assay

Dilution	Absorbance at 550nm			ΔBlank	µg/ml	Corrected conc (mg/ml)
	1	2	Average			
1:10	0.39	0.38	0.38	0.29	560.68	5.61
1:100	0.13	0.13	0.13	0.04	32.37	0.32
1:1000	0.10	0.10	0.10	0.01	-32.81	-0.33

CHAPTER III

PREPARATION OF ANTIBODIES AGAINST HLA-C TO ENHANCE NK CELL FUNCTION

3.1. Introduction

HLA-specific alloantibodies arise following exposure to allogeneic or 'foreign' tissue in the form of blood transfusion, pregnancy or transplantation. The presence of pre-formed HLA Class I and II-specific alloantibodies are now recognised as a direct cause of allograft rejection (Patel and Terasaki, 1969; Terasaki and Cai, 2008). Therefore, this study aims to repurpose HLA Class I-specific alloantibodies, more specifically HLA-C-specific alloantibodies from renal transplant recipient sera for therapeutic use by boosting anti-tumour NK cell-mediated responses.

It was hypothesised that as HLA-C allotypes are the major ligands for the inhibitory KIRs on NK cells, performing HLA-C blockade using HLA-C-specific alloantibodies would enhance NK cell function and thus mediate tumour cell lysis. This chapter focusses on the multiple approaches undertaken to prepare and purify HLA-C-specific alloantibodies from patient sera for HLA-C:KIR blockade in NK cell functional assays. Firstly, HLA-specific alloantibody reactivity was measured against physiological or native HLA molecules present on allogeneic lymphocytes and single HLA-C allele-transfected cell lines. Secondly, commercially available and well-established antibody clones were used to analyse surface expression of HLA Class I and II, HLA-C and HLA-E molecules on target cell lines. Finally, in preparation for further functional analyses, HLA-C1 and HLA-C2 allotype-specific alloantibodies were adsorbed and enriched from patient sera by using immobilised HLA column and single HLA-C allele-transfected cell lines.

3.2. Patient recruitment

Renal transplant patients with detectable levels of HLA-specific antibodies were selected for this study. Following ethics approval, 13 renal transplant patients were recruited between April 2017 and June 2020. The patients at the time of blood donation were receiving dialysis treatment and were enlisted for re-transplantation. During the course of the study, a second blood sample was requested from two patients. One patient initially gave consent for blood sample but refused at the time of donation. Of the 13 patients, two blood samples were obtained from transplant nephrectomised patients, seven days post-allograft removal. Additional samples previously collected from patients in a University Hospitals Coventry and Warwickshire (UHCW) study to investigate HLA-specific antibodies (REC 13/WM/090) were also included.

3.3. Screening and identification of HLA antibodies

The study cohort comprised patients with HLA antibody specificities against a range of HLA-A, -B, -C (groups 1 and 2) and Class II alleles. These data were compiled from the routine luminex platform-based HLA microbead analyses used to detect HLA antibody specificities and monitor antibody levels in the Birmingham Histocompatibility and Immunogenetics laboratory. Single HLA Class I and II antigen-coated luminex beads (One Lambda) were used for high-definition-based routine monitoring of HLA-specific antibody levels. HLA Fusion software was used to analyse the results obtained from the high-definition testing of sera to determine HLA antibody specificities detected within the sample (Figure 3.1).

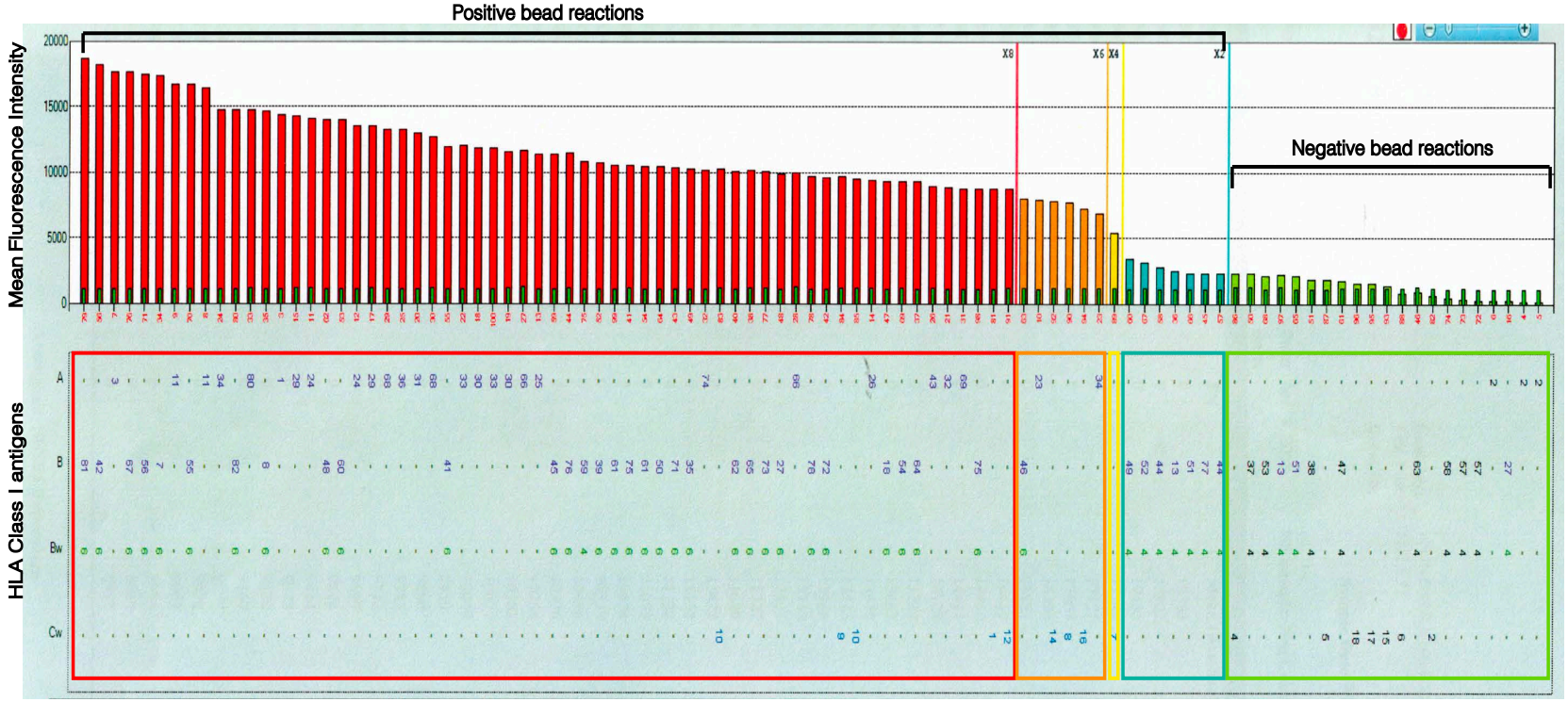

Figure 3.1. | Representative single HLA Class I antigen bead reactivity profile.

LABScreen Class I (One Lambda) single antigen bead (SAB) analysis of patient serum shows reactivity towards a range of HLA-A, -B and -C antigen coated beads. Polystrene SABs embedded with varying ratios of two fluorochromes and coated with single HLA Class I antigens were treated with patient serum, followed by labelling of HLA antibody-bound beads with anti-IgG secondary antibody.. The varying colours represent the MFIs measured based on the strength of bead reactions.

The strength of the HLA antigen-specific bead reaction is demonstrated via mean fluorescence intensity (MFI) values as a qualitative output which are normalised against negative control serum bead reactivity run in the same assay. The single antigen bead (SAB) assay does not offer a direct quantitative measure of HLA alloantibodies in the test sample. The HLA Fusion software utilises different colours to present a visual easy-to-interpret format of the SAB assay results based on the MFI values measured. At NHSBT, Birmingham, HLA antibody MFI values above 2000 is considered clinically positive. High MFI values i.e. >10,000 (red) are strongly positive bead reactions; <10,000 MFI (orange/yellow) is a moderately positive bead reaction; <5,000 MFI is a weak positive bead reaction and <2,000 MFI (green) is a negative reaction.

Patients were selected and later recruited based on their IgG HLA antibody profiles generated from single antigen bead testing (Figure 3.2). Five out of the thirteen patient sera tested were positive for HLA Class I and II-specific antibodies, whilst three patient sera were negative for HLA-C-specific antibodies. As the aim of the study was to modulate the inhibitory interaction between HLA-C and KIRs on NK cells, it was imperative to recruit patients with alloantibodies against the KIR ligand groups (either 1 or 2) of the HLA-C locus.

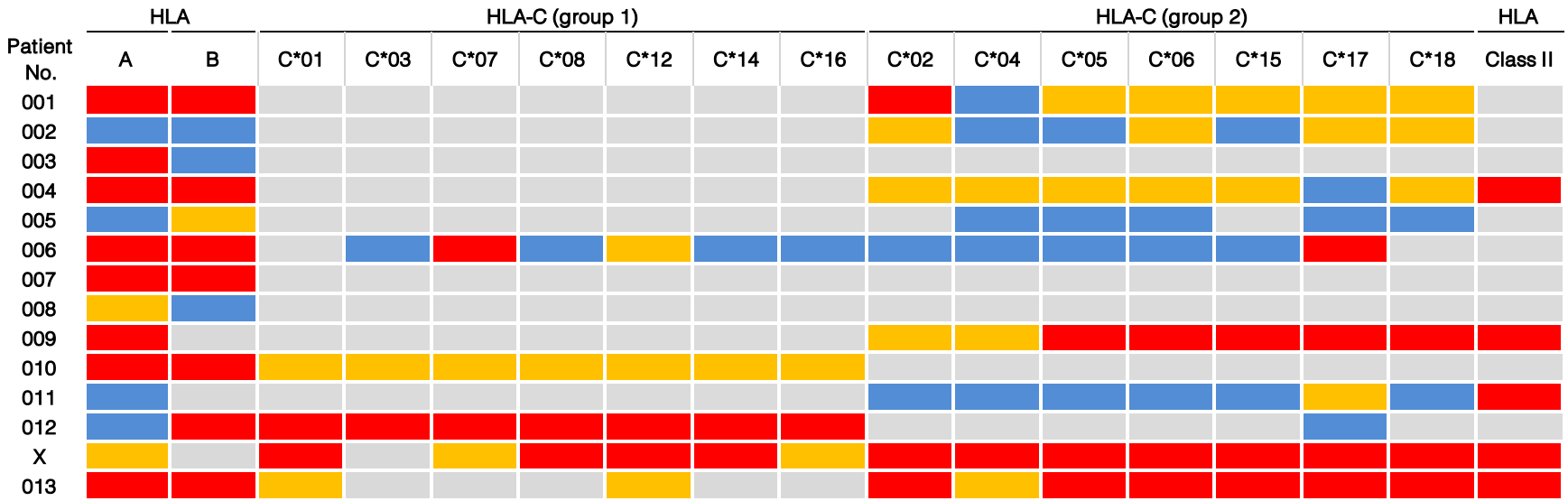

Figure 3.2. | Summary of HLA antibody specificity profiles of renal transplant patient cohort.

HLA antibody specificities were detected using the One Lambda single antigen bead Luminex platform. Polystrene SABs embedded with varying ratios of two fluorochromes and coated with single HLA Class I antigens were treated with patient serum, followed by labelling of HLA antibody-bound beads with anti-IgG secondary antibody. The range of HLA-specific antibody levels measured by median fluorescence intensity are represented by the different colours – MFI >10,000 (red); MFI <10,000 (yellow); MFI >2,000 (blue) and MFI <2,000 (grey). Patients were identified by an assigned number from 001-013. Patient 'X' had been deceased for a number of years prior to this study.

3.4. Cellular reactivity of HLA-specific alloantibodies

3.4.1. HLA-matched PBMCs

Clinically, cross matching is a transplantation-based compatibility test performed between a potential kidney donor PBMCs and recipient serum. This test directly detects antibodies against donor antigens on specific lymphocyte subsets. Using this principle, the reactivity of HLA-specific alloantibodies to target antigens was confirmed by testing patient sera against HLA-matched PBMCs. Fluorescently labelled anti-human IgG antibody was subsequently added to detect any HLA-specific antibody bound PBMCs. Positive or negative cross match was later determined by measuring an increase in median fluorescence intensity (MFI) compared to the control sera.

Lymphocytes isolated from lymph nodes (donor 1), spleen (donor 2) and whole blood (donor 3) from three different individuals were treated with multiple patient sera containing a range of HLA Class I-specific alloantibodies. The antibody specificities were previously determined by the SAB assay. Blood group AB serum was included as a negative control whilst a pan-HLA reactive serum was used as a positive control for this assay. Serological HLA typing data was available only for the HLA-A and -B loci from NHSBT, Birmingham, which was used to identify patient sera expected to react with the donor lymphocytes. Table 3.1 summarises the HLA type of the three sources of lymphocytes and the presence (red) or absence (grey) of HLA-specific alloantibodies specific to the donor HLA antigens, providing an early indication of the expected serum reactivity outcome.

Table 3.1. | HLA matched PBMCs to determine reactivity against patient sera

				Control Sera		Patient Sera			
Source	**Donor**	**HLA**	**Alleles**	**NC**	**PC**	**003**	**007**	**008**	**010**
Lymph Nodes	**1**	A	30, 31						
		B	27, 52						
Spleen	**2**	A	2, 23						
		B	40, 50						
Whole Blood	**3**	A	2, 11						
		B	35, 44						

To determine positive and negative serum reactivity against donor cells via flow cytometry, firstly live $CD14^-$ $CD56^-$ $CD19^-$ single lymphocytes were selected (Figure 3.3A). Serum HLA-specific alloantibody binding to antigens were measured on the $CD3^+$ T cell subset. It was vital to select $CD3^+$ T cells for this analysis as HLA Class I-specific antibodies bind to both $CD3^+$ T cells and $CD19^+$ B cells, while HLA Class II-specific antibodies are known to bind to B cells only (Schinstock et al., 2016). Representative plots show lack of reactivity of negative control serum to $CD3^+$ T cells whereas total $CD3^+$ T cell population was also anti-IgG^+ with positive control serum. Patient serum shows partial reactivity to $CD3^+$ T cells, most likely due to low HLA antigen expression on donor T cells or low antibody levels present in the serum (Figure 3.3B). Compared to control sera, the magnitude in the shifts of MFI following patient serum treatment determine positive or negative cross match results (Figure 3.3C).

For example, co-incubation of lymphocytes from donor 1 with patient 003 serum presented a positive reading by demonstrating strong reactivity with HLA-A and HLA-B-specific antibodies in the serum. Comparatively, either weak or no binding was observed following co-incubation with sera from patients 007, 008 and 010. In contrast, lymphocytes from donor 2 demonstrated weak to strong reactivity to all patient sera compared to negative control serum. Lymphocytes from donor 3 also presented a similar serum antibody

reactivity profile as donor 2. However, due to the lack of HLA-specific antibodies in patient 008 serum corresponding to the HLA Class I genotype of donor 3, anti-IgG reactivity of patient 008 serum was similar to the reactivity observed with negative control serum. This flow cytometry-based detection of HLA-specific alloantibody reactivity to HLA matched lymphocytes confirm the reactivity of antibodies to physiological HLA molecules.

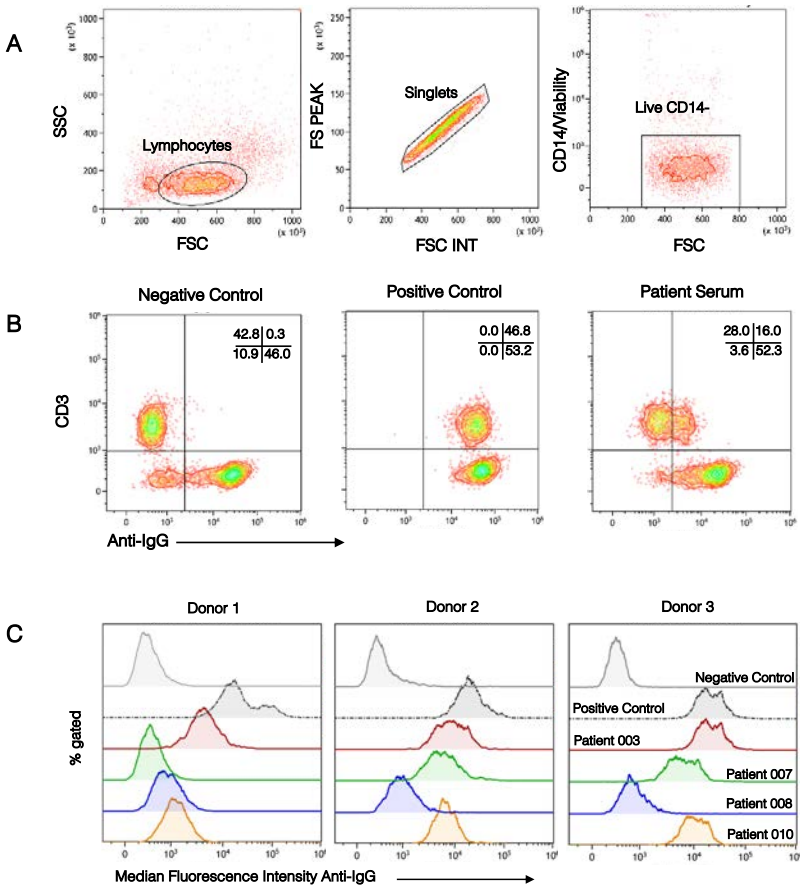

Figure 3.3. | Flow cytometry-based HLA-specific alloantibody reactivity to PBMCs.

A | Sequential gating strategy used to determine positive and negative cross matches. Following the selection of $CD14^-$ live lymphocytes, HLA Class I-specific alloantibody reactivity to donor HLA antigens was detected on $CD3^+$ T cells.

B | Representative plots of control sera (negative and positive) and patient serum reactivity to donor $CD3^+$ T cells detected with anti-human IgG secondary antibody.

C | Overlayed histograms showing serum HLA Class I-specific antibody binding by a measurable increase in anti-IgG-FITC median fluorescence intensity of $CD3^+$ T cells. Sera samples tested include negative control (light grey), positive control (dark grey), patient 003 (red), patient 007 (green), patient 008 (blue) and patient 010 (orange).

3.4.2. HLA-C allele-transfected cell lines

Patient serum reactivity to donor lymphocytes matched to the HLA-specific antibody profile demonstrated antibody binding to multiple target antigens on $CD3^+$ T lymphocyte population. To determine HLA-specific antibody reactivity to a single target antigen, surface expression of HLA Class I-deficient cell lines – 721.221 and K562 and their single HLA-C allele transfected counterparts were analysed and later tested with a range of patient sera. Amino acid sequence alignments of the HLA-C allotypes reveal dimorphisms at positions 77 and 80 defined by serine and asparagine for HLA-C1 alleles and asparagine and lysine for HLA-C2 allotypes, respectively (Colonna et al., 1993b) (Figure 3.4A). HLA-C group 1 comprises HLA-Cw1, Cw3, Cw7, Cw8, Cw12, Cw14 and Cw16 and HLA-C group 2 comprises HLA-Cw2, Cw4, Cw5, Cw6, Cw15, Cw17 and Cw18.

Firstly, HLA expression including HLA Class I (W6/32 clone), HLA-C (DT-9 clone), HLA-E and HLA Class II was analysed on target cell lines (Figures 3.4B and 3.4C). Lack of increase in MFI values confirmed the absence of HLA Class I expression on parental cell lines. Single HLA-C allele expression on transfected cell lines was detected by both W6/32 and DT-9 antibody clones. MFI values deriving from W6/32 binding to K562-HLA-C transfected cell lines were greater than MFIs from DT-9 antibody binding, suggesting W6/32 antibody as a higher affinity antibody clone compared to DT-9. Conversely, DT-9 antibody reactivity was greater on 721.221-HLA-C transfectants in comparison to W6/32. This is most likely due to the presence of HLA-E on 721.221 cell surface, which is also detected by the DT-9 antibody clone. Moreover, as 721.221 cell line originates from B cells, high HLA Class II expression was measured on the parental cells and HLA-C allelic transfectants compared to K562 and HLA-C transfectants.

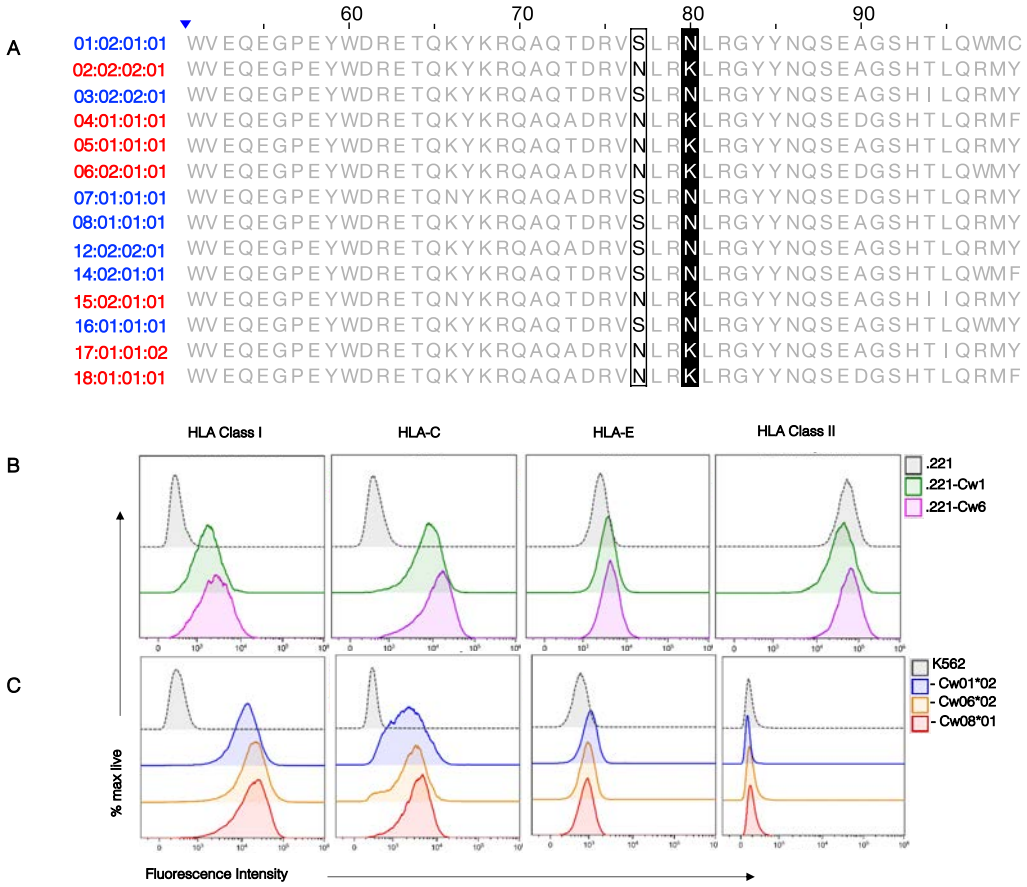

Figure 3.4. | HLA-C allotypes and surface expression on parental and HLA-C-transfected cell lines.

A | Sequence alignment of amino acids between HLA-C allotypes. The sequences shown span from positions 50-100 and are highly conserved. Differences in HLA-C1 (blue) and HLA-C2 (red) allotypes are defined by the amino acid residues at positions 77 and 80 in the α1 helix of the HLA-C molecule. HLA-C1 allotypes share Serine^{77} (S) and Asparagine^{80} (N) whilst HLA-C2 allotypes share Asparagine^{77} (N) and Lysine^{80} (K).

B | Expression of HLA loci including HLA Class I, HLA-C, HLA-E and HLA Class II detected using flow cytometry on 721.221 (grey), 721.221-Cw1 (green) and 721.221-Cw6 (pink) cell lines.

C | Expression of HLA loci including HLA Class I, HLA-C, HLA-E and HLA Class II detected on K562 (grey), K562-Cw01*02 (blue), K562-Cw06*02 (orange) and K562-Cw08*01 (red) cell lines.

Secondly, patient sera containing antibodies against a range of HLA-C antigens were tested against HLA-C1 and -C2-transfected K562 and 721.221 cell lines (Figure 3.5). Using flow cytometry, an increase in anti-IgG MFI was measured as a result of HLA-specific antibody binding. Differential staining patterns were observed against 721.221 and K562 parental cell lines when treated with serum containing HLA Class II-specific antibodies. There was a notable difference in the magnitude of anti-IgG detection towards HLA Class II-expressing 721.221 cell lines compared to HLA Class II-deficient K562 cell lines. For example, the degree of patient 004 serum reactivity to 721.221 target cells, which showed strong reactivity to HLA Class II antigen-coated beads in luminex assay, was drastically increased by two log fold. Similar reactivity patterns were observed with sera from patients 011 and X. In contrast, patient 012 serum reactivity observed against 721.221-Cw1 cells was a result of only HLA-C1-specific alloantibodies present in the serum. The absence of HLA Class II expression on K562 cell surface removed the possibility of confounding effects arising from Class II-specific antibody binding to target cell surface.

The presence of HLA-C2-specific alloantibodies detected using single antigen luminex beads in patient sera (004, 011 and X), was validated by their reactivity to HLA-C2 allele-transfected K562-Cw06*02 cell line only. Conversely, the reactivity of patient 012 serum positive for HLA-C1-specific alloantibodies was detected against HLA-C1-transfected K562-Cw01*02 and K562-Cw08*01 cell lines. No reactivity to the negative control cell line, K562 was observed compared to the HLA-C allele-transfected counterparts. These data demonstrate that HLA-C-specificities, initially detected by using single HLA antigen coated beads, also react to physiological HLA on lymphocytes (Figures 3.4) and cell lines (Figure 3.5) in a similar manner. Testing serum containing HLA-C-specific alloantibodies against HLA-C allelic transfectants not only confirmed the selective reactivity of the antibodies to the two KIR ligand groups, but also confirmed the surface expression of the

cell lines. This further validates the use of K562-HLA-C allele-transfected cell lines for subsequent functional assays (Chapter IV).

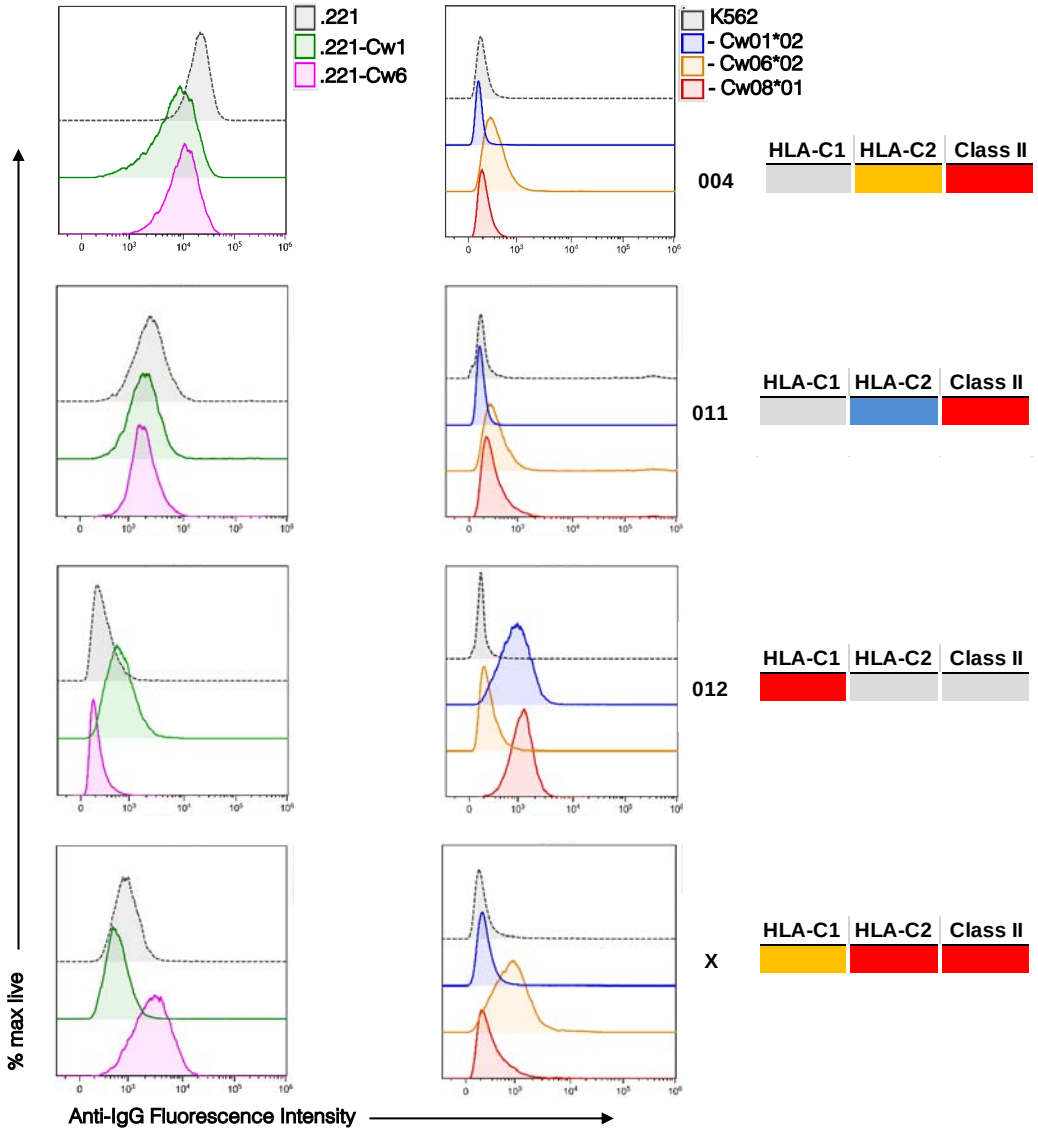

Figure 3.5. | HLA-specific alloantibodies selectively bind to HLA-C alleles.

Renal transplant sera with HLA-C group 1 and 2-specific alloantibodies were co-incubated with target cell lines at 1:2 final dilution, followed by anti-human IgG-FITC secondary antibody.. Alloantibody binding to target antigen was detected by an increase in anti-human IgG-FITC median fluorescence. Representative histogram plots show alloantibody binding to cell lines including parental and HLA-C allele transfected 721.221 (left panel) and K562 (right panel) cell lines. Patients with varying HLA-C and HLA Class II-specific alloantibody MFI values are represented by the different colours – MFI >10,000 (red); MFI <10,000 (yellow); MFI >2,000 (blue) and MFI <2,000 (grey).

3.5. Enrichment of HLA-C-specific alloantibodies from serum

Following the detection of reactivity to target allele-transfected cell lines, HLA-C-specific alloantibodies were adsorbed and enriched from patient sera whilst removing HLA-A, HLA-B and HLA-Class II-specific antibodies. The resulting antibody eluate was subsequently utilised in further functional experiments involving NK cells. Sera with known HLA-C alloantibody specificities were adsorbed using either (i) a single HLA-C allele expressing cell line, or (ii) an immobilised HLA affinity column. The enriched HLA antibody specificities were later confirmed using the single antigen bead assay on the Luminex platform.

3.5.1. Single HLA-C allele transfected cell line

The HLA-C allele-transfected cell line used for antibody adsorption was selected on the basis of serum reactivity pattern towards target cell lines (Figure 3.5). The aim was to remove non-specific antibodies from serum, for example HLA Class II-specific alloantibodies, and to retain HLA-C-specific alloantibodies from the adsorption process. All sera samples were firstly incubated with 721.221 parental cell line. Following centrifugation, the resulting serum supernatant was incubated with 721.221-Cw6 cell line to adsorb HLA-C group 2-specific alloantibodies. To gently dissociate and elute the antibodies, 721.221-Cw6 cells were treated with an IgG elution buffer and subsequently neutralised, resulting in an enriched alloantibody eluate.

Figure 3.6 shows the HLA antigen reactivity of patient serum pre-adsorption and enriched eluate post-adsorption with an HLA-C2 allele-transfected cell line to luminex beads. Representative patient serum demonstrated reactivity predominantly against the HLA-C locus antigens, including HLA-C1 and -C2 alleles. Non-HLA-C-specific alloantibodies i.e. alloantibodies specific for HLA-A, -B and Class II antigens were also studied. Firstly, HLA Class II-specific alloantibodies from 100μl of patient serum were removed using 721.221 cell line (Figure 3.6A). High MFI levels which indicated the HLA Class II antigen reactivity were reduced to the point they were undetectable, following antibody adsorption. For example, HLA-DQ7 bead reactivity in the serum was minimised from over 16,000 MFI to less than 300 MFI in the eluate. These data also validate the use of a high HLA Class II expressing cell line, in this case 721.221, as an effective tool to remove or enrich specific alloantibodies from serum.

Subsequent serum adsorption with HLA-Cw6 transfected 721.221 cell line shows the enrichment of alloantibodies specific to HLA-C2 group variants – Cw2, 4, 5, 6, 15, 17 and 18. HLA-A and HLA-B-specific alloantibodies were completely absent in the eluate (Figure 3.6B) whilst MFI values of less than 2000 were measured against HLA-C group 1 specificities – Cw1, 8, 12, 14 and 16. Together, the enriched antibodies in the eluate predominantly show reactivity to HLA-C group 2 antigens, demonstrating specific adsorption and enrichment of HLA-C2-specific alloantibodies reacting to group 2 allotypes only.

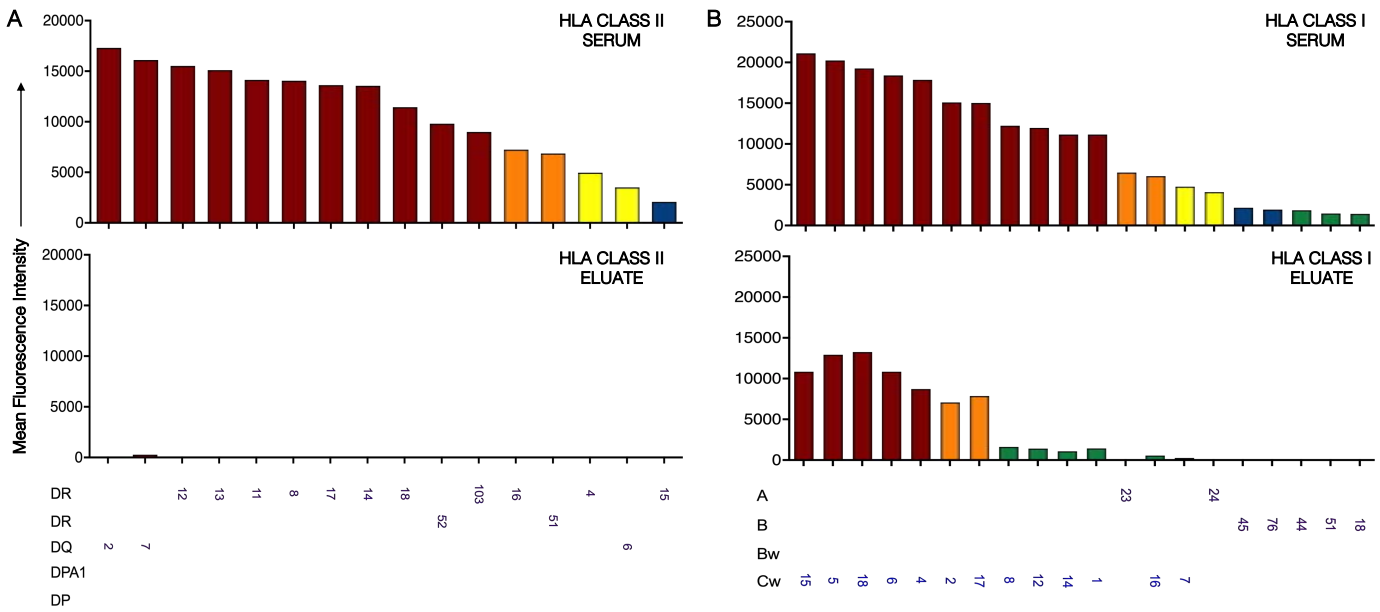

Figure 3.6. | HLA Class I and II analyses of epitope-specific adsorption with cell lines.

A | Patient serum positive for a range of HLA Class II-specific alloantibodies with high MFI values was co-incubated with HLA Class II-expressing 721.221 cell line. Post-adsorption, HLA Class II-specific alloantibodies were removed from the eluate.

B | The Class II alloantibody-depleted supernatant was applied to HLA-Cw6 expressing 721.221 cell line to adsorb and enrich for HLA-C2 epitope sharing antibody. The eluate was neutralised and tested against HLA Class I SABs using the luminex platform.

The Y axes indicate bead MFI value and the X axes present HLA Class I and II antigen specificities. Range of MFI levels are denoted by different colours - MFI >20,000 (red); MFI <10,000 (orange); MFI >5,000 (yellow); MFI >2,000 (blue) and MFI <2,000 (green).

3.5.2. Immobilised HLA column

To selectively adsorb and enrich for HLA-C group 1-specific alloantibodies, up to 2ml of diluted serum was applied to HLA-Cw08*01 protein-coupled column. After multiple wash steps, antibody-bound to the beads was dissociated using an alkaline-based elution step. Following buffer exchange and concentration of the eluted alloantibody, single antigen Luminex analyses were performed on three fractions – (i) fraction resulting from loading the diluted patient serum onto the column, (ii) the accumulation of multiple wash fractions and (iii) the elution fraction containing alloantibodies released from the column (Figure 3.7).

Representative patient serum containing a range of HLA Class I-specific alloantibodies which recognise HLA-B46, 73, HLA-C group 1 and HLA-A antigens was applied to the immobilised HLA column. The serum was negative for HLA Class II-specific alloantibodies. Figure 3.7 shows the HLA-specific antibody profiles of the serum during the load, wash and elution stages of the enrichment process. Luminex microbead analysis of the load phase with flow-through of the diluted serum demonstrate low MFI values for all HLA antigens, suggesting the binding and retention of antibody to the column, including third party HLA-A-specific alloantibodies. Similarly, the wash fraction (total 7ml) show MFI values of less than 5000 for HLA-C group 1 specificities, diluting out the 'weakly' reactive third-party antibodies, thus the lack of detection. Following the release of HLA-Cw08*01 epitope-sharing antibody from the column in 5ml of alkaline solution, the eluted antibody was concentrated to small volumes ranging from 0.5-1ml. The eluate demonstrated specific bead reactivity to HLA-B46, -B73 and HLA-C1 epitope-sharing antigens only. Other third-party antibodies were not detected.

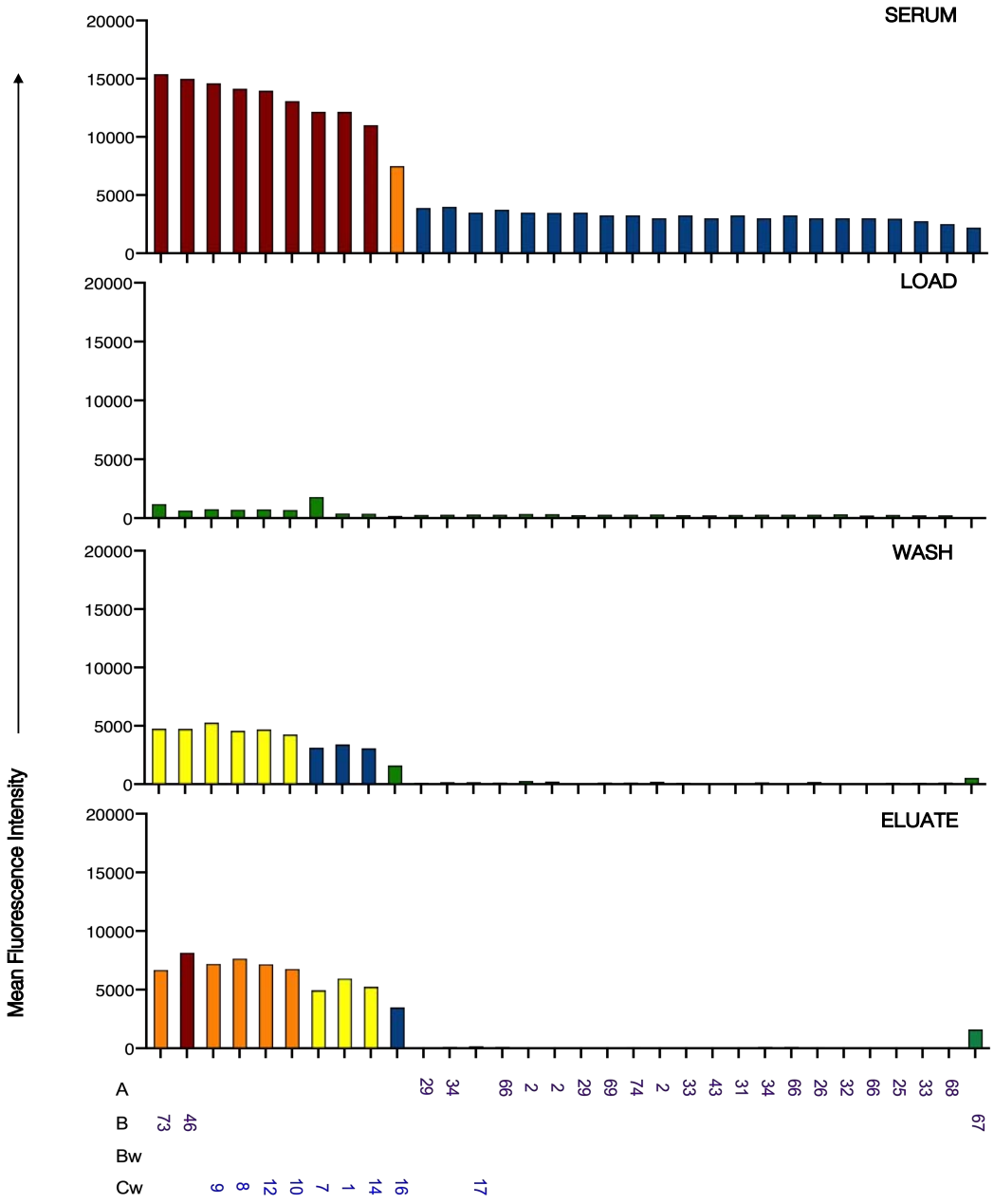

Figure 3.7. | HLA Class I analysis of epitope-specific adsorption with soluble HLA column.

Patient serum positive for a range of HLA Class I-specific alloantibodies, including HLA-C group 1 antigens was applied to HLA-Cw08*01 allele-coupled sepharose column. HLA Class I luminex analysis was performed on three fractions resulting from column-based adsorption – serum load, wash phase and antibody elution phase. Following alloantibody eluate neutralisation and concentration, luminex analysis demonstrated the selective adsorption and retention of HLA-C group 1 epitope specific alloantibody. HLA protein coupled column was kindly gifted by Rico Buchli and colleagues (OneLambda).

3.5.3. Comparing HLA Class I bead reactivity – pre- and post-adsorption

Serum samples from patients with high MFI levels of HLA-C-specific alloantibodies were selected for adsorption. HLA-C group 1-specific alloantibodies were adsorbed with an HLA-Cw8 protein-coupled column, whilst an HLA-C2 allele-transfected cell line was used to adsorb HLA-C group 2-specific alloantibodies. Using these two approaches, the MFI values measured pre- and post-adsorption by single HLA antigen beads were compared to evaluate changes in MFI values (Figure 3.8).

Adsorption with an immobilised HLA-Cw8 column demonstrated comparable bead reactivities for HLA-C group 1 epitope sharing antigens, including HLA-B46 and -B73. A reduction of almost 50% in MFI values was observed post-column-based adsorption, indicating dilution of enriched alloantibodies. MFI values for third-party alloantibodies i.e. HLA-A-specific antibodies were very low (1.7% to 3.2%) (Figure 3.8A).

Similarly, adsorption of antibodies using an HLA-C2 allele-transfected cell line showed an overall reduction in post-adsorption in MFI values, most likely due to the dilution factor of the eluate (Figure 3.8B). Compared to column-based adsorption, however, enriching for HLA-C group 2 epitope-specific antibodies with a cell line demonstrated higher MFI values. For example, HLA-Cw18 eluate MFI value (13,250.0) was reduced by approximately 30% compared to the serum MFI value (19,268.0). Epitope-sharing HLA-Cw5 antigen showed a similar reduction in MFI value post-adsorption (12,924.0). Other HLA-C2 antigen specificities show comparable MFI values, indicating the presence of a second antibody potentially cross-reactive with the remaining HLA-C2 group antigens.

Although the adsorption process with a single HLA-C2 allele-transfected cell line is selective, it was not highly specific, as alloantibody recognising HLA-C1 antigens were also enriched. The MFI values of HLA-C1 bead reactivity were comparatively lower than HLA-C2 bead reactivity with MFI values ranging from 5.4% to 13.1% post-adsorption. Unlike the immobilised HLA column, third-party HLA-A-specific alloantibodies were efficiently removed following cell line-based adsorption.

Together, these data suggest that adsorption of epitope-specific antibodies is more effective when using a cell line transfected with a single antigen of interest as the solid phase. The enrichment of alloantibodies also undergo dilution in the resulting eluate, which is demonstrated by the changes in MFI values.

3.5.4. Reactivity of enriched alloantibodies to target antigens

In comparison to microbead reactivity, alloantibody binding to target cell lines following adsorption was also measured by testing parental K562 and single HLA-C allele transfected K562 cell lines with serum and enriched eluate (Figure 3.9). MHC Class I deficient-K562 and HLA-Cw06*02 allele transfected cell lines show no increase in MFI with both HLA-C1-specific alloantibody containing serum and enriched eluate tests (Figure 3.9A). HLA-C1 allele-transfected cell lines – Cw01*02 and Cw08*01, however demonstrate higher MFI values (1,103.0 and 1,440.0 respectively) when incubated with enriched alloantibodies, compared to serum at 922.0 and 1,190.0 MFI values respectively.

Similarly, co-incubation of patient serum and enriched eluate positive for HLA-C2-specific antibodies with K562 present comparable MFI values at 219.7 and 219.2, respectively (Figure 3.9B). In contrast, HLA-Cw06*02 allele transfected cell line demonstrates strong reactivity to both patient serum (MFI=877.1) and enriched HLA-C2-specific alloantibody eluate (MFI=1,383.9). Moreover, comparison of MFI values based on HLA-C1 (Figure 3.9C; left) and HLA-C2-specific (Figure 3.9C; right) antibody serum and eluate binding to target cell lines suggest that the detection of enriched antibodies bound to target antigens was more sensitive following adsorption and elution processes.

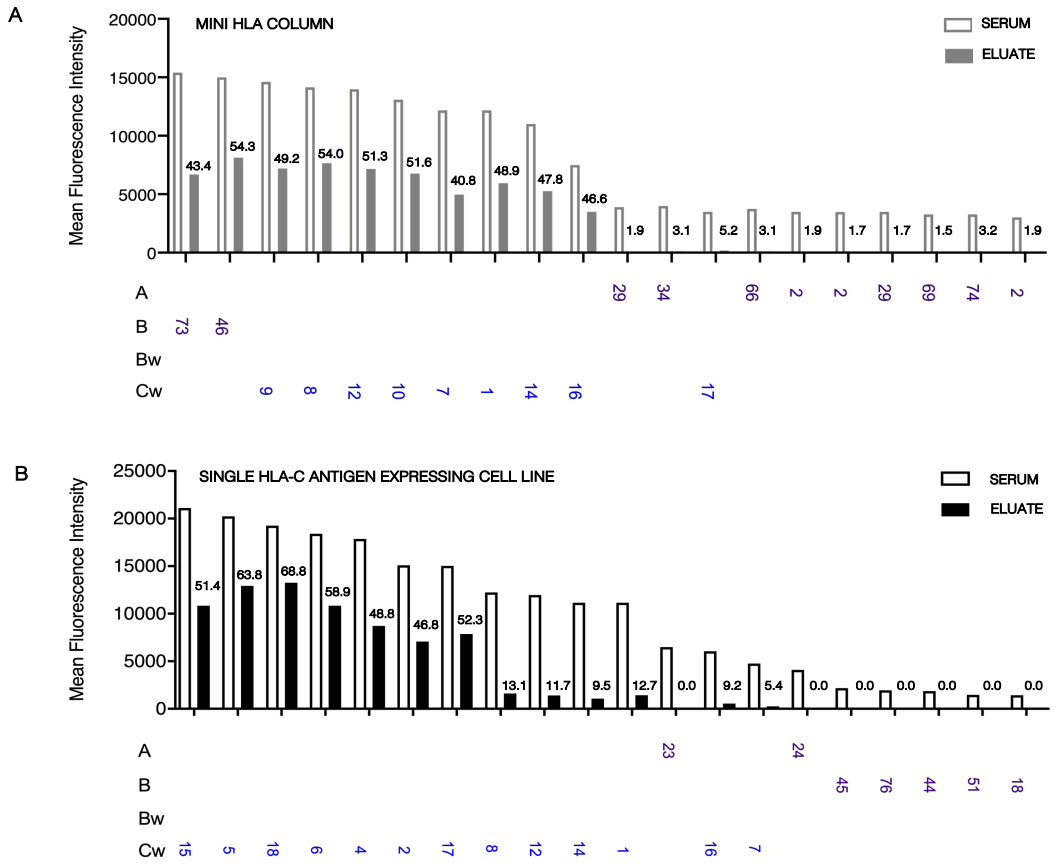

Figure 3.8. | Percentage changes in MFI values pre- and post-adsorption of alloantibody from serum.

HLA-C-specific alloantibodies were adsorbed with an **A |** HLA-Cw8 protein-coupled column or **B |** HLA-C2 allele-transfected cell line. MFI values deriving from the bead reactions were analysed in luminex assays. The numbers represent the percentage changes in MFI values pre and post-adsorption of alloantibody

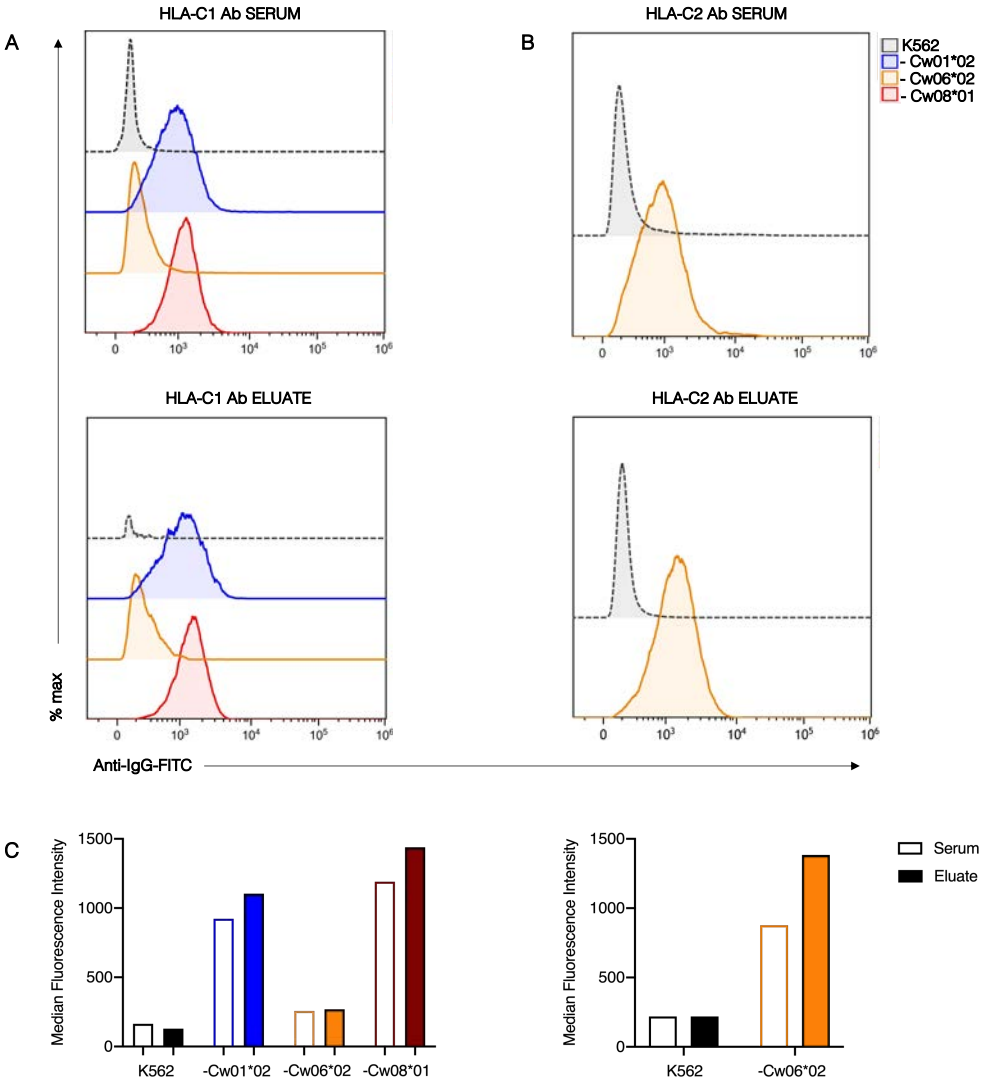

Figure 3.9. | Enriched HLA-C-specific alloantibodies selectively bind to target antigens.

Enriched HLA-C-specific alloantibody serum and eluate were co-incubated with parental and HLA-C allele-transfected K562 cell lines. Antibody reactivity to surface antigens was detected by an increase in anti-IgG-FITC MFI.

A | Histogram overlay plots demonstrate representative HLA-C1-specific alloantibody containing patient serum (above) and enriched eluate (below) reactivity to K562 (grey), HLA-C group 1 allele expressing K562-Cw01*02 (blue) and K562-Cw08*01 (red) and HLA-C group 2 allele expressing K562-Cw06*02 (orange).

B | Histogram overlay plots demonstrate representative HLA-C2-specific alloantibody containing patient serum (above) and enriched eluate (below) reactivity to K562 (grey) and HLA-C group 2 allele expressing K562-Cw06*02 (orange).

C | Median fluorescence intensity values (MFI) of anti-IgG-FITC measured following serum (empty bar) and eluate (filled bar) alloantibody binding. HLA-C1-specific atibody (left) and HLA-C2-specific atibody (right).

3.6. Discussion

The work in this chapter aimed to purify HLA-specific alloantibodies from the sera of renal transplant patients, particularly HLA-C-specific alloantibodies. Emphasis was placed on confirming and validating the HLA-specific antibody specificities on live cells expressing target antigens in their native form. This also included adsorbing and enriching for HLA-C-specific alloantibodies using an HLA-C allele-coupled sepharose column and a single HLA-C allele expressing cell line. Post-adsorption luminex analyses demonstrated that adsorption was specific and third-party alloantibodies were removed. The enrichment of HLA-C-specific alloantibodies of interest from patient sera were performed for subsequent functional assays and to study their function as potential KIR mimics.

3.6.1. Serum HLA-specific alloantibody reactivity to native antigens

Solid organ allograft rejection stimulates HLA-specific alloantibodies which tend to be high titre. This study analysed the sera of renal transplant recipients with a previously failed/rejected graft to determine HLA-specific alloantibody reactivity to native HLA antigens expressed on the cell surface of lymphocytes and cell lines. Solid phase assays using the Luminex platform detect clinically relevant HLA-specific antibodies (Pei et al., 2003). This assay has now taken priority over cell based assays such as Patel and Terasaki's complement dependent cytotoxicity (CDC) assay (Patel and Terasaki, 1969). SAB testing determined HLA-specific antibody presence in the serum and their reactivity to target proteins at the antigenic and allelic levels.

There are, however, underlying issues with this solid phase methodology as commercial kits from vendors have reportedly produced false positive reactions (In et al., 2014; Chacko et al., 2016; Park and Dr, 2017). This limitation is most likely due to errors in the manufacturing process involving purification of HLA antigens and alleles, which are later used to coat the microbeads. Several studies have shown that the generation of allelic proteins using recombinant DNA technology introduces conformational changes to the HLA structure, binding the proteins to the beads in their denatured form. Denatured HLA coated beads, therefore provide an inaccurate measure of donor-specific antibody (DSA), leading to erroneous interpretation of positive and negative bead reactions (Cai et al., 2009; Otten et al., 2013; Grenzi et al., 2013).

It is thought that native HLA antigens purified from EBV immortalised B cell lines are the same or the most closely matching forms of the HLA antigens expressed on cell membranes. Therefore, it can be speculated that native HLA antigen bound beads are more likely to provide a reliable landscape of antibody specificities present within the serum (Gebel and Bray, 2014). In the current study, however, LABScreen Class I and II single antigen beads (One Lambda, Canoga Park, CA) used to detect antibodies in patient sera were coated with recombinant HLA antigens. These proteins consist of intact HLA trimers i.e. HLA heavy chain (HC), β_2-microglobulin (β_2m) and peptide structure, but also free HCs devoid of β_2m and/or peptide (Ravindranath et al., 2017).

Keeping these caveats in mind, the specificities of HLA-specific DSAs initially detected by SABs were validated by testing patient serum in antibody binding assays, including flow cytometry-based crossmatch analysis with HLA-matched lymphocytes and single HLA-C allele-transfected cell lines. HLA-C allele expression was greater on K562-HLA-C-transfected cells as demonstrated by W6/32 staining (Figure 3.4C). As a result, the level

of HLA-C-specific alloantibody reactivity to K562-HLA-C-transfected cells was greater than 721.221-HLA-C-transfected cells, particularly in the absence of HLA Class II-specific alloantibodies (Figure 3.5 – Patient 012). Firstly, this validates the specificity of HLA-specific alloantibodies by SABs as true positives. Secondly, these data demonstrate that HLA-C alleles were expressed in their native form on the cell surface which allowed selective and accurate discrimination between the two KIR ligand groups HLA-C-specific alloantibodies. Finally, HLA-specific alloantibody reactivity to physiological HLA molecules on PBMCs and cell lines confirm their specificities in a cell-based system.

3.6.2. Cross-reactivity of HLA antigens

Cross-reactivity of HLA antigens is a phenomenon characterised by antibodies targeting public or commonly shared epitopes on the surface of HLA antigens – a side effect of originating from a highly polymorphic family of proteins (Rodey et al., 1994). Consequently, an antibody targeting a public epitope will exhibit a positive reaction to other HLA antigens sharing the reactive epitope. For example, in this study, SAB luminex analysis of patient 012 serum shows positive microbead reactions to HLA-B46, B73 and HLA-C group 1 antigens (Figure 3.7 – serum profile).

An in-depth analysis of HLA epitopes by adsorbing and eluting alloantibodies from recombinant HLA antigen-transfected cell lines identified a range of epitope-sharing antigens, including HLA-B*46, HLA-B*73, Cw1, 7, 8, 9, 10, 12, 14 and 16 (epitope 246) (El-Awar et al., 2007). Epitope 246 is defined by certain amino acid residues present at specific positions in the HLA Class I heavy chain. For example, epitope 246 is characterised by 76V + 80N amino acid residues or by a combination of 73T + 76V + 79R. Initial work showed serological cross-reactivity between HLA-Bw46 (Payne et al., 1975)

and HLA-Cw1 and 3 antigens a result of an identical α1 domain as HLA-B*46 (Zemmour et al., 1992). This broad HLA-B/C loci epitope reactivity is retained following antibody adsorption with HLA-Cw08*01 (HLA-C1 allele) bound sepharose mini column. The resulting eluate, therefore, consisted of enriched alloantibody which recognised epitope 246 on the column-bound HLA-C allele and later on the single HLA antigen coated microbeads for the luminex assay (Figure 3.7 – eluate profile). Moreover, HLA-B*46:01 is an HLA-B and HLA-C interlocus recombinant allele which shares HLA-C-specific motif KYRV at residues 66-76 in the α1-domain (Barber et al., 1996; Hilton et al., 2017).

KIR ligand groups 1 and 2 antigens are defined by the presence of specific amino acid residues at positions 77 and 80 in the α1 helix (Figure 3.4A). However, when enriching for HLA-C group 2-specific antibodies using a recombinant cell line (Figure 3.6), the eluate demonstrated reactivity against HLA-C2 specificities. The eluate also showed reactivity to the HLA-C1 alleles (Figure 3.8). Due to the unusually conserved nature of the α1 helix of the HLA-C molecule, the enrichment of HLA-C1-specific antibody alongside HLA-C2-specific antibody indicate the possibility of a non-specific adsorption process. This further demonstrates that allelic dimorphism between the KIR ligand groups must be taken into account when evaluating the efficiency of adsorbing antibodies using recombinant cell lines.

3.6.3. Evaluating changes in MFI values post-alloantibody adsorption

Pre- and post-adsorption HLA-specific antibody detection was performed using the luminex platform. The clinical serology laboratory at NHSBT, Birmingham use MFI values of above 2000 as positive. Therefore, the enriched HLA-C1-specific antibody from Patient X showing reactivity would be concluded negative as the MFI value for each antigen specificity is less than 2000 (Figure 3.6B). Other laboratories have reported using cut off values as low as 300 and 1000 (Zoet et al., 2011). However, for research purposes, the detection of HLA-specific alloantibody by SABs reactive to other HLA-C group specificities were considered positive.

When comparing the enriched HLA-C-specific alloantibody reactivity to the transfected cell lines (Figure 3.9), particularly in the instance of K562-C1 (Cw01*02 and Cw08*01) and K562-C2 (Cw06*02) cells, detection of antibody eluate binding was much more sensitive with higher MFI values than serum binding. This suggests that despite the adsorption and enrichment processes diluting the alloantibody eluate, the specificity of HLA-C1 and HLA-C2-specific antibody was increased, particularly in the absence of other confounding third-party antibodies, making them suitable to utilise in functional experiments.

3.7. Conclusions

HLA-C-specific alloantibodies initially detected using single antigen-coated beads also reacted to HLA molecules on PBMCs and single HLA-C allele-transfected cell lines. Consistent with the HLA-C alleles sequence alignments, HLA-C-specific antibodies detected the differences between the KIR ligand groups of proteins on the target cell surface. This, in turn, facilitated alloantibody adsorption and enrichment from renal transplant recipient sera by using either HLA-C allele-transfected cell lines or an immobilised HLA-C protein-coupled column. Post-adsorption luminex analyses of the diluted antibody eluates revealed lower MFI values, whilst the reactivity of the HLA-C1 and HLA-C2-specific enriched antibodies towards cell lines was improved. Together, these findings show that antibodies against HLA-C can bind to physiological or native forms of HLA-C molecules on the target cell surface, which were enriched from serum in preparation for subsequent use in NK cell functional assays to mimic KIR specificities.

CHAPTER IV

ANTIBODIES AGAINST HLA-C ENHANCE NK CELL FUNCTION

4.1. Introduction

The surface expression levels of HLA-C proteins are thought to be 13 to 18 times lower than HLA-A and HLA-B loci expression (Apps et al., 2015), and yet HLA-C plays an important role in maintaining tolerance to immune cells such as NK cells (Valiante et al., 1997). Key polymorphisms in the α1 helix of the HLA Class I molecule define two distinct groups of HLA-C alleles – group 1 (HLA-C1; Ser^{77} Asn^{80}) and group 2 (HLA-C2; Asn^{77} Lys^{80}) (Colonna et al., 1993b). HLA-C allotypes have largely evolved as the major ligands for the inhibitory receptors KIR2DL1 and KIR2DL2/3 on NK cells (Hilton and Parham, 2017). Functional studies have shown that the lack of HLA-C molecules on target cell surface presents a 'missing-self' scenario to NK cells, resulting in immediate and efficient lysis of target cells (Ljunggren and Kärre, 1990). Whilst the presence of the HLA-C 'self' molecules protects target cells, mainly normal cells from autologous NK cell-mediated lysis (Ciccone et al., 1994).

However, in diseases such as cancer, this inhibitory interplay between HLA-C and KIRs acts to suppress NK cell function and can thereby facilitate tumour cell evasion and support disease progression (Garrido et al., 2012; Jobim et al., 2013; Kowalewski et al., 2015). Therefore, this chapter addresses two questions – (i) Is KIR:HLA-C blockade by HLA-C allele-specific antibodies a potential strategy to enhance NK cell function and to increase target cell lysis? and (ii) What are the possible HLA-C-specific antibody mechanisms of actions involved in enhancing NK cell-mediated cytolysis?

Both activating and inhibitory KIRs can be expressed on the same NK cell. The dominant interaction of ligands with their corresponding KIRs ultimately determines the NK cell functional outcome. Therefore, to identify effector cells with specific KIR expression patterns, firstly the human NK cell inhibitory and activating KIR repertoires in healthy individuals were characterised by flow cytometry.

Secondly, enriched NK cells from healthy individuals with a suitable KIR repertoire were co-incubated with an MHC Class I-negative cell line, K562 and K562 cells that had been transfected with single HLA-C alleles – HLA-Cw08*01 (C1) and HLA-Cw06*02 (C2). An *in vitro* NK cell cytotoxicity model was developed to study the effect of enriched HLA-C-specific alloantibodies (Chapter III) on the inhibitory KIR:HLA-C interaction and thus, NK cell function against target cells.

Thirdly, the HLA-C alloantibody-dependent mechanism of action was investigated. The first approach aimed to confirm the role of HLA-C:KIR blockade in enhancing NK cell activation against target cells by inhibiting IgG-FcγRIIIa ligation using a CD16-specific blocking antibody. The second approach utilised a proteolytic enzyme, IdeS to cleave the Fc fragment of HLA-C-specific antibodies, thereby eliminating ADCC-mediated responses, whilst potentially retaining a cytotoxic response mediated by HLA-C:KIR blockade. The final approach examined the ability of HLA-C-specific antibodies to mediate enhanced NK cell function in the complete absence of FcγRIIIa by harnessing NK cell line effector responses.

4.2. Characterisation of human NK cell KIR repertoires

The functional education and expansion of NK cells is controlled by a profile of activating and inhibitory KIRs that interact with HLA-C ligands to maintain tolerance to normal, healthy 'self' tissue. To characterise the human NK cell KIR repertoire, peripheral blood mononuclear cells (PBMCs) from healthy individuals were immunophenotyped and analysed via flow cytometry. Two multi-parameter flow cytometry panels were designed to perform a phenotypic analysis of KIRs – KIR2DL/KIR2DS (Table 2.6) and KIR3DL/KIR3DS (Table 2.7).

Healthy lab donors (n=5) were recruited with fully informed consent and leucocyte cones, a by-product of the apheresis process during blood donation from healthy volunteers (n=12) were obtained for this study. Following the selection of viable single lymphocytes ($CD14^{neg}$ $CD19^{neg}$), the $CD56^{dim}$ $CD3^{neg}$ NK cell subset was identified for KIR repertoire analysis (Figure 4.1A). $CD56^{bright}$ NK cells were excluded from further analysis as they are reported to lack the expression of specific inhibitory KIRs (Jacobs et al., 2001). The surface expression of nine KIRs – KIR2DL1, KIR2DS4, KIR2DL2/L3/S2, KIR2DL3, KIR3DL1, KIR3DL2 and KIR3DL3 using seven antibodies, was subsequently measured to determine the range of single-KIR frequencies within this cohort (Figure 4.1B).

The expression levels of individual KIRs were highly variable as represented by the range for each KIR frequency and the differences between the KIRs (Figure 4.1C). Despite variability among donors, the most commonly expressed KIR group, KIR2DL2/L3/S2 which was detected by the antibody clone DX27, was present on approximately 30% of the total $CD56^{dim}$ NK cells. The proportions of single $KIR2DL1^{+}$ and $KIR2DL3^{+}$ expressing $CD56^{dim}$ NK cells showed similar frequencies with averages of 18.1% and 19.4%,

respectively. Of note, all donors lacked the expression of KIR3DL3 (mean=0.3%) on CD56^{dim} NK cells. In addition, out of the 17 healthy individuals analysed, five donors showed high frequencies of KIR2DS4 expression, reaching up to 59.5%.

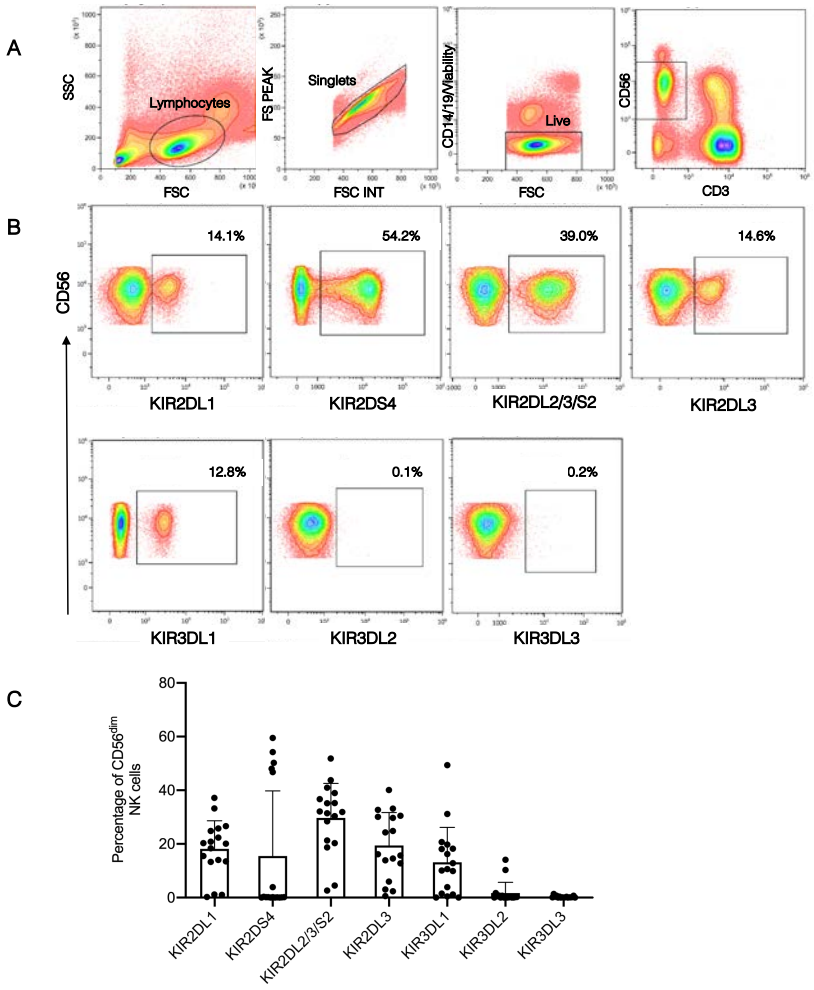

Figure 4.1. | Characterisation of KIR repertoires from healthy individuals.

PBMCs from healthy donors were stained with multiple combinations of KIR-specific antibodies. The data were collected using the Beckman Coulter Gallios flow cytometer and analysed by the Kaluza software.

A | Representative flow cytometry gating strategy to identify viable CD56^{dim} CD14^{neg} CD19^{neg} CD3^{neg} lymphocytes.

B | Representative dot-plots showing single-KIR2DL1, KIR2DS4, KIR2DL2/3/S2, KIR2DL3, KIR3DL1, KIR3DL2 and KIR3DL3 expression on the CD56^{dim} NK cell subset.

C | Summary of the frequencies of inhibitory and activating KIR-expressing CD56^{dim} NK cells in a cohort of 17 healthy individuals. Each dot indicates data from one donor. Bars represent the percentage mean of each KIR population (±SD) across the healthy donor cohort.

Next, a combination of antibodies was used to differentiate between the inhibitory and activating forms of KIRs (Figure 4.2) and to analyse their co-expression for further functional experiment purposes. Firstly, to distinguish between KIR2DL1^{+} (inhibitory) and KIR2DS1^{+} (activating) populations, a combination of REA284 (KIR2DL1) and EB6 (KIR2DL1/2DS1) antibody clones were used. CD56^{dim} NK cells from healthy controls specifically expressing either KIR2DL1 or KIR2DS1 and dual expressing KIR2DL1^{+} KIR2DS1^{+} NK cells were identified. Secondly, the combined use of DX27 (KIR2DL2/L3/S2) and 180701 (KIR2DL3) antibodies enabled the selection of individuals expressing either KIR2DL2 and/or KIR2DS1 and those carrying KIR2DL3 alone (Figure 4.2A). Thirdly, the frequency of either KIR2DL1^{+} (REA284^{+} 180701^{-}) or KIR2DL3^{+} (REA284^{-} 180701^{+}) expression on CD56^{dim} NK cells were assessed within this cohort of healthy individuals (Figure 4.2B). The frequency of KIR2DL1^{+} only NK cells ranged from 0.7% to 22.8%, while KIR2DL3^{+} only NK cells ranged from 0.3% to 36.9%.

Co-expression of KIR2DL1^{+} KIR2DL3^{+} on a proportion of NK cells were comparatively lower, ranging from 0.03% to 20.7%. Of note, one donor (HD002) presented with a very high percentage of KIR2DL1^{+} KIR2DL3^{+} double positive NK cells, reaching up to 26.2% of total CD56^{dim} NK cells (Figure 4.2C – HD002). Therefore, donors with a dominant proportion of CD56^{dim} NK cells expressing KIR2DL1 (e.g. HD001) were used for experiments involving the assessment of HLA-C2:KIR2DL1 interaction, whilst HLA-C1:KIR2DL2/3 interaction was analysed using donors with a high percentage of KIR2DL3^{+} CD56^{dim} NK cells (HD004). The inhibitory KIR:HLA-C interaction was also assessed by selecting donors with a dominant proportion of KIR2DL1^{+} KIR2DL3^{+} double positive NK cells (HD002).

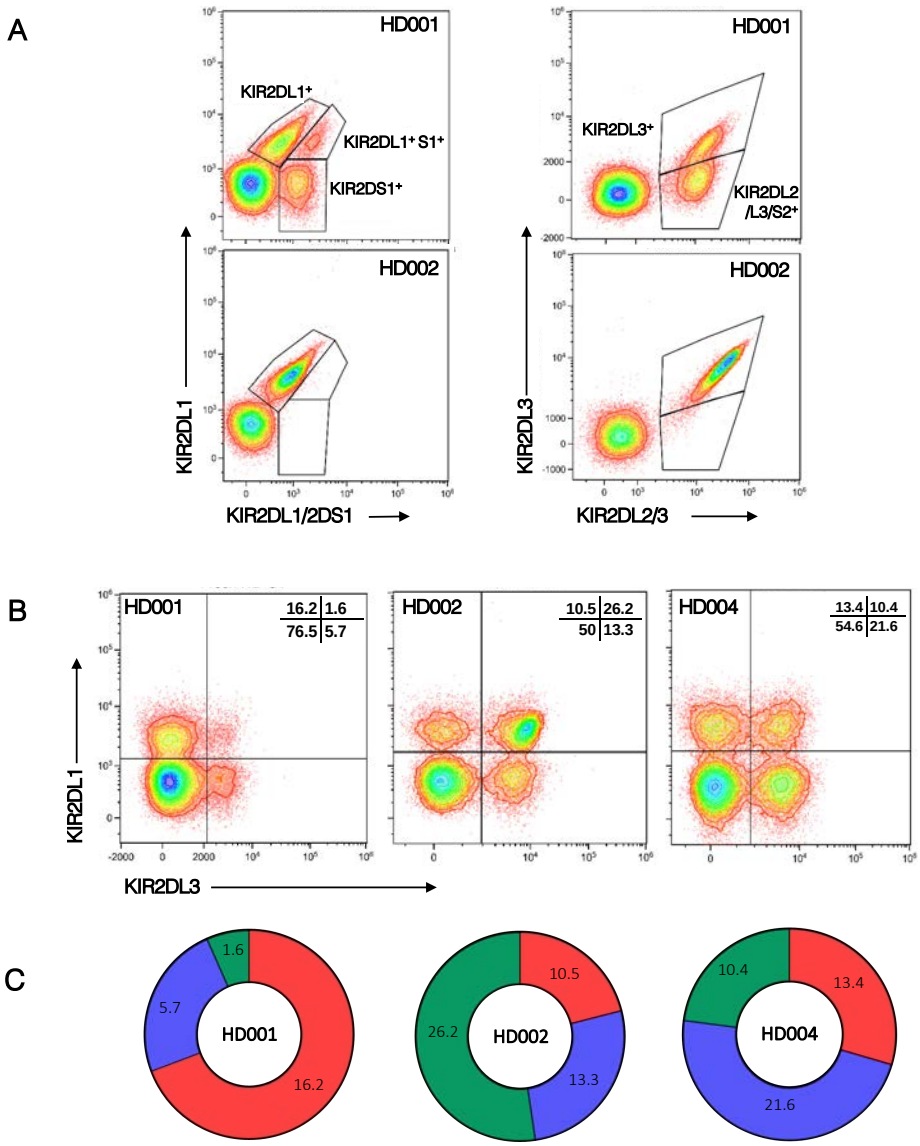

Figure 4.2. | Identification of single KIR-expressing NK cell subsets in healthy individuals.

PBMCs from healthy donors were stained with multiple combinations of KIR-specific antibodies. The data were collected using the Beckman Coulter Gallios flow cytometer and analysed by the Kaluza software.

A | Representative flow cytometry plots identifying KIR2DL1^{+}, KIR2DL1^{-}S1^{+} and KIR2DL1^{+}S1^{+} (left panel), KIR2DL3^{+} and KIR2DL2/3/S2^{+} (right panel) NK cell subsets in two healthy individuals.

B | The observed frequencies of single and dual expression of KIR2DL1 (REA284 clone) and KIR2DL3 (180701 clone) on CD56^{dim} NK cells across three representative healthy individuals.

C | Pie charts depict the composition of KIR2DL1^{+} (red) or KIR2DL3^{+} (blue) or dual KIR2DL1^{+}2DL3^{+} (green) expressing NK cells. The frequency of each population is indicated within the pie chart.

4.3. Flow cytometry-based NK cell cytotoxicity assay

To measure NK cell cytotoxicity against target cells transfected with HLA-C1 and HLA-C2 alleles, a flow cytometry-based cytotoxicity assay was optimised. Firstly, NK cells enriched from healthy individuals were co-incubated with parental K562 target cells to determine the optimal effector-to-target ratio. Secondly, the effect of IFN-α-mediated activation of NK cells was examined. Thirdly, by selecting healthy donors with specific NK-KIR repertoires, the difference in NK cell mediated lysis of HLA-C1/C2-transfected target cells was measured.

4.3.1. Optimisation of NK cell cytotoxicity assay

Using total NK cells enriched from healthy individuals, regardless of NK-KIR repertoires, target cell cytotoxicity was measured by quantifying the number of viable CFSE-labelled K562 target cells, following an overnight incubation with NK cells. K562, an MHC Class I-negative cell line derived from a chronic myelogenous leukaemia patient (Lozzio and Lozzio, 1977), is well known to be susceptible to NK cell-mediated cytolysis due to the lack of HLA Class I proteins and a high density of NK cell activating receptor ligands (Lisovsky et al., 2015). Briefly, NK cells were enriched from healthy donor PBMCs using a magnetic bead-based negative selection enrichment kit. NK cell purity was then assessed using flow cytometry (Figure 4.3A) and IFN-α was added to enriched NK cells for activation.

Following an overnight incubation, the co-culture of NK cells and CFSE-labelled K562 cells was harvested and analysed by flow cytometry. The cell viability dye, propidium iodide was added to the samples to differentiate between viable and non-viable target cells (Figure 4.3B). Countbright counting beads were also included to validate the acquisition and the quantification of viable $CFSE^+$ K562 cells by flow cytometry (see Chapter II).

A representative example in Figure 4.3B shows that in the presence of NK cells at an effector-to-target (E:T) ratio of 1:1, the number of viable K562 cells show a marked reduction from 26,285 cells to 4,641 cells. Conversely, the number of non-viable-CFSE-labelled target cells (1,057) increased following co-incubation with NK cells to 8,385 cells. This assay demonstrates the ability of NK cells from healthy individuals to effectively lyse the MHC Class I-deficient K562 cells.

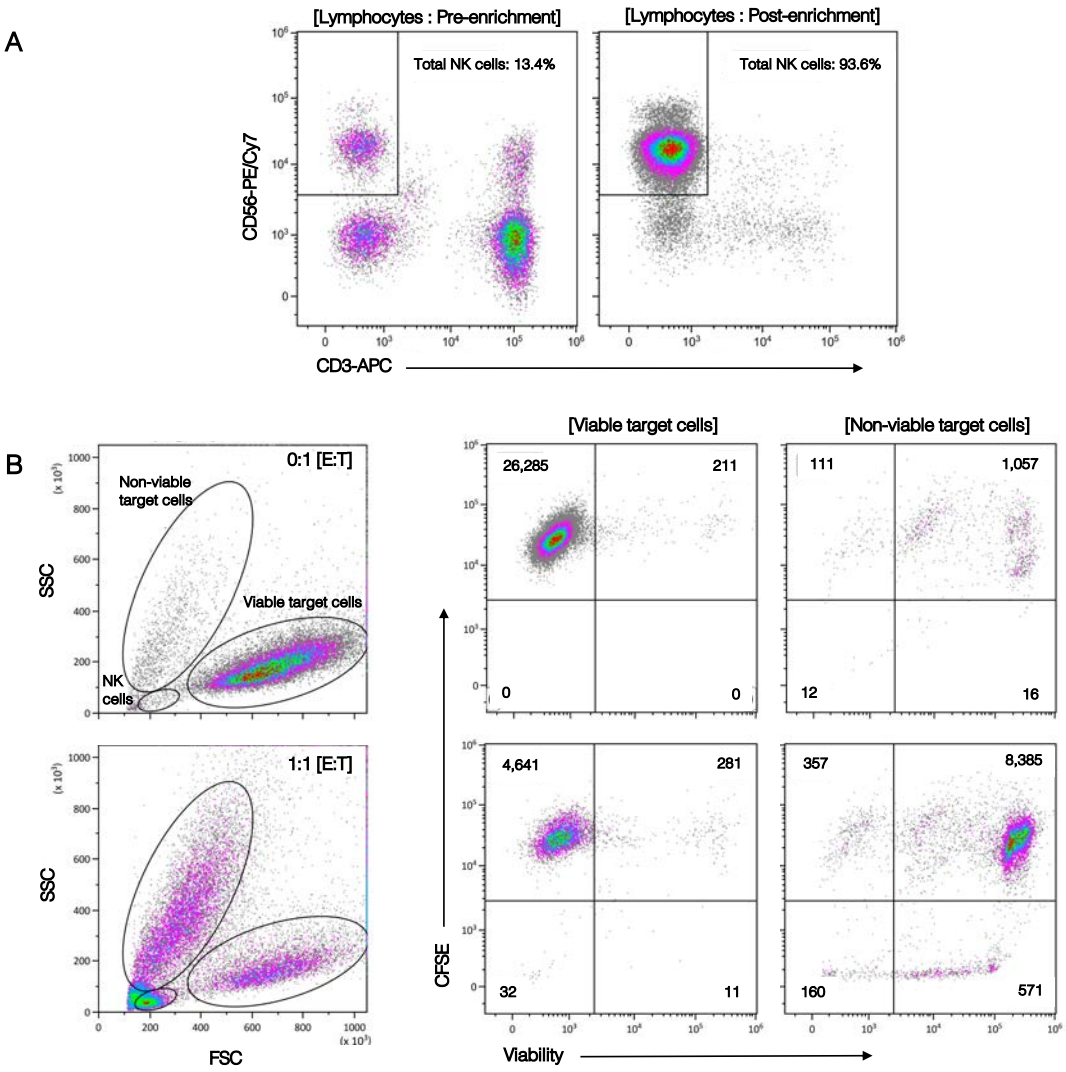

Figure 4.3. | Flow cytometry-based NK cell cytotoxicity assay.

A | Representaive example of NK cell enrichment from healthy donor PBMCs using a negative selection magnetic bead-based kit. Pre-enrichment, representative density plot shows $CD3^{neg}$ $CD56^{pos}$ cell subset constituting 13.4% of total lymphocytes. Post-negative selection, enrichment of $CD3^{neg}$ $CD56^{pos}$ cells was measurable with a purity of 93.6%.

B | Optimisation of flow gating strategy. Forward and side scatter parameters discern between potential viable and non-viable target cell populations. Propidium Iodide (PI), a viability dye enabled the detection and quantification of $CFSE^{pos}$ PI^{neg} viable target cells and $CFSE^{pos}$ PI^{pos} non-viable target cells, in the absence (upper panel) and presence (lower panel) of NK cells.

Next, the NK cell cytotoxicity assay was further optimised by determining the optimal E:T ratio. The effect of pre-activating NK cells with IFN-α was also measured (Figure 4.4). Multiple experimental repeats with NK cells from healthy donors (n=4) revealed an increasing effector cell number-dependent NK cell cytotoxic activity towards K562 cells. A median percentage of target cell cytotoxicity ranging from 30-60% was detected at 0.5:1 E:T ratio, and this was subsequently used for further experiments. Moreover, IFN-α pre-activated NK cells exhibited a more cytotoxic profile, with an enhanced ability to efficiently lyse K562 cells compared to non-activated NK cells. To harness this enhanced effect, IFN-α pre-activated NK cells were used throughout the study.

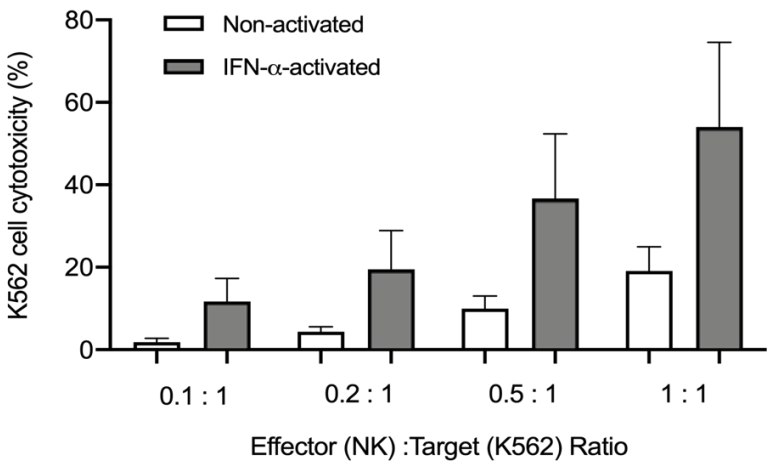

Figure 4.4. | Determining the optimal E:T ratio for NK cell cytotoxicity assay.

Varying number of effector cells (NK cells) were co-incubated with target cells (K562) overnight to determine the optimal E:T ratio. Pre-activation of NK cells with (grey bars) and without (white bars) IFN-α was also compared. The percentage of K562 cell cytotoxicity was calculated using standardised CountBright beads. Bars represent mean ± SEM from four independent experimental repeats. Each condition was performed in triplicate wells.

4.3.2. HLA-C binding to inhibitory KIR affects NK cell function

To study the interaction between HLA-C and inhibitory KIR proteins, healthy individuals with a dominant proportion of KIR2DL3$^+$ or KIR2DL1$^+$ NK cell subsets were selected for co-incubation with CFSE-labelled parental and HLA-C1 (-Cw08*01) or -C2 (Cw06*02) allele-transfected target cells, respectively. It was hypothesised that compared to the MHC Class I deficient K562 cells, HLA-C1 and -C2-transfected target cells would be less susceptible to NK cell-mediated lysis.

The lack of 'self' HLA-C ligands on the parental K562 cell surface mimicked the 'missing-self' scenario in this NK cell-based cytotoxicity assay resulting in cytolysis, regardless of the dominant KIR expression levels (Figure 4.5). However, a large biological variation was observed in NK cell activity whereby some donors were more efficient at lysing parental K562 cells. This effect is shown with two out of four donors with a high proportion of KIR2DL1$^+$ NK cells (Figure 4.5B). With the exception of one donor, NK cells from three donors with a dominant proportion of KIR2DL3$^+$ NK cells demonstrated a reduced cytotoxic function against K562-C1 target cells (mean±SEM=24.9±2.0%) compared to K562 cells (35.6±7.9%) (Figure 4.5A). Similarly, K562-C2 target cells were less susceptible to dominant KIR2DL1$^+$ NK cell-mediated cytotoxicity (17.3±5.0%) than K562 cells (28.7±8.6%) (Figure 4.5B). Due to the high donor variation observed in this experiment, statistically significant reduction in NK cell activity in the presence of HLA-C alleles was not achieved. Despite this observation, a reduced cytolytic effect of K562-HLA-C allele transfected cells was detected. This effect requires further analysis by increasing the number of experimental repeats and healthy donors for NK cells.

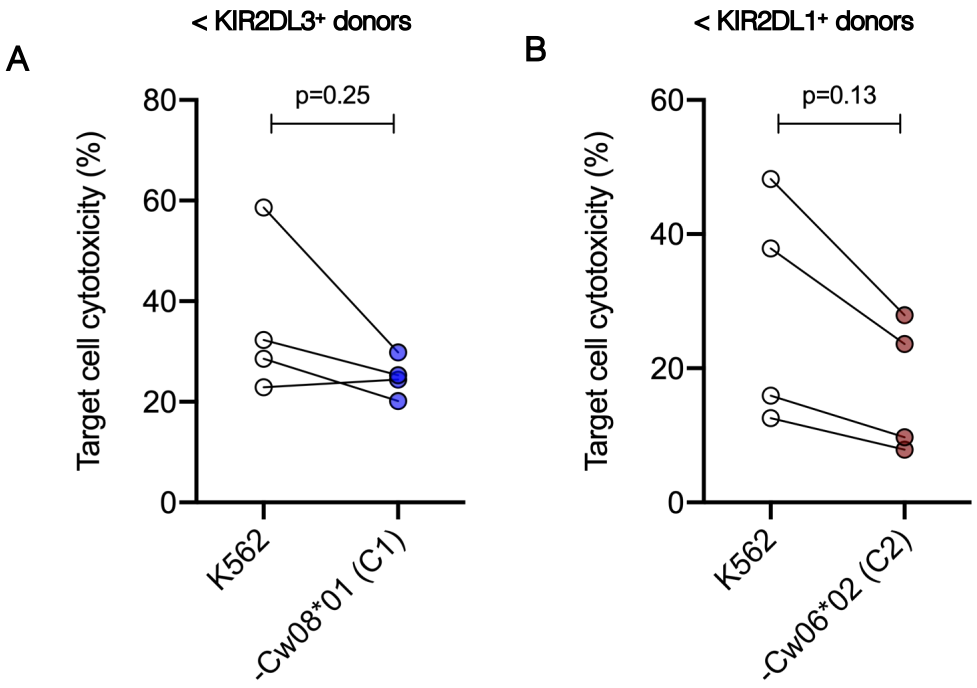

Figure 4.5. | HLA-C allotype binding to inhibitory KIRs affects NK cell-mediated cytotoxicity.

A | IFN-α activated NK cells from multiple healthy donors with a dominant proportion of KIR2DL3 were co-incubated with parental K562 cells (empty circles) and K562-Cw08*01 (HLA-C1 allotype) (blue circles) target cells in an overnight assay. 0.5:1 E:T ratio was used.

B | IFN-α activated NK cells from multiple healthy donors with a dominant proportion of KIR2DL1 were co-incubated with parental K562 cells (empty circles) and K562-Cw06*02 (HLA-C2 allotype) (red circles) target cells in an overnight assay. 0.5:1 E:T ratio was used.

Each connecting line represents one expriment with healthy donor NK cells. Statistical analysis perfomed with Wilcoxon matched-pairs signed rank test. No significant difference in percentage cell cytotoxicity was observed between parental K562 and HLA-C allele-transfected K562 cells. The percentage of target cell cytotoxicity was calculated using standardised CountBright beads.

4.3.3. Blocking the HLA-C and inhibitory KIR interaction

As a control experiment, parental and HLA-C1 and -C2-transfected target cells were treated with purified DT-9 antibody to determine the possible impact on NK cell function. Although its precise epitope reactivity is unknown, the DT-9 antibody clone, which recognises HLA-C and -E (Braud et al., 1998b) was used to block the inhibitory HLA-C and KIR interaction (Figure 4.6).

K562 parental cells do not express HLA-C or HLA-E. However, following DT-9 antibody treatment K562 cytolysis was enhanced from an average of 25.8±6.0% to 36.6±3.7%. This effect was consistent across all experiments using three healthy donor-derived NK cells. In contrast, this increased cytolysis was not observed in relation to K562-C1 target cell lysis (control=25.1±10.6%) following treatment with DT-9 antibody (25.5±10.8%). Although donor variation was the most obvious with K562-C1, DT-9 antibody treatment did not have an affect on K562-C1 cytolysis. Binding of DT-9 antibody to K562-C2 target cells, however, led to a moderate increase in lysis from 19.4±8.0% to 23.5±7.4%, and this effect was observed across all three donors. Despite the increase in K562 and K562-C2 lysis following DT-9 antibody treatment, the difference before and after treatment was not statistically significant. Experimental repeats are required to confirm whether DT-9 antibody reduces or increases the lysis of HLA-C allele transfected cells in the presence of NK cells from healthy donors. Together, these data suggest that DT-9 antibody prevents HLA-C and inhibitory KIR ligation, leading to a modest enhancement of NK cell function.

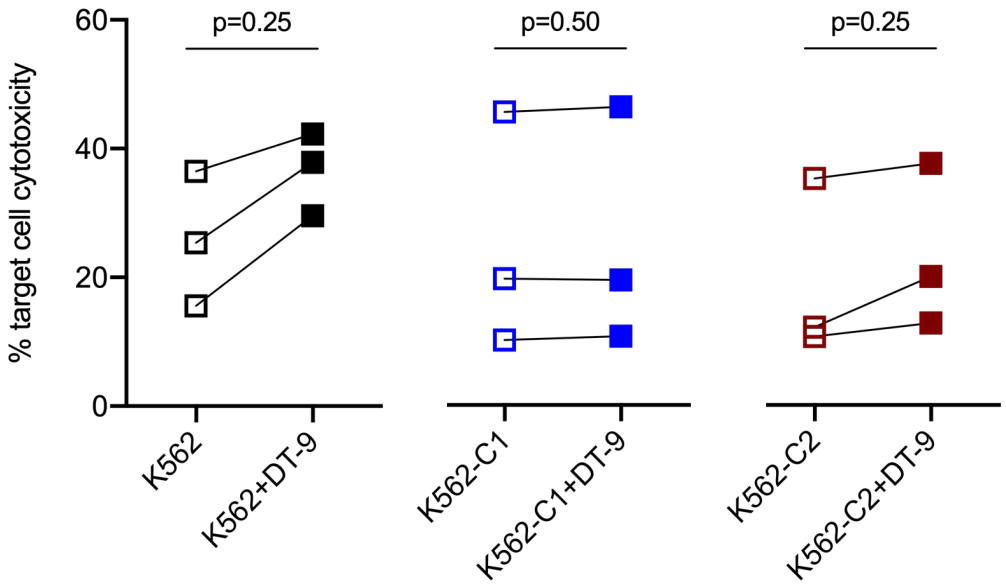

Figure 4.6. | Target cell lysis following blockade of HLA-C and KIR interaction by DT-9 antibody.

IFN-α activated NK cells from healthy donors (n=3) were co-incubated with parental K562 cells (left panel), K562-Cw08*01 (HLA-C1 allotype; middle panel) and K562-Cw06*02 (HLA-C2 allotype; right panel) target cells in an overnight assay. 0.5:1 E:T ratio was used. Prior to NK cell co-incubation, target cells were treated with DT-9 antibody clone for 30mins at room temperature. Open squares indicate control conditions i.e. no DT-9 antibody treatment. Closed squares indicate DT-9 antibody treatment of target cells K562 (black), K562-C1 (blue) and K562-C2 (red). Each connecting line represents one independent experiment. A total of three experimental repeats with NK cells deriving from three healthy donors were conducted. Statistical analysis performed with Wilcoxon matched-pairs signed rank test. The percentage target cell cytotoxicity was calculated using standardised CountBright beads.

4.4. Modulation of NK cell responses by HLA-C-specific alloantibodies

The flow cytometry-based NK cell cytotoxicity assays shown in the previous section were designed to evaluate the potential activity of HLA-C-specific alloantibodies in modulating NK cell lysis against single HLA-C allele-transfected target cells. The study aimed to mask HLA-C recognition from KIRs to harness the NK cell response in favour of activation. To test this strategy, parental and HLA-C1 and -C2 target cells were treated with enriched HLA-C1 or -C2-specific antibodies respectively, followed by an overnight co-incubation with IFN-α NK cells.

4.4.1. HLA-C-specific alloantibodies increase NK cell-mediated target cell lysis

Using two representative examples that analysed the effect of disrupting KIR2DL3:HLA-C1 and KIR2DL1:HLA-C2 interactions in this functional assay, NK cell cytotoxicity towards target cells was evaluated pre- and post-HLA-C-specific antibody treatment (Figure 4.7). Similar to Figure 4.5, Figure 4.7 shows that in comparison to K562 cells, K562-C1 (20.2±4.6%) (left panel) and K562-C2 cells (17.8±2.8%) (right panel) were less susceptible to lysis from NK cells in the absence of HLA-C-specific antibody treatment. NK cells with a high percentage of KIR2DL3 (HD004) (Figure 4.7A; right) and KIR2DL1 (HD001) expression (Figure 4.7B; right), respectively were utilised in these examples.

An increase in K562-C1 cytolysis was observed following HLA-C1-specific antibody treatment (37.1±2.5%). K562 cytolysis was enhanced to 41.8±4.1% after antibody treatment, although both differences were not statistically significant. HLA-C2-specific antibody treatment of K562-C2 cells did, however, result in a significant increase in target cell lysis from 17.8±2.8% to 40.0±1.2% indicating the potential of HLA-C-specific alloantibodies to enhance NK cell function in this *in vitro* functional assay.

Following multiple experiments using NK cells from different healthy donors, the differences in the level of HLA-C-specific antibody-treated target cell cytotoxicity was further analysed. In the representative examples of Figure 4.7, the absolute percentage target cell cytotoxicity was measured to show the effect of HLA-C-specific antibody treatment compared to no treatment on NK cell function. Figure 4.8 presents the data by analysing the average difference (Δ) in percentage of K562 and HLA-C allele transfected K562 cell cytotoxicity, before and after antibody treatment. For example, an increase of 13.2% in K562 cytolysis was measured following antibody treatment. Similarly, K562-C1 cell cytotoxicity was increased from 20.2% to 37.1% (Δ16.9%) (Figure 4.8A). This data analysis strategy was applied to minimise the variation in responses observed due to the use of NK cells from multiple healthy donors in this assay. The differences in target cell cytotoxicity measured following HLA-C1-specific (Figure 4.8B) and HLA-C2-specific (Figure 4.8C) antibody treatment were summarised. In both cases, a modest increase in K562 cytolysis was observed. However, the overall difference in K562-C1 ($P_{Mann\ Whitney}$=0.03) and K562-C2 ($P_{Mann\ Whitney}$=0.06) target cell cytotoxicity, following antibody treatment was statistically significantly greater than K562 cells. These data indicate that HLA-C allele-specific antibodies recognised and reacted with the transfected HLA-C allele, leading to enhanced lysis of specific KIR ligand target cells.

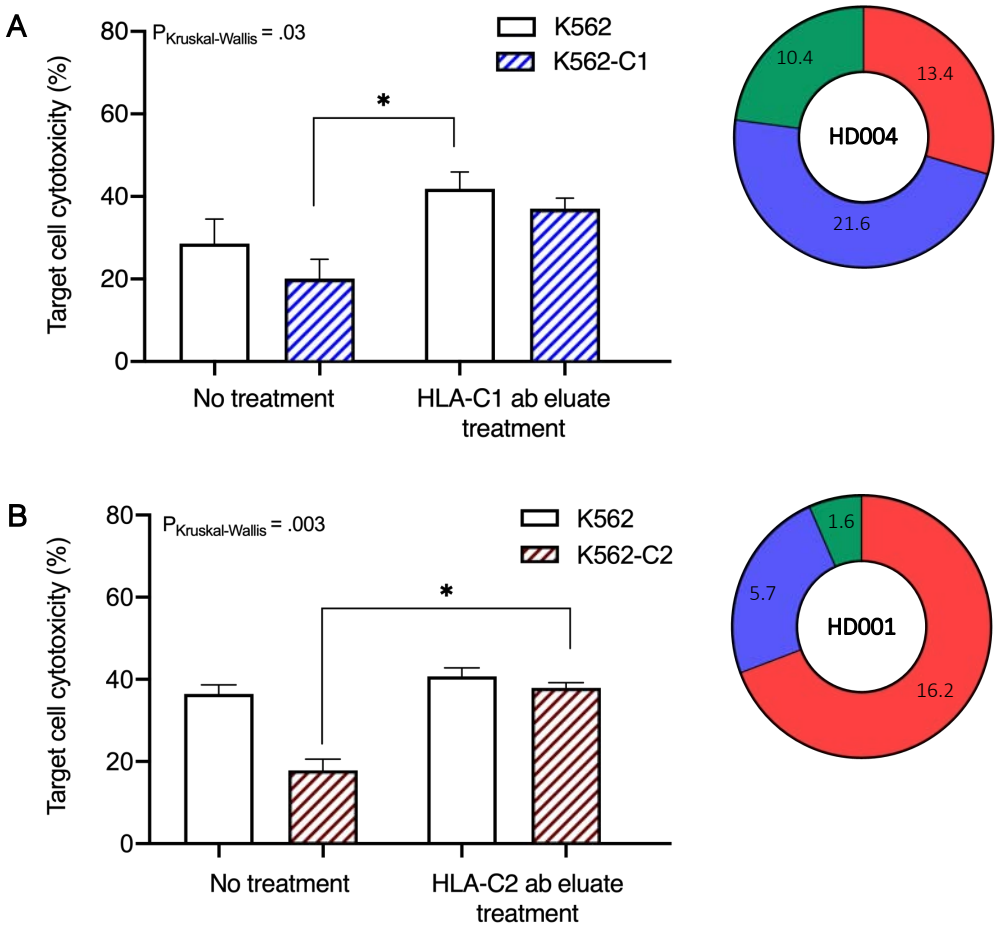

Figure 4.7. | Representative examples of NK cell cytotoxicity assay analyses in the presence or absence of HLA-C-specific antibody treatment.

Target cells were treated with HLA-C-specific enriched alloantibodies for 30mins at room temperature. IFN-α activated NK cells were co-incubated with untreated or alloantibody-treated target cells at 0.5:1 E:T ratio in an overnight assay.

A | K562 and K562-C1 (HLA-Cw08*01) cells were treated with HLA-C1-specific alloantibody. White bars represent K562 cells. Blue shaded bars represent K562-C1 cells. Pie charts depicts the percentage KIR2DL1$^+$ (red) or KIR2DL3$^+$ (blue) or dual KIR2DL1$^+$2DL3$^+$ (green) NK cells from donor HD004.

B | K562 and K562-C2 (HLA-Cw06*02) cells were treated with HLA-C2-specific alloantibody. White bars represent K562 cells. Red shaded bars represent K562-C2 cells. Pie charts depicts the percentage KIR2DL1$^+$ (red) or KIR2DL3$^+$ (blue) or dual KIR2DL1$^+$2DL3$^+$ (green) NK cells from donor HD001.

Each condition was performed in triplicate wells. Bars represent mean±SEM percentage target cell cytotoxicity from six independent experiments (n=6). Statistical analysis performed by One way ANOVA with Kruskal Wallis for non-parametric data with Dunn's multiple comparisons test. The percentage target cell cytotoxicity was calculated using standardised CountBright beads.

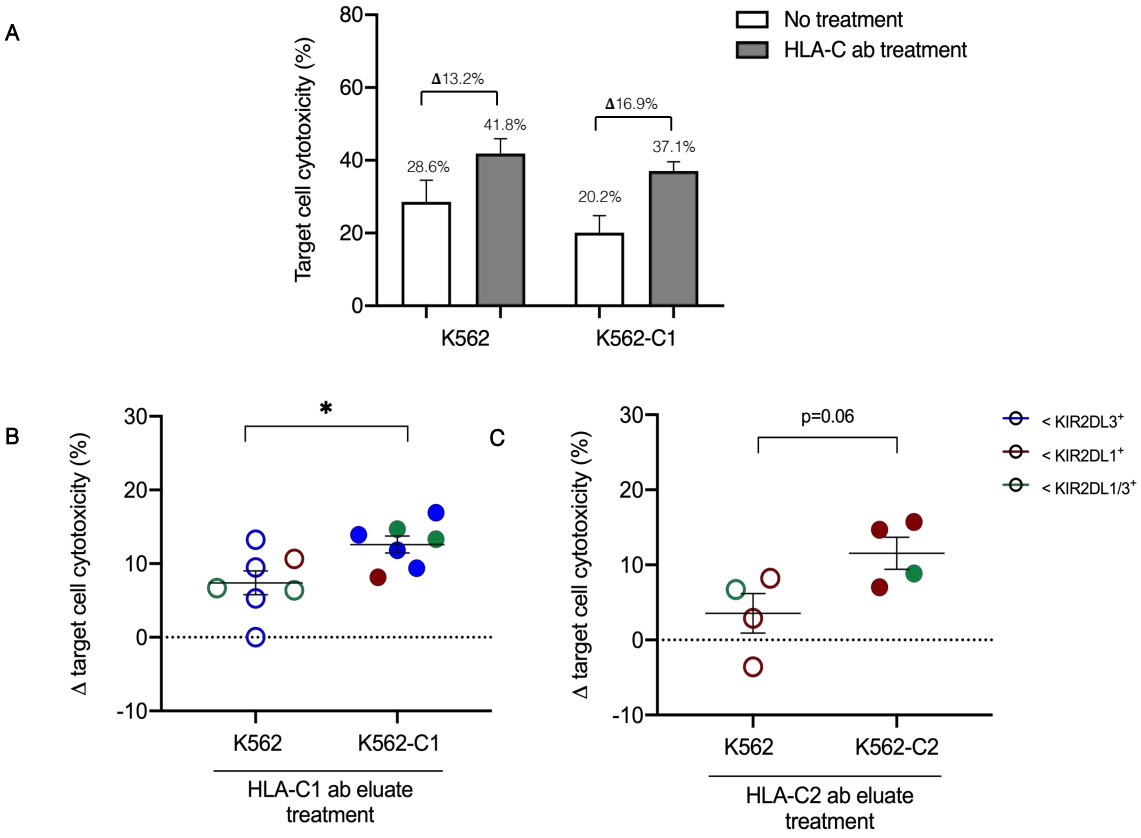

Figure 4.8. | Differences in NK cell-mediated lysis of HLA-C-specific antibody-treated target cells.

A | Representative example shows the difference (Δ) in percentage target cell cytotoxicity measured with HLA-C-specific antibody treatment (grey bar) and no treatment (white bar). The percentage values indicate K562 and K562-C1 target cell cytotoxicity following an overnight incubation with IFN-α activated NK cells at 0.5:1 E:T ratio. Each condition was performed in triplicate wells. Bars represent mean±SEM percentage target cell cytotoxicity from six independent experiments (n=6). The percentage target cell cytotoxicity was calculated using standardised CountBright beads.

B | K562 and K562-C1 (HLA-Cw08*01) cells were treated with HLA-C1-specific alloantibody. The difference (Δ) in percentage target cell cytotoxicity was measured before and after antibody treatment. Each circle represents the average difference calculated from control and treatment responses from one healthy donor (n=7).

C | K562 and K562-C2 (HLA-Cw06*02) cells were treated with HLA-C2-specific alloantibody. The difference (Δ) in percentage target cell cytotoxicity was measured before and after antibody treatment. Each circle represents the average difference calculated from control and treatment responses from one healthy donor (n=4).

The circle colour represents the dominant inhibitory KIR expression on donor NK cells used in each experiment - KIR2DL1+ (red); KIR2DL3+ (blue); KIR2DL1+2DL3+ (green). Statistical analyses performed by Mann Whitney unpaired t-test; * p=0.03.

The effect of HLA-C-specific antibodies on HLA-C allele-transfected K562 target cells was analysed. NK cell-mediated target cell cytotoxicity was compared before and after antibody treatment. In the instance of HLA-C1-specific antibody treated K562-C1 cells (Figure 4.9A), target cell cytotoxicity was significantly greater than no antibody treatment. The same effect was observed with HLA-C2-specific antibody-treated K562-C2 cells (Figure 4.9B). On average, K562-C1 cells were lysed more efficiently by multiple NK cell donors in the absence of antibody treatment (32.1±3.7%) than K562-C2 cells (16.8±4.4%). Similarly, the average increase in target cell lysis following HLA-C-specific antibody treatment was greater with K562-C1 cells (44.7±3.2%) than K562-C2 cells (26.4±6.6%).

Inter-donor variability based on the KIR phenotype of the NK cells utilised in the assays was also observed. For example, NK cells comprising a large population of KIR2DL1$^+$ (red) or dual expressing KIR2DL1$^+$ KIR2DL3$^+$ (green) performed more efficiently at lysing untreated and HLA-C1-specific antibody-treated K562-C1 cells (Figure 4.9A). In contrast, NK cells with a dominant population of KIR2DL1$^+$ cells revealed variable cytotoxic responses towards K562-C2 target cells (Figure 4.9B). It is noteworthy that NK cells from HD002 (Figure 4.2C) with a high percentage of KIR2DL1$^+$ KIR2DL3$^+$ NK cells were more efficient at lysing K562-C1 target cells (28.3±0.8%) than K562-C2 target cells (18.4±2.1%) in the absence of antibody treatment. Following HLA-C-specific antibody treatment, HD002 NK cell-mediated K562-C1 cell cytotoxicity (42.9±1.1%) was greater than K562-C2 cell cytotoxicity (27.3±0.8%).

Together, the data in Figures 4.7 – 4.9 confirm that HLA-C-specific alloantibodies can mediate enhanced NK cell cytotoxic activation. Of note, this effect was more pronounced with the HLA-C1-specific antibody eluate against the K562-C1 cells compared to the use of HLA-C2-specific antibody on K562-C2 cells. Although an increase in K562 cytolysis was also observed following treatment with both antibody eluates, the difference was small compared to the enhancement of K562-C1 and -C2 cytolysis, suggesting a more specific functional ability of HLA-C-specific alloantibodies to induce NK cell hyperresponsiveness against HLA-C transfected target cells.

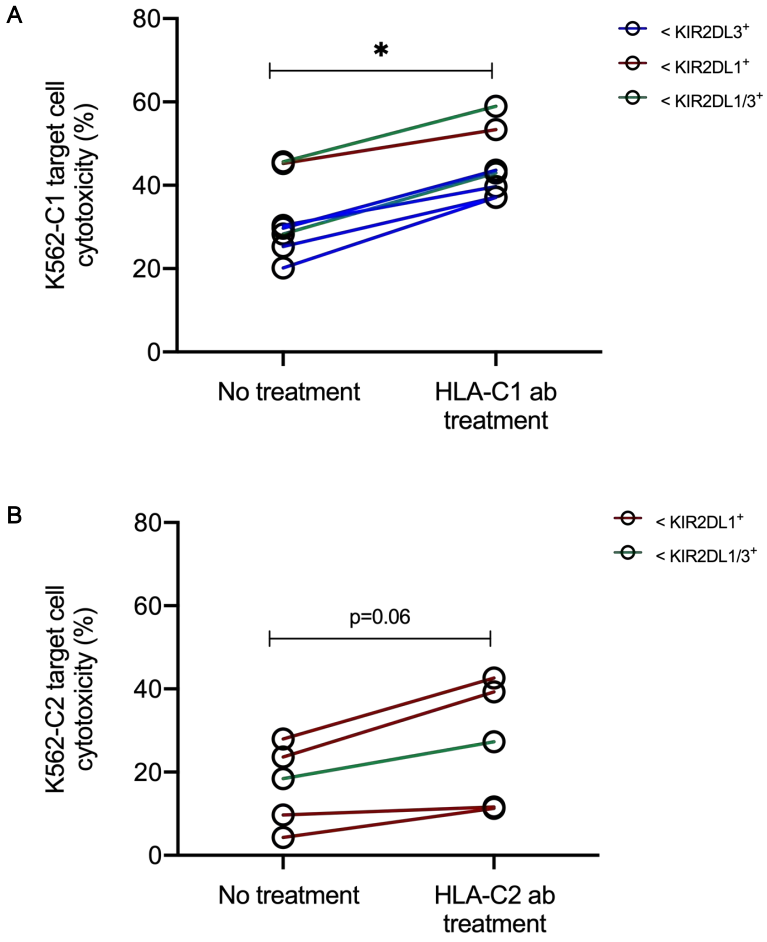

Figure 4.9. | Antibodies against HLA-C enhance NK cell function against HLA-C-transfected cells.

Target cells were treated with HLA-C-specific enriched alloantibodies for 30mins at room temperature. IFN-α activated NK cells were co-incubated with untreated or alloantibody-treated target cells at 0.5:1 E:T ratio in an overnight assay. Each condition was performed in triplicate wells.

A | K562-C1 (HLA-Cw08*01) cells were treated with HLA-C1-specific alloantibody. The percentage target cell cytotoxicity was measured before and after antibody treatment. Each circle represents the percentage target cell cytotoxicity calculated from control and treatment responses from one healthy donor (n=7).

B | K562-C2 (HLA-Cw06*02) cells were treated with HLA-C2-specific alloantibody. The percentage target cell cytotoxicity was measured before and after antibody treatment. Each circle represents the percentage target cell cytotoxicity calculated from control and treatment responses from one healthy donor (n=4).

Line colour represents the dominant inhibitory KIR expression on donor NK cells used in each experiment - KIR2DL1+ (red); KIR2DL3+ (blue); KIR2DL1+2DL3+ (green). The percentage target cell cytotoxicity was calculated using standardised CountBright beads. Statistical analyses performed by Wilcoxon matched-pairs signed rank test; * p=0.02.

4.5. Inhibition of ADCC-regulated NK cell cytotoxicity

Several studies have shown that cross-linking of Fc receptors on NK cells promote the effect of antibody dependent cell cytotoxicity (ADCC) (Binyamin et al., 2008; Borgerding et al., 2010). Therefore, a range of approaches were used to assess whether the effects of HLA-C-specific antibody observed in this study were simply related to ADCC rather than direct and specific inhibition of HLA-C:KIR interaction. To study the extent of FcγRIIIa involvement in facilitating NK cell activation against HLA-C-specific antibody coated target cells, either (i) NK cells were treated with a CD16-specific blocking antibody or (ii) HLA-C-specific alloantibodies were digested by a proteolytic enzyme IdeS, which prevented the ligation of the Fc fragment to CD16. These approaches aimed to limit the effect of ADCC mediated by the cross-linking of Fc receptors.

4.5.1. The effect of CD16 inhibition on NK cell function

The possible role of FcγRIIIa in regulating ADCC under the influence of HLA-C-specific alloantibody binding to target cells was examined. Enriched NK cells were incubated with purified CD16-specific antibody to assess whether the increase in target cell lysis reflected the influence of HLA-C:KIR blockade. Cytotoxicity was measured and compared using untreated (no CD16 blockade) NK cells and CD16-specific antibody-treated NK cells from multiple healthy individuals (Figure 4.10). CD16 blockade reduced cytolysis of HLA-C-specific antibody-treated K562-C1 and K562-C2 target cells compared to untreated NK cells. For example, in the instance of K562-C1, the average target cell cytotoxicity from multiple NK cell donors increased from 32.4±4.3% to 46.0±3.6%.

However, co-incubation of K562-C1 target cells with CD16-specific antibody-treated NK cells consistently led to a decrease in target cell cytotoxicity levels (36.7±2.1%) measured under no antibody treatment (or control) levels (Figure 4.10A). Moreover, the difference between percentage cytotoxicity observed under control and CD16 blockade conditions was not statistically significant ($P_{Friedman}$=0.75), implicating FcγRIIIa involvement in the mechanism by which HLA-C1-specific antibodies potentiate NK cell activation.

Analysis of CD16 blockade effect on lysis of K562-C2 target cells, however, presents a different result (Figure 4.10B). Compared to the no antibody treatment response (17.7±3.1%), increased lysis of K562-C2 cells (30.6±7.3%) following incubation with HLA-C2-specific antibody was largely retained following co-incubation with anti-CD16 treated NK cells (32.2±7.2%). In the case of one donor with a high proportion of NK-KIR2DL1 expression, CD16 blockade of NK cells led to a greater cytotoxic response towards HLA-C2-specific antibody coated K562-C2 cells (51.7±2.2%) compared to untreated NK cells (45.6±0.6%). This effect was observed within two out of three NK cell donors with a similar percentage of KIR2DL1^{+} NK cells. A statistical difference ($P_{Friedman}$=0.04) was observed between control and CD16-specific antibody treated NK cells conditions, suggesting that HLA-C2-specific alloantibodies have the capacity to regulate and enhance NK cell cytotoxic activation by an alternative mechanism to ADCC. These findings also indicate that two HLA-C allotype-specific antibody preparations act differently against corresponding HLA-C transfected alleles K562 target cells.

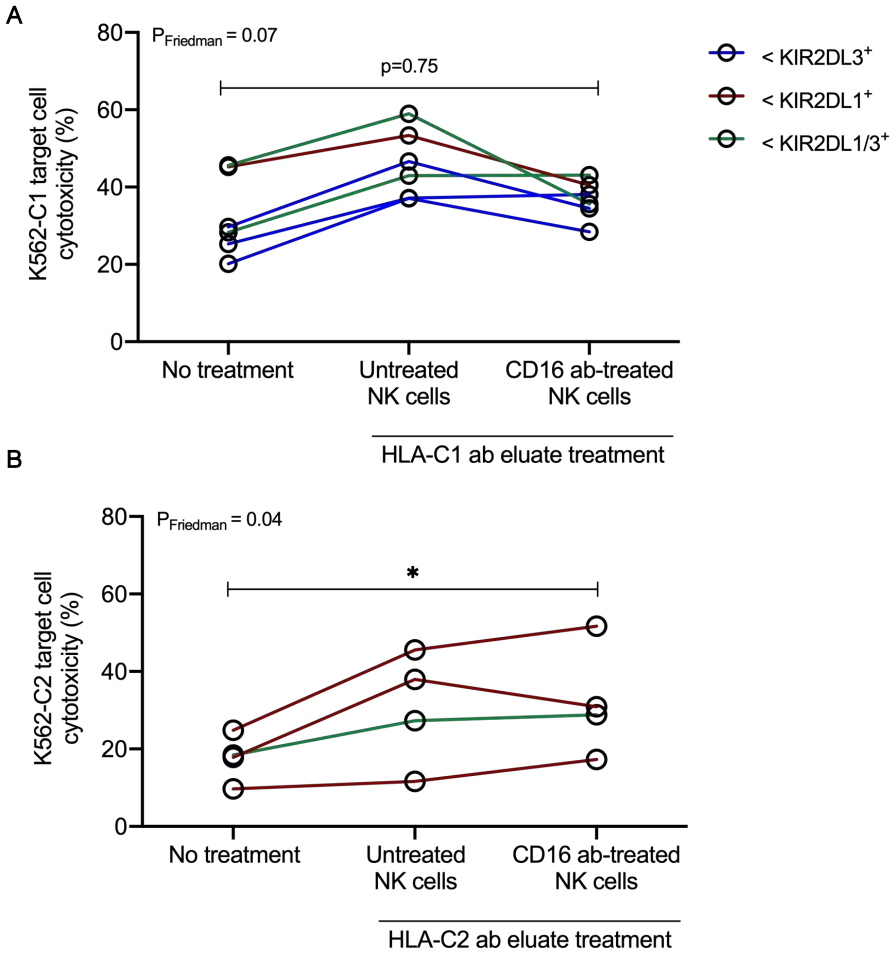

Figure 4.10. | The effect of CD16 blockade on NK cell mediated lysis of HLA-C-specific antibody-treated target cells.

Target cells were treated with HLA-C-specific enriched alloantibodies and NK cells were treated with CD16-specific antibody. NK cells and target cells were co-incubated at 0.5:1 E:T ratio in an overnight assay. Each condition was performed in triplicate wells. The percentage target cell cytotoxicity was measured before and after antibody treatment using untreated and CD16-specific antibody treated NK cells.

A | K562-C1 (HLA-Cw08*01) cells were treated with HLA-C1-specific antibody. Each circle represents the percentage target cell cytotoxicity calculated from control and treatment responses from one healthy donor (n=6).

B | K562-C2 (HLA-Cw06*02) cells were treated with HLA-C2-specific antibody. Each circle represents the percentage target cell cytotoxicity calculated from control and treatment responses from one healthy donor (n=4).

Line colour represents the dominant inhibitory KIR expression on donor NK cells used in each experiment - KIR2DL1+ (red); KIR2DL3+ (blue); KIR2DL1+2DL3+ (green). The percentage target cell cytotoxicity was calculated using standardised CountBright beads. Statistical analyses performed by One way ANOVA for non-parametric data, Friedman test with Dunn's multiple comparisons test; * p = 0.04.

4.5.2. The impact of IdeS-digested HLA-C-specific alloantibodies on NK cell function

As an alternative approach to CD16 blockade in limiting the effect of ADCC, HLA-C-specific alloantibody eluates were treated with Immunoglobulin G-degrading enzyme of *Streptococcus pyogenes* (IdeS). This proteolytic enzyme cleaves IgG at the hinge region, aiming to prevent FcγRIIIa-mediated activation of NK cells in this *in vitro* functional assay. IdeS was, therefore, used to assess the mechanism of action by which HLA-C-specific alloantibodies could increase target cell lysis by NK cells. In particular, if this effect was seen to be IdeS-independent, this would suggest that increased NK cell cytotoxic activation was acting at least partially via inhibitory KIR signalling.

Firstly, to confirm the IgG-cleaving activity of IdeS, HLA-C1 and -C2-specific antibody eluates were incubated with IdeS. Assessment of untreated and IdeS-treated antibodies' reactivity with K562 and HLA-C allele transfected cell lines was detected by flow cytometry (Figure 4.11A). As expected, due to the lack of MHC Class I expression on K562, HLA-C1 and -C2 antibody-specific eluates - untreated and IdeS-treated, showed no staining towards this cell line (Figure 4.11B). Comparatively, antibody binding was observed against the K562-C1 and K562-C2 cell lines (MFI = 5,790.76 and 9,049.04, respectively), but this was markedly reduced following IdeS treatment (MFI = 1,466.19 and 1,150.99, respectively). Furthermore, the lack of Fc fragment detection was also confirmed by single antigen luminex bead analysis. Together, these results reveal the efficient cleavage of enriched HLA-C-specific IgG *in vitro* by the enzyme IdeS.

It would be expected that the absence of the Fc fragment on the intact IgG molecule would prevent cross linking of Fc receptors, thus limiting NK cell activation. K562-C1 and -C2 target cells were exposed to IdeS-treated HLA-C-specific alloantibodies in the presence of NK cells (Figure 4.11C). The cytotoxicity was then measured and compared with other control conditions within the NK cell cytotoxicity assay. This approach aimed to confirm the mechanism of action of HLA-C-specific alloantibodies and the relative impact of ADCC blockade.

Following exposure to IdeS-digested HLA-C1-specific IgG, cytolysis of K562-C1 target cells reduced to levels measured under control conditions (Figure 4.11C; left). This effect is clearly observed in two out of three healthy NK cell donors with a high KIR2DL3 expression. One donor, however, demonstrated a largely retained cytotoxicity response after treatment with IdeS-digested HLA-C1-specific eluate (40.3%) compared to 40.0% cytolysis with untreated HLA-C1-specific eluate. Similarly, the HLA-C2-specific antibody eluate was largely effective at sensitising for lysis of K562-C2 target cells, even after IdeS treatment. Interestingly, this pattern is entirely consistent with that observed with the anti-CD16 treated NK cell activation responses, although no statistical significance was observed in this case (Figure 4.11C; right).

Based on the data generated from CD16 blockade of NK cells and Fc fragment digestion of HLA-C-specific antibodies, it appears that HLA-C1 and HLA-C2-specific antibody eluates are mediating increased target cell lysis via different NK cell activation mechanisms. HLA-C1-specific antibody effect was reduced to almost control levels when K562-C1 cells were exposed to anti-CD16 treated NK cells. A global reduction in K562-C1 target cell cytotoxicity was observed with all NK cell donors. This effect was not replicated by NK cell donors used for CD16 blockade and IdeS-treated antibody assays involving K562-C2 target cells. These data suggest that HLA-C1-specific antibodies mediate effects via ADCC, whilst HLA-C2-specific antibodies act largely through alternative mechanisms, most likely by blocking inhibitory signalling through KIR engagement.

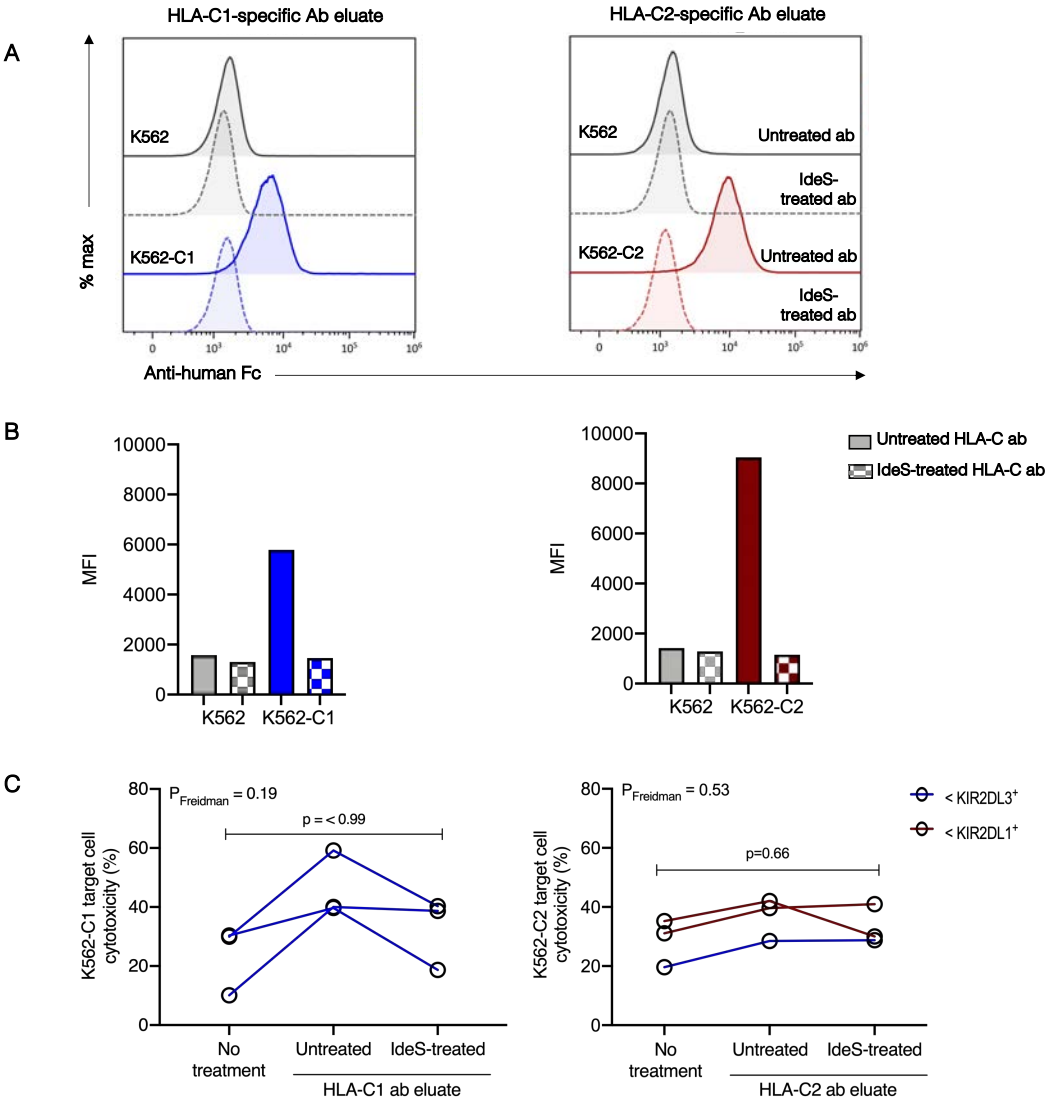

Figure 4.11. | The effect of IdeS on HLA-C-specific potentiation of NK cell function.

A | IdeS was incubated with enriched HLA-C-specific antibody eluates. Intact HLA-C1 (left panel) and HLA-C2-specific (right panel) IgG (solid lines) and IdeS-digested HLA-C antibody (dotted lines) were incubated with parental and HLA-C allotype transfected K562 cells followed by staining with anti-human Fc secondary antibody flow cytometry analysis.

B | Corresponding MFI values derived from flow cytometry analyses show the intact HLA-C-specific antibody reactivity against K56-C1 (left panel) and K562-C2 (right panel) in comparison to negative control cell line (K562) following IdeS-treatment. Solid bars represent intact HLA-C-specific IgG. Checkered bars represent IdeS-treated HLA-C-specific antibody.

C | Target cells were treated with either intact or IdeS-treated HLA-C1-specific (left) and HLA-C2-specific (right) enriched alloantibodies, and co-incubated with NK cells at 0.5:1 E:T ratio in an overnight assay. Each condition was performed in triplicate wells. Line colour represents the dominant inhibitory KIR expression on donor NK cells used in each experiment - KIR2DL1+ (red) or KIR2DL3+ (blue). The percentage target cell cytotoxicity was calculated using standardised CountBright beads. Statistical analyses performed by Two way ANOVA non-parametric Friedman test with Dunn's multiple comparisons test.

4.6. Functional recognition of inhibitory KIR2DL1 and HLA-C2 ligand using an NK cell line

To further determine the impact of HLA-C-specific alloantibodies in mediating increased target cell lysis, in the presence and absence of CD16, the NK92 cell line was used as an alternative source of effector cells in the *in vitro* assays. NK92 is a highly cytotoxic human NK cell line of lymphoma origin that does not express KIRs or CD16 (Gong et al., 1994). The cytotoxic function and sustained growth of NK92 cells are strictly dependent upon interleukin-2 (IL-2). Firstly, the lack of KIR expression on NK92 was confirmed by flow cytometry (Figure 4.12). Secondly, the NK cell line was transduced using either a lentiviral or retrovirus system to stably express inhibitory KIRs – *2DL1, 2DL2* and *2DL3* (Figure 4.13). Thirdly, the impact of single inhibitory KIR expression on recognition of HLA-C allele-transfected targets in the presence and absence of HLA-C-specific antibody was measured (Figure 4.14).

4.6.1. Generation of single KIR-expressing human NK cell lines

To confirm the absence of KIR expression on NK92 and NKL cell lines, antibodies against KIR2DL1/S1/S3/S5, KIR2DL2/3, KIR3DL1 and KIR3DL2 were used for flow cytometry analysis (Figure 4.12A). In comparison to unstained cells, both human NK cell lines showed no KIR antibody binding, thus confirming the lack of expression. Next, using lentiviral and retroviral transduction technology, single inhibitory KIRs were introduced into NK92 cells. *KIR2DL2* and *KIR2DL3* were transduced separately into NK92 cells whilst *KIR2DL1* and *GFP* were transduced to generate stably expressing KIR cell lines, respectively.

Following lentiviral transduction, low KIR2DL3-NK92 expression level was measured, whereas no KIR2DL2 expression was observed on transduced NK92 cells (Figure 4.12B). *KIR2DL1*, however, was introduced into NK92 using a retroviral system, whilst green fluorescent protein (*GFP*) enabled a measure of efficiency (Figure 4.12C). Next, using FACS, pure KIR^+ NK92 cell populations were obtained which were subsequently propagated and maintained in culture. Unfortunately, *KIR2DL3* gene transduced NK92 cells failed to survive in culture post-FACS due to low cell number. Approximately 0.5% of NK92-KIR2DL1-GFP^+ population was selected post-transduction and sorted via FACS (Figure 4.12C). This KIR-expressing population was propagated in culture until >75% of the total cell line population were dual KIR2DL1 and GFP-expressors. CD16-negative, NK92-KIR2DL1-GFP cells were subsequently used as effectors for flow cytometry-based cytotoxicity assay (Figure 4.12D).

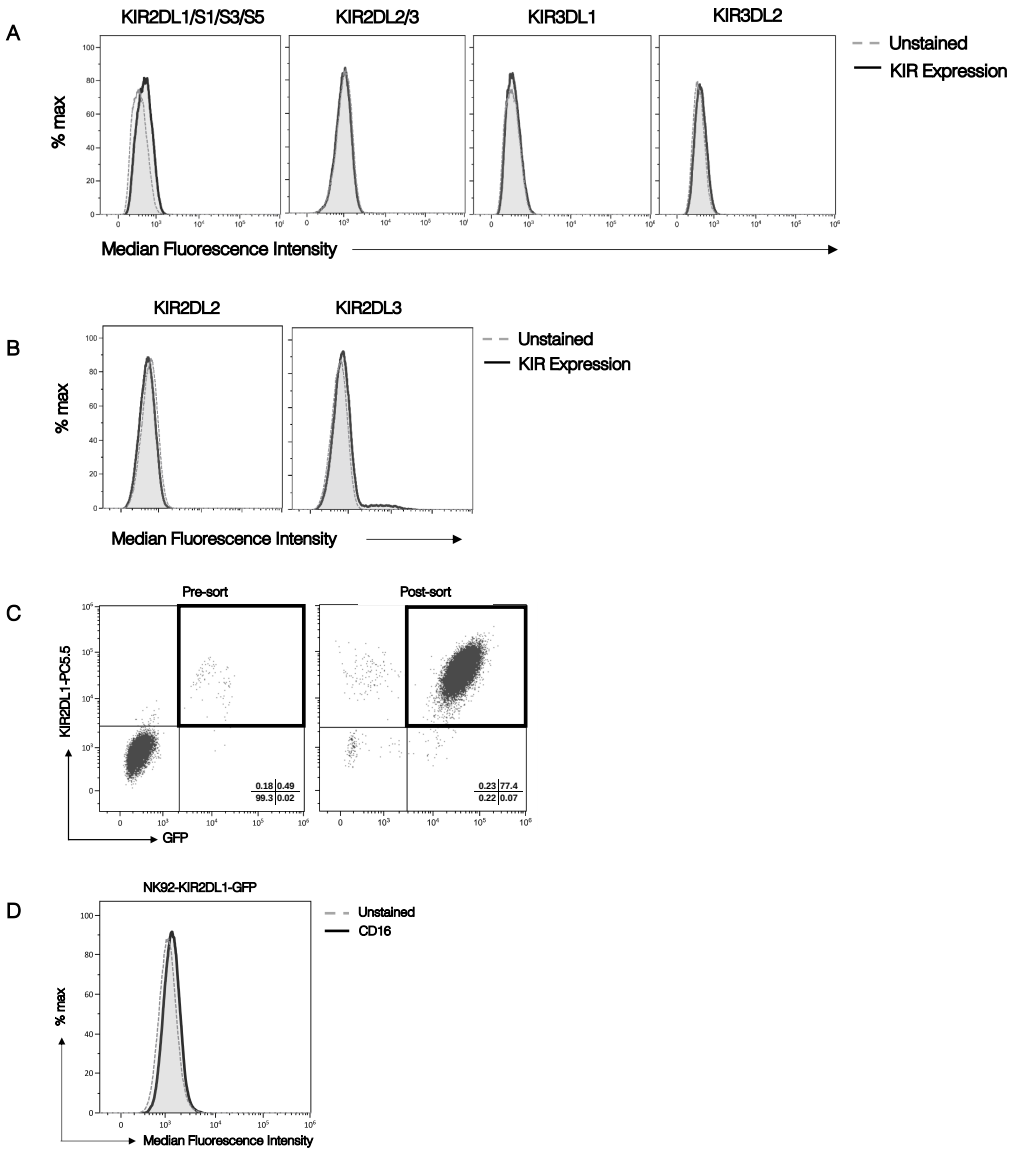

Figure 4.12. | Single inhibitory *KIR* gene transduction into NK92 cell line.

A | Characterisation of KIR expression on NK92 cell line using flow cytometry. KIR2DL1/S1/S3/S5, KIR2DL2/3, KIR3DL1 and KIR3DL2 surface expression on NK92 cells were analysed.

B | Following lentiviral vector transduction, no KIR2DL2 expression (left panel) but KIR2DL3 expression (right panel) was detected (solid black line) on NK92 cells compared to unstained cells (dashed grey line).

C | KIR2DL1 and GFP were transduced into NK92 cell line using the retroviral vector system. Dual KIR2DL1 and GFP-expressing NK92 cells (0.49%) were sorted via FACS and propagated into a cell line.

D | Confirmation of lack of CD16 expression (black solid line) on KIR2DL1-expressing NK92 cell line by flow cytometry compared to unstained cells (dashed grey line).

4.6.2. Optimisation of an NK92-KIR2DL1 cell line-based functional assay

To determine the optimal E:T ratio, K562 target cells were co-cultured with different concentrations of NK92 cells. The effect of IL-2 pre-conditioning on NK92 cell activation toward K562 cells was also investigated (Figure 4.13A). Following co-incubation of K562 cells with NK92 at E:T ratios ranging from 1:1 to 20:1, effector cells cultured with IL-2 conditioned medium displayed higher levels of target cell lysis. Maximal cytotoxicity was observed at 20:1 E:T ratio under IL-2-independent stimulation (62.2±2.6%) whilst IL-2-dependent NK92 cells were more efficient at 10:1 E:T ratio with 81.9±0.7% K562 cytolysis. This functional assay confirmed the importance of IL-2 in NK92 cell line activation and function.

Based on these findings, the NK92-KIR2DL1 cell line, also pre-conditioned with IL-2, was co-incubated with K562-C2 target cells. This assay determined the sub-optimal E:T ratio required to assess functional significance of single KIR2DL1 and HLA-C2 ligand interactions (Figure 4.13B). A sub-optimal K562-C2 percentage cytotoxicity (34.8±3.1%) was detected at an E:T ratio of 5:1, which was selected to potential measurement of HLA-C2-specific potentiation of K562-C2 cytolysis.

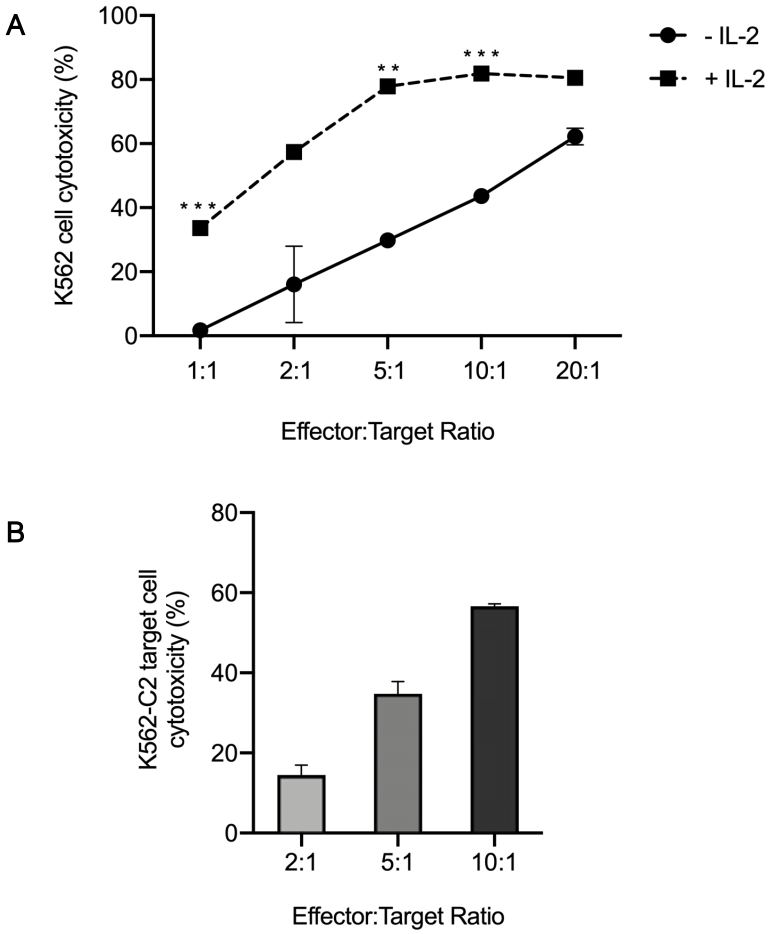

Figure 4.13. | Determining the optimal E:T ratio for NK92-KIR2DL1 cell line-based cytotoxicity assay.

A | Varying number of parental NK92 cells, pre-conditioned with IL-2 (square) or control (circle) medium were incubated with K562 cells overnight to determine the effect of IL-2 on NK92 cell cytotoxic function. Each condition was performed in triplicate wells. The average percentage K562 cell cytotoxicity displayed with standard error of the mean. Statistical significance obtained by two way ANOVA with multiple comparisons mixed model analysis; ** $p < 0.01$; *** $p < 0.001$. Data indicates one independent experiment (n=1).

B | IL-2 conditioned NK92-KIR2DL1 cells were co-incubated with K562-C2 target cells to determine optimal E:T ratio for cytotoxicity assays. The percentage target cell cytotoxicity was calculated using standardised CountBright beads. Bars represent mean ± SEM. Each condition was performed in triplicate wells. Data indicates one independent experiment (n=1).

4.6.3. HLA-C2-specific alloantibody-dependent NK92-KIR2DL1 responses

To determine whether HLA-C2-specific alloantibodies could enhance the cytotoxic activity of NK92-KIR2DL1 against K562-C2 target cells, a functional assay similar to that utilising healthy donor NK cells as effectors in the previous sections was performed. Live eFluor670-labelled K562-C2 cells were quantified using flow cytometry, following exposure to HLA-C2-specific alloantibodies and co-cultured overnight with NK92-KIR2DL1 cells. Percentage target cell cytotoxicity was calculated by using counting beads as a standard.

In the first approach, K562 and K562-C2 target cell cytotoxicity was measured after HLA-C1 and -C2-specific alloantibody treatment (Figure 4.14A). In the absence of HLA-C alloantibody exposure, K562-C2 cytolysis was significantly lower (3.0±2.7%) confirming functional inhibitory recognition of the HLA-C2 ligand by KIR2DL1. Treatment with HLA-C1-specific alloantibodies increased K562-C2 lysis to 7.2±2.3%. In contrast, K562 cytolysis was reduced from 22.6±1.6% to 18.0±1.5%. Importantly, compared to control conditions, HLA-C2-specific antibody-treated K562-C2 cells showed an increase to 15.0±2.9% in NK92-KIR2DL1-mediated lysis, whilst K562 cell lysis response remained similar to control levels (20.8±0.6%).

Next, K562-C2 cells were exposed to untreated and IdeS-treated HLA-C2-specific alloantibody and subsequently co-cultured with NK92-KIR2DL1 cells (Figure 4.14B). This assay aimed to further confirm and validate the functional capacity of HLA-C2-specific alloantibody to inhibit KIR2DL1 and HLA-C2 interaction, and to assess the importance of ADCC. HLA-C2-specific antibody-coated K562-C2 cells were lysed more efficiently (28.7±3.2%) than control target cells (19.3±6.0%). This effect was highly reproducible. Moreover, this response persisted with IdeS-digested HLA-C2-specific IgG (28.0±6.9%) demonstrating that antibody binding to HLA-C most likely modulates NK92 cell cytotoxicity by blocking the HLA-C:KIR interaction in the absence of ADCC responses.

These data confirm that HLA-C2 expression on target cells reduces lysis by NK92 cells which express KIR2DL1. In addition, treatment of these target cells with a negative control HLA-C1-specific alloantibody eluate does not significantly increase cytolysis. However, HLA-C2-specific alloantibodies demonstrate an increase in target cell cytotoxicity by 12%. Finally, the lack of CD16 expression on NK92-KIR2DL1 cells confirms that the ability of HLA-C-specific alloantibodies to stimulate effector cell function is independent of ADCC and most likely acts via blockade of KIR engagement.

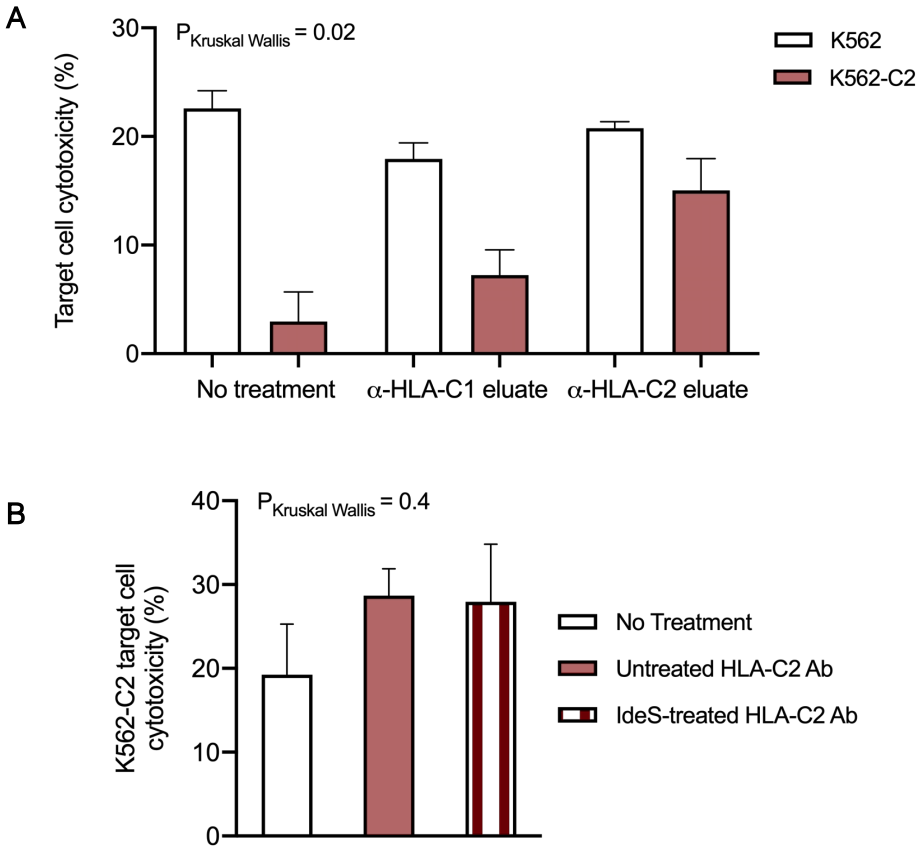

Figure 4.14. | HLA-C-specific antibody modulation of NK92-KIR2DL1 cytotoxicity.

A | K562 (white bar) and K562-C2 (red bar) were treated with HLA-C1 and HLA-C2-specific enriched antibodies. IL-2 conditioned KIR2DL1-NK92 cells were co-incubated with antibody-treated target cells at 5:1 E:T ratio in an overnight assay. Percentage target cell cytotoxicity was analysed using flow cytometry and calculated using standardised CountBright beads. Bars represent mean ± SEM from one independent experiment (n=1). Each condition was performed in triplicate wells.

B | K562-C2 target cells were treated with HLA-C2-specific enriched antibody. IL-2 conditioned KIR2DL1-NK92 cells were co-incubated with untreated (white bar); intact IgG (red bar) and IdeS-treated IgG (striped bar) target cells at 5:1 E:T ratio in an overnight assay. Percentage target cell cytotoxicity was analysed using flow cytometry and calculated using standardised CountBright beads. Bars represent mean±SEM from four independent experiments (n=4). Each condition was performed in triplicate wells.Statistical analysis performed with One way ANOVA with Kruskal Wallis for non-parametric data with Dunn's multiple comparisons test.

4.7. Discussion

The main objective of this chapter was to develop *in vitro* functional assays that assess the function of antibodies against HLA-C in impacting NK cell-mediated target cell cytotoxicity. Using a standardised flow cytometry-based NK cell cytotoxicity assay, the findings show that HLA-C-specific alloantibodies enhance NK cell activation. These data highlight a potential value for HLA-C-specific antibodies in enhancing NK cell function in diseases such as cancer to induce tumour cell deletion.

4.7.1. NK cell KIR repertoires

A number of studies have implicated specific HLA-C-KIR combinations as risk factors for diseases, including autoimmunity, infection, pregnancy and cancer (Hiby et al., 2004; Khakoo et al., 2004; Jobim et al., 2013; Machado-Sulbaran et al., 2019). These combinations appear to influence the susceptibility to, or the severity of the disease by modulating immune function. To select suitable healthy NK cell donors with specific inhibitory KIR expression for analysing KIR:HLA-C interactions in the NK cell functional assays, the NK cell KIR repertoire was characterised by flow cytometry for this study. Traditionally, donors are genotyped using single specific primer-polymerase chain reaction (SSP-PCR) to determine KIR gene expression for an accurate analysis. The results from KIR SSP-PCR are subsequently confirmed by an extensive flow cytometry phenotypic analysis (Uhrberg, 2005; David et al., 2009; Czaja et al., 2014). The lack of ethics approval to sequence DNA from healthy individuals limited investigation into their KIR genotypes.

Although the *KIR* gene cluster is highly polymorphic (Parham and Guethlein, 2018), in the current study, the highest level of expression of inhibitory KIRs was observed for the KIR2DL2/3/S2 cluster. This finding may partly reflect the fact that these KIRs were all identified by one antibody clone. In contrast, the level of KIR3DL3 expression was virtually undetectable on $CD56^{dim}$ NK cells from the healthy donor cohort. Phenotypically, KIR3DL3 surface expression is either very low or rarely detectable on peripheral blood NK cells (Trundley et al., 2006) due to the epigenetic silencing of the *KIR3DL3* gene (Trompeter et al., 2005).

Interestingly, five donors revealed a large population of $CD56^{dim}$ NK cells (>50%) as $KIR2DS4^{+}$. Despite the high frequency of $KIR2DS4^{+}$ NK cells, this subset was highly unlikely to play a role in this study of HLA-C allotypes and inhibitory KIR interactions. This study utilised target cells transfected with HLA-C1 allotype C*08:01 or HLA-C2 allotype C*06:02 which are not recognised by KIR2DS4. Therefore, the lack of stimulation, which would otherwise lead to NK cell activation, was absent and thus unlikely to influence the overall NK cell functional response.

Although the inhibitory KIR repertoire is thought to be highly variable, the average frequency of $KIR2DL1^{+}$ or $KIR2DL3^{+}$ NK cells in the healthy donor cohort was similar. KIR acquisition and expression is primarily characterised by two models which support either random or sequential acquisition of KIRs (Held et al., 1996; Raulet et al., 1997). The extent of HLA Class I molecules involved in KIR acquisition and expression is unclear (Andersson et al., 2009), but there is a strong possibility that cognate HLA-C ligands impact KIR repertoires at the genetic and protein expression levels, as has been described for KIR2DL1 (Yawata et al., 2006). Moreover, the range of single $KIR2DL1^{+}$ or $KIR2DL3^{+}$ NK cell subset frequency was variable between healthy donors.

Low frequencies of single KIR2DL1$^+$ or KIR2DL3$^+$ NK cells can possibly be explained by high donor HLA-C expression, which is also known for affecting NK cell functional responses (Sips et al., 2016). By taking advantage of these proposed hypotheses, the current study utilised NK cells from healthy donors with a dominant proportion of either KIR2DL1$^+$ or KIR2DL3$^+$ NK cells. The aim was to maximise the NK cell cytotoxic effect when HLA-C-specific antibodies prevented NK cell ligation to cognate KIR ligand on target cells.

4.7.2. HLA-C and inhibitory KIR interactions

The strength of inhibition hypothesis characterises the strength of the HLA-C-KIR interaction, and therefore the resulting level of inhibitory signalling will determine the ultimate NK cell functional outcome (Rajagopalan and Long, 2005). The KIR2DL1:HLA-C2 interaction is thought to be of higher affinity than the interaction between KIR2DL3 and HLA-C1. Therefore, weaker inhibitory interactions induce a greater NK cell activating response and less inhibition. This effect is reflected in this study as K562-C1 cells were lysed more efficiently than K562-C2 cells (Figure 4.5), despite K562-C1 cells being co-incubated overnight with NK cells comprising a dominant proportion of KIR2DL3$^+$ effectors.

Perhaps the efficiency of NK cell mediated lysis of single HLA-C allele-transfected cells might also be dependent upon the HLA-C ligand density on target cell surface i.e. the inhibition threshold. Due to the variegated KIR expression on NK cells, KIR2DL1 levels have shown to determine the inhibition threshold involving HLA-Cw6 ligand (Almeida et al., 2011). This observation is further supported by the 'rheostat' model whereby the activation of each NK cell is quantitatively tuned by the number of inhibitory signals

received during education (Brodin et al., 2009b). However, to test this proposed hypothesis effectively, it is vital to determine degranulation responses and/or IFN-γ secretion following NK cell stimulation which were not evaluated in this study. Instead the HLA-C ligand density on surface of target cells was tested by HLA loci-specific antibodies (Chapter III). Median fluorescence intensity (MFI) values derived from HLA-C-specific antibody staining (DT-9 clone) showed comparable HLA-C1 (MFI = 3,610.5) and HLA-C2 (MFI = 2,724.5) surface expression. This suggests that HLA-C ligand density was not a major determinant of the differences that were observed in relation to the ability of the two HLA-C allotypes to inhibit NK cell mediated cytotoxicity.

It can be speculated that licensing of NK cells during differentiation is likely to act as a determinant of their functional activity as licensed NK cells degranulate with a greater capacity in the absence of cognate HLA-C ligands (Yu et al., 2007) . Sim et al. (2016), however, have shown that KIR2DL1 and KIR2DL3 confer a similar impact on licensing and that the number of ligands is not important for NK cell education. Therefore, the influence of the 'strength of inhibition' on NK cell licensing i.e. weak HLA-C licensing imparting a weak NK cell response is not likely to play a role in the differences observed between K562-C1 and -C2 target cell lysis.

It may be the case that the differences observed in inhibition of NK cell cytotoxicity was most likely to result from the individual strength of HLA-C1 and HLA-C2 interactions with KIR proteins. It is important to account for the inter-donor variability observed in NK cell responses, but the general trend observed in the current study points to K562-C1 target cells being more susceptible to NK cell-mediated lysis than K562-C2 target cells.

Interestingly, even in the presence of a dominant percentage of KIR ligand mismatched NK cells, e.g. K562-C1 cells co-incubated with NK cells from HD002 (< KIR2DL1$^+$ KIR2DL3$^+$) or HD001 (< KIR2DL1$^+$), NK cell cytotoxicity of K562-C1 cells was significantly greater than the donors with dominant KIR2DL3$^+$ NK cell population. This effect was not observed with K562-C2 target cells. Therefore, more experiments with multiple KIR ligand mismatched NK cell donors are required to establish an alloreactive effect against target cells.

4.7.3. HLA-C-specific antibodies increase NK cell responses

Prior to analysing the effect of enriched HLA-C1 or HLA-C2-specific antibodies on NK cell function, DT-9 antibody treatment of K562 cells demonstrated a greater cytotoxicity response compared to K562-C1 and K562-C2 cells. This suggested that DT-9 antibody enhanced NK cell function against K562 cells. However, K562 cell line is considered as MHC Class I-deficient and is a prime example of target cells to study NK cell cytotoxicity responses. Nonetheless, low HLA-C expression on K562 cells has been reported (Le Bouteiller et al., 2002), whilst Boegel et al. (2014) confirmed HLA-C*05 (HLA-C2) expression by RNA sequencing. Together, these data indicate that DT-9 antibody possibly masked HLA-C*05 recognition by KIRs, enhancing NK cell activation. Although DT-9 antibody binding to K562 cells (MFI = 345.0) was much lower than K562-C2 (MFI = 2,724.5), a modest increase in K562-C2 lysis was also observed after DT-9 antibody treatment. However, K562-C1 and K562-C2 cytolysis was not as high as K562 cytolysis, indicating that DT-9 antibody-coated K562 cells caused a non-specific increase in NK cell activation. It can be further speculated that the presence of an HLA-C ligand on target cell surface prevented a non-specific increase in K562-C1 and K562-C2 cell lysis.

Compared to enriched HLA-C-specific antibodies, DT-9 antibody was unable to enhance NK cell cytotoxic function to the same level. A consistent increase in target cell lysis was observed when NK cells were exposed to HLA-C-specific antibody-coated target cells. These results are in line with published data utilising murine monoclonal antibodies (Lobo and Spencer, 1989) and human HLA Class I antibodies (Nathan and Scobell, 2012; Legris et al., 2016). Importantly, the increase in the lysis of HLA-C1 allele transfected target cells was more significant ($p < 0.05$) than the cytotoxicity observed with HLA-C2 allele expressing target cells ($p = 0.06$) (Figure 4.7A). Similar to the effect observed with DT-9 antibody-treated K562 cells, an increase in cytolysis was measured following HLA-C-specific antibody treatment, though this response was likely to be non-specific.

In the instance of K562-C1 antibody treatment (Figure 4.9A), two NK cell donors categorised as alloreactive or KIR ligand mismatched were used in the functional assays. It can be speculated that these alloreactive NK cells readily lysed K562-C1 target cells due to the absence of cognate HLA-C2 ligand, particularly in the case of KIR2DL1$^+$ NK cells (red), whilst KIR2DL1$^+$ KIR2DL3$^+$ NK cells (green) received insufficient inhibitory signalling. NK cells from multiple healthy donors with a high KIR2DL3$^+$ frequency performed comparably under control conditions as well as post-HLA-C1-specific antibody treatment of K562-C1 target cells. Thus far, these findings indicate that HLA-C-specific antibodies can render target cells more susceptible to NK cells by 'masking' relevant surface antigens that are normally responsible for maintaining tolerance to NK cells. However, mechanisms by which these antibodies were enhancing NK cell function in this *in vitro* model were unclear.

In addition to ADCC, antibodies are known to function by activating the complement cascade but as this model utilised NK cells enriched from PBMCs, the resulting co-cultures of HLA-C antibody-bound target cells and NK cells were absent of complement proteins, preventing cascade activation. Therefore, the effect of ADCC mediated by the ligation of Fc receptors to the Fc fragment of HLA-C IgG and the impact on NK cell function was examined in detail.

4.7.4. Influence of FcγR and intracellular NK cell signalling on effector cell function

Two experiments were performed to limit the ADCC effect. Firstly, CD16 blockade with a CD16-specific antibody significantly abrogated the enhanced NK cell mediated lysis of target cells coated with HLA-C-specific antibodies, though inter-donor variability was observed (Figure 4.10). Whilst some donors demonstrated a complete abrogation of antibody-dependent enhanced NK cell activation, others retained a threshold of increased function. Human FcγRIIIa and b polymorphisms on NK cells can influence ligand binding e.g. inefficient interaction with IgG, which in turn, impact NK cell function (Deeg et al., 1997) in autoimmunity and anti-cancer therapeutics, notably with rituximab treatment (Capuano et al., 2015). This effect is also observed in the current study with rituximab-treated primary B-CLL cells in the presence of CD16-specific antibody-treated NK cells (Chapter V; Figure 5.10). Moreover, some NK cell donors did retain enhanced NK cell function despite CD16 blockade. This indicates that although ADCC plays a role in enhancing NK cell activity, another mechanism of action of HLA-C-specific antibodies may also be in operation.

Secondly, to study the effect of the Fc region of HLA-C-specific alloantibodies, the enzyme, IdeS was used to digest the antibody at the hinge region to separate the Fab and Fc fragments. Although the Fab fragment retained reactivity to the HLA-C molecule, the cleavage of the Fc fragment reduced NK cell function in some cases (Nathan and Scobell, 2012). In this study, enhanced NK cell function mediated by HLA-C1-specific antibodies was maximally abrogated, but the same effect was not observed in the presence of HLA-C2-specific antibodies (Figure 4.11C).

To further examine the potential importance of CD16 engagement and ADCC in antibody mediated potential of NK cell cytotoxicity, NK cell line NK92, which lacks CD16 expression was utilised. The transduction of single inhibitory KIR proteins facilitated a more detailed analysis of the responses observed in this study. The enhanced cytolysis of K562-C2 target cells following HLA-C2-specific antibody exposure was not due to increased target cell-effector cell complex formation i.e. HLA-C-specific antibody and CD16 ligation, but an effect of increased NK cell signalling favouring activation as KIR2DL1 was not engaged. This ADCC-independent response was further confirmed through the use of IdeS-digested HLA-C2-specific antibody (Figure 4.14B).

Taken together, these data indicate that HLA-C-specific antibody-dependent enhanced NK cell responses in this biologically variable system are partially mediated through ADCC, but this is dependent on the HLA-C allotype specificity of the antibody. HLA-C1-specific antibody eluate cytotoxicity data suggests the antibody preparation to be working in an ADCC-dependent manner, whilst HLA-C2-specific antibody eluate retains NK cell-mediated target cytotoxicity following CD16 blockade and Fc fragment removal in an ADCC-independent response.

In line with the strength of inhibition hypothesis, as KIR2DL1:HLA-C2 interaction is of higher affinity compared to KIR2DL3:HLA-C1, the retained NK cell activation against K562-C2 cells was a consequence of the balance of signals within NK cells skewed towards activation. This effect persisted as KIR2DL1 did not recognise and bind to the antibody masked HLA-C2 ligand. Further detailed analyses are required to determine the impact of HLA-C-specific antibodies on NK cell function and the antibody binding affinity to HLA-C allotypes.

4.8. Conclusions

This chapter aimed to investigate the potential of HLA-C blockade in enhancing NK cell function. Phenotypic analyses of NK-KIR repertoires identified suitable donors with a high proportion of NK cells expressing either single HLA-C2 ligand-specific KIR2DL1 or HLA-C1 ligand-specific KIR2DL3 and dual-expressing KIR2DL1 and KIR2DL3 NK cell subsets. These NK cells were subsequently utilised in functional assays to study NK cell function in response to HLA-C allele-specific alloantibodies disrupting HLA-C ligand and inhibitory KIR interactions. Both HLA-C1-specific and HLA-C2-specific alloantibodies significantly enhanced lysis of K562-C1 and K562-C2 target cells, respectively, demonstrating the potential of HLA-C blockade at boosting NK cell function. Further assessment of mechanism of actions involved in HLA-C-specific alloantibody-dependent responses revealed that HLA-C-specific antibodies act to enhance NK cell mediated cytotoxicity through two mechanisms – ADCC-dependent which is likely to be HLA-C1 antibody eluate-specific, whilst the cell line adsorbed HLA-C2 antibody eluate appears to maintain NK cell-mediated cytotoxicity through direct inhibition of HLA-C:KIR engagement. These findings suggest that HLA-C1 and HLA-C2-specific antibody preparations behave differently due to the particular antibody repertoire and epitopes being recognised. Moreover, these data strongly lend support to antibodies against HLA-C harnessing the inhibitory KIR and NK cell intracellular signalling to shift inhibition signals towards activation and enhancing NK cell function.

CHAPTER V

THERAPEUTIC POTENTIAL OF HLA-C-SPECIFIC ANTIBODIES IN CANCER

5.1. Introduction

Loss or downregulation of HLA Class I in cancer is a phenomenon that facilitates tumour escape and has been reported in a number of invasive tumours, including cancers of breast, colon, melanoma and pancreas (Garrido et al., 1997) and tumour cell lines (Seliger et al., 2002). Whilst these strategies primarily promote escape from T cell mediated attack, the absence of 'self'-HLA ligands render tumour cells susceptible to NK cells. However, tumour cells have evolved to avoid NK immune surveillance by engaging in several different strategies that ultimately aim to reduce NK cell function. These strategies include greater surface density of HLA Class I molecules (Classen et al., 2003; Kowalewski et al., 2015), particularly HLA-C which often leads to increased association with their receptors, promoting disease progression (Naumova et al., 2005; Campillo et al., 2013; Jobim et al., 2013). Other upregulated inhibitory ligands include HLA-E (lo Monaco et al., 2011) and HLA-G (Lin and Yan, 2015). Therefore, the interaction between NK cell inhibitory receptors and HLA-C/-E/-G ligands prevent tumour cell deletion.

Recent studies have shed light on a new form of 'checkpoints' for NK cell-based immunotherapy that target NK cell dysfunction in cancer. Anti-NKG2A antibody inhibits interaction with cognate HLA-E ligand and has demonstrated a boost in anti-tumour NK cell responses (André et al., 2018). HLA-G ligand blockade increased tumour cell susceptibility to NK cells (Maki et al., 2008). Anti-KIR therapy is considered as an attractive alternative strategy to ADCC which inhibits HLA-C and iKIR interaction to unleash NK cells from a state of inhibition. Limitations to KIR blockade therapy include trogocytosis of surface KIR2D molecules and hyporesponsive NK cells (Carlsten et al., 2016). Therefore, this study aimed to target the same HLA-C-iKIR pathway but with human HLA-C-specific alloantibodies to investigate their therapeutic potential against tumour cells.

In this chapter, HLA expression on solid tumour cell lines and leukaemia cells from Chronic Lymphocytic Leukaemia (CLL) patients was characterised. This included total HLA Class I, HLA-C and HLA-E expression analysis by flow cytometry. HLA-C allelic variant expression was analysed using HLA-C1 and -C2-specific alloantibodies enriched from renal transplant patient sera. Following determination of HLA-C allotype expression, cytotoxicity assays were performed using primary NK cells from healthy donors or KIR2DL1-expressing NK92 cells as effector cells. Solid tumour cell lines and primary B-CLL cells were exposed to relevant HLA-C allele-specific alloantibodies and subsequently co-incubated with effector cells. HLA-C-specific alloantibody mechanism of action was also examined by performing CD16 blockade on NK cells or with Fc fragment-deficient HLA-C-specific alloantibodies.

5.2. HLA Class I expression on solid tumour cell lines

5.2.1. Characterisation of HLA Class I expression

To analyse the surface expression of HLA Class I proteins, particularly HLA-C, four ovarian cancer, three pancreatic cancer, one epidermoid carcinoma and one melanoma cell lines were immunophenotyped via flow cytometry. Monoclonal antibody clone W6/32 specific for pan-HLA Class I proteins and DT-9 antibody clone directed against HLA-C were used. The expression levels were shown as the relative MFI value compared with the isotype antibody control staining.

All tumour cell lines revealed high surface HLA Class I (HLA-A, -B and -C) expression levels (Figure 5.1A). Comparatively, HLA-C expression was weakly positive across most cell lines with the exception of SKOV-3 (ovarian) and A431 (epidermoid carcinoma), where high HLA-C expression was observed (Figure 5.1B). Overall, the MFI staining of DT-9 antibody staining of all solid tumour cell lines revealed a range of low/weakly positive and moderately positive staining patterns (Figure 5.1C). For example, cell lines including CAOV-1, SUIT-2 and A375 showed low or no HLA-C expression with relative MFI value of less than 1. Moderate HLA-C expression levels with MFI value of less than 2 were observed in A2780 and OVCAR-3 (ovarian) and PANC-1 (pancreatic) cell lines. Increase in DT-9 staining MFI values of A431 and SKOV-3 cell lines were distinctly greater than other cell lines (relative MFI = 2.47 and 2.97, respectively).

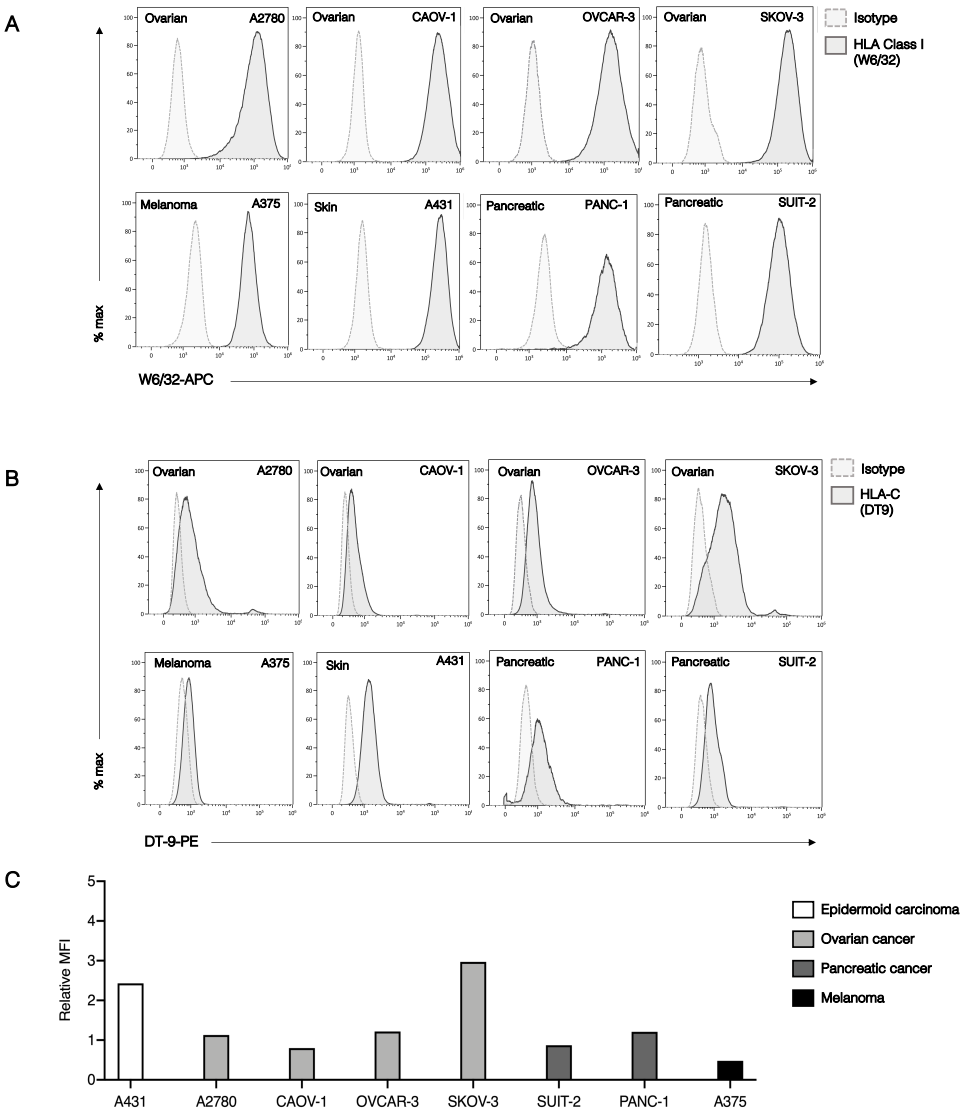

Figure 5.1. | HLA Class I expression on solid tumour cell lines.

Various solid tumour cell lines were stained with W6/32-APC or DT-9-PE antibodies. The data were collected using the Beckman Coulter Gallios flow cytometer and analysed by the Kaluza software.

A | W6/32-APC antibody (solid grey line) and mouse IgG2a, κ isotype control (dotted grey line) were used to determine HLA Class I expression.

B | DT-9-PE antibody (solid grey line) and mouse IgG2b, κ isotype control (dotted grey line) was used to determine HLA-C expression.

C | Relative median fluorescence intensity values of DT-9 staining compared to isotype control staining for all solid tumour cell lines – A431 (epidermoid skin; white bar); A2780, CAOV-1, OVCAR-3 and SKOV-3 (ovarian cancer; light grey bars); SUIT-2 and PANC-1 (pancreatic cancer; dark grey bars) and A375 (melanoma; black bar).

5.2.2. Characterisation of HLA-C locus variant expression

In addition to HLA-C expression, HLA-C groups 1 and 2 allotype expression on all cell lines were analysed using enriched HLA-C antibody eluates (Chapter III). Antibody eluate staining was compared to unstained target cells. Most ovarian and pancreatic tumour cell lines demonstrated similar anti-IgG staining to unstained counterparts (Figure 5.2A). Two cell lines, however, A431 and A375 revealed distinct reactivity patterns to HLA-C antibody eluates (Figure 5.2B). A431, a skin epidermoid carcinoma cell lines exhibited stronger reactivity to HLA-C1-specific antibody eluate (relative MFI = 6.4) than HLA-C2-specific antibody eluate (relative MFI = 0.87). Conversely, A375, a melanoma cell line which initially demonstrated low HLA-C expression levels (Figure 5.1), showed almost four times greater reactivity with HLA-C2-specific antibody eluate (MFI=1.89) than HLA-C1-specific antibody eluate (MFI=0.51) when compared with unstained cells. SKOV-3, an ovarian cancer cell line which demonstrated the highest HLA-C expression within the studied tumour cell lines, exhibited comparable reactivity patterns to HLA-C1 (MFI=0.49) and HLA-C2 (MFI=0.77) specific antibody eluates (Figure 5.2C).

Together, these data present strongly positive staining of HLA Class I expression with W6/32 antibody clone. HLA-C expression levels were also detected by the DT-9 antibody clone. Further phenotypic analyses of HLA-C groups 1 and 2 expression on solid tumour cell lines with enriched antibody eluates revealed differential reactivity patterns with either comparable or higher MFI values indicating greater HLA-C1 (A431) or HLA-C2 (A375) expression.

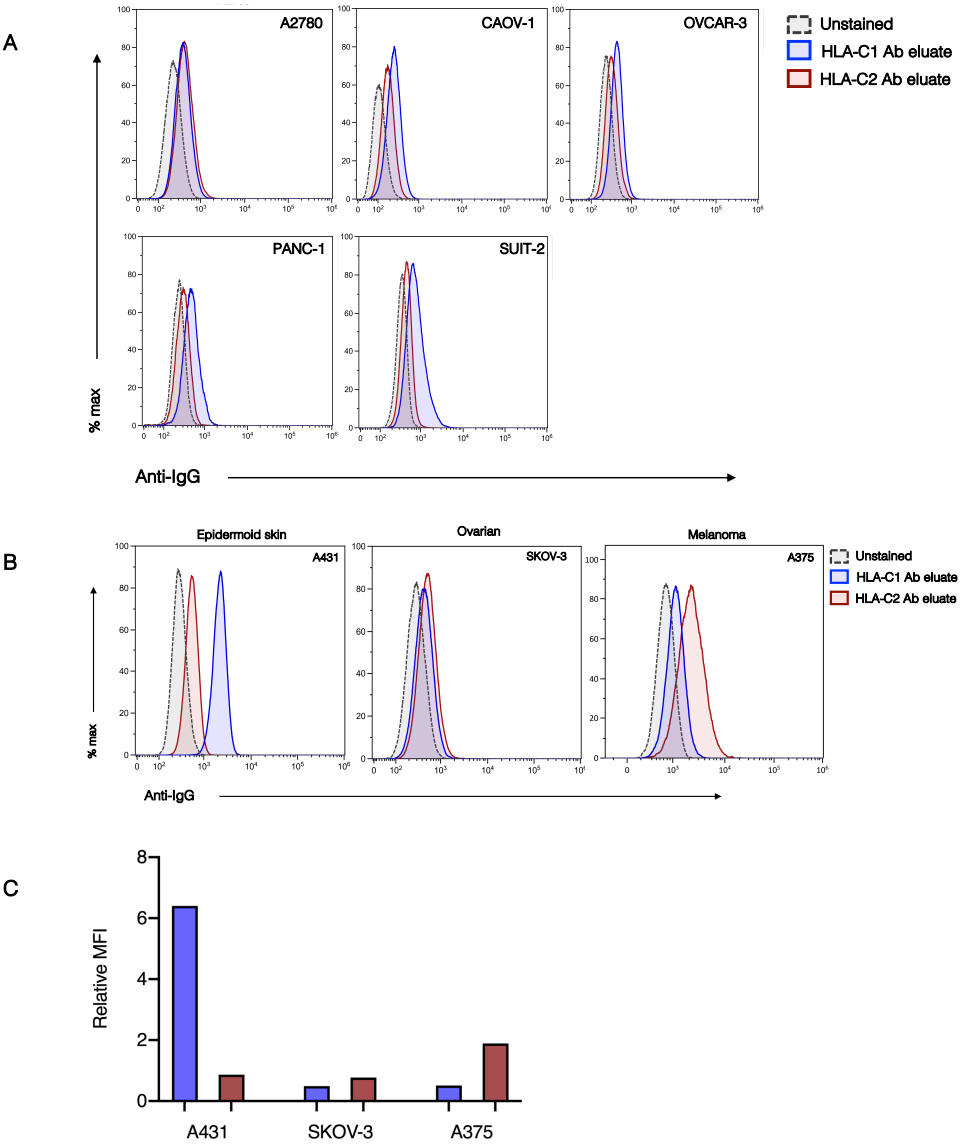

Figure 5.2. | HLA-C locus variant expression on solid tumour cell lines.

Solid tumour cell lines were stained with HLA-C group 1 or group 2-specific enriched antibodies. Anti-human IgG secondary antibody (solid lines) was used to detect expression compared to unstained cells (dotted line). The data were collected using the Beckman Coulter Gallios flow cytometer and analysed by the Kaluza software.

A | Overlayed histogram analyses of HLA-C groups 1 (blue) and 2 (red)-specific antibody eluates staining of A2780, CAOV-1, OVCAR-3 (ovarian cancer) and PANC-1 and SUIT-2 (pancreatic cancer) cell lines.

B | Representative examples of cell lines A431 (epidermoid skin), SKOV-3 (ovarian) and A375 (melanoma) exhibiting distinct reactivity to HLA-C antibody eluate staining.

C | Comparison of relative median fluorescence intensity values of enriched HLA-C1 (blue bar) and HLA-C2 (red bar) specific antibody staining compared to unstained cells for A431, SKOV-3 and A375 cell lines.

5.3. The effect of HLA-specific alloantibodies on solid tumour cell lines

Following the detection of variable HLA-C expression on tumour cell lines, A431 (epidermoid skin cancer) and A375 (melanoma) target cells were treated with enriched HLA-C-specific antibodies prior to co-incubation with effector cells in the cytotoxicity assay. This study aimed to analyse the potential of enhanced NK cell mediated responses towards target tumour cells. Similar to the NK cell cytotoxicity functional assays discussed in Chapter IV, negatively selected NK cells from healthy donors were co-incubated with A431 target cells (Figure 5.3). In contrast, to determine ADCC-independent target cytolysis, HLA-C2-specific KIR2DL1 gene transduced NK92 cells were used as effectors and co-incubated with A375 cells (Figure 5.4).

To identify optimal effector-to-target (E:T) ratio, cellular cytotoxicity was determined by the colorimetric lactate dehydrogenase (LDH) assay. A431 target cells were co-incubated with enriched IFN-α-activated NK cells from a healthy donor at varying E:T ratios including 1:1, 2:1, 5:1 and 10:1 (Figure 5.3A). Based on the HLA-C groups 1 or 2 expression analyses (Figure 5.2C), healthy donors with a dominant proportion of KIR2DL3$^+$ NK cells were selected as effector cells for A431 target cells. Cytotoxicity responses of IFN-α-activated NK cells revealed that an increased number of effector cell number led to a greater NK cell cytotoxic activity towards A431 cells. An average of 11.2±5.1% A431 cytotoxicity was measured at 5:1 E:T ratio, which was used in subsequent functional experiment involving HLA-C-specific antibodies.

NK cell cytotoxic function was substantially enhanced when target cells were pre-treated with HLA-C-specific antibody eluates. At E:T ratio of 5:1, A431 cytolysis (n=1) increased from 4.6% (control) to 10.1% following HLA-C1-specific antibody treatment. HLA-C2-specific antibody weakly enhanced the killing capacity of NK cells to 6.4% (Figure 5.3B). These data suggest that lower A431 cellular cytotoxicity possibly results from high cognate HLA-C1 ligand expression ligating with KIR2DL3, modulating inhibition of NK cell activity. Treatment with HLA-C1-specific antibody, however, led to an increase in NK cell activation and thus increased A431 target cell lysis.

In comparison, A375 target cells were co-incubated with IL-2 conditioned KIR2DL1-expressing NK92 cells, respectively at varying E:T ratios including 1:1, 2:1, 5:1 and 10:1 (Figure 5.4A). A375 target cell cytolysis was comparatively greater than the responses observed with primary NK cell mediated A431 cytotoxicity. For example, at 10:1 E:T ratio, an average of 60.7±11.2% A375 cytotoxicity was measured compared to 21.4±9.8% A431 cytotoxicity, suggesting that A375 cells were more susceptible to cytolysis. NK92-KIR2DL1 cytotoxicity capacity was greater than the cytokine-activated NK cells (Figure 5.3B, n=6).

A similar effect was observed with co-cultures of HLA-C-specific antibody treated-A375 target cells and NK92-KIR2DL1 effector cells. This cytotoxic capacity was improved from an average of 29.4±6.7% (no treatment) to 50.1±15.2% following A375 target cells pre-treatment with HLA-C2-specific antibody eluate (n=5) (Figure 5.4B). A small increase in A375 cellular cytotoxicity was also observed with HLA-C1-specific antibody eluate (37.7±7.8%). The lack of CD16 on NK92-KIR2DL1 cell surface (Chapter IV, Figure 4.12D), confirm the enhanced effector cell function was indeed mediated in the absence of ADCC responses. Overall, these data confirm that masking HLA-C recognition on solid tumour cell lines from inhibitory KIRs augment NK cell function to increase target cell lysis.

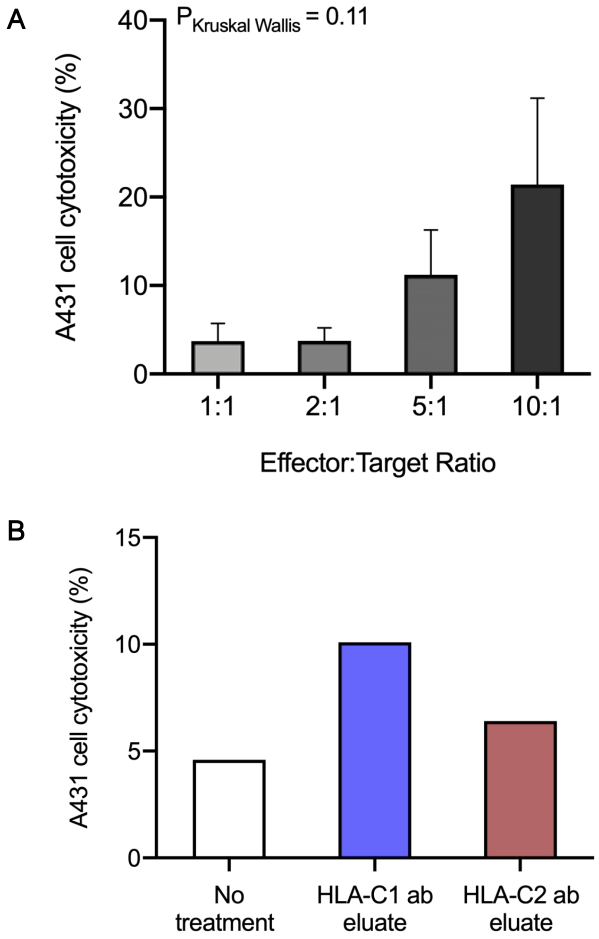

Figure 5.3. | The effect of HLA-C-specific antibodies on NK cytotoxicity against A431 tumour cell line.

Target cell cytotoxicity was measured using the colorimetric LDH assay. Culture supernatants were mixed with general medium at a 1:10 dilution. LDH reaction mix was added to each well and absorbance values were measured at 490nm after 15 minutes.

A | IFN-α-activated NK cells from a healthy donor were incubated with A431 cells overnight at varying E:T ratios – 1:1, 2:1, 5:1 and 10:1. Bars represent mean±SEM calculated from two independent experiments (n=2). Each assay condition was performed in triplicate wells. Statistical analysis for non-parametric data performed by one way ANOVA, Kruskal-Wallis test with Dunn's multiple comparisons analysis.

B | Primary NK cell mediated cytotoxicity of A431 target cells was measured under no treatment/control conditions (white bar); HLA-C1-specific antibody treatment (blue bar) and HLA-C2-specific antibody treatment (red bar). Bars represent mean±SEM calculated from one experiment (n=1). Each assay condition was performed in triplicate wells.

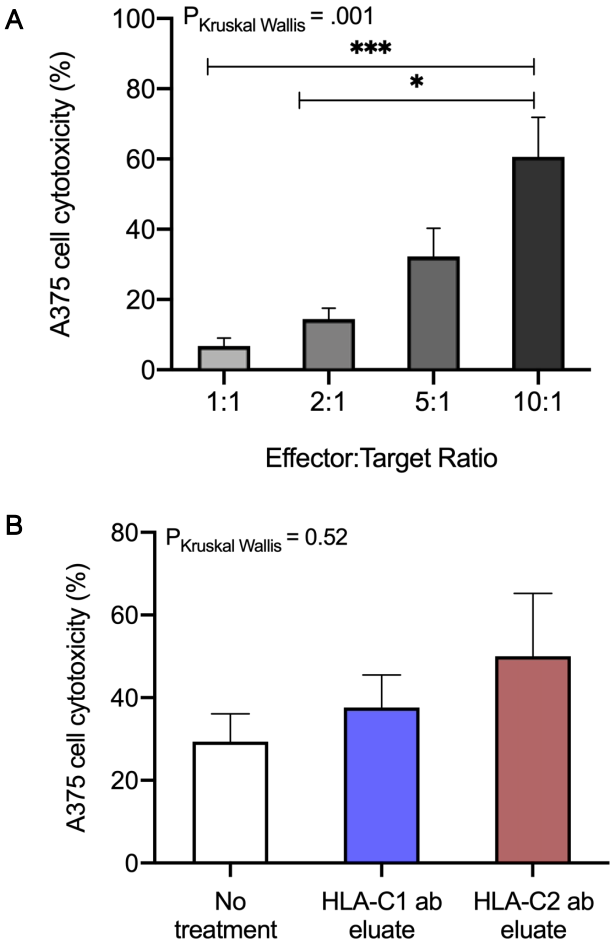

Figure 5.4. | The effect of HLA-C-specific antibodies on NK cytotoxicity against A375 tumour cell line.

Target cell cytotoxicity was measured using the colorimetric LDH assay. Culture supernatants were mixed with general medium at a 1:10 dilution. LDH reaction mix was added to each well and absorbance values were measured at 490nm after 15 minutes.

A | IL-2 conditioned NK92-KIR2DL1 cells were incubated with A375 cells overnight at varying E:T ratios – 1:1, 2:1, 5:1 and 10:1. Bars represent mean±SEM calculated from six independent experiments (n=6). Each assay condition was performed in triplicate wells. Statistical analysis for non-parametric data performed by one way ANOVA, Kruskal-Wallis test with Dunn's multiple comparisons analysis; * $p < 0.05$; *** $p < 0.001$.

B | NK92-KIR2DL1 cell mediated cytotoxicity of A375 target cells was measured under no treatment/control conditions (white bar); HLA-C1-specific antibody treatment (blue bar) and HLA-C2-specific antibody treatment (red bar). Bars represent mean±SEM calculated from five independent experiments (n=5). Each assay condition was performed in triplicate wells. Statistical analysis for non-parametric data performed by one way ANOVA, Kruskal-Wallis test with Dunn's multiple comparisons analysis.

5.4. Characterisation of HLA-C expression on primary tumour cells

To determine the HLA Class I expression levels on primary tumour cells, patients with Chronic Lymphocytic Leukaemia (CLL) were recruited for this study. The aim was to analyse HLA-C expression levels on the tumour cell subset and to examine the susceptibility of tumour cells coated with HLA alloantibodies to NK cell effector function. Functional analyses of HLA alloantibodies focussed on the possible therapeutic potential of enriched HLA-C-specific antibodies in the treatment of CLL.

In therapy-naïve CLL patients, normal B cells ($CD5^-CD19^+$) and tumour cells ($CD5^+CD19^+$) were immunophenotyped using three multi-parameter flow cytometry panels. HLA-C (DT-9 clone), HLA-A/-B/-C (W6/32 clone) and HLA-E (3D12 clone) surface expression were quantified by utilising median fluorescence intensity (MFI) ratios. As an internal control, MFI values deriving from the autologous $CD3^+$ T cell subset were used to calculate MFI ratios for HLA-C, HLA-A/-B/-C and HLA-E on $CD5^+CD19^+$ tumour cells.

5.4.1. Defining tumour cell population in B-CLL patients

CLL is characterised by the clonal expansion of $CD5^+$ B cells, normally a minor subset of B lymphocytes in healthy individuals. CD5 expression on normal B cells has been described as 'dim' compared to the levels observed on T cells. The differences between the proportion of $CD5^-$ and $CD5^+$ B cells in healthy individuals and untreated B-CLL patients were defined by flow cytometry (Figure 5.5A).

On average, CD5-expressing $CD19^+$ cells constituted 5.6% of the total B cells in healthy individuals whereas in B-CLL patients, more than half of the B cell subset (63.3%) can be identified as the neoplastic $CD5^+$ $CD19^+$ cells (Figure 5.5B). The percentage of normal, healthy $CD5^-$ $CD19^+$ cells was four times greater (mean=17.7%) than their counterparts in B-CLL patients (mean=4.4%). These differences in the proportion of B cell subsets in healthy individuals and B-CLL patients validate the over-expression of CD5 on B cells as an appropriate phenotypic marker to detect leukaemic cells via flow cytometry. This also confirms that whilst the percentage of $CD5^+$ $CD19^+$ leukaemic cells is variable within the patient cohort, on average their proportion is significantly greater than healthy $CD5^+$ $CD19^+$ cells.

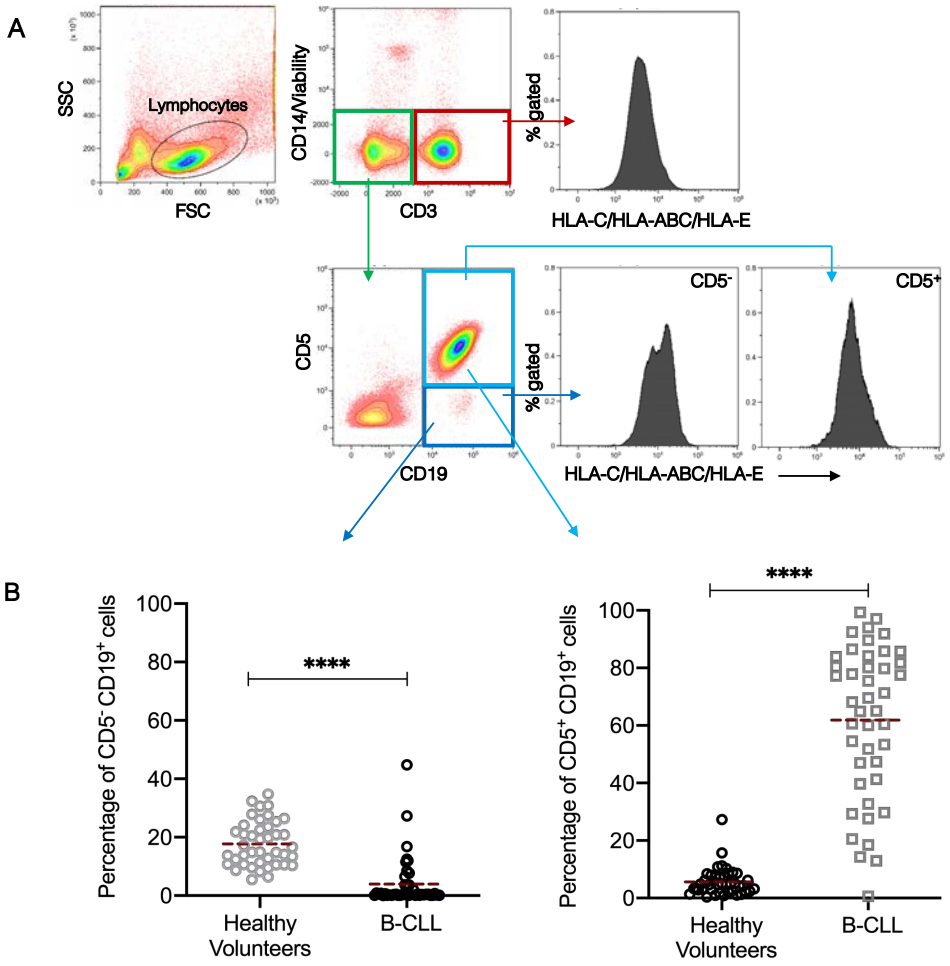

Figure 5.5. | Defining normal and B-CLL tumour populations by flow cytometry.

PBMCs were stained with antibodies for flow cytometry analysis. The data were collected using the Beckman Coulter Gallios flow cytometer and analysed by the Kaluza software.

A | Flow cytometry gating strategy to identify viable $CD14^{neg}$ CD3 T cells (red box) and $CD5^{pos}$ $CD19^{pos}$ (green box) cell subsets. Representative histogram plots showing HLA Class I, HLA-C and HLA-E expression on $CD3^{pos}$ and CD19-expressing $CD5^{neg}$ (dark blue box) and $CD5^{pos}$ (light blue box) subsets.

B | The percentage of $CD19^{pos}$ $CD5^{neg}$ B cell subsets were compared between healthy volunteers (grey circle) and B-CLL patients (black circle) (left). Greater percentage of neoplastic dual expressing $CD19^{pos}$ $CD5^{pos}$ B cells were observed in B-CLL patients (right). Dashed red line indicates mean. Statistical significance was obtained via Mann Whitney unpaired t-test for non-parametric data; **** $p < 0.0001$. Healthy volunteers (n=42) and B-CLL patients (n=43).

5.4.2. Primary B-CLL cells show an increase in HLA-C surface expression

To analyse HLA-C, HLA Class I and HLA-E expression on total $CD19^+$ B cell subset, fresh PBMCs from healthy donors (n=42) and untreated B-CLL patients (n=43) were stained with DT-9, W6/32 and 3D12 antibody clones, respectively (Figure 5.6A). No significant differences were found in HLA-E expression levels between healthy donors and B-CLL patients. Total HLA Class I levels were upregulated on $CD19^+$ B cells from CLL patients (mean MFI ratio = 2.39) compared to healthy donors (1.86) ($p < 0.001$). Similarly, MFI ratios related to HLA-C expression were significantly higher on $CD19^+$ B-CLL cells (2.92) than those from healthy individuals (2.42) ($p=0.03$).

To further analyse the HLA-C expression, total $CD19^+$ B cells were divided into $CD5^-$ and $CD5^+$ subsets (Figure 5.6B; left). The MFI ratios calculated from autologous $CD3^+$ T cells revealed HLA-C expression variability on $CD5^-$ and $CD5^+$ B cells in both cohorts. The average HLA-C MFI ratio on CD5-negative B-CLL cells was greater (mean MFI ratio = 3.69) than the level of HLA-C on the same subset in healthy individuals (2.61). Similarly, HLA-C surface expression levels on tumour $CD5^+$ $CD19^+$ cells were significantly increased (2.96) compared to normal $CD5^+$ $CD19^+$ counterparts (1.91) ($p < 0.001$). Moreover, both cohorts demonstrated greater HLA-C expression on CD5-negative B cells than the dual $CD5^+$ $CD19^+$ cell subset.

Total HLA-A/-B/-C expression was measured on $CD5^-$ and $CD5^+$ B cells (Figure 5.6B; middle). In healthy volunteers, the average HLA-A/-B/-C levels on $CD5^-$ (2.56) and $CD5^+$ (1.89) B cells were relatively similar to HLA-C expression (2.61 and 1.91, respectively). On $CD5^+$ $CD19^+$ B-CLL cells, however, HLA-A/-B/-C levels were similar (1.84) to levels observed in healthy volunteers, indicating that unlike HLA-C, the clonally expanded $CD5^+$ B cells retain stable levels of HLA Class I molecules. The same effect was observed with $CD5^-$ cells in B-CLL patients as the mean MFI ratio (2.83) was similar to that in healthy volunteers.

To consider the potential cross-reactive effect of the DT-9 antibody clone, HLA-E-locus specific antibody (3D12) was used (Figure 5.6B; right). In line with the literature, on average HLA-E levels on healthy $CD5^-$ (1.11) and $CD5^+$ (0.97) B cells were two times lower than HLA-C and HLA-A/-B/-C expression levels. Primary B-CLL cells demonstrate slightly higher HLA-E expression (1.29 and 1.07, respectively) but no significant difference was observed between the leukaemic $CD5^+$ $CD19^+$ B cells and those from healthy donors. This further confirmed that the higher MFI ratios measured in B-CLL patients by DT-9 antibody was due to the upregulation of HLA-C surface expression levels.

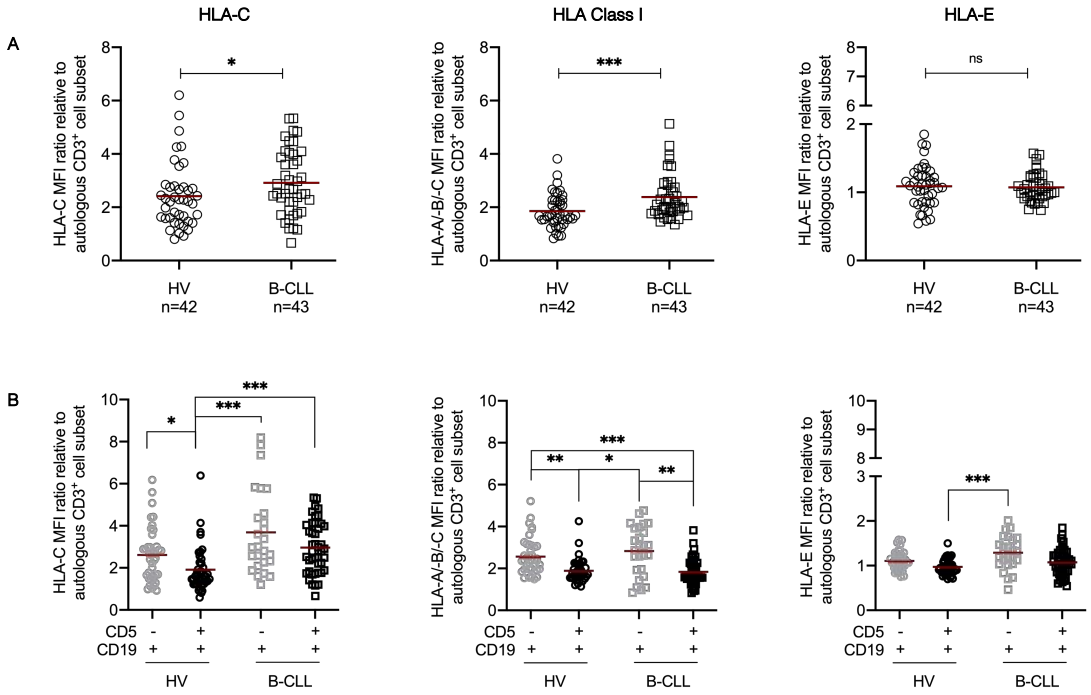

Figure 5.6. | HLA Class I expression on B cell subsets in healthy donors and B-CLL patients. HLA-C (left), HLA Class I (middle) and HLA-E (right) expression levels were analysed by the Beckman Coulter Gallios flow cytometer by using DT-9, W6/32 and 3D12 antibody clones, respectively.

A | Comparison of HLA Class I allele expression was analysed on total $CD19^{pos}$ B cells and compared between healthy donors (circles) and B-CLL patients (squares). Statistical significance was obtained via Mann Whitney unpaired t-test for non-parametric data; * $p < 0.05$; *** $p < 0.001$.

B | Total B cell subsets from healthy donors and B-CLL patients were further divided into $CD5^{pos}$ (black) and $CD5^{neg}$ (grey) subsets for HLA Class I expression analysis. Every symbol represents the individual MFI ratio for each antibody determined by dividing MFI expressed on leukaemic ($CD5^{pos}$) or normal ($CD5^{neg}$) B lymphocytes with MFI expressed on autologous T lymphocytes. The solid red line indicates mean. Statistical significance was obtained by Mann Whitney unpaired t-test for non-parametric data; * $p < 0.05$; ** $p < 0.01$, *** $p < 0.001$. Healthy volunteers (n=42) and B-CLL patients (n=43).

5.4.3. HLA-C expression is selectively increased on B-CLL cells compared to other HLA Class I proteins

The median age for the incidence of CLL is 70 years. Healthy volunteers used in this study of CD5-expressing B cells were not age-matched to the B-CLL patients. The ages of the healthy volunteers ranged from 21 to 74 years. A simple linear regression analysis was performed to determine if the increase in HLA-C expression is dependent upon age in healthy volunteers (Figure 5.7A). Using the MFI ratios derived from $CD5^+$ B cells, the results of the regression analysis indicate that HLA-C (r^2=0.04), HLA-A/-B/-C (r^2=0.02) and HLA-E (r^2=0.02) expression levels do not increase with age in healthy individuals. This suggests that the increase in HLA-C expression observed in primary B-CLL cells is therefore, a characteristics of the disease.

To further confirm the increased HLA-C expression in B-CLL, MFI ratios of CD5-expressing B cells deriving from healthy volunteers aged 50 years and above (a subset of the healthy cohort in Figure 5.6) were compared with their counterparts from B-CLL patients. Similar to previous results, HLA-C expression was elevated on $CD5^+$ $CD19^+$ tumour cells ($p < 0.001$) (Figure 5.7B), unlike HLA-A/-B/-C (Figure 5.7C) and HLA-E (Figures 5.7D) expression levels.

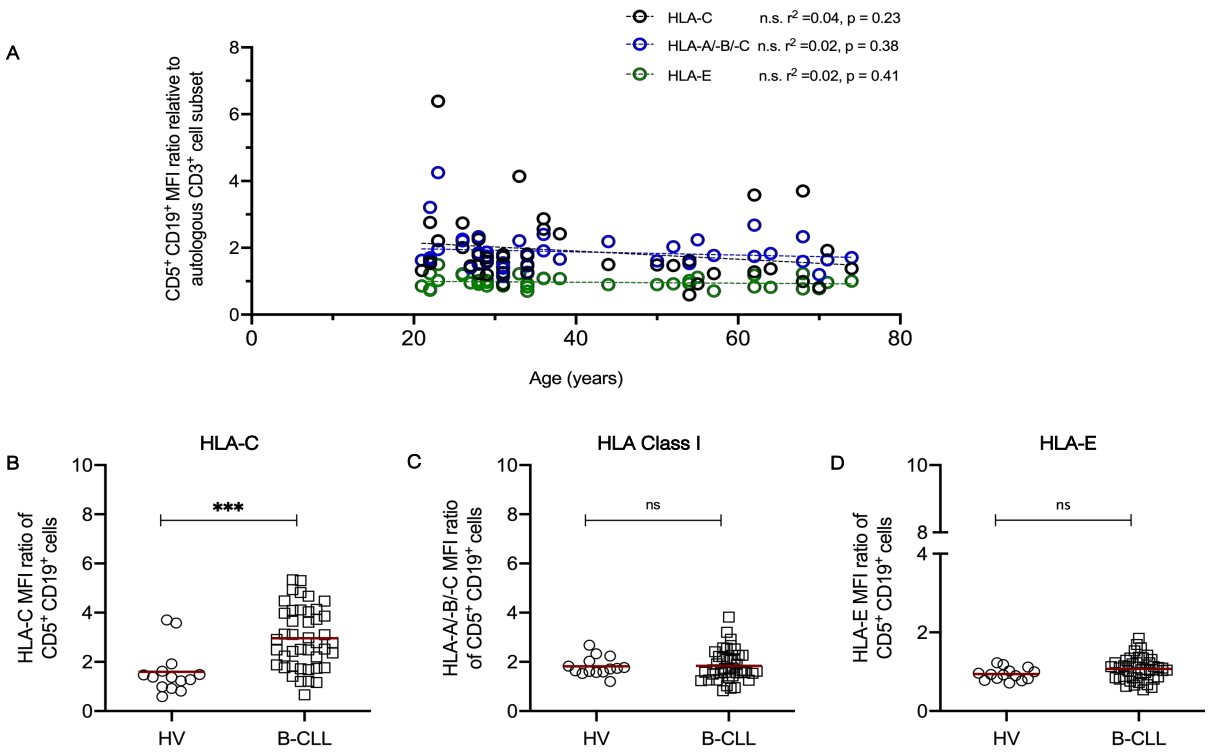

Figure 5.7. | Upregulation of HLA-C expression is disease-dependent in B-CLL.

A | The expression of HLA-C (black circle), HLA Class I (blue circle) and HLA-E (green circle) were analysed on the $CD5^+$ $CD19^+$ cell subset in healthy donors. Lines represent linear regression. Statistical analysis via simple linear regression analysis.

B | HLA-C (left), HLA Class I (middle) and HLA-E (right) expression levels were analysed on $CD5^+$ $CD19^+$ cell subset from B-CLL patients (square) healthy donors aged 50 years and above (circle). Every symbol represents the individual MFI ratio for each antibody determined by dividing MFI expressed on $CD5^{pos}$ B lymphocytes with MFI expressed on autologous T lymphocytes. The solid red line indicates mean. Statistical significance obtained via Mann Whitney unpaired t-test for non-parametric data; *** $p < 0.001$. Healthy volunteers (n=14) and B-CLL patients (n=43).

5.4.4. HLA-C serological typing of B-CLL cells

To assess the functional potential of HLA-C-specific alloantibodies, allogeneic NK cell-mediated lysis of leukaemic cells was investigated. Firstly, B-CLL patients were serologically typed for their HLA-C expression to select patient PBMCs for *in vitro* NK cell functional assays. Terasaki HLA typing trays were used to assign HLA-C antigen type to randomly selected cryopreserved PBMCs from ten B-CLL patients (Table 5.1). The tray wells contain anti-sera or monoclonal antibodies specific to the HLA-C locus. Also known as the microlymphocytotoxicity assay, the detection of antigen-antibody complement reaction by phase-contrast illumination involves visually scoring viable and non-viable cells between 1 and 8. The greater the cell death, the higher the score and therefore, a highly specific (or positive) reaction against the antibodies in the well. Using this score key, three patients were identified as HLA-C group 1 homozygous; one patient as HLA-C group 2 homozygous; four patients were assigned as HLA-C heterozygous whilst the HLA-C type for two patients were uninterpretable, with one patient (*) demonstrating extreme sensitivity to complement.

Table 5.1. | Terasaki HLA-C allele specificity reaction scores for ten B-CLL patients

			HLA-C allele specificities (-Cw)																											
Patient ID	NC	PC	1	1	1/3	2	2	2	3	3	9 +/- 10	9	4	4	4	5	5/ B18	5	6 +/- 4	6 +/- 2/15	6/2	4/6	17	7 +/- 17	7/ 17	7	7	8	8	8	Conclusion
210JB	0	8	0	1	0	0	0	0	0	0	0	0	0	0	0	0	0	0	0	0	0	0	0	1	6	0	0	2	0	0	U/I
208PM	0	8	6	1	1	0	0	1	1	1	1	1	0	0	0	1	6	2	2	1	4	1	2	8	8	8	8	8	6	6	C1+ C1+
199DJ	0	8	1	0	6	0	0	2	8	0	0	0	0	0	2	0	6	1	0	0	0	0	0	6	4	4	2	4	2	1	C1+ C1+
120PL	0	8	8	8	6	0	0	0	0	1	0	0	0	0	0	0	6	4	2	1	0	0	0	8	8	6	4	4	1	1	C1+ C1+
56AT	0	8	8	8	6	0	0	1	1	2	8	1	0	4	1	1	1	1	1	1	1	1	6	6	8	4	2	2	1	1	C1+ C2+
166DA	0	8	2	0	0	0	0	1	0	0	6	0	0	0	0	0	8	4	6	6	8	0	0	8	8	8	2	1	4	0	C1+ C2+
197JH	0	8	6	0	0	6	4	6	0	1	0	0	6	6	6	0	0	0	6	1	8	6	1	1	0	0	1	4	1	1	C2+ C2+
186KN	0	8	0	0	0	8	4	4	2	0	0	0	0	0	0	0	6	2	0	0	6	0	0	6	6	2	4	6	2	0	C1+ C2+
*251LH	4	8	8	6	8	0	0	2	2	8	6	2	8	8	8	1	2	2	8	8	8	8	2	8	8	4	6	8	8	2	U/I
31RH	0	8	4	1	8	0	0	4	6	8	6	2	0	0	4	0	2	2	8	6	6	2	0	2	8	0	1	6	2	1	C1+ C2+

NC = negative control; PC = positive control; U/I = uninterpretable

*extreme sensitivity to complement reaction; HLA-C type unclear

5.4.5. Characterisation of HLA-C locus variant expression on B-CLL cells

Secondly, to limit potential discrepancies arising from interpreting serological typing data, the assigned HLA-C type of the ten B-CLL patient PBMCs were further validated. Enriched HLA-C groups 1 and 2-specific antibodies from renal transplant recipients were used to phenotype surface HLA-C locus variant expression on $CD5^+$ $CD19^+$ B cell subset from three patients. HLA-C serological typing concluded 199DJ as C1/C1 homozygous, 186KN as C1/C2 heterozygous and 197JH as C2/C2 homozygous (Table 5.1). Using an anti-human IgG secondary antibody, the reactivity of the HLA-C antibody eluates with $CD5^+$ $CD19^+$ tumour cells was measured by flow cytometry (Figure 5.8A).

In line with the serological typing analysis, Figure 5.8B shows 199DJ (C1/C1) B-CLL tumour cells exhibiting increased reactivity to HLA-C1-specific antibody eluate (MFI=6,695.97) than to HLA-C2-specific antibody eluate (MFI=4,187.82). Conversely, C2/C2 homozygous 197JH donor demonstrated a distinct increase in anti-IgG MFI following staining with HLA-C2-specific antibody eluate (MFI=9,306.27) compared to the less reactive HLA-C1-specific antibody eluate (MFI=4,042.45). Phenotyping for HLA-C1 and HLA-C2 antigen expression on tumour cell subset from C1/C2 heterozygous patient 186KN, revealed similar reactivity and anti-IgG MFI values following staining with HLA-C1 (MFI = 4,594.85) and HLA-C2 (MFI = 5,250.90) specific antibody eluates. This phenotype analysis of HLA-C allotype expression on primary B-CLL cells confirms and validates the serologically assigned HLA-C allotype.

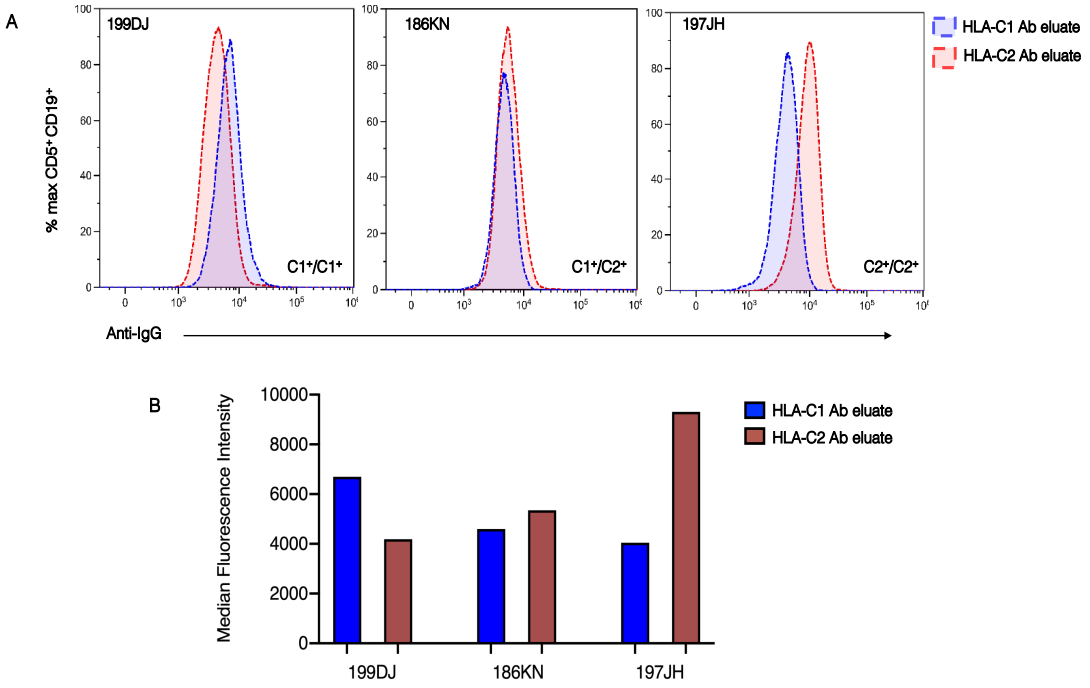

Figure 5.8. | HLA-C allelic surface expression analysis on B-CLL cells.

PBMCs from B-CLL patients were stained with HLA-C group 1 (blue dotted line) or group 2 (red dotted line) specific enriched antibodies. Anti-human IgG secondary antibody (solid lines) was used to detect expression. The data were collected using the Beckman Coulter Gallios flow cytometer and analysed by the Kaluza software.

A | Three B-CLL patients serologically typed as HLA-C1/C1 homozygous (199DJ – left); HLA-C1/C2 heterozygous (186KN – middle); HLA-C2/C2 homozygous (197JH – right) were co-incubated with enriched HLA-C1 (blue) or -C2 (red) specific alloantibodies. Using an anti-IgG secondary antibody, reactivity to HLA-C1 or -C2-specific alloantibodies were measured by flow cytometry. Overlayed histogram plots represent specific antibody binding on $CD5^+$ $CD19^+$ cell subset which support HLA-C serological typing results.

B | The MFI values quantified from HLA-C1 (blue bar) or -C2 (red bar) -specific alloantibody reactivity for each B-CLL patient is represented in a bar chart.

5.5. Can HLA-specific alloantibodies increase B-CLL cytolysis?

5.5.1. Optimisation of flow cytometry based CLL cytotoxicity assay

The functional potential of HLA-C alloantibodies to reverse the dampened NK cell cytotoxic response against primary tumour cells was investigated. Using 5:1 E:T ratio, enriched B cells from CLL patient PBMCs were exposed to varying concentrations of an anti-CD20 antibody, rituximab (Figure 5.9A). The cytotoxicity assays performed in this chapter with primary B-CLL samples quantified viable (propidium iodide negative) $CD5^+$ $CD19^+$ B cells as a measure of NK cell-mediated target cell cytotoxicity. Rituximab is used as a primary treatment for CLL and was included in these functional assays as a positive control. Representative examples in Figure 5.9B show that co-incubation with allogeneic NK cells at an effector-to-target ratio of 5:1 reduces the number of viable $CD5^+$ $CD19^+$ tumour cells from 5,693 cells to 3,275 cells. A marked increase in cytolysis of $CD5^+$ $CD19^+$ tumour cells was observed following treatment with rituximab (0.1μg/ml) (351 live target cells) and HLA-C2-specific antibody eluate (381 live target cells).

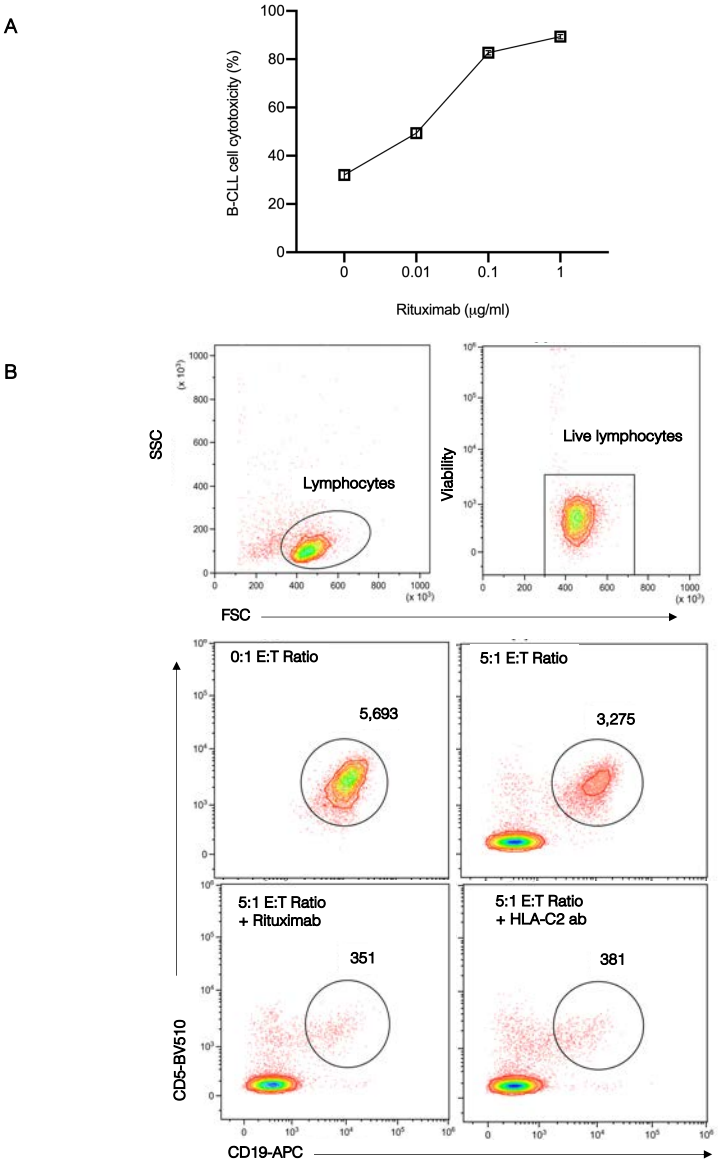

Figure 5.9. | Optimisation of B-CLL and NK cell cytotoxicity assay.

A | The optimal 5:1 E:T ratio was determined and dose-dependent analysis of rituximab-coated LCLs and NK cells was performed. Data shown as mean±SEM of triplicate wells and are representative of one experiment. Each square represents the average percentage cytotoxicity calculated from triplicate wells for each assay condition.

B | Representative flow gating strategy to quantify the number of live leukaemic $CD5^+$ $CD19^+$ cells in the absence of effector cells (0:1 E:T); presence of effector cells (5:1 E:T), treatment with rituximab at 0.1μg/ml (5:1 E:T) and HLA-C2-specific antibody treatment (5:1 E:T).

5.5.2. HLA-C-specific alloantibodies enhance primary B-CLL cell lysis

B-CLL tumour cells from two untreated patients – C1/C1 (199DJ) and C2/C2 (197JH) homozygous were treated with HLA-C1 and -C2-specific antibody eluates, respectively. Allogeneic healthy NK cells with a high proportion of $CD56^{dim}$ cells expressing either KIR2DL3 (HLA-C1 ligand-specific) or KIR2DL1 (HLA-C2 ligand-specific) were co-incubated with enriched B cells from C1/C1 and C2/C2 PBMCs, respectively at 5:1 effector-to-target ratio (Figure 5.9).

Under control conditions i.e. no HLA-C-specific antibody treatment, C1/C1 (Figure 5.10A) and C2/C2 (Figure 5.10B) B cells demonstrated reduced susceptibility to NK cell lysis compared to HLA-C-specific antibody treatment. This pattern was observed in all functional experiments utilising NK cells from healthy donors, regardless of the KIR phenotype of the effector cells. Following HLA-C-specific antibody treatment, a significant increase in C1/C1 and C2/C2 $CD5^{+}$ $CD19^{+}$ tumour cell lysis was observed. For example, in Figure 5.10A, one donor with a high proportion of $KIR2DL3^{+}$ NK cells (blue line) demonstrated enhanced function towards HLA-C1-specific antibody-coated C1/C1 B cells by increasing target cell cytotoxicity from an average of 20.5±4.5% to 73.0±6.0%. Similarly, multiple NK cells donors with high $KIR2DL1^{+}$ expression (red) revealed augmented NK cell activation towards HLA-C2-specific antibody-bound C2/C2 B cells to approximately 100% cytolysis (Figure 5.10B). Compared to enriched HLA-C1-specific antibody, HLA-C2-specific antibody generated a more potent response in tumour cell lysis by preventing HLA-C2 ligation to specific KIR2DL1, and thus promoting NK cell activation.

Two healthy donors with a high proportion of dual expressing KIR2DL1 and KIR2DL3 NK cells (green) revealed a small increase in percentage target cell cytotoxicity following co-incubation with HLA-C1-specific antibody treated C1/C1 B cells (Figure 5.10A). Interestingly, a comparable increase in reactivity responses were observed with both donors i.e. 40.4±5.6% and 36.9±2.4%. In the presence of non-specific HLA-C ligand expressing tumour cells, high KIR2DL1$^+$ (red) or KIR2DL3$^+$ (blue) NK cells lacking their cognate HLA-C ligand demonstrated similar increase in activation. For example, the activity of high KIR2DL3$^+$ NK cells was enhanced, leading to an increase of 38% in C2/C2 B-CLL cell cytolysis. In comparison, to HLA-C2 ligand specific KIR2DL1$^+$ NK cells, an average of 45.9% increase in C1/C1 target cell cytotoxicity was observed.

Overall, these results confirm allogeneic NK cell function is suppressed in the presence of untreated B cells enriched from B-CLL patient PBMCs in comparison to HLA-C-specific antibody-treated B cells. Treating HLA-C1/C1 or HLA-C2/C2 B cells with enriched specific HLA alloantibodies leads to enhanced NK cell function, irrespective of the KIR phenotype and significantly increased lysis of CD5$^+$ CD19$^+$ tumour cells.

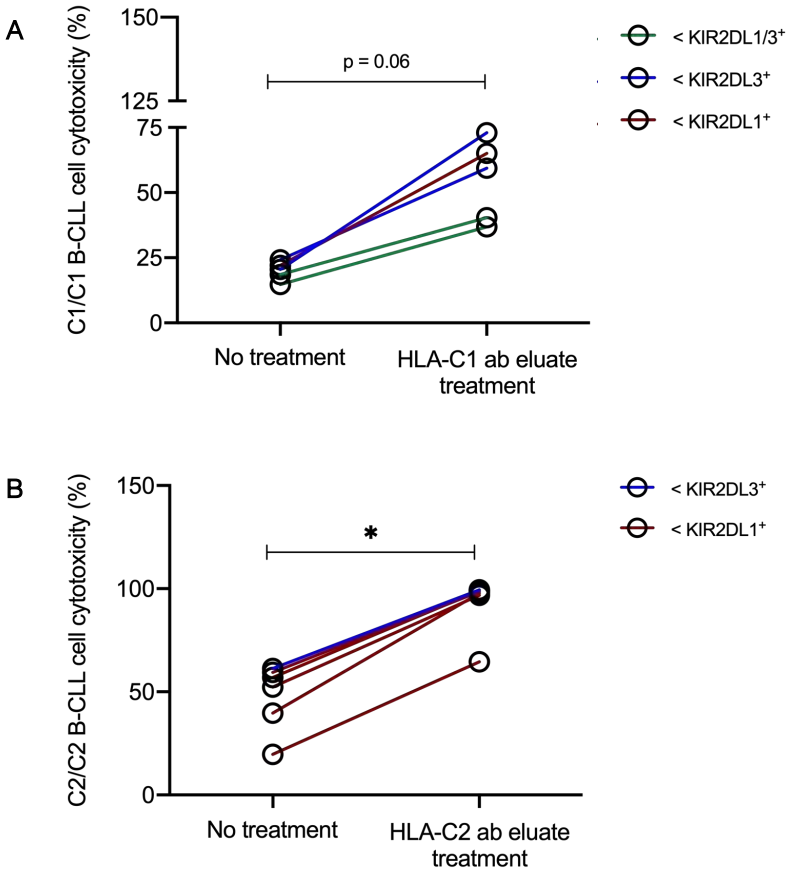

Figure 5.10. | HLA-C-specific alloantibodies enhance primary B-CLL cell lysis.

Enriched B cells were treated with HLA-C-specific enriched alloantibodies for 30mins at room temperature. IFN-α activated NK cells were co-incubated with untreated or alloantibody-treated B cells at 5:1 E:T ratio in an overnight assay. Each condition was performed in triplicate wells. Each circle represents percentage target cell cytotoxicity derived from one experiment from individual healthy donors or an average from multiple experimental repeats with the same healthy donor NK cells.

A | Treatment of HLA-C1/C1 homozygous CLL patient (199DJ) leukaemic $CD5^+$ $CD19^+$ cells with HLA-C1-specific alloantibodies. The percentage target cell cytotoxicity was measured before and after antibody treatment. Each circle represents the percentage target cell cytotoxicity calculated from control and treatment responses from one healthy donor (n=5).

B | Treatment of HLA-C2/C2 homozygous CLL patient (197JH) leukaemic $CD5^+$ $CD19^+$ cells with HLA-C2-specific alloantibodies. The percentage target cell cytotoxicity was measured before and after antibody treatment. Each circle represents the percentage target cell cytotoxicity calculated from control and treatment responses from one healthy donor (n=6)

Line colour represents the dominant inhibitory KIR expression on donor NK cells used in each experiment - $KIR2DL1^+$ (red); $KIR2DL3^+$ (blue); $KIR2DL1^+2DL3^+$ (green). Statistical analyses performed by Wilcoxon matched-pairs signed rank test; * p=0.03.

5.5.3. Promoting ADCC-independent NK cell cytotoxicity against primary tumours

As discussed in Chapter IV, two approaches were utilised to elucidate the mechanism of action of HLA-C alloantibodies in this *in vitro* functional model. Firstly, NK cells were treated with FcγRIII (CD16)-blocking antibody to limit the potential effect of antibody-dependent cell cytotoxicity (ADCC). Secondly, the Fc fragments of the HLA-C-specific antibodies were digested using the proteolytic enzyme IdeS, to detect a retained cytotoxic effect independent of ADCC-mediated responses. These approaches aimed to potentiate NK cell activating function by inhibiting intracellular signalling mediated by KIR:HLA-C interactions towards tumour cell lysis.

To optimise these approaches rituximab was used as a positive control in the functional assays. Rituximab primarily functions via ADCC whereby the Fc fragment ligates with CD16 on NK cells initiating intracellular signalling to activate NK cells. Inhibition of CD16 by CD16-specific antibody aimed to limit this potent response. Rituximab was also treated with IdeS to remove the humanised Fc fragment and prevent ADCC-mediated NK cell responses.

Figure 5.11 shows two representative examples of testing these approaches in the NK cell-based functional assay. As expected, rituximab treatment of B cells and co-culture with untreated NK cells (Figure 5.11A) led to a significant increase in $CD5^+$ $CD19^+$ B cell cytotoxicity from 40.0±1.0% to 82.3±1.2% (mean±SEM). Co-incubation with CD16-inhibited NK cells, however, reduced B-CLL cytotoxicity (50.0±2.0%) to almost control levels. Figure 5.11B examined the effect of intact rituximab on $CD5^+$ $CD19^+$ B-CLL cells compared to IdeS-treated rituximab. Similar to Figure 5.11A, an increase in target cell

cytotoxicity was observed from 47.0±5.5% to 94.0±1.0%, in the presence of intact rituximab treated-B cells and untreated NK cells. B cells exposed to Fc fragment-digested rituximab demonstrated a reduction in NK cell mediated cytotoxicity to 53.0±4.2%.

These approaches were further validated by including rituximab control in each NK cell-based functional assay performed using B-CLL patient samples. The data are summarised in Figure 5.12. Rituximab treatment of enriched B cells undoubtedly increased target cell susceptibility to NK cell mediated cytotoxicity, although inter-donor NK cell response variability and B-CLL patient dependent differences were observed. In most cases, CD16 blockade of NK cells reversed the increased susceptibility of rituximab-treated B-CLL cells to control (i.e. no rituximab treatment) levels ($P_{Dunn's} = 0.07$; ns) (Figure 5.12A). Similarly, IdeS-treated rituximab showed a reduction in target cell lysis. Despite the general reduction in B-CLL cytotoxicity with CD16-inhibited NK cells and IdeS-treated rituximab, a few B-CLL patient-healthy donor NK cell combinations demonstrated a retained cytotoxicity effect in B-CLL cells.

Together, the data in Figures 5.11 and 5.12 confirm that rituximab treatment of B-CLL cells increases susceptibility to NK cell mediated lysis. Therefore, the inhibition of CD16 and the removal of Fc fragment of rituximab antibody are both validated as effective approaches that limit ADCC to further facilitate ADCC-independent NK cell responses.

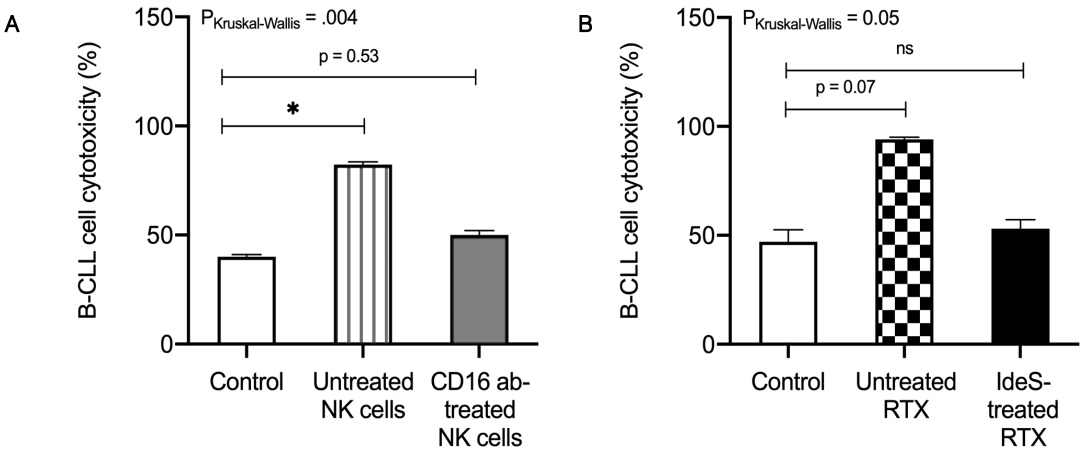

Figure 5.11. | Optimisation of an ADCC-independent B-CLL and NK cell cytotoxicity assay.

Enriched B cells were co-incubated with IFN-α activated NK cells at 5:1 E:T ratio in an overnight assay. Cultures were harvested, data were collected by using the Beckman Coulter Gallios flow cytometer and analysed using the Kaluza software. Data shown as mean±SEM of triplicate wells and are representative of one experiment. Statistical analyses performed with by one way ANOVA for non-parametric data, Kruskal-Wallis test with Dunn's multiple comparisons analysis; * $p < 0.05$. RTX = rituximab

A | Bar chart comparing the effects of IFN-α-activated untreated NK cells and CD16-inhibited NK cells following overnight co-incubation with rituximab-coated B cells from CLL patient. Percentage B-CLL cytotoxicity was measured in the absence of treatment i.e. untreated B cells and NK cells (white bar); rituximab-treated B cells and untreated NK cells (striped bar) and rituximab-treated B cells and CD16-inhibited NK cells (grey bar).

B | Bar chart comparing the effects of untreated rituximab and Fc fragment-digested with IdeS rituximab on B-CLL cell cytotoxicity following overnight co-incubation with NK cells. Percentage B-CLL cytotoxicity was measured in the absence of treatment i.e. untreated B cells and NK cells (white bar); intact rituximab-treated B cells and untreated NK cells (black and white bar) and IdeS-treated rituximab-treated B cells and untreated NK cells (black bar).

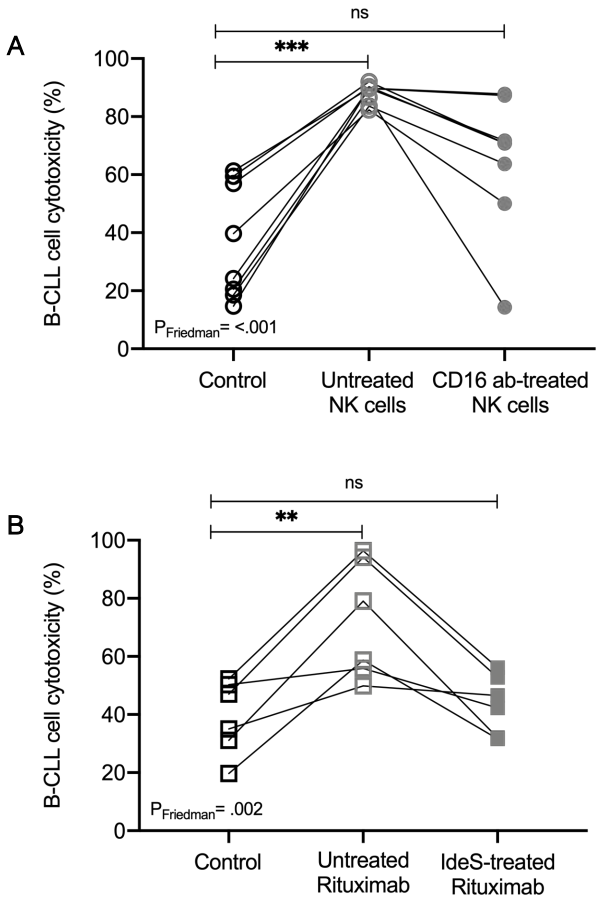

Figure 5.12. | Validation of ADCC-independent B-CLL and NK cell cytotoxicity assays.

Enriched B cells were co-incubated with IFN-α activated NK cells at 5:1 E:T ratio in an overnight assay. Cultures were harvested, data were collected by using the Beckman Coulter Gallios flow cytometer and analysed using the Kaluza software. Data shown as mean±SEM of triplicate wells. Statistical analyses performed with by One way ANOVA for non-parametric data, Friedman test with Dunn's multiple comparisons analysis; * p <0.05; ** p <0.01; *** p <0.001.

A | The effects of IFN-α-activated untreated NK cells and CD16-inhibited NK cells following overnight co-incubation with rituximab-coated B cells from multiple CLL patients. Percentage B-CLL cytotoxicity was measured in the absence of treatment i.e. untreated B cells and NK cells (white circle); rituximab-treated B cells and untreated NK cells (grey outline circle) and rituximab-treated B cells and CD16-inhibited NK cells (grey circle). Each circle represents the percentage B-CLL cell cytotoxicity calculated from one healthy donor (n=8).

B | The effects of untreated rituximab and Fc fragment-digested with IdeS rituximab on B-CLL cell cytotoxicity following overnight co-incubation with NK cells. Percentage B-CLL cytotoxicity was measured in the absence of treatment i.e. untreated B cells and NK cells (white square); intact rituximab-treated B cells and untreated NK cells (grey outline square) and IdeS-treated rituximab-treated B cells and untreated NK cells (grey square). Each square represents the percentage B-CLL cell cytotoxicity calculated from one healthy donor (n=6).

5.5.5. HLA-C-specific alloantibodies and CD16 blockade

To investigate whether HLA-C-specific alloantibodies can enhance NK cell function in the absence of ADCC, HLA-C group 1 or group 2-specific alloantibody bound enriched B cells were co-incubated overnight with untreated and CD16 antibody-treated NK cells. Figure 5.13A shows a representative bar graph presenting tumour cell resistance to NK cell cytotoxicity under control conditions. Tumour cell susceptibility increases following treatment with enriched HLA-C2-specific antibody from an average of 40.0±1.0% to 97.7±0.3%. Co-incubation with CD16-inhibited NK cells reduced target cell cytotoxicity to 67.3±2.3%. A retained NK cell cytotoxic effect was observed, indicating ADCC-independent modulation of NK cell function. Similarly, retained NK cell cytotoxic responses were observed ($P_{Dunn's}$ = 0.03) following co-incubation C1/C1 B-CLL cell treatment with HLA-C group 1 specific antibody and CD16-inhibited NK cells from multiple healthy donors (Figure 5.13B). Likewise, lysis of HLA-C2/C2 tumour cells treated with HLA-C2-specific alloantibody in the presence of CD16-inhibited NK cells exhibited reduced B-CLL cytotoxicity, but not completely reaching control levels ($P_{Dunn's}$ = 0.47; ns) (Figure 5.13C). These data have demonstrated that there are potentially two mechanisms involved in enhancing NK cell cytotoxicity responses by HLA-C-specific alloantibodies – ADCC and blockade of HLA-C:KIR mediated inhibitory signalling to favour activation.

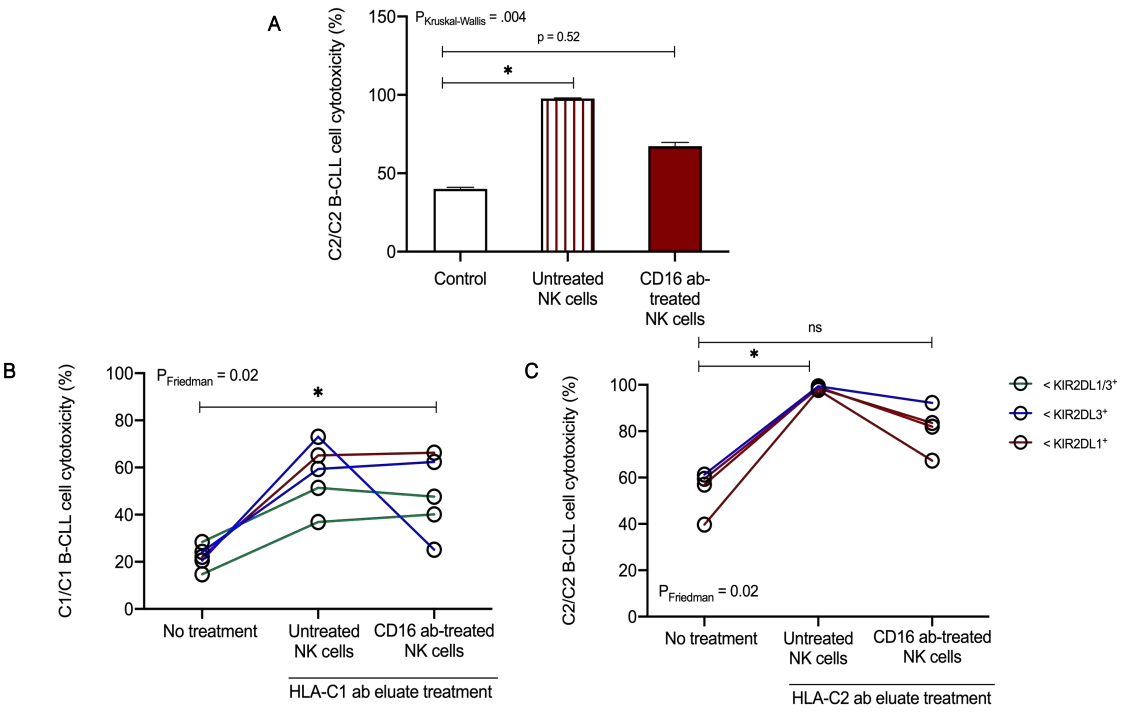

Figure 5.13. | The effect of CD16 blockade on HLA-C-specific alloantibody treated B-CLL cells.

A | Representative bar chart comparing the effects of IFN-α-activated untreated NK cells and CD16-inhibited NK cells following overnight co-incubation with HLA-C2-specific antibody-coated B cells from C2/C2 homozygous CLL patient at 5:1 E:T ratio. Percentage B-CLL cytotoxicity was measured in the absence of treatment i.e. untreated B cells and NK cells (white bar); antibody-treated B cells and untreated NK cells (red striped bar) and antibody-treated B cells and CD16-inhibited NK cells (red bar). Data shown as mean±SEM of triplicate wells from one experiment. Statistical analyses performed with by one way ANOVA for non-parametric data, Kruskal-Wallis test with Dunn's multiple comparisons analysis; * $p < 0.05$.

B | The effects of IFN-α-activated untreated NK cells and CD16-inhibited NK cells following overnight co-incubation with HLA-C1-specific antibody-coated B cells from C1/C1 homozygous CLL patient. Percentage B-CLL cytotoxicity was measured in the absence of treatment i.e. untreated B cells and NK cells, antibody-treated B cells and untreated NK cells and antibody-treated B cells and CD16-inhibited NK cells. Each circle represents the percentage B-CLL cell cytotoxicity calculated from one healthy donor (n=5).

C | The effects of IFN-α-activated untreated NK cells and CD16-inhibited NK cells following overnight co-incubation with HLA-C2-specific antibody-coated B cells from C2/C2 homozygous CLL patient. Percentage B-CLL cytotoxicity was measured in the absence of treatment i.e. untreated B cells and NK cells, antibody-treated B cells and untreated NK cells and antibody-treated B cells and CD16-inhibited NK cells. Each circle represents the percentage B-CLL cell cytotoxicity calculated from one healthy donor (n=4).

Statistical significance analysed with Friedman test with Dunn's multiple comparisons analysis; * $p < 0.05$. Line colour represents the dominant inhibitory KIR expression on donor NK cells used in each experiment - KIR2DL1$^+$ (red); KIR2DL3$^+$ (blue) and KIR2DL1$^+$2DL3$^+$ (green).

5.5.6. The effects of HLA-C2-specific alloantibody lacking the Fc fragment

Thus far, the findings of this work have shown that following CD16 blockade of NK cells, HLA-C-specific alloantibodies maintain an enhanced NK cell function towards target tumour cells, which suggests that by inhibiting Fc fragment ligation to CD16, NK cell activity persists against target cells. To further confirm these results, HLA-C2/C2 B-CLL cells were treated with HLA-C2-specific antibody lacking the Fc fragment.

Figure 5.14A shows the increased target cell lysis observed with HLA-C2-specific antibody treatment (96.7±0.3%) reduced to 46.0±2.1% with IdeS-digested alloantibody. The significant reduction in cytotoxicity responses was comparable to control i.e. no treatment level (40.0±1.0%). Next, multiple experimental repeats to show NK cell donor variation (Figure 5.14B) revealed similar reduction in responses following treatment with IdeS-digested HLA-C2-specific antibodies ($P_{Dunn's}$ = >0.99; ns), with the exception of one donor which showed retained target cell cytotoxicity under the IdeS-treated HLA-C2-specific antibody condition. These results indicate that HLA-C2-specific alloantibodies enhance NK cell function mostly by ADCC but the direct effect on inhibition of KIR:HLA-C interaction by the HLA-C-specific antibodies cannot be completely ruled out.

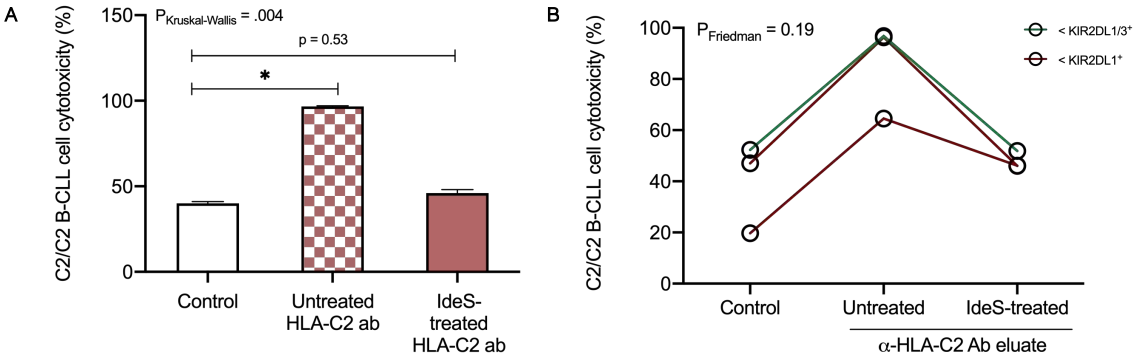

Figure 5.14. | The effect of Fc fragment-digested HLA-C2-specific alloantibody on B-CLL cells.

A | Representative bar chart comparing the effects of intact HLA-C2-specific antibody and Fc fragment-digested antibody with IdeS on B-CLL cell cytotoxicity following overnight co-incubation with NK cells at 5:1 E:T ratio. Percentage B-CLL cytotoxicity was measured in the absence of treatment i.e. untreated B cells and NK cells (white bar); intact antibody-treated B cells and untreated NK cells (red and white bar) and IdeS-treated antibody-bound B cells and untreated NK cells (red bar). Data shown as mean±SEM of triplicate wells from one experiment. Statistical analyses performed with by one way ANOVA for non-parametric data, Kruskal-Wallis test with Dunn's multiple comparisons analysis; * $p < 0.05$.

B | A summary of the effects of IFN-α-activated untreated NK cells and CD16-inhibited NK cells from multiple healthy donors following overnight co-incubation with HLA-C2-specific antibody-coated B cells from a C2/C2 homozygous CLL patient. The percentage target cell cytotoxicity was measured in the absence of treatment, intact HLA-C2-specific antibody treatment of B cells and Fc fragment-digested HLA-C2-specific antibody treatment in the presence of untreated NK cells. Each circle represents the percentage target cell cytotoxicity calculated from one healthy donor (n=3).

Statistical significance analysed with Friedman test with Dunn's multiple comparisons analysis; * $p < 0.05$. Line colour represents the dominant inhibitory KIR expression on donor NK cells used in each experiment - KIR2DL1$^+$ (red) and KIR2DL1$^+$2DL3$^+$ (green).

5.6. Harnessing patient autologous NK cell function against cancer

To limit possible additional cytotoxicity effect mediated by the use of allogeneic NK cells in these *in vitro* functional assays, autologous NK cells from B-CLL patients were utilised. Two B-CLL patients' tumour cell subset were phenotyped for their HLA-C locus variant expression and were concluded as HLA-C2/C2 homozygous (Figure 5.15A). Compared to HLA-C1-specific antibody eluate staining, patients 349GC and 151RG tumour cells exhibited distinct increase in anti-IgG reactivity with enriched HLA-C2-specific antibody eluate (MFI = 8.922.5 and 5.761.6, respectively).

Next, B cells and NK cells from the same B-CLL patient PBMCs were negatively enriched. IFN-α-activated autologous NK cells were co-incubated with HLA-C2-specific antibody-bound enriched patient B cells. Results in Figure 5.15B show that in the absence of antibody treatment, NK cell activity against tumour cells was poor, particularly in the case of patient 151RG (mean cytotoxicity 3.0±1.0%). Treatment of B cells with HLA-C2-specific antibody lead to a significantly enhanced cytolytic function of NK cells. For example, an increase of 34% (349GC) and 24.3% (151RG) in target cell cytotoxicity was measured. IdeS-treated HLA-C2-specific antibody eluate, however, revealed a reduction in the improved NK cell function by 17.5% and 11.6%, respectively.

These results show that similarly to allogeneic NK cells from healthy donors, the cytolytic potential of patient autologous NK cells can be harnessed by inhibiting self HLA-C2 ligand binding to KIR2DL1 with HLA-C2-specific alloantibody. The increase in the activation of NK cells was retained with HLA-C2-specific alloantibodies lacking the Fc fragment, further demonstrating that HLA-C-specific alloantibodies can modulate the NK cell state of responsiveness to favour activation. Moreover, these data support previous findings that indicate the involvement of an additional mechanism of HLA-C-specific antibodies by which NK cell cytotoxicity is enhanced in the absence of ADCC. Together, these findings support the therapeutic potential of HLA-C-specific alloantibodies to prevent HLA-C/KIR interaction i.e. self-recognition and prime patient autologous NK cells to generate an enhanced cytolytic response towards tumour cells expressing KIR ligands.

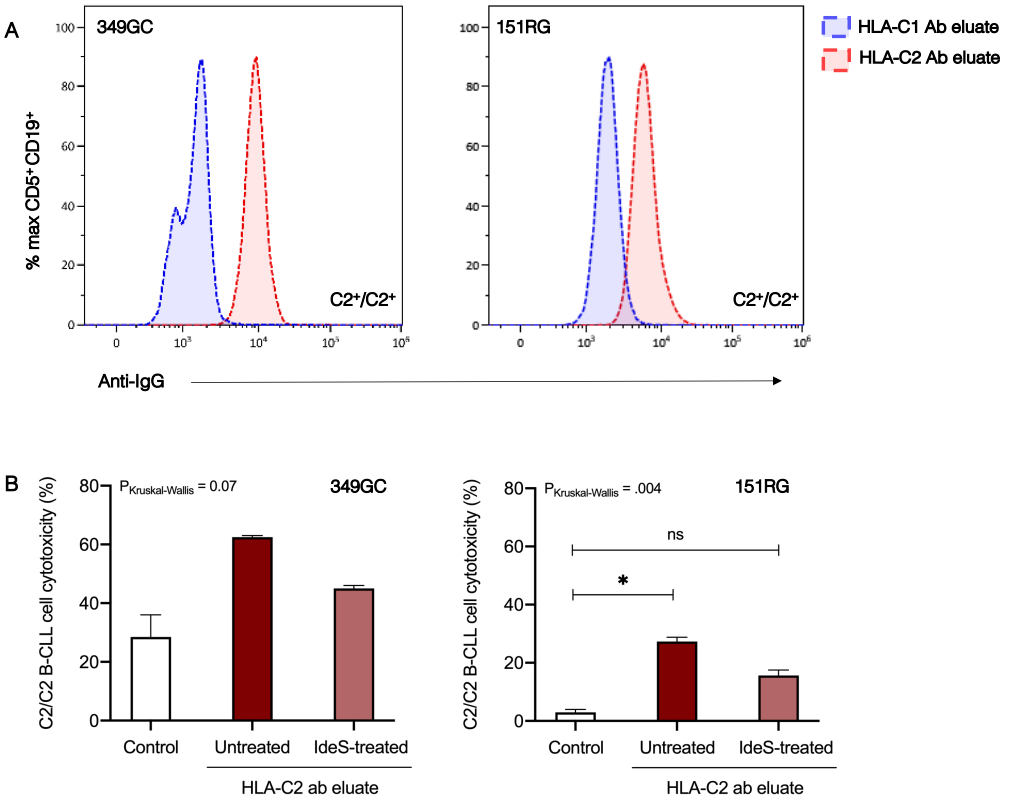

Figure 5.15. | Harnessing autologous NK cell cytotoxic function from B-CLL patients.

A | Two B-CLL patients – 349GC (left) and 151RG (right), were co-incubated with enriched HLA-C1 (blue) or -C2 (red) specific alloantibodies. Using an anti-IgG secondary antibody, reactivity to HLA-C1 or -C2-specific alloantibodies were measured by flow cytometry. Overlayed histogram plots represent specific antibody binding on $CD5^+$ $CD19^+$ cell subset to show greater HLA-C2 allelic expression. The data were collected using the Beckman Coulter Gallios flow cytometer and analysed by the Kaluza software.

B | The effect of HLA-C2-specific alloantibody treatment of B-CLL cells – 349GC (left) and 151RG (right) and autologous IFN-α-activated NK cells was measured in an overnight assay. Percentage B-CLL cytotoxicity was measured in the absence of treatment i.e. untreated B cells and NK cells (white bar); intact antibody-treated B cells and untreated NK cells (dark red bar) and IdeS-treated antibody-bound B cells and untreated NK cells (light red bar). Data shown as mean±SEM from duplicate (349GC) or triplicate (151RG) wells and are representative of one experiment per B-CLL patient. Statistical analyses performed with by one way ANOVA for non-parametric data, Kruskal-Wallis test with Dunn's multiple comparisons analysis; * $p < 0.05$.

5.7. Discussion

This chapter described the profile of HLA-C expression, and additional HLA Class I proteins on solid tumour cell lines and primary B-CLL cells by using a range of flow cytometry-based antibody panels, including enriched HLA-C-specific alloantibodies from the sera of renal transplant recipients. Differential HLA-C expression on solid tumour cell lines revealed suitable target cells to test with HLA-C-specific alloantibodies, which showed the ability to promote NK cell function. In addition, increased HLA-C expression on $CD5^+$ $CD19^+$ B-CLL tumour cell subset presented an opportunity to investigate the therapeutic potential of HLA-C alloantibodies in a primary tumour cell model. Firstly, the HLA-C-specific alloantibodies enhanced NK cell mediated lysis of primary B-CLL cells. Secondly, this increase in cytotoxicity was partially retained, even after the blockade of ADCC pathway. These findings confirmed that two mechanisms were involved in the enhanced NK cell cytotoxic function by HLA-C-specific antibodies.

5.7.1. Characterising HLA-C expression on solid tumour cell lines

The role of HLA expression in various human cancers has been well studied. It is generally accepted that total HLA expression, particularly HLA Class I is downregulated in tumours, primarily to escape T cell mediated attack (Demanet et al., 2004). As a major tumour escape mechanism, loss or downregulation of HLA Class I or an altered HLA Class I phenotype has been reported in a number of invasive tumours, including cancers of breast, colon, melanoma and pancreas (Garrido et al., 1997) and tumour cell lines (Seliger et al., 2002). These observations, however, were mostly based on immunohistochemistry (IHC) analyses as direct flow cytometry analysis was difficult due to the availability of primary samples.

A range of solid tumour cell lines were phenotyped for HLA Class I and HLA-C expression by using W6/32 and DT-9 antibodies, respectively. Whilst high levels of total HLA Class I was observed in all cell lines, HLA-C was differentially expressed, resulting in low to moderate expression compared to HLA Class I. As W6/32 is a pan-HLA Class I antibody, staining pattern included HLA-A, -B and -C antigens and thus higher MFI values were measured. Comparatively, lower MFI values from DT-9 staining can be possibly explained by selective HLA-C locus loss or downregulation as an immune evasion mechanism. On the other hand, given that HLA-C levels on normal cells are up to 18 times lower than HLA-A and -B levels (Apps et al., 2015), low to moderate staining by DT-9 antibody is not so surprising. Moreover, higher MFI values deriving from DT-9 staining e.g. SKOV-3, requires the antibody specificity for HLA-E locus to be taken into consideration. Hence, the HLA-C locus variant expression on tumour cell lines was analysed by using enriched HLA-C1 and HLA-C2-specific alloantibodies.

Most cell lines including SKOV-3 did not demonstrate distinct reactivity patterns, but A431 (epidermoid carcinoma) and A375 (melanoma) cell lines revealed high MFI values following staining with HLA-C1 and -C2-specific alloantibodies, respectively. A431 and A375 cell line reactivity to the enriched alloantibodies were highly selective as the binding specificities were in line with the published HLA-C types of the two cell lines – A431 (HLA-C*07:02 homozygous – C1) and A375 (HLA-C*16:02 (C1) and HLA-C*06:02 (C2)) (Boegel et al., 2014).

Although HLA-C1 (-C*16:02) positive, lower A375 reactivity to HLA-C1-specific antibody eluate was similar to the eluate reactivity observed with HLA-Cw16 antigen coated luminex beads. Figure 3.7 (Chapter III) shows the MFI values for cross-reactive epitopes comprising HLA-B46, 73 and HLA-C1 antigens, including Cw16, following enrichment of HLA-C1-specific alloantibodies from patient serum. Similar to the physiological reactivity

of A375 cells, HLA-Cw16 coated bead reactivity was less than 5000, potentially explaining the weaker HLA-C1-specific antibody reactivity profile than HLA-C2-specific antibody.

The number of reports describing HLA-C levels in melanoma and epidermoid carcinomas are limited. In line with the findings of the current study (Figure 5.2), low HLA-C levels were also measured on a range of melanoma cell lines (Chang et al., 2015). Likewise, HLA Class I expression at the mRNA and protein levels are lower in A375 cells (Johnson et al., 2016). Moreover, to the best of my knowledge, the findings in the current study are the first to confirm and validate HLA-C locus allele variant expression of in A375 and A431 by enriched HLA-C allotype-specific alloantibodies by flow cytometry.

In contrast to melanoma, 30-35% of epidermoid carcinomas (A431) express higher levels of HLA Class I proteins, presenting a more heterogeneous tumour landscape (García-Plata et al., 1993). This is also evident from the high MFI values measured from W6/32 staining for HLA Class I proteins and DT-9 staining for HLA-C (Figure 5.1). A431 cells also express HLA-E at detectable levels (Io Monaco et al., 2011), but the confounding effects were irrelevant as HLA-C1-specific antibody not only confirmed HLA-C expression but also HLA-C*07:02 (C1 allotype) allelic specificity.

5.7.2. HLA-C-specific alloantibodies and solid tumour cell cytolysis

Next, it was hypothesised that despite the heterogeneity of the HLA-expressing A431 and A375 target cells, disrupting the HLA-C:KIR interaction with HLA-C alloantibodies would lead to enhanced NK cell function and thus, increased target cell cytotoxicity. This hypothesis was proven by the improved activity of polyclonal NK cells (enriched from healthy donor PBMCs with a dominant proportion of KIR2DL3^{+} NK cells) towards A431 cells and KIR2DL1-gene (HLA-C2-specific) transduced NK92 cell line towards A375 cells.

In agreement with the findings of the A431-NK cell cytotoxicity assay, previous studies have also shown A431 as resistant to NK cell-mediated lysis (Galea-Lauri et al., 1999; Veluchamy et al., 2016). Lutz and Kurago (1999) demonstrated that lysis of squamous cell carcinoma cells (i.e. epidermoid carcinoma) was increased in the presence of HLA Class I-specific antibody and NK-92 subclones expressing KIRs. In the current study, however, polyclonal NK cell function was enhanced in the presence of HLA-C1-specific antibody-coated A431 cells. Although these results were observed in a single experiment, they indicate that the NK cell-resistant A431 cells were susceptible to cytolysis when HLA-C recognition was masked from KIR recognition.

Similar to A431 cells, Pende et al. (1998) have shown that primary melanoma cells with IFN-γ-stimulated HLA Class I expression offers protection from NK cell mediated lysis. In lieu of polyclonal effector cells, this study used KIR2DL1-transduced NK92 cells as effectors to demonstrate that HLA-C2 ligand (HLA-C*06:02) ligation with KIR2DL1 on NK92 cells suppressed A375 target cell lysis. Disruption of this HLA-C:KIR interaction led to increased A375 target cytolysis, which was further enhanced with HLA-C2-specific alloantibody as well as, unexpectedly, HLA-C1-specific alloantibody treatment. Sim et al., (2017) have reported that two HLA-bound peptides promote HLA-C2 allotype-specific, KIR2DL1 cross-reactive binding to HLA-C1 allotypes, which in this case is HLA-C*16:02. Moreover, in evolutionary terms, C2-epitope specific KIR2DL1 evolved much later from C1-epitope specific KIR (Hilton et al., 2012). Therefore, it is plausible to speculate that HLA-C1-specific alloantibody binding to HLA-C*16:02 mimicked HLA-C2-specific alloantibody binding to HLA-C*06:02, leading to enhanced NK92-KIR2DL1 function.

5.7.3. HLA-C expression on primary B-CLL cells

To gain a better understanding of HLA-C levels on primary CLL leukaemic blasts, total $CD19^+$ cell subset was further selected on the basis of CD5 expression. B-CLL occurs in the elderly and is characterised by the clonal expansion and accumulation of heterogenous malignant $CD5^+$ $CD19^+$ B cell clones (Kampalath, MD et al., 2003). More than 90% of B cells in early life predominantly express CD5, which later range between 10-20% in healthy adults (Gadol and Ault, 1986; Bhat et al., 1992). These frequencies, however, were not observed in the current study. The healthy volunteer cohort (aged 21-74 years) recruited to investigate HLA-C expression on specific B cell subsets demonstrated a much lower percentage (5.7±4.8%) of CD5-expressing B cells. In this study, the $CD5^+$ B cell subset in healthy volunteers aged 50 years and above (mean age 61.5 years), amounted to an average of 5.6±3.4%, which was comparable to 6.5% reported in healthy donors with a mean age of 66.7 years (Höffkes et al., 1996). Moreover, these findings contradict the flow cytometry analyses of B lymphocytes by Stewart and Stewart (1993) who found 2.7±1.9% of $CD5^+$ $CD19^+$ B cell population in the peripheral blood from healthy donors. The ages of the donors recruited for the study were not discussed in the published study.

Although co-expression of CD5 and CD19 has been previously used to phenotypically characterise B-CLL cells (Zheng et al., 2002), CD23 is also considered as a 'required' marker for flow cytometry-based analysis, particularly in B-CLL diagnosis (Rawstron et al., 2018). The current study did not include CD23 as a marker for analysis as CD23 is expressed at comparable densities on $CD5^+$ $CD19^+$ B cells from healthy adults and CLL patients (Damle et al., 2002).

To date, HLA Class I expression, particularly the HLA-C locus has not been studied in treatment-naïve, CD5-expressing $CD19^+$ B cells from CLL patients, but the total $CD19^+$ subset was analysed. In contrast to healthy donors, an average of 61.9±26.4% of $CD5^+$ $CD19^+$ cells were representative of the total B cell population in the B-CLL cohort. This study is the first to investigate HLA-C levels on both $CD5^-$ and $CD5^+$ $CD19^+$ cells in B-CLL and to report upregulation of HLA-C expression on the leukaemic $CD5^+$ B cell subset ($p < .001$) when compared with healthy individuals. HLA-E ($p = 0.32$) and total HLA Class I expression ($p > 0.99$) remained unchanged. These results, however, are contradictory to previously published research reporting loss or downregulation of HLA Class I expression in haematological malignancies, including AML, ALL and CLL (Brouwer et al., 2002; Masuda et al., 2007; Verheyden et al., 2009).

For example, Verheyden et al. (2009) examined total HLA Class I and HLA-allele specific expression on 20 B-CLL patients and reported downregulation of HLA-A and -B expression on $CD19^+$ cells. HLA-C expression was analysed at the allelic level by using antibodies recognising HLA-C1 allotypes – HLA-Cw1, -Cw3, -Cw*08:01, -Cw*12:02, -Cw*14:02 and HLA-C2 allotype HLA-Cw4 (Mulder et al., 1998). Total HLA-C2 allotype expression on leukaemic blasts was largely ignored. In contrast, this study used the DT-9 antibody clone to analyse HLA-C expression on both total $CD19^+$ subset and the malignant $CD5^+$ $CD19^+$ cells. The discrepancy between published findings and the results from the current study is likely to be a consequence of (i) the antibodies used to investigate HLA-C expression, and/or (ii) the patient criteria used for the B-CLL cohort. Linear regression analysis of HLA-C expression in healthy donors (Figure 5.7A) did not increase with age and indicated that higher cell surface HLA-C levels on $CD5^+$ $CD19^+$ cells is a consequence of the disease rather than increasing age. However, all patients were at an early stage of the disease suggesting that increased HLA-C expression is present at an early point in the natural history of the disorder.

5.7.4. HLA-E and HLA Class I expression on primary B-CLL cells

The caveat to using DT-9 antibody to measure HLA-C levels is the cross-reactivity to the HLA-E locus. Therefore, 3D12 antibody clone specific to HLA-E only was used to study the expression separately. Moreover, NK cell immune evasion mechanisms in B-CLL include upregulation of HLA-G (Erikci et al., 2009) and HLA-E (Wagner et al., 2017). In this study, HLA-E levels on both total $CD19^+$ subset and the malignant $CD5^+$ $CD19^+$ cells were comparable to healthy donors. This finding is not supported by published data which overwhelmingly report increased surface HLA-E and soluble HLA-E levels in CLL patients (Veuillen et al., 2012; McWilliams et al., 2016; Wagner et al., 2017). The methodological differences between published literature and this study could be responsible for no changes observed in HLA-E expression. As all the aforementioned studies analysed expression almost exclusively on $CD19^+$ B cells, this study also analysed the same population and found no difference in expression (Figure 5.6A). By further subdividing the $CD19^+$ population into the malignant $CD5^+$ B cell subset, also did not reveal any changes in HLA-E expression when compared with counterpart subset from healthy donors (Figure 5.6B). More importantly, to account for the genetic variability in HLA expression between individuals, MFI ratios and not raw MFI values were used for the phenotype analysis. Therefore, the MFI values deriving from a population of interest were divided by the MFI values deriving from autologous normal T cells ($CD3^+$) (Verheyden et al., 2009). This approach was not utilised by other studies analysing HLA-E expression, giving rise to discrepancies in data analysis.

Selecting malignant $CD5^+$ B cells from total $CD19^+$ B cells revealed no difference in total HLA Class I expression when compared to $CD5^+$ $CD19^+$ cells from healthy donors (Figure 5.6). This finding is consistent with other studies where comparable HLA Class I levels were observed in B-CLL patients (Masuda et al., 2007; Kowalewski et al., 2015). Increased

HLA Class I levels were measured in this study but on total $CD19^+$ B cells ($p < .00001$). It can be speculated that the upregulation of total HLA Class I was a consequence of a possibly greater $CD19^+$ B cell subset in CLL patients due to the clonal proliferation of leukaemic cells and thus increased tumour burden.

5.7.5. HLA-C-specific alloantibodies increase B-CLL tumour cytolysis

Due to the increased HLA-C levels on B-CLL cells, the therapeutic potential of HLA-C-specific alloantibodies to enhance NK cell function was investigated. Increased surface HLA Class I expression of drug resistant leukaemia cell line confers NK cell cytotoxicity resistance (Classen et al., 2003). In B-CLL, the functional capacity of NK cells is reportedly very poor, which often leads to reduced cytotoxic potential (Jewell et al., 1992; Veuillen et al., 2012; Parry et al., 2016). The same effect was observed in this study where NK cells exhibited poor cytotoxic activity against autologous B-CLL cells (Figure 5.15). This impaired functionality is usually accompanied by downregulation of NK cell activating receptors such as NKG2D (Huergo-Zapico et al., 2014), DNAM-1 and NCRs (Costello et al., 2012; Parry et al., 2016) as well as shedding of activating ligands from the surface of leukaemic cells (Hilpert et al., 2012). Reduced activity of NK cells has been shown to improve with either IL-2 (Kay and Zarling, 1987) or IFN-α treatment (Jewell et al., 1992). Therefore, enriched NK cells from healthy donors and B-CLL patients were pre-activated with IFN-α overnight. Consistent with previous findings, allogeneic NK cells from healthy donors demonstrate a greater cytotoxic function compared with NK cells deriving from CLL patients (Hofland et al., 2019).

The tolerogenic state of B-CLL cells is partially attributed to HLA-G, which like HLA-E, is upregulated on leukaemic blasts, facilitating escape from NK cells (Nückel et al., 2005). Due to the high antigen density, HLA-G blockade has shown to increase tumour cell susceptibility to NK cell mediated lysis (Maki et al., 2008). Using the same principle, enriched HLA-C1 or -C2-specific alloantibodies were used to perform blockade of KIR ligands on primary $CD5^+$ $CD19^+$ cells. Similar to HLA-G blockade, masking HLA-C recognition led to enhanced NK cell function and thus increased tumour cytolysis. This is the first study to use enriched HLA-C allotype-specific antibodies as a novel combination of tools to phenotype HLA-C allelic expression on B-CLL cells by recognising reactive epitopes at position 80. The same antibodies were subsequently used for HLA-C blocking experiments and augmenting NK cell function.

It is undoubtedly clear from this study that HLA-C-specific alloantibodies enhance allogeneic patient autologous NK cell activity. The differences in enhanced tumour cytolysis, however, was dependent on allogeneic NK cells and their specific KIR repertoires. Similar to the findings from Chapter IV, in the presence of KIR ligand mismatched NK cells, HLA-C-specific antibody coated B cells were lysed as effectively as in the presence of KIR ligand matched NK cells (Figures 5.10 and 5.13). This suggests that following HLA-C-specific alloantibody-dependent stimulation, KIR ligand mismatched or alloreactive NK cells act as potently as KIR ligand matched NK cells because they were present in the equivalent of a 'non-self' system. Moreover, as HLA-C allotypes are cross-reactive e.g. KIR2DL3 can also bind to HLA-C2 allotypes but with a lower affinity (Moesta et al., 2008), masking potential HLA-C ligand recognition is effectively mimicking an HLA-C-deficient target cell primed for NK cell activation.

Of note, whole NK cells from healthy donors with a dominant proportion of single KIR2DL1$^+$ (red) or KIR2DL3$^+$ (blue) NK cells were used in the HLA-C blocking functional assays. Co-expression with other inhibitory KIRs such as KIR2DL2, which also binds HLA-C1 ligands was not characterised. Therefore, it is possible for potential unaccounted inhibitory NK cell receptors to also impact the overall NK cell response to susceptible target cells. A limitation to these findings is that only one KIR ligand mismatched NK cell donor was utilised in HLA-C1 and -C2 blocking experiments with primary B-CLL cells. Therefore, to gain a better understanding of the functional capacity of KIR ligand educated and uneducated NK cells following HLA-C-specific alloantibody stimulation requires multiple experimental repeats with different NK cell donors.

Nevertheless, an increase in B-CLL cytotoxicity was observed using patient autologous NK cells (Figure 5.15). Although only two B-CLL patients were tested, HLA-C2-specific antibody treatment of B cells in both cases demonstrated enhanced NK cell function. As NK cells and B cells derived from the same patient, NK cells were KIR ligand matched. This finding further proves and validates the potential use of HLA-C-specific antibodies as therapy on tumour cells with upregulated HLA-C expression.

5.7.6. HLA-C-specific alloantibodies – mechanism of action

Leukaemic cells are thought to have evolved immune surveillance escape mechanisms by favouring inhibitory over activating KIR signalling (Verheyden et al., 2004; Verheyden and Demanet, 2006). This hypothesis is supported by the increased HLA-C levels on leukaemic blasts reported in this study. Moreover, by using HLA-C-specific alloantibodies, anti-tumour NK cell immune responses can be boosted as HLA-KIR interactions were inhibited. As discussed in Chapter IV, the mechanism of action of HLA-C-specific

alloantibodies was also investigated to potentially harness ADCC-independent NK cell responses.

Following inhibition of CD16 on NK cells, a retained cytotoxic function against HLA-C1 and -C2 antibody-specific treated B-CLL cells was demonstrated (Figure 5.13). CD16 blockade was efficient as positive control rituximab responses included in every experiment reached near control levels (Figure 5.12). In addition to the potential involvement of FCγRIIIa polymorphisms affecting NK cell responses, a study by Isitman et al. (2016) reported that single inhibitory KIR^{+} (iKIR) NK cells i.e. KIR2DL1, KIR2DL3 or KIR3DL1, expressed CD16 at a lower frequency than $iKIR^{-}$ NK cells. Moreover, poor NK cell effector function for ADCC was observed due to lower CD16 expression. The primary B-CLL-NK cell cytotoxicity assays utilised NK cells from healthy donors with a high percentage of KIR2DL1 or KIR2DL3 expression on NK cells. CD16 expression was not analysed (Chapter IV). Therefore, with the assumption of low CD16 expression together with preserved NK cell function against target cells after CD16 blockade offers a plausible reasoning for maintaining increased NK cell responses, not by ADCC but an alternative mechanism. This may involve modulating intracellular NK cell signalling to favour activation in the absence of ligation with HLA-C ligand.

Although single positive iKIR NK cells express CD16 at a lower frequency, it is still present on the cell surface. Therefore, it is noteworthy that regardless of CD16 surface density, Fc fragment of the HLA-C-specific alloantibodies engaging with CD16 would lead to NK cell activation. In an effort to counteract this variable, HLA-C-specific alloantibodies were treated with IdeS to digest and remove the Fc fragment from the hinge region of the antibody structure, preventing CD16 activation.

In contrast to the findings from CD16 blockade, IdeS-treated HLA-C-specific alloantibodies indicate a dominant role of ADCC in enhanced NK cell responses observed in these functional assays. Of note, not all NK cell donors demonstrated a significant reduction in target cell cytotoxicity, once again suggesting that the retained cytotoxic response is likely to partially result from NK cell intracellular signalling favouring activation. This effect is more evident in functional assays utilising HLA-C2/C2 B-CLL patient autologous NK cells.

Due to the limited availability of patient samples and the number of PBMCs isolated, these assays were performed with two B-CLL patients only. Both patients show that the increase in NK cell function and tumour cell lysis was preserved in the absence of CD16 engagement, which is similar to the effect observed in Chapter IV using K56-2C2 target cells. Taken together, these findings lend support to the hypothesis that unengaged iKIRs on NK cells leads to the dominance of activating signals over inhibitory signals, which in the absence of ADCC-dependent responses also enhance NK cell cytotoxic function against HLA-C2-specific antibody-coated target cells.

5.8. Conclusions

This preliminary study of HLA-C-specific alloantibodies as potential cancer therapeutics demonstrate promising, but variable *in vitro* activity that enhance anti-tumour NK cell activity by specifically blocking HLA-C-KIR interactions on solid and haematological tumour cells. In addition to the therapeutic potential, HLA-C-specific alloantibodies proved to be multi-functional as a novel tool for investigating HLA-C allelic expression on tumour cells. Allogeneic NK cells from healthy donors present a poor cytotoxic response to B-CLLs which was significantly enhanced by HLA-C allotype-specific alloantibodies. The HLA-C-specific alloantibodies mechanism of action indicate the potential role of harnessing NK cell intracellular activating signalling and limiting ADCC-dependent responses to possibly prevent off-target effects *in vivo*. This was also the case involving patient autologous NK cells. The action of HLA-C-specific antibodies included two mechanisms – (i) ADCC and (ii) NK cell activation mediated by HLA-C:KIR interaction blockade. In some cases, the influence of NK cell intracellular activating signalling with limited ADCC-dependent responses would suggest minimal off-target effects *in vivo*. The complete therapeutic potential of HLA-C-specific alloantibodies for cancer therapy and possibly other disease areas require additional robust and detailed analyses.

CHAPTER VI

GENERATION OF HLA-SPECIFIC MONOCLONAL ANTIBODIES FROM SINGLE B CELLS

6.1. Introduction

The findings from the previous chapters within this thesis demonstrate the functional potential of HLA-C-specific antibodies. The antibodies act as KIR mimics but disrupt the inhibitory interaction between the KIRs on NK cells and HLA-C ligands, which in turn, enhance NK cell-mediated lysis of target cells. To perform the functional experiments, HLA-C-specific antibodies were isolated from the sera of sensitised renal transplant recipients awaiting re-transplantation. Moreover, HLA-C group 1 or group 2-specific antibodies were efficiently enriched using either an immobilised HLA-protein coupled column or an HLA-C group 2 allele-transfected cell line, respectively. Although the adsorption processes were specific, the enriched antibody eluate likely contained a polyclonal mix of antibodies reactive to multiple epitopes on the HLA-C molecule. Therefore, monoclonal antibodies generated from single B cells of interest presented a more favourable alternative to repeated cycles of antibody enrichment, particularly from a limited amount of sera.

Several methods are available by which human monoclonal antibodies can be produced from memory, short-lived antibody-secreting or antigen-specific B cells. These methods include fusion of an antibody-producing B cell and myeloma cell to produce hybridomas (Köhler and Milstein, 1975); phage display technology (McCafferty et al., 1990); immortalisation of B cells by EBV (Traggiai et al., 2004) and direct amplification of immunoglobulin genes from short-lived antibody-secreting B cells to express monoclonal antibodies in a mammalian system (Tiller et al., 2008; Smith et al., 2009).

This chapter aimed to generate HLA Class I, particularly HLA-C-specific monoclonal antibodies from single B cells deriving from the PBMCs of renal transplant recipients (Figure 6.1). Firstly, to identify HLA-specific antibody producing B cells, flow cytometry-based selection tools such as HLA Class I-specific tetramers or single HLA antigen coated beads were tested and optimised for this study using PBMCs from non-sensitised and sensitised individuals. These tools were later used to isolate HLA-specific memory B cells which were cultured for a short period of time and culture supernatants were screened to determine antibody specificities.

Secondly, two approaches involving short-term culture of B cells were examined. The first approach aimed to isolate HLA-specific monoclonal antibodies by stimulating B cells with CD40-L and cytokines IL-2 and IL-21 to induce an antibody-secreting phenotype of B cells. The culture supernatants were tested for IgG using an ELISA while antibody specificities were tested using single HLA antigen coated luminex beads. The second approach involved large-scale immortalisation of B cells by EBV. Screening of culture supernatants for antibody specificities were performed using alloreactive PHA blasts from healthy donor PBMCs.

Finally, a more direct approach was undertaken to generate HLA-specific antibodies from renal transplant patients by isolating the plasmablast population seven days after transplant nephrectomy. At first, the immunoglobulin genes were successfully amplified by PCR from single plasmablasts and sequenced. Next, paired heavy and light chain DNA deriving from the same plasmablast were cloned into respective expression vectors and transiently expressed in a mammalian cell line system. The recombinant antibodies were tested against a number of cell lines and HLA Class I antigen-coated beads in a luminex assay to determine specificity.

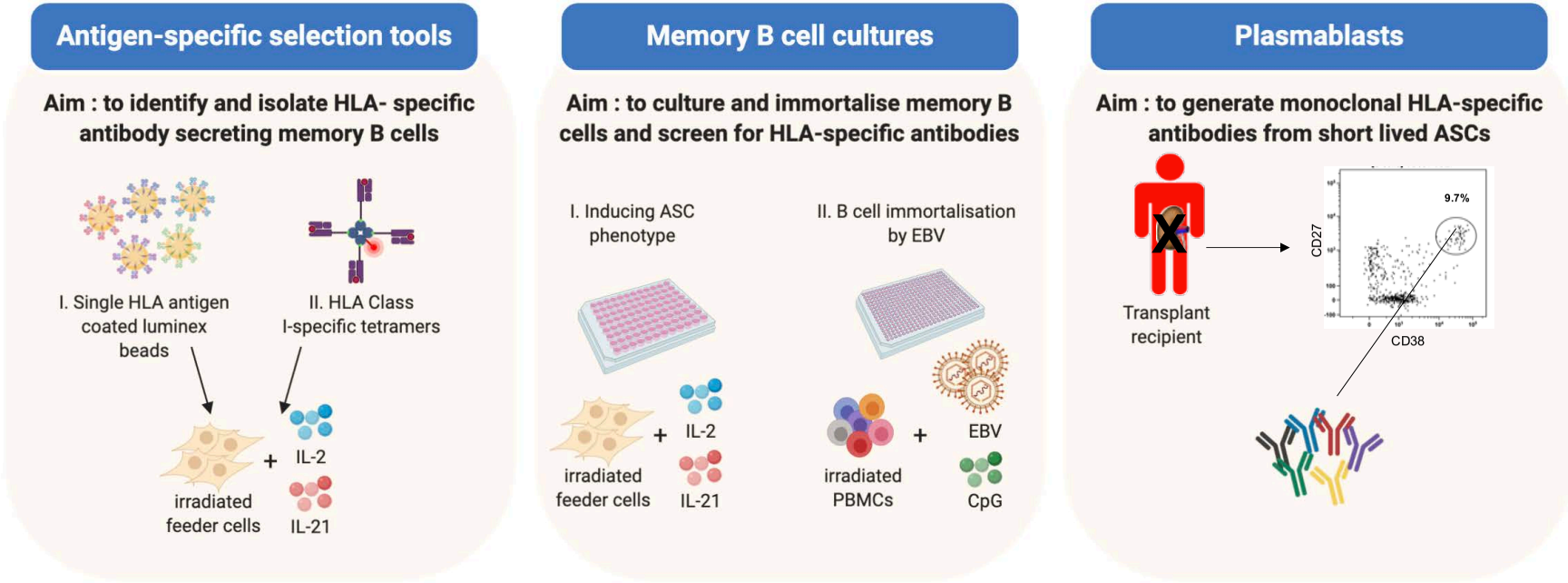

Figure 6.1. | Overview of the methods used to generate HLA-specific monoclonal antibodies.

To identify and isolate HLA-specific antibody secreting memory B cells, selection tools such as HLA Class I-specific tetramers and single HLA antigen coated luminex beads were used in the absence and presence of a short-term B cell culture system that aimed to induce an antibody secreting B cell phenotype. Alternatively, B cells were immortalised using EBV and a B cell activating culture system, involving irradiated alloegeneic PBMCs and CpG. To generate recombinant antibodies *in vitro* from single B cells, low-affinity antibody secreting plasmablast population was identified from two transplant nephrectomised patients. Using FACS, plasmablasts were sorted at the single cell level to amplify the immunoglobulin genes for transient expression in a mammalian system.

6.2. Optimisation of methods to isolate HLA-specific antibody secreting B cells

6.2.1. Culturing memory B cells to produce antibodies

The method to rapidly expand and enhance memory B cells in culture to isolate human monoclonal antibodies (Huang et al., 2013) was optimised for this study. This approach aimed to enhance antigen-specific memory B cell survival or proliferation on a CD40 ligand (CD40-L) expressing feeder cell system supplemented with IL-2 and IL-21 to produce IgG over 12 days. At the end of this culture system, the supernatants may be harvested for screening or neutralisation assays, and the expanded memory B cells may be collected for recombinant antibody production (see Section 6.5). In the current study, this method was firstly optimised using memory B cells isolated from PBMCs from a healthy donor. This process of optimisation included seeding cells at various densities per well and harvesting supernatants to detect and quantify total IgG using ELISA.

Figure 6.2 illustrates the flow cytometry-based gating strategy used to isolate $CD19^+$ $CD27^+$ memory B cell subset of interest from PBMCs. IgG^+ $CD19^+$ B cells were negatively enriched by excluding viable $CD19^+$ B cells also expressing IgD, IgM and IgA. Next, IgG^+ $CD19^+$ $CD27^+$ memory B cells were added to a layer of CD40-L expressing feeder cells at varying cell densities per well – 1, 2, 4, 10, 20, 50 and 100. After 12 days, supernatants from rows plated with the same number of B cells were harvested and pooled at a final 1:10 dilution. Total IgG production was determined using an IgG-specific ELISA.

Figure 6.3A reveals varying IgG concentrations measured at different cell densities. Using the standard curve generated for IgG detection, the total IgG from pooled supernatants ranged from 8.7-22.7ng/mL. When 2 or 4 cells per well were plated, a comparable concentration of IgG was measured at 16.5 and 17.1ng/mL, respectively. Moreover, similar IgG levels (~23.0ng/mL) were observed when 10, 20, 50 and 100 cells were plated per well, suggesting saturation of the IgG ELISA.

Therefore, the method was further optimised by seeding one memory B cell per well (Figure 6.3B) across three 96 well plates. Pooled supernatants from wells containing one cell also demonstrated median IgG concentration of 16.9ng/mL (ranging from 11.8-22.7ng/mL). Reducing the cell density from 2 cells to 1 cell per well revealed similar levels of total IgG production with 16.5ng/mL and 16.9ng/mL, respectively. Taken together, these data show that achieving a seeding density between 1 and 4 cells per well is optimal to detect IgG in culture supernatants. Lower cell densities would also facilitate an efficient downstream process of antibody cloning. Moreover, measuring total IgG in supernatants from wells with high cell density saturate the IgG ELISA assay, leading to unreliable and inaccurate measurement.

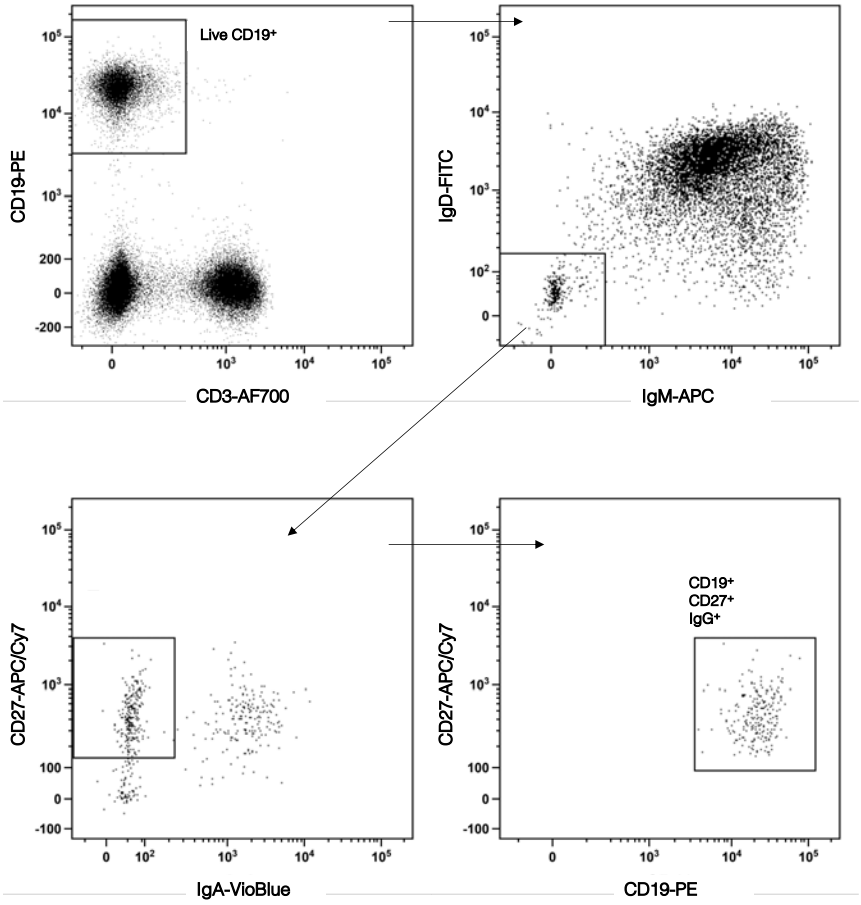

Figure 6.2. | Representative flow gating strategy to isolate IgG-expressing memory B cells.

PBMCs were gated on viable $CD19^+$ B cells and excluded $CD3^+$ T cells from further analysis. Negative isolation strategy was adopted to gate out B cells expressing IgD, IgM and IgA, leaving with IgG^+ B cells. IgG-expressing memory B cells were identified as $CD19^+$ $CD27^+$ and were subsequently sorted into wells using FACS for further analyses.

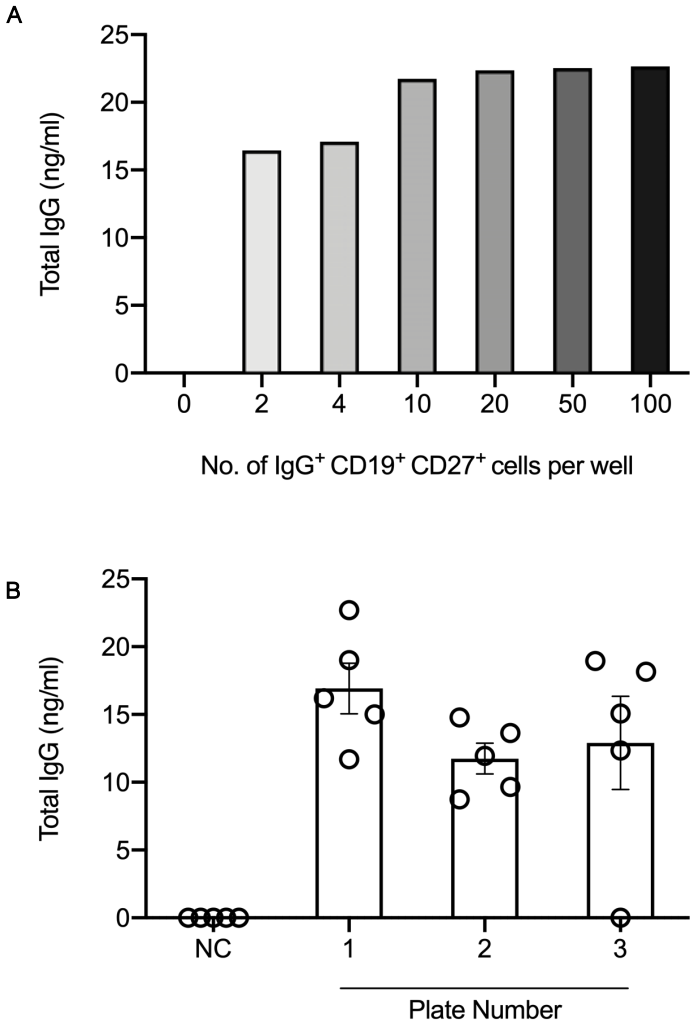

Figure 6.3. | Total IgG concentrations measured after 12 days of culture by ELISA.

A | IgG^+ $CD19^+$ $CD27^+$ B cells were seeded at densities of 0, 2, 4, 10, 20, 50 and 100 cells per well containing a layer of CD40-L expressing feeder cell line and medium conditioned with IL-2 and IL-21. Total IgG (ng/mL) was quantified by ELISA. Data represent a single experiment.

B | IgG^+ $CD19^+$ $CD27^+$ B cells were seeded at density of 1 cell per well in three 96 well plates containing a layer of CD40-L expressing feeder cell line and medium conditioned with IL-2 and IL-21. Each circle represents IgG concentration measured from pooled supernatants of 10 individual wells containing single B cell cultures. Five pooled supernatants were tested per plate, including a row of negative control which contained no B cells. Total IgG (ng/mL) was quantified by ELISA. Bars indicate mean±SEM. Data represent a single experiment.

6.2.2. Isolation and culture of HLA Class I-specific tetramer$^+$ B cells

HLA Class I-specific tetramers have shown to be effective tools in selecting and isolating HLA Class I-specific antibody secreting B cells from women immunised by pregnancy (Mulder et al., 2003) and transplantation (Zachary et al., 2007). Therefore, the use of HLA Class I-specific tetramers was optimised as a selection tool for the current study. The aim was to use the tetramers, irrespective of the CMV-specific peptide bound in the grooves, to identify and isolate HLA Class I-specific alloreactive B cells from renal transplant recipients with a previously failed allograft. Short-term cultures using the CD40-L, IL-2 and IL-21 system were also established to promote proliferation of single tetramer-bound alloreactive B cells.

Two patients – Allomab 003 and 008 with high levels of HLA-A and HLA-B-specific alloantibodies were selected for this method (Figure 6.4). PBMCs from patients were co-incubated with cell surface staining antibodies and fluorophore-conjugated HLA-A1, -A3, -B7, -B8 and -B35-specific tetramers. Using FACS, negatively enriched IgG-expressing CD19$^+$ CD27$^+$ memory B lymphocytes were further selected on the basis of tetramer reactivity (Figure 6.5A). Patient 003 serum HLA-specific antibody profile demonstrated reactivity to HLA-A1 (MFI=16,088.0) and HLA-B7 (MFI=5,000.0) antigen-coated beads only (Figure 6.5B). However, HLA-A1 and HLA-B7-specific tetramers and negative control HLA-A3 and HLA-B35-specific tetramers all revealed reactivity to IgG$^+$ CD19$^+$ CD27$^+$ B cells (Figure 6.5C). Likewise, patient 008 presenting with HLA-B7-specific antibody (MFI=1,000.0) (Figure 6.5D) showed binding to HLA-A1, -A3, -B7, -B8-specific tetramers (Figure 6.5E). These results strongly indicate non-specific binding with the tetramers in this assay. The HLA-specific tetramer-bound alloreactive B cells were subsequently sorted at the single cell level onto a culture system comprising CD40-L expressing feeder cells, IL-2 and IL-21.

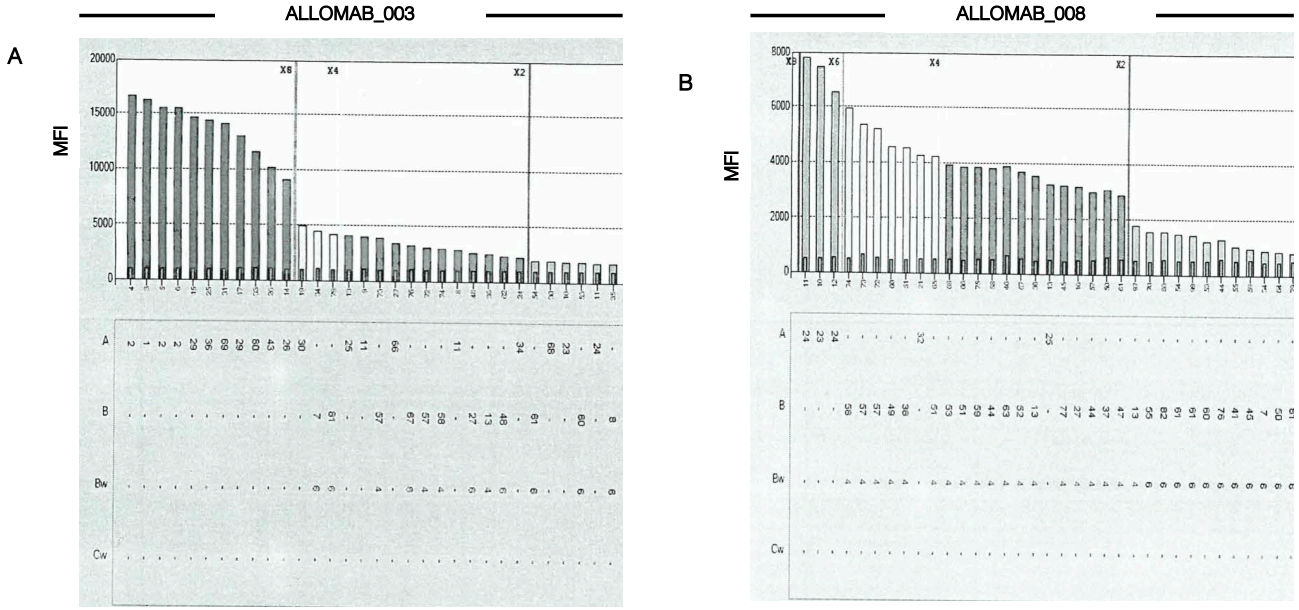

Figure 6.4. | HLA Class I antigen bead reactivity profiles of Allomab patients 003 and 008.

LABScreen Class I (One Lambda) single antigen bead (SAB) analysis of patient serum shows reactivity towards a range of HLA-A, -B and -C antigen coated beads. Polystrene SABs embedded with varying ratios of two fluorochromes and coated with single HLA Class I antigens were treated with patient serum, followed by labelling of antibody-bound beads with anti-IgG secondary antibody. The range of HLA-specific antibody levels were measured by median fluorescence intensity values (MFI).

A | Patient 003 serum presents an antibody profile predominantly reactive to HLA-A antigens with MFI values above 10,000, and a few HLA-B antigens with MFI values below 5,000.

B | Patient 008 serum presents an antibody profile highly reactive to HLA-A antigens with MFI values above 6,000, and HLA-B antigens with MFI values ranging between 2,000 and 6,000.

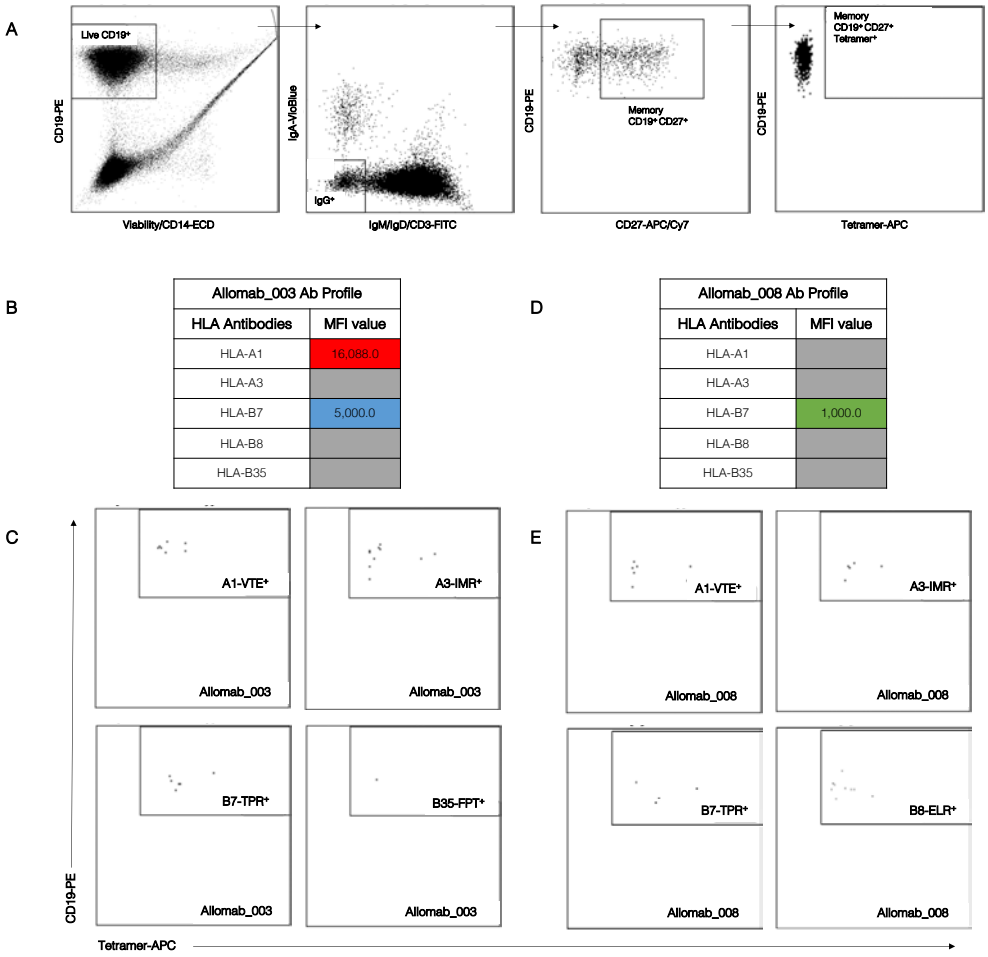

Figure 6.5. | Identification and isolation of HLA-tetramer+ memory B cells.

A | Representative flow gating strategy showing selection of viable CD19+ B cells and exclusion of CD3+ T cells. Negative isolation strategy was adopted to gate out B cells expressing IgD, IgM and IgA. IgG-expressing memory B cells were identified as CD19+ CD27+ tetramer+.

B | A summary of HLA-specific antibody profile of patient 003 with high MFI value (red) against HLA-A1-coated beads and low MFI value (blue) against HLA-B7-coated beads. No bead reactions (grey) were detected against HLA-A*03, HLA-B*08 and HLA-B*35.

C | FACS analysis of HLA Class I-specific tetramer binding to patient 003 IgG+ memory B cells. Binding was detected against HLA-A*01 (VTE), HLA-A*03 (IMR), HLA-B*07 (TPR) and HLA-B*35 (FPT). B cells were seeded at density of 1 cell per well containing a layer of CD40-L expressing feeder cell line and medium conditioned with IL-2 and IL-21.

D | A summary of HLA-specific antibody profile of patient 008 with detectable reactivity (green) against HLA-B*07-coated beads. No bead reactions (grey) were detected against HLA-A*01, HLA-A*03, HLA-B*08 and HLA-B*35.

E | FACS analysis of HLA Class I-specific tetramer binding to patient 008 IgG+ memory B cells. Binding was detected against HLA-A*01 (VTE), HLA-A*03 (IMR), HLA-B*07 (TPR) and HLA-B*08 (ELR). B cells were seeded at density of 1 cell per well containing a layer of CD40-L expressing feeder cell line and medium conditioned with IL-2 and IL-21.

After 12 days, the collected culture supernatants were tested for IgG production by ELISA. Figure 6.6A shows that absorbance values similar to the negative control (0.05) were measured predominantly for tetramer$^+$ memory B lymphocytes, irrespective of tetramer specificity for each patient. Patient 003, however, revealed greater absorbance values deriving from HLA-A*01 and HLA-A*03 single B cells, compared to the negative control. The concentrations of IgG secreted by HLA-A*01 B cells were variable, which ranged from 8.2-20.0 ng/mL, whilst 13.2ng/mL total IgG was detected in the supernatant deriving from HLA-A*03 B cell culture (Figure 6.6B).

To further confirm and validate the presence of IgG in the harvested supernatants, light chain specificity ELISA was performed (Figure 6.6C). Higher absorbance values were detected for kappa chain IgG compared to lambda chain IgG, demonstrating that their detection is mutually exclusive. Furthermore, the detection of single light chain specificity confirmed the presence of monoclonal antibodies obtained from single B cell cultures. Although B cells from patient PBMCs showed binding to HLA Class I-specific tetramers corresponding to the respective antibody profile, they also demonstrated non-specific reactivity to irrelevant tetramers. Therefore, a more selective tool was required to identify and isolate B lymphocytes secreting HLA-specific antibodies of interest.

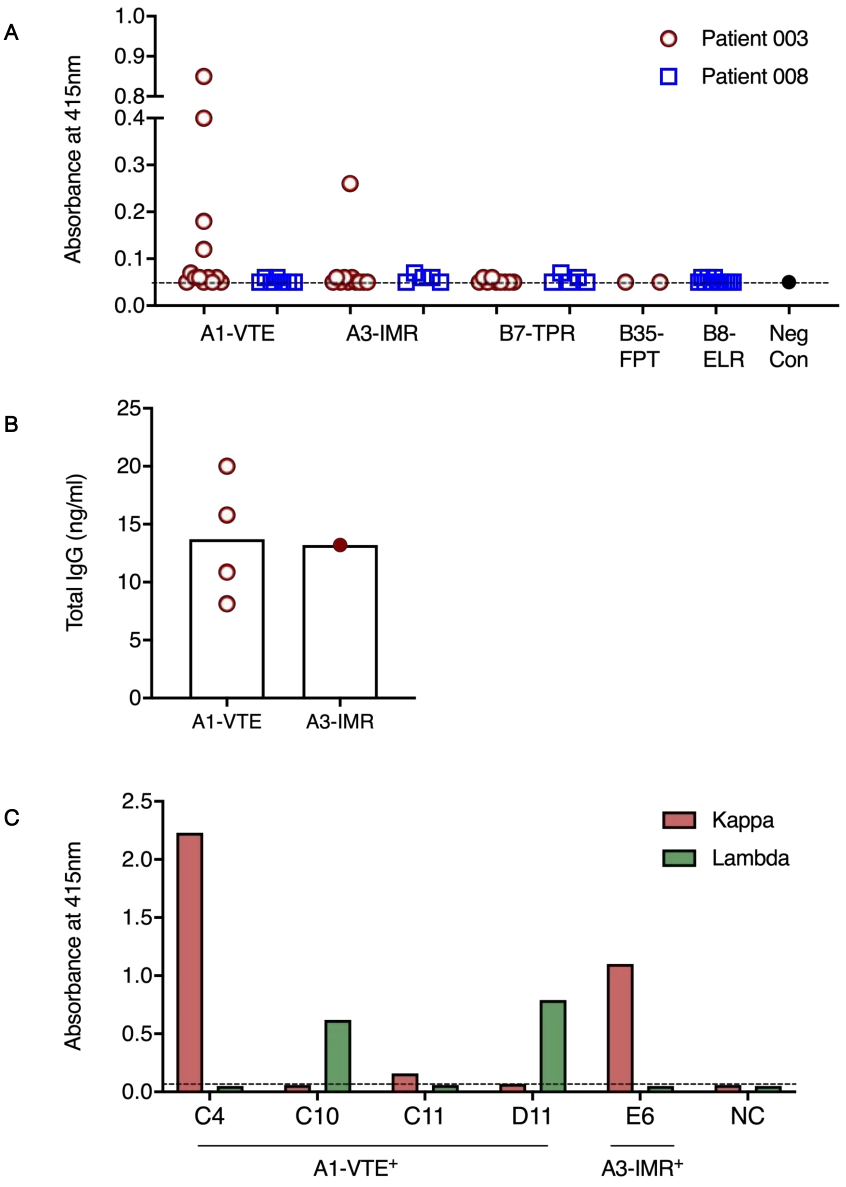

Figure 6.6. | Total IgG concentrations measured after 12 days of HLA-tetramer+ B cell culture.

A | Absorbance values at 415nm were measured for individual wells containing HLA-tetramer+ IgG+ CD19+ CD27+ B cells. Red circles indicate IgG measured from patient 003 B cell cultures. Blue squares indicate IgG measured from patient 008 B cell cultures. Dotted line represents the negative control well absorbance value.

B | Total IgG (ng/mL) was quantified by ELISA for wells with high absorbance values from patient 003 B cell cultures. Red outline circles represent IgG concentrations of wells containing HLA-A1-specific tetramer+ B cells. Red circle represents IgG concentration of well containing HLA-A3-specific tetramer+ B cell.

C | Light chain specificity ELISA was performed using supernatants from wells containing HLA-A1 and HLA-A3-specific tetramer+ B cells Red bars indicate kappa light chain specificity. Green bars indicate lambda light chain specificity.

6.2.3. Detection of HLA Class I-specific SAB-bound B cells

As an alternative selection tool, the use of HLA Class I antigen-coated single antigen beads (SABs) was optimised. To determine the presence of HLA Class I-specific antibody secreting B cells, PBMCs from healthy donors were co-incubated with LIFECODES single HLA Class I antigen-coated luminex beads (Immucor, USA). Figure 6.7A is a schematic representation of isolated PBMCs from healthy donors labelled with a cell surface CD19-specific fluorochrome conjugated antibody, followed by co-incubation with SABs before flow cytometry-based analysis. To detect B cell binding to SABs, the flow gating strategy in Figure 6.7B was used during HLA Class I-SAB immunostaining analysis.

Firstly, all single PBMCs were identified based upon their forward scatter area and height parameters. Secondly, forward and side scatter profiles of the single cells were separated into the unbound Class I beads and Bead-B cell rosette (BBR) populations. The BBR gate included SAB-bound B cells whilst the unbound PBMCs were easily identifiable by their intermediate forward scatter and low side scatter profiles. Unbound SABs, however, were identified at low forward scatter and high side scatter parameters. Therefore, the BBR gate was set directly above the PBMC population with intermediate forward scatter and high side scatter profiles. Thirdly, the addition of propidium iodide (PI) allowed exclusion of dead cells within the BBR population and live B cells were selected for CD19 expression. Finally, the optimal working conditions of the unbound beads were confirmed by the skewed representation of histogram analysis of each fluorochrome (Figure 6.7C). Each HLA Class I antigen-specific bead population projecting to a specific region based on distinct fluorochrome ratios was evaluated by viewing one fluorochrome-equivalent fluorescence channel against the other.

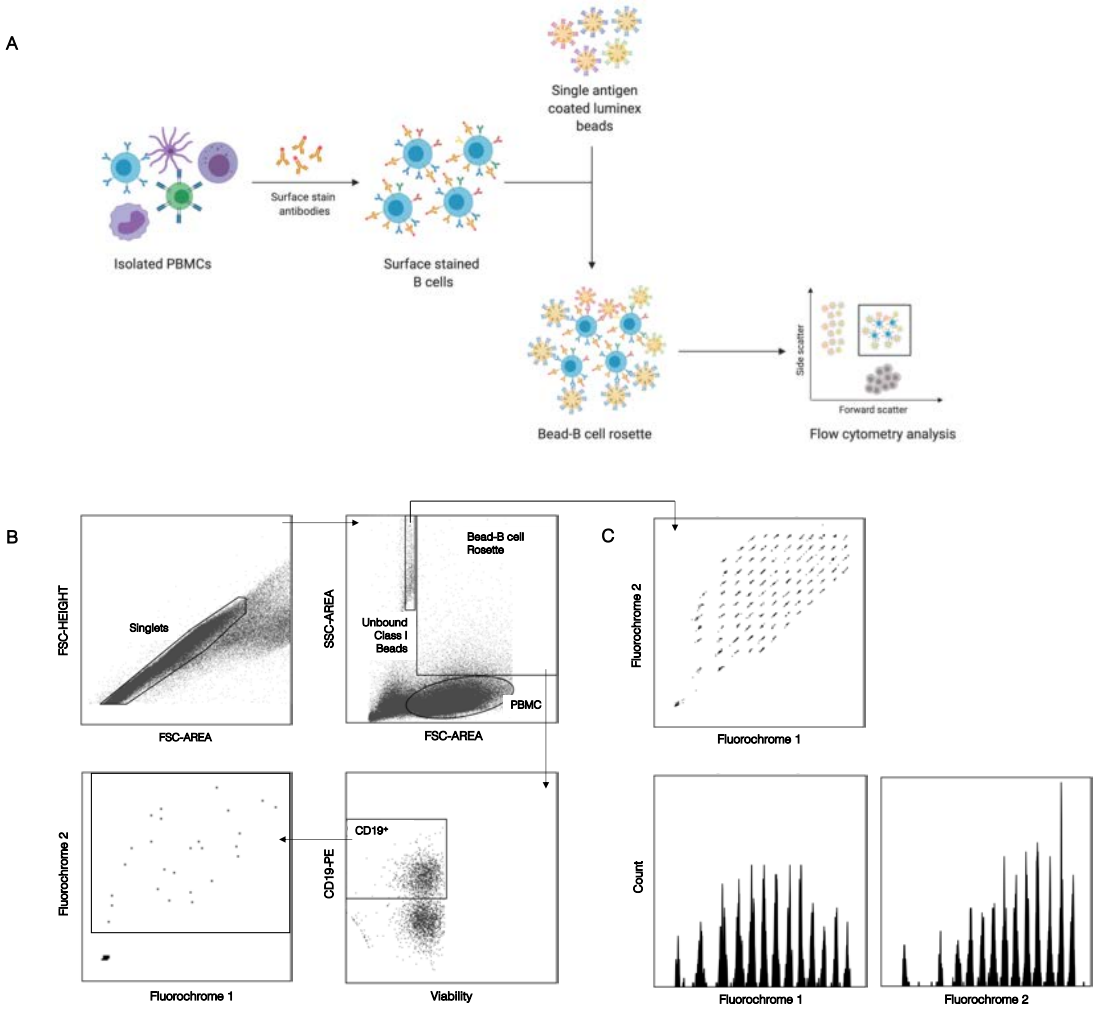

Figure 6.7. | HLA Class I-specific antibody secreting B cell binding to single antigen coated beads.

A | Schematic showing the principle of B cells binding to SABs. PBMCs were labelled with cell surface antibodies and co-incubated with HLA Class I antigen-coated beads. Labelled B cells secreting HLA-specific antibodies bind to SABs and form a bead-B cell rosette (BBR). Flow cytometry identified unbound SABs and PBMCs and BBRs for further analysis.

B | Flow gating strategy used to analyse and detect the presence of antigen-specific B cells in healthy individuals. Single cell population was divided into unbound Class I beads, bead-B cell rosette and PBMC populations. Live $CD19^{+}$ B cells from the BBR gate were selected and bead reactivity was analysed by their internal fluorochrome ratio profiles.

C | Distinct allele-specific Class I bead populations are observed when each fluorochrome is viewed against the other. Skewed histogram plot represents the varying ratios of each fluorochrome within total beads population.

The frequency of live $CD19^+$ B cells specifically interacting with SABs was determined by analysing the percentage of $CD19^+$ and bead fluorochromes 1^+ and 2^+ B cells. Varying volumes of Class I-antigen coated beads – 1µL, 2µL and 3µL were co-incubated with CD19-labelled B cells to identify an optimal volume of SABs to use in this assay. To limit non-specific binding to SABs, B cells were pre-treated with autologous serum and subsequently incubated with SABs.

Figure 6.8 demonstrates that varying volumes of beads show different levels of reactivity towards B cells. Under no serum treatment (-), the largest percentage of Class I bead-positive B cell population was detected with 2µL of beads (median=0.02%), whilst 1µL and 3µL both showed a median of 0.01%. Treatment with donor autologous serum (+), however demonstrated that the percentage frequency of Class I bead+ B cells increased as the volume of beads added for co-incubation was also increased, in the order of 1µL, 2µL and 3µL (median = 0.01%, 0.03% and 0.035%, respectively). Mann Whitney unpaired t-test revealed that there was no statistical difference between no serum (-) and serum (+) treatment at the various bead volumes used to identify HLA-specific antibody secreting alloreactive B cells. This shows that treating PBMCs with serum prior to co-incubation with beads does not directly affect binding to SABs. Moreover, using high volume of beads (3µL), in the absence of serum treatment, to react with PBMCs demonstrated similar frequency of SAB-bound B cells as beads at a lower volume (1µL). This suggested that using 1µL of SABs was sufficient to detect HLA-specific antibody secreting B cells.

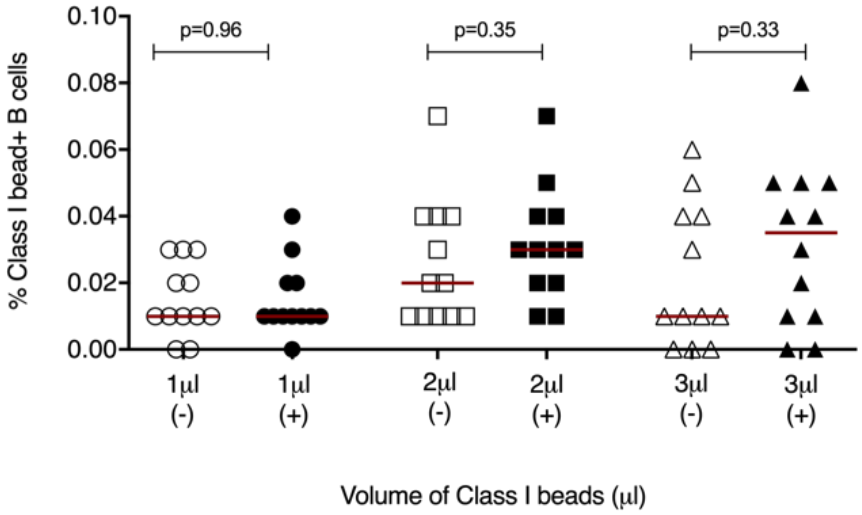

Figure 6.8. | Optimisation of single HLA coated beads and serum treatment for staining assay.

Varying volumes of SABs – 1µL, 2µL and 3µL were tested for B cell reactivity during co-incubation with donor autologous serum untreated (left; open symbols) and pre-treated (right; closed symbols) $CD19^+$ B cells. The percentage frequency of Class I bead-bound B cells were measured. The effect of serum treatment compared to untreated B cells was measured for all SAB volumes used in this immunoassay. Mann Whitney t-test for nonparametric data revealed no overall significant difference between the treatments. Red line indicates median; n=12 per group.

6.3. Isolation and culture of HLA-specific antibody-secreting B cells

By combining the approaches covered in section 6.2, HLA Class I-specific antibody-producing memory B cells were isolated with HLA Class I SABs for *in vitro* expansion. Using the gating strategy in Figure 6.7B, $CD19^+$ B cells of interest were detected in PBMCs from healthy donors and renal transplant recipients. Representative examples in Figure 6.9 illustrates a greater frequency of SAB-bound B cells in PBMCs from a healthy donor (15.8%) (Figure 6.9A) compared to PBMCs analysed from four patients, where less than 12.0% SAB-bound B cells were observed (Figure 6.9B). With the exception of patient 001 (11.8%), patients 002, 003 and 004 presented a more selective bead binding pattern and thus, lower frequencies of HLA Class I-specific bead-B cell rosette were detected at 0.9%, 3.0% and 6.9%, respectively. Therefore, compared to the higher frequencies of SAB-bound B cells observed in healthy donors, lower frequencies from patients implies potentially more specific binding of HLA-specific antibody secreting B cells.

To isolate HLA Class I-specific antibody secreting B cells, patient 007 with HLA-A and HLA-B-specific antibodies was selected (Figure 6.10A). Cell surface labelled-patient PBMCs were co-incubated with HLA Class I-specific SABs. The bead-B cell rosette was further selected for live $CD19^+$ $CD27^+$ memory B cell phenotype. IgG^+ memory B cells were negatively selected during flow cytometry analysis by excluding IgD^+ IgM^+ IgA^+ B cells. Finally, the IgG^+ $CD19^+$ $CD27^+$ B cells bound to SABs (15.4%) were identified (Figure 6.10B) and sorted at the single cell level onto a layer CD40-L expressing feeder cells and medium conditioned with IL-2 and IL-21 for *in vitro* B cell expansion. The same process was repeated using PBMCs from a healthy donor. In total, 13 IgG^+ $CD19^+$ $CD27^+$ B cells

bound to SABs were isolated from healthy donor PBMCs (Figure 6.10C) and 8 IgG$^+$ CD19$^+$ CD27$^+$ bead-B cells were isolated from patient 007 PBMCs (Figure 6.10D).

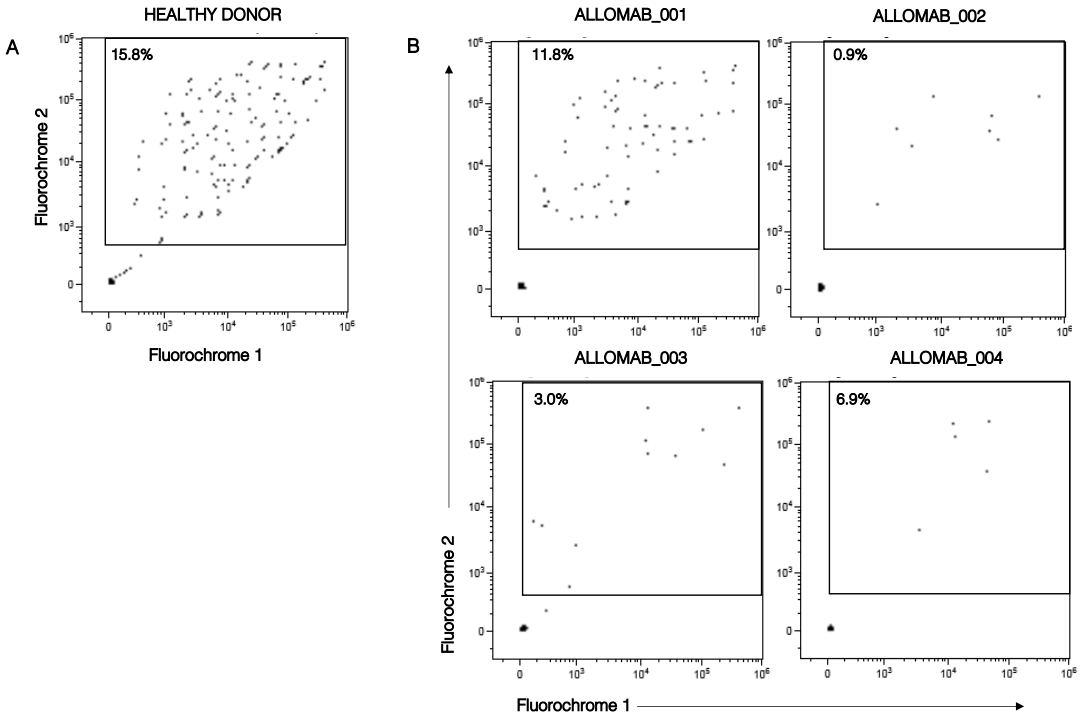

Figure 6.9. | Optimisation of single HLA antigen coated beads reactivity against PBMCs.

A | CD19-labelled B cells were co-incubated with single HLA antigen coated beads and analysed by flow cytometry using the gating strategy from figure 6.7. Representative flow plot demonstrating the total percentage reactivity of CD19$^+$ B cells from healthy donor PBMCs towards HLA SABs. Distinct HLA antigen-specific bead populations were observed when the bead-B cell rosette was visualised using the two fluorochrome parameters of the beads.

B | CD19-labelled B cells from renal transplant patients 001-004 were co-incubated with single HLA antigen coated beads and analysed by flow cytometry. Flow plots demonstrate the total percentage reactivity of CD19$^+$ B cells from patient PBMCs towards HLA SABs. Differential patterns of HLA antigen-specific bead populations were observed when the bead-B cell rosette was visualised using the two fluorochrome parameters of the beads.

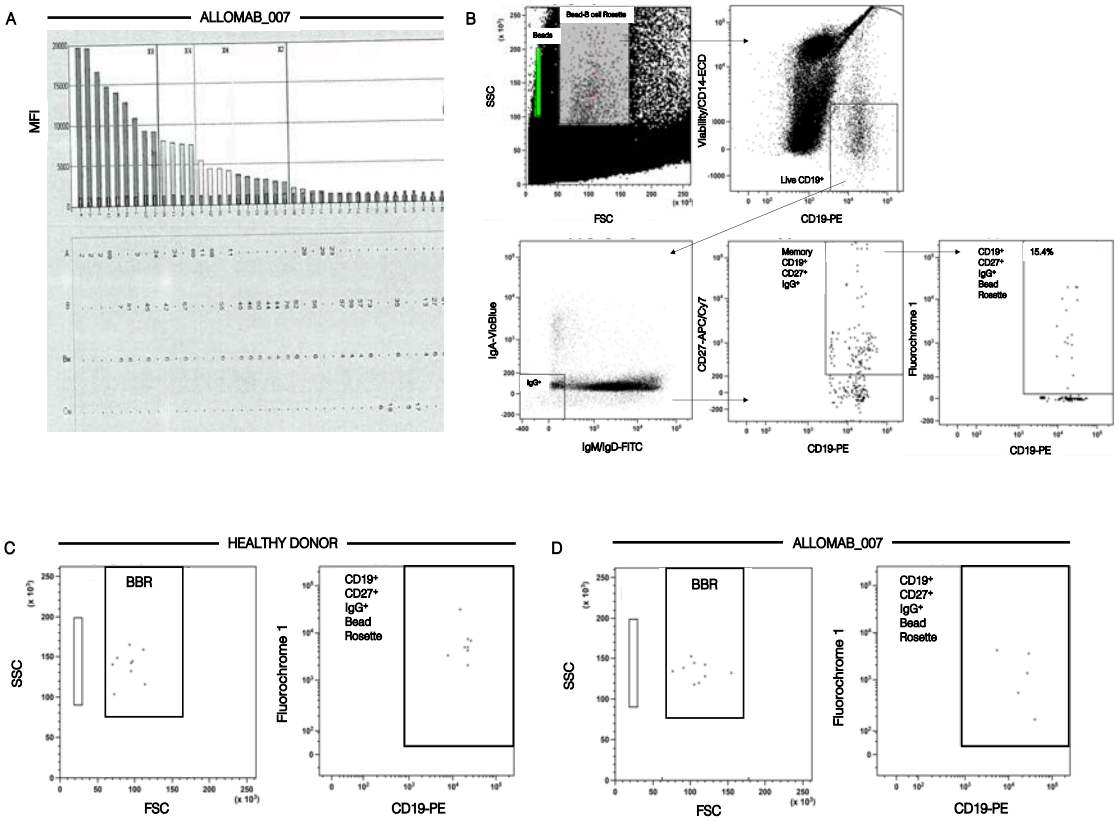

Figure 6.10. | Detection of HLA-specific antibody secreting B cells using SABs.

A | LABScreen Class I (One Lambda) single antigen bead (SAB) analysis of patient 007 serum shows reactivity towards predominantly HLA-A and HLA-B antigen-coated beads. The range of HLA-specific antibody levels were measured by median fluorescence intensity values (MFI).

B | Representative flow gating strategy used to identify HLA SAB-bound B cells (bead-B cell rosette). Negative isolation strategy was adopted to gate out B cells expressing IgD, IgM and IgA. IgG-expressing bead bound-B cells were identified as $CD19^{+}$ $CD27^{+}$ and were subsequently sorted at the single cell level into wells containing a layer of CD40-L expressing feeder cell line and medium conditioned with IL-2 and IL-21.

C | HLA Class I antigen coated bead bound-B cell rosettes (BBR) from healthy donor PBMCs were further selected on the basis of IgG, CD19 and CD27 expression. BBRs display intermediate forward scatter and low side scatter. The two fluorochrome parameters of the SABs were used to visualise the target cell population for FACS.

D | HLA Class I antigen coated bead bound-B cell rosettes (BBR) from patient 007 PBMCs were further selected on the basis of IgG, CD19 and CD27 expression. BBRs display intermediate forward scatter and low side scatter. The two fluorochrome parameters of the SABs were used to visualise the target cell population for FACS.

After 12 days in culture, supernatants from each well were harvested and analysed for IgG production using ELISA. The absorbance values measured at 415nm from individual wells containing B cells from healthy donor or patient 007 PBMCs were comparable to the negative control (no B cells plated) (Figure 6.11A). Two wells containing patient IgG^+ $CD19^+$ $CD27^+$ B cells, however, demonstrated higher absorbance values at 0.17 and 0.21 compared to the negative control well (0.05), indicating the presence of IgG. Total IgG was subsequently measured and quantified as 17.5ng/mL and 23.7ng/mL, respectively (Figure 6.11B). Furthermore, approximately 4.0ng/mL IgG was also detected in another well containing patient IgG^+ $CD19^+$ $CD27^+$ B cell. Similar to the absorbance values, healthy donor IgG^+ $CD19^+$ $CD27^+$ memory B cells did not reveal greater concentrations of IgG indicating the culture supernatants did not contain secreted IgG.

Supernatants from three IgG^+ wells – D6, D7 and D9 were tested for the light chain specificity by ELISA (Figure 6.12A). Using either anti-human kappa or lambda chain secondary antibody, wells D7 and D9 revelated lambda chain specificity with absorbance values of 0.21 and 0.11, respectively. Culture supernatants from well D6 and negative control demonstrated no reactivity to light chain-specific secondary antibodies. Next, supernatants were tested for HLA Class I antigen specificities following co-incubation with SABs (Figure 6.12B). Compared to the positive control, wells D6, D7 and D9 did not exhibit strong binding to the HLA Class I-specific SABs, indicating that either the secreted IgG was not HLA Class I-specific or that total IgG concentration was very low to detect binding.

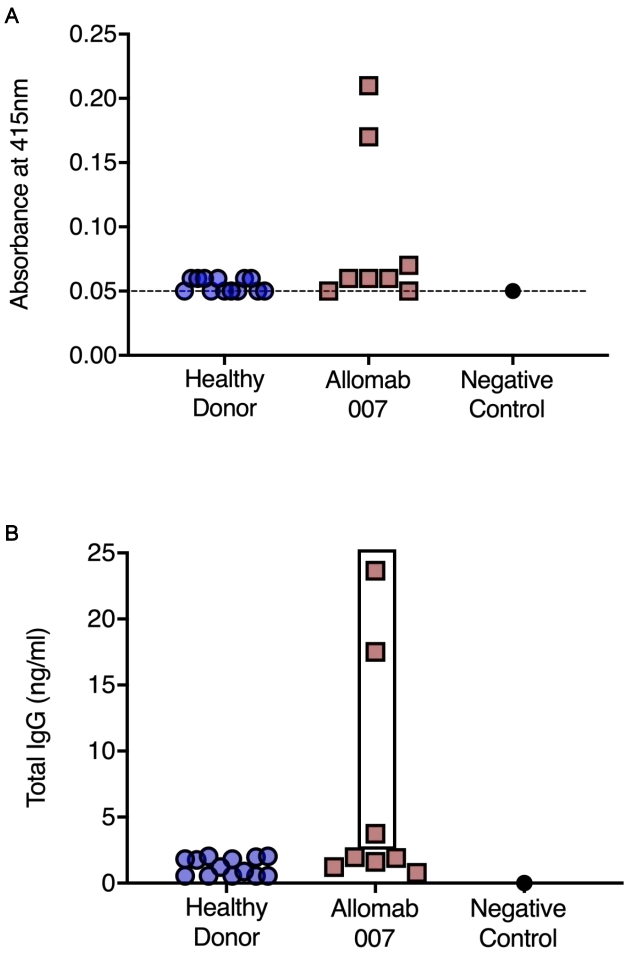

Figure 6.11. | Total IgG concentrations measured after 12 days of HLA SAB$^+$ B cell culture.

A | Absorbance values at 415nm were measured by ELISA using supernatants from individual wells containing SAB$^+$ IgG$^+$ CD19$^+$ CD27$^+$ B cells isolated from healthy donor (blue circle) and patient 007 (red square) PBMCs. Dotted line represents the absorbance value measured from the supernatant dervining from the negative control well (black circle). Data represent a single experiment.

B | Total IgG (ng/mL) was quantified by ELISA for all wells containing single cell culutres of SAB$^+$ IgG$^+$ CD19$^+$ CD27$^+$ B cells from healthy donor (blue circle) and patient 007 (red square). Supernatant from negative control well (with no B cell culture; black circle) was also tested. The black box highlight three individual supernatants with high detectable levels of IgG compared to negative control. Data represent a single experiment.

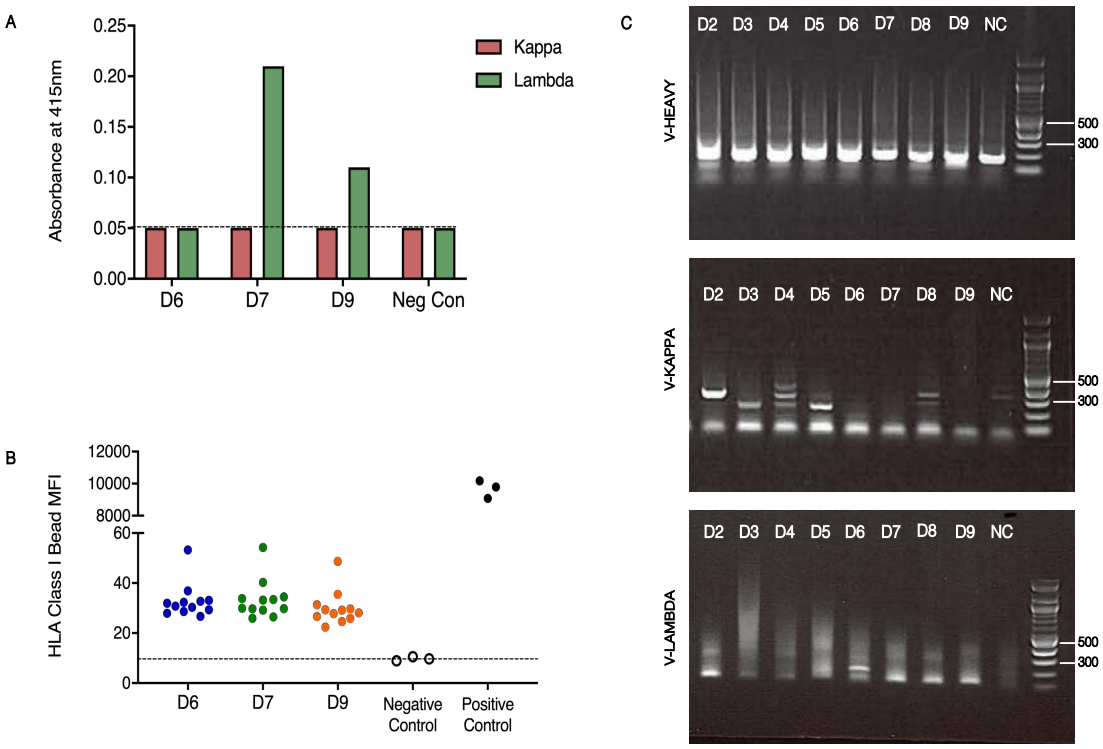

Figure 6.12. | Additional analyses of SAB⁺ IgG⁺ CD19⁺ CD27⁺ B cell culture supernatants.

A | Light chain specificity ELISA was performed using supernatants from wells D6, D7 and D9 containing SAB⁺ IgG⁺ CD19⁺ CD27⁺ B cells isolated from patient 007 PBMCs. Red bars indicate kappa light chain specificity. Green bars indicate lambda light chain specificity.

B | Supernatants were tested against single HLA Class I antigen-coated beads in a luminex assay. Polystrene SABs embedded with varying ratios of two fluorochromes were treated with culture supernatants, followed by labelling of antibody-bound beads with anti-IgG secondary antibody. Negative control (A/B serum) and positive control (pan HLA reactive) sera were included in the assay. The range of HLA-specific antibody levels were measured by median fluorescence intensity values (MFI).

C | Amplification of heavy and light chain variable regions using nested polymerase chain reaction (PCR). Eight single B cell cultures were harvested and PCR products of IgH (380-450bp), IgK (510-540bp) and Igλ (405-450bp) were observed.

After harvesting the supernatants for IgG detection and antigen specificity screening assay, the cultured B cells were collected by adding catch buffer containing RNA inhibitor, RNAsin to each well. The immunoglobulin variable genes – heavy (V_H), kappa (V_K) and lambda (V_λ) were amplified (described in section 6.5) from the expanded patient B cells (Figure 6.12C). Single bands indicating amplified gene product at 380-450bp (V_H) 510-540bp (V_K), and 405-450bp (V_λ) were not observed, which suggests that either the B cells were not viable following 12 days in culture or that the RNA was not preserved efficiently.

Taken together, these data show that PBMCs from renal transplant recipients demonstrate a more selective binding pattern with single HLA Class I antigen coated beads compared to PBMCs from a healthy donor. As a result, IgG-producing memory B cells bound to SABs were isolated and cultured over two weeks. The lack of IgG production by isolated B cells from healthy donor revealed non-specific reactivity to SABs as the donor did not experience any immunisation events during their lifetime. Although low levels of IgG were detected in the supernatants from three wells containing one patient memory B cell, the supernatants did not react strongly to the HLA Class I-specific SABs by luminex testing. Furthermore, attempts to recover the immunoglobulin genes from candidate wells were not successful and due to time restrictions, this experiment could not be repeated.

6.4. Immortalisation of B cells by Epstein-Barr Virus

Early studies have shown that Epstein-Barr virus (EBV) immortalisation of B cells leads to the production of human monoclonal antibodies (Steinitz et al., 1977; Tiebout et al., 1984). In the current study, as limited success was achieved with targeted approaches i.e. MHC Class I-specific tetramers and single antigen beads, a broader approach was undertaken to immortalise B cells from renal transplant recipients with failed allografts and screen for monoclonal antibodies specific to HLA antigens of interest. The work described in section 6.4.1. was carried out in collaboration with Professor Antonio Lanzavecchia and colleagues at the Institute of Research in Biomedicine (IRB), Bellinzona, Switzerland. Using the same protocol, a second study described in section 6.4.2. was carried out at the University of Birmingham (UoB) to analyse immortalised B cell clones. The secreted antibodies were subsequently analysed using two assays – (i) staining of alloreactive PHA blasts generated from healthy donor PBMCs expressing the HLA genotype corresponding to the patient HLA-specific antibody profile and (ii) HLA Class I and II single antigen coated luminex bead assay.

6.4.1. Immortalisation of B cells by EBV – IRB

6.4.1.1. Detection of HLA-specific antibody reactivity from patient serum

Sera and PBMCs from two Allomab patients – 010 and 012 were transported to the Institute of Research in Biomedicine (IRB) for large-scale immortalisation of B cells with EBV. Patient 010 presented with an antibody profile with high levels of reactivity to predominantly HLA-A and HLA-B antigens (Figure 6.13A), whilst patient 012 was selected to isolate HLA-C-specific antibodies demonstrated by the luminex analyses (Figure 6.13B). Both patients did not show reactivity to HLA Class II antigens. Therefore, healthy donors with the corresponding HLA type to the patient antibody profiles were selected (Figure 6.13C).

Firstly, to demonstrate patient-derived HLA Class I-specific antibody reactivity, alloreactive PHA blasts generated from healthy donors (Figure 6.13C) were co-incubated with patient serum, A/B serum (negative control) and pan HLA-reactive serum (positive control) at varying three-fold dilution range. Expi293 cells were used as a control cell line in this assay which is HLA-C1/C1 homozygous (C*07:02/C*07:02) (Boegel et al., 2014) (Figure 6.14A). This assay was performed to establish patient serum reactivity to allogeneic PHA blasts with HLA type that corresponded to the patient HLA antibody profiles. Therefore, it was expected that the patient serum would react strongly to the healthy donor PHA blasts, whilst showing variable reactivity to the Expi293 cells due to the presence of HLA-A and HLA-B antigens.

A

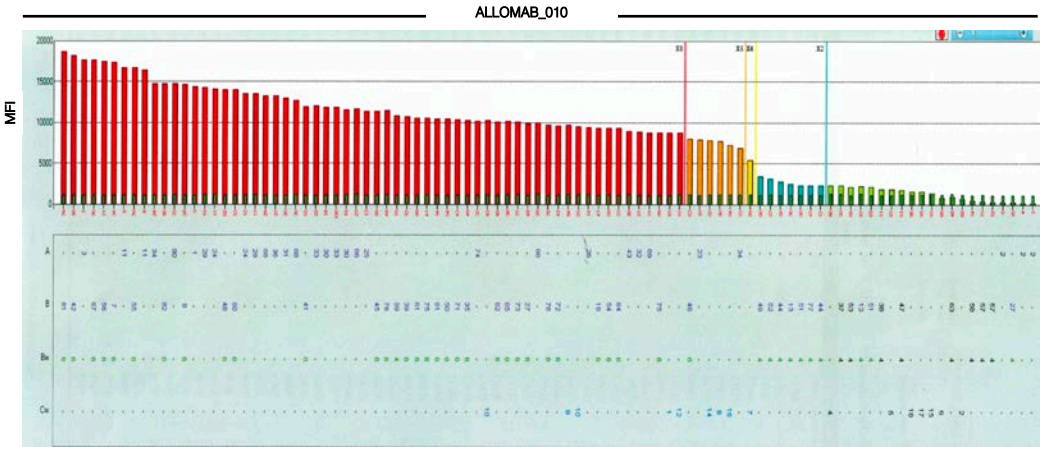

B

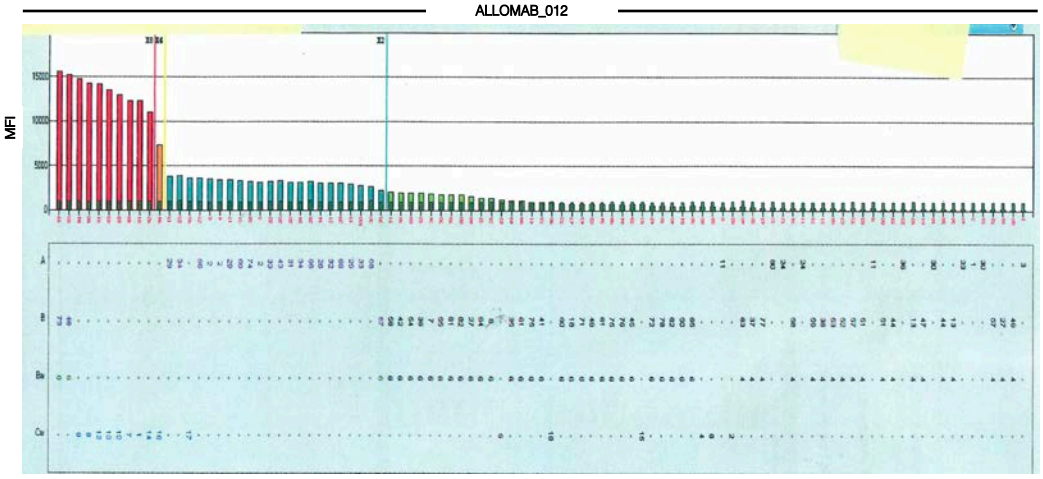

C

ALLOMAB_010 SCREEN

	HLA Type		
Donor	**A**	**B**	**C**
HD92	1, 3	8, 38	7, 12
HD15	11, 32	15, 53	3, 4
HD56	3, 68	14, 37	6, 8

ALLOMAB_012 SCREEN

	HLA Type		
Donor	**A**	**B**	**C**
HD37	24, 32	8, 56	1, 7
HD22	2, 68	14	8
HD80	24, 30	13, 38	6, 12

Figure 6.13. | HLA Class I-specific antibody specificities detected in patients 010 and 012 sera.

LABScreen Class I (One Lambda) single antigen bead (SAB) analysis of patient serum shows reactivity towards a range of HLA-A, -B and -C antigen coated beads by labelling of antibody-bound beads with anti-IgG secondary antibody. The range of HLA-specific antibody levels were measured by median fluorescence intensity values (MFI).

A | Patient 010 serum presents an antibody profile predominantly reactive to HLA-A and HLA-B antigens with MFI values above 10,000. HLA-C group 1-specific bead reactions were observed.

B | Patient 012 serum presents an antibody profile predominantly reactive to epitope-sharing HLA-B and HLA-C group 1 antigens with MFI values above 10,000. Lower MFI values were observed against HLA-A antigens.

C | Summary of healthy donor HLA genotypes corresponding to patient serum antibody profiles. Three donors were selected per patient to generate alloreactive PHA blasts for HLA-specific antibody screening from large-scale B cell cultures.

Patient 10 serum reactivity was observed across the three PHA blasts deriving from healthy donor PBMCs – HD56, HD15 and HD92 (Figure 6.14A). Positive control serum reacted more strongly than the patient serum to the PHA blasts and Expi293 cells, particularly at lower dilutions (1:2-1:54). Weak but positive binding to both T cell clones and Expi293 cells, compared to patient and positive control sera, was also observed with negative control serum indicating non-specific binding.

As patient 10 presented high MFI values, predominantly against the HLA-A antigen-coated luminex beads, healthy donors with corresponding HLA type were selected to test patient serum reactivity. Compared to HD15 and HD56, the HLA type of HD92 was the most suited to patient 10 serum antibody profile (Figure 6.13), and thus, serum reactivity was expected to the strongest. However, PHA blasts from HD56 demonstrated strong reactivity to patient 10 serum following 1:162 dilution as the total percentage of anti-IgG$^+$ T cells were greater (8.2%) than anti-IgG$^+$ Expi293 cells (0.74%), HD15 (1.94%) and HD92 (0.8%) (Figure 6.14A; green box). In contrast, PHA blasts from all three donors presented a strongly positive serum binding patterns at lower dilutions (1:2-1:54) than HD92.

The total percentage of anti-IgG$^+$ T cells reduced significantly at higher patient 10 serum dilutions. For example, at 1:486, 1.2% of T cells from HD15 were anti-IgG$^+$, while HD92 presented 1.4% and 0.6% of anti-IgG$^+$ T cells at 1:486 and 1:1,458 dilutions, respectively. A high proportion of anti-IgG$^+$ T cells (3.55%) from HD15 were observed at 1:1,458 dilution which was most likely a result of technical error. In comparison, total percentage of anti-IgG$^+$ T cells from HD56 showing persistent reactivity with patient 10 serum was also evident at higher dilutions (1:486 – 2.2%; 1:1,458 – 1.69%).

Compared to patient 010, patient 012 serum reacted with a limited number of HLA Class I antigens that share cross-reactive epitopes – HLA-B*46, -B*73 and HLA-C1 alleles (discussed in Chapter III), which also presented lower MFI values. As a result, patient 012 serum reactivity to corresponding HLA-matched PHA or T cell blasts (Figure 6.14B) was weaker than the strong reactivity patterns observed with patient 010 serum. For example, based on the antibody profile, patient 012 serum was expected to react strongly to PHA blasts deriving from HD22 and HD37 compared to HD80 (Figure 6.13C).

At the lowest dilution, (1:2), the total percentage of anti-IgG$^+$ T cells from HD22 (24.1%) and HD37 (38.5%) were greater than HD80 (7.51%). However, at 1:6 dilution, the total percentage of anti-IgG$^+$ T cell population from HD22 (4.60%) and HD37 (4.85%) were significantly reduced, which were similar to HD80 (5.82%) (Figure 6.14B; red box). Non-specific patient 012 serum binding to Expi293 cells at lower dilutions (1:2-1:54) was observed which titrated out to control levels (no serum control) at 1:162 dilution across the three T cell blast donors. HD37 demonstrated persistent reactivity to patient 012 serum at the highest dilution (1:1,1458) with 1.91% anti-IgG$^+$ T cells compared to anti-IgG$^+$ K562 cells (0.56%) and anti-IgG$^+$ T cells from HD22 (0.44%) and HD80 (0.99%).

Positive and negative control sera binding to alloreactive PHA blasts deriving from HD22, HD37 and HD80 were similar to the patterns observed with PHA blasts deriving from HD92, HD15 and HD56 used for patient 010 serum reactivity (Figure 6.14A). Strong reactivity profiles of positive control serum were observed at lower dilutions (1:2-1:54), which reduced to control levels at higher dilutions (1:162-1:1,458) against both T cells and K562 cells. In some instances, negative control serum unexpectedly demonstrated binding to alloreactive PHA or T cell blasts (HD37 and HD80), even at higher dilutions of 1:486 and 1:1,458.

These data confirm that patient 010 and 012 sera containing HLA Class I-specific antibodies recognise and bind to physiological HLA proteins on PHA or T cell blasts. In the instance of patient 012 serum, low MFI values representing antibodies specific to a limited number of HLA Class I antigens, combined with generally low HLA-C cell surface expression is likely responsible for the weak serum reactivity patterns observed against the PHA blasts.

In contrast, patient 010 serum containing a range of antibodies against the HLA-A and HLA-B antigens, combined with higher cell surface expression of HLA-A and HLA-B loci than HLA-C demonstrated stronger serum reactivity against the PHA blasts. Moreover, patient sera binding was observed against the negative control Expi293 cells which titrated out to control levels at dilutions between 1:162-1:1,458, most likely due to the HLA expression on this cell line. Nonetheless, these data also confirm and validate the use of staining PHA blasts as a method of screening antibodies deriving from EBV-B cell culture supernatants.

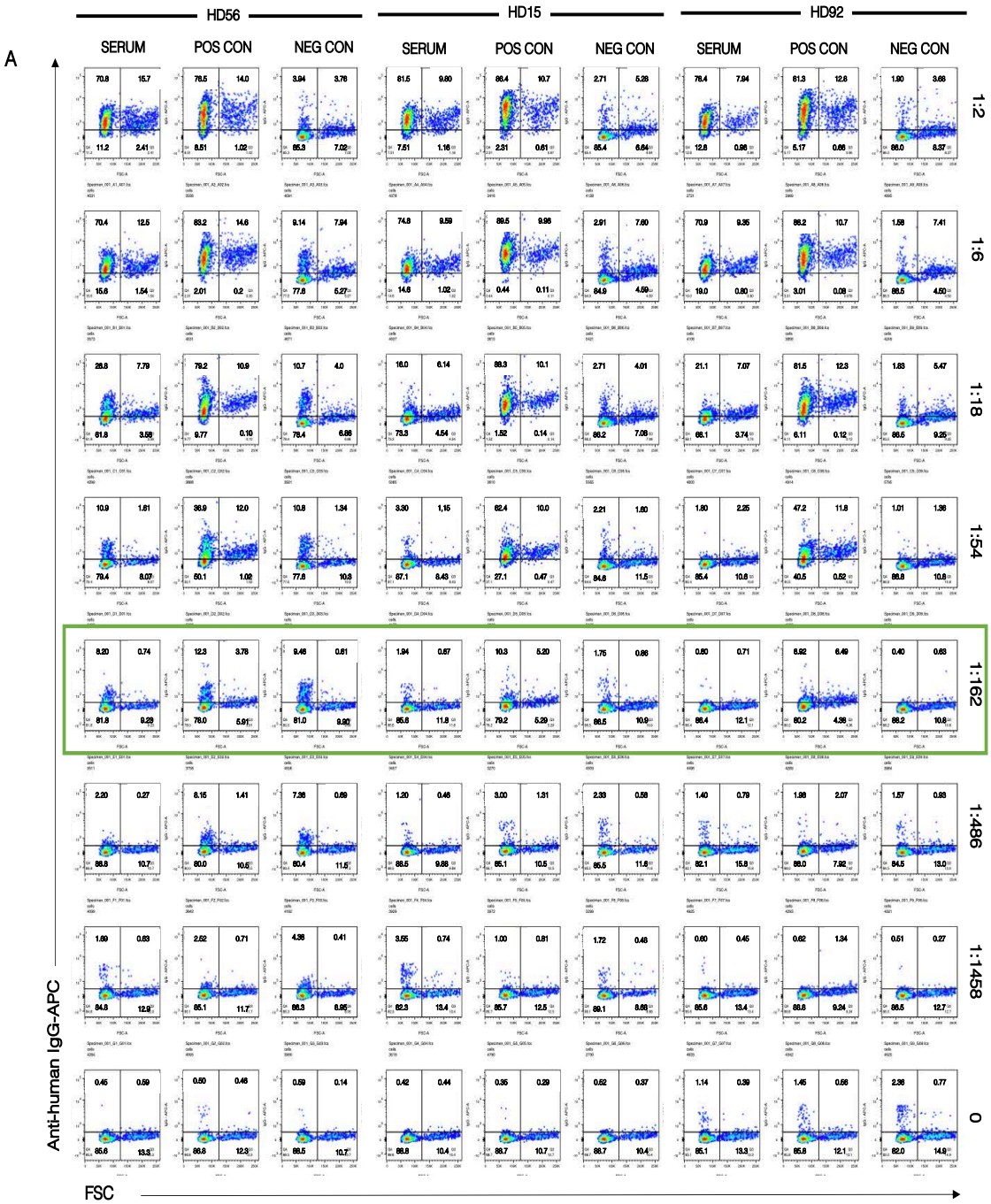
A
HD56
HD15
HD92
SERUM
POS CON
NEG CON
SERUM
POS CON
NEG CON
SERUM
POS CON
NEG CON
1:2
1:6
1:18
1:54
1:162
1:486
1:1458
0
Anti-human IgG-APC
FSC

Figure 6.14. | Validation of HLA-specific serum antibody binding to PHA blasts.

PHA blasts from individual healthy donors were co-incubated with patient serum, A/B serum (negative control) and pan-HLA reactive (positive control) at varying three-fold dilutions. Anti-human IgG secondary antibody was added to detect serum antibody to PHA blasts by flow cytometry. Negative control cell line, K562 was included in each test. K562 cells (high forward scatter) and PHA blasts (low forward scatter) were differentiated upon the basis of forward scatter parameter. Differential patient sera antibody binding patterns were observed against individual alloreactive PHA blasts with **A |** patient 010 and **B |** patient 012 sera.

6.4.1.2. Culturing EBV-B cells and screening supernatants for antibodies

Using FACS, IgG^+ $CD19^+$ B cells were isolated from the patient PBMCs and plated onto a layer of irradiated allogeneic PBMCs and medium supplemented with EBV and CpG ODN. In total, 4,000 IgG^+ $CD19^+$ B cells were sorted from patient 010 PBMCs which were plated at 1.5 cell density per well in seven 384 well plates. From patient 012, 20,000 IgG^+ $CD19^+$ B cells were isolated and plated at 3 cells per well in a total of nineteen 384 well plates. After 14 days in culture, supernatants from a set number of wells across multiple plates were pooled using a robotic liquid transfer system. For example, 5μl of supernatant from well A1 in plates 1-7 were combined to test the specificities of the antibodies secreted by the B cells against the alloreactive PHA blasts. K562 cell line was included as the negative control.

Similar to patient sera testing, reactivity to HLA antigens on the pooled alloreactive PHA blasts from three healthy donors per patient was identified by an increase in percentage of anti-IgG^+ PHA blasts in comparison to negative control (Figure 6.15A). A total of 1,536 pooled supernatants from both patient 010 and 012 B cell cultures were screened against alloreactive PHA blasts. Two pools from wells M7 and N2 specific to patient 010 B cell cultures, showed a high proportion of anti-IgG^+ PHA blasts (3.10% and 5.55%, respectively). Similarly, an increase in anti-IgG^+ K562 cells (2.7% and 5.38%, respectively) was observed (Figure 6.15B). Pooled supernatants from patient 012 B cell cultures demonstrated greater reactivity to the combined PHA blasts. Figure 6.15C shows an increased frequency of anti-IgG^+ PHA blasts. Two wells, B6 and O7 revealed greater proportion of anti-IgG^+ PHA blasts at 9.82% and 9.12%, respectively compared to anti-IgG^+ K562 cells (1.84% and 1.85%, respectively). Together, these data show that three pooled culture supernatants were strongly reactive against the alloreactive PHA blasts, suggesting the antibodies in the supernatants specific towards the HLA proteins.

Next, the three pooled supernatants containing potential HLA-specific antibodies were tested against SABs (Figure 6.16). Co-incubation of pooled supernatant from well N2 of the patient 010 B cell screen with single HLA Class I antigen coated luminex beads revealed reactivity towards specific HLA antigens (Figure 6.16A). Moderately positive bead reactions with MFI values less than 6,000 were observed against HLA-B7 and HLA-B81 coated beads. MFI values less than 5,000 showed weakly positive bead reactions to other HLA-B antigens including HLA-B42, -B56, -B67, -B35 and -B82 as well as HLA-A3 and HLA-A11. The supernatant was also reactive against other HLA-A and HLA-B antigens (MFI <2,000). This demonstrated that the pooled supernatants from well N2 comprised antibodies specific to the HLA Class I antigens. Pooled antibody supernatant candidates from patient 012 B cell screen – wells B6 and O7 were not reactive against the SABs as MFI values less than 2.0 were observed (Figures 6.16B and 6.16C).

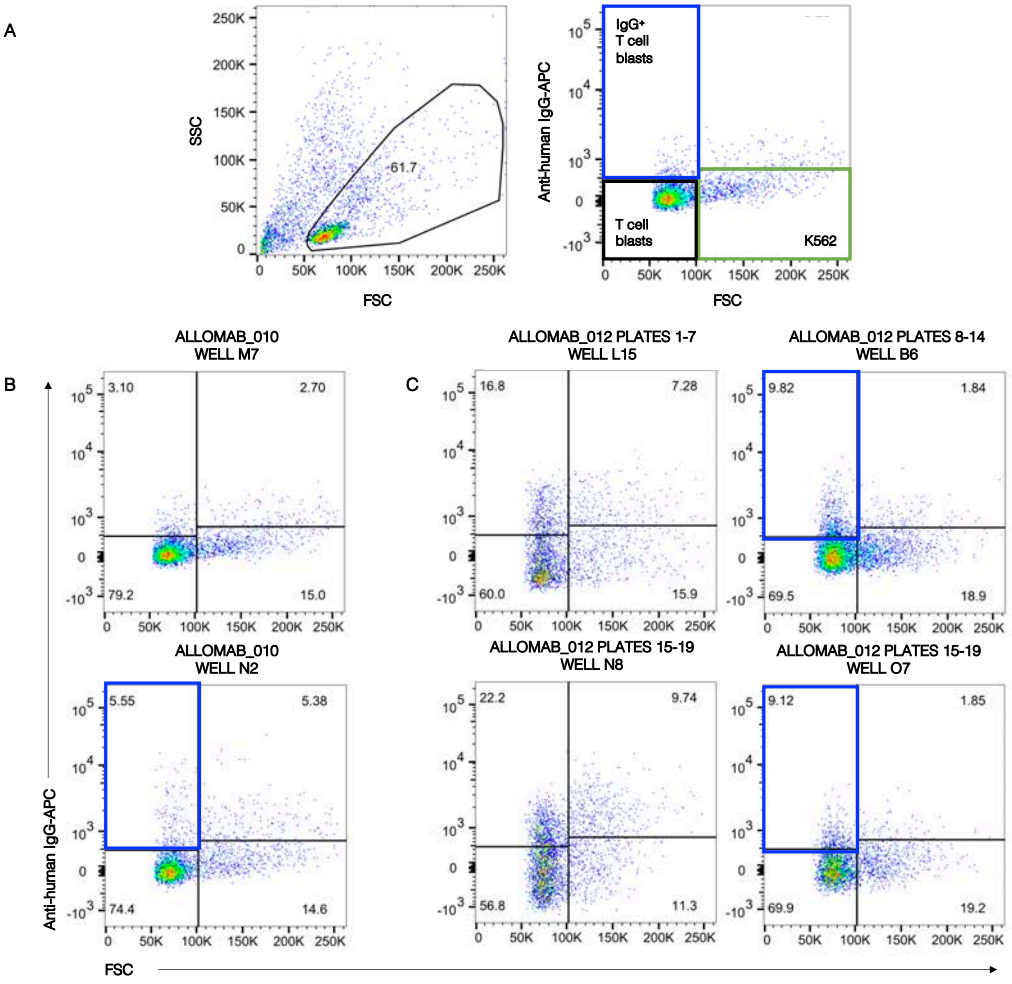

Figure 6.15. | Screening of pooled supernatants from EBV-transformed B cell cultures against alloreactive PHA blasts.

A | Representative flow gating strategy shows that PHA blasts were identified based on forward (FSC) and side scatter (SSC) profiles. The normal lymphocyte gate was extended further to include the increased size of K562 cells. PHA blasts with bound antibody from the supernatants were identified by analysing the gated cells based on forward scatter and anti-human IgG-APC parameters. Unbound PHA blasts (black quadrant); unbound K562 cells (green quadrant) and IgG antibody-bound PHA blasts (blue quadrant).

B | Two pooled supernatant candidates from patient 010 B cell culture screen were identified with greater percentage of anti-IgG$^+$ PHA blast population compared to anti-IgG$^+$ K562 population. Supernatant from well N2 was selected for further analysis.

C | Four pooled supernatant candidates from patient 012 B cell culture screen were identified with greater percentage of anti-IgG$^+$ PHA blast population compared to anti-IgG$^+$ K562 population. Supernatants from wells B6 and O7 were selected for further analysis.

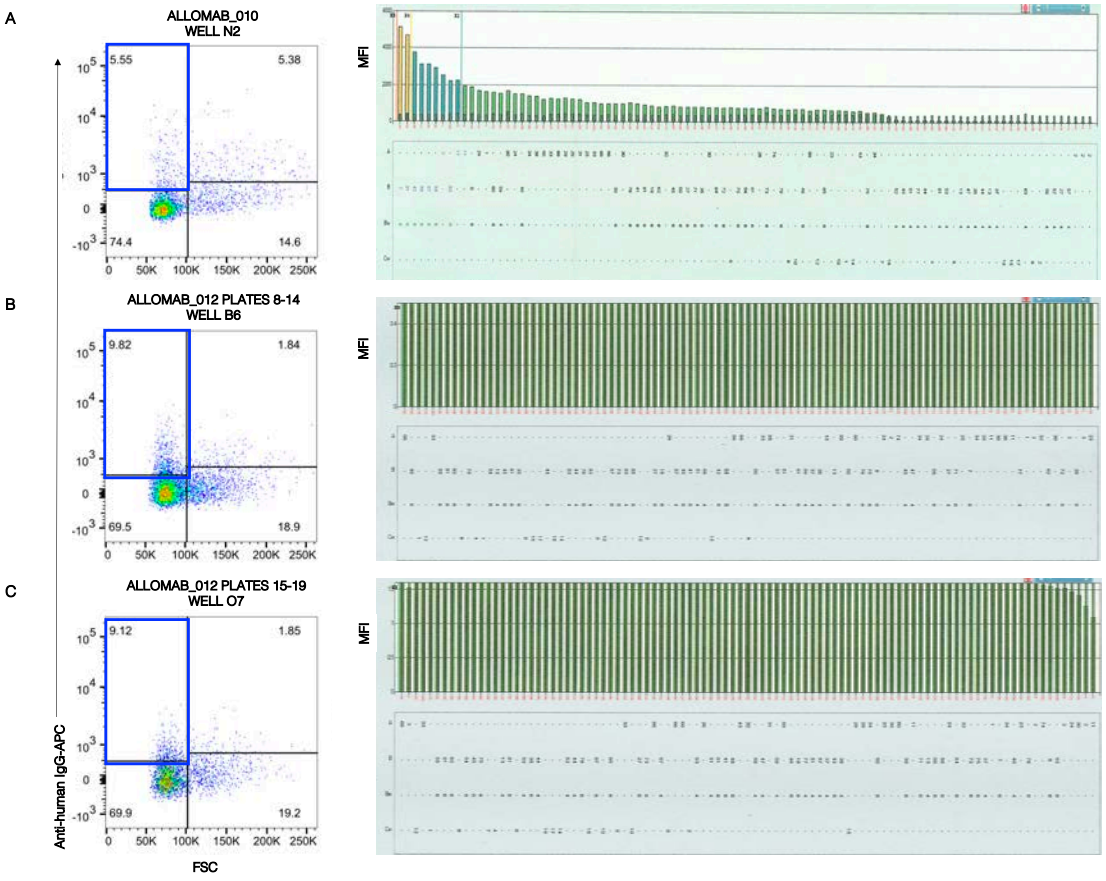

Figure 6.16. | Screening of candidate pooled supernatants of EBV-transformed B cell cultures against single HLA antigen coated beads.

Candidate pooled supernatants containing antibodies that reacted with PHA blasts were identified in the blue quadrant. LABScreen Class I (One Lambda) single antigen bead (SAB) analysis of pooled supernatants was detected by labelling of antibody-bound beads with anti-IgG secondary antibody. The range of HLA-specific antibody levels were measured by median fluorescence intensity values (MFI).

A | Candidate pooled supernatants from well N2 of patient 010 screen demonstrated reactivity against HLA Class I antigen-coated beads. Varying MFI values were measured for specific HLA-A and HLA-B antigen bead reactions.

B | Candidate pooled supernatants from well B6 of patient 012 screen did not show reactivity towards HLA Class I antigen-coated beads.

C | Candidate pooled supernatants from well O7 of patient 012 screen did not show reactivity towards HLA Class I antigen-coated beads.

6.4.1.3. Screening supernatants from individual wells for HLA-specific antibodies

Following the luminex analyses, supernatants from the seven individual wells comprising each pool of supernatants were tested against the alloreactive PHA blasts to identify the EBV-transformed B cells secreting HLA-specific antibodies. Each supernatant was also co-incubated separately with PHA blasts from healthy donors to analyse antibody reactivity towards different HLA Class I proteins. Similar to the luminex analyses, the supernatants from B6 (Figure 6.17A) and O7 (Figure 6.17B) individual wells from patient 012 screen did not demonstrate an increase in anti-IgG reactivity of PHA blasts as the percentage total of anti-IgG$^+$ PHA blasts remained comparable to K562 reactivity levels. Interestingly, supernatants from well B6 of Plate 6 (Figure 6.17A) revealed binding to CFSE-labelled K562 cells with similar percentage total of anti-IgG$^+$ K562 cells observed across the three PHA blast donors at 3.11% (HD80), 3.51% (HD37) and 3.60% (HD22). This culture supernatant potentially comprises antibody specific against K562 cell surface antigens.

Testing of individual N2 wells from patient 010 EBV-B cell cultures, however, showed that supernatant from Plate 4 was strongly reactive against the three alloreactive PHA blasts as well as the negative control, K562 cells (Figure 6.17C). The average total percentage of anti-IgG$^+$ PHA blasts was greater (24.1±1.4%) than anti-IgG$^+$ K562 cells (15.0±1.9%). This observation corresponds with the screening of the pooled supernatants (Figure 6.16A). Further luminex analysis of this particular candidate supernatant revealed a broadly reactive HLA Class I-specific antibody profile (Figure 6.18). Strong to weakly positive bead reactions were detected against a range of HLA Class I antigens. Moreover, the antibody profile deriving from the supernatant from a single well was visually similar to the patient 010 serum antibody profile (Figure 6.13A), suggesting the presence of either more than one HLA-specific antibody or an HLA epitope-specific cross-reactive antibody.

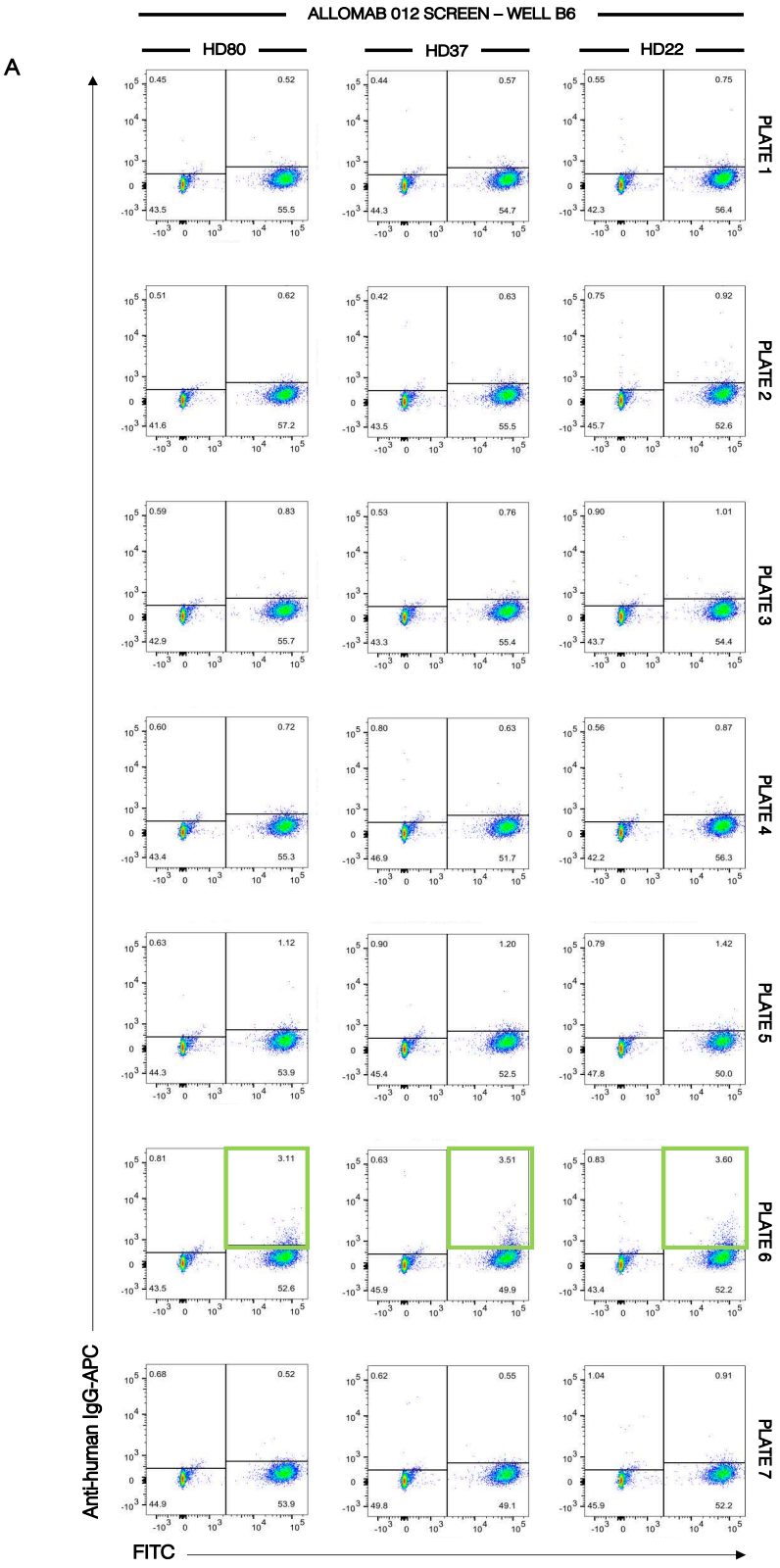
A
ALLOMAB 012 SCREEN – WELL B6
HD80
HD37
HD22
PLATE 1
PLATE 2
PLATE 3
PLATE 4
PLATE 5
PLATE 6
PLATE 7
Anti-human IgG-APC
FITC

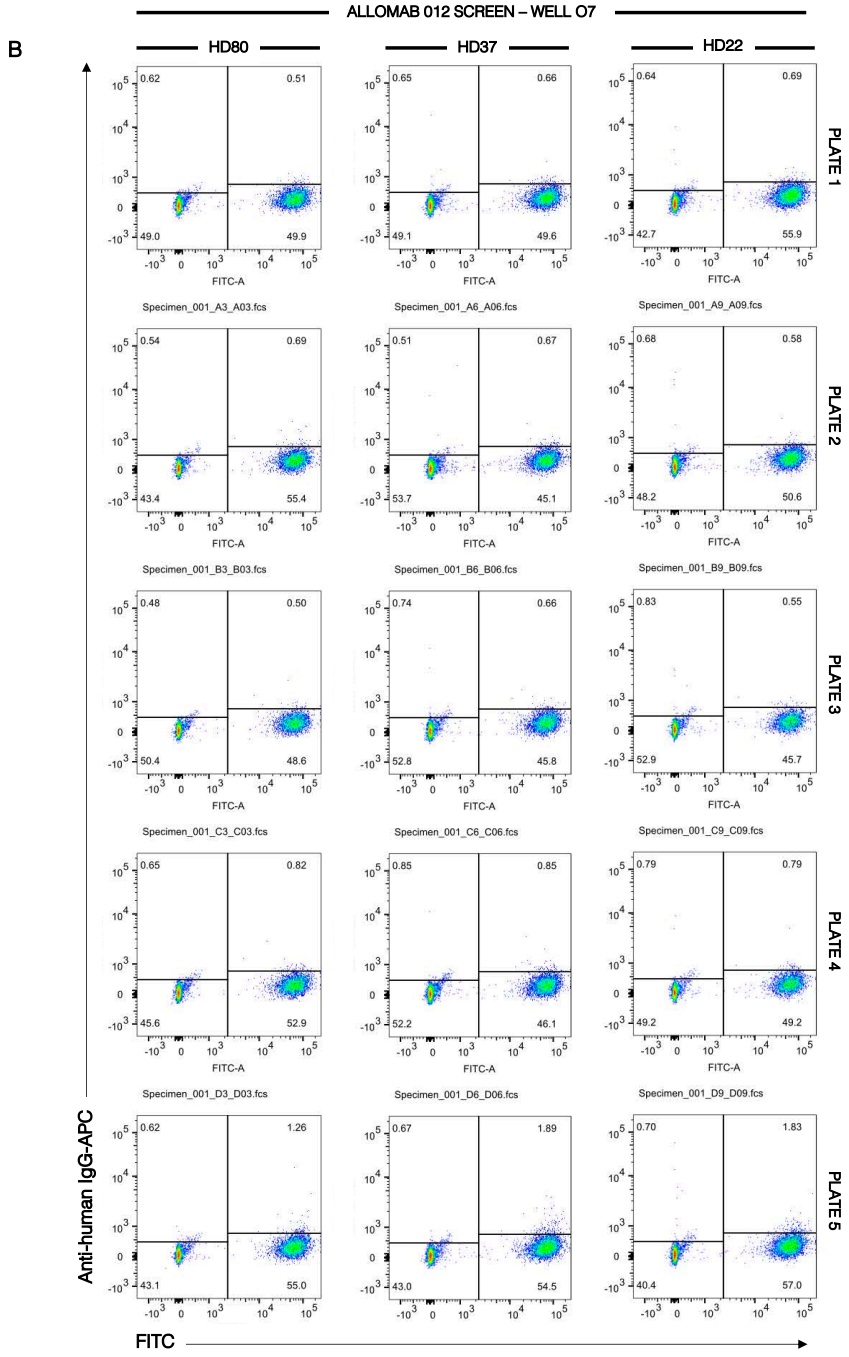
ALLOMAB 012 SCREEN – WELL O7
B
HD80
HD37
HD22
PLATE 1
PLATE 2
PLATE 3
PLATE 4
PLATE 5
0.62
0.51
49.0
49.9
0.65
0.66
49.1
49.6
0.64
0.69
42.7
55.9
Specimen_001_A3_A03.fcs
Specimen_001_A6_A06.fcs
Specimen_001_A9_A09.fcs
0.54
0.69
43.4
55.4
0.51
0.67
53.7
45.1
0.68
0.58
48.2
50.6
Specimen_001_B3_B03.fcs
Specimen_001_B6_B06.fcs
Specimen_001_B9_B09.fcs
0.48
0.50
50.4
48.6
0.74
0.66
52.8
45.8
0.83
0.55
52.9
45.7
Specimen_001_C3_C03.fcs
Specimen_001_C6_C06.fcs
Specimen_001_C9_C09.fcs
0.65
0.82
45.6
52.9
0.85
0.85
52.2
46.1
0.79
0.79
49.2
49.2
Specimen_001_D3_D03.fcs
Specimen_001_D6_D06.fcs
Specimen_001_D9_D09.fcs
0.62
1.26
43.1
55.0
0.67
1.89
43.0
54.5
0.70
1.83
40.4
57.0
FITC-A
Anti-human IgG-APC
FITC

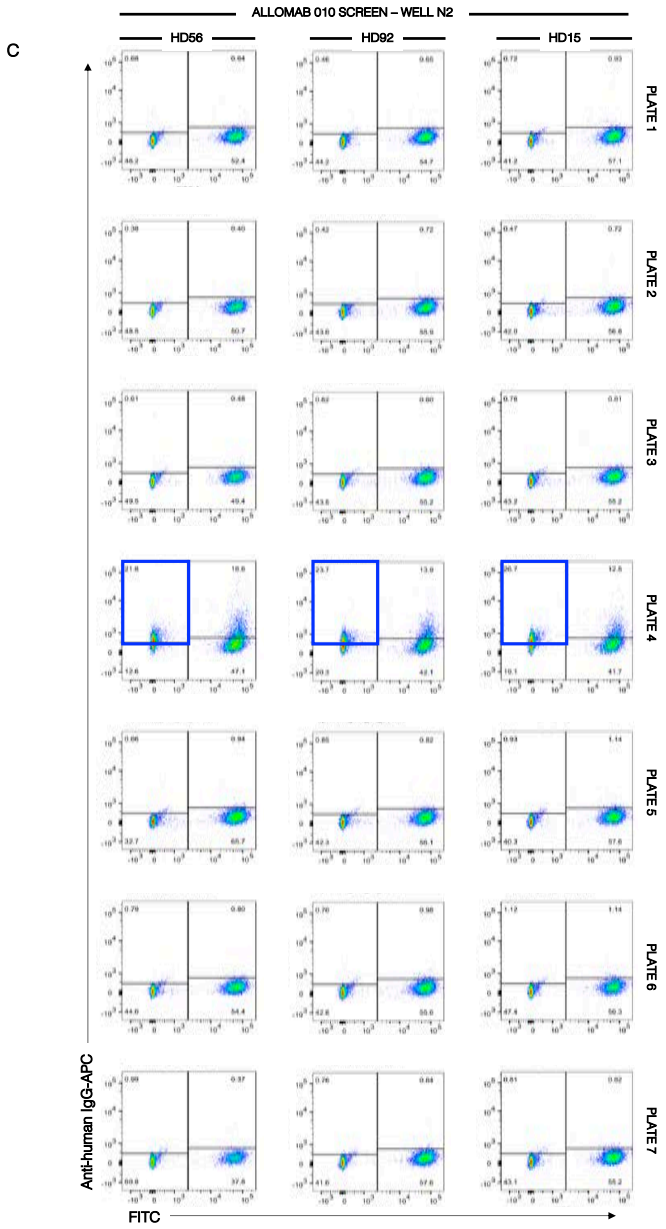

Figure 6.17. | Screening of individual supernatants from EBV-transformed B cell cultures against alloreactive PHA blasts.

A | Individual supernatants from well B6 (patient 012) across seven plates were tested against alloreactive PHA blasts from three healthy donors. Well B6 from plate 6 demonstrated a greater percentage of anti-IgG$^+$ CFSE-labelled K562 population (green quadrant) compared to anti-IgG$^+$ T cell blast population.

B | Individual supernatants from well O7 (patient 012) across five plates were tested against alloreactive PHA blasts from three healthy donors. No increase in percentage of anti-IgG$^+$ PHA blast population was observed.

C | Individual supernatants from well N2 (patient 010) across seven plates were tested against alloreactive T cell blasts from three healthy donors. Well N2 from plate 4 demonstrated a greater percentage of anti-IgG$^+$ PHA blast population (green quadrant) compared to anti-IgG$^+$ CFSE-labelled K562 population.

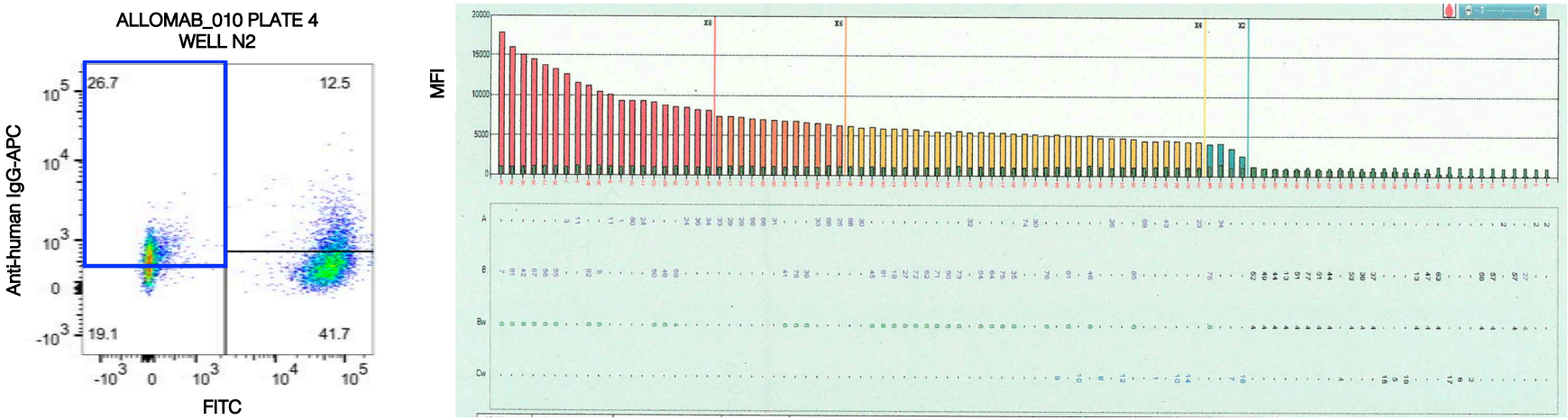

Figure 6.18. | Screening of individual candidate supernatants of EBV-transformed B cell cultures against single HLA antigen coated beads.

A greater percentage of anti-IgG$^+$ T cell blast population (blue qaudrant) compared to anti-IgG$^+$ CFSE-labelled K562 cells was measured when supernatant from well N2 of plate 4 from patient 010 screen was analysed. LABScreen Class I (One Lambda) single antigen bead (SAB) analysis of well N2 supernatant from plate 4 was detected by labelling of antibody-bound beads with anti-IgG secondary antibody. A range of HLA Class I antigen-specific antibody levels were measured by median fluorescence intensity values (MFI).

To analyse the EBV-B cells from this candidate culture potentially producing HLA-reactive antibodies, colleagues at the IRB harvested the B cells for immunoglobulin gene amplification and recombinant antibody production. Following nested PCR (section 6.6), no heavy and light chain genes were obtained, limiting further downstream analyses. Taken together, this collaborative attempt to immortalise HLA-specific antibody producing B cells from renal transplant patients was met with relative success. Therefore, the methodology was repeated at UoB to successfully isolate HLA-specific antibody producing alloreactive B cells and obtain the immunoglobulin genes to attempt recombinant antibody production *in vitro*.

6.4.2. Immortalisation of B cells by EBV – University of Birmingham

6.4.2.1. Detection of HLA-specific antibody reactivity from patient serum

For the second study using EBV to immortalise alloreactive B cells, patient 013 was recruited. Luminex analyses revealed the presence of HLA Class I (Figure 6.19A) and HLA Class II-specific antibodies (Figure 6.19B) in the serum. Strongly positive bead reactions were detected for HLA-DR and HLA-DP antigens as the observed MFI values were more than 10,000. Similarly, high MFI values (>10,000) were measured against the HLA-C2 antigen coated beads – HLA-C*18, C*15, C*05, C*02, C*06 and C*17, followed by strongly positive HLA-A2 antigen-specific bead reactions. Reactivity to several HLA-B antigens was also detected. With the HLA Class I and II-specific antibody profiles in mind, alloreactive PHA blasts were also generated from healthy donor PBMCs carrying the corresponding HLA genotype (Figure 6.19C). Emphasis was placed on selecting healthy donors based on the HLA Class I genotype, particularly HLA-C and as the healthy donors carried HLA-C group 2 antigens, strong antibody reactivity to the PHA or T cell blasts was expected.

A

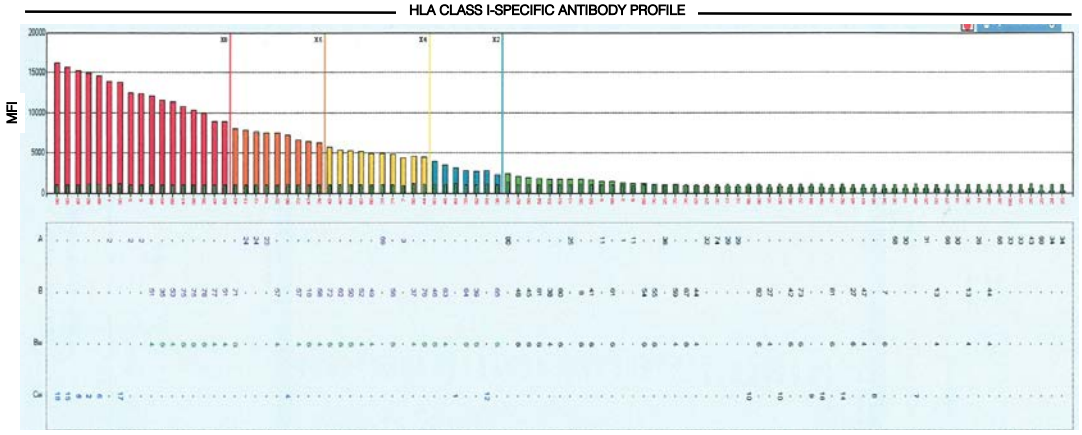

B

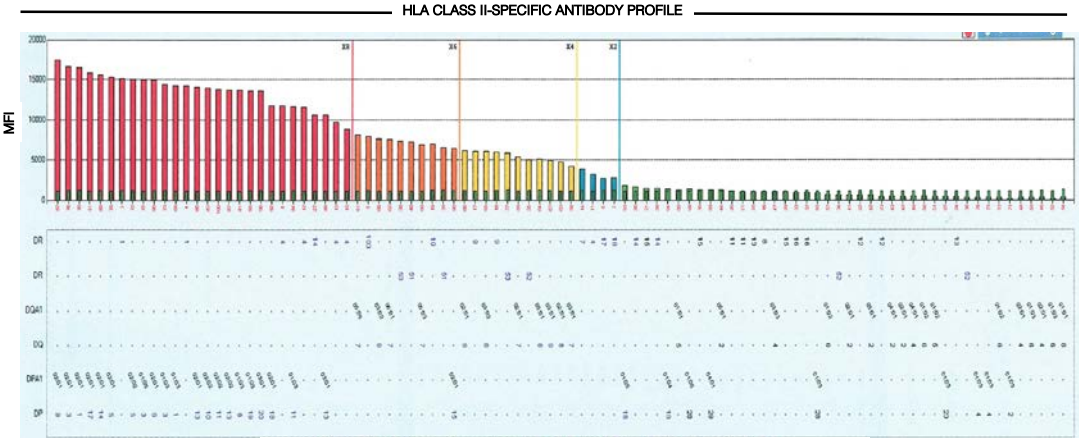

C

ALLOMAB_013 SCREEN

	HLA Type				
Donor	**A**	**B**	**C**	**DRβ1**	**DQβ1**
HD54	2	35, 44	4, 5	4, 7	
HD60	2, 3	7, 44	5, 15	11, 13	3, 6
HD84	2, 23	45, 53	4, 6	13	

Figure 6.19. | HLA Class I-specific antibody specificities detected in patient 013 serum.

LABScreen Class I (One Lambda) single antigen bead (SAB) analysis of patient serum shows reactivity towards a range of HLA-A, -B and -C antigen coated beads by labelling of antibody-bound beads with anti-IgG secondary antibody. The range of HLA-specific antibody levels were measured by median fluorescence intensity values (MFI).

A | Patient 013 serum presents an HLA Class I-specific antibody profile with strong bead reactions against HLA-C group 2 antigens, HLA-A and HLA-B antigens.

B | Patient 013 serum also showed reactivity to a range of HLA-DR and HLA-DP antigen-coated beads confirming the presence of HLA Class II-specific antibodies in the serum.

C | Summary of healthy donor HLA Class I and II genotypes corresponding to patient 013 serum antibody profile. Three donors were selected to generate alloreactive PHA blasts for HLA-specific antibody screening from large-scale B cell cultures.

To determine patient 013 serum reactivity, alloreactive PHA blasts from three healthy donors were combined and co-incubated with patient serum at varying dilutions (Figure 6.20). K562 cells were CFSE-labelled and included as a negative control as in the previous experiments. Similar to patient 010 and 012 sera (Figure 6.14), strong patient 013 serum antibody binding to pooled PHA blasts and K562 cells was observed at lower dilutions (1:2-1:18). Reactivity to PHA or T cell blasts was reduced to control levels at 1:486 dilution. Serum binding to K562 cells, however, persisted at higher dilutions (1:1,458). Due to the low number of PHA blasts in culture, positive and negative control sera were not tested.

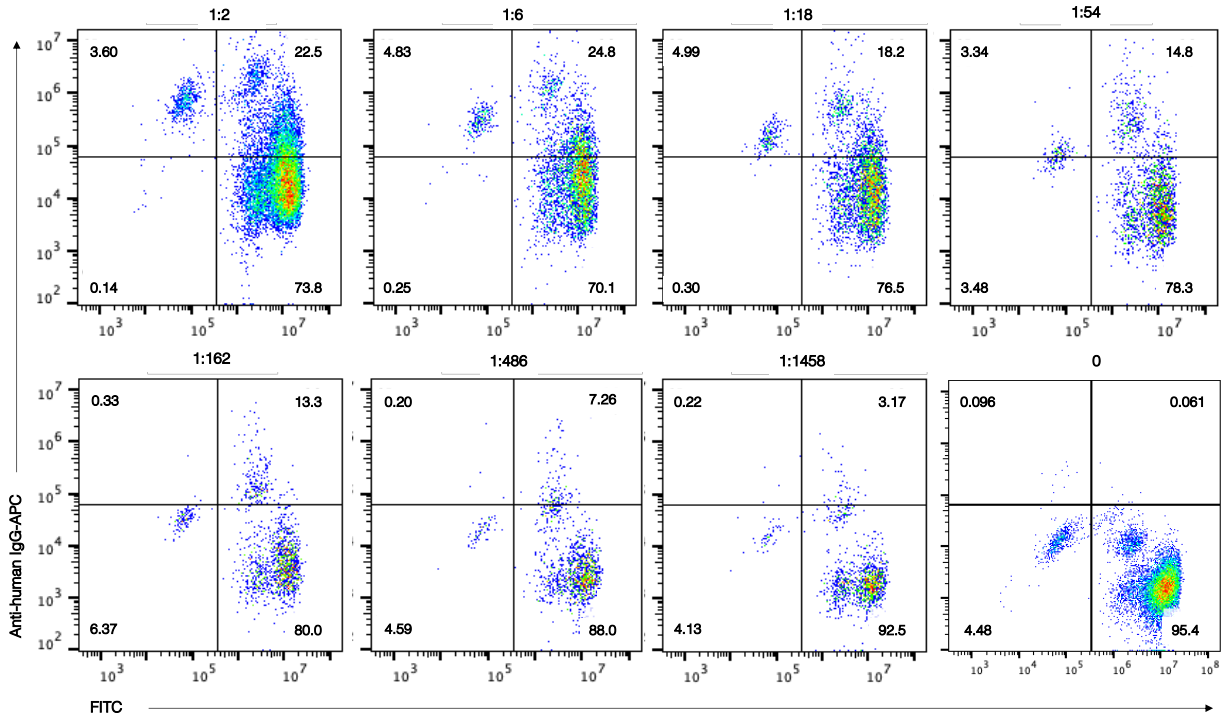

Figure 6.20. | Validation of HLA-specific patient 013 serum antibody binding to pooled alloreactive PHA blasts.

PHA blasts from individual healthy donors were combined and co-incubated with patient 013 serum at varying three-fold dilutions. Anti-human IgG secondary antibody was added to detect serum antibody to PHA blasts by flow cytometry. Negative control cell line, K562 was labelled with CFSE and included in each test. K562 cells (high forward scatter) and PHA blasts (low forward scatter) were differentiated upon the basis of forward scatter parameter. Differential patient serum antibody binding patterns were observed against the pooled alloreactive PHA or T cell blasts and CFSE-labelled K562 cells.

6.4.2.2. Culturing EBV-B cells and screening supernatants for antibodies

In contrast to patients 010 and 012, PBMCs from patient 013 were freshly isolated from whole blood and labelled with cell surface antibodies for flow cytometry analysis. IgD, IgM and IgA expressing $CD19^+$ B cells were excluded and IgG^+ $CD19^+$ $CD27^+$ memory B cells were isolated using FACS (Figure 6.21A). Approximately 12,000 IgG^+ $CD19^+$ $CD27^+$ B cells were sorted and subsequently plated at 3 cells per well containing allogeneic irradiated feeder cells and medium supplemented with EBV and CpG ODN. A total of ten 384 well plates were set up for *in vitro* culture of two weeks.

Similar to the protocol described in section 6.4.1., following short-term culture of B cells, supernatants were collected and pooled manually and screened against combined alloreactive PHA blasts to detect IgG reactivity. Approximately 768 supernatant pools were screened of which three pools – wells B24, O8 and P1, demonstrated reactivity to the PHA blasts (Figure 6.21B). Compared to K562 cells, the pooled culture supernatants revealed an increase in total percentage of anti-IgG^+ PHA blasts with 0.50%, 0.12% and 0.29%, respectively. These candidate supernatants pools were also tested against HLA Class I (Figure 6.22) and II antigen coated luminex beads. No binding was detected against the SABs indicating that the antibodies secreted in the cultures were not HLA-specific or that the antibody titres in the pooled supernatants were low due to the dilution factor (1:10), thus limiting the detection of potential HLA-specific antibodies.

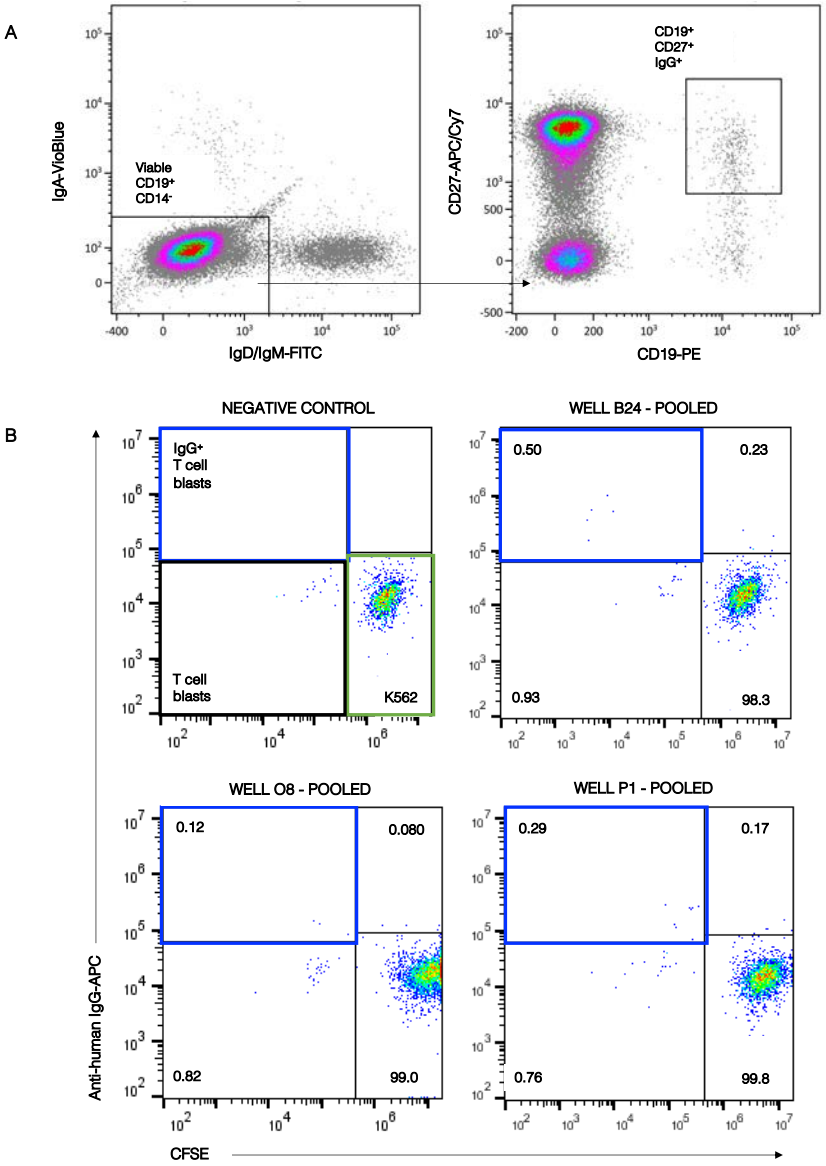

Figure 6.21. | Screening of pooled supernatants from EBV-transformed B cell cultures against alloreactive PHA blasts – UoB.

A | Representative flow gating strategy shows that CD14+ monocytes were excluded and viable CD19+ B cells were further analysed. Negative isolation strategy was adopted to gate out B cells expressing IgD, IgM and IgA. IgG-expressing CD19+ CD27+ were bulk sorted and manually plated at 3 cells per well density into wells containing irradiated alloegenic PBMCs and medium supplemented with EBV and CpG ODN.

B | PHA blasts and CFSE-labelled K562 cells (negative control) were co-incubated with pooled supernatants and analysed based on forward scatter and anti-human IgG-APC parameters. Unbound PHA blasts (black quadrant); unbound K562 cells (green quadrant) and IgG antibody-bound PHA blasts (blue quadrant) can be identified in the dot plot.Three pooled supernatant candidates from patient 013 B cell culture screen were identified – B24, O8 and P1 with greater percentage of anti-IgG+ T cell blast population compared to anti-IgG+ K562 population.

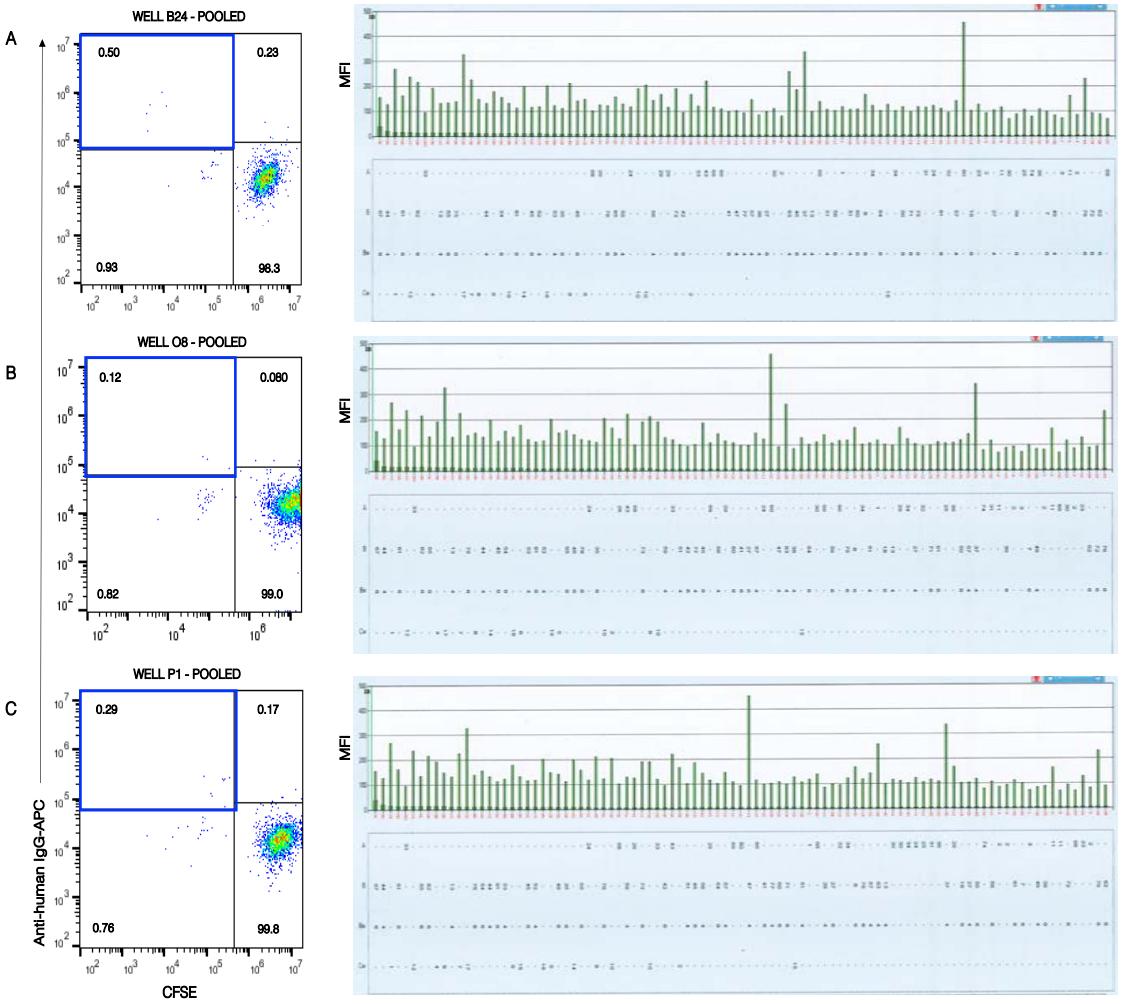

Figure 6.22. | Screening of candidate pooled supernatants of EBV-transformed B cell cultures against single HLA antigen coated beads – UoB.

Candidate pooled supernatants containing antibodies that reacted with PHA blasts were identified in the blue quadrant. LABScreen Class I (One Lambda) single antigen bead (SAB) analysis of pooled supernatants was detected by labelling of antibody-bound beads with anti-IgG secondary antibody. The range of HLA-specific antibody levels were measured by median fluorescence intensity values (MFI). Candidate pooled supernatants from **A |** well B24, **B |** well O8, and **C |** well P1 did not show reactivity towards HLA Class I antigen-coated beads.

6.4.2.3. Amplification of immunoglobulin genes from EBV-B cell cultures

Next, supernatants from individual wells comprising one pool of supernatant were co-incubated with the combined alloreactive PHA blasts. Figure 6.23 shows multiple individual tests of wells B24, O8 and P1 where a modest increase in total percentage of anti-IgG$^+$ PHA blasts were detected. Compared to K562 cells, noticeable supernatant reactivity was observed from well B24 from Plate 1 (0.11%) and Plate 5 (0.24%); well O8 from Plate 8 (0.26%) and well P1 from Plate 7 (0.15%).

EBV-B cell cultures from the candidate wells were harvested. Using RT-PCR and nested PCR, the antibody genes were amplified on a per well basis from a total of 29 wells. Single bands indicating amplified gene product at 380-450bp (V_H) (Figure 6.24A), 510-540bp (V_K) (Figure 6.24B), and 405-450bp (V_λ) (Figure 6.24C) were observed from several wells. In total, paired heavy and light chain DNA deriving from the same well was obtained from two EBV-B cell cultures – well B24 from Plate 1 and well 08 from Plate 2 (Figure 6.24D). Several wells were positive for kappa and lambda light chain DNA which is to be expected as 3 B cells per well were seeded and thus, the antibody containing supernatants derived from polyclonal EBV-B cell cultures.

Further analyses involving sequencing the PCR products of variable heavy and light chain regions, expression vector cloning and transient co-transfection into a mammalian system were not performed due to time restrictions. Therefore, the specificities of the secreted antibodies by the EBV-B cell cultures could not be confirmed.

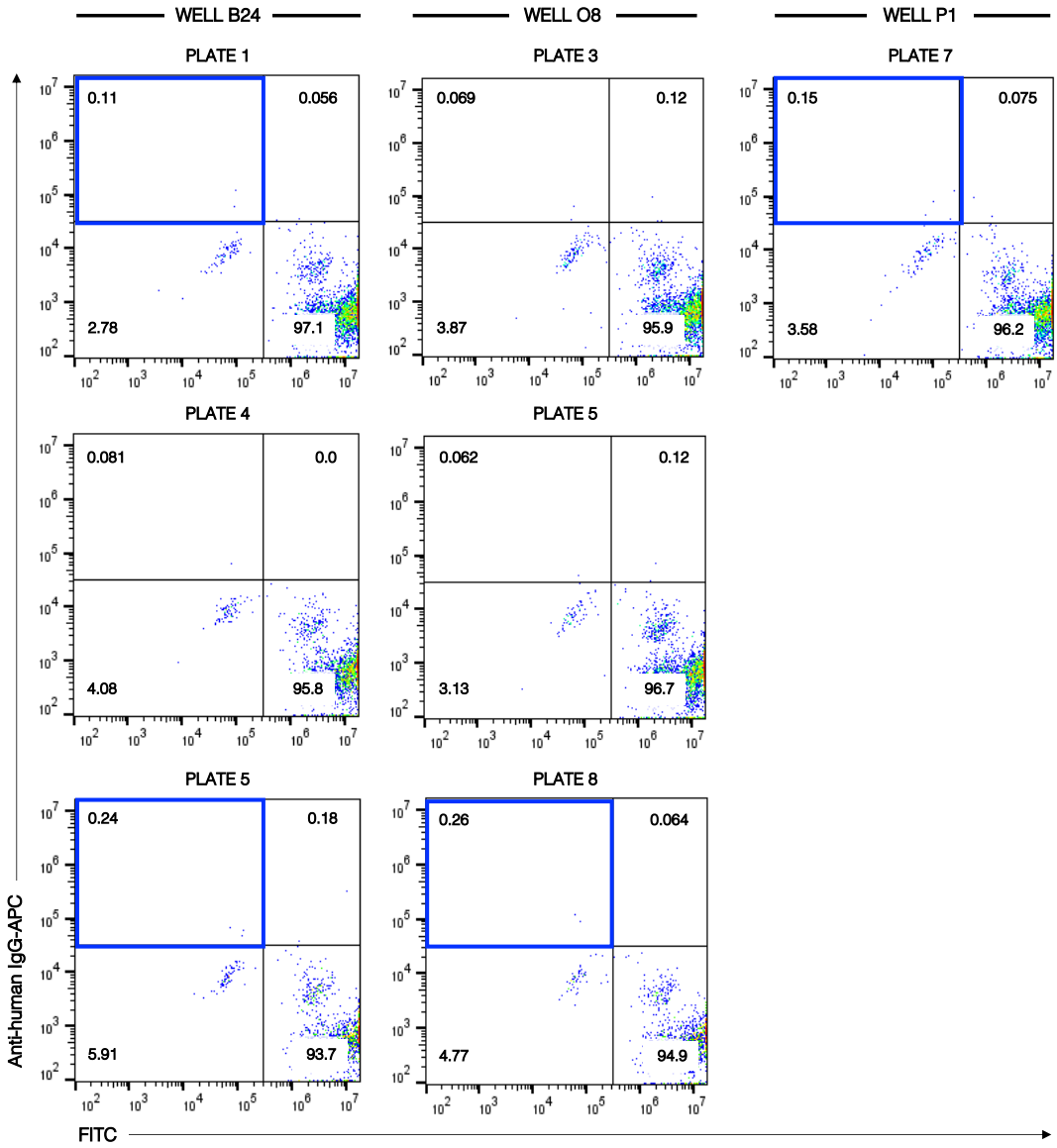

Figure 6.23. | Screening of individual supernatants from EBV-transformed B cell cultures against alloreactive PHA blasts – UoB.

PHA blasts and CFSE-labelled K562 cells (negative control) were co-incubated with a selection of individual supernatants from wells B24, O8 and P1 and analysed based on FITC channel and anti-human IgG-APC parameters. Supernatants demonstrating a greater percentage of anti-IgG$^+$ T cell blast population (blue quadrant) compared to anti-IgG$^+$ CFSE-labelled K562 population are shown.

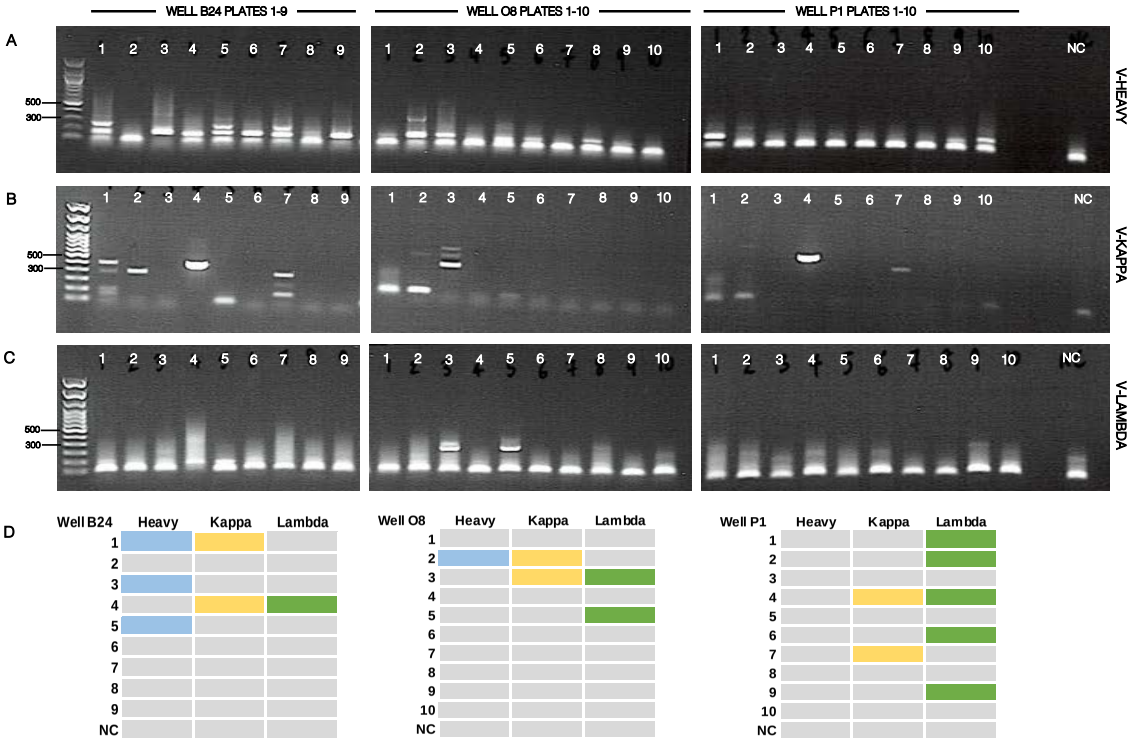

Figure 6.24. | Amplification of immunoglobulin genes from EBV-B cell cultures using PCR.

Amplification of heavy and light chain variable regions using nested polymerase chain reaction (PCR). Nine individual EBV-B cell cultures from well B24 (plates 1-9) were harvested and ten individual EBV-B cell cultures from well O8 (plates 1-10) and well P1 (plates 1-10) were harvested. Following RT-PCR and nested PCR, gene products were visualised on 1% w/v agarose gel. PCR products specific to **A |** IgH (380-450bp), **B |** IgK (510-540bp) and **C |** Igλ (405-450bp) were observed. **D |** Summary of paired heavy and light chain genes amplified from EBV-B cell cultures. Blue indicates the presence of IgH product, yellow indicates the presence of IgK product and green indicates the presence of Igλ product. No PCR product is indicated as grey.

6.5. Generation of alloreactive antibodies from plasmablasts

Plasmablasts are short-lived antibody secreting cells that appear transiently and persist in circulation for up to 10 days after antigen exposure. To generate alloreactive HLA-specific monoclonal antibodies, two renal transplant recipients who had rejected their allograft and were due to undergo transplant nephrectomy (TN) were recruited. The approach aimed to isolate activated plasmablasts, seven days post-TN at the peak of the immune response. It was hypothesised that following the withdrawal of immunosuppression treatment, the antibodies secreted by this B cell subset would be predominantly alloreactive, and therefore specific to the surface antigens on the allograft, including HLA molecules. This method relied on sorting single plasmablasts into PCR plates and amplifying immunoglobulin (Ig) genes i.e. heavy and light chain variable regions from each cell. Following Ig expression vector cloning of heavy and light chain sequences, transient co-transfection into mammalian system was performed to produce recombinant monoclonal antibodies (Figure 6.25).

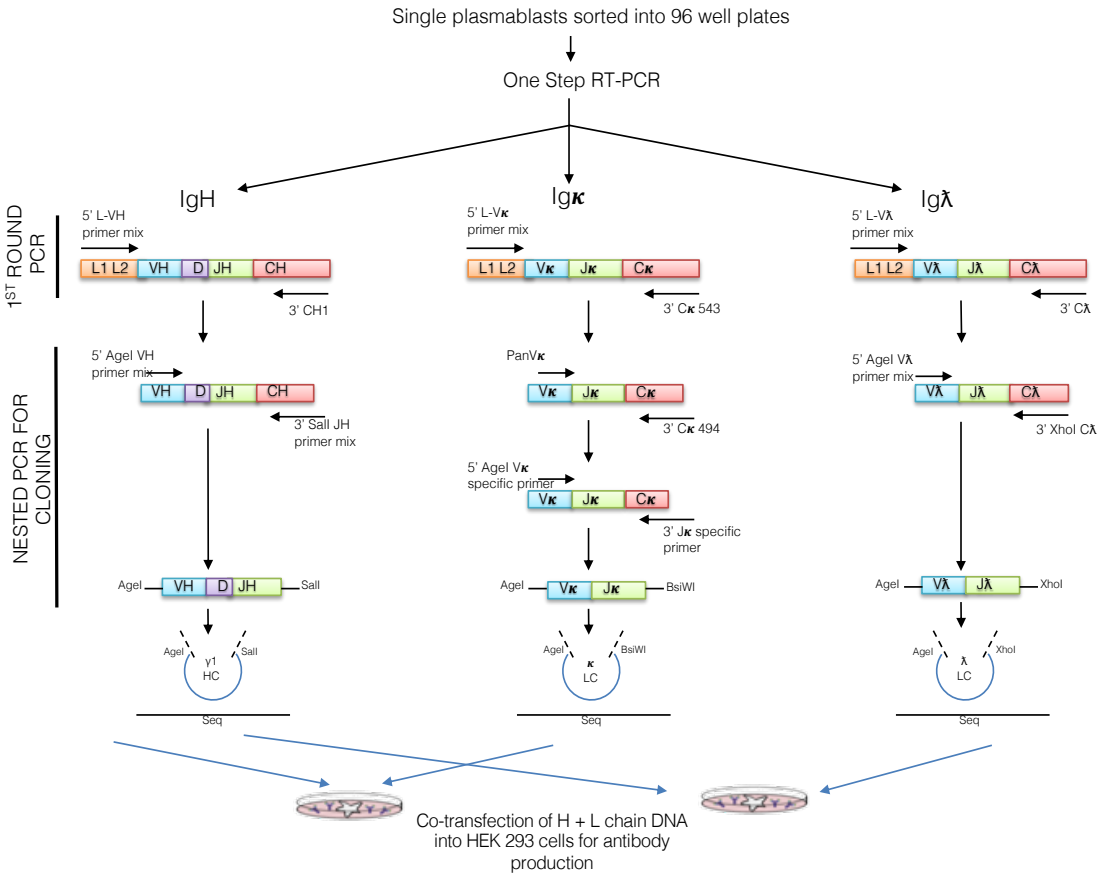

Figure 6.25. | Schematic of antibody cloning and expression process from single B cells.

Heavy and light chain genes were amplified by nested PCR from single plasmablasts. The first PCR round involves amplifying the leader region using forward primer mixes and constant region using reverse primer mixes specific to IgH, IgK and Igλ genes. The nested PCRs were performed using FWR1-specific forward primer mixes and J-gene or constant regions-specific reverse primer mixes. This PCR step also incorporates restriction sites to the PCR products to facilitate sequencing and expression vector cloning. Recombinant antibody production was performed by transiently co-transfecting heavy and light chain plasmids into HEK293 cells. The secreted antibodies in the supernatants were collected after 5 days in culture for further analyses. Adapted from Tiller et. al, (2008).

6.5.1. Detection of plasmablast subset by flow cytometry

To detect short-lived antibody secreting cells (ASCs) i.e. plasmablasts, PBMCs were isolated from whole blood collected from healthy donors, seven days after vaccination or from TN-experienced renal transplant patients. Using flow cytometry, monocytes ($CD14^+$), NK cells ($CD56^+$) and T cells ($CD3^+$) were excluded from analysis. Live $CD19^+$ B cells were further selected into the high CD27 and CD38-expressing plasmablasts (Figure 6.26A). A healthy donor with no recent history of vaccination with an immunogen presented with a low frequency of plasmablasts (0.29%) in the periphery (Figure 6.26A; right panel). Two healthy donors vaccinated against Hepatitis B or flu were recruited to analyse the plasmablast population frequency, seven days after vaccination (Figure 6.26B). The percentages of $CD27^+$ $CD38^+$ ASCs observed within the vaccinated healthy donors were greater (0.42% and 0.66%, respectively) compared to non-vaccinated healthy donor.

In contrast, seven days following TN and withdrawal of immunosuppression treatment, the renal transplant patients revealed significantly greater frequency of $CD27^+$ $CD38^+$ ASCs at 1.48% and 9.65% in the periphery (Figure 6.26C). Plasmablasts were sorted at the single cell level into PCR plates containing catch buffer supplemented with RNase inhibitor for immunoglobulin gene amplification.

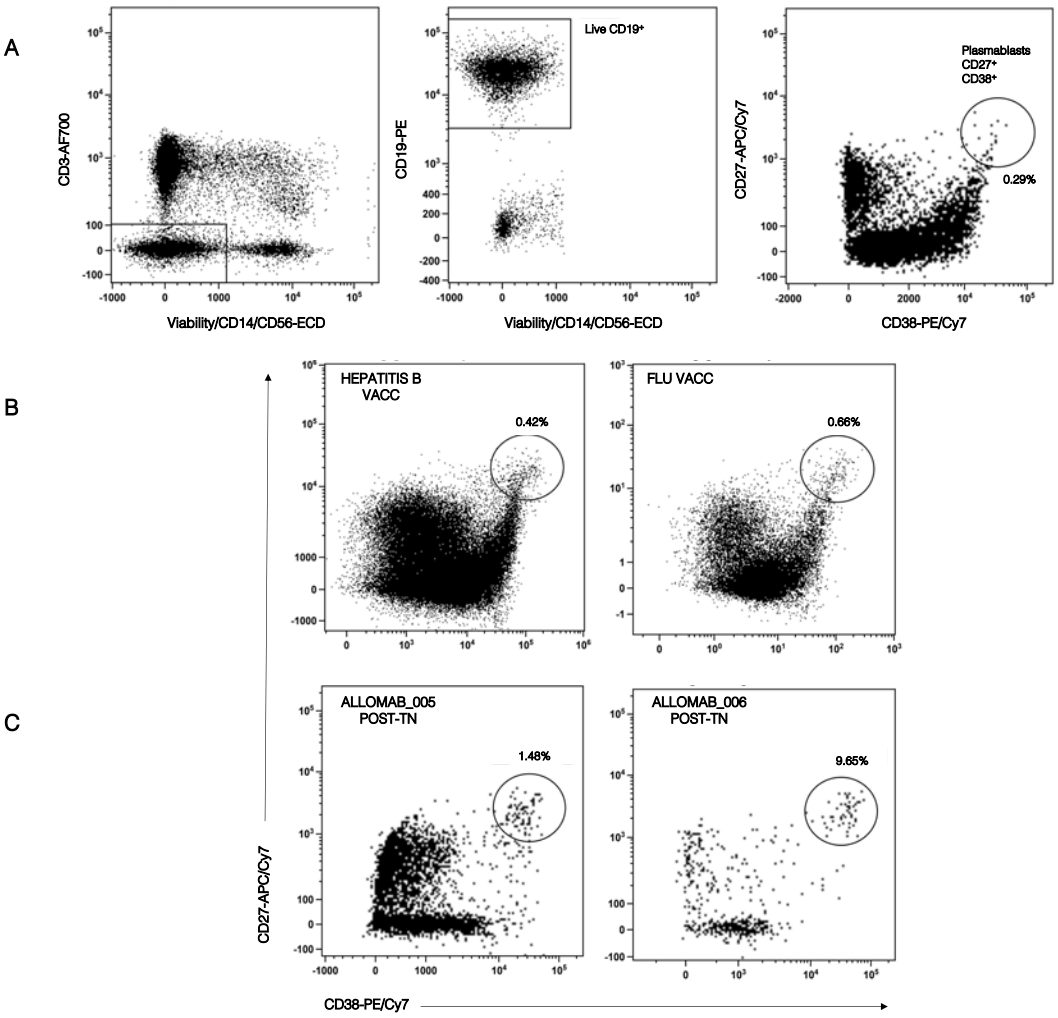

Figure 6.26. | Transplant nephrectomy induces a potent plasmablast response.

A | Representative flow gating strategy used to exclude CD14+ monocytes; CD56+ NK cells and CD3+ T cells from further analysis. Viable CD19+ B cells were selected to identify dual CD27+ CD38+ plasmablast population.

B | The plasmablast response (CD27+ CD38+) in two healthy donors vaccinated against Hepatitis B and flu was analysed 7 days after vaccination.

C | Following transplant nephrectomy, two patients 005 and 006 demonstrate a potent plasmablast response compared to vaccinated healthy donors. Using the gate indicated in the flow plots, dual CD27+ CD38+ plasmablasts were isolated by FACS at the single cell level into PCR plates.

6.5.2. Amplification of immunoglobulin genes from single plasmablasts

To generate recombinant monoclonal antibodies, RT-PCR and semi-nested PCR were performed and the antibody genes from a single plasmablast were amplified. RT-PCR included the synthesis of cDNA and the amplification of IgG-specific heavy and light chain variable genes. The final 'cloning' nested PCR step incorporated restricted sites to the Ig genes for expression vector cloning (Figure 6.24). The amplified heavy and light chain genes from a single cell were determined by visualising single bands at approximately 380-450bp (V_H) (Figure 6.27A), 510-540bp (V_K) (Figure 6.27B) and 405-450bp (V_λ) (Figure 6.27C) on 1% w/v agarose gel. Representative example of paired V_H and V_L genes from a PCR plate is summarised in Figure 6.28.

The semi-nested PCR for cloning uses a cocktail of primers for V_H and V_L chain region amplification. Due to the closely related V_K cloning PCR primer sequences, the amplified V_K genes were purified and sequenced. The data were analysed to determine the correct 5' and 3' V_K-specific primers to incorporate the appropriate restriction sites for cloning. Figure 6.29 shows a representative example of detailed V_K gene sequence analysis. The V_K nucleotide sequence was compared with the sequences in the online IMGT/V-QUEST reference directory sets of the human IgK locus. Firstly, the results summary (Figure 6.29A) revealed the functionality of the sequence i.e. productive IgK rearranged sequence with no stop codon and in-frame junction detected. Secondly, the V-GENE and allele (IGKV3-20*01) and J-GENE and allele (IGKJ1*01) were indicated with a percentage identity of more than 92%. However, further analysis of the V_K region by protein translation was performed to identify the most suitable primers (Figure 6.29B). The 5' V_K-specific primer V_K3-20/3D-20 (EIVLTQS) and the 3' V_K-specific primer J_K3 (DIKRTV) were identified for the cloning PCR (Figure 6.29C). Finally, these specific primers were used to add restriction sites to the V_K gene for subsequent expression vector cloning.

A

V_H region amplification

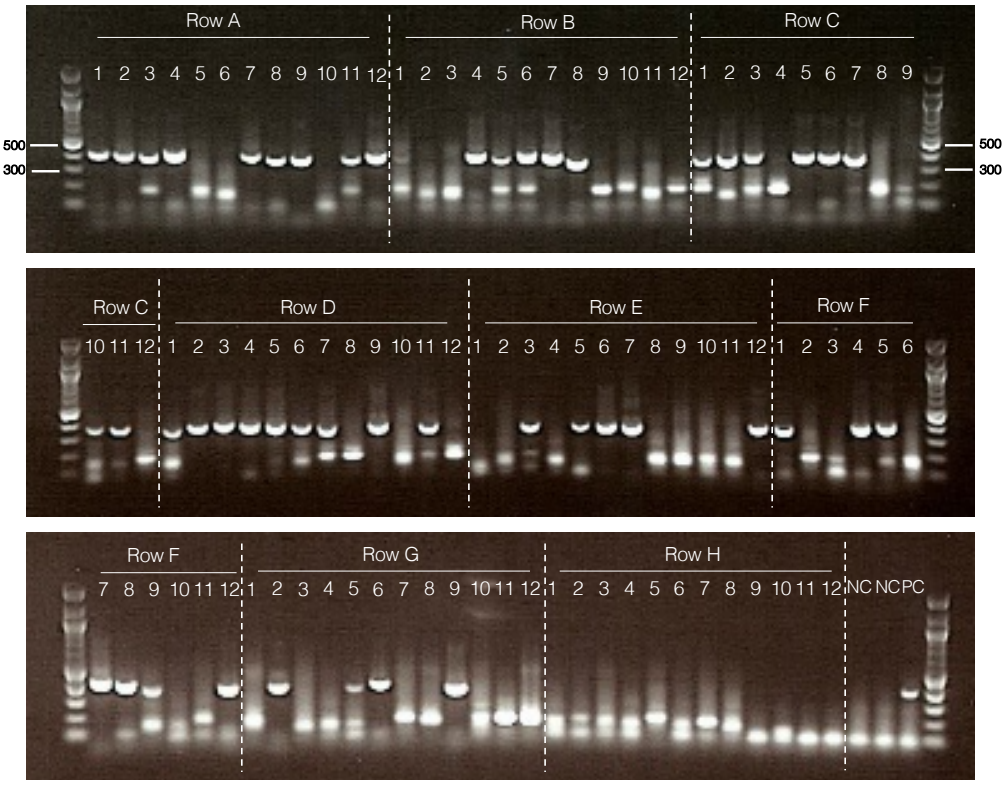

B

V_K region amplification

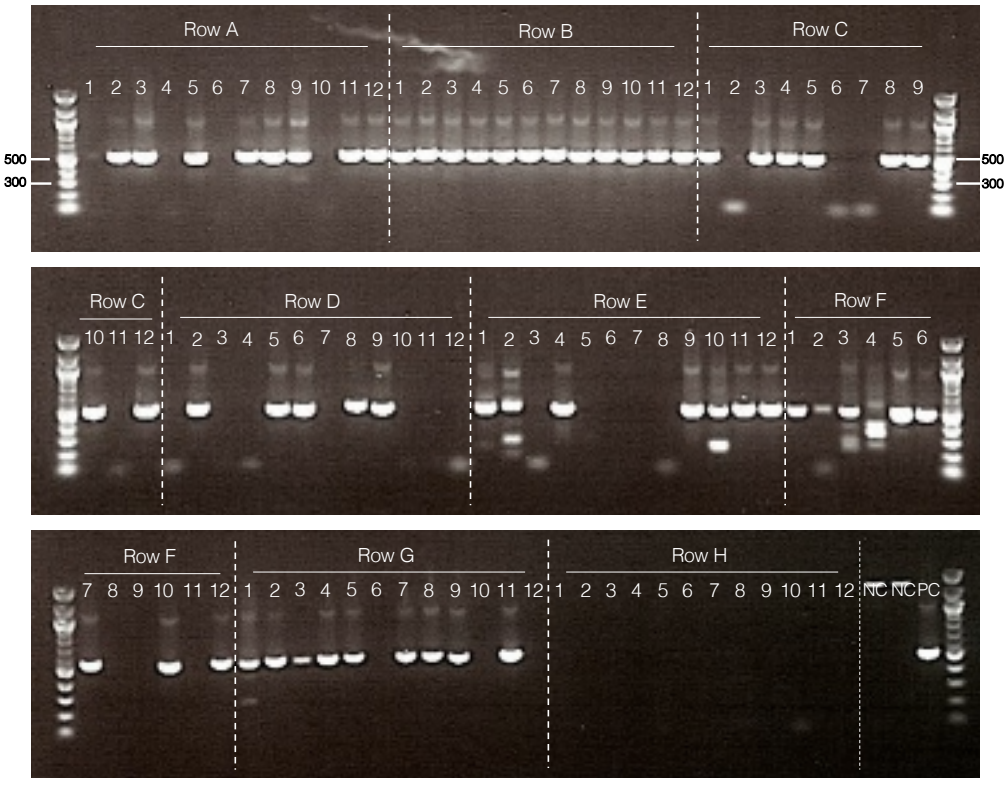

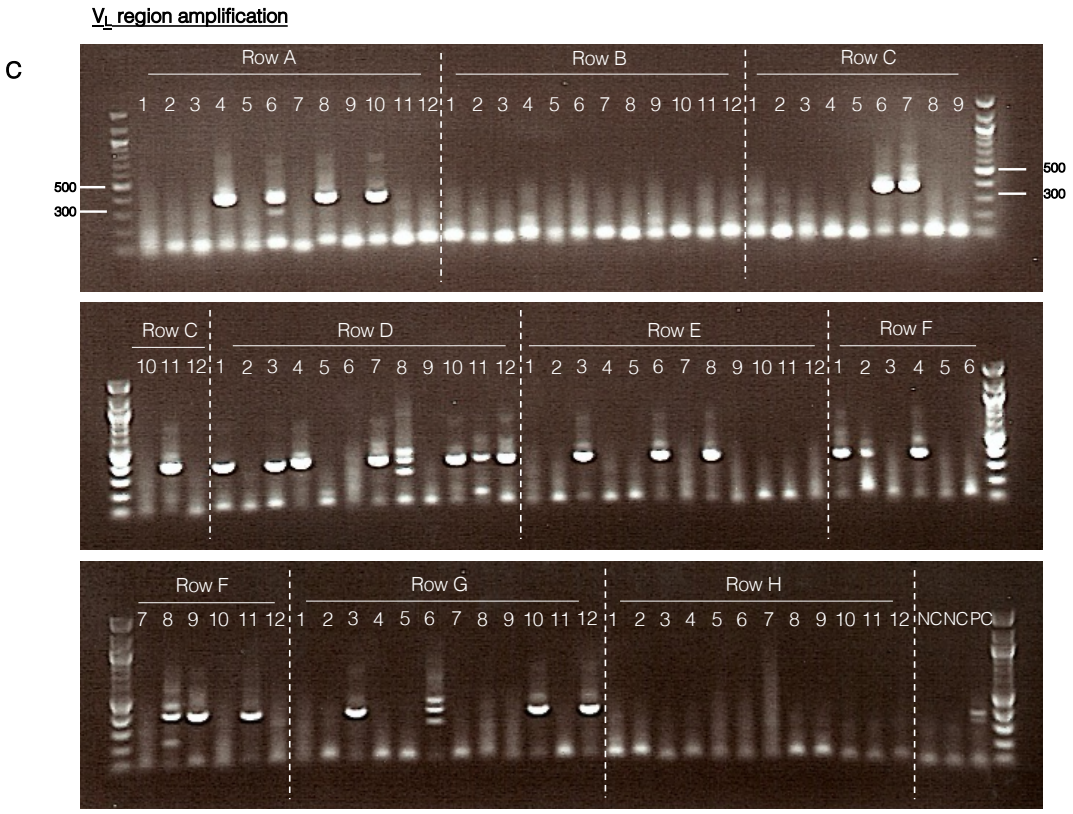

Figure 6.27. | Amplification of immunoglobulin genes from single isolated plasmablasts using PCR.

Representative example shows the amplification of heavy and light chain variable regions from a total of 84 plasmablasts using polymerase chain reaction (PCR) . Single plasmablasts were sorted directly into wells containing RNAse-inhibiting RT-PCR catch buffer. Following RT-PCR and nested PCR, gene products were visualised on 1% w/v agarose gel. PCR products indicating variable regions specific to **A |** IgH (380-450bp), **B |** IgK (510-540bp) and **C |** Igλ (405-450bp) were observed. Positive control (PC) using cDNA from B cells and negative control (NC) containing no B cell were also included in each PCR step.

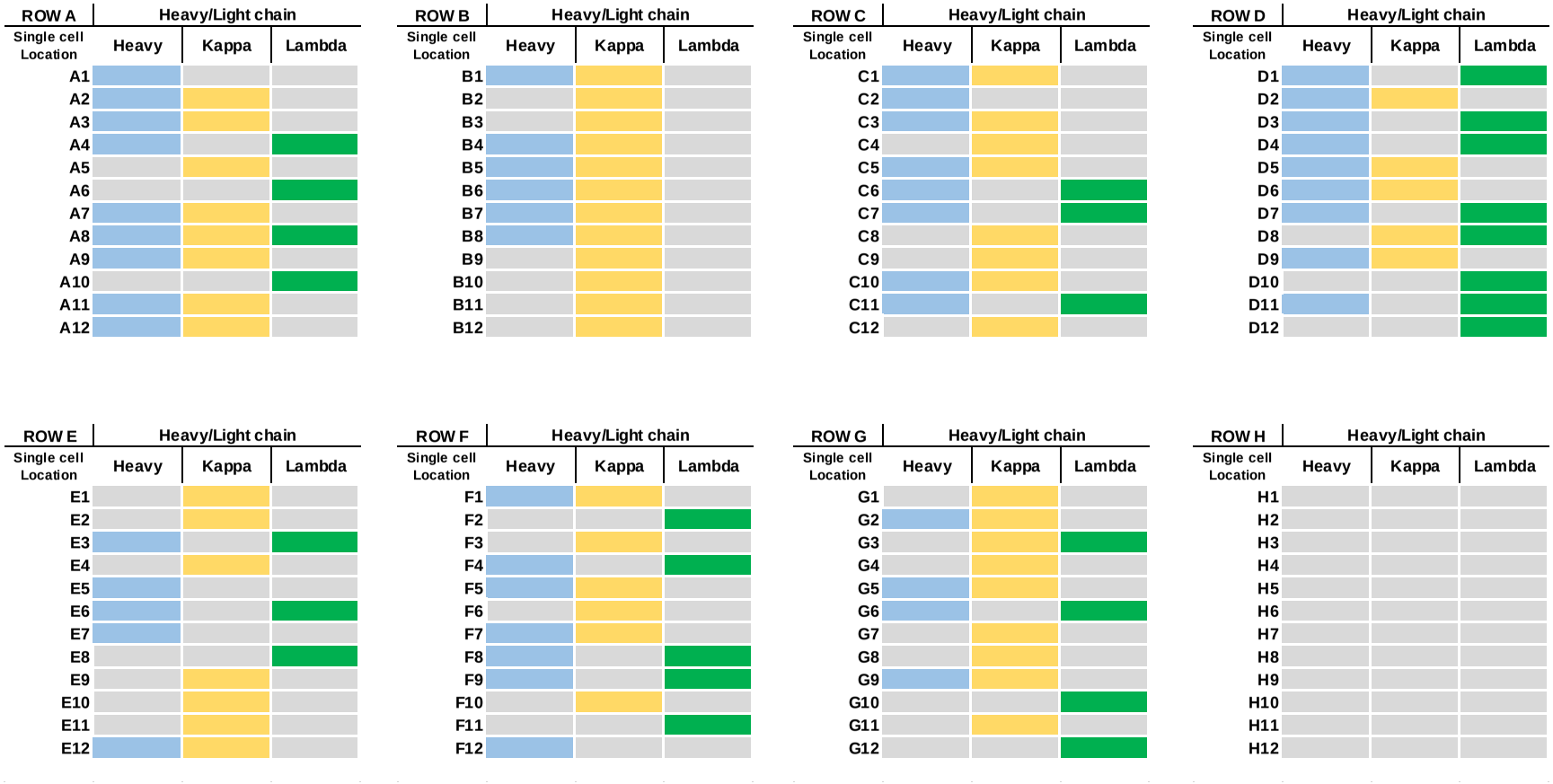

Figure 6.28. | Summary of paired heavy and light chain genes amplified from a total of 84 single plasmablasts.

Single plasmablasts were sorted into rows A-G of a 96 well PCR plate. Row H represents the negative control row which did not contain any plasmablasts. Blue indicates the presence of IgH product, yellow indicates the presence of IgK product and green indicates the presence of Igλ product. No PCR product is indicated as grey.

A

>G03_Kappa_B10.ab1
gctcccagcctcctcatstatggtgcatccagaagggccactggcagcccmgacaggttc
agkggcagtgggtytggggcagacttcactctcaccatyagcagagtggagcctgaagat
tttgcagtgtattactgtcagcagtatggtggctcaccgacgttyggccaagggaccaag
gtggacatcaaacgaactgtggctgcaccatctgtcttyatcttcccgccatytgatgag
cagttgaaatctggaactgcctctgttgtgtgcctgctgaataacttctatcccagagag
gccaaagtacagtggaaggtggataacgccctccaattcggkwaytaccmagrrkkryms
scc

Result summary:	Productive IGK rearranged sequence (no stop codon and in-frame junction)		
V-GENE and allele	Homsap IGKV3-20*01 F	score = 661	identity = 92.81% (142/153 nt)
J-GENE and allele	Homsap IGKJ1*01 F	score = 157	identity = 94.29% (33/35 nt)
FR-IMGT lengths, CDR-IMGT lengths and AA JUNCTION	[X.7.36.10]	[X.3.8]	CQQYGGSPTF

B

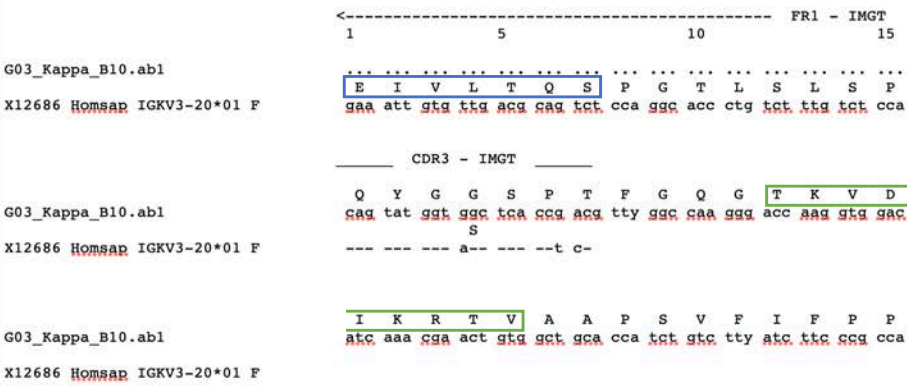

C

Forward primers		
5'AgeIVk1	CTGCAACCGGTGTACATTCTGACATCCAGATGACCCAGTC	ATGVHSDIQMTQ
5'AgeIVk1_9_1–13	TTGTGCTGCAACCGGTGTACATTCAGACATCCAGTTGACCCAGTCT	CAATGVHSDIQLTQS
5'AgeIVk1D_43_1_8	CTGCAACCGGTGTACATTGTGCCATCCGGATGACCCAGTC	ATGVHCAIRMTQ
5'AgeIVk2	CTGCAACCGGTGTACATGGGGATATTGTGATGACCCAGAC	ATGVHGDIVMTQ
5'AgeIVk2_28_2_30	CTGCAACCGGTGTACATGGGGATATTGTGATGACTCAGTC	ATGVHGDIVMTQ
5'AgeVk3_11_3D_11	TTGTGCTGCAACCGGTGTACATTCAGAAATTGTGTTGACACAGTC	CAATGVHSEIVLTQ
5'AgeVk3_15_3D_15	CTGCAACCGGTGTACATTCAGAAATAGTGATGACGCAGTC	ATGVHSEIVMTQ
5'AgeVk3_20_3D_20	TTGTGCTGCAACCGGTGTACATTCAGAAATTGTGTTGACGCAGTCT	CAATGVHSEIVLTQS
5'AgeVk4_1	CTGCAACCGGTGTACATTCGGACATCGTGATGACCCAGTC	ATGVHSDIVMTQ
Reverse primers		
3'BsiWIJk1_2_4	GCCACCGTACGTTTGATYTCCACCTTGGTC	TKVXIKRTV
3'BsiWIJk3	GCCACCGTACGTTTGATATCCACTTTGGTC	TKVDIKRTV
3'BsiWIJk5	GCCACCGTACGTTTAATCTCCAGTCGTGTC	TRLEIKRTV

Figure 6.29. | Representative example of kappa PCR product sequencing analysis.

Kappa PCR products were sequenced to determine the correct forward and reverse primers for nested PCR stage and to incorporate restriction sites for expression vector cloning.

A | Kappa PCR nucleotide sequence was analysed using IMGT/V-QUEST online tool. The results summary of the green highlighted sequence provides information about the productivity of the sequence and sequence identity similarity to the reference sequence datasets in the tool directory. The software suggested primer sequences for forward sequence (V-GENE and allele) and reverse sequence (J-GENE and allele) are also provided (blue text).

B | The V-REGION was translated and aligned with the closest germLine V-GENE. The complete translation of the input sequence has not been shown. The amino acid sequence for the forward primer (blue box) and for the reverse primer (green box) have been highlighted.

C | Summary of the forward and reverse primers used for IgK nested PCR for cloning. The nucleotide (second column) and translated sequences (third column) are provided for 5' VK3-20/3D-20 (blue) and 3' Jk3 (green) primers.

6.5.3. Expression vector cloning and transient co-transfection

Heavy and light chain regions were ligated with respective vectors. Following growth of vectors in bacterial cultures, plasmid DNA was extracted. To determine positive bacterial clones carrying the respective V_H, V_K and V_λ gene insert, a diagnostic analysis was performed by digesting the plasmid DNA with specific restriction enzymes. The positive clones were visualised on 1% w/v agarose gel with single bands at 400-600bp (Figure 6.30A).

To test the recombinant antibody expression system, both heavy and light chain plasmids were transiently co-transfected into HEK293T cells. Culture supernatants harvested after five days were analysed for the presence of IgG and total IgG concentration using an IgG ELISA. Small scale transfections (24 well plate) of multiple heavy and light chain plasmid DNA deriving from the same single cell were analysed. Representative example of total IgG concentrations from small-scale supernatants were measured at a range of 3.0-45.0μg/mL (Figure 6.30B). Large-scale transfections whereby supernatants ranging from 50-100mL were concentrated to small volumes of up to 0.5mL by centrifugal filter units, yielded up to ~6.0mg/mL IgG (Figure 6.30C).

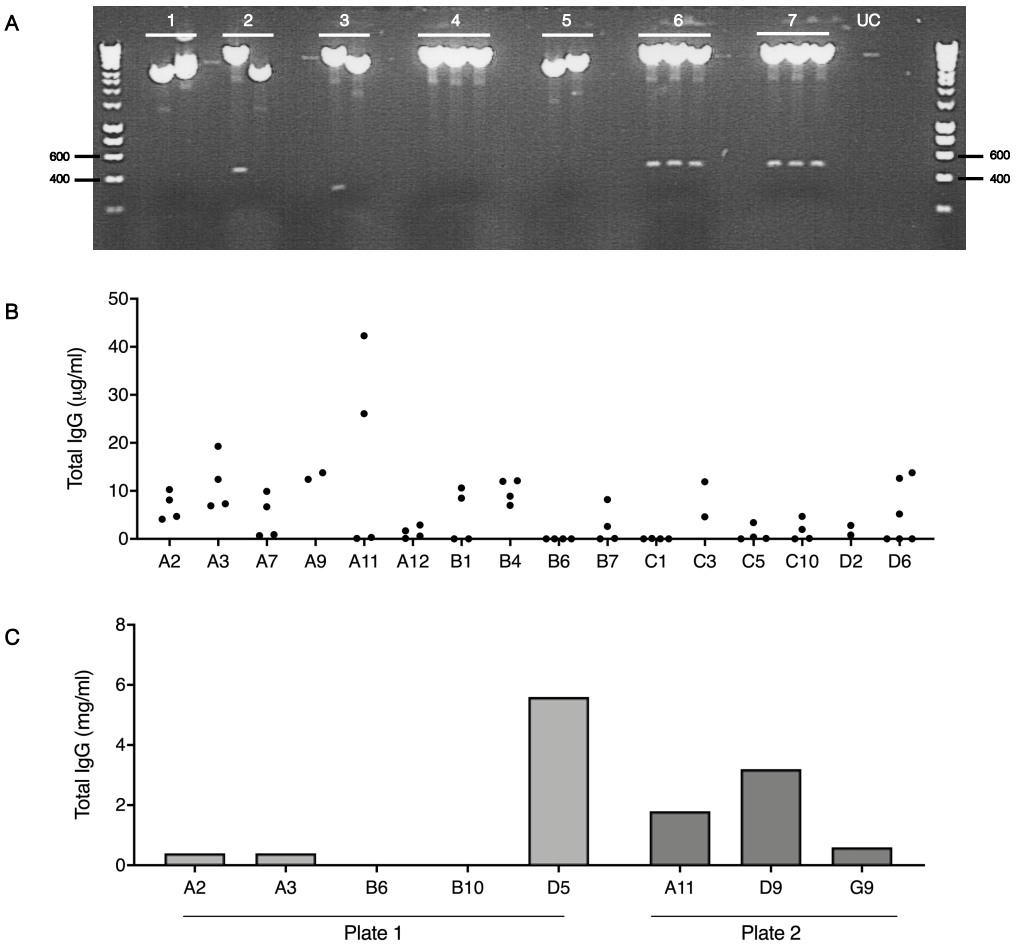

Figure 6.30. | Expression vector cloning and recombinant antibody production.

A | Plasmid DNA containing heavy or light chain inserts were digested to test for positive clones. Representative example shows the presence of IgH inserts at 400-500bp compared to uncut (UC) plasmid DNA. Several clones did not contain IgH insert.

B | Representative example of total IgG from small-scale transfections quantified by ELISA. Heavy and light chain DNA were co-transfected into HEK293T cells in 24 well plates. Transfection medium was replaced with 0.5mL of protein-free medium and HEK293T cells were cultured for 5 days. Supernatants were collected and tested for IgG by ELISA. Each dot represents multiple combinations of heavy and light chain transfections deriving from a single well based on the number of positive heavy/light chain gene-containing bacterial clones detected.

C | Representative example of total IgG from large-scale transfections quantified by bicinchoninic acid assay (BCA). Heavy and light chain DNA were co-transfected into HEK293T cells in 150cm^2 tissue culture plates. Transfection medium was replaced with 25mL of protein-free medium and HEK293T cells were cultured for 5 days. Supernatants were collected and tested for total protein concentration using the BCA assay.

To detect the antigen specificity of the recombinantly generated antibodies, the harvested supernatants were tested against a number of cell lines, including HEK293T, a kidney epithelial cell line. As the plasmablasts derived from a renal transplant patient undergoing chronic rejection, it was speculated that most of the ASCs would be HLA alloreactive and specific to kidney allograft. Therefore, antibody supernatants were co-incubated with HEK293T and reactivity was detected with anti-human IgG secondary antibody. However, no increase in anti-IgG fluorescence was detected from a number of recombinant antibodies generated from two plates of sorted ASCs (Figure 6.31A). This suggests that the antibodies did not recognise or bind to HEK293 surface antigens. Moreover, HLA Class I mixed bead luminex screen of 34 heavy and light chain co-transfections from Plate 1 did not react with the antibody supernatants (Figure 6.31B).

Large scale culture supernatants containing secreted antibody clones from Plate 1 were tested against the parental K562 cell line and HLA-A*02 and HLA-A*24 plasmid-transfected K562 cells. Two antibody clones deriving from a single cell in wells A2 and B6 demonstrated reactivity to the parental and HLA-A antigen transfected cell lines. (Figure 6.31C). Antibody clone from well A2 showed the greatest reactivity to K562 cells (MFI=324.4), followed by K562-A2 (MFI=318.9) and HLA-A24 (MFI=255.9). In contrast, antibody clone from well B6 demonstrated increased anti-IgG MFI values against HLA-A2 and HLA-A24 cells (MFI=272.9 and 222.4, respectively) compared to K562 (MFI=196.4). Moreover, further sequencing analysis of the V_H and V_L chain regions revealed that the antibody clones encoded different V(D)J segments, suggesting that the isolated single plasmablast clones and the recombinantly expressed antibodies were unique (Table 6.1).

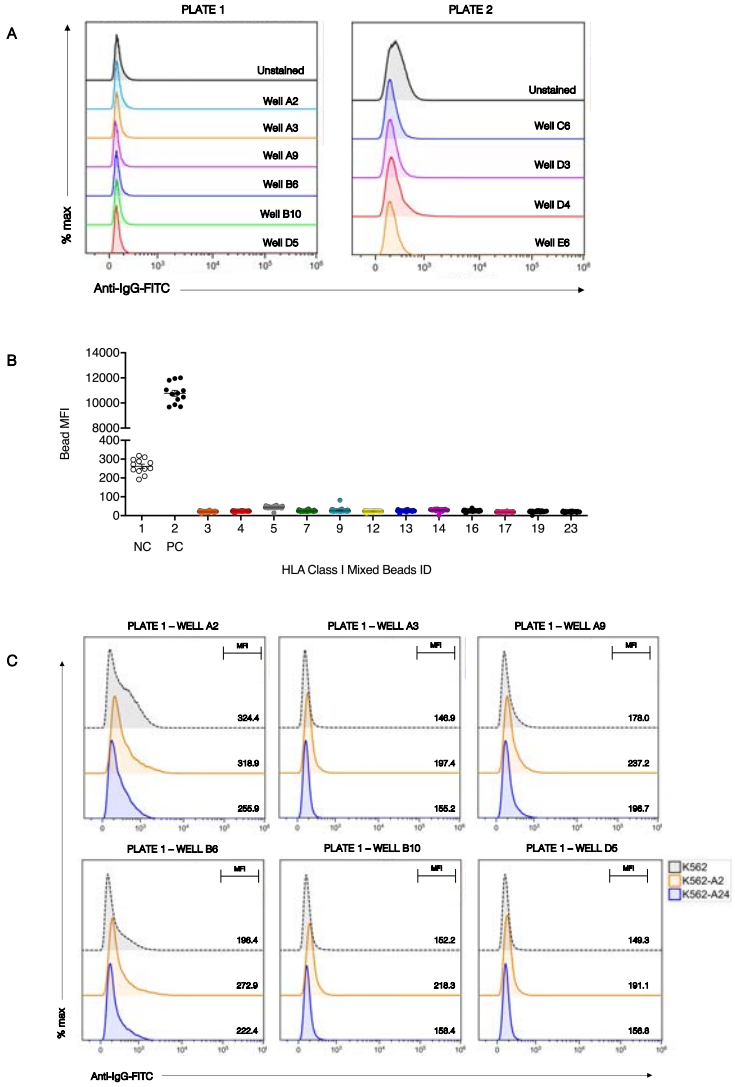

Figure 6.31. | Detection of recombinantly expressed antibody specificities.

A | Antibodies generated from single plasmablasts from two PCR plates were tested against HEK293T cells to determine antigen specificity. Antibody supernatants from small-scale transfections were co-incubated with HEK293T cells and subsequently labelled with anti-human IgG-FITC secondary antibody for flow cytometry analysis. An increase in anti-IgG-FITC indicated antibody binding to HEK293T cells.

B | Supernatants were tested against mixed HLA Class I antigen-coated beads in a luminex assay. Polystrene SABs coated with multiple HLA antigens and embedded with varying ratios of two fluorochromes were treated with culture supernatants, followed by labelling of antibody-bound beads with anti-IgG secondary antibody. Negative control (A/B serum) and positive control (pan HLA reactive) sera were included in the assay. The range of HLA-specific antibody levels were measured by median fluorescence intensity values (MFI).

C | Antibodies generated from six single plasmablasts from PCR Plate 1 were tested against parental and HLA-A2 and HLA-A24 transfected K562 cells to determine antigen specificity. Antibody supernatants from large-scale transfections were co-incubated with target cell lines and subsequently labelled with anti-human IgG-FITC secondary antibody for flow cytometry analysis. An increase in anti-IgG-FITC indicated antibody binding to target cell lines.

Table 6.1. | Summary of V(D)J genes and CDR3 regions of antibody clones

	Heavy chain					Light chain		
Clone	**V**	**D**	**J**	**CDR3**	**K/L**	**V**	**J**	**CDR3**
A2	V3-21*01	D3-10*01	J6*02	ARAQEFGSVIIYYYYGMDVW	**Kappa**	V1-39*01	J1*01	QQTYTLPWTF
A3	V3-49*04	D1-26*01	J3*01	TRSTHSEALXVW	**Kappa**	V2-28*01	J3*01	MASYPVPPTF
A9	V4-34*01	D4-23*01	J2*01	ARGIRTNDYGGLTSHWYFDLW	**Kappa**	V1-12*01	J4*01	QQTNSFPLTF
B6	V4-59*08	D3-10*01	J3*02	ARSLWFGNLNDVFDI	**Lambda**	V1-40*01	J3*02	XXYXGRXGXPG (PHE 118 not identified)
B10	V4-30-2*01	D6-13*01	J1*01	ARGAAVSGXAAAGWFEXW	**Kappa**	V3-20*01	J1*01	QQYGGSPTF
D5	V3-23*01	D1-1*01	J3*01	AKATGSIDPFDV	**Lambda**	V2-14*01	J2*01	RLNXSGHHXV

Collectively, these data from the plasmablast study in section 6.5 demonstrate that recombinant antibodies can be successfully generated from a single B cell. The number of experiments performed to determine antibody specificities were limited, mostly due to time restrictions and lack of resources. Therefore, additional experiments were planned to identify the specificities of the antibodies deriving from single plasmablasts. One approach involved continuing large-scale production of antibodies to obtain high concentrations and test against (i) HLA antigen-coated luminex beads, (ii) autologous patient kidney biopsies and (iii) glomerular endothelial cell lines. Another approach involved testing the antibodies against a commercial kidney cell lysate carrying the HLA type that corresponded to the patient HLA-specific antibody profile to determine the antibody specificities using mass spectroscopy.

6.6. Discussion

The main objective of the work in this chapter was to isolate HLA-specific antibody producing B cells from sensitised renal transplant recipients. There was particular interest in isolating HLA-C-specific antibody secreting B cells to generate recombinant antibodies *in vitro* and further investigate the functional interaction between HLA-C ligands and KIRs on NK cells.

A combination of selection tools and *in vitro* culture methods were used to detect antibody-secreting peripheral B cells. Memory B cells of interest were identified using targeted approaches such as single HLA antigen-coated beads and HLA Class I-specific tetramers as well as a global approach by immortalising the memory B cell population using EBV, followed by screening of individual culture supernatants for HLA-specific antibodies. Similarly, isolation of single plasmablasts from transplant nephrectomy-experienced patients provided an alternative approach to identify HLA-specific alloreactive B cells.

Enrichment of antigen-specific B cells using either HLA antigen-coated beads or HLA Class I-specific tetramers presented inconsistent and unreliable results due to high background levels of staining observed, even with PBMCs from healthy donors. Immortalisation of B cells by EBV method was relatively successful as HLA-specific antibodies were detected in culture supernatants, indicating the presence of HLA-specific alloreactive B cells in large scale EBV-B cell cultures. Although attrition was observed, from the two plates (144 cells) analysed for the plasmablast study, heavy and light chain genes were amplified from 52 cells, of which 37 antibodies were successfully cloned and expressed in a culture system. Monoclonal antibodies were generated recombinantly at both small and large scales *in vitro*, but the specificities need to be determined.

6.6.1. Methods to detect HLA-specific antibody secreting B cells

Due to the heterogeneity of the memory B cell population, enrichment of antigen-specific B cells is a commonly used strategy to isolate B cells of interest and clone the antibody genes. Previous studies have identified and isolated HLA-specific antibody secreting B cells from sensitised individuals by using monomeric HLA (Barnardo et al., 2000); tetrameric HLA (Mulder et al., 2003; Zachary et al., 2007; Ouisse et al., 2017) and single HLA antigen coated beads (Degauque et al., 2013). Therefore, by taking advantage of these established methods, the most suitable approach to meet the objectives of the current study were tested.

In this study, targeted approaches involving tetrameric HLA and single HLA antigen beads were used. Both approaches demonstrated the presence of HLA alloreactive B cells in renal transplant patients and healthy individuals. The frequency of HLA tetramer$^+$ B cells was low, which was most likely to result from the initial low frequency of HLA-specific memory B cells (Mulder et al., 2001, 2003) combined with a low starting number of PBMCs. It is also possible that the peptide bound in the groves of the tetramers influences binding to specific and non-specific B cells. Mulder et al., (2005) have shown that the bound peptide is decisive for the binding of HLA-specific antibodies. Although further detailed analyses were not performed, it can be speculated that the low frequency of HLA tetramer$^+$ B cells was potentially a reflection of poor binding to the peptide in the HLA monomers.

Consistent with previous studies (Pape et al., 2011; Taylor et al., 2012), non-specific tetramer binding was also observed as patient B cells demonstrated reactivity to HLA Class I-specific tetramers for which antibody specificities were not detected in the serum. Background levels of non-specific tetramer binding is likely to arise from binding to soluble

immunoglobulin antigen receptor (Zachary et al., 2007). Moreover, IgG was not detected in the supernatants deriving from the non-specific tetramer^{+} B cells. Although luminex analyses are extremely sensitive, there is a possibility that antibody levels-specific to the irrelevant tetramer were below the level of detection of the luminex assay.

Similarly, varying levels of non-specific binding was observed between B cells from healthy individuals and HLA SABs. This finding suggests that a proportion of circulating peripheral blood B cells in non-immunised or sensitised individuals secrete HLA Class I-specific antibodies (Degauque et al., 2013). Low frequencies of HLA-specific antibodies in healthy non-sensitised males (Morales-Buenrostro et al., 2008; El-Awar et al., 2009) and females (Triulzi et al., 2009) have been previously reported. The rise of HLA-specific antibodies in individuals with no prior sensitisation events are likely to result from natural immunising events such as infections, allergies, ingestion of specific proteins and vaccines (D'Orsogna et al., 2011).

Interestingly, the total percentage of SAB-bound B cells from renal transplant patient PBMCs was much lower than the values observed in healthy individuals. Whilst this finding further confirms the non-specific binding property of SABs to B cells from healthy donors, it can be speculated that a more selective and definitive binding pattern towards HLA alloreactive B cells from sensitised patients was demonstrated. However, it was difficult to assign the HLA antigen specificity of the bead-B cell rosette based on the position of detection due to the lack of information from the manufacturer product sheets.

Similar to the non-specific HLA tetramer^{+} B cells, SAB-bound B cells from healthy donors also did not secrete IgG. These findings confirm that using HLA-specific tetramers and SABs present with strong background binding that also includes non-specific B cells in the enriched antigen-specific B cell population. Although tetrameric HLA and SABs have

previously proven useful to identify and isolate HLA-specific antibody secreting B cells, the findings of this study provide an insight into the potential pitfalls of binding non-specific B cells and their impact on the overall experimental outcome.

6.6.2. Short-term cultures of B cells

It was in the interest of the current study to attempt to expand memory B cells over a short period of time and maximise recovery of a clonal culture for immunoglobulin genes amplification and allow the screening of HLA-specific antibodies from cultured B cells. The first B cell culture method used was adapted from Huang et al., (2013), which was particularly favourable as it did not involve transformation or fusion of B cells to achieve monoclonal antibody production. The aim was to screen supernatants for HLA antibody specificities and potentially harvest a monoclonal cell culture deriving from a single B cell. Although IgG was detected in the supernatants, this method did not provide a more robust response in the expansion of memory B cells. Moreover, the collection of cultures to amplify heavy and light chain genes for antibody production was unsuccessful, suggesting either technical inefficiency or non-viable clonal cultures.

During FACS, however, a negative isolation strategy was adopted whereby IgG-expressing B cells were not selected on the basis of the IgG marker. This strategy limited activation-induced cell death, which was used for almost all B cell culture experiments in this study. However, it is also true that the HLA tetramer^{+} B cells and SAB-bound B cells were isolated from previously frozen PBMCs, which possibly affected the overall viability of B cells in cultures despite the short-term stimulation (Jourdan et al., 2009). Therefore, factors including the proapoptotic state of B cells post-recovery of PBMCs and activation for up to two weeks have to be considered to optimise the survival of clonal cultures.

In comparison to the methods used to detect and subsequently culture HLA-specific antibody secreting B cells, an alternative approach was adopted whereby the global memory B cell subset was analysed. The method of B cell immortalisation by EBV in the presence of a B cell activator was met with relative success (section 6.4). The data generated from the collaboration with IRB demonstrated that this method is efficient to analyse the alloreactive memory B cell repertoire of a renal transplant patient. Although the heavy and light chain genes were not obtained, the screening process identified B cell clones producing HLA-specific antibodies. As this procedure was rapid and highly efficient which was completed in less than four weeks, the method was replicated at UoB.

The aim was to recover B cell clones and produce HLA-specific antibodies *in vitro* to interrogate specificity and favourable functional properties. Unfortunately, the second attempt at this method was not as successful as the first attempt at IRB. Technical problems led to fewer alloreactive PHA blasts propagated in culture, which affected the overall screening process. Although clear and noticeable binding was observed in some cases, particularly with pooled supernatant screening of wells B24 and P1, they could not be considered completely reliable, most likely due to the low number of alloreactive PHA blasts available per test.

Despite the positive staining observed with PHA blasts, HLA Class I luminex analyses were negative suggesting that either the antibody titre was very low that HLA bead reactivity was undetectable or that the antibodies were not HLA-specific. Nonetheless, the lack of reactivity points to an inefficient process of B cell immortalisation by EBV during the second attempt. This is evident from further screening of supernatants from individual wells and the limited success in recovering V_H and V_L genes from each EBV-B cell culture. Amplified kappa and lambda-chain specific DNA deriving from the same well was observed, which was likely to be a result of polyclonal B cell cultures from seeding three

B cells per well. Despite the limited success of the second EBV-B cell culture experiment, paired immunoglobulin genes were amplified from two B cell cultures, subsequent cloning and *in vitro* generation of recombinant antibodies will allow further large-scale production of these antibodies to determine their specificities.

The FACS process at the IRB involved isolating $CD19^+$ IgG^+ B cells for immortalisation, whereas during the second attempt at UoB, additional stages were included e.g. negative isolation of IgG-expressing B cells and selecting for $CD27^+$ memory B cells. It is possible that plating memory B cells for transformation by EBV reduced the efficiency of the cloning process, particularly as memory lymphocytes, compared to naïve cells, are known to have a reduced capacity to proliferate (Pinna et al., 2009). Other factors such as the optimal functional ability of EBV to transform was routinely tested by the IRB for B cell culture experiments, which was not replicated at UoB, potentially affecting the overall transformation efficiency.

There are advantages and disadvantages when comparing the two short-term B cell culture methods such as inducing antibody secreting cell (ASC) phenotype (section 6.3) or B cell immortalisation by EBV (section 6.4) were used in this thesis. The induction of ASC phenotype during short-term B cell culture was used as a more specific method performed following enrichment of antigen-specific B cells. The enriched B cells, however, are more likely to be in a poor condition at the end of 12 days due to chronic activating state of the culture system. Compared to immortalisation by EBV, the short-term induction of ASC phenotype experiment in this study was more cost effective and less labour intensive. Whilst antigen-specific B cells can also be immortalised by EBV, this selection step was not used in the current study. Instead, this approach was performed on a large scale whereby the total IgG^+ memory B cell population was isolated and cultured in over thirty 384-well plates. Although the EBV-B cell culture approach was extremely labour

intensive, it yielded some success in identifying potentially HLA-specific B cells. As these experiments were carried out on a much larger scale than the induced ASC phenotype cultures, they were more likely to provide a positive outcome by immortalising B cells of interest, allowing more time and resources to perform downstream experiments to maximise antibody gene recovery.

6.6.3. Recombinant antibody production from single plasmablasts

Another limitation to this approach included the patient samples used in this study. Most of the patients recruited for this study were awaiting re-transplantation. Therefore, at the time of blood donation, the alloreactive memory B cell pool of the patients was essentially resting in the periphery and not primed or activated by another sensitising event. Although memory B lymphocytes represent the immunisation history over the lifetime of a host, serum antibody levels specific to the immunogens are also maintained (Bernasconi et al., 2002). Moreover, peripheral memory B lymphocytes and/or other B cell subsets are not likely to be involved in persistent alloantibody production, but rather express the immunoglobulins at the cell surface levels (Perry et al., 2008). Therefore, a boost in alloantigen exposure would lead to a short-term increase in HLA-specific antibody levels. This presents the perfect opportunity to interrogate the memory B cell pool and perform a large-scale screen to access antibody specificities of interest. Hence, recruiting patients with a recently failed allograft may offer a more favourable and useful pool of antibody secreting candidates to facilitate detailed analyses of the HLA-specific antibody secreting peripheral blood memory B cells.

Transient antibody secreting cells (ASCs), i.e. plasmablasts were isolated from TN-experienced patients demonstrating a boost in their immune response following allograft removal and withdrawal of immunosuppression treatment. This leads to the differentiation

of memory B cells into low-affinity antibody producing plasmablasts ($CD27^{++}$ $CD38^{++}$) (Stegall et al., 2009). It was hypothesised that the plasmablast population would be enriched for HLA-specific antibody secreting B cells as the patients were undergoing chronic rejection prior to allograft removal. Moreover, the withdrawal of immunosuppression treatment, usually prescribed to suppress graft rejection, further potentiated the antibody-mediated immune response post-TN. However, an antigen-specific selection step was not incorporated during FACS, which led to the isolation of single plasmablasts secreting antibodies specific to other antigens. It has been reported that depending on individual donors and the response generated to vaccination or other immunising events can vary, thus 10-30% of ASCs could be antigen-specific (Smith et al., 2009). Although plasmablasts were not isolated based on their antigen specificities, variation in plasmablast frequency was observed in the current study as patient 006 demonstrated a higher frequency of $CD27^{++}$ $CD38^{++}$ population (9.65%) compared to patient 005 (1.48%) per 10^5 flow events.

Amplification of immunoglobulin genes from a half plate (48 wells) of single plasmablasts yielded ~25% of paired heavy and light chain combinations. A full plate (84 wells as Row H was identified as the control row), paired heavy and light chain genes were obtained from ~50% of single cells. However, the recovery of V_H and V_L regions from a single cell did not always translate into an antibody, as several antibodies were lost during the cloning process indicating high attrition.

Following transient co-transfection of paired antibody genes into HEK293T cells, the secreted IgG levels were variable, which ranged from 3.0-45.0μg/mL. several individual transfections produced low amounts of IgG, indicating the presence of non-functional antibodies (Tiller et al., 2008). This is evident from one antibody clone B6, which failed to provide the CDR3 sequence for the light chain region (Table 6.1). Moreover, large-scale

transfection of heavy and light chain DNA deriving from the single plasmablast in well B6 did not produce detectable levels of IgG.

To the best of our knowledge, this is the first study that analysed the ASCs from a transplant nephrectomised patient. Although several antibodies were successfully generated *in vitro,* the specificities are unknown. Surface staining of K562 cells with antibody supernatants revealed two potential antibody clones with demonstrated reactivity. As K562 is an MHC Class I-deficient cell line, the antibodies are unlikely to be HLA-specific. Therefore, a number of antibody clones were produced on a large scale to determine the antigen specificity by mass spectroscopy in the near future. Further experiments involving testing recombinantly generated antibodies against HLA Class I SABs, autologous patient kidney biopsies and cell lines of kidney origin would be approaches of interest to determine antibody specificities. Collectively, these findings highlight the potential of analysing the plasmablast antibody repertoire following transplant nephrectomy to further identify and characterise alloreactive B cell subsets in addition to the memory B cell pool.

6.7. Conclusions

The findings of this chapter show that HLA-specific antibody secreting B cells were identified, isolated and cultured from sensitised renal transplant recipients. Using MHC Class I-specific tetramers and single HLA antigen coated beads, memory B lymphocytes of interest were selected, though varying levels of background and non-specific binding was observed. Short-term activation of B cells with CD40-L, IL-2 and IL-21 led to detectable levels of IgG from single B cell cultures. To date, however, the specificities of the secreted antibodies are undefined, most likely due to low antibody titres. Transformation of B cells by EBV yielded some success in identifying HLA-specific antibody secreting B cell clones but the downstream antibody expression requires further exploration. Isolation of single plasmablasts from TN-experienced patients facilitated the *in vitro* expression of recombinant antibodies, providing an alternative approach for analysing the alloreactive antibody repertoire during an active immune response.

CHAPTER VII

GENERAL

DISCUSSION

In the current study, the role of HLA-C-specific antibodies was investigated in enhancing NK cell mediated responses against target cells. The findings of this study are the first to demonstrate that human HLA-C-specific alloantibodies enriched from the sera of highly sensitised renal transplant recipients can inhibit the KIR:HLA-C interaction. To meet the aims and objectives of the study, firstly allelic specificities of the human HLA-C-specific alloantibodies in sera were screened and confirmed using luminex microbead assays and flow cytometry-based cell line surface staining. Secondly, this work has successfully demonstrated that HLA-C1 and HLA-C2-specific alloantibodies can recognise and mask HLA-C molecules to block the interaction with relevant KIRs and subsequently boost NK cell function against HLA-C allele-transfected cell lines and primary tumour cells. Investigations into the actions of HLA-C-specific antibodies reveal the possibility of two mechanisms – ADCC mediated NK cell responses and the masking of HLA-C molecules to skew HLA-C-driven KIR signalling towards NK cell activation, which were largely dependent on the HLA-C allotype-specific antibody preparations used in this study. Several approaches were also undertaken to identify and isolate HLA-C-specific antibody secreting B cells from resting PBMCs and short-lived activated plasmablasts during an immune response.

7.1. Similarities of *in vitro* model to pregnancy

The *in vitro* NK cell-based cytotoxicity assay used throughout this study involved inducing 'missing-self' model to test the enriched human HLA-C-specific alloantibodies. Multiple cell lines with either no HLA-C expression or single HLA-C allele transfectants were used to analyse the interaction with KIRs on NK cells. This *in vitro* model highlighted the importance of HLA-C:KIR interaction in conferring resistance to NK cell effector function. It was also biologically relevant as it represented what may happen as a result of exposure to allogeneic HLA antigens during pregnancy. Although the primary villous trophoblast

cells are HLA-deficient, the extravillous trophoblast cells express the classical and polymorphic HLA-C and non-classical HLA-E and HLA-G molecules (Apps et al., 2009). During the early stages of pregnancy, foetal HLA-C interacts with maternal KIRs on uterine NK cells to regulate the process of placentation.

These immunological adjustments that take place between the mother and the foetus carrying non-self paternal HLA antigens also serve as a source of allorecognition by maternal immune cells via mechanisms not clearly understood, leading to the generation of HLA-C-specific alloreactive antibodies. In addition to combinations of specific *HLA-C* and *KIR* genes, the cross-over of maternally-produced foetal HLA-C-specific alloantibodies pose a great risk of foetal rejection by recurrent miscarriages and preeclampsia (Hiby et al., 2004; Meuleman et al., 2016). This principle can also be applied to using HLA-C-specific antibodies as therapeutic agents against cancer.

As discussed in chapter V, tumour cells upregulate the expression of HLA-E and HLA-G inhibitory ligands alongside HLA-C to escape NK cell immunosurveillance. This is also observed in pregnancy to accommodate non-self foetal growth by mediating maternal tolerance. Nonetheless, HLA-C-specific antibody mediated foetal rejection demonstrates the potential of immunoregulatory maternal uterine NK cells to override other inhibitory signalling provided by the nonclassical foetal HLA Class I molecules. A similar HLA-C-specific antibody-mediated rejection effect was observed in the *in vitro* model by improving the effector function of NK cells.

7.2. Variation in alloantibody-mediated enhanced NK cell function

One major observation of this study showed that although intact HLA-C-specific alloantibodies enhanced NK cell function against target cells, this was not a dominant effect. The increase in the magnitude of NK cell cytotoxicity activity in some donors was greater than others, which did not reduce even following CD16 blockade (Figures 4.10 and 5.13). There are two possible explanations for this observed effect.

Fc receptor polymorphisms reportedly affect monoclonal antibody therapy in a range of diseases, including cancer (Binstadt et al., 2003; Mellor et al., 2013). Therefore, polymorphisms in the FcγRIII were likely responsible for the variations observed in the NK cell activity. Interestingly, FcγRIIIα does not bind IgG efficiently but amino acid substitutions of phenylalanine to valine in the Ig-like domain of the receptor demonstrate an increased affinity for IgG_1, IgG_3, and IgG_4 (Wu et al., 1997). Therefore, correlation of CD16 polymorphisms and their impact on HLA-C-specific alloantibody mediated enhanced NK cell activity can potentially explain this hypothesis.

Additionally, as it has been discussed previously (Chapters IV and V), enhanced NK cell cytotoxicity following HLA-C blockade was potentially mediated through an ADCC-independent mechanism. Fc polymorphisms may affect the binding affinity of the IgG Fc fragment to FcγRIIIα, the $F(ab')_2$ fragment of HLA-C-specific alloantibodies following IdeS-digestion would nevertheless recognise and mask the HLA-C molecule. This, in turn, would prevent HLA-C ligation to KIRs and induce NK cell activation as demonstrated by the retained ADCC-independent NK cell cytotoxicity against target cells (Figures 4.11 and 5.14). The magnitude of this effect was also variable between different NK cell donors, suggesting that perhaps KIR genotypes and NK cell education may play a role in the

range of enhanced NK cell cytotoxic activities measured in this study. The effect of ADCC-independent improved NK cell activity was further validated by the *in vitro* experiments involving Fc receptor-deficient *KIR2DL1* gene-transduced NK92 cells and IdeS-digested HLA-C-specific alloantibodies (Figures 4.14 and 5.4).

In addition to FcγRIIIα polymorphisms, antigen:antibody ratios influence the effector activity of antibodies (Pierson et al., 2007; Temming et al., 2019). An excess or shortage of antibodies are likely to disrupt the composition of immune complexes required to induce NK cell effector function. This is an important factor involving the functional experiments as the aim was to enhance NK cell function, which would also require optimal levels of antibodies to mediate FcR-crosslinking. Moreover, this factor may potentially be linked to the antibody preparations used in this study that affected retained NK cell cytotoxicity against target cells. A limitation to this study is the lack of total IgG quantification of the enriched alloantibody eluates due to the potentially low titre of antibodies in the serum and uncertainty of the eluate purity. Dose-response analyses of the enriched alloantibodies would have established an optimal antibody concentration required to drive the activation of NK cell effector activity against target cell lines and primary tumour cells. Moreover, the dose of enriched alloantibodies could have been adjusted to accommodate for the variation in ADCC-dependent and -independent NK cell responses observed with multiple donors.

7.3. Therapeutic potential of HLA-C-specific antibodies

It has been hypothesised that the selective downregulation of HLA-A and HLA-B loci allow tumour cell evasion from T cell mediated attack, whereas retaining or even upregulating HLA-C expression facilitates escape from NK cells (Demanet et al., 2004). One of the major findings of this work shows that treatment-naïve Binet stage A CLL patients present increased HLA-C expression on the $CD5^+$ $CD19^+$ tumour cell subset. Moreover, this increase in expression was a consequence of the disease. This study has shown that by masking HLA-C molecules by HLA-C-specific antibodies on target cells, including primary CLL cells led to enhanced NK cell cytotoxic function. It was undoubtedly clear that in every case, HLA-C-specific antibody bound target cells became more susceptible to lysis. Therefore, the potential of HLA-C-specific antibodies as a research tool or as a therapy cannot be ignored.

The magnitude of NK cell-mediated responses, however, is also impacted by the antigen density. Thus, the low surface expression of HLA-C may influence the efficiency of antibodies against HLA-C as a therapy. Recent studies indicate that increased HLA-C:KIR interactions in cancer lead to disease pathogenesis (described in section 1.6) and reduced tumour susceptibility to NK cell cytolysis (Pende et al., 2005; Jobim et al., 2013). In addition to the findings of the current study in a cohort of CLL patients, published reports further suggest that HLA-C expression on tumour cells is key in maintaining resistance to NK cell cytotoxicity. By extension, increased HLA-C expression on tumour cells would provide a substantial density of HLA-C antigens to induce alloantibody-mediated HLA-C:KIR blockade. Therefore, masking HLA-C molecules with human HLA-C-specific antibodies and thus preventing HLA-C and KIR ligation presents as an attractive form of therapy to restore and boost NK cell function.

With regards to the antibody specificities administered to potential patients would depend on the *HLA-C* genotype of the individuals, providing a basis for a more personalised form of antibody therapy. It is quite evident from the findings of this study that in the absence of ADCC-dependent NK cell responses, HLA-C-specific antibody treatment of target cells also led to enhanced NK cell function. Moreover, it is highly likely that HLA-C-specific alloantibodies as therapeutic agents would be administered in combination with another therapy to maximise the cytotoxic effect against tumour cells e.g. anti-CD20 rituximab treatment and patient HLA-C-specific antibody. To achieve an equally or more potent NK cell response, a dual treatment approach including HLA-C-specific antibody therapy would be required. This form of combinatorial approach involving KIR blockade is currently underway for many disease indications.

7.4. Potential adverse effects of HLA-C-specific antibodies

This study has shown that HLA-C allotype-specific antibodies can be enriched from serum based on the binding determinant at position 80 in the α1 helix of the HLA-C molecule. In contrast, lirilumab (IPH2102) the 'first-in-class' antibody for KIR blockade is a cross-reactive antibody which recognises KIR2DL1, KIR2DL2 and KIR2DL3, but lacks clinical efficacy. Comparatively, the findings of the current study have shown HLA-C-specific antibody treatment of target cells result in hyperresponsive NK cells and this increased effect is partially retained in the absence of ADCC-mediated responses.

One of the main concerns about using HLA-C-specific antibodies as a therapy involves the potential of off-target effects arising from non-specific binding. Whilst tumour cells may experience enhanced NK cell mediated cytolysis, the surrounding healthy tissue may be subject to a similar effect. As self-MHC Class I molecules are expressed ubiquitously on nucleated cells in the host, HLA-C expression is thought to be approximately 10% or less

than HLA-A and HLA-B levels (Blais et al., 2011). Therefore, it is possible that due to the ubiquitous yet low expression level, HLA-C-specific antibodies may not elicit a global adverse response in the host. Similar to HLA-C blockade, off-target effects would also arise due to KIR blockade, resulting in breaking immune tolerance to healthy cells. However, in addition to enhancing NK cell reactivity against HLA-C-expressing tumour cells, KIR blockade did not break tolerance to healthy tissue (Vahlne et al., 2010). Instead, the threshold of NK cell activation was lowered *in vitro* due to the inhibition of KIR2DL signalling. Moreover, healthy cells are unlikely to express NK cell activating ligands such as MICA, MICB and ULBP proteins which are crucial in triggering NK cell activation. Increased levels of these activating ligands are usually a sign of stress or DNA damage and most often found on virally infected or malignant cells.

Therefore, considering the generally low expression of HLA-C combined with low levels of activating NK cell ligands on healthy tissue, it is highly likely that the extent of off-target or adverse events will be limited. KIR blockade studies have shown that inhibition of KIR signalling does not result in attack on normal cells. To utilise HLA-C-specific antibodies as therapeutic agent, a screening process that identify cancer patients with high HLA-C levels on tumour cells can be implemented to maximise the efficacy of these antibodies and minimise off-target effects. Together with the presence of NK cell activating ligands, HLA-C-specific antibody therapeutic strategy would involve restoring NK cell function by harnessing the HLA-C-driven inhibitory KIR signalling to favour activation. Moreover, using HLA-C allotype-specific antibodies would offer a more personalised approach to antibody therapy, but to address concerns of adverse events and further validate the therapeutic potential of these antibodies, more extensive *in vitro* and *in vivo* studies are required.

7.5. Future directions

The work in this thesis has shown that antibodies against the HLA-C proteins that significantly enhance NK cell activation to increase target cell lines and primary tumour cell lysis. It will be in the interest of this project to consider the impact of FcγRIIIα polymorphisms that are likely to be responsible for the variable NK cell responses observed with different healthy donors and HLA-C-specific antibodies. To address this, wildtype and low/high affinity FcγRIIIα could be transduced into a single *KIR* gene expressing NK cell line. These experiments would offer a better understanding of FcγRIIIα ligation to the Fc fragments of the enriched HLA-C allotype-specific antibodies, and perhaps provide an insight into altering Fc domain interactions by introducing mutations (Jefferis, 2012) in the FcγRIIIα binding site to reduce ADCC-dependent NK cell activity. This strategy can also be used as a potential biomarker to predict the therapeutic efficacy of HLA-C-specific antibodies in different patients.

The therapeutic potential of HLA-C-specific $F(ab')_2$ fragments also require further exploration as this study has demonstrated their ability to enhance NK cell function. Therefore, the effect that HLA-C-specific $F(ab')_2$ fragments mediate via HLA-C:KIR blockade against other types of tumour cells as a monotherapeutic agent and possibly as a treatment for combinatorial antibody therapy require additional analyses.

As discussed in chapter I, the role of KIRs is important during NK cell licensing, which also contributes to the magnitude of the NK cell response to stimuli. Therefore, instead of relying on phenotype analysis to determine the KIR repertoire of NK cells from healthy donors, upon ethics approval, KIR genotyping by SSP-PCR could be performed, followed by an extensive phenotype analysis to determine the proportion of NK cells expressing

one or two and more KIR combinations. This approach would provide a more informed basis for selecting the most suitable NK cell donors for *in vitro* functional experiments.

In addition to their development as a therapy, enriched HLA-C-specific antibodies have also proved their potential as tools for research and diagnostics by investigating the HLA-C allotype expression on tumour cell lines and primary CLL cells. HLA-C1 allotype-specific antibodies were enriched using an immobilised HLA-Cw08 protein column, while HLA-C2 allotype-specific antibodies were selected using a cell line. Although the cell lines were transfected with single HLA-Cw06*02 allele, potential antibodies against other cell surface antigens were likely to have been enriched during the process. Perhaps, an immobilised HLA-C2 protein column would help minimise the risk of enriching non-specific or third-party antibodies that are likely to interfere with the *in vitro* functional investigations of these antibodies.

To avoid such confounding factors involved in enriching antibodies from serum, several attempts were made to generate HLA Class I-specific antibodies from single antigen-specific B cells. Although a variety of methods and B cell selection tools were used to identify B cells of interest, a recombinantly produced antibody specific to target antigens was not achieved. PBMCs isolated from renal transplant recipients with circulating HLA Class I-specific antibodies were sent to Professor Antonio Lanzavecchia at the IRB, Bellinzona, Switzerland in attempt to immortalise alloreactive B cells by EBV and subsequently propagate them into cell lines. However, it was not possible to establish cell lines from EBV-transformed B cells in this study, despite the detection of HLA Class I-specific antibodies in the culture supernatants. In the future, it would be in the interest of the project to repeat the B cell-EBV immortalisation experiments by using B cells from renal transplant recipients shortly after experiencing an immunising event e.g. acute rejection or a transplant, prior to immunosuppression treatment. The search for sources

with a high frequency of alloreactive B cells could be expanded to females immunised by pregnancy as circulating HLA Class I-specific memory B cells have previously been detected and analysed in multiparous females (Mulder et al., 2001, 2003). These strategies would identify more candidates positive for alloreactive B cells against a range of polymorphic HLA-C antigens.

Another area of interest for future work would be to determine the specificities of antibodies deriving from single plasmablasts. This particular part of the study holds great potential in identifying alloreactive antibodies against allograft antigens, including HLA Class I proteins. As this study is possibly the first to analyse the low affinity antibody-secreting plasmablast population following transplant nephrectomy (TN), confirming the specificities of the recombinantly generated antibodies is vital. To this end, there were plans to test the antibodies against a range of kidney endothelial cell lines and the transplant kidney biopsy tissue from the same TN patient. In addition, to characterise the plasmablast-derived antibodies, plans to test the antibodies against allogeneic kidney cell lysate and possibly K562 cell line lysate by mass spectrometry were discussed, particularly as a few antibodies demonstrated reactivity towards HLA Class I-deficient K562 cells. By performing these additional analyses to complement and build on the findings of this study would further confirm and validate the potential of antibodies against HLA-C as therapeutic and research and diagnostic agents.

CONCLUSIONS

In this study, HLA-C-specific antibodies were successfully enriched from the sera of renal transplant recipients, which also recognised key polymorphic determinants on the physiological and native forms of HLA-C molecules. More importantly, the findings of this study have demonstrated that HLA-C-specific antibodies enhance NK cell-mediated responses against a range of target cell lines and primary tumour cells.

Using NK cells from healthy donors with specific inhibitory KIR repertoires, functional analyses investigating the role of antibodies against HLA-C in enhancing NK cell activity confirmed that HLA-C:KIR blockade increased the lysis of HLA-C allele-transfected K562 cells. The same cytolytic effect was observed with B cells enriched from HLA-C1/C1 and HLA-C2/C2 homozygous B-CLL patients with increased surface HLA-C expression on the tumour cell subset. To elucidate the potential mechanism of actions involved in HLA-C-specific antibody-mediated NK cell responses, CD16 blockade on NK cells and antibody Fc fragment digestion revealed ADCC-dependent and -independent enhanced NK cell activity which were conditional to the different HLA-C-specific antibody preparations. In the absence of ADCC, the direct inhibition of HLA-C:KIR engagement implied that the lack of inhibitory KIR signalling led to the dynamic balance of signals within an NK cell to favour activation. ADCC-independent NK cell cytotoxicity against HLA-C allele-transfected K562 cells and solid tumour cell line was further confirmed by using FcγRIIIα-deficient KIR2DL1-expressing NK92 cells as effector cells.

HLA-specific memory B cells were identified and isolated from renal transplant recipients using HLA Class I-specific tetramers and single HLA antigen coated beads. Attempts at immortalising B cells using EBV led to the detection of alloreactive HLA Class I-specific antibodies, confirming the presence of circulating HLA-alloreactive memory B cells. The alloreactive antibody repertoire during an active immune response was analysed by generating recombinant antibodies from single plasmablasts. To determine the antibody specificities, additional experiments are required.

Collectively, the findings of the current study provide an encouraging insight into human HLA-C-specific antibodies potentially as another form of immune checkpoint blockade therapeutics that target NK cell immune responses. Going forward, future studies will aim to identify HLA Class I-specific antibody secreting B cells to generate recombinant antibodies as well as enrich for antibodies that are specific to the different HLA-C allotypes from the sera of sensitised individuals. Thus, the HLA-C and KIR relationship can be further interrogated by these antibodies to ultimately modulate and harness NK cell activity against cancer.

BIBLIOGRAPHY

Abbas, A.K., Lichtman, A.H., Pillai, S., et al. (2015) Basic immunology : functions and disorders of the immune system. 5th ed.

Van Acker, H.H., Capsomidis, A., Smits, E.L., et al. (2017) CD56 in the immune system: More than a marker for cytotoxicity? Frontiers in Immunology. 8 (JUL) p. 892. doi:10.3389/fimmu.2017.00892. Actor, J.K. (2014) "A Functional Overview of the Immune System and Immune Components." In Introductory Immunology. Elsevier. pp. 1–15. doi:10.1016/b978-0-12-420030-2.00001-9.

Afzali, B., Lombardi, G. and Lechler, R.I. (2008) Pathways of major histocompatibility complex allorecognition. Current Opinion in Organ Transplantation, 13 (4): 438–444. doi:10.1097/MOT.0b013e328309ee31.

Akira, S., Uematsu, S. and Takeuchi, O. (2006) Pathogen recognition and innate immunity. Cell. 124 (4) pp. 783–801. doi:10.1016/j.cell.2006.02.015.

Akkaya, M., Kwak, K. and Pierce, S.K. (2020) B cell memory: building two walls of protection against pathogens. Nature Reviews Immunology. 20 (4) pp. 229–238. doi:10.1038/s41577-019-0244-2.

Albrechtsen, D., Jervell, J., Solheim, B.G., et al. (1978) Significance of Hla-D/Dr Matching in Renal Transplantation. The Lancet, 312 (8100): 1126–1127. doi:10.1016/S0140-6736(78)92278-X.

Alegre, E., Rizzo, R., Bortolotti, D., et al. (2014) Some basic aspects of HLA-G biology. Journal of Immunology Research, 2014. doi:10.1155/2014/657625.

Almeida, C.R., Ashkenazi, A., Shahaf, G., et al. (2011) Human NK cells differ more in their KIR2DL1-dependent thresholds for HLA-Cw6-mediated inhibition than in their maximal killing capacity Zimmer, J. (ed.). PLoS ONE, 6 (9): e24927. doi:10.1371/journal.pone.0024927.

Alter, G., Malenfant, J.M. and Altfeld, M. (2004) CD107a as a functional marker for the identification of natural killer cell activity. Journal of Immunological Methods, 294 (1–2): 15–22. doi:10.1016/j.jim.2004.08.008.

Andersson, S., Fauriat, C., Malmberg, J.A., et al. (2009) KIR acquisition probabilities are independent of self-HLA class I ligands and increase with cellular KIR expression. Blood, 114 (1): 95–104. doi:10.1182/blood-2008-10-184549.

André, P., Denis, C., Soulas, C., et al. (2018) Anti-NKG2A mAb Is a Checkpoint Inhibitor that Promotes Anti-tumor Immunity by Unleashing Both T and NK Cells. Cell, 175 (7): 1731-1743.e13. doi:10.1016/j.cell.2018.10.014.

Anegón, I., Cuturi, M.C., Trinchieri, G., et al. (1988) Interaction of Fc receptor (CD16) ligands induces transcription of interleukin 2 receptor (CD25) and lymphokine genes and expression of their products in human natural killer cells. Journal of Experimental Medicine, 167 (2): 452–472. doi:10.1084/jem.167.2.452.

Anfossi, N., André, P., Guia, S., et al. (2006) Human NK Cell Education by Inhibitory Receptors for MHC Class I. Immunity, 25 (2): 331–342. doi:10.1016/j.immuni.2006.06.013.

Anfossi, N., Doisne, J.-M., Peyrat, M.-A., et al. (2004) Coordinated Expression of Ig-Like Inhibitory MHC Class I Receptors and Acquisition of Cytotoxic Function in Human CD8 + T Cells . The Journal of Immunology, 173 (12): 7223–7229. doi:10.4049/jimmunol.173.12.7223.

Antony Nolan Research Institute (n.d.) HLA Nomenclature @ hla.alleles.org. Available at: http://hla.alleles.org/nomenclature/naming.html (Accessed: 23 May 2020).

Apps, R., Meng, Z., Del Prete, G.Q., et al. (2015) Relative Expression Levels of the HLA Class-I Proteins in Normal and HIV-Infected Cells. The Journal of Immunology, 194 (8): 3594–3600. doi:10.4049/jimmunol.1403234.

Apps, R., Murphy, S.P., Fernando, R., et al. (2009) Human leucocyte antigen (HLA) expression of primary trophoblast cells and placental cell lines, determined using single antigen beads to characterize allotype specificities of anti-HLA antibodies. Immunology, 127 (1): 26–39. doi:10.1111/j.1365-2567.2008.03019.x.

Augusto, D.G. (2016) The impact of KIR polymorphism on the risk of developing cancer: Not as strong as imagined? Frontiers in Genetics, 7 (JUN): 121. doi:10.3389/fgene.2016.00121.

Bachelet, T., Couzi, L., Guidicelli, G., et al. (2011) Anti-Cw donor-specific alloantibodies can lead to positive flow cytometry crossmatch and irreversible acute antibody-mediated rejection. American Journal of Transplantation, 11 (7): 1543–1544. doi:10.1111/j.1600-6143.2011.03584.x.

Baker, M. (2005) Upping the ante on antibodies. Available at: http://www.nature.com/naturebiotechnology (Accessed: 3 July 2020).

Balan, V., Ruppert, K., Demetris, A.J., et al. (2008) Long-term outcome of human leukocyte antigen mismatching in liver transplantation: Results of the National institute of diabetes and digestive and kidney diseases liver transplantation database. Hepatology, 48 (3): 878–888. doi:10.1002/hep.22435.

Ball, S. and Dallman, M. (2014) Kidney Transplantation–Principles and Practice. Chapter 2 - Immunology of Graft Rejection. Seventh. Morris, P.J. and Knechtle, S.J. (eds.). Available at: https://doi.org/10.1016/B978-1-4557-4096-3.00002-7.

Barber, L.D., Percival, L., Valiante, N.M., et al. (1996) The inter-locus recombinant HLA-B*4601 has high selectivity in peptide binding and functions characteristic of HLA-C. Journal of Experimental Medicine, 184 (2): 735–740. doi:10.1084/jem.184.2.735.

Barbié, V. and Lefranc, M.P. (1998) The human Immunoglobulin Kappa Variable (IGKV) Genes and Joining (IGKJ) Segments. Experimental and Clinical Immunogenetics, 15 (3): 171–183. doi:10.1159/000019068.

Barnardo, M.C.N.M., Harmer, A.W., Shaw, O.J., et al. (2000) Detection of HLA-specific IGG antibodies using single recombinant HLA alleles: The monoLISA assay. Transplantation, 70 (3): 531–536. doi:10.1097/00007890-200008150-00023.

Beck, A., Goetsch, L., Dumontet, C., et al. (2017) Strategies and challenges for the next generation of antibody–drug conjugates. doi:10.1038/nrd.2016.268.

Beck, S. and Trowsdale, J. (2000) The Human Major Histocompatibility Complex : Lessons from the DNA Sequence . Annual Review of Genomics and Human Genetics, 1 (1): 117–137. doi:10.1146/annurev.genom.1.1.117.

Becker, S., Kiessling, R., Lee, N., et al. (1978) Modulation of Sensitivity to Natural Killer Cell Lysis After in Vitro Explantation of a Mouse Lymphoma - PubMed. Journal of the National Cancer Institute, 61 (6): 1495–1498.

Beers, S.A., Glennie, M.J. and White, A.L. (2016) Influence of immunoglobulin isotype on therapeutic antibody function. Blood, 127 (9): 1097–1101. doi:10.1182/blood-2015-09-625343.

Benson, D.M., Bakan, C.E., Zhang, S., et al. (2011) IPH2101, a novel anti-inhibitory KIR antibody, and lenalidomide combine to enhance the natural killer cell versus multiple myeloma effect. Blood, 118 (24): 6387–6391. doi:10.1182/blood-2011-06-360255.

Benson, D.M. and Caligiuri, M.A. (2014) Killer immunoglobulin-like receptors and tumor immunity. Cancer immunology research. 2 (2) pp. 99–104. doi:10.1158/2326-6066.CIR-13-0219.

Benson, D.M., Cohen, A.D., Jagannath, S., et al. (2015) A phase I trial of the anti-KIR antibody IPH2101 and lenalidomide in patients with relapsed/refractory multiple myeloma. Clinical Cancer Research, 21 (18): 4055–4061. doi:10.1158/1078-0432.CCR-15-0304.

Bergholtz, B.O. and Thorsby, E. (1977) Macrophage-Dependent Response of Immune Human T Lymphocytes to PPD In Vitro Influence of HLA-D Histocompatibility. Scandinavian Journal of Immunology, 6 (8): 779–786. doi:10.1111/j.1365-3083.1977.tb02151.x.

Bernard Amos, D. (1991) Fundamental antigens of HLA. Human Immunology, 30 (4): 236–246. doi:10.1016/0198-8859(91)90002-Q.

Bernasconi, N.L., Traggiai, E. and Lanzavecchia, A. (2002) Maintenance of serological memory by polyclonal activation of human memory B cells. Science, 298 (5601): 2199–2202. doi:10.1126/science.1076071.

Bhat, N.M., Teng, N.N.H., Bieber, M.M., et al. (1992) The ontogeny and functional characteristics of human b-1 (Cd5 + b) cells. International Immunology, 4 (2): 243–252. doi:10.1093/intimm/4.2.243.

Biassoni, R., Falco, M., Cambiaggi, A., et al. (1995) Amino acid substitutions can influence the natural killer (nk)-mediated recognition of hla-c molecules. role of serine-77 and lysine-80 in the target cell protection from lysis mediated by “group 2” or “group 1” nk clones. Journal of Experimental Medicine, 182 (2): 605–609. doi:10.1084/jem.182.2.605.

Biassoni, R., Pessino, A., Malaspina, A., et al. (1997) Role of amino acid position 70 in the binding affinity of p50.1 and p58.1 receptors for HLA-Cw4 molecules. European Journal of Immunology, 27 (12): 3095–3099. doi:10.1002/eji.1830271203.

Binstadt, B.A., Geha, R.S. and Bonilla, F.A. (2003) IgG Fc receptor polymorphisms in human disease: Implications for intravenous immunoglobulin therapy. Journal of Allergy and Clinical Immunology. 111 (4) pp. 697–703. doi:10.1067/mai.2003.1380.

Binyamin, L., Alpaugh, R.K., Hughes, T.L., et al. (2008) Blocking NK Cell Inhibitory Self-Recognition Promotes Antibody-Dependent Cellular Cytotoxicity in a Model of Anti-Lymphoma Therapy. The Journal of Immunology, 180 (9): 6392–6401. doi:10.4049/jimmunol.180.9.6392.

Birrer, M.J., Moore, K.N., Betella, I., et al. (2019) Antibody-Drug Conjugate-Based Therapeutics: State of the Science. Journal of the National Cancer Institute, 111 (6): 538–549. doi:10.1093/jnci/djz035.

Bjorkman, P.J., Saper, M.A., Samraoui, B., et al. (1987a) Structure of the human class I histocompatibility antigen, HLA-A2. Nature, 329 (6139): 506–512. doi:10.1038/329506a0.

Bjorkman, P.J., Saper, M.A., Samraoui, B., et al. (1987b) The foreign antigen binding site and T cell recognition regions of class I histocompatibility antigens. Nature, 329 (6139): 512–518. doi:10.1038/329512a0.

Blackwell, J.M., Jamieson, S.E. and Burgner, D. (2009) HLA and infectious diseases. Clinical Microbiology Reviews. 22 (2) pp. 370–385. doi:10.1128/CMR.00048-08.

Blais, M.E., Dong, T. and Rowland-Jones, S. (2011) HLA-C as a mediator of natural killer and T-cell activation: Spectator or key player? Immunology. 133 (1) pp. 1–7. doi:10.1111/j.1365-2567.2011.03422.x.

Bléry, M., Delon, J., Trautmann, A., et al. (1997) Reconstituted killer cell inhibitory receptors for major histocompatibility complex class I molecules control mast cell activation induced via immunoreceptor tyrosine-based activation motifs. Journal of Biological Chemistry, 272 (14): 8989–8996. doi:10.1074/jbc.272.14.8989.

Blokhuis, J.H., Hilton, H.G., Guethlein, L.A., et al. (2017) KIR2DS5 allotypes that recognize the C2 epitope of HLA-C are common among Africans and absent from Europeans. Immunity Inflammation and Disease, 5 (4): 461–468. doi:10.1002/iid3.178.

Boegel, S., Löwer, M., Bukur, T., et al. (2014) A catalog of HLA type, HLA expression, and neoepitope candidates in human cancer cell lines. OncoImmunology, 3 (8): e954893. doi:10.4161/21624011.2014.954893.

Bonilla, F.A. and Oettgen, H.C. (2010) Adaptive immunity. Journal of Allergy and Clinical Immunology, 125 (2 SUPPL. 2): S33–S40. doi:10.1016/j.jaci.2009.09.017.

Bonneville, M., Moreau, J.F., Blokland, E., et al. (1988) T lymphocyte cloning from rejected human kidney allograft. Recognition repertoire of alloreactive T cell clones. Journal of immunology (Baltimore, Md. : 1950), 141 (12): 4187–95.

Borgerding, A., Hasenkamp, J., Engelke, M., et al. (2010) B-lymphoma cells escape rituximab-triggered elimination by NK cells through increased HLA class I expression. Experimental Hematology, 38 (3): 213–221. doi:10.1016/j.exphem.2009.12.007.

Borrego, F. (2006) The First Molecular Basis of the "Missing Self" Hypothesis. The Journal of Immunology, 177 (9): 5759–5760. doi:10.4049/jimmunol.177.9.5759.

Borrego, F., Masilamani, M., Kabat, J., et al. (2005) The cell biology of the human natural killer cell CD94/NKG2A inhibitory receptor. Molecular Immunology. 42 (4 SPEC. ISS.) pp. 485–488. doi:10.1016/j.molimm.2004.07.031.

Bosch, A., Llorente, S., Eguia, J., et al. (2014) HLA-C antibodies are associated with irreversible rejection in kidney transplantation: Shared molecular eplets characterization. Human Immunology, 75 (4): 338–341. doi:10.1016/j.humimm.2014.01.010.

Bottino, C., Vitale, M., Pende, D., et al. (1995) Receptors for hla class i molecules in human nk cells. Seminars in Immunology, 7 (2): 67–73. doi:10.1006/smim.1995.0010.

Boudreau, J.E. and Hsu, K.C. (2018a) Natural Killer Cell Education and the Response to Infection and Cancer Therapy: Stay Tuned. Trends in Immunology. 39 (3) pp. 222–239. doi:10.1016/j.it.2017.12.001.

Boudreau, J.E. and Hsu, K.C. (2018b) Natural killer cell education in human health and disease. Current Opinion in Immunology. 50 pp. 102–111. doi:10.1016/j.coi.2017.11.003.

Boudreau, J.E., Liu, X.R., Zhao, Z., et al. (2016) Cell-Extrinsic MHC Class I Molecule Engagement Augments Human NK Cell Education Programmed by Cell-Intrinsic MHC Class I. Immunity, 45 (2): 280–291. doi:10.1016/j.immuni.2016.07.005.

Le Bouteiller, P., Barakonyi, A., Giustiniani, J., et al. (2002) Engagement of CD160 receptor by HLA-C is a triggering mechanism used by circulating natural killer (NK) cells to mediate cytotoxicity. Proceedings of the National Academy of Sciences of the United States of America, 99 (26): 16963–16968. doi:10.1073/pnas.012681099.

Boyington, J.C., Motykat, S.A., Schuckt, P., et al. (2000) Crystal structure of an NK cell immunoglobulin-like receptor in complex with its class I MHC ligand. Nature, 405 (6786): 537–543. doi:10.1038/35014520.

Boyington, J.C. and Sun, P.D. (2002) A structural perspective on MHC class I recognition by killer cell immunoglobulin-like receptors. doi:10.1016/S0161-5890(02)00030-5.

Braud, V.M., Allan, D.S.J., O'Callaghan, C.A., et al. (1998a) HLA-E binds to natural killer cell receptors CD94/NKG2A, B and C. Nature, 391 (6669): 795–799. doi:10.1038/35869.

Braud, V.M., Allan, D.S.J., Wilson, D., et al. (1998b) TAP- and tapasin-dependent HLA-E surface expression correlates with the binding of an MHC class I leader peptide. Current Biology, 8 (1): 1–10. doi:10.1016/S0960-9822(98)70014-4.

Bräuninger, A., Goossens, T., Rajewsky, K., et al. (2001) Regulation of immunoglobulin light chain gene rearrangements during early B cell development in the human. European Journal of Immunology, 31 (12): 3631–3637.

Brodin, P., Kärre, K. and Höglund, P. (2009a) NK cell education: not an on-off switch but a tunable rheostat. Trends in Immunology, 30 (4): 143–149. doi:10.1016/j.it.2009.01.006.

Brodin, P., Lakshmikanth, T., Johansson, S., et al. (2009b) The strength of inhibitory input during education quantitatively tunes the functional responsiveness of individual natural killer cells. Blood, 113 (11): 2434–2441. doi:10.1182/blood-2008-05-156836.

Brouwer, R.E., Van Der Heiden, P., Schreuder, G.M.T., et al. (2002) Loss or downregulation of HLA class I expression at the allelic level in acute leukemia is infrequent but functionally relevant, and can be restored by interferon. Human Immunology, 63 (3): 200–210. doi:10.1016/S0198-8859(01)00381-0.

Brown, J.H., Jardetzky, T.S., Gorga, J.C., et al. (1993) Three-dimensional structure of the human class II histocompatibility antigen HLA-DR1. Nature, 364 (6432): 33–39. doi:10.1038/364033a0.

Bryceson, Y.T., March, M.E., Ljunggren, H.G., et al. (2006) Activation, coactivation, and costimulation of resting human natural killer cells. Immunological Reviews. 214 (1) pp. 73–91. doi:10.1111/j.1600-065X.2006.00457.x.

Burshtyn, D.N., Scharenberg, A.M., Wagtmann, N., et al. (1996) Recruitment of tyrosine phosphatase HCP by the killer cell inhibitory receptor. Immunity, 4 (1): 77–85. doi:10.1016/S1074-7613(00)80300-3.

Burton, D.R., Williamson, R.A. and Parren, P.W.H.I. (2000) Antibody and virus: Binding and neutralization. Virology, 270 (1): 1–3. doi:10.1006/viro.2000.0239.

Cai, J., Terasaki, P.I., Anderson, N., et al. (2009) Intact HLA not β2m-free heavy chain-specific HLA class I antibodies are predictive of graft failure. Transplantation, 88 (2): 226–230. doi:10.1097/TP.0b013e3181ac6198.

Campbell, K.S. and Purdy, A.K. (2011) Structure/function of human killer cell immunoglobulin-like receptors: Lessons from polymorphisms, evolution, crystal structures and mutations. Immunology. 132 (3) pp. 315–325. doi:10.1111/j.1365-2567.2010.03398.x.

Campillo, J.A., Legaz, I., López-Álvarez, M.R., et al. (2013) KIR gene variability in cutaneous malignant melanoma: Influence of KIR2D/HLA-C pairings on disease susceptibility and prognosis. Immunogenetics, 65 (5): 333–343. doi:10.1007/s00251-013-0682-0.

Cao, Y., Gordic, M., Kobold, S., et al. (2010) An optimized assay for the enumeration of antigen-specific memory B cells in different compartments of the human body. Journal of Immunological Methods, 358 (1–2): 56–65. doi:10.1016/j.jim.2010.03.009.

Capuano, C., Romanelli, M., Pighi, C., et al. (2015) Anti-CD20 therapy acts via FcγRIIIA to diminish responsiveness of human natural killer cells. Cancer Research, 75 (19): 4097–4108. doi:10.1158/0008-5472.CAN-15-0781.

Cardarelli, F., Pascual, M., Tolkoff-Rubin, N., et al. (2005) Prevalence and significance of anti-HLA and donor-specific antibodies long-term after renal transplantation. Transplant International, 18 (5): 532–540. doi:10.1111/j.1432-2277.2005.00085.x.

Carlsten, M., Korde, N., Kotecha, R., et al. (2016) Checkpoint inhibition of KIR2D with the monoclonal antibody IPH2101 induces contraction and hyporesponsiveness of NK cells in patients with myeloma. Clinical Cancer Research, 22 (21): 5211–5222. doi:10.1158/1078-0432.CCR-16-1108.

Cassatella, M.A., Anegon, I., Cuturi, M.C., et al. (1989) FcγR(CD16) interaction with ligand induces Ca2+ mobilization and phosphoinositide turnover in human natural killer cells. Role of Ca2+ in FcγR(CD16)-induced transcription and expression of lymphokine genes. Journal of Experimental Medicine, 169 (2): 549–567. doi:10.1084/jem.169.2.549.

Cella, M., Longo, A., Ferrara, G.B., et al. (1994) NK3-specific natural killer cells are selectively inhibited by Bw4-positive HLA alleles with isoleucine 80. Journal of Experimental Medicine, 180 (4): 1235–1242. doi:10.1084/jem.180.4.1235.

Cerwenka, A., Baron, J.L. and Lanier, L.L. (2001) Ectopic expression of retinoic acid early inducible-1 gene (RAE-1) permits natural killer cell-mediated rejection of a MHC class I-bearing tumor in vivo. Proceedings of the National Academy of Sciences of the United States of America, 98 (20): 11521–11526. doi:10.1073/pnas.201238598.

Chacko, M.P., Augustin, A., David, V.G., et al. (2016) Nonspecific positivity on the Luminex crossmatch assay for anti-human leukocyte antigen antibodies due to antibodies directed against the antibody coated beads. Indian Journal of Nephrology, 26 (2): 134–137. doi:10.4103/0971-4065.159305.

Chan, C.J., Smyth, M.J. and Martinet, L. (2014) Molecular mechanisms of natural killer cell activation in response to cellular stress. Cell Death and Differentiation, 21 (1): 5–14. doi:10.1038/cdd.2013.26.

Chang, C.C., Pirozzi, G., Wen, S.H., et al. (2015) Multiple structural and epigenetic defects in the human leukocyte antigen class I antigen presentation pathway in a recurrent metastatic melanoma

following immunotherapy. Journal of Biological Chemistry, 290 (44): 26562–26575. doi:10.1074/jbc.M115.676130.

Chapman, J.R., Taylor, C., Ting, A., et al. (1986) Hyperacute rejection of a renal allograft in the presence of anti–hla–cw5 antibody. Transplantation, 42 (1): 91–93. doi:10.1097/00007890-198607000-00022.

Chess, A. (1998) Expansion of the allelic exclusion principle? Science. 279 (5359) pp. 2067–2068. doi:10.1126/science.279.5359.2067.

Cheung, W.C., Beausoleil, S.A., Zhang, X., et al. (2012) A proteomics approach for the identification and cloning of monoclonal antibodies from serum. Nature Biotechnology. 30 (5) pp. 447–452. doi:10.1038/nbt.2167.

Choo, S.Y. (2007) The HLA system: Genetics, immunology, clinical testing, and clinical implications. Yonsei Medical Journal, 48 (1): 11–23. doi:10.3349/ymj.2007.48.1.11.

Ciccone, E., Pende, D., Viale, O., et al. (1992) Involvement of HLA Class I Alleles in Natural Killer (NK) Cell-specific Functions: Expression of HLA-Cw3 Confers Selective Protection from Lysis by Alloreactive NK Clones Displaying a Defined Specificity (Specificity 2). Journal of Experimental Medicine, 176 (4): 963–971. doi:10.1084/jem.176.4.963.

Ciccone, E., Pende, D., Vitale, M., et al. (1994) Self class I molecules protect normal cells from lysis mediated by autologous natural killer cells. European Journal of Immunology, 24 (4): 1003–1006. doi:10.1002/eji.1830240434.

Claas, F.H.J., Roelen, D.L., Mulder, A., et al. (2006) Differential Immunogenicity of HLA Class I Alloantigens for the Humoral versus the Cellular Immune Response: “Towards Tailor-Made HLA Mismatching.” Human Immunology. 67 (6) pp. 424–429. doi:10.1016/j.humimm.2006.03.004.

Classen, C.F., Falk, C.S., Friesen, C., et al. (2003) Natural killer resistance of a drug-resistant leukemia cell line, mediated by up-regulation of HLA class I expression. Haematologica, 88 (5): 509–521.

Clatworthy, M.R., Espeli, M., Torpey, N., et al. (2010) The generation and maintenance of serum alloantibody. Current Opinion in Immunology. 22 (5) pp. 669–681. doi:10.1016/j.coi.2010.08.018.

Cohn, M. (2004) If the “adaptive” immune system can recognize a significant portion of the pathogenic universe to which the “innate” immune system is blind, then. . . Scandinavian Journal of Immunology. 60 (1) pp. 1–2. doi:10.1111/j.0300-9475.2004.01449.x.

Collins, A.M. and Watson, C.T. (2018) Immunoglobulin light chain gene rearrangements, receptor editing and the development of a self-tolerant antibody repertoire. Frontiers in Immunology. 9 (OCT) p. 2249. doi:10.3389/fimmu.2018.02249.

Colonna, M., Borsellino, G., Falco, M., et al. (1993a) HLA-C is the inhibitory ligand that determines dominant resistance to lysis by NK1- and NK2-specific natural killer cells. Proceedings of the National Academy of Sciences of the United States of America, 90 (24): 12000–12004. doi:10.1073/pnas.90.24.12000.

Colonna, M., Borsellino, G., Falco, M., et al. (1993b) HLA-C is the inhibitory ligand that determines dominant resistance to lysis by NK1- and NK2-specific natural killer cells. Proceedings of the National Academy of Sciences of the United States of America, 90 (24): 12000–12004. doi:10.1073/pnas.90.24.12000.

Cook, M.A., Milligan, D.W., Fegan, C.D., et al. (2004) The impact of donor KIR and patient HLA-C genotypes on outcome following HLA-identical sibling hematopoietic stem cell transplantation for myeloid leukemia. Blood, 103 (4): 1521–1526. doi:10.1182/blood-2003-02-0438.

Cooper, M.A., Fehniger, T.A. and Caligiuri, M.A. (2001a) The biology of human natural killer-cell subsets. Trends in Immunology. 22 (11) pp. 633–640. doi:10.1016/S1471-4906(01)02060-9.

Cooper, M.A., Fehniger, T.A., Turner, S.C., et al. (2001b) Human natural killer cells: A unique innate immunoregulatory role for the CD56bright subset. Blood, 97 (10): 3146–3151. doi:10.1182/blood.V97.10.3146.

Corti, D. and Lanzavecchia, A. (2014) Efficient Methods To Isolate Human Monoclonal Antibodies from Memory B Cells and Plasma Cells. Microbiology Spectrum, 2 (5). doi:10.1128/microbiolspec.aid-0018-2014.

Costello, R.T., Knoblauch, B., Sanchez, C., et al. (2012) Expression of natural killer cell activating receptors in patients with chronic lymphocytic leukaemia. Immunology, 135 (2): 151–157. doi:10.1111/j.1365-2567.2011.03521.x.

Croce, C.M., Shander, M., Martinis, J., et al. (1979) Chromosomal location of the genes for human immunoglobulin heavy chains. Proceedings of the National Academy of Sciences of the United States of America, 76 (7): 3416–3419. doi:10.1073/pnas.76.7.3416.

Crotty, S. and Ahmed, R. (2004) Immunological memory in humans. Seminars in Immunology, 16 (3): 197–203. doi:10.1016/j.smim.2004.02.008.

Crotty, S., Aubert, R.D., Glidewell, J., et al. (2004) Tracking human antigen-specific memory B cells: A sensitive and generalized ELISPOT system. Journal of Immunological Methods, 286 (1–2): 111–122. doi:10.1016/j.jim.2003.12.015.

Curry, A.J., Pettigrew, G.J., Negus, M.C., et al. (2007) Dendritic cells internalise and re-present conformationally intact soluble MHC class I alloantigen for generation of alloantibody. European Journal of Immunology, 37 (3): 696–705. doi:10.1002/eji.200636543.

Cyster, J.G., Ansel, K.M., Reif, K., et al. (2000) Follicular stromal cells and lymphocyte homing to follicles. Immunological Reviews. 176 pp. 181–193. doi:10.1034/j.1600-065X.2000.00618.x.

Czaja, K., Borer, A.S., Schmied, L., et al. (2014) A comprehensive analysis of the binding of anti-KIR antibodies to activating KIRs. Genes and Immunity, 15 (1): 33–37. doi:10.1038/gene.2013.58.

D'Andrea, A., Chang, C., Franz-Bacon, K., et al. (1995) Molecular cloning of NKB1. A natural killer cell receptor for HLA-B allotypes. Journal of immunology (Baltimore, Md.: 1950), 155 (5): 2306–10.

D'Orsogna, L.J.A., Van Besouw, N.M., Van Der Meer-Prins, E.M.W., et al. (2011) Vaccine-induced allo-hla-reactive memory T cells in a kidney transplantation candidate. Transplantation, 91 (6): 645–651. doi:10.1097/TP.0b013e318208c071.

Damle, R.N., Ghiotto, F., Valetto, A., et al. (2002) B-cell chronic lymphocytic leukemia cells express a surface membrane phenotype of activated, antigen-experienced B lymphocytes. Blood, 99 (11): 4087–4093. doi:10.1182/blood.V99.11.4087.

Daniel, C., Horvath, S. and Allen, P.M. (1998) A basis for alloreactivity: MHC helical residues broaden peptide recognition by the TCR. Immunity, 8 (5): 543–552. doi:10.1016/S1074-7613(00)80559-2.

David, G., Morvan, M., Gagne, K., et al. (2009) Discrimination between the main activating and inhibitory killer cell immunoglobulin-like receptor positive natural killer cell subsets using newly characterized monoclonal antibodies. Immunology, 128 (2): 172–184. doi:10.1111/j.1365-2567.2009.03085.x.

Deeg, H.J., Koene, H.R., Kleijer, M., et al. (1997) Fc gammaRIIIa-158V/F polymorphism influences the binding of IgG by natural killer cell Fc gammaRIIIa, independently of the Fc gammaRIIIa-48L/R/H phenotype. Blood, 90 (3): 1109–1114. doi:10.1182/blood.v90.3.1109.1109_1109_1114.

Degauque, N., Ngono, A.E., Akl, A., et al. (2013) Characterization of antigen-specific B cells using nominal antigen-coated flow-beads. PLoS ONE, 8 (12). doi:10.1371/journal.pone.0084273.

Dekosky, B.J., Ippolito, G.C., Deschner, R.P., et al. (2013) High-throughput sequencing of the paired human immunoglobulin heavy and light chain repertoire. Nature Biotechnology, 31 (2): 166–169. doi:10.1038/nbt.2492.

DeKosky, B.J., Kojima, T., Rodin, A., et al. (2015) In-depth determination and analysis of the human paired heavy- and light-chain antibody repertoire. Nature Medicine, 21 (1): 86–91. doi:10.1038/nm.3743.

Delves, P.J. and Roitt, I.M. (2000) The immune system. First of two parts. New England Journal of Medicine. 343 (1) pp. 37–49. doi:10.1056/NEJM200007063430107.

Demanet, C., Mulder, A., Deneys, V., et al. (2004) Down-regulation of HLA-A and HLA-Bw6, but not HLA-Bw4, allospecificities in leukemic cells: An escape mechanism from CTL and NK attack? Blood, 103 (8): 3122–3130. doi:10.1182/blood-2003-07-2500.

Dendrou, C.A., Petersen, J., Rossjohn, J., et al. (2018) HLA variation and disease. Nature Reviews Immunology. 18 (5) pp. 325–339. doi:10.1038/nri.2017.143.

Diefenbach, A. and Raulet, D.H. (1999) Natural killer cells: Stress out, turn on, tune in. Current Biology, 9 (22): R851–R853. doi:10.1016/s0960-9822(00)80044-5.

Diefenbach, A. and Raulet, D.H. (2003) Innate immune recognition by stimulatory immunoreceptors. Current Opinion in Immunology. 15 (1) pp. 37–44. doi:10.1016/S0952-7915(02)00007-9.

Dorak, M.T. (2002) Basic Immunology: Functions and Disorders of the Immune System. doi:10.1093/aje/155.2.185-a.

Dranoff, G. (2004) Cytokines in cancer pathogenesis and cancer therapy. Nature Reviews Cancer. 4 (1) pp. 11–22. doi:10.1038/nrc1252.

Drukker, M., Katz, G., Urbach, A., et al. (2002) Characterization of the expression of MHC proteins in human embryonic stem cells. Proceedings of the National Academy of Sciences of the United States of America, 99 (15): 9864–9869. doi:10.1073/pnas.142298299.

Dulberger, C.L., McMurtrey, C.P., Hölzemer, A., et al. (2017) Human Leukocyte Antigen F Presents Peptides and Regulates Immunity through Interactions with NK Cell Receptors. Immunity, 46 (6): 1018-1029.e7. doi:10.1016/j.immuni.2017.06.002.

Edelman, G.M. and Gally, J.A. (1962) The nature of Bence-Jones proteins. Chemical similarities to polypetide chains of myeloma globulins and normal gamma-globulins. The Journal of experimental medicine, 116 (2): 207–227. doi:10.1084/jem.116.2.207.

El-Awar, N., Terasaki, P.I., Nguyen, A., et al. (2009) Epitopes of human leukocyte antigen class I antibodies found in sera of normal healthy males and cord blood. Human Immunology, 70 (10): 844–853. doi:10.1016/j.humimm.2009.06.020.

El-Awar, N.R., Akaza, T., Terasaki, P.I., et al. (2007) Human leukocyte antigen class I epitopes: Update to 103 total epitopes, including the C locus. Transplantation, 84 (4): 532–540. doi:10.1097/01.tp.0000278721.97037.1e.

Elgueta, R., Benson, M.J., De Vries, V.C., et al. (2009) Molecular mechanism and function of CD40/CD40L engagement in the immune system. Immunological Reviews. 229 (1) pp. 152–172. doi:10.1111/j.1600-065X.2009.00782.x.

Elgueta, R., De Vries, V.C. and Noelle, R.J. (2010) The immortality of humoral immunity. Immunological Reviews. 236 (1) pp. 139–150. doi:10.1111/j.1600-065X.2010.00924.x.

Elgundi, Z., Reslan, M., Cruz, E., et al. (2017) The state-of-play and future of antibody therapeutics. Advanced Drug Delivery Reviews, 122: 2–19. doi:10.1016/j.addr.2016.11.004.

Elliott, J.M., Wahle, J.A. and Yokoyama, W.M. (2010) MHC class I-deficient natural killer cells acquire a licensed phenotype after transfer into an MHC class I-sufficient environment. Journal of Experimental Medicine, 207 (10): 2073–2079. doi:10.1084/jem.20100986.

Erikci, A.A., Karagoz, B., Ozyurt, M., et al. (2009) HLA-G expression in B chronic lymphocytic leukemia: A new prognostic marker? Hematology, 14 (2): 101–105. doi:10.1179/102453309X385197.

Erikson, J., Martinis, J. and Croce, C.M. (1981) Assignment of the genes for human λ immunoglobulin chains to chromosome 22. Nature, 294 (5837): 173–175. doi:10.1038/294173a0.

European Bioinformatics Institute (2020) Statistics < IMGT/HLA < IPD < EMBL-EBI. Available at: https://www.ebi.ac.uk/ipd/imgt/hla/stats.html (Accessed: 25 May 2020).

Fadda, L., Borhis, G., Ahmed, P., et al. (2010) Peptide antagonism as a mechanism for NK cell activation. Proceedings of the National Academy of Sciences of the United States of America, 107 (22): 10160–10165. doi:10.1073/pnas.0913745107.

Fan, Q.R., Long, E.O. and Wiley, D.C. (2001) Crystal structure of the human natural killer cell inhibitory receptor KIR2DL1-HLA-Cw4 complex. Nature Immunology, 2 (5): 452–460. doi:10.1038/87766.

Faure, M. and Long, E.O. (2002) KIR2DL4 (CD158d), an NK Cell-Activating Receptor with Inhibitory Potential. The Journal of Immunology, 168 (12): 6208–6214. doi:10.4049/jimmunol.168.12.6208.

Fearon, D.T. and Locksley, R.M. (1996) The instructive role of innate immunity in the acquired immune response. Science, 272 (5258): 50–54. doi:10.1126/science.272.5258.50.

Fernandez, N.C., Treiner, E., Vance, R.E., et al. (2005) A subset of natural killer cells achieves self-tolerance without expressing inhibitory receptors specific for self-MHC molecules. Blood, 105 (11): 4416–4423. doi:10.1182/blood-2004-08-3156.

Foley, B., De Santis, D., Lathbury, L., et al. (2008) KIR2DS1-mediated activation overrides NKG2A-mediated inhibition in HLA-C C2-negative individuals. International Immunology, 20 (4): 555–563. doi:10.1093/intimm/dxn013.

Forrest, C., Hislop, A.D., Rickinson, A.B., et al. (2018) Proteome-wide analysis of CD8+ T cell responses to EBV reveals differences between primary and persistent infection. PLOS Pathogens, 14 (9): e1007110. doi:10.1371/journal.ppat.1007110.

Forslund, E., Sohlberg, E., Enqvist, M., et al. (2015) Microchip-Based Single-Cell Imaging Reveals That CD56 dim CD57 − KIR − NKG2A + NK Cells Have More Dynamic Migration Associated with Increased Target Cell Conjugation and Probability of Killing Compared to CD56 dim CD57 − KIR − NKG2A − NK Cells . The Journal of Immunology, 195 (7): 3374–3381.

Förster, R., Mattis, A.E., Kremmer, E., et al. (1996) A putative chemokine receptor, BLR1, directs B cell migration to defined lymphoid organs and specific anatomic compartments of the spleen. Cell, 87 (6): 1037–1047. doi:10.1016/S0092-8674(00)81798-5.

Freund-Brown, J., Chirino, L. and Kambayashi, T. (2018) Strategies to enhance NK cell function for the treatment of tumors and infections. Critical Reviews in Immunology, 38 (2): 105–130. doi:10.1615/CritRevImmunol.2018025248.

Frohn, C., Fricke, L., Puchta, J.C., et al. (2001) The effect of HLA-C matching on acute renal transplant rejection. Nephrology Dialysis Transplantation, 16 (2): 355–360. doi:10.1093/ndt/16.2.355.

Furukawa, H., Yabe, T., Watanabe, K., et al. (1999) Tolerance of NK and LAK activity for HLA class I-deficient targets in a TAP1-deficient patient (bare lymphocyte syndrome type I). Human Immunology, 60 (1): 32–40. doi:10.1016/S0198-8859(98)00097-4.

Gadol, N. and Ault, K.A. (1986) Phenotypic and Functional Characterization of Human LEUI (CD5) B Cells. Immunological Reviews, 93 (1): 23–34. doi:10.1111/j.1600-065X.1986.tb01500.x.

Galea-Lauri, J., Darling, D., Gan, S.U., et al. (1999) Expression of a variant of CD28 on a subpopulation of human NK cells: implications for B7-mediated stimulation of NK cells. Journal of immunology (Baltimore, Md. : 1950), 163 (1): 62–70.

Garcia-Beltran, W.F., Hölzemer, A., Martrus, G., et al. (2016) Open conformers of HLA-F are high-affinity ligands of the activating NK-cell receptor KIR3DS1. Nature Immunology, 17 (9): 1067–1074. doi:10.1038/ni.3513.

Garcia-Plata, D., Mozos, E., Carrasco, L., et al. (1993) HLA molecule expression in cutaneous squamous cell carcinomas: An immunopathological study and clinical-immunohistopathological correlations.

Garrido, C., Paco, L., Romero, I., et al. (2012) MHC class I molecules act as tumor suppressor genes regulating the cell cycle gene expression, invasion and intrinsic tumorigenicity of melanoma cells. Carcinogenesis, 33 (3): 687–693. doi:10.1093/carcin/bgr318.

Garrido, F., Ruiz-Cabello, F., Cabrera, T., et al. (1997) Implications for immunosurveillance of altered HLA class I phenotypes in human tumours. Immunology Today. 18 (2) pp. 89–95. doi:10.1016/S0167-5699(96)10075-X.

Gebel, H.M. and Bray, R.A. (2014) HLA antibody detection with solid phase assays: Great expectations or expectations too great? American Journal of Transplantation. 14 (9) pp. 1964–1975. doi:10.1111/ajt.12807.

Geller, A. and Yan, J. (2019) The role of membrane bound complement regulatory proteins in tumor development and cancer immunotherapy. Frontiers in Immunology. 10 (MAY). doi:10.3389/fimmu.2019.01074.

Georgiou, G., Ippolito, G.C., Beausang, J., et al. (2014) The promise and challenge of high-throughput sequencing of the antibody repertoire. Nature Biotechnology. 32 (2) pp. 158–168. doi:10.1038/nbt.2782.

Goldstein, L.D., Chen, Y.J.J., Wu, J., et al. (2019) Massively parallel single-cell B-cell receptor sequencing enables rapid discovery of diverse antigen-reactive antibodies. Communications Biology, 2 (1): 1–10. doi:10.1038/s42003-019-0551-y.

Gong, J.H., Maki, G. and Klingemann, H.G. (1994) Characterization of a human cell line (NK-92) with phenotypical and functional characteristics of activated natural killer cells. Leukemia, 8 (4): 652–658.

Goodnow, C.C., Vinuesa, C.G., Randall, K.L., et al. (2010) Control systems and decision making for antibody production. Nature Immunology. 11 (8) pp. 681–688. doi:10.1038/ni.1900.

Goodridge, J.P., Burian, A., Lee, N., et al. (2010) HLA-F Complex without Peptide Binds to MHC Class I Protein in the Open Conformer Form. The Journal of Immunology, 184 (11): 6199–6208. doi:10.4049/jimmunol.1000078.

Goodridge, J.P., Burian, A., Lee, N., et al. (2013) HLA-F and MHC Class I Open Conformers Are Ligands for NK Cell Ig-like Receptors. The Journal of Immunology, 191 (7): 3553–3562. doi:10.4049/jimmunol.1300081.

Goodridge, J.P., Jacobs, B., Saetersmoen, M.L., et al. (2019) Remodeling of secretory lysosomes during education tunes functional potential in NK cells. Nature Communications, 10 (1): 1–15. doi:10.1038/s41467-019-08384-x.

Goulmy, E., Termijtelen, A., Bradley, B.A., et al. (1977) Y-antigen killing by T cells of women is restricted by HLA [26]. Nature. 266 (5602) pp. 544–545. doi:10.1038/266544a0.

Grenzi, P.C., de Marco, R., Silva, R.Z.R., et al. (2013) Antibodies against denatured HLA class II molecules detected in luminex-single antigen assay. Human Immunology, 74 (10): 1300–1303. doi:10.1016/j.humimm.2013.06.035.

Gumperz, J.E., Litwin, V., Phillips, J.H., et al. (1995) The Bw4 public epitope of HLA-B molecules confers reactivity with natural killer cell clones that express NKB1, a putative HLA receptor. Journal of Experimental Medicine, 181 (3): 1133–1144. doi:10.1084/jem.181.3.1133.

Han, M., Rogers, J.A., Lavingia, B., et al. (2009) Peripheral blood B cells producing donor-specific HLA antibodies in vitro. Human Immunology, 70 (1): 29–34. doi:10.1016/j.humimm.2008.10.013.

Hansasuta, P., Dong, T., Thananchai, H., et al. (2004) Recognition of HLA-A3 and HLA-A11 by KIR3DL2 is peptide-specific. European Journal of Immunology, 34 (6): 1673–1679. doi:10.1002/eji.200425089.

Harding, F.A., Stickler, M.M., Razo, J., et al. (2010) The immunogenicity of humanized and fully human antibodies: Residual immunogenicity resides in the CDR regions. mAbs, 2 (3): 256–265. doi:10.4161/mabs.2.3.11641.

Heidt, S., Roelen, D.L., De Vaal, Y.J.H., et al. (2012) A novel ELISPOT assay to quantify HLA-specific B cells in HLA-immunized individuals. American Journal of Transplantation, 12 (6): 1469–1478. doi:10.1111/j.1600-6143.2011.03982.x.

Held, P.J., Kahan, B.D., Hunsicker, L.G., et al. (1994) The impact of hla mismatches on the survival of first cadaveric kidney transplants. New England Journal of Medicine, 331 (12): 765–770. doi:10.1056/NEJM199409223311203.

Held, W., Dorfman, J.R., Wu, M.F., et al. (1996) Major histocompatibility complex class I-dependent skewing of the natural killer cell Ly49 receptor repertoire. European Journal of Immunology, 26 (10): 2286–2292. doi:10.1002/eji.1830261003.

Hiby, S.E., Walker, J.J., O'Shaughnessy, K.M., et al. (2004) Combinations of maternal KIR and fetal HLA-C genes influence the risk of preeclampsia and reproductive success. Journal of Experimental Medicine, 200 (8): 957–965. doi:10.1084/jem.20041214.

Hickey, M.J., Valenzuela, N.M. and Reed, E.F. (2016) Alloantibody generation and effector function following sensitization to human leukocyte antigen. Frontiers in Immunology, 7 (FEB): 30. doi:10.3389/fimmu.2016.00030.

Hilpert, J., Grosse-Hovest, L., Grünebach, F., et al. (2012) Comprehensive Analysis of NKG2D Ligand Expression and Release in Leukemia: Implications for NKG2D-Mediated NK Cell Responses. The Journal of Immunology, 189 (3): 1360–1371. doi:10.4049/jimmunol.1200796.

Hilton, H.G., McMurtrey, C.P., Han, A.S., et al. (2017) The Intergenic Recombinant HLA-B∗46:01 Has a Distinctive Peptidome that Includes KIR2DL3 Ligands. Cell Reports, 19 (7): 1394–1405. doi:10.1016/j.celrep.2017.04.059.

Hilton, H.G. and Parham, P. (2017) Missing or altered self: human NK cell receptors that recognize HLA-C. Immunogenetics, 69 (8–9): 567–579. doi:10.1007/s00251-017-1001-y.

Hilton, H.G., Vago, L., Older Aguilar, A.M., et al. (2012) Mutation at Positively Selected Positions in the Binding Site for HLA-C Shows That KIR2DL1 Is a More Refined but Less Adaptable NK Cell Receptor Than KIR2DL3. The Journal of Immunology, 189 (3): 1418–1430.

Höffkes, H.G., Schmidtke, G., Uppenkamp, M., et al. (1996) Multiparametric immunophenotyping of B cells in peripheral blood of healthy adults by flow cytometry. Clinical and Diagnostic Laboratory Immunology, 3 (1): 30–36. doi:10.1128/cdli.3.1.30-36.1996.

Hoffman, W., Lakkis, F.G. and Chalasani, G. (2016) B cells, antibodies, and more. Clinical Journal of the American Society of Nephrology, 11 (1): 137–154. doi:10.2215/CJN.09430915.

Hofland, T., Endstra, S., Gomes, C.K.P., et al. (2019) Natural Killer Cell Hypo-responsiveness in Chronic Lymphocytic Leukemia can be Circumvented In Vitro by Adequate Activating Signaling. HemaSphere, 3 (6): e308. doi:10.1097/hs9.0000000000000308.

Hourmant, M., Cesbron-Gautier, A., Terasaki, P.I., et al. (2005) Frequency and clinical implications of development of donor-specific and non-donor-specific HLA antibodies after kidney transplantation. Journal of the American Society of Nephrology, 16 (9): 2804–2812. doi:10.1681/ASN.2004121130.

Hu, W., Wang, G., Huang, D., et al. (2019) Cancer immunotherapy based on natural killer cells: Current progress and new opportunities. Frontiers in Immunology. 10 (MAY) p. 1205. doi:10.3389/fimmu.2019.01205.

Huang, J., Doria-Rose, N.A., Longo, N.S., et al. (2013) Isolation of human monoclonal antibodies from peripheral blood B cells. Nature Protocols, 8 (10): 1907–1915. doi:10.1038/nprot.2013.117.

Huang, S., Armstrong, E.A., Benavente, S., et al. (2004) Dual-agent molecular targeting of the epidermal growth factor receptor (EGFR): Combining anti-EGFR antibody with tyrosine kinase inhibitor. Cancer Research, 64 (15): 5355–5362. doi:10.1158/0008-5472.CAN-04-0562.

Huergo-Zapico, L., Acebes-Huerta, A., Gonzalez-Rodriguez, A.P., et al. (2014) Expansion of NK cells and reduction of NKG2D expression in chronic lymphocytic leukemia.Correlation with progressive disease. PLoS ONE, 9 (10): e108326. doi:10.1371/journal.pone.0108326.

Hurley, C.K. (2020) Naming HLA diversity: A review of HLA nomenclature. Human immunology. doi:10.1016/j.humimm.2020.03.005.

Hwang, W.Y.K. and Foote, J. (2005) Immunogenicity of engineered antibodies. Methods, 36 (1): 3–10. doi:10.1016/j.ymeth.2005.01.001.

Imai, K. and Takaoka, A. (2006) Comparing antibody and small-molecule therapies for cancer. Nature Reviews Cancer. 6 (9) pp. 714–727. doi:10.1038/nrc1913.

In, J.W., Rho, E.Y., Shin, S., et al. (2014) False-positive reactions against HLA class II molecules detected in luminex single-antigen bead assays. Annals of Laboratory Medicine, 34 (5): 408–410. doi:10.3343/alm.2014.34.5.408.

Isitman, G., Tremblay-McLean, A., Lisovsky, I., et al. (2016) NK cells expressing the inhibitory killer immunoglobulin-like receptors (iKIR) KIR2DL1, KIR2DL3 and KIR3DL1 are less likely to be CD16+ than their iKIR negative counterparts Wainberg, M.A. (ed.). PLoS ONE, 11 (10): e0164517. doi:10.1371/journal.pone.0164517.

Jacobs, R., Hintzen, G., Kemper, A., et al. (2001) CD56bright cells differ in their KIR repertoire and cytotoxic features from CD56dim NK cells. European Journal of Immunology, 31 (10): 3121–3126. doi:10.1002/1521-4141(2001010)31:10<3121::AID-IMMU3121>3.0.CO;2-4.

Jain, A. and Pasare, C. (2017) Innate Control of Adaptive Immunity: Beyond the Three-Signal Paradigm. The Journal of Immunology, 198 (10): 3791–3800. doi:10.4049/jimmunol.1602000.

Janeway, C.A. (1989) “Approaching the asymptote? Evolution and revolution in immunology.” In Cold Spring Harbor Symposia on Quantitative Biology. 1989. pp. 1–13. doi:10.1101/sqb.1989.054.01.003.

Janeway, C.A. and Medzhitov, R. (2002) I Nnate I Mmune R Ecognition . Annual Review of Immunology, 20 (1): 197–216. doi:10.1146/annurev.immunol.20.083001.084359.

Jefferis, R. (2012) Isotype and glycoform selection for antibody therapeutics. Archives of Biochemistry and Biophysics. 526 (2) pp. 159–166. doi:10.1016/j.abb.2012.03.021.

Jewell, A.P., Worman, C.P., Giles, F.J., et al. (1992) Resistance of chronic lymphocytic leukaemia cells to interferon-α generated lymphokine activated killer cells. Leukemia and Lymphoma, 7 (5–6): 473–480. doi:10.3109/10428199209049804.

Jewett, A. and Bonavida, B. (1995) Interferon-α activates cytotoxic function but inhibits interleukin-2-mediated proliferation and tumor necrosis factor-α secretion by immature human natural killer cells. Journal of Clinical Immunology, 15 (1): 35–44. doi:10.1007/BF01489488.

Jin, P. and Wang, E. (2003) Polymorphism in clinical immunology - From HLA typing to immunogenetic profiling. Journal of Translational Medicine. 1 p. 8. doi:10.1186/1479-5876-1-8.

Jobim, M.R., Jobim, M., Salim, P.H., et al. (2013) Analysis of KIR gene frequencies and HLA class I genotypes in breast cancer and control group. Human Immunology, 74 (9): 1130–1133. doi:10.1016/j.humimm.2013.06.021.

Johnson, D.B., Estrada, M. V., Salgado, R., et al. (2016) Melanoma-specific MHC-II expression represents a tumour-autonomous phenotype and predicts response to anti-PD-1/PD-L1 therapy. Nature Communications, 7 (1): 1–10. doi:10.1038/ncomms10582.

Johnson, D.B., Peng, C. and Sosman, J.A. (2015) Nivolumab in melanoma: Latest evidence and clinical potential. Therapeutic Advances in Medical Oncology, 7 (2): 97–106. doi:10.1177/1758834014567469.

Jones, P.T., Dear, P.H., Foote, J., et al. (1986) Replacing the complementarity-determining regions in a human antibody with those from a mouse. Nature, 321 (6069): 522–525. doi:10.1038/321522a0.

Jonsson, A.H., Yang, L., Kim, S., et al. (2010) Effects of MHC Class I Alleles on Licensing of Ly49A + NK Cells . The Journal of Immunology, 184 (7): 3424–3432. doi:10.4049/jimmunol.0904057.

Jourdan, M., Caraux, A., De Vos, J., et al. (2009) An in vitro model of differentiation of memory B cells into plasmablasts and plasma cells including detailed phenotypic and molecular characterization. Blood, 114 (25): 5173–5181. doi:10.1182/blood-2009-07-235960.

Jucaud, V., Shaked, A., DesMarais, M., et al. (2018) The Relative Immunogenicity of HLA Mismatches in Adult Liver Transplant Patients from the ITN A-WISH Trial. Transplantation, 102: S623. doi:10.1097/01.tp.0000543527.25918.d0.

Kampalath, B., Barcos, M.P. and Stewart, C. (2003) Phenotypic Heterogeneity of B Cells in Patients With Chronic Lymphocytic Leukemia/Small Lymphocytic Lymphoma. American Journal of Clinical Pathology, 119 (6): 824–832. doi:10.1309/4agu-t3lk-eurd-7t7k.

Kannabhiran, D., Lee, J., Schwartz, J.E., et al. (2015) Characteristics of circulating donor human leukocyte antigen-specific immunoglobulin G antibodies predictive of acute antibody-mediated rejection and kidney allograft failure. Transplantation, 99 (6): 1156–1164. doi:10.1097/TP.0000000000000511.

Karahan, G.E., Claas, F.H.J. and Heidt, S. (2017a) B cell immunity in solid organ transplantation. Frontiers in Immunology. 7 (JAN) p. 686. doi:10.3389/fimmu.2016.00686.

Karahan, G.E., Krop, J., Wehmeier, C., et al. (2019) An easy and sensitive method to profile the antibody specificities of HLA-specific memory b cells. Transplantation, 103 (4): 716–723. doi:10.1097/TP.0000000000002516.

Karahan, G.E., de Vaal, Y.J.H., Krop, J., et al. (2017b) A Memory B Cell Crossmatch Assay for Quantification of Donor-Specific Memory B Cells in the Peripheral Blood of HLA-Immunized Individuals. American Journal of Transplantation, 17 (10): 2617–2626. doi:10.1111/ajt.14293.

Karlsson Hedestam, G.B., Fouchier, R.A.M., Phogat, S., et al. (2008) The challenges of eliciting neutralizing antibodies to HIV-1 and to influenza virus. Nature Reviews Microbiology. 6 (2) pp. 143–155. doi:10.1038/nrmicro1819.

Kärre, K., Ljunggren, H.G., Piontek, G., et al. (1986) Selective rejection of H-2-deficient lymphoma variants suggests alternative immune defence strategy. Nature, 319 (6055): 675–678. doi:10.1038/319675a0.

Katz, G., Gazit, R., Arnon, T.I., et al. (2004) MHC Class I-Independent Recognition of NK-Activating Receptor KIR2DS4. The Journal of Immunology, 173 (3): 1819–1825.

Katz, G., Markel, G., Mizrahi, S., et al. (2001) Recognition of HLA-Cw4 but Not HLA-Cw6 by the NK Cell Receptor Killer Cell Ig-Like Receptor Two-Domain Short Tail Number 4. The Journal of Immunology, 166 (12): 7260–7267. doi:10.4049/jimmunol.166.12.7260.

Kawasaki, T. and Kawai, T. (2014) Toll-like receptor signaling pathways. Frontiers in Immunology. 5 (SEP) p. 461. doi:10.3389/fimmu.2014.00461.

Kay, N.E. and Zarling, J. (1987) Restoration of impaired natural killer cell activity of B-chronic lymphocytic leukemia patients by recombinant interleukin-2. American Journal of Hematology, 24 (2): 161–167. doi:10.1002/ajh.2830240207.

Khakoo, S.I. and Jamil, K.M. (2011) KIR/HLA interactions and pathogen immunity. Journal of Biomedicine and Biotechnology, 2011: 298348. doi:10.1155/2011/298348.

Khakoo, S.I., Thio, C.L., Martin, M.P., et al. (2004) HLA and NK cell inhibitory receptor genes in resolving hepatitis C virus infection. Science, 305 (5685): 872–874. doi:10.1126/science.1097670.

Khan, T.A., Friedensohn, S., De Vries, A.R.G., et al. (2016) Accurate and predictive antibody repertoire profiling by molecular amplification fingerprinting. Science Advances, 2 (3): e1501371. doi:10.1126/sciadv.1501371.

Kiessling, R., Klein, E., Pross, H., et al. (1975) "Natural" killer cells in the mouse. II. Cytotoxic cells with specificity for mouse Moloney leukemia cells. Characteristics of the killer cell. European Journal of Immunology, 5 (2): 117–121. doi:10.1002/eji.1830050209.

Kim, H.J., Choi, H.B., Jang, J.P., et al. (2014) HLA-Cw polypmorphism and killer cell immunoglobulin-like receptor (KIR) gene analysis in Korean colorectal cancer patients. International Journal of Surgery, 12 (8): 815–820. doi:10.1016/j.ijsu.2014.06.012.

Kim, S., Poursine-Laurent, J., Truscott, S.M., et al. (2005) Licensing of natural killer cells by host major histocompatibility complex class I molecules. Nature, 436 (7051): 709–713. doi:10.1038/nature03847.

Klee, G.G. (2000) Human anti-mouse antibodies. Archives of Pathology and Laboratory Medicine, 124 (6): 921–923. doi:10.1007/978-3-662-49054-9_1489-1.

Köhler, G. and Milstein, C. (1975) Continuous cultures of fused cells secreting antibody of predefined specificity. Nature, 256 (5517): 495–497. doi:10.1038/256495a0.

Kohrt, H.E., Thielens, A., Marabelle, A., et al. (2014) Anti-KIR antibody enhancement of anti-lymphoma activity of natural killer cells as monotherapy and in combination with anti-CD20 antibodies. Blood, 123 (5): 678–686. doi:10.1182/Blood-2013-08-519199.

Kolfschoten, M.V.D.N., Schuurman, J., Losen, M., et al. (2007) Anti-inflammatory activity of human IgG4 antibodies by dynamic Fab arm exchange. Science, 317 (5844): 1554–1557. doi:10.1126/science.1144603.

Kovaltsuk, A., Krawczyk, K., Galson, J.D., et al. (2017) How B-cell receptor repertoire sequencing can be enriched with structural antibody data. Frontiers in Immunology. 8 (DEC) p. 1. doi:10.3389/fimmu.2017.01753.

Kowalewski, D.J., Schuster, H., Backert, L., et al. (2015) HLA ligandome analysis identifies the underlying specificities of spontaneous antileukemia immune responses in chronic lymphocytic leukemia (CLL). Proceedings of the National Academy of Sciences of the United States of America, 112 (2): E116–E175. doi:10.1073/pnas.1416389112.

Kuchen, S., Robbins, R., Sims, G.P., et al. (2007) Essential Role of IL-21 in B Cell Activation, Expansion, and Plasma Cell Generation during CD4 + T Cell-B Cell Collaboration . The Journal of Immunology, 179 (9): 5886–5896. doi:10.4049/jimmunol.179.9.5886.

Kulkarni, S., Martin, M.P. and Carrington, M. (2008) The Yin and Yang of HLA and KIR in human disease. Seminars in Immunology, 20 (6): 343–352. doi:10.1016/j.smim.2008.06.003.

Kumbala, D. and Zhang, R. (2013) Essential concept of transplant immunology for clinical practice. World Journal of Transplantation, 3 (4): 113. doi:10.5500/wjt.v3.i4.113.

Kwaa, A.K.R., Talana, C.A.G. and Blankson, J.N. (2018) Interferon Alpha Enhances NK Cell Function and the Suppressive Capacity of HIV-Specific CD8 + T Cells . Journal of Virology, 93 (3). doi:10.1128/jvi.01541-18.

Kwakkenbos, M.J., van Helden, P.M., Beaumont, T., et al. (2016) Stable long-term cultures of self-renewing B cells and their applications. Immunological Reviews, 270 (1): 65–77. doi:10.1111/imr.12395.

Labrijn, A.F., Aalberse, R.C. and Schuurman, J. (2008) When binding is enough: nonactivating antibody formats. Current Opinion in Immunology. 20 (4) pp. 479–485. doi:10.1016/j.coi.2008.05.010.

Labrijn, A.F., Buijsse, A.O., Van Den Bremer, E.T.J., et al. (2009) Therapeutic IgG4 antibodies engage in Fab-arm exchange with endogenous human IgG4 in vivo. Nature Biotechnology, 27 (8): 767–771. doi:10.1038/nbt.1553.

Lakkis, F.G. and Lechler, R.I. (2013) Origin and biology of the allogeneic response. Cold Spring Harbor Perspectives in Medicine, 3 (8). doi:10.1101/cshperspect.a014993.

Lanier, L.L. (2005) Nk Cell Recognition. Annual Review of Immunology, 23 (1): 225–274. doi:10.1146/annurev.immunol.23.021704.115526.

Lanier, L.L., Le, A.M., Civin, C.I., et al. (1986) The relationship of CD16 (Leu-11) and Leu-19 (NKH-1) antigen expression on human peripheral blood NK cells and cytotoxic T lymphocytes. Journal of immunology (Baltimore, Md. : 1950), 136 (12): 4480–6.

Lanier, L.L., Ruitenberg, J.J. and Phillips, J.H. (1988) Functional and biochemical analysis of CD16 antigen on natural killer cells and granulocytes. Journal of immunology (Baltimore, Md. : 1950), 141 (10): 3478–85. Available at: http://www.ncbi.nlm.nih.gov/pubmed/2903193 (Accessed: 19 January 2020).

Lanoue, A., Batista, F.D., Stewart, M., et al. (2002) Interaction of CD22 with α2,6-linked sialoglycoconjugates: Innate recognition of self to dampen B cell autoreactivity? European Journal of Immunology, 32 (2): 348–355.

Lanzavecchia, A. (1985) Antigen-specific interaction between T and B cells. Nature, 314 (6011): 537–539. doi:10.1038/314537a0.

Laux, G. and Opelz, G. (2004) Immunological relevance of CREG matching in cadaver kidney transplantation. Transplantation, 78 (3): 442–446. doi:10.1097/01.TP.0000128615.41964.BC.

Lavinder, J.J., Wine, Y., Giesecke, C., et al. (2014) Identification and characterization of the constituent human serum antibodies elicited by vaccination. Proceedings of the National Academy of Sciences of the United States of America, 111 (6): 2259–2264. doi:10.1073/pnas.1317793111.

Lazar, G.A., Dang, W., Karki, S., et al. (2006) Engineered antibody Fc variants with enhanced effector function. Proceedings of the National Academy of Sciences of the United States of America, 103 (11): 4005–4010. doi:10.1073/pnas.0508123103.

Lechler, R.I. and Batchelor, J.R. (1982) Restoration of immunogenicity to passenger cell-depleted kidney allografts by the addition of donor strain dendritic cells. Journal of Experimental Medicine, 155 (1): 31–41. doi:10.1084/jem.155.1.31.

Lee, H.T., Lee, S.H. and Heo, Y.S. (2019) Molecular interactions of antibody drugs targeting PD-1, PD-L1, and CTLA-4 in immuno-oncology. Molecules. 24 (6). doi:10.3390/molecules24061190.

Lee, N., Llano, M., Carretero, M., et al. (1998) HLA-E is a major ligand for the natural killer inhibitory receptor CD94/NKG2A. Proceedings of the National Academy of Sciences of the United States of America, 95 (9): 5199–5204. doi:10.1073/pnas.95.9.5199.

Lee, P.C., Terasaki, P.I., Takemoto, S.K., et al. (2002) All chronic rejection failures of kidney transplants were preceded by the development of HLA antibodies. Transplantation, 74 (8): 1192–1194. doi:10.1097/00007890-200210270-00025.

Leeaphorn, N., Pena, J.R.A., Thamcharoen, N., et al. (2018) HLA-DQ mismatching and kidney transplant outcomes. Clinical Journal of the American Society of Nephrology, 13 (5): 763–771. doi:10.2215/CJN.10860917.

Legris, T., Picard, C., Todorova, D., et al. (2016) Antibody-dependent NK cell activation is associated with late kidney allograft dysfunction and the complement-independent alloreactive potential of donor-specific antibodies. Frontiers in Immunology, 7 (AUG).

Lin, A. and Yan, W.H. (2015) Human leukocyte antigen-G (HLA-G) expression in cancers: Roles in immune evasion, metastasis and target for therapy. Molecular Medicine. 21 (1) pp. 782–791. doi:10.2119/molmed.2015.00083.

Lisovsky, I., Isitman, G., Bruneau, J., et al. (2015) Functional analysis of NK cell subsets activated by 721.221 and K562 HLA-null cells. Journal of Leukocyte Biology, 97 (4): 761–767. doi:10.1189/jlb.4ab1014-499r.

Liu, J., Xiao, Z., Ko, H.L., et al. (2014) Activating killer cell immunoglobulin-like receptor 2DS2 binds to HLA-A 11. Proceedings of the National Academy of Sciences of the United States of America, 111 (7): 2662–2667. doi:10.1073/pnas.1322052111.

Liu, Y. -J, Oldfield, S. and Maclennan, I.C.M. (1988) Memory B cells in T cell-dependent antibody responses colonize the splenic marginal zones. European Journal of Immunology, 18 (3): 355–362. doi:10.1002/eji.1830180306.

Ljunggren, H.G. and Kärre, K. (1990) In search of the "missing self": MHC molecules and NK cell recognition. Immunology Today, 11 (C): 237–244. doi:10.1016/0167-5699(90)90097-S.

Lobo, P.I. and Spencer, C.E. (1989) Use of anti-HLA antibodies to mask major histocompatibility complex gene products on tumor cells can enhance susceptibility of these cells to lysis by natural killer cells. Journal of Clinical Investigation, 83 (1): 278–287. doi:10.1172/JCI113870.

Lombardi, G., Barber, L., Sidhu, S., et al. (1991) The specificity of alloreactive T cells is determined by MHC polymorphisms which contact the T cell receptor and which influence peptide binding. International Immunology, 3 (8): 769–775. doi:10.1093/intimm/3.8.769.

Long, E.O., Sik Kim, H., Liu, D., et al. (2013) Controlling Natural Killer Cell Responses: Integration of Signals for Activation and Inhibition. Annual Review of Immunology, 31 (1): 227–258. doi:10.1146/annurev-immunol-020711-075005.

Lozzio, B.B. and Lozzio, C.B. (1977) Letter to the editor. International Journal of Cancer, 19 (1): 136–136. doi:10.1002/ijc.2910190119.

Lu, D.R., Tan, Y.C., Kongpachith, S., et al. (2014) Identifying functional anti-Staphylococcus aureus antibodies by sequencing antibody repertoires of patient plasmablasts. Clinical Immunology, 152 (1–2): 77–89. doi:10.1016/j.clim.2014.02.010.

Lucas, D.P., Leffell, M.S. and Zachary, A.A. (2015) Differences in Immunogenicity of HLA Antigens and the Impact of Cross-Reactivity on the Humoral Response. Transplantation, 99 (1): 77–85. doi:10.1097/TP.0000000000000355.

Lúcia, M., Luque, S., Crespo, E., et al. (2015) Preformed circulating HLA-specific memory B cells predict high risk of humoral rejection in kidney transplantation. Kidney International, 88 (4): 874–887. doi:10.1038/ki.2015.205.

Lutz, C.T. and Kurago, Z.B. (1999) Human leukocyte antigen class I expression on squamous cell carcinoma cells regulates natural killer cell activity. Cancer Research, 59 (22): 5793–5799. Available at: http://www.ncbi.nlm.nih.gov/pubmed/10582701

Machado-Sulbaran, A.C., Ramírez-Dueñas, M.G., Navarro-Zarza, J.E., et al. (2019) KIR/HLA gene profile implication in systemic sclerosis patients from Mexico. Journal of Immunology Research, 2019. doi:10.1155/2019/6808061.

Mailliard, R.B., Alber, S.M., Shen, H., et al. (2005) IL-18-induced CD83+CCR7+ NK helper cells. Journal of Experimental Medicine, 202 (7): 941–953. doi:10.1084/jem.20050128.

Main, E.K., Lampson, L.A., Hart, M.K., et al. (1985) Human neuroblastoma cell lines are susceptible to lysis by natural killer cells but not by cytotoxic T lymphocytes. Journal of immunology (Baltimore, Md. : 1950), 135 (1): 242–6.

Maki, G., Hayes, G.M., Naji, A., et al. (2008) NK resistance of tumor cells from multiple myeloma and chronic lymphocytic leukemia patients: Implication of HLA-G. Leukemia, 22 (5): 998–1006. doi:10.1038/leu.2008.15.

Malcolm, S., Barton, P., Murphy, C., et al. (1982) Localization of human immunoglobulin κ light chain variable region genes to the short arm of chromosome 2 by in situ hybridization. Proceedings of the National Academy of Sciences of the United States of America, 79 (16 I): 4957–4961. doi:10.1073/pnas.79.16.4957.

Malnati, M.S.;, Peruzzi, M.;, Parker, K.C.;, et al. (1995) Peptide specificity in the recognition of MHC Class I by natural killer cell clones.

Mandelboim, O., Reyburn, H.T., Valés-Gómez, M., et al. (1996) Protection from lysis by natural killer cells of group 1 and 2 specificity is mediated by residue 80 in human histocompatibility leukocyte antigen C alleles and also occurs with empty major histocompatibility complex molecules. Journal of Experimental Medicine, 184 (3): 913–922. doi:10.1084/jem.184.3.913.

Markey, K.A., Koyama, M., Gartlan, K.H., et al. (2014) Cross-Dressing by Donor Dendritic Cells after Allogeneic Bone Marrow Transplantation Contributes to Formation of the Immunological Synapse and Maximizes Responses to Indirectly Presented Antigen. The Journal of Immunology, 192 (11): 5426–5433. doi:10.4049/jimmunol.1302490.

Marrari, M. and Duquesnoy, R.J. (2010) Detection of donor-specific HLA antibodies before and after removal of a rejected kidney transplant. Transplant Immunology, 22 (3–4): 105–109. doi:10.1016/j.trim.2009.12.005.

Maruyama, M., Lam, K.P. and Rajewsky, K. (2000) Memory B-cell persistence is independent of persisting immunizing antigen. Nature, 407 (6804): 636–642. doi:10.1038/35036600.

Masuda, K., Hiraki, A., Fujii, N., et al. (2007) Loss or down-regulation of HLA class I expression at the allelic level in freshly isolated leukemic blasts. Cancer Science, 98 (1): 102–108. doi:10.1111/j.1349-7006.2006.00356.x.

McBlane, J.F., van Gent, D.C., Ramsden, D.A., et al. (1995) Cleavage at a V(D)J recombination signal requires only RAG1 and RAG2 proteins and occurs in two steps. Cell, 83 (3): 387–395. doi:10.1016/0092-8674(95)90116-7.

McCafferty, J., Griffiths, A.D., Winter, G., et al. (1990) Phage antibodies: filamentous phage displaying antibody variable domains. Nature, 348 (6301): 552–554. doi:10.1038/348552a0.

McCutcheon, J.A., Gumperz, J., Smith, K.D., et al. (1995) Low HLA-C expression at cell surfaces correlates with increased turnover of heavy chain mRNA. Journal of Experimental Medicine, 181 (6): 2085–2095. doi:10.1084/jem.181.6.2085.

McHeyzer-Williams, L.J. and McHeyzer-Williams, M.G. (2005) Antigen-specific memory B cell development. Annual Review of Immunology, 23 (1): 487–513.

McKenna, R.M. and Takemoto, S.K. (2000) Improving HLA matching for kidney transplantation by use of CREGs. Lancet. 355 (9218) pp. 1842–1843. doi:10.1016/S0140-6736(00)02283-2.

McKenzie, L.M., Pecon-Slattery, J., Carrington, M., et al. (1999) Taxonomic hierarchy of HLA class I allele sequences. Genes and Immunity, 1 (2): 120–129. doi:10.1038/sj.gene.6363648.

McMurtrey, C., Lowe, D., Buchli, R., et al. (2014) Profiling antibodies to class II HLA in transplant patient sera. Human Immunology, 75 (3): 261–270. doi:10.1016/j.humimm.2013.11.015.

McVicar, D.W., Taylor, L.S., Gosselin, P., et al. (1998) DAP12-mediated signal transduction in natural killer cells: A dominant role for the Syk protein-tyrosine kinase. Journal of Biological Chemistry, 273 (49): 32934–32942. doi:10.1074/jbc.273.49.32934.

McWilliams, E.M., Mele, J.M., Cheney, C., et al. (2016) Therapeutic CD94/NKG2A blockade improves natural killer cell dysfunction in chronic lymphocytic leukemia. OncoImmunology, 5 (10). doi:10.1080/2162402X.2016.1226720.

Mehra, N.K., Gurvinder Kaur., McCluskey, J., et al. (2010) The HLA complex in biology and medicine : a resource book. Jaypee Bros. Medical Publishers.

Mellor, J.D., Brown, M.P., Irving, H.R., et al. (2013) A critical review of the role of Fc gamma receptor polymorphisms in the response to monoclonal antibodies in cancer. Journal of Hematology and Oncology. 6 (1) p. 1. doi:10.1186/1756-8722-6-1.

Meuleman, T., van Beelen, E., Kaaja, R.J., et al. (2016) HLA-C antibodies in women with recurrent miscarriage suggests that antibody mediated rejection is one of the mechanisms leading to recurrent miscarriage. Journal of Reproductive Immunology, 116: 28–34. doi:10.1016/j.jri.2016.03.003.

Milner, J., Melcher, M.L., Lee, B., et al. (2016) HLA Matching Trumps Donor Age. Transplantation Direct, 2 (7): e85. doi:10.1097/txd.0000000000000597.

Milongo, D., Kamar, N., Del Bello, A., et al. (2017) Allelic and Epitopic Characterization of Intra–Kidney Allograft Anti-HLA Antibodies at Allograft Nephrectomy. American Journal of Transplantation, 17 (2): 420–431. doi:10.1111/ajt.13958.

Moen, T., Albrechtsen, D., Flatmark, A., et al. (1980) Importance of HLA-DR Matching in Cadaveric Renal Transplantation: A Prospective One-Center Study of 170 Transplants. New England Journal of Medicine, 303 (15): 850–854. doi:10.1056/NEJM198010093031504.

Moesta, A.K., Norman, P.J., Yawata, M., et al. (2008) Synergistic Polymorphism at Two Positions Distal to the Ligand-Binding Site Makes KIR2DL2 a Stronger Receptor for HLA-C Than KIR2DL3. The Journal of Immunology, 180 (6): 3969–3979. doi:10.4049/jimmunol.180.6.3969.

lo Monaco, E., Tremante, E., Cerboni, C., et al. (2011) Human leukocyte antigen E contributes to protect tumor cells from lysis by natural killer cells. Neoplasia, 13 (9): 822–830. doi:10.1593/neo.101684.

Morales-Buenrostro, L.E., Terasaki, P.I., Marino-Vázquez, L.A., et al. (2008) "Natural" human leukocyte antigen antibodies found in nonalloimmunized healthy males. Transplantation, 86 (8): 1111–1115. doi:10.1097/TP.0b013e318186d87b.

Morales-Estevez, C., De la Haba-Rodriguez, J., Manzanares-Martin, B., et al. (2016) KIR genes and their ligands predict the response to anti-EGFR monoclonal antibodies in solid tumors. Frontiers in Immunology, 7 (DEC): 561. doi:10.3389/fimmu.2016.00561.

Morandi, F., Rizzo, R., Fainardi, E., et al. (2016) Recent advances in our understanding of HLA-G biology: Lessons from a wide spectrum of human diseases. Journal of Immunology Research, 2016. doi:10.1155/2016/4326495.

Morrison, B.J., Roman, J.A., Luke, T.C., et al. (2017) Antibody-dependent NK cell degranulation as a marker for assessing antibody-dependent cytotoxicity against pandemic 2009 influenza A(H1N1) infection in human plasma and influenza-vaccinated transchromosomic bovine intravenous immunoglobulin therapy. Journal of Virological Methods, 248: 7–18.

Morrison, S.L., Johnson, M.J., Herzenberg, L.A., et al. (1984) Chimeric human antibody molecules: Mouse antigen-binding domains with human constant region domains. Proceedings of the National Academy of Sciences of the United States of America, 81 (21 I): 6851–6855. doi:10.1073/pnas.81.21.6851.

Motley, M.P. and Fries, B.C. (2017) A New Take on an Old Remedy: Generating Antibodies against Multidrug-Resistant Gram-Negative Bacteria in a Postantibiotic World. mSphere, 2 (5). doi:10.1128/msphere.00397-17.

Mulder, A., Eijsink, C., Kardol, M.J., et al. (2003) Identification, Isolation, and Culture of HLA-A2-Specific B Lymphocytes Using MHC Class I Tetramers. The Journal of Immunology, 171 (12): 6599–6603. doi:10.4049/jimmunol.171.12.6599.

Mulder, A., Eijsink, C., Kester, M.G.D., et al. (2005) Impact of Peptides on the Recognition of HLA Class I Molecules by Human HLA Antibodies. The Journal of Immunology, 175 (9): 5950–5957. doi:10.4049/jimmunol.175.9.5950.

Mulder, A., Kardol, M.J., Kamp, J., et al. (2001) Determination of the frequency of HLA antibody secreting B-lymphocytes in alloantigen sensitized individuals. Clinical and Experimental Immunology, 124 (1): 9–15. doi:10.1046/j.1365-2249.2001.01497.x.

Mulder, A., Kardol, M.J., Uit Het Broek, C.M., et al. (1998) A human monoclonal antibody against HLA-Cw1 and a human monoclonal antibody against an HLA-A locus determinant derived from a single uniparous female. Tissue Antigens, 52 (4): 393–396. doi:10.1111/j.1399-0039.1998.tb03062.x.

Murata, K. and Baldwin, W.M. (2009) Mechanisms of complement activation, C4d deposition, and their contribution to the pathogenesis of antibody-mediated rejection. Transplantation Reviews, 23 (3): 139–150. doi:10.1016/j.trre.2009.02.005.

Muro, M., González-Soriano, M.J., Salgado, G., et al. (2010) Specific “intra-allele” and “intra-broad antigen” human leukocyte antigen alloantibodies in kidney graft transplantation. Human Immunology, 71 (9): 857–860. doi:10.1016/j.humimm.2010.05.018.

Murphy, K. and Weaver, C. (2017) Janeway’s Immunobiology. Ninth. New York: Garland Science (Taylor & Francis Group). doi:10.1086/696793.

Nadel, B. and Feeney, A.J. (1997) Nucleotide deletion and P addition in V(D)J recombination: a determinant role of the coding-end sequence. Molecular and Cellular Biology, 17 (7): 3768–3778. doi:10.1128/mcb.17.7.3768.

Natsume, A., In, M., Takamura, H., et al. (2008) Engineered antibodies of IgG1/IgG3 mixed isotype with enhanced cytotoxic activities. Cancer Research, 68 (10): 3863–3872. doi:10.1158/0008-5472.CAN-07-6297.

Natsume, A., Shimizu-Yokoyama, Y., Satoh, M., et al. (2009) Engineered anti-CD20 antibodies with enhanced complement-activating capacity mediate potent anti-lymphoma activity. Cancer Science, 100 (12): 2411–2418. doi:10.1111/j.1349-7006.2009.01327.x.

Naumova, E., Mihaylova, A., Stoitchkov, K., et al. (2005) Genetic polymorphism of NK receptors and their ligands in melanoma patients: Prevalence of inhibitory over activating signals. Cancer Immunology, Immunotherapy, 54 (2): 172–178. doi:10.1007/s00262-004-0575-z.

Nemazee, D. (2006) Receptor editing in lymphocyte development and central tolerance. Nature Reviews Immunology. 6 (10) pp. 728–740. doi:10.1038/nri1939.

Nückel, H., Rebmann, V., Dürig, J., et al. (2005) HLA-G expression is associated with an unfavorable outcome and immunodeficiency in chronic lymphocytic leukemia. Blood, 105 (4): 1694–1698. doi:10.1182/blood-2004-08-3335.

O’Connor, G.M., Vivian, J.P., Gostick, E., et al. (2015) Peptide-Dependent Recognition of HLA-B*57:01 by KIR3DS1. Journal of Virology, 89 (10): 5213–5221. doi:10.1128/jvi.03586-14.

O’Shea, J.J., Weissman, A.M., Kennedy, I.C.S., et al. (1991) Engagement of the natural killer cell IgG Fc receptor results in tyrosine phosphorylation of the ζ chain. Proceedings of the National Academy of Sciences of the United States of America, 88 (2): 350–354. doi:10.1073/pnas.88.2.350.

Oettinger, M.A., Schatz, D.G., Gorka, C., et al. (1990) RAG-1 and RAG-2, adjacent genes that synergistically activate V(D)J recombination. Science, 248 (4962): 1517–1523. doi:10.1126/science.2360047.

Okuda, T., Ishikawa, T., Azhipa, O., et al. (2002) Early passenger leukocyte migration and acute immune reactions in the rat recipient spleen during liver engraftment: With particular emphasis on donor major histocompatibility complex class II+ cells. Transplantation, 74 (1): 103–111. doi:10.1097/00007890-200207150-00018.

Opelz, G., Döhler, B., Middleton, D., et al. (2017) HLA Matching in Pediatric Kidney Transplantation: HLA Poorly Matched Living Donor Transplants Versus HLA Well-Matched Deceased Donor Transplants. Transplantation, 101 (11): 2789–2792. doi:10.1097/TP.0000000000001811.

Opelz, G. and Wujciak, T. (1994) The influence of HLA compatibility on graft survival after heart transplantation. New England Journal of Medicine, 330 (12): 816–819. doi:10.1056/NEJM199403243301203.

Orr, M.T., Murphy, W.J. and Lanier, L.L. (2010) “Unlicensed” natural killer cells dominate the response to cytomegalovirus infection. Nature Immunology, 11 (4): 321–327. doi:10.1038/ni.1849.

Otagiri, M. and Giam Chuang, V.T. (2016) Albumin in medicine: Pathological and clinical applications. Albumin in Medicine: Pathological and Clinical Applications, pp. 1–277. doi:10.1007/978-981-10-2116-9.

Otten, H.G., Verhaar, M.C., Borst, H.P.E., et al. (2013) The significance of pretransplant donor-specific antibodies reactive with intact or denatured human leucocyte antigen in kidney transplantation. Clinical and Experimental Immunology, 173 (3): 536–543. doi:10.1111/cei.12127.

Ouisse, L.H., Gautreau-Rolland, L., Devilder, M.C., et al. (2017) Antigen-specific single B cell sorting and expression-cloning from immunoglobulin humanized rats: A rapid and versatile method for the generation of high affinity and discriminative human monoclonal antibodies. BMC Biotechnology, 17 (1): 3. doi:10.1186/s12896-016-0322-5.

Pallares, N., Frippiat, J.P., Giudicelli, V., et al. (1998) The human immunoglobulin lambda variable (IGLV) genes and joining (IGLJ) segments. Experimental and Clinical Immunogenetics. 15 (1) pp. 8–18. doi:10.1159/000019054.

Pape, K.A., Taylor, J.J., Maul, R.W., et al. (2011) Different B cell populations mediate early and late memory during an endogenous immune response. Science, 331 (6021): 1203–1207. doi:10.1126/science.1201730.

Parham, P. (2005) MHC class I molecules and KIRS in human history, health and survival. Nature Reviews Immunology. 5 (3) pp. 201–214. doi:10.1038/nri1570.

Parham, P. and Guethlein, L.A. (2018) Genetics of Natural Killer Cells in Human Health, Disease, and Survival. Annual Review of Immunology, 36 (1). doi:10.1146/annurev-immunol-042617-053149.
Park, Y. and Dr, H.-S.K. (2017) Meaning of HLA Antibodies Frequently Detected by Single Antigen Bead Assay. Transplantation, 101: S39. doi:10.1097/01.tp.0000520355.70691.06.

Parry, H.M., Stevens, T., Oldreive, C., et al. (2016) NK cell function is markedly impaired in patients with chronic lymphocytic leukaemia but is preserved in patients with small lymphocytic lymphoma. Oncotarget, 7 (42): 68513–68526. doi:10.18632/ONCOTARGET.12097.

Pascual, V. and Capra, J.D. (1991) Human Immunoglobulin Heavy-Chain Variable Region Genes: Organization, Polymorphism, and Expression. Advances in Immunology, 49 (C): 1–74. doi:10.1016/S0065-2776(08)60774-9.

Patel, R. and Terasaki, P.I. (1969) Significance of the positive crossmatch test in kidney transplantation. The New England journal of medicine, 280 (14): 735–739. doi:10.1056/NEJM196904032801401.

Patnaik, A., Kang, S.P., Rasco, D., et al. (2015) Phase i study of pembrolizumab (MK-3475; Anti-PD-1 monoclonal antibody) in patients with advanced solid tumors. Clinical Cancer Research, 21 (19): 4286–4293. doi:10.1158/1078-0432.CCR-14-2607.

Paulson, J.C., MacAuley, M.S. and Kawasaki, N. (2012) Siglecs as sensors of self in innate and adaptive immune responses. Annals of the New York Academy of Sciences. 1253 (1) pp. 37–48. doi:10.1111/j.1749-6632.2011.06362.x.

Pauza, M.E., Rehmann, J.A. and LeBien, T.W. (1993) Unusual patterns of immunoglobulin gene rearrangement and expression during human B cell ontogeny: Human B cells can simultaneously express cell surface κ and λ light chains. Journal of Experimental Medicine, 178 (1): 139–149. doi:10.1084/jem.178.1.139.

Payne, R., Radvany, R., Grumet, F.C., et al. (1975) “Two third series antigens transmitted together - A possible fourth SD locus?” In Kissmeyer-Nielsen, F. (ed.). Histocompatibility Testing 1975. Copenhagen, 1975. Munksgaard. pp. 343–347.

PAYNE, R., TRIPP, M., WEIGLE, J., et al. (1964) a New Leukocyte Isoantigen System in Man. Cold Spring Harbor symposia on quantitative biology, 29: 285–295. doi:10.1101/SQB.1964.029.01.031.

Pei, J., Akatsuka, Y., Anasetti, C., et al. (2001) Generation of HLA-C-specific cytotoxic T cells in association with marrow graft rejection: Analysis of alloimmunity by T-cell cloning and testing of T-cell-receptor rearrangements. Biology of Blood and Marrow Transplantation, 7 (7): 378–383. doi:10.1053/bbmt.2001.v7.pm11529487.

Pei, R., Lee, J.H., Shih, N.J., et al. (2003) Single human leukocyte antigen flow cytometry beads for accurate identification of human leukocyte antigen antibody specificities. Transplantation, 75 (1): 43–49. doi:10.1097/00007890-200301150-00008.

Pelletier, R.P., Hennessy, P.K., Adams, P.W., et al. (2002) Clinical significance of MHC-reactive alloantibodies that develop after kidney or kidney-pancreas transplantation. American Journal of Transplantation, 2 (2): 134–141. doi:10.1034/j.1600-6143.2002.020204.x.

Pende, D., Accame, L., Pareti, L., et al. (1998) The susceptibility to natural killer cell-mediated lysis of HLA class I-positive melanomas reflects the expression of insufficient amounts of different HLA class I alleles. European Journal of Immunology, 28 (8): 2384–2394. doi:10.1002/(SICI)1521-4141(199808)28:08<2384::AID-IMMU2384>3.0.CO;2-L.

Pende, D., Biassoni, R., Cantoni, C., et al. (1996) The natural killer cell receptor specific for HLA-A allotypes: A novel member of the p58/p70 family of inhibitory receptors that is characterized by three immunoglobulin-like domains and is expressed as a 140-kD disulphide- linked dimer. Journal of Experimental Medicine, 184 (2): 505–518. doi:10.1084/jem.184.2.505.

Pende, D., Spaggiari, G.M., Marcenaro, S., et al. (2005) Analysis of the receptor-ligand interactions in the natural killer-mediated lysis of freshly isolated myeloid or lymphoblastic leukemias: Evidence for the involvement of the Polio virus receptor (CD 155) and Nectin-2 (CD 112). Blood, 105 (5): 2066–2073. doi:10.1182/blood-2004-09-3548.

Perry, D.K., Pollinger, H.S., Burns, J.M., et al. (2008) Two novel assays of alloantibody-secreting cells demonstrating resistance to desensitization with IVIG and rATG. American Journal of Transplantation, 8 (1): 133–143. doi:10.1111/j.1600-6143.2007.02039.x.

Peruzzi, M., Parker, K.C., Long, E.O., et al. (1996) Peptide sequence requirements for the recognition of HLA-B*2705 by specific natural killer cells. Journal of immunology (Baltimore, Md.: 1950), 157 (8): 3350–6.

Peter, H.H., Pavie-Fischer, J., Fridman, W.H., et al. (1975) Cell-mediate cytotoxicity in vitro of human lymphocytes against a tissue culture melanoma cell line (igr3). Journal of immunology (Baltimore, Md.: 1950), 115 (2): 539–48.

Petersdorf, E. (2011) The HLA Complex in Biology and Medicine: A Resource Book. Jaypee Bros. Medical Publishers. doi:10.1038/bmt.2010.259.

Phan, T.G., Paus, D., Chan, T.D., et al. (2006) High affinity germinal center B cells are actively selected into the plasma cell compartment. Journal of Experimental Medicine, 203 (11): 2419–2424. doi:10.1084/jem.20061254.

Pierson, T.C., Xu, Q., Nelson, S., et al. (2007) The Stoichiometry of Antibody-Mediated Neutralization and Enhancement of West Nile Virus Infection. Cell Host and Microbe, 1 (2): 135–145. doi:10.1016/j.chom.2007.03.002.

Pietra, B.A., Wiseman, A., Bolwerk, A., et al. (2000) CD4 T cell-mediated cardiac allograft rejection requires donor but not host MHC class II. Journal of Clinical Investigation, 106 (8): 1003–1010. doi:10.1172/JCI10467.

Pinna, D., Corti, D., Jarrossay, D., et al. (2009) Clonal dissection of the human memory B-cell repertoire following infection and vaccination. European Journal of Immunology, 39 (5): 1260–1270. doi:10.1002/eji.200839129.

Ploegh, H.L. (2007) Bridging B Cell and T Cell Recognition of Antigen. The Journal of Immunology, 179 (11): 7193–7193. doi:10.4049/jimmunol.179.11.7193.

Poljak, R.J., Amzel, L.M., Avey, H.P., et al. (1973) Three dimensional structure of the Fab' fragment of a human immunoglobulin at 2.8 Å resolution. Proceedings of the National Academy of Sciences of the United States of America, 70 (12). doi:10.1073/pnas.70.12.3305.

Prugnolle, F., Manica, A., Charpentier, M., et al. (2005) Pathogen-driven selection and worldwide HLA class I diversity. Current Biology, 15 (11): 1022–1027. doi:10.1016/j.cub.2005.04.050.

Putnam, F.W., Liu, Y.S. and Low, T.L. (1979) Primary structure of a human IgA1 immunoglobulin. IV. Streptococcal IgA1 protease digestion, Fab and Fc fragments, and the complete amino acid sequence of the α1 heavy chain. The Journal of biological chemistry, 254 (8): 2865–74.

Rajagopalan, S. and Long, E.O. (1997) The direct binding of a p58 killer cell inhibitory receptor to human histocompatibility leukocyte antigen (HLA)-Cw4 exhibits peptide selectivity. Journal of Experimental Medicine, 185 (8): 1523–1528. doi:10.1084/jem.185.8.1523.

Rajagopalan, S. and Long, E.O. (2005) Understanding how combinations of HLA and KIR genes influence disease. Journal of Experimental Medicine, 201 (7): 1025–1029. doi:10.1084/jem.20050499.

Rajagopalan, S. and Long, E.O. (2012) KIR2DL4 (CD158d): An activation receptor for HLA-G. Frontiers in Immunology, 3 (AUG): 258. doi:10.3389/fimmu.2012.00258.

Raulet, D.H., Held, W., Correa, I., et al. (1997) Specificity, tolerance and developmental regulation of natural killer cells defined by expression of class I-specific Ly49 receptors. Immunological Reviews, 155 (1): 41–52. doi:10.1111/j.1600-065X.1997.tb00938.x.

Raulet, D.H. and Vance, R.E. (2006) Self-tolerance of natural killer cells. Nature Reviews Immunology. 6 (7) pp. 520–531. doi:10.1038/nri1863.

Raulet, D.H., Vance, R.E. and McMahon, C.W. (2001) Regulation of the Natural Killer Cell Receptor Repertoire . Annual Review of Immunology, 19 (1): 291–330.

Ravindranath, M.H., Jucaud, V. and Ferrone, S. (2017) Monitoring native HLA-I trimer specific antibodies in Luminex multiplex single antigen bead assay: Evaluation of beadsets from different manufacturers. Journal of Immunological Methods, 450: 73–80. doi:10.1016/j.jim.2017.07.016.

Rawstron, A.C., Kreuzer, K.A., Soosapilla, A., et al. (2018) Reproducible diagnosis of chronic lymphocytic leukemia by flow cytometry: An European Research Initiative on CLL (ERIC) & European Society for Clinical Cell Analysis (ESCCA) Harmonisation project. Cytometry Part B - Clinical Cytometry, 94 (1): 121–128. doi:10.1002/cyto.b.21595.

de Rham, C., Ferrari-Lacraz, S., Jendly, S., et al. (2007) The proinflammatory cytokines IL-2, IL-15 and IL-21 modulate the repertoire of mature human natural killer cell receptors. Arthritis Research and Therapy, 9 (6): R125. doi:10.1186/ar2336.

Rock, K.L., Benacerraf, B. and Abbas, A.K. (1984) Antigen presentation by hapten-specific b lymphocytes: I. Role of surface immunoglobulin receptors. Journal of Experimental Medicine, 160 (4): 1102–1113. doi:10.1084/jem.160.4.1102.

Rodey, G.E., Neylan, J.F., Whelchel, J.D., et al. (1994) Epitope specificity of HLA class I alloantibodies I. Frequency analysis of antibodies to private versus public specificities in potential transplant recipients. Human Immunology, 39 (4): 272–280. doi:10.1016/0198-8859(94)90270-4.

Romagné, F., André, P., Spee, P., et al. (2009) Preclinical characterization of 1-7F9, a novel human anti-KIR receptor therapeutic antibody that augments natural killer-mediated killing of tumor cells. Blood, 114 (13): 2667–2677. doi:10.1182/blood-2009-02-206532.

VAN ROODJ and VAN LEEUWEN (1963) Leukocyte Grouping. a Method and Its Application. The Journal of clinical investigation, 42 (9): 1382–1390. doi:10.1172/jci104822.

Sasazuki, T., Juji, T., Morishima, Y., et al. (1998) Effect of matching of class I HLA alleles on clinical outcome after transplantation of hematopoietic stem cells from an unrelated donor. New England Journal of Medicine, 339 (17): 1177–1185. doi:10.1056/NEJM199810223391701.

Saulquin, X., Gastinel, L.N. and Vivier, E. (2003) Crystal structure of the human natural killer cell activating receptor KIR2DS2 (CD158j). Journal of Experimental Medicine, 197 (7): 933–938. doi:10.1084/jem.20021624.

Schinstock, C.A., Gandhi, M.J. and Stegall, M.D. (2016) Interpreting anti-HLA antibody testing data: A practical guide for physicians. Transplantation, 100 (8): 1619–1628.

Schroeder, H.W. and Cavacini, L. (2010) Structure and function of immunoglobulins. Journal of Allergy and Clinical Immunology, 125 (2 SUPPL. 2). doi:10.1016/j.jaci.2009.09.046.

Schultheiß, C., Paschold, L., Simnica, D., et al. (2020) Next-Generation Sequencing of T and B Cell Receptor Repertoires from COVID-19 Patients Showed Signatures Associated with Severity of Disease. Immunity, 53 (2): 442-455.e4. doi:10.1016/j.immuni.2020.06.024.

Seliger, B., Cabrera, T., Garrido, F., et al. (2002) HLA class I antigen abnormalities and immune escape by malignant cells. Seminars in Cancer Biology, 12 (1): 3–13. doi:10.1006/scbi.2001.0404.

Senju, H., Kumagai, A., Nakamura, Y., et al. (2018) Effect of IL-18 on the expansion and phenotype of human natural killer cells: Application to cancer immunotherapy. International Journal of Biological Sciences, 14 (3): 331–340. doi:10.7150/ijbs.22809.

Sharma, N., Benechet, A.P., Lefrancois, L., et al. (2015) CD8 T Cells Enter the Splenic T Cell Zones Independently of CCR7, but the Subsequent Expansion and Trafficking Patterns of Effector T Cells after Infection Are Dysregulated in the Absence of CCR7 Migratory Cues. The Journal of Immunology, 195 (11): 5227–5236. doi:10.4049/jimmunol.1500993.

Sherman, L.A. and Chattopadhyay, S. (1993) The Molecular Basis of Allorecognition. Annual Review of Immunology, 11 (1): 385–402. doi:10.1146/annurev.iy.11.040193.002125.

Shields, R.L., Namenuk, A.K., Hong, K., et al. (2001) High Resolution Mapping of the Binding Site on Human IgG1 for FcγRI, FcγRII, FcγRIII, and FcRn and Design of IgG1 Variants with Improved Binding to the FcγR. Journal of Biological Chemistry, 276 (9): 6591–6604. doi:10.1074/jbc.M009483200.

Shih, T.A.Y., Roederer, M. and Nussenzweig, M.C. (2002) Role of antigen receptor affinity in T cell-independent antibody responses in vivo. Nature Immunology, 3 (4): 399–406. doi:10.1038/ni776.

Shiroishi, M., Tsumoto, K., Amano, K., et al. (2003) Human inhibitory receptors Ig-like transcript 2 (ILT2) and ILT4 compete with CD8 for MHC class I binding and bind preferentially to HLA-G. Proceedings of the National Academy of Sciences of the United States of America, 100 (15): 8856–8861. doi:10.1073/pnas.1431057100.

Sim, M.J.W., Malaker, S.A., Khan, A., et al. (2017) Canonical and cross-reactive binding of NK cell inhibitory receptors to HLA-C allotypes is dictated by peptides bound to HLA-C. Frontiers in Immunology, 8 (MAR): 193. doi:10.3389/fimmu.2017.00193.

Sim, M.J.W., Rajagopalan, S., Altmann, D.M., et al. (2019) Human NK cell receptor KIR2DS4 detects a conserved bacterial epitope presented by HLA-C. Proceedings of the National Academy of Sciences of the United States of America, 116 (26): 12964–12973. doi:10.1073/pnas.1903781116.

Sim, M.J.W., Stowell, J., Sergeant, R., et al. (2016) KIR2DL3 and KIR2DL1 show similar impact on licensing of human NK cells. European Journal of Immunology, 46 (1): 185–191. doi:10.1002/eji.201545757.

Simmonds, M. and Gough, S. (2009) The HLA Region and Autoimmune Disease: Associations and Mechanisms of Action. Current Genomics, 8 (7): 453–465. doi:10.2174/138920207783591690.

Sips, M., Liu, Q., Draghi, M., et al. (2016) HLA-C levels impact natural killer cell subset distribution and function. Human Immunology, 77 (12): 1147–1153. doi:10.1016/j.humimm.2016.08.004.

Sivaganesh, S., Harper, S.J., Conlon, T.M., et al. (2013) Copresentation of Intact and Processed MHC Alloantigen by Recipient Dendritic Cells Enables Delivery of Linked Help to Alloreactive CD8 T Cells by Indirect-Pathway CD4 T Cells. The Journal of Immunology, 190 (11): 5829–5838. doi:10.4049/jimmunol.1300458.

Smith, G.P. (1985) Filamentous fusion phage: Novel expression vectors that display cloned antigens on the virion surface. Science, 228 (4705): 1315–1317. doi:10.1126/science.4001944.

Smith, K., Garman, L., Wrammert, J., et al. (2009) Rapid generation of fully human monoclonal antibodies specific to a vaccinating antigen. Nature Protocols, 4 (3): 372–384. doi:10.1038/nprot.2009.3.

Smith, S.A., Zhou, Y., Olivarez, N.P., et al. (2012) Persistence of Circulating Memory B Cell Clones with Potential for Dengue Virus Disease Enhancement for Decades following Infection. Journal of Virology, 86 (5): 2665–2675. doi:10.1128/jvi.06335-11.

Snanoudj, R., Claas, F.H.J., Heidt, S., et al. (2015) Restricted specificity of peripheral alloreactive memory B cells in HLA-sensitized patients awaiting a kidney transplant. Kidney International, 87 (6): 1230–1240. doi:10.1038/ki.2014.390.

Solheim, B.G., Flatmark, A., Enger, E., et al. (1977) Influence of HLA-A, -B, -C, and -D matching on the outcome of clinical kidney transplantation. Transplantation Proceedings, 9 (1): 475–478. Available at: http://www.ncbi.nlm.nih.gov/pubmed/141132 (Accessed: 21 January 2020).

Stegall, M.D., Dean, P.G. and Gloor, J. (2009) Mechanisms of Alloantibody Production in Sensitized Renal Allograft Recipients. American Journal of Transplantation, 9 (5): 998–1005. doi:10.1111/j.1600-6143.2009.02612.x.

Steinitz, M., Klein, G., Koskimies, S., et al. (1977) EB virus-induced B lymphocyte cell lines producing specific antibody. Nature, 269 (5627): 420–422. doi:10.1038/269420a0.

Steinman, R.M., Bonifaz, L., Fujii, S.I., et al. (2005) "The innate functions of dendritic cells in peripheral lymphoid tissues." In Advances in Experimental Medicine and Biology. 2005. Springer, Boston, MA. pp. 83–97. doi:10.1007/0-387-24180-9_12.

Steinmuller, D. (1980) Passenger leukocytes and the immunogenicity of skin allografts. Journal of Investigative Dermatology, 75 (1): 107–115. doi:10.1111/1523-1747.ep12521331.

Stewart, C.A., Laugier-Anfossi, F., Vély, F., et al. (2005) Recognition of peptide-MHC class I complexes by activating killer immunoglobulin-like receptors. Proceedings of the National Academy of Sciences of the United States of America, 102 (37): 13224–13229. doi:10.1073/pnas.0503594102.

Stewart, C.C. and Stewart, S.J. (1993) Immunological Monitoring Utilizing Novel Probes. Annals of the New York Academy of Sciences, 677 (1): 94–112. doi:10.1111/j.1749-6632.1993.tb38769.x.

Storkus, W.J., Alexander, J., Payne, J.A., et al. (1989a) Reversal of natural killing susceptibility in target cells expressing transfected class I HLA genes. Proceedings of the National Academy of Sciences of the United States of America, 86 (7): 2361–2364. doi:10.1073/pnas.86.7.2361.

Storkus, W.J., Alexander, J., Payne, J.A., et al. (1989b) The alpha 1/alpha 2 domains of class I HLA molecules confer resistance to natural killing. Journal of immunology (Baltimore, Md.: 1950), 143 (11): 3853–7.

Storkus, W.J., Salter, R.D., Alexander, J., et al. (1991) Class I-induced resistance to natural killing: identification of nonpermissive residues in HLA-A2. Proceedings of the National Academy of Sciences of the United States of America, 88 (14): 5989–92. doi:10.1073/pnas.88.14.5989.

Takemoto, S.K., Terasaki, P.I., Gjertson, D.W., et al. (2000) Twelve years' experience with national sharing of HLA-matched cadaveric kidneys for transplantation. New England Journal of Medicine, 343 (15): 1078–1084. doi:10.1056/NEJM200010123431504.

Tan, Y.C., Blum, L.K., Kongpachith, S., et al. (2014) High-throughput sequencing of natively paired antibody chains provides evidence for original antigenic sin shaping the antibody response to influenza vaccination. Clinical Immunology, 151 (1): 55–65. doi:10.1016/j.clim.2013.12.008.

Taylor, A.L., Negus, S.L., Negus, M., et al. (2007) Pathways of Helper CD4 T Cell Allorecognition in Generating Alloantibody and CD8 T Cell Alloimmunity. Transplantation, 83 (7): 931–937. doi:10.1097/01.tp.0000257960.07783.e3.

Taylor, J.J., Pape, K.A. and Jenkins, M.K. (2012) A germinal center-independent pathway generates unswitched memory B cells early in the primary response. Journal of Experimental Medicine, 209 (3): 597–606. doi:10.1084/jem.20111696.

Temming, A.R., de Taeye, S.W., de Graaf, E.L., et al. (2019) Functional Attributes of Antibodies, Effector Cells, and Target Cells Affecting NK Cell–Mediated Antibody-Dependent Cellular Cytotoxicity. The Journal of Immunology, 203 (12): 3126–3135. doi:10.4049/jimmunol.1900985.

Terasaki, P.I. and Cai, J. (2008) Human leukocyte antigen antibodies and chronic rejection: From association to causation. Transplantation, 86 (3): 377–383. doi:10.1097/TP.0b013e31817c4cb8.

Thomas, A., Teicher, B.A. and Hassan, R. (2016) Antibody–drug conjugates for cancer therapy. The Lancet Oncology. 17 (6) pp. e254–e262. doi:10.1016/S1470-2045(16)30030-4.

Thomas, K.A., Valenzuela, N.M. and Reed, E.F. (2015) The perfect storm: HLA antibodies, complement, FcγRs, and endothelium in transplant rejection. Trends in Molecular Medicine. 21 (5) pp. 319–329. doi:10.1016/j.molmed.2015.02.004.

Tiebout, R.F., Stricker, E.A.M., Hagenaars, R., et al. (1984) Human lymphoblastoid cell line producing protective monoclonal IgG1, χ anti-tetanus toxin. European Journal of Immunology, 14 (5): 399–404. doi:10.1002/eji.1830140504.

Tiller, T., Meffre, E., Yurasov, S., et al. (2008) Efficient generation of monoclonal antibodies from single human B cells by single cell RT-PCR and expression vector cloning. Journal of Immunological Methods, 329 (1–2): 112–124. doi:10.1016/j.jim.2007.09.017.

Tinckam, K.J., Rose, C., Hariharan, S., et al. (2016) Re-examining risk of repeated HLA mismatch in kidney transplantation. Journal of the American Society of Nephrology, 27 (9): 2833–2841. doi:10.1681/ASN.2015060626.

Tonegawa, S. (1983) Somatic generation of antibody diversity. Nature, 302 (5909): 575–581. doi:10.1038/302575a0.

Topham, N.J. and Hewitt, E.W. (2009) Natural killer cell cytotoxicity: How do they pull the trigger? Immunology. 128 (1) pp. 7–15. doi:10.1111/j.1365-2567.2009.03123.x.

Torres, M.A. and Moraes, M.E.H. (2011) Nomenclature for factors of the HLA system Nomenclatura dos fatores do sistema HLA. Available at: www.ebi. (Accessed: 25 May 2020).

Townsend, A.R.M., Rothbard, J., Gotch, F.M., et al. (1986) The epitopes of influenza nucleoprotein recognized by cytotoxic T lymphocytes can be defined with short synthetic peptides. Cell, 44 (6): 959–968. doi:10.1016/0092-8674(86)90019-X.

Toyoda, M., Ge, S., Suviolahti, E., et al. (2012) IFNγ production by NK cells from HLA-sensitized patients after in vitro exposure to allo-antigens. Transplant Immunology, 26 (2–3): 107–112. doi:10.1016/j.trim.2011.11.001.

Traggiai, E., Becker, S., Subbarao, K., et al. (2004) An efficient method to make human monoclonal antibodies from memory B cells: Potent neutralization of SARS coronavirus. Nature Medicine, 10 (8): 871–875. doi:10.1038/nm1080.

Trapani, J.A. (1995) Target cell apoptosis induced by cytotoxic T cells and natural killer cells involves synergy between the pore-forming protein, perforin, and the serine protease, granzyme B. Australian and New Zealand Journal of Medicine, 25 (6): 793–799. doi:10.1111/j.1445-5994.1995.tb02883.x.

Trinchieri, G., Santoli, D., Dee, R.R., et al. (1978) Anti-viral activity induced by culturing lymphocytes with tumor-derived or virus-transformed cells: Identification of the anti-viral activity as interferon andcharacterization of the human effector lymphocyte subpopulation*. Journal of Experimental Medicine, 147 (5): 1299–1313. doi:10.1084/jem.147.5.1299.

Triulzi, D.J., Kleinman, S., Kakaiya, R.M., et al. (2009) The effect of previous pregnancy and transfusion on HLA alloimmunization in blood donors: Implications for a transfusion-related acute lung injury risk reduction strategy. Transfusion, 49 (9): 1825–1835. doi:10.1111/j.1537-2995.2009.02206.x.

Trompeter, H.-I., Gómez-Lozano, N., Santourlidis, S., et al. (2005) Three Structurally and Functionally Divergent Kinds of Promoters Regulate Expression of Clonally Distributed Killer Cell Ig-Like Receptors (KIR), of KIR2DL4 , and of KIR3DL3 . The Journal of Immunology, 174 (7): 4135–4143. doi:10.4049/jimmunol.174.7.4135.

Trowsdale, J. (2001) Genetic and functional relationships between MHC and NK receptor genes. Immunity. 15 (3) pp. 363–374. doi:10.1016/S1074-7613(01)00197-2.

Trundley, A.E., Hiby, S.E., Chang, C., et al. (2006) Molecular characterization of KIR3DL3. Immunogenetics, 57 (12): 904–916. doi:10.1007/s00251-005-0060-7.

Uhrberg, M. (2005) The KIR gene family: Life in the fast lane of evolution. European Journal of Immunology, 35 (1): 10–15. doi:10.1002/eji.200425743.

Uhrberg, M., Valiante, N.M., Shum, B.P., et al. (1997) Human diversity in killer cell inhibitory receptor genes. Immunity, 7 (6): 753–763. doi:10.1016/S1074-7613(00)80394-5.

Vahlne, G., Lindholm, K., Meier, A., et al. (2010) In vivo tumor cell rejection induced by NK cell inhibitory receptor blockade: Maintained tolerance to normal cells even in the presence of IL-2. European Journal of Immunology, 40 (3): 813–823. doi:10.1002/eji.200939755.

Valenzuela, N.M. and Reed, E.F. (2015) Antibodies to HLA Molecules Mimic Agonistic Stimulation to Trigger Vascular Cell Changes and Induce Allograft Injury. Current Transplantation Reports, 2 (3): 222–232. doi:10.1007/s40472-015-0065-6.

Valiante, N.M., Uhrberg, M., Shilling, H.G., et al. (1997) Functionally and structurally distinct NK cell receptor repertoires in the peripheral blood of two human donors. Immunity, 7 (6): 739–751. doi:10.1016/S1074-7613(00)80393-3.

Velardi, A. (2008) Role of KIRs and KIR ligands in hematopoietic transplantation. Current Opinion in Immunology, 20 (5): 581–587. doi:10.1016/j.coi.2008.07.004.

Veluchamy, J.P., Spanholtz, J., Tordoir, M., et al. (2016) Combination of NK cells and cetuximab to enhance anti-tumor responses in RAS mutant metastatic colorectal cancer. PLoS ONE, 11 (6). doi:10.1371/journal.pone.0157830.

Verheyden, S., Bernier, M. and Demanet, C. (2004) Identification of natural killer cell receptor phenotypes associated with leukemia. Leukemia, 18 (12): 2002–2007. doi:10.1038/sj.leu.2403525.

Verheyden, S. and Demanet, C. (2006) Susceptibility to myeloid and lymphoid leukemia is mediated by distinct inhibitory KIR-HLA ligand interactions [2]. Leukemia. 20 (8) pp. 1437–1438. doi:10.1038/sj.leu.2404279.

Verheyden, S., Ferrone, S., Mulder, A., et al. (2009) Role of the inhibitory KIR ligand HLA-Bw4 and HLA-C expression levels in the recognition of leukemic cells by Natural Killer cells. Cancer Immunology, Immunotherapy, 58 (6): 855–865. doi:10.1007/s00262-008-0601-7.

Veuillen, C., Aurran-Schleinitz, T., Castellano, R., et al. (2012) Primary B-CLL resistance to NK cell cytotoxicity can be overcome in vitro and in vivo by priming NK cells and monoclonal antibody therapy. Journal of Clinical Immunology, 32 (3): 632–646. doi:10.1007/s10875-011-9624-5.

Vey, N., Bourhis, J.H., Boissel, N., et al. (2012) Aphase 1 trial of the anti-inhibitory KIR mAb IPH2101 for AML in complete remission. Blood, 120 (22): 4317–4323. doi:10.1182/blood-2012-06-437558.

Vey, N., Dumas, P.-Y., Recher, C., et al. (2017) Randomized Phase 2 Trial of Lirilumab (anti-KIR monoclonal antibody, mAb) As Maintenance Treatment in Elderly Patients (pts) with Acute Myeloid Leukemia (AML): Results of the Effikir Trial. Blood, 130 (Supplement 1): 889–889. doi:10.1182/BLOOD.V130.SUPPL_1.889.889.

Vilches, C. and Parham, P. (2002) KIR : Diverse, Rapidly Evolving Receptors of Innate and Adaptive Immunity. Annual Review of Immunology, 20 (1): 217–251.

Vitale, M., Sivori, S., Pende, D., et al. (1995) Coexpression of two functionally independent p58 inhibitory receptors in human natural killer cell clones results in the inability to kill all normal allogeneic target cells. Proceedings of the National Academy of Sciences of the United States of America, 92 (8): 3536–3540. doi:10.1073/pnas.92.8.3536.

Vitale, M., Zimmer, J., Castriconi, R., et al. (2002) Analysis of natural killer cells in TAP2-deficient patients: Expression of functional triggering receptors and evidence for the existence of inhibitory receptor(s) that prevent lysis of normal autologous cells. Blood, 99 (5): 1723–1729. doi:10.1182/blood.V99.5.1723.

Vivier, E., Nunès, J.A. and Vély, F. (2004) Natural killer cell signaling pathways. Science. 306 (5701) pp. 1517–1519. doi:10.1126/science.1103478.

Vivier, E., Ugolini, S., Blaise, D., et al. (2012) Targeting natural killer cells and natural killer T cells in cancer. Nature Reviews Immunology. 12 (4) pp. 239–252. doi:10.1038/nri3174.

Wagner, B., da Silva Nardi, F., Schramm, S., et al. (2017) HLA-E allelic genotype correlates with HLA-E plasma levels and predicts early progression in chronic lymphocytic leukemia. Cancer, 123 (5): 814–823. doi:10.1002/cncr.30427.

Wagtmann, N., Biassoni, R., Cantoni, C., et al. (1995) Molecular clones of the p58 NK cell receptor reveal immunoglobulin-related molecules with diversity in both the extra- and intracellular domains. Immunity, 2 (5): 439–449. doi:10.1016/1074-7613(95)90025-X.

Waltari, E., McGeever, A., Friedland, N., et al. (2019) Functional Enrichment and Analysis of Antigen-Specific Memory B Cell Antibody Repertoires in PBMCs. Frontiers in Immunology, 10 (JUN): 1452. doi:10.3389/fimmu.2019.01452.

Wardemann, H., Yurasov, S., Schaefer, A., et al. (2003) Predominant autoantibody production by early human B cell precursors. Science, 301 (5638): 1374–1377. doi:10.1126/science.1086907.

Wasowska, B.A., Lee, C.Y., Halushka, M.K., et al. (2007) New concepts of complement in allorecognition and graft rejection. Cellular Immunology, 248 (1): 18–30. doi:10.1016/j.cellimm.2007.04.009.

Weiner, G.J. (2015) Building better monoclonal antibody-based therapeutics. Nature Reviews Cancer, 15 (6): 361–370. doi:10.1038/nrc3930.

Weinstein, J.A., Jiang, N., White, R.A., et al. (2009) High-throughput sequencing of the zebrafish antibody repertoire. Science, 324 (5928): 807–810. doi:10.1126/science.1170020.

Williams, R.C., Opelz, G., McGarvey, C.J., et al. (2016) The risk of transplant failure with hla mismatch in first adult kidney allografts from deceased donors. Transplantation, 100 (5): 1094–1102. doi:10.1097/TP.0000000000001115.

Winter, C.C., Gumperz, J.E., Parham, P., et al. (1998) Direct binding and functional transfer of NK cell inhibitory receptors reveal novel patterns of HLA-C allotype recognition. Journal of immunology (Baltimore, Md. : 1950), 161 (2): 571–7.

Winter, C.C. and Long, E.O. (1997) A single amino acid in the p58 killer cell inhibitory receptor controls the ability of natural killer cells to discriminate between the two groups of HLA-C allotypes. Journal of immunology (Baltimore, Md. : 1950), 158 (9): 4026–8.

Wrammert, J., Smith, K., Miller, J., et al. (2008) Rapid cloning of high-affinity human monoclonal antibodies against influenza virus. Nature, 453 (7195): 667–671. doi:10.1038/nature06890.

Wu, C.H., Liu, I.J., Lu, R.M., et al. (2016) Advancement and applications of peptide phage display technology in biomedical science. Journal of Biomedical Science, 23 (1): 8. doi:10.1186/s12929-016-0223-x.

Wu, J., Edberg, J.C., Redecha, P.B., et al. (1997) A novel polymorphism of FcγRIIIa (CD16) alters receptor function and predisposes to autoimmune disease. Journal of Clinical Investigation, 100 (5): 1059–1070. doi:10.1172/JCI119616.

Wyatt, R.C., Lanzoni, G., Russell, M.A., et al. (2019) What the HLA-I!—Classical and Non-classical HLA Class I and Their Potential Roles in Type 1 Diabetes. Current Diabetes Reports. 19 (12) pp. 1–11. doi:10.1007/s11892-019-1245-z.

Xu, J.L. and Davis, M.M. (2000) Diversity in the CDR3 region of V(H) is sufficient for most antibody specificities. Immunity, 13 (1): 37–45. doi:10.1016/S1074-7613(00)00006-6.

Xu, M., Hadinoto, V., Appanna, R., et al. (2012) Plasmablasts Generated during Repeated Dengue Infection Are Virus Glycoprotein–Specific and Bind to Multiple Virus Serotypes. The Journal of Immunology, 189 (12): 5877–5885. doi:10.4049/jimmunol.1201688.

Yang, W., Yoon, A., Lee, S., et al. (2017) Next-generation sequencing enables the discovery of more diverse positive clones from a phage-displayed antibody library. Experimental and Molecular Medicine, 49 (3): 308. doi:10.1038/emm.2017.22.

Yawata, M., Yawata, N., Draghi, M., et al. (2006) Roles for HLA and KIR polymorphisms in natural killer cell repertoire selection and modulation of effector function. Journal of Experimental Medicine, 203 (3): 633–645. doi:10.1084/jem.20051884.

Yeager, M. and Hughes, A.L. (1996) Interallelic recombination has not played a major role in the history of the HLA-C locus. Immunogenetics, 44 (2): 128–133. doi:10.1007/s002510050100.

Yokoyama, W.M. and Kim, S. (2006) Licensing of natural killer cells by self-major histocompatibility complex class I. Immunological Reviews. 214 (1) pp. 143–154. doi:10.1111/j.1600-065X.2006.00458.x.

Young, J.D.E., Hengartner, H., Podack, E.R., et al. (1986) Purification and characterization of a cytolytic pore-forming protein from granules of cloned lymphocytes with natural killer activity. Cell, 44 (6): 849–859. doi:10.1016/0092-8674(86)90007-3.

Yu, J., Heller, G., Chewning, J., et al. (2007) Hierarchy of the Human Natural Killer Cell Response Is Determined by Class and Quantity of Inhibitory Receptors for Self-HLA-B and HLA-C Ligands. The Journal of Immunology, 179 (9): 5977–5989. doi:10.4049/jimmunol.179.9.5977.

Yu, X., Tsibane, T., McGraw, P.A., et al. (2008) Neutralizing antibodies derived from the B cells of 1918 influenza pandemic survivors. Nature, 455 (7212): 532–536. doi:10.1038/nature07231.

Yusa, S. and Campbell, K.S. (2003) Src Homology Region 2-Containing Protein Tyrosine Phosphatase-2 (SHP-2) Can Play a Direct Role in the Inhibitory Function of Killer Cell Ig-Like Receptors in Human NK Cells. The Journal of Immunology, 170 (9): 4539–4547. doi:10.4049/jimmunol.170.9.4539.

Zachary, A.A., Kopchaliiska, D., Montgomery, R.A., et al. (2007) HLA-specific B cells: I. A method for their detection, quantification, and isolation using HLA tetramers. Transplantation, 83 (7): 982–988. doi:10.1097/01.tp.0000259017.32857.99.

Zappacosta, F., Borrego, F., Brooks, A.G., et al. (1997) Peptides isolated from HLA-Cw*0304 confer different degrees of protection from natural killer cell-mediated lysis. Proceedings of the National Academy of Sciences of the United States of America, 94 (12): 6313–6318. doi:10.1073/pnas.94.12.6313.

van der Zee, J.S., van Swieten, P. and Aalberse, R.C. (1986) Inhibition of complement activation by IgG4 antibodies. Clinical and experimental immunology, 64 (2): 415–22. Available at: http://www.ncbi.nlm.nih.gov/pubmed/3488859.

Zemmour, J., Gumpert, J.E., Hlldebrand, W.H., et al. (1992) The molecular basis for reactivity of anti-Cw1 and anti-Cw3 alloantisera with HLA-B46 haplotypes. Tissue Antigens, 39 (5): 249–257. doi:10.1111/j.1399-0039.1992.tb01943.x.

Zhang, J., Scordi, I., Smyth, M.J., et al. (1999) Interleukin 2 receptor signaling regulates the perforin gene through signal transducer and activator of transcription (Stat)5 activation of two enhancers. Journal of Experimental Medicine, 190 (9): 1297–1307. doi:10.1084/jem.190.9.1297.

Zhao, X.Y., Chang, Y.J., Xu, L.P., et al. (2014) HLA and KIR genotyping correlates with relapse after T-cell-replete haploidentical transplantation in chronic myeloid leukaemia patients. British journal of cancer, 111 (6): 1080–1088. doi:10.1038/bjc.2014.423.

Zheng, Z., Venkatapathy, S., Rao, G., et al. (2002) Expression profiling of B cell chronic lymphocytic leukemia suggests deficient CD1-mediated immunity, polarized cytokine response, altered adhesion and increased intracellular protein transport and processing of leukemic cells. Leukemia, 16 (12): 2429–2437. doi:10.1038/sj.leu.2402711.

Ziegler, K. and Unanue, E.R. (1981) Identification of a macrophage antigen-processing event required for I-region-restricted antigen presentation to T lymphocytes. Journal of immunology (Baltimore, Md. : 1950), 127 (5): 1869–75.

Zinkernagel, R.M. and Doherty, P.C. (1974) Restriction of in vitro T cell-mediated cytotoxicity in lymphocytic choriomeningitis within a syngeneic or semiallogeneic system. Nature, 248 (5450): 701–702. doi:10.1038/248701a0.

Zoet, Y.M., Brand-Schaaf, S.H., Roelen, D.L., et al. (2011) Challenging the golden standard in defining donor-specific antibodies: Does the solid phase assay meet the expectations? Tissue Antigens, 77 (3): 225–228. doi:10.1111/j.1399-0039.2010.01608.x.